Non-overlapping domain decomposition methods with non-local transmission operators for harmonic wave propagation problems

Émile Parolin

INSTITUT POLYTECHNIQUE DE PARIS

ENSTA

IP PARIS

NNT : 2020IPPAE011

Thèse de doctorat

Méthodes de décomposition de domaine sans recouvrement avec opérateurs de transmission non-locaux pour des problèmes de propagation d'ondes harmoniques

Thèse de doctorat de l'Institut Polytechnique de Paris
préparée à l'ENSTA Paris

École doctorale n°574 Mathématiques Hadamard (EDMH)
Spécialité de doctorat : Mathématiques appliquées

Thèse présentée et soutenue à Palaiseau, le 4 décembre 2020, par

Emile Parolin

Composition du Jury :

Annalisa Buffa Professeure, École polytechnique fédérale de Lausanne	Présidente
Bruno Després Professeur, Sorbonne Université (LJLL)	Rapporteur
Martin Gander Professeur, Université de Genève	Rapporteur
Patrick Ciarlet Professeur, ENSTA Paris (POEMS)	Examinateur
Xavier Claeys Maître de conférence, Sorbonne Université (LJLL)	Examinateur
Nicole Spillane Chargée de recherche, École polytechnique (CMAP)	Examinatrice
Patrick Joly Directeur de recherche, INRIA (POEMS)	Directeur de thèse
Matthieu Lecouvez Ingénieur de recherche, CEA	Invité

Remerciements

En premier lieu, j'aimerais exprimer mes profonds remerciements à mon directeur de thèse Patrick Joly pour ses conseils, sa patience ainsi que sa rigueur scientifique. Cette thèse doit également beaucoup à Xavier Claeys et je tiens sincèrement à le remercier pour la confiance qu'il m'a accordée en me partageant tout au long de ce travail ses idées, d'une richesse scientifique remarquable. Je remercie aussi chaleureusement Francis Collino pour sa disponibilité, sa culture scientifique et ses morceaux de code qui ont grandement contribué à la qualité de ce travail. Je mesure la chance que j'ai eue de pouvoir travailler avec eux trois et j'espère que notre collaboration se poursuivra au-delà de cette première expérience.

Je tiens également à remercier profondément mes deux rapporteurs, Bruno Després et Martin Gander, qui m'ont fait l'honneur de relire avec beaucoup d'attention ce manuscrit. Un grand merci aux autres membres du jury, et tout d'abord à Annalisa Buffa pour avoir accepté d'en être la présidente. Merci également à Patrick Ciarlet, Matthieu Lecouvez, et Nicole Spillane pour l'intérêt et l'attention qu'ils ont portés à mes travaux.

Un doctorant ne serait rien sans un labo, et j'ai eu la chance de travailler pendant trois ans dans un environnement particulièrement stimulant et à taille humaine. Sans les citer tous, je voudrais pour cela remercier les membres de l'équipe Poems, incarnée par sa directrice Anne-Sophie, et plus largement les membres de l'Uma qui ont su créer une ambiance agréable et accueillante pour les doctorants.

Je tiens maintenant à saluer quelques compagnons de route dans cette thèse, dont les discussions ont pu me changer les idées, ils se reconnaîtront : Corinne, Fabio, Florian, Luiz, Maria, Martin, Maryna, Yohannes. Un immense merci aussi à Sonia qui, en plus d'avoir été à l'initiative de ma rencontre avec l'équipe Poems, a toujours eu une attention particulière à mon égard. Un merci particulier à Laure (et par transitivité Clémentine et Bibou), pour son soutien dans cette aventure. Enfin, merci à Émilie, pour tout.

Acknowledgements

This work was conducted as part of the project NonLocalDD funded by the French National Research Agency, grant ANR–15–CE23–0017–01, whose project leader was Xavier Claeys.

Abstract

Keywords: Domain decomposition methods, harmonic waves, junction points.

The pioneering work of B. Després then M. Gander, F. Magoules and F. Nataf have shown that it is mandatory, at least in the context of wave equations, to use impedance type transmission conditions in the coupling of subdomains in order to obtain convergence of non-overlapping domain decomposition methods (DDM). In the standard approach considered in the literature, the impedance operator involved in the transmission conditions is local and leads to algebraic convergence of the DDM in the best cases. In later works, F. Collino, S. Ghanemi and P. Joly then F. Collino, P. Joly and M. Lecouvez have observed that using non local impedance operators such as integral operators with suitable singular kernels could lead to a geometric convergence of the DDM.

This thesis extends these works (that mainly concerned the scalar Helmholtz equation) with the extension of the analysis to electromagnetic wave propagation. Besides, the numerical analysis of the method is performed for the first time, proving the stability of the convergence rate with respect to the discretization parameter, hence the robustness of the approach. Several integral operators are then proposed as transmission operators for Maxwell equations in the spirit of those constructed for the acoustic setting. An alternative to integral operators, based on the resolution of elliptic auxiliary problems, is also advocated and analyzed. Extensive numerical results are conducted, illustrating the high potential of the new approach. Based on a recent work by X. Claeys, the last part of this work consists in exploiting the multi-trace formalism to extend the convergence analysis to the case of partitions with junction points, which is a difficult problem that attracted a lot of attention recently. The new approach relies on a new operator that communicates information between sub-domains, which replaces the classical point-to-point exchange operator. A proof of geometrical convergence of the associated iterative algorithm, again uniform with respect to the discretization parameter, is available and we show that one recovers the standard algorithm in the absence of junction points.

Résumé

Mots clés : Méthodes de décomposition de domaine, ondes harmoniques, points de jonction.

Les premiers travaux de B. Després, puis M. Gander, F. Magoules et F. Nataf ont montré qu'il est nécessaire, du moins dans le contexte des équations d'ondes, d'utiliser des conditions de transmission de type impédante pour le couplage des sous-domaines afin d'obtenir la convergence des méthodes de décomposition de domaine sans-recouvrement. L'approche standard considérée dans la littérature utilise un opérateur d'impédance local permettant une convergence algébrique dans les meilleurs cas. Des travaux ultérieurs dus à F. Collino, S. Ghanemi et P. Joly puis F. Collino, P. Joly et M. Lecouvez ont permis de montrer que l'utilisation d'opérateurs d'impédance non-locaux, comme par exemple des opérateurs intégraux avec des noyaux singuliers adaptés, peut permettre une convergence géométrique des méthodes de décomposition de domaine.

Cette thèse prolonge ces travaux (qui ont principalement concerné l'équation de Helmholtz scalaire) pour dans un premier temps étendre l'analyse au cas de la propagation d'ondes électromagnétiques. De plus, l'analyse numérique de la méthode est pour la première fois effectuée, démontrant la stabilité du taux de convergence par rapport au paramètre de discrétisation, et ainsi la robustesse de l'approche. Plusieurs opérateurs intégraux sont ensuite proposés comme opérateurs de transmission pour les équations de Maxwell dans le même esprit que ceux construits pour le cas de l'acoustique. Une alternative aux opérateurs intégraux, fondée sur la résolution de problèmes auxiliaires elliptiques, est par ailleurs proposée et étudiée. De nombreuses expériences numériques ont été menées, illustrant le haut potentiel de cette nouvelle approche. À partir de récents travaux de X. Claeys, la dernière partie de ce travail consiste à exploiter le formalisme multi-trace afin d'étendre l'analyse au cas des partitions comportant des points de jonction, problème ayant attiré beaucoup d'attention récemment. Cette nouvelle approche met en jeu un nouvel opérateur permettant la communication d'informations entre sous-domaines, qui a vocation à remplacer l'opérateur point-à-point classique. Une preuve de convergence géométrique de l'algorithme itératif associé, également uniforme par rapport au paramètre de discrétisation, est disponible et l'on montre que l'on retrouve l'algorithme classique en l'absence de point de jonction.

Contents

List of Symbols

d	Embedding medium dimension $\in \{1, 2, 3\}$
ν	Outward unit normal vector
ω	Frequency
κ_0	Wave number of reference medium
a	Variable coefficient (dimensionless)
n	Variable coefficient (dimensionless)
D	Differential operator
D^*	Adjoint of D
L	Elliptic operator
U	Hilbert space (3.8)
U_Γ	Hilbert space with a regular trace on Γ (3.68)
V_h	Discrete Hilbert space (4.1)
$\mathbb{U}$	Broken Hilbert space (3.92)
$\mathbb{U}_\Gamma$	Broken Hilbert space with a regular trace on Γ (3.93)
$\mathbb{V}_h$	Broken discrete Hilbert space (4.27)
γ_0	Dirichlet trace operator (3.29)
γ_1	Neumann trace operator (3.29)
$\boldsymbol{\gamma}_{0,\parallel}$	Dirichlet multi trace operator (3.123)
$\boldsymbol{\gamma}_{1,\parallel}$	Neumann multi trace operator (3.123)
$\boldsymbol{\gamma}_\parallel$	Multi trace operator (3.123)
$\boldsymbol{\gamma}_{0,\times}$	Dirichlet multi trace operator (9.9)
$\boldsymbol{\gamma}_{1,\times}$	Neumann multi trace operator (9.9)
$\boldsymbol{\gamma}_\times$	Multi trace operator (9.9)
$\boldsymbol{\gamma}_{0,h,\parallel}$	Discrete Dirichlet multi trace operator (4.35)
$\boldsymbol{\gamma}_{0,h,\times}$	Discrete Dirichlet multi trace operator (10.2)
X_0	Dirichlet trace space (3.25)
$\mathrm{X}_{1/2}$	Pivot space between trace space (3.46)
X_1	Neumann trace space (3.25)
X	Trace space (3.71)
$\mathrm{X}_{0,h}$	Dirichlet discrete trace space (4.5)
$\mathrm{X}_{1,h}$	Neumann discrete trace space (4.7)
X_h	Discrete trace space (4.11)
$\mathbb{M}_{0,\parallel}$	Dirichlet multi trace space (3.120)
$\mathbb{M}_{1/2,\parallel}$	Pivot space between the multi trace space (3.120)
$\mathbb{M}_{1,\parallel}$	Neumann multi trace space (3.120)
$\mathbb{M}_\parallel$	Multi trace space (3.120)
$\mathbb{M}_{0,\times}$	Dirichlet multi trace space (9.6)

$\mathbb{M}_{1/2,\times}$	Pivot space between the multi trace space (9.6)
$\mathbb{M}_{1,\times}$	Neumann multi trace space (9.6)
$\mathbb{M}_{\times}$	Multi trace space (9.6)
$\mathbb{M}_{0,h,\parallel}$	Discrete Dirichlet multi trace space (4.32)
$\mathbb{M}_{1,h,\parallel}$	Discrete Neumann multi trace space (4.32)
$\mathbb{M}_{h,\parallel}$	Discrete multi trace space (4.32)
$\mathbb{M}_{0,h,\times}$	Discrete Dirichlet multi trace space (10.1)
$\mathbb{M}_{1,h,\times}$	Discrete Neumann multi trace space (10.1)
$\mathbb{M}_{h,\times}$	Discrete multi trace space (10.1)
$\mathbb{C}_{\parallel}$	Cauchy trace space (3.132)
$\mathbb{C}_{\times}$	Cauchy trace space (9.17)
$\mathbb{C}_{h,\parallel}$	Discrete Cauchy trace space (4.43)
$\mathbb{C}_{h,\times}$	Discrete Cauchy trace space (10.10)
$\mathbb{S}_{0,\parallel}$	Dirichlet single trace space (3.140)
$\mathbb{S}_{1,\parallel}$	Neumann single trace space (3.140)
$\mathbb{S}_{\parallel}$	Single trace space (3.140)
$\mathbb{S}_{0,\times}$	Dirichlet single trace space (9.24)
$\mathbb{S}_{1,\times}$	Neumann single trace space (9.24)
$\mathbb{S}_{\times}$	Single trace space (9.24)
$\mathbb{S}_{0,h,\parallel}$	Discrete Dirichlet single trace space (4.45)
$\mathbb{S}_{1,h,\parallel}$	Discrete Neumann single trace space (4.45)
$\mathbb{S}_{h,\parallel}$	Discrete single trace space (4.45)
$\mathbb{S}_{0,h,\times}$	Discrete Dirichlet single trace space (10.12)
$\mathbb{S}_{1,h,\times}$	Discrete Neumann single trace space (10.12)
$\mathbb{S}_{h,\times}$	Discrete single trace space (10.12)
$\mathbf{T}_{0,\parallel}$	Transmission operator (3.172)
$\mathbf{T}_{1,\parallel}$	Transmission operator (3.172)
$\mathbf{T}_{1/2,\parallel}$	Transmission operator (3.172)
$\mathbf{Z}$	Impedance operator (3.173)
$\mathbf{T}_{0,\times}$	Transmission operator (9.65)
$\mathbf{T}_{1,\times}$	Transmission operator (9.65)
$\mathrm{t}_{0,\parallel}$	Scalar product on Dirichlet multi-trace (3.228)
$\mathrm{t}_{1,\parallel}$	Scalar product on Neumann multi-trace (3.228)
$\mathrm{t}_{1/2,\parallel}$	Scalar product on multi-trace pivot space (3.228)
$\mathrm{t}_{0,\times}$	Scalar product on Dirichlet multi-trace (9.67)
$\mathrm{t}_{1,\times}$	Scalar product on Neumann multi-trace (9.67)
$\mathrm{t}_{0,h,\parallel}$	Discrete transmission operator (4.82)
$\mathrm{t}_{1,h,\parallel}$	Discrete transmission operator (4.82)
z_{h}	Discrete transmission operator (4.84)
$\mathrm{t}_{0,h,\times}$	Discrete transmission operator (10.39)
$\mathbf{P}_{0,\times}$	Projector on the Dirichlet single trace space (9.79)
$\mathbf{P}_{1,\times}$	Projector on the Neumann single trace space (9.79)
$\mathbf{P}_{0,h,\times}$	Discrete projector (10.67)
$\mathbf{\Pi}_{\parallel}$	Exchange operator (3.184)
$\mathbf{\Pi}_{0,\times}$	Communication operator in Dirichlet multi trace (9.80)
$\mathbf{\Pi}_{1,\times}$	Communication operator in Neumann multi trace (9.80)
$\mathbf{\Pi}_{0,h,\times}$	Discrete communication operator (10.68)
$\mathbf{S}_{1,\parallel}$	Scattering operator (3.176)
$\mathbf{S}_{0,\times}$	Scattering operator (9.71)

Introduction

Contents

Motivation for domain decomposition

Historically, Domain Decomposition (DD) methods were invented by Schwarz [125]. The purpose was to prove existence of solution of Laplace equation in domains that are unions of sub-domains with simple shapes, for which existence proofs were known. Nowadays, the interest in DD methods has somehow shifted from a theoretical tool to a practical numerical strategy, able to leverage the increasing power of modern parallel supercomputers. Broadly speaking, the main motivation is now to be able to accurately compute numerical solutions to increasingly more complex problems. DD methods generally refer to a coupling strategy for different Partial Differential Equations (PDE) models and/or discretization methods in adjacent sub-domains. In this work, however, we focus only on the situation where we want to solve only one type of equation, related to *time-harmonic wave propagation problems*, posed in a *large* domain.

Mechanically, as the size of the domain of interest grows, the size of the associated linear systems, obtained using standard numerical methods such as the finite element method (FEM), also increases. At some point, the size of the linear system will become so big that using a direct solver will not be feasible for a given machine. A possible approach could then be to use an iterative solver (e.g. Krylov solvers) to solve the problem. However, for the propagative (and even elliptic) problems we consider, the linear systems are often ill-conditioned. For a typical mesh size h, the condition number is of the order of $\mathcal{O}(h^{-2})$ [127, Section 1.2]. So the iterative solver would struggle to solve the large system without a preconditioner.

For wave propagation problems, the conditioning issue is often tied to mesh requirements induced by the wave propagation phenomena. Indeed, as the wavelength λ decreases, the mesh shall be refined to capture the finer oscillations. One expects to decrease h at least linearly with λ. However, the so-called pollution effect makes the situation even worse since the finite element error actually increases with the frequency when the number of points per wavelength is kept constant. Besides, the additional inherent difficulty of wave propagation problems, in

comparison to elliptic ones, mainly lies in the (a priori) indefiniteness of the wave equation and therefore of the related linear systems after discretization.

DD methods appear as one possible way to tackle the issue of large problems by applying the 'divide and conquer' strategy. The main idea is to divide the domain in many small sub-domains, small enough so that the PDE can be solved easily in each sub-domain by means of a direct method for instance. Moreover, each local solve in the sub-domains can be done independently and in parallel on different machines or cluster nodes, thereby harvesting the power of modern distributed architectures. These independent local solves alone will not yield the global solution. However one can hope to construct a convergent sequence of local solutions by iteratively solving the local sub-problems and letting sub-domains exchange some (boundary) information in-between successive solves. The art of domain decomposition is precisely to devise efficient methods to doing so and in particular on the adequate prescription of transmission conditions between sub-domains.

Overlapping and non-overlapping strategies

In the large class of DD methods, there are two important sub-classes: the *overlapping* and *non-overlapping* strategies, which refer to the type of underlying partition of the domain on which the DD method is built. Roughly speaking, in an overlapping partition each sub-domain shares a set of non-zero measure with its neighbours, whereas in a non-overlapping partition two adjacent sub-domains are separated by an interface of inferior dimension.

If the initial algorithm of Schwarz [125] is based on an overlapping partition and the convergence proof of Lions [94] actually rests on the existence of the overlap, overlapping strategies possess many drawbacks in practical numerical implementations. First of all, the size of the local sub-problems is increased by the size of the overlap, making the local solves somehow unnecessarily more expensive. In addition, the generation of overlapping mesh partitions and the implementation of overlapping domain decomposition methods are more involved than non-overlapping strategies. Finally, we also point out that when DD methods are used to couple two different PDE models, the non-overlapping strategies are much more natural to consider.

All these limitations are not prohibitive and many successful methods are built on overlapping partitions, however this work is only dedicated to non-overlapping configurations.

Impedance-based domain decomposition methods

In classical Schwarz methods, the information coming from adjacent sub-domains is incorporated in the local sub-problems in the form of either non-homogeneous Dirichlet (as proposed by Schwarz [125]) or Neumann boundary conditions. However, such classical Schwarz algorithms suffer from two issues

- they do not converge for Helmholtz type problems, even with overlap;
- they do not converge in a non-overlapping configuration, even for a coercive problem.

The breakthrough idea, proposed independently by Lions [96] for the Laplace equation and Després [49] for the Helmholtz equation, is to combine Dirichlet and Neumann traces to form Robin transmission conditions. One can use a scalar coefficient to compute the Robin quantity, but this can be generalized easily to a (local or non-local) boundary operator. Such an operator is referred to as the *transmission* or *impedance* operator. The term impedance is justified by the fact that such an operator has the homogeneity of an impedance. We shall use both terms

indifferently. Two key benefits of such transmission conditions are that, first, they make Schwarz-type algorithms applicable for Helmholtz-like propagation problems [49], and second, do not require overlapping to actually converge [96]. Furthermore, for elliptic problems with overlapping, compared to the classical Schwarz algorithm, the convergence rate is always improved [67, Th. 1].

Many refinements on this original idea have been proposed, which mainly consist in using more sophisticated transmission or impedance operators to construct the generalized Robin condition. In the following, we shall distinguish different domain decomposition methods by the transmission operator that is used. When designing a transmission operator, the main objective is of course to obtain faster convergence, i.e. the minimum number of iterations, without increasing the computation cost of one iteration too much. However, as far as the mathematical analysis is concerned, the first question that arises and which we shall ask ourselves is the following:

Given a transmission operator, are the local sub-problems well-posed?

It is in general difficult to answer this question directly, since it does not only depend on the type of transmission operator but also on the nature of the problem, on the regularity of the interface and so on. Broadly speaking, for wave propagation problems, a sufficient condition to ensure that the sub-problems will be well-posed is if the real-part (to be defined) of the operator is positive, at least for a regular enough interface. At the discrete level, this will translate as invertible matrices, at least for sufficiently refined meshes. To try to answer the above question more precisely, we can classify the transmission operators found in the literature into three broad categories:

- The *identity operator* of Després [49] deserves its own category. It yields properly defined transmission conditions and the associated local sub-problems are always well-defined.
- *High-order local operators*, by which we mean second-order surface differential operators but also rational fractions of such operators.

  Second order operators have been proposed by Gander, Magoules and Nataf [72] for the Helmholtz equation. Numerical experiments suggest that they improve the convergence rates of the relaxed Jacobi algorithm, provided that the parameters involved in the definition of the transmission operators are properly tuned. If the second-order differential operator is positive and the interface is regular enough, the local sub-problems will be in general well-posed.

  The use of higher-order or rational fractions of surface differential operators was advocated by Boubendir, Antoine and Geuzaine [17] for the Helmholz equation and El Bouajaji, Thierry, Antoine and Geuzaine in [61] for Maxwell equations, in an attempt to approximate transparent or absorbing boundary conditions. For such operators, the convergence analysis is incomplete. In particular, they do not satisfy the sufficient condition of positivity so that the well-posedness of local sub-problems remains in general an open problem and depends on the configuration.
- *Non-local operators*: their interest in domain decomposition methods, which lies in the theoretical guarantees of convergence, was first advocated in [78] for the Helmholtz equation, despite their increased computational cost. Among other properties, positivity is explicitly required for such impedance operators in order to ensure the well-posedness of local sub-problems.

Note that we only cited above a few references, a more complete and detailed review of the literature is conducted in the first chapter.

The domain decomposition methods based on impedance conditions are often referred to as 'Optimized Schwarz Methods' (OSM) in the literature. The term seems to have been introduced in [69] for symmetric positive definite problems. The 'optimized' term refers to the possibility to tune the free parameters (which can be generalized to a boundary operator) that comes into play when one combines the Dirichlet and Neumann quantities together. The goal of this tuning is to decrease the convergence factor (i.e. improve the convergence rate) of the Jacobi iterative algorithm, as was done for instance in [67, 72, 75, 97] for the Helmholtz equation in non-overlapping configurations.

Convergence analysis: the utility of non-local operators

Domain decomposition methods are by nature iterative methods. The simplest iterative algorithms are often considered for the theoretical analysis of convergence, namely fixed-point algorithms such as the (relaxed) Jacobi or the Gauss-Seidel algorithms. However in practice one typically uses Krylov acceleration techniques, for instance the GMRES algorithm, since for wave propagation problems the matrices are in general indefinite. Note that the convergence of the relaxed Jacobi algorithm implies the convergence of the corresponding GMRES algorithm, even for the restarted version (the converse is not true). In this respect, it is important to study theoretically the relaxed Jacobi algorithm.

Several important questions arise when we consider the mathematical analysis of the convergence of domain decomposition algorithms:

> Is the algorithm convergent to the solution of the original problem?
>
> What is the convergence rate?
>
> After discretization, how does the convergence rate depend on the parameter h?

A highly desirable property for domain decomposition methods often encountered in the literature is the notion of *optimality*, in the sense of Toselli and Widlund [127, Def. 1.2, Sec. 1.3], i.e. *"a rate of convergence to the exact solution independent of the size of the system"*, which is related to the third question above.

The answers to these questions vary again greatly depending on the transmission operator that is used. We use our previous classification to structure the discussion on this matter:

- *Identity operator*: The relaxed Jacobi algorithm is provably convergent, with an algebraic convergence [49] and the convergence is guaranteed both in the continuous and discrete settings. The proof is based on the decrease of a pseudo-energy. However the convergence rate is not h-uniform for both the Jacobi and GMRES algorithm.

- *High-order local operators*: Domain decomposition methods based on high-order local operator or rational fractions of local operators lack a general convergence analysis. Some partial proofs are available but concern specific geometries amenable to Fourier or modal analysis [17, 61]. However, the actual implementations of the method seem to perform rather well.

  The convergence proof based on energy considerations can be extended in some particular cases to several (positive) second-order differential operators, as was done for instance by Piacentini and Rosa [117] or by Després, Nicolopoulos and Thierry in a recent paper [52], both for the acoustic case.

- *Non-local operators*: The main motivation for considering non-local operators comes from the guaranteed *geometric* convergence of the relaxed Jacobi algorithm [78, 91]. Besides, the convergence rate is observed to be stable with the discretization.

Junctions and cross-points

In non-overlapping configurations, the special points (in 2D) or lines (in 3D) where strictly more than two domains abut are termed 'junctions' or 'cross-points', depending on the authors. We shall use both terms indifferently, although the term 'cross-points' is strictly speaking more applicable to two-dimensional configurations. Besides, it is important to distinguish such *interior* cross-points with the points (in 2D) or lines (in 3D) that mark the intersection of an interface between two sub-domains with the physical boundary of the global domain, and which are termed *boundary* cross-points. The union of all junctions lines in 3D is sometimes referred to as the 'wire-basket'.

For realistic large scale applications, domain decomposition methods should be applicable to domain partitions with junctions, whose presence is in general inevitable if an automatic mesh partitioner is used. However, the presence of junctions can be an issue both at the theoretical level for the convergence analysis of the method and in practice in numerical implementations.

The nature of the issue posed by junctions varies depending on the type of transmission operators that are used. We review below the literature on the subject, mainly for the Helmholtz equation as it is rather scarce for the electromagnetic case:

- *Identity operator*: There is no additional issue in presence of junctions to define and analyse the DD method at the continuous level. In addition, the convergence proof based on energy estimates [49] still stands in presence of junction points. At the discrete level, one possible route that avoids the junction problem altogether is to use a mixed-hybrid finite element formulation as in the original work of Després [49]. The advantage of the approach is that no degree of freedom is associated to cross-points.

  In contrast, delicate questions may arise in the definition of transmission conditions at cross-points in the case where nodal discretizations are used and for which degrees of freedom are associated to cross-points. For instance, Gander and Kwok [71] pointed out, already for elliptic problems, that straightforward nodal discretizations (for which degrees of freedom are associated to cross-points) can diverge and that the continuous proof (based on energy estimates) fails to carry over to the discrete setting in general.

  Some ad-hoc treatment of the problem at the discrete level has been developed by Bendali and Boubendir [13, 15] which introduces additional global unknowns at the junction points effectively coupling all sub-domains. This leads to a global indefinite system posed on the reunion of all junctions that needs to be solved at each iteration.

  More recently, Gander and Santugini [73] introduced two techniques, termed 'auxiliary variable' and 'complete communication', to treat the issue. They present the strategies for elliptic problems but we believe that the approach could be extended to wave propagation problems.

- *High-order local operators*: When second or higher-order impedance operators are used, the implementation difficulties in continuous Lagrange finite element methods still stands, but the junction points are already troublesome at the continuous level. The main additional issue is the presence of a 'corner', which raises a definition issue due to the use of high-order operators (for instance Laplace-Beltrami operators) on open surfaces. One needs some compatibility conditions to be enforced at the corners to ensure the well-posedness of the problems with such transmission conditions, a problem that is somehow overlooked in many papers.

  Modave *et al* [105] reported non-consistency issue in the absence of treatment of junction points with physical boundaries in the context of high-order absorbing boundary conditions.

They presented a discrete treatment of cross-points for high-order transmission operators. However, the approach is only valid on cartesian-like partition of the mesh, allowing only to treat cross- points where an even number of domains abut.

The issue has been addressed recently by Després, Nicolopoulos and Thierry [52] for a class of second-order transmission operators. Quasi-continuity relations are used at the corners to obtain a transmission operator suited for broken line interfaces. The convergence of the algorithm is proven by using energy estimate techniques.

- *Non-local operators*: In presence of junctions, DD methods using non-local operators can be properly defined at the continuous level, and are provably convergent [78]. However, the geometric convergence proof [42, 44, 91] is not valid in presence of cross-points. Besides, numerical experiments suggest that the convergence is in fact *not* geometric, and we shall provide some numerical evidence of this fact.

Research direction and main contributions

First, let us point out that the work we present here is the latest development in a long standing research effort on domain decomposition methods for wave propagation problems that dates back to the PhD thesis of Bruno Després in 1991 [49], already under the supervision of Patrick Joly, and from which the idea to use Robin transmission conditions to obtain convergence of domain decomposition algorithms for the Helmholtz equation firstly emerged. This initial work was later completed in the course of Souad Ghanemi PhD in 1996 [78], also advised by Patrick Joly and in which Francis Collino took also part. The idea to use non-local transmission operators was then developed and the geometric convergence of the associated relaxed Jacobi and Gauss-Seidel algorithms was proven. More recently, the subject was revived during the PhD of Matthieu Lecouvez in 2015 [91], still supervised by Patrick Joly, with Francis Collino also involved. Several integral operators were proposed and analyzed for the Helmholtz equation, and tested numerically in 2D. These different contributions were the main starting point of the ANR project 'NonLocal DD' led by Xavier Claeys, which funded this work.

The first purpose of this work is to extend the convergence analysis of non-overlapping domain decomposition methods with *non-local* transmission operators that was available for the Helmholtz equation [42, 43, 44, 78, 91] to the electromagnetic setting. We achieve this by providing an abstract framework that includes both the acoustic and electromagnetic settings and which is the subject of Part I of this manuscript.

The second purpose of this work is to combine the convergence analysis with the actual construction of suitable non-local impedance operators for Maxwell equations that satisfy the requirements of the theory. This is the subject of Part II of this manuscript. The natural idea was to extend the work of Lecouvez [91] where integral-based transmission operators adapted to the acoustic case where advocated and numerically tested. This task proved to be rather difficult. First on the theoretical side, since the functional setting associated to the Maxwell equations is more intricate. Second, on the numerical implementation of the operators which required great care. Despite the amount of work dedicated to these aspects and which is reported in this manuscript for completeness, the outcome of the numerical tests in 3D is rather disappointing. However, these difficulties motivated the investigation of a new route to construct suitable non-local operators which proved in turn to be rather successful in our numerical experiments. These operators are no longer integral operators (which were discretized using the boundary element method) but rather involve solving auxiliary elliptic problems which are more easily solved numerically and do not require sophisticated technologies. We provide a generic definition, with simple adaptations to the acoustic or electromagnetic settings, which includes

the case of heterogeneous media. The parameters appearing in the definition are easy to choose and do not require complicated tuning to get efficiency. Besides, these transmission operators can be used in sub-domains of arbitrary geometry, including ones with rough boundaries generated by automatic graph partitioners, without any additional treatment.

A third research direction for this work was to prove the stability with respect to the discretization parameter of the geometric convergence of domain decomposition methods using suitable non-local impedance operators. This was a conjecture, largely supported by numerical evidence, made for instance in [91]. We rigorously proved this result in the acoustic case, see the numerical analysis of Part I (the case of Maxwell equations is only partially covered by our analysis). This axis of research led to the published work [30].

Finally, the last research direction concerned by this work is the investigation of the cross-point issue, namely the fact that cross-points break the geometric convergence proof. Using the multi-trace formalism and leveraging the ideas proposed by Xavier Claeys in a recent paper [29] we provide an answer to the problem by defining a new communication operator that exchanges information between sub-domains. The geometric convergence proof is recovered if suitable non-local transmission operators are used and remains stable after discretization. Importantly, the method is found to be a generalization of the previously described method in absence of junction points. This axis of research led to the preprint work [33].

Let us summarize below the outcome of this work, in what we believe are our four main contributions:

1. The description and analysis of a large class of non-overlapping domain decomposition methods for wave propagation problems, including both the Helmholtz equation and **3D time-harmonic Maxwell's equations**, with suitable non-local transmission operators. This is completed by an actual implementation and testing of the method for a standard finite element discretization;

2. The design of a **novel transmission operator** based on auxiliary elliptic problems which satisfies the requirements of the convergence theory and can be generalized to a large class of wave propagation problems including both the acoustic and electromagnetic settings;

3. The numerical analysis of a finite-element based Galerkin discretization of the domain decomposition method applied to the Helmholtz equation. We proved the h**-uniform stability** of the geometric convergence for the relaxed Jacobi algorithm;

4. The description and analysis, supported by extensive numerical results, of a specific domain decomposition method that performs a clean treatment of configurations with **junction points**, allowing to recover the geometric convergence of the algorithm if suitable non-local transmission operators are used.

We acknowledge, in addition to Patrick Joly as PhD-advisor, the participation throughout this work of two additional collaborators. Xavier Claeys, leader of the ANR project that funded this work, who came up in particular with the breakthrough ideas regarding the fourth contribution above. Francis Collino, also enrolled in the ANR project, who participated actively in the development (and implementation) of new non-local transmission operators, in particular regarding the second contribution above.

Outline of the work

There are two preliminary chapters:

1. Chapter 1: we conduct an overview of the literature from our perspective, i.e. the emphasis is on domain decomposition methods that can be applied to time-harmonic wave propagation problems.

2. Chapter 2: in this chapter we try to motivate in a simple two-domain configuration our usage of the Multi-Trace (MTF) formalism [83, 84, 32, 38] for domain decomposition methods. This is intended as an introduction to the main concepts that we will extensively manipulate in subsequent chapters. The basic foundation of our treatment of junction points is also laid out.

The rest of the manuscript is organized as follows:

1. **Part I: we describe and analyse an abstract generalization of a class of non-overlapping domain decomposition methods for some time-harmonic wave propagation problems.** This contribution builds on previous works that were mainly concerned with acoustic wave propagation [42, 43, 44, 78, 91]. The initial aim was to generalize the method to the electromagnetic setting. We extend the formalism to a wider class of wave-type problems, provided that some simple abstract assumptions hold, that includes both the Helmholtz and Maxwell equations. The domain decomposition methods we consider belong to the family of impedance-based methods and our focus is on the derivation of sufficient conditions on the impedance or transmission operators to ensure fast (geometric) convergence of iterative algorithms.

    - Chapter 3: the abstract domain decomposition method is firstly defined and analysed at the continuous level. We write and prove the equivalence between our (abstract) model problem and an (abstract) decomposed problem. We then show how to recast the formulation as an interface problem posed on the skeleton of the partition before describing some iterative algorithms that can be applied to solve it. The convergence analysis is conducted and sufficient conditions on the transmission operator for geometric convergence of the relaxed Jacobi algorithm are provided. The last section of the chapter establishes that our abstract framework is valid for the two main applications we have in mind, namely acoustic and electromagnetic harmonic wave propagation problems.
    - Chapter 4: this chapter is devoted to the numerical analysis of a particular choice of discretization of the previously described method, namely conformal Galerkin discretization. We show that the discrete problem can also be decomposed and reformulated equivalently on the skeleton. Besides, we settle the crucial question of uniform stability of the geometric convergence of the iterative domain decomposition method, which was recognized before this work as an open question in [91, Rem. 3, Chap. 6]. Indeed, we prove that the convergence factor of the discrete Jacobi algorithm is uniformly bounded above with respect to the discretization parameter, upon using transmission operators with suitable uniform continuity and coercivity properties. This important result rests on the theoretical existence of a continuous and stable discrete Dirichlet lifting, constructed from the Scott-Zhang interpolator. We show that widely used discretization methods for Helmholtz equation using standard finite elements fall in our abstract discrete framework.

2. **Part II: we advocate several new transmission operators that satisfy the requirements of the theory.** We can further structure the work in this direction into two main branches:

   - Chapters 5, 6 and 7: we focus our attention on *integral* operators (of convolution type). Similar transmission operators were studied in earlier works such as [44, 91] for the acoustic setting and [34] for the electromagnetic setting.
     - Chapter 5: we propose and construct several candidate transmission operators based on potential theory with adequate theoretical properties, both for Helmholtz and Maxwell equations. Our main concern is to propose, for the Maxwell case, impedance operators for which we know techniques that reduce the computational burden of non-local operators without compromising their essential properties.
     - Chapter 6: we use modal analysis for spherical geometries in the electromagnetic setting to compare more quantitatively the operators previously described. This completes the theoretical analysis and provides further confidence in our propositions of suitable transmission operators.
     - Chapter 7: the numerical implementation of the previously introduced operators is discussed and numerical experiments are conducted. Numerical experiments with the newly proposed operators in 3D are however disappointing. Our investigations suggest that the issue lies in the discretization method that is used to compute the integral operators, namely the boundary element method (BEM) which would not cope well with the finite element method (FEM) that is used to solve the equation in the domain.
   - Chapter 8: in this chapter we propose a novel realisation of a suitable non-local transmission operator based on elliptic auxiliary problems. This idea, which can be applied seamlessly either to the acoustic or the electromagnetic setting, appears to be new. If the underlying continuous operator is of very similar nature as the operators based on integral representations discussed in the preceding chapters, we show in our numerical experiments that it behaves much better in practice. The implementation of this operator exonerates from the need to interface (or implement) a boundary element code and can be carried out so that to have a reduced computational footprint. To do so, the geometric domain in which the auxiliary problem is solved is restricted to a strip whose boundary coincides on one side with the transmission interface and is a fictitious boundary on the other side. We discuss and carefully compare the behaviour of the operator for various boundary conditions on the fictitious boundary as the width of the strip is shrunk. Based on our numerical experiments this operator seems particularly well-suited for heterogeneous media.

3. **Part III: we describe and analyse a generalization of the domain decomposition that allows the presence of junction points.** We build upon the multi-trace formalism and the breakthrough idea proposed in [29] which provides a new point of view on the classical point-to-point exchange operator. This is the product of a joint work with Xavier Claeys who provided most of the theoretical foundation in the analysis.

   - Chapter 9: the novel domain decomposition strategy that permits the presence of interior junction points (still excluding junction points with the physical boundary for the sake of simplicity) is described at the continuous level. The presentation follows the same abstract route as what was done in Chapter 3, highlighting in the process the key features that permit to handle cross points. We show that under some mild

conditions on the transmission operators the method falls back to the one described in Chapter 3 in the absence of junction points. In addition, we provide again sufficient conditions on the transmission operators to guarantee the geometric convergence of the relaxed Jacobi algorithm.

- Chapter 10: the numerical analysis of a discrete version of the previously described domain decomposition strategy is considered in full generality (i.e. the method allows for interior as well as boundary cross points). Again, the discrete solution of the original discrete problem is a fixed point of the interface problem posed on the skeleton. We show for the acoustic setting that this new method also enjoys h-uniform bounds on the convergence rate of the relaxed Jacobi algorithm, upon using transmission operators with suitable uniform continuity and coercivity properties.
- Chapter 11: extensive numerical experiments are provided to support the theory. We show numerical illustrations of the h-uniform stability of the convergence rate when using non-local operators. The robustness of the method is demonstrated through numerical tests with increasing frequency and in heterogeneous media. Strong and weak scalability tests are also performed. Besides, we demonstrate numerically that the novel exchange of data between sub-domains can be performed efficiently.

Chapter 1

State of the art

Contents

Domain decomposition is a very active field of research and the associated literature is vast, particularly regarding the design and analysis of methods for the numerical simulation of elliptic problems. See for instance the books [58, 118, 113, 127] for a general reference, and [68] for an historic of the field. Note that our review is mainly focused on methods for time-harmonic wave propagation problems, which is the subject of this work, and more precisely on the literature that views (as we do) domain decomposition methods at the PDE level. This bias actually excludes a large body of valuable references that adopt a more algebraic point of view.

The chapter is organized in three sections. In the first section we provide some brief computations which we find enlightening. It indicates the interest in using Robin-type transmission conditions for wave propagation problems in a non-overlapping configuration. This is a clear difference with the original overlapping Schwarz algorithm which relies only on Dirichlet conditions. The second section is devoted to an overview of the different transmission operators that one can use to define (non-overlapping) domain decomposition methods for wave propagation problems. In the third section we review several treatments that have been proposed to address the different issues that arise in the presence of cross-points.

1.1 A revisit of the initial Schwarz algorithm

The purpose of this section is to motivate the use of (non-overlapping) impedance-based domain decomposition methods. We show that the initial algorithm of Schwarz does not converge when either the sub-problems do not overlap or the problem is no longer elliptic.

In his celebrated paper from 1870 [125], Schwarz considers the existence of a solution to the following Dirichlet problem

$$\begin{cases} -\Delta u = 0, & \text{in } \Omega = \Omega_1 \cup \Omega_2, \\ u = g, & \text{on } \partial\Omega. \end{cases} \tag{1.1}$$

where Ω_1 and Ω_2 are two *overlapping* sub-domains.

The solution is proved to exist as the (well-defined) limit of the sequence of local solutions $(u_1^n,\, u_2^n)$, constructed for $n \geq 1$ and two initial guesses u_1^0 and u_2^0 as follows,

$$\begin{cases} -\Delta u_1^n = 0, & \text{in } \Omega_1, \\ u_1^n = g, & \text{on } \partial\Omega \cap \partial\Omega_1, \\ u_1^n = u_2^{n-1}, & \text{on } \partial\Omega_1 \cap \partial\Omega_2, \end{cases} \qquad \begin{cases} -\Delta u_2^n = 0, & \text{in } \Omega_2, \\ u_2^n = g, & \text{on } \partial\Omega \cap \partial\Omega_2, \\ u_2^n = u_1^n, & \text{on } \partial\Omega_1 \cap \partial\Omega_2. \end{cases} \tag{1.2}$$

This is called the *Schwarz alternating algorithm.*

Note that the above algorithm is not parallel since the local problem in the sub-domain Ω_1 must be solved before the local problem in the sub-domain Ω_2. The parallel version was proposed by Lions in a series of three articles published more than a century later from 1988 to 1990 [94, 95, 96] that revived the interest for domain decomposition methods. We shall study in this section the parallel version, which is closer to our target applications.

1.1.1 A 1D model problem with the classical Schwarz algorithm

We show now on a 1D model problem that the classical Schwarz algorithm with Dirichlet transmission conditions does not converge: first, for elliptic problems in the non-overlapping case; and then, for propagative problems, even in the overlapping case.

Elliptic problem We consider first the model (elliptic) problem, for a positive and real parameter η,

$$\left(-\Delta + \eta^2\right) u = f, \qquad \text{in } \Omega = \mathbb{R}, \tag{1.3}$$

where we require the solution u to decay at infinity and f is the source term, in $L^2(\mathbb{R})$ for instance. Let us consider a modified version of the above classical Schwarz algorithm where the unbounded domain $\mathbb{R}$ is split into two overlapping half-spaces $\Omega_1 = (-\infty, \delta)$ and $\Omega_2 = (0, +\infty)$ for an overlapping parameter $\delta \geq 0$ (the case $\delta = 0$ allowing to recover the non-overlapping case).

The classical (parallel) Schwarz algorithm, for $n \geq 1$ and two initial guesses u_1^0 and u_2^0, is written as

$$\begin{cases} \left(-\partial_{xx} + \eta^2\right) u_1^n = f, & \text{in } \Omega_1, \\ u_1^n = u_2^{n-1}, & \text{at } \delta, \end{cases} \qquad \begin{cases} \left(-\partial_{xx} + \eta^2\right) u_2^n = f, & \text{in } \Omega_2, \\ u_2^n = u_1^{n-1}, & \text{at } 0, \end{cases} \tag{1.4}$$

where we require the local solutions u_1^n and u_2^n to decay at infinity. By linearity, it is enough to consider the case $f \equiv 0$ and analyze the convergence to the zero solution.

Standard computations then yield

$$\begin{cases} u_1^n(x) = u_2^{n-1}(\delta)\, e^{\eta(x-\delta)}, & x < \delta, \\ u_2^n(x) = u_1^{n-1}(0)\, e^{-\eta x}, & x > 0, \end{cases} \tag{1.5}$$

and by induction one can prove that

$$\begin{cases} u_1^{2n}(0) = \rho_{c,+}^n\, u_1^0(0), \\ u_2^{2n}(\delta) = \rho_{c,+}^n\, u_2^0(\delta), \end{cases} \tag{1.6}$$

where the convergence factor (over two iterations) is

$$\rho_{c,+} := e^{-2\eta\delta}. \tag{1.7}$$

It is readily seen that in the non-overlapping case ($\delta = 0$), the convergence factor $\rho_{c,+}$ is identically equal to 1 and the algorithm does not converge. In contrast, if the overlapping parameter is not trivial ($\delta > 0$) the convergence is guaranteed since the convergence factor $\rho_{c,+} < 1$. This is not surprising, it is clear that by exchanging only Dirichlet data at the common interface, the algorithm for the error is stationary.

Propagation problem We consider now the model problem for wave propagation, for a positive and real parameter κ, and a source term in L^2 with compact support

$$\left(-\Delta - \kappa^2\right) u = f, \qquad \text{in } \Omega = \mathbb{R}, \tag{1.8}$$

where we require the solution u to satisfy the Sommerfeld radiation condition at infinity (our time convention is $e^{-\mathrm{i}\omega t}$)

$$\lim_{r \to +\infty} \left(\partial_r - \mathrm{i}\kappa\right) u = 0, \qquad r = |x|. \tag{1.9}$$

The classical Schwarz algorithm, for $n \geq 1$ and two initial guesses u_1^0 and u_2^0, is written as

$$\begin{cases} \left(-\partial_{xx} - \kappa^2\right) u_1^n = f, & \text{in } \Omega_1, \\ u_1^n = u_2^{n-1}, & \text{at } \delta, \end{cases} \qquad \begin{cases} \left(-\partial_{xx} - \kappa^2\right) u_2^n = f, & \text{in } \Omega_2, \\ u_2^n = u_1^{n-1}, & \text{at } 0, \end{cases} \tag{1.10}$$

where we also require the local solutions u_1^n and u_2^n to satisfy the Sommerfeld radiation condition at infinity. Standard computations then yield

$$\begin{cases} u_1^n(x) = u_2^{n-1}(\delta)\, e^{-\mathrm{i}\kappa(x-\delta)}, & x < \delta, \\ u_2^n(x) = u_1^{n-1}(0)\, e^{\mathrm{i}\kappa x}, & x > 0, \end{cases} \tag{1.11}$$

and by induction one can prove that

$$\begin{cases} u_1^{2n}(0) = \rho_c^n\, u_1^0(0), \\ u_2^{2n}(\delta) = \rho_c^n\, u_2^0(\delta), \end{cases} \tag{1.12}$$

where the (now complex) convergence factor (over two iterations) is

$$\rho_c := e^{-2\mathrm{i}\kappa\delta}. \tag{1.13}$$

Again, in the non-overlapping case ($\delta = 0$), the convergence factor ρ_c is identically equal to 1 and the algorithm does not converge (which was predicted). However this time, even if the overlapping is not trivial ($\delta > 0$), we see that the convergence factor ρ_c is equal to 1 in modulus, from the presence of the imaginary unit in the exponential factor.

1.1.2 The interest of the Robin transmission conditions

We show now on the same model problems that using Robin transmission conditions one can restore the lost convergence previously observed.

Elliptic problem Introducing a Robin boundary condition, parameterized by a complex t to be chosen later, the (*optimized*) Schwarz algorithm, for $n \geq 1$ and two initial guesses u_1^0 and u_2^0, is written as

$$\begin{cases} \left(-\partial_{xx} + \eta^2\right) u_1^n = f, & \text{in } \Omega_1, \\ \left(\partial_x + t\right) u_1^n = \left(\partial_x + t\right) u_2^{n-1}, & \text{at } \delta, \end{cases} \quad \begin{cases} \left(-\partial_{xx} + \eta^2\right) u_2^n = f, & \text{in } \Omega_2, \\ \left(-\partial_x + t\right) u_2^n = \left(-\partial_x + t\right) u_1^{n-1}, & \text{at } 0, \end{cases} \tag{1.14}$$

where we require the local solutions u_1^n and u_2^n to decay at infinity. Note that we could consider two different Robin parameters, one for each sub-domain, but it is enough to introduce only one parameter for our purposes.

Note that by taking formally the limit $t \to +\infty$ one recovers the previous case with Dirichlet transmission conditions and by setting $t = 0$ one gets Neumann transmission conditions (which yield similar pathological behavior as the Dirichlet case).

Standard computations then yield

$$\begin{cases} u_1^n(x) = u_2^{n-1}(\delta) \left(\frac{t-\eta}{t+\eta}\right) e^{\eta(x-\delta)}, & x < \delta, \\ u_2^n(x) = u_1^{n-1}(0) \left(\frac{t-\eta}{t+\eta}\right) e^{-\eta x}, & x > 0, \end{cases} \tag{1.15}$$

and by induction one can prove that

$$\begin{cases} u_1^{2n}(0) = \rho_{o,+}^n \, u_1^0(0), \\ u_2^{2n}(\delta) = \rho_{o,+}^n \, u_2^0(\delta), \end{cases} \tag{1.16}$$

where the convergence factor (over two iterations) is

$$\rho_{o,+} := \left(\frac{t-\eta}{t+\eta}\right)^2 \, e^{-2\eta\delta}. \tag{1.17}$$

It is readily seen that for any Robin parameter t with a real and positive real part, the convergence factor $\rho_{c,+}$ is strictly lower than 1 in modulus and the algorithm does converge independently of the overlap (albeit with a faster rate with a larger overlap). In fact, the best parameter is $t = \eta$ which yields convergence in two iterations. This is an optimal result, which is valid in the one-dimensional case. In higher dimensions (see [74] for instance), the optimal parameter is a (pseudo-differential) operator.

Propagation problem Introducing a Robin boundary condition, parameterized by a complex t to be chosen later, the (*optimized*) Schwarz algorithm, for $n \geq 1$ and two initial guesses u_1^0 and u_2^0, is written as

$$\begin{cases} \left(-\partial_{xx} - \kappa^2\right) u_1^n = f, & \text{in } \Omega_1, \\ \left(\partial_x - t\right) u_1^n = \left(\partial_x - t\right) u_2^{n-1}, & \text{at } \delta, \end{cases} \quad \begin{cases} \left(-\partial_{xx} - \kappa^2\right) u_2^n = f, & \text{in } \Omega_2, \\ \left(-\partial_x - t\right) u_2^n = \left(-\partial_x - t\right) u_1^{n-1}, & \text{at } 0, \end{cases} \tag{1.18}$$

where we require the local solutions u_1^n and u_2^n to satisfy the Sommerfeld radiation condition at infinity. Standard computations then yield

$$\begin{cases} u_1^n(x) = u_2^{n-1}(\delta) \left(\frac{t-\mathrm{i}\kappa}{t+\mathrm{i}\kappa}\right) e^{-\mathrm{i}\kappa(x-\delta)}, & x < \delta, \\ u_2^n(x) = u_1^{n-1}(0) \left(\frac{t-\mathrm{i}\kappa}{t+\mathrm{i}\kappa}\right) e^{\mathrm{i}\kappa x}, & x > 0, \end{cases} \tag{1.19}$$

and by induction one can prove that

$$\begin{cases} u_1^{2n}(0) = \rho_o^n \, u_1^0(0), \\ u_2^{2n}(\delta) = \rho_o^n \, u_2^0(\delta), \end{cases} \tag{1.20}$$

where the convergence factor (over two iterations) is

$$\rho_o := \left(\frac{t - \mathrm{i}\kappa}{t + \mathrm{i}\kappa}\right)^2 \, e^{-2\mathrm{i}\kappa\delta}. \tag{1.21}$$

The situation is formally similar to the previous case. We observe that the overlapping parameter plays no role in the convergence and for any Robin parameter t with a real and positive imaginary part, the convergence factor $\rho_{c,+}$ is strictly lower than 1 in modulus. The optimal parameter in this case is $t = \mathrm{i}\kappa$, which is valid in the one-dimensional case. In higher dimensions (see [72] for instance), the optimal parameter is also a (pseudo-differential) operator.

1.2 DDM for propagative problems

We provide in this section an overview of the different transmission operators that one can use to define (non-overlapping) domain decomposition methods for wave propagation problems.

1.2.1 The original transmission conditions of Després

The idea proposed by Després [47, 49, 48, 51, 50] is to consider the physical transmission conditions at the interface and to rewrite them equivalently as Robin conditions.

1.2.1.1 Helmholtz

Let us consider a partition with two sub-domains Ω_1 and Ω_2 separated by an interface Σ, with respective outward unit normals ν_1 and ν_2. We denote by u_1 and u_2 their respective local solutions, satisfying the Helmholtz equation, introducing the wavenumber κ,

$$\left(-\Delta - \kappa^2\right) u_j = 0, \qquad \text{in } \Omega_j, \ j = 1, 2. \tag{1.22}$$

For simplicity we assume that the source term comes from a non-homogeneous physical boundary condition which is omitted. The continuity conditions, which correspond to the continuity of the

trace of the solution and the trace of its normal derivative, are

$$\begin{cases} u_1 = u_2, \\ \partial_{\nu_1} u_1 = -\partial_{\nu_2} u_2, \end{cases} \qquad \text{on } \Sigma, \tag{1.23}$$

and can be recast as Robin conditions as follows

$$\begin{cases} +\partial_{\nu_1} u_1 - \mathrm{i}\kappa\, u_1 = -\partial_{\nu_2} u_2 - \mathrm{i}\kappa\, u_2, \\ +\partial_{\nu_2} u_2 - \mathrm{i}\kappa\, u_2 = -\partial_{\nu_1} u_1 - \mathrm{i}\kappa\, u_1, \end{cases} \qquad \text{on } \Sigma. \tag{1.24}$$

It is clear that the conditions (1.23) and (1.24) are equivalent.

Remark 1.1. *In the case were the medium of propagation is heterogeneous, the coefficient* $\mathrm{i}\kappa$ *can be modified, for instance by taking into account a simple local average of the varying coefficients of the PDE from both sides of the interface, see [49, Sec. 4.3].*

Formal generalization To help compare different choices of transmission operators, let us rewrite the transmission conditions (1.24) for two general transmission operators T_s, $s \in \{1, 2\}$, as

$$\begin{cases} +\partial_{\nu_1} u_1 - \mathrm{T}_1\, u_1 = -\partial_{\nu_2} u_2 - \mathrm{T}_1\, u_2, \\ +\partial_{\nu_2} u_2 - \mathrm{T}_2\, u_2 = -\partial_{\nu_1} u_1 - \mathrm{T}_2\, u_1, \end{cases} \qquad \text{on } \Sigma. \tag{1.25}$$

With this convention, the conditions of Després consists in using

$$\mathrm{T}_1 = \mathrm{T}_2 = \mathrm{i}\kappa\, \mathrm{Id}. \tag{1.26}$$

The first equation of (1.25) will be used as a Robin condition for the local sub-problem written in the domain Ω_1 and the second one for the local sub-problem written in the domain Ω_2.

In the actual implementation of the domain decomposition method, such transmission conditions will imply that one will need to solve local sub-problems of the form (omitting the physical boundary condition)

$$\begin{cases} \left(-\Delta - \kappa^2\right) u_j = 0, & \text{in } \Omega_j, \\ +\partial_{\nu_j} u_j - \mathrm{i}\kappa\, \mathrm{T}_j\, u_j = x_j, & \text{on } \Sigma, \end{cases} \qquad j = 1, 2, \tag{1.27}$$

where x_j, $j = 1, 2$ are given. Usually this data will incorporate information coming from the adjacent sub-domain and will be computed with the solution obtained at the previous iteration. For instance, if the relaxed Jacobi algorithm is used, this data reads

$$\begin{cases} x_1 := +r\, \left[+\partial_{\nu_1} u_1 - \mathrm{i}\kappa\, \mathrm{T}_1\, u_1\right] + (1 - r)\, \left[-\partial_{\nu_2} u_2 - \mathrm{i}\kappa\, \mathrm{T}_1\, u_2\right], \\ x_2 := +r\, \left[+\partial_{\nu_2} u_2 - \mathrm{i}\kappa\, \mathrm{T}_2\, u_2\right] + (1 - r)\, \left[-\partial_{\nu_1} u_1 - \mathrm{i}\kappa\, \mathrm{T}_2\, u_1\right], \end{cases} \tag{1.28}$$

where $0 \leq r < 1$ is the relaxation parameter and the quantities used are computed at the previous iteration.

Convergence analysis The first advantage in using Després method is that the local sub-domain problems are always well-posed which translates in the discrete setting as the fact that the local matrices are always invertible. This feature is not always guaranteed if Dirichlet or Neumann conditions are used instead of the Robin boundary conditions proposed by Després. When used in the static (elliptic) problem, using the Robin condition corresponds to suppressing the so-called "rigid body modes".

The second advantage of using Després method is that the convergence of the relaxed Jacobi algorithm iterative algorithm is always guaranteed. Note that the relaxation is necessary in the general case, although the classical Jacobi algorithm (without relaxation) may nevertheless converge in some particular configurations. For a proof of this convergence result, we refer the reader to [49] and more precisely to Theorem 4.1 for the continuous setting and to Theorem 7.1 for the corresponding discrete result in the case of a discretization based on a mixed-hybrid finite element formulation. These proofs are based on the decay of a pseudo-energy estimate defined on the interface.

1.2.1.2 Maxwell

The extension of the original idea for Helmholtz to Maxwell was considered by Després, Joly and Roberts [49, 51]. In the electromagnetic setting, the local solutions $\mathbf{E}_1$ and $\mathbf{E}_2$ satisfy

$$\left(\mathbf{curl}\,\mathbf{curl} - \kappa^2\right)\mathbf{E}_j = 0, \qquad \text{in } \Omega_j,\ j = 1, 2. \tag{1.29}$$

The continuity conditions are

$$\begin{cases} \nu_1 \times (\mathbf{E}_1 \times \nu_1) = \nu_2 \times (\mathbf{E}_2 \times \nu_2), \\ \mathbf{curl}\,\mathbf{E}_1 \times \nu_1 = -\,\mathbf{curl}\,\mathbf{E}_2 \times \nu_2, \end{cases} \qquad \text{on } \Sigma, \tag{1.30}$$

and can be recast as Robin conditions as follows

$$\begin{cases} +\,\mathbf{curl}\,\mathbf{E}_1 \times \nu_1 - \mathrm{i}\kappa\,\nu_1 \times (\mathbf{E}_1 \times \nu_1) = -\,\mathbf{curl}\,\mathbf{E}_2 \times \nu_2 - \mathrm{i}\kappa\,\nu_2 \times (\mathbf{E}_2 \times \nu_2), \\ +\,\mathbf{curl}\,\mathbf{E}_2 \times \nu_2 - \mathrm{i}\kappa\,\nu_2 \times (\mathbf{E}_2 \times \nu_2) = -\,\mathbf{curl}\,\mathbf{E}_1 \times \nu_1 - \mathrm{i}\kappa\,\nu_1 \times (\mathbf{E}_1 \times \nu_1), \end{cases} \qquad \text{on } \Sigma. \tag{1.31}$$

Formal generalization Again, to help compare different choices of transmission operators, let us rewrite the transmission conditions (1.31) for two general transmission operators T_s, $s \in \{1, 2\}$, as

$$\begin{cases} +\,\mathbf{curl}\,\mathbf{E}_1 \times \nu_1 - \mathrm{T}_1\,\nu_1 \times (\mathbf{E}_1 \times \nu_1) = -\,\mathbf{curl}\,\mathbf{E}_2 \times \nu_2 - \mathrm{T}_1\,\nu_2 \times (\mathbf{E}_2 \times \nu_2), \\ +\,\mathbf{curl}\,\mathbf{E}_2 \times \nu_2 - \mathrm{T}_2\,\nu_2 \times (\mathbf{E}_2 \times \nu_2) = -\,\mathbf{curl}\,\mathbf{E}_1 \times \nu_1 - \mathrm{T}_2\,\nu_1 \times (\mathbf{E}_1 \times \nu_1), \end{cases} \qquad \text{on } \Sigma. \tag{1.32}$$

With this convention, the conditions of Després consists in using

$$\mathrm{T}_1 = \mathrm{T}_2 = \mathrm{i}\kappa\,\mathrm{Id}. \tag{1.33}$$

In the actual implementation of the domain decomposition method, the local sub-problems are of the form (omitting the physical boundary condition)

$$\begin{cases} \left(\mathbf{curl}\,\mathbf{curl} - \kappa^2\right)\mathbf{E}_j = 0, & \text{in } \Omega_j, \\ +\,\mathbf{curl}\,\mathbf{E}_j \times \nu_j - \mathrm{i}\kappa\,\mathrm{T}_j\,\nu_j \times (\mathbf{E}_j \times \nu_j) = \mathbf{x}_j & \text{on } \Sigma, \end{cases} \qquad j = 1, 2, \tag{1.34}$$

where $\mathbf{x}_j$, $j = 1, 2$ are given data incorporating information coming from the neighbouring subdomain.

Convergence analysis This choice of transmission conditions yields well-posed local subproblems and a convergence analysis formally similar to the one devised in the acoustic setting is also applicable, see for instance [49, Th. 9.1] or [51, Th. 2.5]. Besides, a mixed-hybrid finite element formulation of the method inherits the convergence properties from the continuous setting and is therefore a well-adapted discretization strategy, at the price of an increased computational cost.

1.2.2 The "exact" transmission operator

It is worth mentioning the existence of an "exact" transmission operator which provides *optimal* domain decomposition methods in the sense that it yields convergence in J iterations if J is the number of sub-domains in the decomposition. This result is valid in the special configuration where the sub-domains satisfy a chain-like configuration (one-dimensional splitting). For the proof of this result, we refer the reader to [44, Sec. 1.3.2] for a two-domain configuration and [74, Th. 17] for a configuration with J serially connected sub-domains. In [39, Th. 6.2], it is shown for a slightly more general configuration (still excluding cross-points) that the number of iterations to convergence (or nilpotence index) is equal to the depth of the adjacency graph of the partition plus one iteration.

In the acoustic setting, the "exact" transmission operator T_1 that shall be used in the Robin boundary condition imposed for the problem in the sub-domain Ω_1 is the so-called Dirichlet-to-Neumann (DtN) map associated to the sub-domain Ω_2. More specifically, we define for a given Dirichlet trace x on the interface Σ

$$\mathrm{T}_1 x := \partial_{\nu_2} v_2, \tag{1.35}$$

where v_2 is solution to (omitting the physical boundary)

$$\begin{cases} \left(-\Delta - \kappa^2\right) v_2 = 0, & \text{in } \Omega_2, \\ v_2 = x, & \text{on } \Sigma. \end{cases} \tag{1.36}$$

The definition of the operator T_2 is formally similar, with a DtN map defined in the sub-domain Ω_1. Note that these maps are not always well-defined, for instance if κ is a Dirichlet eigenvalue of the Laplacian operator. The extension to the electromagnetic setting is straightforward and uses Electric-to-Magnetic maps. The generalization if this idea to more sub-domains requires to solve auxiliary problems in the complementary of each sub-domain.

At the discrete level, the "exact" transmission operator can be viewed as a Schur complement matrix for the degrees of freedom that lies on the transmission interface. In [98] for instance, the authors compute a sparse approximation of the (dense) Schur complement matrix to derive an algebraic DD method.

This strong result is however mainly of theoretical interest since actually computing this ideal operator is (almost) as difficult than solving the original problem. It is nevertheless clear that this could be used as a guide for the construction of efficient transmission operators and this is the idea behind some DD methods as we have already seen.

Connection with absorbing boundary conditions In some cases the above "exact" transmission conditions coincide with transparent or absorbing boundary conditions. The construction of (artificial) absorbing boundary conditions (ABC) is an old subject, first formalized in 1977 in a paper by B. Engquist and E. Majda [63]. In this paper, the Helmholtz equation is considered and the "exact" transmission condition given by the Dirichlet-to-Neumann (DtN) map is studied for the case of the exterior half-space problem in homogeneous media. It corresponds to the following pseudo-differential impedance operator

$$\mathrm{i}\kappa \sqrt{\mathrm{Id} + \frac{1}{\kappa^2}\Delta_\Sigma}\,, \tag{1.37}$$

where Δ_Σ is the Laplace-Beltrami tangential operator. This operator is sometimes referred to in the literature as the "square-root operator".

For the electromagnetic setting, the exact transparent operator formally corresponds to the following pseudo-differential impedance operator

$$\mathrm{i}\kappa \left(\mathrm{Id} + \frac{1}{\kappa^2}\boldsymbol{\Delta}_\Sigma\right)^{-1/2} \left(\mathrm{Id} - \frac{1}{\kappa^2}\,\mathbf{curl}_\Sigma \,\mathrm{curl}_\Sigma\right). \tag{1.38}$$

For a proof of this result, see for instance [59, Prop. 1].

The transmission conditions of Després are commonly reinterpreted as a zeroth order Taylor approximation of (1.37) in the small parameter $|\boldsymbol{\xi}|/\kappa$ if we denote by $\boldsymbol{\xi}$ the Fourier parameter. This approximation yields the following absorbing boundary condition for a general surface Σ with outward unit vector ν (our time convention is $e^{-\mathrm{i}\omega t}$)

$$\partial_\nu u - \mathrm{i}\kappa\, u = 0, \qquad \text{on } \Sigma, \tag{1.39}$$

for the Helmholtz equation and

$$\mathbf{curl}\,\mathbf{E} \times \nu - \mathrm{i}\kappa\, \nu \times (\mathbf{E} \times \nu) = 0 \qquad \text{on } \Sigma, \tag{1.40}$$

for the Maxwell case. This is the reason why the DDM using Després transmission conditions is sometimes referred to as *TO0* for "Taylor Order 0". This reinterpretation also explains the choice of parameter $\mathrm{i}\kappa$ in the transmission conditions.

The point of view of this work We emphasize that, in this work and in contrast to some other works, we do *not* try to approximate these "exact" transmission conditions. The approach that we adopt is to try to derive a method which is provably convergent (with hopefully a fast convergence rate) and to provide sufficient conditions on its ingredients (mainly the transmission operator) to do so. In particular, we will always consider real positive definite transmission operators and this "exact" operator does *not* in general fall into this class of operators. However, one common characteristic shared by both the transmission operators we advocate and this "exact" operator is that they will be both of the same order when considered as pseudo-differential operators.

1.2.3 Zeroth-order transmission operators

In the continuous setting To try to improve the convergence of the iterative algorithms, one can consider alternatives to the choice of the parameter $\mathrm{i}\kappa$ involved in the definition of the Robin conditions. The common approach to do so is based on the splitting of $\mathbb{R}^3$ or $\mathbb{R}^2$ into two half-spaces. This particular geometry allows to use Fourier analysis to compute explicitly a modal convergence rate in Fourier space of the classical Jacobi algorithm (no relaxation is considered). In the continuous setting and for a non-overlapping configuration, such an analysis will reveal that for any choice of the free parameter, the convergence rate in Fourier space will always tend to 1 as the modulus of the Fourier parameter goes to infinity. Any optimization strategy at the continuous level is therefore hopeless.

In the discrete setting The situation changes if one consider the discrete problem. The key idea is to consider only the Fourier frequencies that can be represented on the mesh. Typically this means for a Fourier parameter smaller than $\frac{\pi}{h}$, where h is the discretization parameter. The coefficient in the transmission conditions is then optimized by solving $\min - \max$ problems for Fourier frequencies only in the bandwidth of the mesh discretization. Since the strategy is based on an optimization process with zeroth order transmission operators, the methods described below are sometimes referred to as "Optimized Order 0" (*OO0*) methods.

A first step in this direction was proposed by Gander, Magoules and Nataf in [72], where the authors propose to use, for a parameter $\alpha \in \mathbb{C}$ to be optimized,

$$\mathrm{T}_1 = \mathrm{T}_2 = \alpha \,\mathrm{Id}. \tag{1.41}$$

Note that the parameter α must be chosen with a strictly positive imaginary part to ensure the well-posedness of the local sub-problems. For the optimized value of the coefficient α, which depends on h, the convergence factor of the classical Jacobi algorithm for the half-space problem is of the form $\tau_h = 1 - \mathcal{O}\left(h^{1/2}\right)$ [72, Th. 4.1]. We also note that Magoules, Iványi and Topping proposed an alternative optimization strategy, based on the same form of transmission conditions, see [97, 99] for the details.

A further generalization of these conditions was later considered by Gander, Halpern and Magoules in [75], which are referred to as the *"two-sided Robin transmission conditions"*, by opposition to the *"one-sided"* version described above. The transmission operators are defined as, for two (dimensionless) parameters α_1, $\alpha_2 \in \mathbb{C}$

$$\mathrm{T}_s = \alpha_s \,\mathrm{Id}, \qquad s \in \{1, 2\}. \tag{1.42}$$

Again, the parameters α_1 and α_2 must be chosen with a strictly positive imaginary part to ensure the well-posedness of the local sub-problems [75, Th. 2.1]. For the optimized value of the coefficients α_1 and α_2 the convergence factor of the classical Jacobi algorithm for the half-space problem is of the form $\tau_h = 1 - \mathcal{O}\left(h^{1/4}\right)$ [75, Th. 4.1].

1.2.4 Second-order transmission operators

1.2.4.1 Helmholtz

Various improvements have been made on the original idea of Després. Several authors have proposed to use higher order surface differential operators defined on the boundary. We readily see that this approach may raise difficulties when the boundary is not smooth. The presence of 'corners' requires dedicated care, which is not specific to domain decomposition methods, see for instance [10, 88].

Second-order Taylor approximation A first idea, if one sees Després operator as the zeroth-order approximation of an absorbing boundary condition (ABC) is to use a higher-order approximation of (1.37). Since the Helmholtz operator is self-adjoint, the next order considered is a second-order Taylor approximation (sometimes referred to as *TO2* for "Taylor Order 2") and reads

$$\partial_\nu u - \mathrm{i}\kappa \left(\mathrm{Id} + \frac{1}{2\kappa^2}\Delta_\Sigma\right) u = 0, \qquad \text{on } \Sigma. \tag{1.43}$$

Transmission conditions based on this ABC are not (often) considered though, because the well-posedness of the local sub-problems are not guaranteed, since the operator $\mathrm{Id} + \frac{1}{2\kappa^2}\Delta_\Sigma$ is not coercive.

Using a positive operator For this reason, Piacentini and Rosa consider a second-order approximation, with the upsetting sign flipped, to obtain a coercive operator [117], namely

$$\partial_\nu u - \mathrm{i}\kappa \left(\mathrm{Id} - \frac{1}{2\kappa^2}\Delta_\Sigma\right) u = 0, \qquad \text{on } \Sigma. \tag{1.44}$$

Besides, they introduced two real and positive tuning parameters α and β, so that their transmission operators are written as

$$\mathrm{T}_1 = \mathrm{T}_2 = \mathrm{i}\kappa\,\beta\left(\mathrm{Id} - \frac{\alpha}{\kappa^2}\Delta_\Sigma\right). \tag{1.45}$$

This choice ensures the well-posedness of the local sub-problems, at least for a regular enough interface. The convergence of the associated iterative algorithm can be proved by extending the proof of Després based on a pseudo-energy estimate [117].

Optimization The optimization approach based on the Fourier analysis of the splitting of $\mathbb{R}^3$ into two half-spaces can also be considered with second-order transmission operators by introducing free-parameters in the definition of the operators. Such methods are sometimes referred to as "Optimized Order 2" (*OO2*) methods.

The optimization of second order operators for Helmholtz problems without overlap was considered in [67, 72], for two parameters $\alpha, \beta \in \mathbb{C}$ to be tuned, the transmission operators read

$$\mathrm{T}_1 = \mathrm{T}_2 = \alpha\mathrm{Id} + \beta\Delta_\Sigma. \tag{1.46}$$

For the optimized values of the free parameters, the convergence factor of the classical Jacobi algorithm for the half-space problem is of the form $\tau_h = 1 - \mathcal{O}\left(h^{1/4}\right)$ for the propagative modes and $\tau_h = 1 - \mathcal{O}\left(h^{1/2}\right)$ for the evanescent modes [72, Th. 4.2]. We also note that Magoules, Iványi and Topping proposed an alternative optimization strategy, based on the same form of transmission conditions, see [97, 99] for the details.

A "two-sided" version was considered in [76], but for an overlapping configuration.

1.2.4.2 Maxwell

Using a positive operator In [41] (and [26]), the idea to adapt a second-order approximation of the transparent operator (1.38) for the half-space is again considered for the Maxwell setting. It is clear that due to the presence of two operators, different second order approximation can be used. The square-root operator is commonly approximated by a constant so that the simplest approximation reads

$$\mathbf{curl}\,\mathbf{E}\times\nu - \mathrm{i}\kappa\left(\mathrm{Id} - \frac{1}{\kappa^2}\,\mathbf{curl}_\Sigma\,\mathbf{curl}_\Sigma\right)\,\nu\times(\mathbf{E}\times\nu) = 0, \qquad \text{on } \Sigma, \tag{1.47}$$

but is troublesome due to the presence of a non coercive operator. The sign can however be modified accordingly, to obtain [41]

$$\mathbf{curl}\,\mathbf{E}\times\nu - \mathrm{i}\kappa\left(\mathrm{Id} + \frac{1}{\kappa^2}\,\mathbf{curl}_\Sigma\,\mathbf{curl}_\Sigma\right)\,\nu\times(\mathbf{E}\times\nu) = 0, \qquad \text{on } \Sigma, \tag{1.48}$$

which can be seen as a straightforward adaptation to the electromagnetic setting of (1.44). Besides, the authors introduce two real and positive tuning parameters α and β, so that their transmission operators are written as

$$\mathrm{T}_1 = \mathrm{T}_2 = \mathrm{i}\kappa\,\beta\left(\mathrm{Id} + \frac{\alpha}{\kappa^2}\,\mathbf{curl}_\Sigma\,\mathbf{curl}_\Sigma\right). \tag{1.49}$$

This choice ensures the well-posedness of the local sub-problems, at least for regular enough interfaces.

Optimization The first analytic optimization of second-order operators in the context of Maxwell equations was considered by Rodriguez and Gerardo-Giorda [121], in the spirit of the techniques used in [72]. They provide an optimized value for the one-parameter transmission conditions ($\alpha > 0$)

$$\mathrm{T}_1 = \mathrm{T}_2 = \mathrm{i}\kappa\,\alpha\left(\mathrm{Id} - \frac{1}{\kappa^2}\,\mathbf{curl}_\Sigma\,\mathbf{curl}_\Sigma\right), \tag{1.50}$$

and two-parameters transmission conditions ($\alpha_1, \alpha_2 > 0$)

$$\begin{cases} \mathrm{T}_1 = \kappa\,\alpha_1\left(\mathrm{Id} - \dfrac{1}{\kappa^2}\,\mathbf{curl}_\Sigma\,\mathbf{curl}_\Sigma\right), \\ \mathrm{T}_2 = \mathrm{i}\kappa\,\alpha_2\left(\mathrm{Id} - \dfrac{1}{\kappa^2}\,\mathbf{curl}_\Sigma\,\mathbf{curl}_\Sigma\right). \end{cases} \tag{1.51}$$

One can however be wary of such conditions, since the well-posedness of such operators is not guaranteed in a general configuration.

In [114], Peng, Rawat and Lee improve the conditions (1.50) by considering a complex coefficient $\alpha \in \mathbb{C}$ and by making a distinction between the transverse electric (TE) and transverse magnetic (TM) modes. The approach is then further improved in [119], where two second-order transmission operators are used ($\alpha, \beta \in \mathbb{C}$)

$$\mathrm{T}_1 = \mathrm{T}_2 = \mathrm{i}\kappa\left(\mathrm{Id} + \frac{\alpha}{\kappa^2}\,\mathbf{grad}_\Sigma\,\mathrm{div}_\Sigma\right)^{-1}\left(\mathrm{Id} - \frac{\beta}{\kappa^2}\,\mathbf{curl}_\Sigma\,\mathbf{curl}_\Sigma\right). \tag{1.52}$$

Similar optimized transmission conditions with second-order operators were also considered in [57] for Maxwell equations written as a first order system and subsequently studied in [56] where a connection between the two-fields and one-field versions is established. Different families of operators are proposed and a convergence factor of the form $\tau_h = 1 - \mathcal{O}\left(h^{1/4}\right)$ was proved for two classes of operators using Fourier analysis [57, Tab. 3]. See also [116, 115] for additional work using second-order tangential operators in transmission conditions, including numerical illustrations on test cases of practical interest.

For the damped Maxwell equations, written as a first-order system, the optimization was treated first in [62] for one-parameter families of operators and further extended in [60] where two-parameters operators are considered.

1.2.5 Rational fraction of local operators

There is a widespread belief in the domain decomposition community that good absorbing boundary conditions (ABC) make for good transmission conditions. As we have already seen, there are indeed connections, at least formally, in the types of transmission operators that are used, even if several transmission conditions have nothing to do with ABC [117, 41]. Note that a first usage of ABC for domain decomposition can perhaps be traced back to [82] and [64], but for Laplace's equation, with zeroth and second order operators. The first use in the context of the Helmholtz equation can be found in [109]. The pinnacle of the approach consisting to use ABC as transmission conditions is probably the work of Boubendir, Antoine and Geuzaine [17] for the Helmholtz equation and then El Bouajaji, Thierry, Antoine and Geuzaine [61] for the Maxwell case. For a review of ABC (and PML, not considered here) techniques, see for instance [108].

If the performance of such domain decomposition methods are rather impressive in the numerical illustrations presented in the literature [17, 61], the approach lacks a general analysis. In particular, it is unclear if the local sub-problems are unconditionally well-posed and if the convergence of the iterative algorithm is guaranteed. Some partial convergence results are available,

see [17, Prop. 3] and [61, Th. 1], but in particular geometries (the case of spherical domains is treated) and without taking into consideration the Padé approximation actually used to compute the transmission operators.

1.2.5.1 Helmholtz

The approach of [17] consists in using the high-order ABC introduced in [3] for the Helmholtz equation. The starting point is the Fourier analysis that provides an exact transmission operator, see (1.37), in the case of the splitting of the whole space $\mathbb{R}^3$ into two half-spaces. To avoid resonances, the operator (1.37) is conveniently regularized by the formal substitution of the wavenumber κ by a complex version $\kappa_\epsilon := \kappa + \mathrm{i}\epsilon$,

$$\mathrm{i}\kappa \sqrt{\mathrm{Id} + \frac{1}{\kappa_\epsilon^2}\Delta_\Sigma}\,, \tag{1.53}$$

where ϵ is a tunable damping parameter, possibly varying on the surface Σ. Some heuristics can be proposed to tune ϵ based on the local curvature of the interface Σ. However, the operator (1.53) remains non-local and expensive to compute. A local approximation of this operator is therefore considered. The idea, borrowed from [9, 81], is to approximate (1.53) using Padé approximation. The $(2N+1)$th-order Padé approximation of the square root is

$$\sqrt{1+x} \;\approx\; 1 + \frac{2}{2N+1}\sum_{j=1}^{N} c_1 \left(1 - \frac{c_1+1}{c_1+1+x}\right), \qquad c_1 = \operatorname{cotan}^2\left(\frac{\mathrm{i}\pi}{2N+1}\right). \tag{1.54}$$

In addition, following [103], the efficiency of the approximant is enhanced by a suitable rotation by some angle ϕ of the branch cut of the square root which is enabled by a change of variable. We have

$$\sqrt{1+x} \;\approx\; \alpha\left[1 + \frac{2}{2N+1}\sum_{j=1}^{N} c_1 \left(1 - \frac{\alpha^2(c_1+1)}{\alpha^2 c_1+1+x}\right)\right], \qquad \alpha = e^{\mathrm{i}\phi}. \tag{1.55}$$

The real approximation (1.54) provides a good approximation for the propagative modes, while the complex approximation (1.55) improves the approximation of the evanescent modes but deteriorates the one of the propagative modes. The rotation angle should be tuned in order to hit the sweet spot.

The transmission operators $\mathrm{T}_1 = \mathrm{T}_2$ are evaluated by the formal substitution of x by $\kappa_\epsilon^{-2}\Delta_\Sigma$ in (1.55). We readily see that the inverse of several local operators must be evaluated in order to compute the action of the operator. This is dealt with by introducing adequate auxiliary variables. For more detail on the reformulation of Padé approximants using auxiliary fields, we refer to [104, Appendix A] and the reference therein.

Note that the above high-order ABC is valid (and efficient) for planar boundaries or regular curved boundaries. Specific treatments shall be applied in presence of corners and were recently derived in [104] and applied in the context of domain decomposition in [105].

1.2.5.2 Maxwell

The approach of [61] consists in using the high-order ABC introduced in [59] for Maxwell equations, on the model of what was previously done for the acoustic case. In the electromagnetic setting the transparent operator for the half-space splitting is given in (1.38). Using again the

formal substitution of the wavenumber κ by a complex version $\kappa_\epsilon := \kappa + \mathrm{i}\epsilon$, the aim is to construct transmission operators $\mathrm{T}_1 = \mathrm{T}_2$ which approximate the operator

$$\mathrm{i}\kappa \left(\mathrm{Id} + \frac{1}{\kappa_\epsilon^2} \boldsymbol{\Delta}_\Sigma \right)^{-1/2} \left(\mathrm{Id} - \frac{1}{\kappa_\epsilon^2} \mathbf{curl}_\Sigma \, \mathrm{curl}_\Sigma \right). \tag{1.56}$$

The high-order ABC considered is more clearly understood written in the following form

$$\sqrt{\mathrm{Id} + \frac{1}{\kappa_\epsilon^2} \boldsymbol{\Delta}_\Sigma} \; \mathbf{curl}\, \mathbf{E} \times \nu - \mathrm{i}\kappa \left(\mathrm{Id} - \frac{1}{\kappa^2} \mathbf{curl}_\Sigma \, \mathbf{curl}_\Sigma \right) \nu \times (\mathbf{E} \times \nu) = 0, \qquad \text{on } \Sigma, \tag{1.57}$$

and the square-root is again approximated as in the acoustic setting using Padé approximants.

1.2.6 Non-local transmission operators

The analysis of domain decomposition methods for Helmholtz equation using non-local operators dates back to the PhD thesis of Ghanemi [78, 42] and was subsequently extended during the PhD thesis of Lecouvez [91, 43, 44].

The approach adopted in those works consists in deriving sufficient conditions on the transmission operators to ensure both the well-posedness of the local sub-problems and the fastest convergence of the iterative algorithms. In particular, if the transmission operators in (1.25) are such that

$$\begin{cases} \mathrm{T}_1 \text{ is continuous from } H^{1/2}(\Sigma) \text{ to } H^{-1/2}(\Sigma), \\ \mathrm{T}_2 = \mathrm{T}_1^*, \qquad \text{(the adjoint)} \\ \mathrm{T}_1 + \mathrm{T}_2 \text{ is positive and injective,} \end{cases} \tag{1.58}$$

then the local sub-problems are well-posed, see [78, Th. 3.1], [42, Th. 1], [91, Lem. 1] and [44, Lem. 2.5]. Moreover, if

$$\begin{cases} \Sigma \text{ is closed (no junction points),} \\ \mathrm{T}_1 + \mathrm{T}_2 \text{ is an isomorphism from } H^{1/2}(\Sigma) \text{ to } H^{-1/2}(\Sigma), \end{cases} \tag{1.59}$$

then the convergence of the relaxed Jacobi algorithm is geometrical, see [78, Th. 3.3], [42, Th. 7], [91, Th. 1] and [44, Th. 2.1], by which we mean that the error between the iterative solution and the exact solution at the iteration n is proportional to τ^n, with the convergence factor $\tau < 1$. Note that (1.59) is not necessary to ensure the convergence of the relaxed Jacobi algorithm, only the geometric convergence. Several integral operators satisfying the above requirements have been analysed in [91, Chap. 4 and 5] and tested numerically (in 2D). More recently, similar ideas and integral operators were also used in [19].

It is the purpose of this document to pursue those works, namely extend the convergence analysis to the electromagnetic setting and propose suitable transmission operators, analyse the dependence of the convergence rate with the discretization parameter and finally lift the absence of junction point assumption.

1.3 The junction issue and available treatments

As we already mentioned in the introduction, the presence of junctions can be an issue both at the theoretical level for the convergence analysis of the method and in practice in numerical implementations. We shall mention that the junction issue is not exclusive to wave propagation problems, in fact it is also present for elliptic problems.

The nature of the issue posed by junctions varies depending on the type of transmission operators that are used. For zeroth-order transmission operators, difficulties arise at the discrete level for nodal finite element discretizations, in the definition of transmission conditions at cross-points. When second or higher-order impedance operators are used, the main difficulty comes from the presence of a 'corner', which raises a definition issue due to the use of high order operators (for instance Laplace-Beltrami operators) on open surfaces, already at the continuous level. In presence of junctions, DD methods using non-local operators can be properly defined but the geometric convergence proof is not valid.

We review below some of the literature available on the cross point issue.

1.3.1 Zeroth-order transmission operators

As we already mentioned in the introduction, there is no additional issue in presence of junctions to define and analyse the DD method at the continuous level when using the identity operator (or other zeroth-order transmission operators). In addition, the continuous convergence proof based on energy estimates [49] still stand in presence of junction points. However, the discretization of the method must be handled with great care, and was the subject of some attention. We review below several strategies that have been proposed at the discrete level to cope with junction points.

1.3.1.1 Mixed-hybrid and mortar methods

Mixed-hybrid or mortar finite element formulations introduce naturally the two Dirichlet and Neumann traces, which are both explicitly discretized. Mixed-hybrid methods seem as a result particularly adapted to the discretization of domain decomposition methods we consider. This was recognized as a decisive feature in early works on the subject [49] which therefore considered such formulations as the preferred discretization method. For a general reference on mixed hybrid methods see [120].

The mixed-hybrid strategy leads to solve local saddle point problems. The main idea, borrowed from [49, Chap. 7] as it was originally constructed, is as follows. Let $f \in L^2(\Omega)$ and $x \in H^{1/2}(\Sigma)$ and suppose we are set to solve the simple model problem

$$\begin{cases} -\Delta p - \kappa^2 p = f, & \text{in } \Omega, \\ (\partial_\nu - ik)\, p = x, & \text{on } \Sigma, \end{cases} \tag{1.60}$$

where $\Sigma = \partial\Omega$ is the transmission interface. We introduce two auxiliary unknowns: $\mathbf{u}$ which is intended to represent ∇p and λ which is intended to represent the natural trace $p|_\Sigma$. The variational form of the problem is

$$\begin{cases} \text{Find } p,\ \mathbf{u},\ \lambda \in L^2(\Omega) \times \mathbf{H}(\mathrm{div};\Omega) \times H^{1/2}(\Sigma) \text{ such that} & \\ -(\mathrm{div}\,\mathbf{u},\ q)_{L^2(\Omega)} - \kappa^2 (p,\ q)_{L^2(\Omega)} = (f,\ q)_{L^2(\Gamma)}, & \forall q \in L^2(\Omega), \\ (\mathbf{u},\ \mathbf{v})_{L^2(\Omega)^3} - (p,\ \mathrm{div}\,\mathbf{v})_{L^2(\Omega)} - \langle \mathbf{v}\cdot\mathbf{n},\ \lambda\rangle_\Sigma = 0, & \forall \mathbf{v} \in \mathbf{H}(\mathrm{div},\Omega), \\ \langle \mathbf{u}\cdot\mathbf{n},\ \mu\rangle_\Sigma - \mathrm{i}\kappa\,\langle \lambda,\ \mu\rangle_\Sigma = \langle x,\ \mu\rangle_\Sigma\,, & \forall \mu \in H^{1/2}(\Sigma), \end{cases} \tag{1.61}$$

where we noted $\langle\cdot,\cdot\rangle_\Sigma$ the duality product on $H^{-1/2}(\Sigma)\times H^{1/2}(\Sigma)$. Note that $\mathbf{u} \in \mathbf{H}(\mathrm{div},\Omega)$ has a natural trace $\mathbf{u}\cdot\mathbf{n}$ in $H^{-1/2}(\Sigma)$.

After discretization, the three unknowns p, $\mathbf{u}$ and λ are respectively represented using $\mathbb{P}_0(\Omega)$, $\mathrm{RT}(\Omega)$ and $\mathbb{P}_0(\Sigma)$ elements (this is the lowest order approximation). The discretization of λ is

therefore non-conformal. The notations $\mathbb{P}_0(\Omega)$ and $\mathbb{P}_0(\Sigma)$ refer respectively to piecewise constant approximation spaces in the volume and on the interface, the notation $\mathrm{RT}(\Omega)$ refer to approximation spaces built on Raviart-Thomas finite elements in the volume.

The key thing to note is that with those approximation spaces the degrees of freedom are located at the interior of either the elements or the interfaces between two elements and thus cannot be shared by more than two subdomains. It follows that none of these degrees of freedom is associated to the cross-points in 2D or junction lines in 3D. It follows that there is no issue in the definition of the transmission conditions, since there is always a point-to-point correspondence between the degrees of freedom of two given sub-domains at their common interface. Besides, this particular choice of discrete approximation strategy allows to inherit the convergence result from the continuous analysis which therefore extends to the actual discrete process.

Independently of the cross-point issue, numerical implementations based on mixed-hybrid formulations suffer from an increased computational cost compared to the usual one field equation based on a nodal discretization. Even if we eliminate some variables, we are left with at least a system of size the number of edges in 2D (or the number of triangles in 3D) which is three (respectively two) times bigger than the corresponding $\mathbb{P}_1$ system.

In addition, it is of interest to be able to devise DD methods applicable to nodal-based discretizations, at least in order to be applicable to already existing codes. It would be particularly irksome that successful DD methods cannot cope well with widely popular discretization methods and must be restricted to only special methods.

1.3.1.2 Boubendir and Bendali strategy for nodal discretizations

In a series of articles [13, 14, 15], an innovative treatment of cross-points was proposed by Boubendir and Bendali. The main idea of the method is to leave untouched the finite elements unknowns and equations related to the cross-points while on the transmission boundaries, standard Robin transmission conditions between sub-domains are enforced.

Since the junction points and associated degrees of freedom are kept in common for all subdomains, a strong coupling is maintained between all local sub-problems at these nodes. This is dealt with by using a Schur complement procedure by solving the local sub-problems with a Dirichlet condition at the cross-points and a Neumann condition for the other nodes located at the transmission interfaces. A global (still indefinite) system remains to be solved at each iteration, which is of the size of the number of degrees of freedom at cross-points. The size of this problem remains moderate since the number of such degrees of freedom is relatively small compared to the size of the local sub-problems.

The method leads to provably well-posed local sub-problems [15, Th. 3.2] and a convergence analysis is available which states that the relaxed Jacobi algorithm converges [15, Th. 3.3]. Numerical results illustrating the suitability of the approach can be found in [12, 18].

It shall be mentioned that this technique builds on ideas that were already available for elliptic problems. Algebraic DD techniques such as the FETI method [100] introduce additional unknowns at cross-points which leads to under-determined systems of interface unknowns (so-called redundant matching conditions) and requires Krylov acceleration techniques to actually converge. The FETI-DP algorithm [66, 90] avoids the problem altogether by replacing the dual variables of the Lagrange multiplier defined on the transmission interface with primal ones. It follows that solving the local problems amounts to performing a Schur complement for the degrees of freedom associated to the junction points, hence relies on the positivity and semi-definiteness of the local matrices.

1.3.1.3 Gander and Santugini strategy for nodal discretizations

For the Poisson equation, it is reported in [70] that the Robin parameter shall be modified in the presence of cross-points in order to avoid divergence of stationary point algorithms. Moreover, Gander and Kwok [71] pointed out that straightforward nodal discretizations of OSM can diverge and that the continuous proof of convergence fails to carry over to the discrete setting in general.

To address this issue, two different approaches are described in [73]. The first strategy consists in introducing auxiliary variables allowing to construct a consistent discretization of the Neumann traces at cross-points which yields provably convergent fixed point iterative algorithms. The use of auxiliary variable is avoided in the second strategy proposed but relies on communication between all neighbouring sub-domains that share a common junction point.

Although developed for the elliptic problem, it seems to us that these approaches are promising and could be extended to wave propagation problems without difficulties, but we are not aware of available work in this direction.

1.3.2 Second-order transmission operator

When tangential second-order (or any higher-order) operators are used in the transmission condition, the cross-points are first troublesome because of the presence of geometric singularities on the transmission boundary and at which the tangential differential operators are not well-defined. Recently, a new corner treatment for absorbing boundary conditions using second order tangential operators defined on polygonal boundaries has been introduced, which paves the way for successful domain decomposition methods [111, 52]. The case of boundary junction points is treated but the work is on-going for interior junction points. The idea is to substitute the classical second order operator, namely $\left(\mathrm{Id} + \frac{1}{2\kappa^2}\Delta_\Sigma\right)$, by an operator with the same second order Taylor approximation (for low Fourier frequencies) but with the correct sign to obtain well posed local sub-problems. The associated second order ABC is

$$\partial_\nu u - \mathrm{i}\kappa \left(\mathrm{Id} - \frac{1}{2\kappa^2}\Delta_\Sigma\right)^{-1} u = 0, \qquad \text{on } \Sigma, \tag{1.62}$$

or equivalently

$$\left(\mathrm{Id} - \frac{1}{2\kappa^2}\Delta_\Sigma\right) \partial_\nu u - \mathrm{i}\kappa\, u = 0, \qquad \text{on } \Sigma. \tag{1.63}$$

Moreover, the authors derive quasi-continuity relations at the corners of the polygonal boundary to complement the above ABC with corner conditions which takes the form of a system of linear ordinary differential equations defined on the flat edges of the boundary. This yields well-defined local sub-problems [52, Th. 2]. The ABC with the corner conditions is then adapted to defined transmission conditions and construct domain decomposition methods. The convergence of the relaxed Jacobi algorithm is guaranteed and the proof relies on a skeleton energy estimate which is provably decreasing [52, Lem. 8].

1.3.3 Rational fraction of local operators

Again, the presence of corners (more than the nature of the cross-point) is troublesome when using Padé-based transmission conditions because tangential differential operators are involved in the definition of the transmission condition. In [104] the authors apply Padé-type high-order ABCs to computational domains with non-smooth (polygonal or polyhedral) boundaries. The proposed treatment relies on compatibility relations which are derived for the case of right-angles. The technique is subsequently applied to more general corners at the price of making

additional approximations or using a regularization of the boundary. The treatment involve auxiliary unknowns which satisfy linear systems of differential equations posed on the flat edges of the boundary.

The approach is then applied in the context of domain decomposition methods in [105] to treat the cross point issue. Numerical results illustrate the efficiency of the approach on a nodal finite element discretization and both boundary and interior cross-points are taken care of.

Notice that such a treatment is limited to special types of partitions where only an even number of sub-domains can meet at a cross-point. Besides, the degrees of freedom associated to cross-points are duplicated as many times as there are sub-domains and this results in an under-determined system in the number of interface unknowns to be solved for. Finally, we point out that the approach lacks a general analysis on the well-posedness of the local sub-problems and the convergence of the iterative algorithms, but this is not specific to the cross-point treatment that is applied.

1.3.4 Non-local transmission operators

In the continuous setting In presence of junctions, DD methods using non-local operators can be properly defined and are provably convergent [78]. However, the geometric convergence proof [42, 44, 91] is *not* valid in presence of cross points. Notice that the proof fails both with interior cross points, but also with boundary cross points.

Besides, the transmission operators based on integral operators proposed in [91] lose their continuity properties on open boundaries. An adequate treatment is therefore required, as proposed in [19] for instance, where the authors use cut-off functions to suitably regularize the integral operators and as a result deal with cross-points.

In the discrete setting In her thesis [78], S. Ghanemi reported numerical results showing the h-uniform stability of the convergence of the relaxed Jacobi algorithm in presence of *boundary* junctions, see Fig. 3.8 in Chap. 6 for the 2D results and Fig. 4.7 in Chap. 9 for the 3D results. The numerical results are obtained using a mixed-hybrid finite element formulation. If other tests presented are obtained in presence of *interior* junctions, no result are provided that shows the degradation of the h-uniformity of the convergence.

In contrast, it is mentioned in [91, Sec. 9.2] that numerical experiments in 2D using a nodal discretization show, at least for the integral operator tested, that the geometric convergence deteriorates with decreasing mesh parameter in the presence of *boundary* junctions. Besides, the numerical error seems to be concentrated near the cross points. Given the previous results using a mixed-hybrid formulation we just mentioned, the issue seems however to be due to the type of non-local operator used, which, as we already mentioned, loses its adequate mapping properties on open boundaries.

Note that several of the above strategies developed for zeroth-order transmission operators could, in theory, be applicable to DD methods using non-local operators. We are not aware of any attempt in this direction though.

Chapter 2

Motivations for a multi-trace formalism

Contents

This chapter is intended as a self contained introduction to domain decomposition and the main important ideas later presented in the thesis. We wish to describe our approach to domain decomposition in a toy configuration with two non-overlapping sub-domains to help the reader grasp the essential concepts. In particular, our goal is to develop intuition on the reasons behind some of the abstract definitions we will later introduce. Subsequent chapters will consider generalizations of the ideas presented below, in a more abstract way. Note that our viewpoint is to first interpret domain decomposition methods at the PDE level, before any discretization method is considered.

2.1 Standard approach for a two-domain decomposition

We consider a model configuration with a non-overlapping partition consisting of two sub-domains, excluding the presence of (boundary) junction points.

2.1.1 A first introduction to domain decomposition method

2.1.1.1 Model problem

We consider the Helmholtz equation in 2D in a (regular) domain Ω with a first order absorbing boundary condition imposed on the boundary Γ of Ω. The model problem is then

$$\begin{cases} \text{Find } u \in H^1(\Omega) \text{ such that} & \\ \left(-\Delta - \kappa^2\right) u = f, & \text{in } \Omega, \\ \left(\partial_\nu - \mathrm{i}\kappa\right) u = g, & \text{on } \Gamma, \end{cases} \tag{2.1}$$

where $f \in L^2(\Omega)$ and $g \in L^2(\Gamma)$ represent the source, κ denotes the wavenumber and ν is the outward unit normal vector to Γ.

2.1.1.2 Decomposition

We consider a non-overlapping partition in two domains, excluding the presence of (boundary) junction points, by introducing a (closed) interface Σ that splits the domain Ω into an interior domain Ω_1 and exterior domain Ω_2. Our assumption on the geometry of the partition yields that the boundary of Ω_1 is made of one component Σ while the boundary of Ω_2 is made of two (disconnected) components Σ and Γ, see Figure 2.1.

The domain decomposition method consists in considering the two local sub-problems

$$\begin{cases} \text{Find } u_1 \in H^1(\Omega_1) \text{ such that} & \\ \left(-\Delta - \kappa^2\right) u_1 = f|_{\Omega_1}, & \text{in } \Omega_1, \end{cases}$$

$$\text{and} \quad \begin{cases} \text{Find } u_2 \in H^1(\Omega_2) \text{ such that} & \\ \left(-\Delta - \kappa^2\right) u_2 = f|_{\Omega_2}, & \text{in } \Omega_2, \\ \left(\partial_\nu - \mathrm{i}\kappa\right) u_2 = g, & \text{on } \Gamma, \end{cases} \tag{2.2}$$

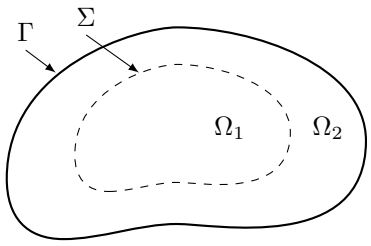

Figure 2.1: Geometric partition in two non-overlapping sub-domains.

which are equivalent to the model problem provided they are coupled by the following transmission conditions, expressing the continuity of the two traces (Dirichlet and Neumann) at the interface Σ

$$\begin{cases} u_1|_\Sigma = u_2|_\Sigma, \\ \partial_{\nu_1} u_1 = -\partial_{\nu_2} u_2, \end{cases} \tag{2.3}$$

where we denoted by ν_1 (respectively ν_2) the outward unit normal vector to Ω_1 (respectively Ω_2) at the interface Σ.

2.1.1.3 Transmission operator and generalized Robin quantities

Using the two equations (2.3) in a domain decomposition method yields algorithms that fail to converge. This is why impedance-like transmission conditions have been developed.

Introducing a boundary operator T on Σ (often referred to as a *transmission* or *impedance* operator) and taking two linear combinations of the transmission conditions (2.3) we get

$$\begin{cases} (+\partial_{\nu_1} - \mathrm{i}\kappa T)\, u_1 = (-\partial_{\nu_2} - \mathrm{i}\kappa T)\, u_2, \\ (-\partial_{\nu_1} - \mathrm{i}\kappa T)\, u_1 = (+\partial_{\nu_2} - \mathrm{i}\kappa T)\, u_2, \end{cases} \quad \text{on } \Sigma. \tag{2.4}$$

It is readily checked that if the operator T is *injective*, the set of equations (2.4) is equivalent to (2.3).

Using the above transmission conditions (2.4), we can rewrite the decomposed problem in the form of the (still coupled) two following local sub-problems

$$\begin{cases} \text{Find } u_1 \in H^1(\Omega_1) \text{ such that} & \\ \left(-\Delta - \kappa^2\right) u_1 = f|_{\Omega_1}, & \text{in } \Omega_1, \\ (+\partial_{\nu_1} - \mathrm{i}\kappa T)\, u_1 = (-\partial_{\nu_2} - \mathrm{i}\kappa T)\, u_2, & \text{on } \Sigma, \end{cases}$$

$$\text{and} \quad \begin{cases} \text{Find } u_2 \in H^1(\Omega_2) \text{ such that} & \\ \left(-\Delta - \kappa^2\right) u_2 = f|_{\Omega_2}, & \text{in } \Omega_2, \\ (\partial_\nu - \mathrm{i}\kappa)\, u_2 = g, & \text{on } \Gamma, \\ (+\partial_{\nu_2} - \mathrm{i}\kappa T)\, u_2 = (-\partial_{\nu_1} - \mathrm{i}\kappa T)\, u_1, & \text{on } \Sigma. \end{cases} \tag{2.5}$$

Assuming that the operator T is *positive definite*, one can prove that the above two local sub-problems are well posed.

2.1.1.4 A first (naive) iterative algorithm

Starting from an initial guess (for instance $u_\pm^0 \equiv 0$), one can construct two sequences $\left(u_\pm^n\right)_{n\in\mathbb{N}}$ of local solutions defined iteratively, for $n \geq 0$, as

$$\text{and} \quad \begin{cases} \text{Find } u_1^{n+1} \in H^1(\Omega_1) \text{ such that} & \\ \left(-\Delta - \kappa^2\right) u_1^{n+1} = f|_{\Omega_1}, & \text{in } \Omega_1, \\ \left(+\partial_{\nu_1} - \mathrm{i}\kappa T\right) u_1^{n+1} = \left(-\partial_{\nu_2} - \mathrm{i}\kappa T\right) u_2^n, & \text{on } \Sigma, \end{cases} \quad \begin{cases} \text{Find } u_2^{n+1} \in H^1(\Omega_2) \text{ such that} & \\ \left(-\Delta - \kappa^2\right) u_2^{n+1} = f|_{\Omega_2}, & \text{in } \Omega_2, \\ \left(\partial_{\nu} - \mathrm{i}\kappa\right) u_2^{n+1} = g, & \text{on } \Gamma, \\ \left(+\partial_{\nu_2} - \mathrm{i}\kappa T\right) u_2^{n+1} = \left(-\partial_{\nu_1} - \mathrm{i}\kappa T\right) u_1^n. & \text{on } \Sigma, \end{cases} \tag{2.6}$$

Note that the above local sub-problems are no longer coupled, since we use in the right-hand-side the data from the previous iteration. We see here how the decomposition of the original problem into smaller local sub-problems can be used to compute iteratively the solution of the model problem.

This is the simplest algorithm that one can write, but as we shall see this is not actually how the method is implemented and analysed. To see this, we shall first reformulate the volume transmission problem as a problem at the interface Σ, which is the subject of the next section.

2.1.2 Reformulation at the interface

2.1.2.1 Interface problem

Before starting the reformulation, let us introduce (w_1, w_2) a lifting of the source defined as follows

$$\text{and} \quad \begin{cases} \text{Find } w_1 \in H^1(\Omega_1) \text{ such that} & \\ \left(-\Delta - \kappa^2\right) w_1 = f|_{\Omega_1}, & \text{in } \Omega_1, \\ \left(+\partial_{\nu_1} - \mathrm{i}\kappa T\right) w_1 = 0, & \text{on } \Sigma, \end{cases} \quad \begin{cases} \text{Find } w_2 \in H^1(\Omega_2) \text{ such that} & \\ \left(-\Delta - \kappa^2\right) w_2 = f|_{\Omega_2}, & \text{in } \Omega_2, \\ \left(\partial_{\nu} - \mathrm{i}\kappa\right) w_2 = g, & \text{on } \Gamma, \\ \left(+\partial_{\nu_2} - \mathrm{i}\kappa T\right) w_2 = 0, & \text{on } \Sigma. \end{cases} \tag{2.7}$$

By linearity, finding (u_1, u_2) is equivalent to find (v_1, v_2) such that

$$\text{and} \quad \begin{cases} \text{Find } v_1 \in H^1(\Omega_1) \text{ such that} & \\ \left(-\Delta - \kappa^2\right) v_1 = 0, & \text{in } \Omega_1, \\ \left(+\partial_{\nu_1} - \mathrm{i}\kappa T\right) v_1 = \left(-\partial_{\nu_2} - \mathrm{i}\kappa T\right) v_2 + \left(-\partial_{\nu_2} - \mathrm{i}\kappa T\right) w_2, & \text{on } \Sigma, \end{cases} \quad \begin{cases} \text{Find } v_2 \in H^1(\Omega_2) \text{ such that} & \\ \left(-\Delta - \kappa^2\right) v_2 = 0, & \text{in } \Omega_2, \\ \left(\partial_{\nu} - \mathrm{i}\kappa\right) v_2 = 0, & \text{on } \Gamma, \\ \left(+\partial_{\nu_2} - \mathrm{i}\kappa T\right) v_2 = \left(-\partial_{\nu_1} - \mathrm{i}\kappa T\right) v_1 + \left(-\partial_{\nu_1} - \mathrm{i}\kappa T\right) w_1, & \text{on } \Sigma. \end{cases} \tag{2.8}$$

It is natural to introduce the following operators, often referred to as local *scattering* operators

$$\begin{aligned} & S_1 \ : \ x_1 \mapsto (-\partial_{\nu_1} - \mathrm{i}\kappa T)\, v_1 \quad \text{where} \quad \begin{cases} v_1 \in H^1(\Omega_1) \text{ is such that} & \\ \left(-\Delta - \kappa^2\right) v_1 = 0, & \text{in } \Omega_1, \\ (+\partial_{\nu_1} - \mathrm{i}\kappa T)\, v_1 = x_1, & \text{on } \Sigma, \end{cases} \\ \text{and} \qquad & S_2 \ : \ x_2 \mapsto (-\partial_{\nu_2} - \mathrm{i}\kappa T)\, v_2 \quad \text{where} \quad \begin{cases} v_2 \in H^1(\Omega_2) \text{ is such that} & \\ \left(-\Delta - \kappa^2\right) v_2 = 0, & \text{in } \Omega_2, \\ (\partial_{\nu} - \mathrm{i}\kappa)\, v_2 = 0, & \text{on } \Gamma, \\ (+\partial_{\nu_2} - \mathrm{i}\kappa T)\, v_2 = x_2, & \text{on } \Sigma. \end{cases} \end{aligned} \tag{2.9}$$

Using the above definition, we obtain from our coupled system that

$$\begin{aligned} & \begin{cases} (+\partial_{\nu_1} - \mathrm{i}\kappa T)\, v_1 = S_2\, (+\partial_{\nu_2} - \mathrm{i}\kappa T)\, v_2 + (-\partial_{\nu_2} - \mathrm{i}\kappa T)\, w_2, \\ (+\partial_{\nu_2} - \mathrm{i}\kappa T)\, v_2 = S_1\, (+\partial_{\nu_1} - \mathrm{i}\kappa T)\, v_1 + (-\partial_{\nu_1} - \mathrm{i}\kappa T)\, w_1, \end{cases} \\ \Leftrightarrow \qquad & \left(\begin{bmatrix} \mathrm{Id} & 0 \\ 0 & \mathrm{Id} \end{bmatrix} - \begin{bmatrix} 0 & S_2 \\ S_1 & 0 \end{bmatrix} \right) \begin{bmatrix} (+\partial_{\nu_1} - \mathrm{i}\kappa T)\, v_1 \\ (+\partial_{\nu_2} - \mathrm{i}\kappa T)\, v_2 \end{bmatrix} = \begin{bmatrix} (-\partial_{\nu_2} - \mathrm{i}\kappa T)\, w_2 \\ (-\partial_{\nu_1} - \mathrm{i}\kappa T)\, w_1 \end{bmatrix}. \end{aligned} \tag{2.10}$$

Noting that, by construction,

$$\begin{cases} (+\partial_{\nu_1} - \mathrm{i}\kappa T)\, w_1 = 0, \\ (+\partial_{\nu_2} - \mathrm{i}\kappa T)\, w_2 = 0, \end{cases} \tag{2.11}$$

we have in fact

$$\left(\begin{bmatrix} \mathrm{Id} & 0 \\ 0 & \mathrm{Id} \end{bmatrix} - \begin{bmatrix} 0 & S_2 \\ S_1 & 0 \end{bmatrix} \right) \begin{bmatrix} (+\partial_{\nu_1} - \mathrm{i}\kappa T)\, u_1 \\ (+\partial_{\nu_2} - \mathrm{i}\kappa T)\, u_2 \end{bmatrix} = \begin{bmatrix} (-\partial_{\nu_2} - \mathrm{i}\kappa T)\, w_2 \\ (-\partial_{\nu_1} - \mathrm{i}\kappa T)\, w_1 \end{bmatrix}. \tag{2.12}$$

To have more compact notations, we introduce

$$\mathbf{S} := \begin{bmatrix} S_1 & 0 \\ 0 & S_2 \end{bmatrix}, \qquad \mathbf{\Pi} := \begin{bmatrix} 0 & \mathrm{Id} \\ \mathrm{Id} & 0 \end{bmatrix}, \tag{2.13}$$

and

$$\mathbb{x} = \begin{bmatrix} x_1 \\ x_2 \end{bmatrix} := \begin{bmatrix} (+\partial_{\nu_1} - \mathrm{i}\kappa T)\, u_1 \\ (+\partial_{\nu_2} - \mathrm{i}\kappa T)\, u_2 \end{bmatrix}, \qquad \mathbb{b} := \begin{bmatrix} (-\partial_{\nu_2} - \mathrm{i}\kappa T)\, w_2 \\ (-\partial_{\nu_1} - \mathrm{i}\kappa T)\, w_1 \end{bmatrix}. \tag{2.14}$$

so that we obtain that $\mathbb{x}$ is solution to

$$(\mathrm{Id} - \mathbf{\Pi S})\, \mathbb{x} = \mathbb{b}. \tag{2.15}$$

The operator $\mathbf{S}$ is the *global* scattering operator and the operator $\mathbf{\Pi}$ is referred to as the *exchange* operator since its action consists in swapping information between the two sub-domains.

We have therefore established that if (u_1, u_2) satisfy the decomposed problem (2.5) then its (incoming) Robin trace $\mathbb{x}$ satisfy the interface problem (2.15).

Reciprocally, we see that if $\mathbb{x} := (x_1, x_2)$ satisfy the interface problem (2.15), and if (v_1, v_2)

are defined as the solution to the local problems

$$\begin{cases} \text{Find } v_1 \in H^1(\Omega_1) \text{ such that} & \\ \left(-\Delta - \kappa^2\right) v_1 = 0, & \text{in } \Omega_1, \\ \left(+\partial_{\nu_1} - \mathrm{i}\kappa T\right) v_1 = x_1, & \text{on } \Sigma, \end{cases}$$
$$\text{and} \quad \begin{cases} \text{Find } v_2 \in H^1(\Omega_2) \text{ such that} & \\ \left(-\Delta - \kappa^2\right) v_2 = 0, & \text{in } \Omega_2, \\ \left(\partial_{\nu} - \mathrm{i}\kappa\right) v_2 = 0, & \text{on } \Gamma, \\ \left(+\partial_{\nu_2} - \mathrm{i}\kappa T\right) v_2 = x_2, & \text{on } \Sigma, \end{cases} \tag{2.16}$$

then $(u_1, u_2) := (v_1 + w_1, v_2 + w_2)$ is solution to the decomposed problem (2.5).

2.1.2.2 Iterative algorithms

One of the simplest iterative method to solve (2.15) is the (relaxed) Jacobi algorithm. Let $\mathbb{x}^0 \in \mathbb{M}$ and a relaxation parameter $0 < r \leq 1$ be given, a sequence $(\mathbb{x}^n)_{n\in\mathbb{N}}$ in $\mathbb{M}$ is constructed using the (relaxed) Jacobi algorithm as follows

$$\mathbb{x}^{n+1} = [(1-r)\mathrm{Id} + r\boldsymbol{\Pi}\mathbf{S}]\,\mathbb{x}^n + r\,\mathbb{b}, \qquad n \in \mathbb{N}. \tag{2.17}$$

The standard Jacobi algorithm (2.6) can be recovered by setting $r = 1$. We shall provide in a subsequent chapter a complete convergence analysis for this algorithm.

Alternatively, a more efficient algorithm to use in practice is the GMRES algorithm [122]. The convergence analysis of such an algorithm is however more delicate to conduct.

2.2 The Multi-Trace point of view

The formalism and terminology adopted below and in the rest of this manuscript is inspired by the Multi-Trace Formalism (MTF) initially introduced in [83, 84, 32, 38] in the context of boundary integral equations. As we shall see, this formalism brings a new point of view on the derivation of domain decomposition methods which will be a fertile ground to develop a new approach to tackle the junction issue. Note that there already exists some literature making connections between the MTF and domain decomposition methods [7, 35, 31, 55].

Spaces We shall need in the following several spaces, for which we recall the definitions. For a Lipschitz domain $\Omega \subset \mathbb{R}^2$, we set

$$\begin{aligned} H^1(\Omega) &:= \left\{ u \in L^2(\Omega),\ \mathbf{grad}\, u \in L^2(\Omega)^2 \right\}, \\ \mathbf{H}(\mathrm{div};\Omega) &:= \left\{ \mathbf{u} \in L^2(\Omega)^2,\ \mathrm{div}\, \mathbf{u} \in L^2(\Omega) \right\}, \\ H^1(\Delta;\Omega) &:= \left\{ u \in H^1(\Omega),\ \Delta u \in L^2(\Omega) \right\}, \end{aligned} \tag{2.18}$$

equipped with the usual norms. The Dirichlet trace space $H^{1/2}(\partial\Omega)$ will be defined as the range of the Dirichlet trace operator, extension to elements of $H^1(\Omega)$ of $u \mapsto u|_{\partial\Omega}$, and equipped with the graph norm. The Neumann trace space $H^{-1/2}(\partial\Omega)$ will be defined as its dual, equipped with the canonical dual norm.

2.2.1 Multi-trace spaces

2.2.1.1 Dirichlet multi-trace space

We introduce the following notation

$$\mathbb{u} := \begin{bmatrix} u_1 \\ u_2 \end{bmatrix} \in H^1(\Omega_1) \times H^1(\Omega_2), \tag{2.19}$$

which is intended to denote a couple of local solutions. Such a couple $\mathbb{u} = (u_1, u_2)$ will be identified (by concatenation) as an element of $L^2(\Omega)$ (i.e. of the whole domain) in a obvious way, and conversely an element of $L^2(\Omega)$ will be identified with its local restrictions to the sub-domains. We introduce the Dirichlet *multi-trace* space,

$$\mathbb{M}_D := H^{1/2}(\Sigma) \times H^{1/2}(\Sigma), \tag{2.20}$$

and we denote by

$$\boldsymbol{\gamma}_D \ : H^1(\Omega_1) \times H^1(\Omega_2) \to \mathbb{M}_D, \tag{2.21}$$

the extension to elements of $H^1(\Omega_1) \times H^1(\Omega_2)$ of the restriction operator defined for regular fields as

$$\mathbb{u} = \begin{bmatrix} u_1 \\ u_2 \end{bmatrix} \mapsto \begin{bmatrix} u_1|_\Sigma \\ u_2|_\Sigma \end{bmatrix}. \tag{2.22}$$

Using standard trace theorems, it is clear that the operator $\boldsymbol{\gamma}_D$ is a continuous and surjective mapping from $H^1(\Delta;\Omega_1) \times H^1(\Delta;\Omega_2)$ to $\mathbb{M}_D$.

The terminology "multi-trace" is borrowed from the Multi-Trace Formalism. The term can be understood in reference to the fact that an element of those spaces represent multiple traces (here from both sides, hence in fact two values) on a single interface Σ.

2.2.1.2 Neumann multi-trace space

Similarly, we introduce the following notation

$$\mathbb{u} := \begin{bmatrix} \mathbf{u}_1 \\ \mathbf{u}_2 \end{bmatrix} \in \mathbf{H}(\mathrm{div};\Omega_1) \times \mathbf{H}(\mathrm{div};\Omega_2), \tag{2.23}$$

which is intended to denote a couple of gradients of local solutions. Again, such a couple $\mathbb{u} = (\mathbf{u}_1, \mathbf{u}_2)$ will be identified as an element of $\mathbf{L}^2(\Omega) := L^2(\Omega)^2$ (i.e. of the whole domain) in a obvious way, and conversely an element of $\mathbf{L}^2(\Omega)$ will be identified with its local restrictions to the sub-domains. We introduce the Neumann *multi-trace* space,

$$\mathbb{M}_N := H^{-1/2}(\Sigma) \times H^{-1/2}(\Sigma), \tag{2.24}$$

and we denote by

$$\boldsymbol{\gamma}_n \ : \mathbf{H}(\mathrm{div};\Omega_1) \times \mathbf{H}(\mathrm{div};\Omega_2) \to \mathbb{M}_N, \tag{2.25}$$

the extension to elements of $\mathbf{H}(\mathrm{div};\Omega_1) \times \mathbf{H}(\mathrm{div};\Omega_2)$ of the normal trace operator defined for regular fields as

$$\mathbb{u} := \begin{bmatrix} \mathbf{u}_1 \\ \mathbf{u}_2 \end{bmatrix} \mapsto \begin{bmatrix} (\nu_1 \cdot \mathbf{u}_1)\,|_\Sigma \\ (\nu_2 \cdot \mathbf{u}_2)\,|_\Sigma \end{bmatrix}. \tag{2.26}$$

Using standard trace theorems, it is also clear that the operator $\boldsymbol{\gamma}_n$ is a continuous and surjective mapping from $\mathbf{H}(\mathrm{div};\Omega_1) \times \mathbf{H}(\mathrm{div};\Omega_2)$ to $\mathbb{M}_N$.

The space $\mathbb{M}_N$ does deserve the qualifying adjective *Neumann* since it is the range of the Neumann operator defined as

$$\begin{aligned} \boldsymbol{\gamma}_N \ &: H^1(\Delta;\Omega_1) \times H^1(\Delta;\Omega_2) \to \mathbb{M}_N, \\ \mathbb{u} = \begin{bmatrix} u_1 \\ u_2 \end{bmatrix} &\mapsto \boldsymbol{\gamma}_n \begin{bmatrix} \mathbf{grad}\, u_1 \\ \mathbf{grad}\, u_2 \end{bmatrix}. \end{aligned} \tag{2.27}$$

2.2.1.3 Multi-trace space

We set

$$\mathbb{M} := \mathbb{M}_D \times \mathbb{M}_N, \tag{2.28}$$

and we introduce the continuous multi-trace operator

$$\boldsymbol{\gamma} := (\boldsymbol{\gamma}_D, \boldsymbol{\gamma}_N) \ : \ H^1(\Delta;\Omega_1) \times H^1(\Delta;\Omega_2) \to \mathbb{M}, \tag{2.29}$$

so that (for sufficiently regular fields) we have

$$\boldsymbol{\gamma}\mathbb{u} := \begin{bmatrix} u_1|_\Sigma \\ u_2|_\Sigma \\ (\partial_{\nu_1} u_1)\,|_\Sigma \\ (\partial_{\nu_2} u_2)\,|_\Sigma \end{bmatrix} \in \mathbb{M}. \tag{2.30}$$

2.2.2 Cauchy-trace space

2.2.2.1 Definition

We define the Cauchy-trace space $\mathbb{C}$ (the clash with the set of complex numbers is unfortunate) as the subspace of the multi-trace space $\mathbb{M}$ whose elements are the two Dirichlet and two Neumann traces of a broken solution $\mathbb{u} = (u_1, u_2) \in H^1(\Omega_1) \times H^1(\Omega_2)$ that satisfies the homogeneous Helmholtz equation in the sub-domains (with the physical boundary condition on Γ, but nothing prescribed on Σ).

More precisely

$$\begin{aligned} & \mathbb{x} \in \mathbb{C} \\ \Leftrightarrow \quad & \exists \mathbb{u} = (u_1, u_2) \in H^1(\Omega_1) \times H^1(\Omega_2) \\ & \text{such that} \qquad \mathbb{x} = \boldsymbol{\gamma}\mathbb{u} = \begin{bmatrix} u_1|_\Sigma \\ u_2|_\Sigma \\ (\partial_{\nu_1} u_1)\,|_\Sigma \\ (\partial_{\nu_2} u_2)\,|_\Sigma \end{bmatrix} \quad \text{with} \quad \begin{cases} \left(-\Delta - \kappa^2\right) u_1 = 0, & \text{in } \Omega_1, \\ \left(-\Delta - \kappa^2\right) u_2 = 0, & \text{in } \Omega_2, \\ \left(\partial_\nu - \mathrm{i}\kappa\right) u_2 = 0, & \text{on } \Gamma. \end{cases} \end{aligned} \tag{2.31}$$

2.2.2.2 A first useful characterization

We formally define two (generalized) Robin operators that couple Dirichlet and Neumann traces using the transmission operator T introduced above as follows

$$\mathbf{R}^{\pm} := \begin{bmatrix} -\mathrm{i}\kappa T & 0 & \pm\mathrm{Id} & 0 \\ 0 & -\mathrm{i}\kappa T & 0 & \pm\mathrm{Id} \end{bmatrix}. \tag{2.32}$$

These operators are continuous mappings from $\mathbb{M} = \mathbb{M}_D \times \mathbb{M}_N$ to $\mathbb{M}_N$.

Using the above notations, we have for a $\mathbb{u} = (u_1, u_2) \in H^1(\Delta;\Omega_1) \times H^1(\Delta;\Omega_2)$

$$\mathbf{R}^{\pm}\boldsymbol{\gamma}\mathbb{u} = \begin{bmatrix} (\pm\partial_{\nu_1} - \mathrm{i}\kappa T)\, u_1 \\ (\pm\partial_{\nu_2} - \mathrm{i}\kappa T)\, u_2 \end{bmatrix}. \tag{2.33}$$

It is then an exercise to show the following characterization of the Cauchy-trace space using the scattering operators (see (2.9) and (2.13)) and the above Robin operators

$$\mathbb{C} = \mathrm{Ker}\left(\mathbf{R}^- - \mathbf{S}\mathbf{R}^+\right). \tag{2.34}$$

2.2.3 Single-trace spaces

2.2.3.1 Definition

The Dirichlet and Neumann *single-trace* spaces are respective subsets of the Dirichlet and Neumann multi-trace spaces and consists of those elements that match (in some sense) at the interface Σ, namely we define

$$\mathbb{S}_D := \{(x_1, x_2) \in \mathbb{M}_D \mid x_1 = x_2\}, \qquad \mathbb{S}_N := \{(x_1, x_2) \in \mathbb{M}_N \mid x_1 = -x_2\}, \tag{2.35}$$

and we set

$$\mathbb{S} := \mathbb{S}_D \times \mathbb{S}_N. \tag{2.36}$$

The term "single-trace" now clearly refers to the matching condition that characterize elements of these spaces.

2.2.3.2 A second useful characterization

The interest of considering such spaces comes from the fact that then one can equivalently reformulate the continuity requirements expressed in (2.3) in the compact form

$$\begin{cases} \gamma_D\mathbb{u} \in \mathbb{S}_D, \\ \gamma_N\mathbb{u} \in \mathbb{S}_N, \end{cases} \qquad \Leftrightarrow \qquad \boldsymbol{\gamma}\mathbb{u} \in \mathbb{S}. \tag{2.37}$$

Besides, we can readily rewrite the transmission conditions (2.4) in the compact form

$$\mathbf{R}^+\boldsymbol{\gamma}\mathbb{u} = \boldsymbol{\Pi}\mathbf{R}^-\boldsymbol{\gamma}\mathbb{u}. \tag{2.38}$$

We recall now that imposing on an element $\mathbb{u} \in H^1(\Delta;\Omega_1) \times H^1(\Delta;\Omega_2)$ to satisfy the continuity requirements of (2.3) (or equivalently the transmission conditions (2.4)) is equivalent to require $\mathbb{u}$ to be an element of $H^1(\Delta,\Omega)$. To summarize, we can state that

$$\begin{aligned} &\forall \mathbb{u} = (u_1, u_2) \in H^1(\Delta;\Omega_1) \times H^1(\Delta;\Omega_2), \\ &\Big(\mathbb{u} \in H^1(\Delta;\Omega) \qquad \Leftrightarrow \qquad \boldsymbol{\gamma}\mathbb{u} \in \mathbb{S} = \mathrm{Ker}\left(\mathbf{R}^+ - \boldsymbol{\Pi}\mathbf{R}^-\right)\Big). \end{aligned} \tag{2.39}$$

2.2.4 A new derivation of the interface problem

2.2.4.1 Interface problem

Before starting the reformulation, let us recall that we introduced (w_1, w_2) a lifting of the source defined as follows

$$\begin{cases} \text{Find } w_1 \in H^1(\Omega_1) \text{ such that} & \\ \left(-\Delta - \kappa^2\right) w_1 = f|_{\Omega_1}, & \text{in } \Omega_1, \\ \left(+\partial_{\nu_1} - \mathrm{i}\kappa T\right) w_1 = 0, & \text{on } \Sigma, \end{cases}$$
$$\text{and} \quad \begin{cases} \text{Find } w_2 \in H^1(\Omega_2) \text{ such that} & \\ \left(-\Delta - \kappa^2\right) w_2 = f|_{\Omega_2}, & \text{in } \Omega_2, \\ \left(\partial_{\nu} - \mathrm{i}\kappa\right) w_2 = g, & \text{on } \Gamma, \\ \left(+\partial_{\nu_2} - \mathrm{i}\kappa T\right) w_2 = 0, & \text{on } \Sigma. \end{cases} \tag{2.40}$$

It follows with our notations, that

$$\mathbf{R}^+\boldsymbol{\gamma}(w_1, w_2) = \begin{bmatrix} \left(+\partial_{\nu_1} - \mathrm{i}\kappa T\right) w_1 \\ \left(+\partial_{\nu_2} - \mathrm{i}\kappa T\right) w_2 \end{bmatrix} = 0. \tag{2.41}$$

Using this lifting, the decomposed problem is

$$\begin{array}{l} \text{Find } u_1, u_2 \in H^1(\Omega_1) \times H^1(\Omega_2) \text{ such that} \\ \begin{cases} \left(-\Delta - \kappa^2\right)(u_1 - w_1) = 0, & \text{in } \Omega_1, \\ \left(-\Delta - \kappa^2\right)(u_2 - w_2) = 0, & \text{in } \Omega_2, \\ \left(\partial_{\nu} - \mathrm{i}\kappa\right)(u_2 - w_2) = 0, & \text{on } \Gamma, \end{cases} \\ \begin{cases} u_1|_{\Sigma} = u_2|_{\Sigma}, \\ \partial_{\nu_1} u_1 = -\partial_{\nu_2} u_2, \end{cases} \quad \text{on } \Sigma. \end{array} \tag{2.42}$$

Using the two characterizations (2.34) and (2.39) we readily obtain that

$$\begin{cases} \boldsymbol{\gamma}(u_1 - w_1, u_2 - w_2) \in \mathbb{C} = \mathrm{Ker}\left(\mathbf{R}^- - \mathbf{S}\mathbf{R}^+\right), \\ \boldsymbol{\gamma}(u_1, u_2) \in \mathbb{S} = \mathrm{Ker}\left(\mathbf{R}^+ - \boldsymbol{\Pi}\mathbf{R}^-\right), \end{cases} \tag{2.43}$$

Using (2.41) we get

$$\begin{cases} \mathbf{R}^-\boldsymbol{\gamma}(u_1, u_2) = \mathbf{S}\mathbf{R}^+\boldsymbol{\gamma}(u_1, u_2) + \mathbf{R}^-\boldsymbol{\gamma}(w_1, w_2), \\ \mathbf{R}^+\boldsymbol{\gamma}(u_1, u_2) = \boldsymbol{\Pi}\mathbf{R}^-\boldsymbol{\gamma}(u_1, u_2). \end{cases} \tag{2.44}$$

Eliminating $\mathbf{R}^-\boldsymbol{\gamma}(u_1, u_2)$ it is then immediate that

$$\mathbf{R}^+\boldsymbol{\gamma}(u_1, u_2) = \boldsymbol{\Pi}\mathbf{S}\mathbf{R}^+\boldsymbol{\gamma}(u_1, u_2) + \boldsymbol{\Pi}\mathbf{R}^-\boldsymbol{\gamma}(w_1, w_2), \tag{2.45}$$

hence we get that the Robin quantity $\mathbb{x} := \mathbf{R}^+\boldsymbol{\gamma}(u_1, u_2)$ satisfies the interface problem (2.15) if we set $\mathbb{b} := \boldsymbol{\Pi}\mathbf{R}^-\boldsymbol{\gamma}(w_1, w_2)$.

2.2.4.2 Decomposition of the multi-trace space

We finish this section with a key result that will be useful when proving convergence result in the following.

We have the following direct sum

$$\mathbb{M} = \mathbb{C} \oplus \mathbb{S}. \tag{2.46}$$

We give below the idea of the proof, which rests on elementary results.

Null intersection. It is clear that an element of $\mathbb{x} \in \mathbb{C}$ is the trace of a broken solution $\mathbb{u} = (u_1, u_2) \in H^1(\Omega_1) \times H^1(\Omega_2)$ which satisfies the homogeneous Helmholtz equation in each sub-domain. Since in addition $\mathbb{x} \in \mathbb{S}$, the solution $\mathbb{u}$ is continuous in its Dirichlet and Neumann traces at the interface Σ, so it satisfies the homogeneous Helmholtz equation in the whole domain Ω. It follows from the well-posedness of the model problem that $\mathbb{u}$ is identically zero, and so are its two traces.

Decomposition. We will prove the decomposition for any element

$$\mathbb{x} := \begin{bmatrix} x_{1,D} \\ x_{2,D} \\ x_{1,N} \\ x_{2,N} \end{bmatrix} \in \mathbb{M}. \tag{2.47}$$

The proof then rests on the well-posedness [44, Lem. 2.4] of the following classical transmission problem

$$\begin{cases} \mathbb{u} = (u_1, u_2) \in H^1(\Omega_1) \times H^1(\Omega_2) \text{ such that,} & \\ \left(-\Delta - \kappa^2\right) u_1 = 0, & \text{in } \Omega_1, \\ \left(-\Delta - \kappa^2\right) u_2 = 0, & \text{in } \Omega_2, \\ \left(\partial_\nu - \mathrm{i}\kappa\right) u_2 = 0, & \text{on } \Gamma, \\ u_1 - u_2 = x_{1,D} - x_{2,D}, & \text{on } \Sigma, \\ \partial_{\nu_1} u_1 + \partial_{\nu_2} u_2 = x_{1,N} + x_{2,N}, & \text{on } \Sigma. \end{cases} \tag{2.48}$$

Set

$$\mathbb{y} = \begin{bmatrix} y_{1,D} \\ y_{2,D} \\ y_{1,N} \\ y_{2,N} \end{bmatrix} := \boldsymbol{\gamma}\mathbb{u} = \begin{bmatrix} u_1|_\Sigma \\ u_2|_\Sigma \\ \left(\partial_{\nu_1} u_1\right)|_\Sigma \\ \left(\partial_{\nu_2} u_2\right)|_\Sigma \end{bmatrix} \in \mathbb{C}, \tag{2.49}$$

which is in $\mathbb{C}$ by construction, and

$$\mathbb{z} := \mathbb{x} - \mathbb{y}. \tag{2.50}$$

The conditions on Σ in the transmission problem are rewritten as

$$\begin{cases} x_{1,D} - y_{1,D} = x_{2,D} - y_{2,D}, \\ x_{1,N} - y_{1,N} = -x_{2,N} + y_{2,N}, \end{cases} \quad \Leftrightarrow \quad \begin{cases} z_{1,D} = z_{2,D}, \\ z_{1,N} = -z_{2,N}, \end{cases} \tag{2.51}$$

which proves that $\mathbb{z} \in \mathbb{S}$.

2.3 Towards a treatment for cross-points

The new point of view brought by the multi-trace formalism, as it was described in Section 2.2, allows us to explain the rationale behind our treatment of junction points. It is clear that the characterization (2.34) will generalize easily in presence of junctions. On the contrary, the classical exchange operator Π is awkward to define in presence of junctions. In the following, we obtain the characterization (2.39) by a method of proof that will easily generalize to an arbitrary setting. Importantly though, the operator $\boldsymbol{\Pi}$ involved will be different in presence of junctions but falls back on the usual exchange operator otherwise.

2.3.1 Properties of the single-trace elements

Elements of the single-trace spaces enjoy several easy but nevertheless interesting properties that we are going to review now.

1. First, they are characterized as the traces of functions that are globally "regular" in a Sobolev sense (the identification between a global function and a couple of local functions is used implicitly here):
$$\begin{aligned} \mathbb{S}_D &= \boldsymbol{\gamma}_D \, H^1(\Omega), \\ \mathbb{S}_N &= \boldsymbol{\gamma}_n \, \mathbf{H}(\mathrm{div};\Omega). \end{aligned} \tag{2.52}$$
This characterization will actually become of importance when we consider junction points, in fact, it will serve as a definition for the single trace spaces.

2. A second key property is the orthogonality between the Dirichlet and Neumann single-trace spaces for the (natural) duality pairing defined on the multi-trace spaces as
$$\begin{aligned} \langle\!\langle \cdot, \cdot \rangle\!\rangle_\Sigma \; &: \mathbb{M}_N \times \mathbb{M}_\mathbb{D} \to \mathbb{C}, \\ &\left(\begin{bmatrix} x_{1,N} \\ x_{2,N} \end{bmatrix}, \begin{bmatrix} x_{1,D} \\ x_{2,D} \end{bmatrix} \right) \mapsto \langle x_{1,N}, x_{1,D} \rangle_\Sigma + \langle x_{2,N}, x_{2,D} \rangle_\Sigma. \end{aligned} \tag{2.53}$$
We readily have
$$\begin{aligned} &\forall \mathbb{x}_N = \begin{bmatrix} x_N \\ -x_N \end{bmatrix} \in \mathbb{S}_N, \; \mathbb{x}_D = \begin{bmatrix} x_D \\ x_D \end{bmatrix} \in \mathbb{S}_D, \\ &\langle\!\langle \mathbb{x}_N, \mathbb{x}_D \rangle\!\rangle_\Sigma = \langle x_N, x_D \rangle_\Sigma + \langle -x_N, x_D \rangle_\Sigma = 0. \end{aligned} \tag{2.54}$$
Note that this duality pairing respects in some sense the Cartesian product nature of the multi-trace spaces. It is easy to see that such a property can be used as yet another characterization of the single-trace spaces, namely we have
$$\begin{aligned} &\forall \mathbb{x}_D \in \mathbb{M}_D, \qquad (\mathbb{x}_D \in \mathbb{S}_D \quad \Leftrightarrow \quad \langle\!\langle \mathbb{x}_N, \mathbb{x}_D \rangle\!\rangle_\Sigma = 0, \; \forall \mathbb{x}_N \in \mathbb{S}_N), \\ &\forall \mathbb{x}_N \in \mathbb{M}_N, \qquad (\mathbb{x}_N \in \mathbb{S}_N \quad \Leftrightarrow \quad \langle\!\langle \mathbb{x}_N, \mathbb{x}_D \rangle\!\rangle_\Sigma = 0, \; \forall \mathbb{x}_D \in \mathbb{S}_D). \end{aligned} \tag{2.55}$$

This last property might seems very trivial at first sight. Indeed, it mainly rests on the simple identification of the Dirichlet and Neumann multi-trace spaces with $\mathbb{R}^2$ and the simple remark that an alternative orthonormal (for the Euclidian scalar product) basis for $\mathbb{R}^2$ is provided by the two vectors $(1,1)$ and $(1,-1)$. The subspaces generated by these two vectors being themselves easily identified with the Dirichlet and Neumann single-trace spaces. However, we feel like these simple remarks are enlightening to understand the more abstract framework we are going to develop in the subsequent chapters.

2.3.2 Introducing orthogonal projectors

Transmission operator Let us suppose that T is a self-adjoint positive isomorphism from $H^{1/2}(\Sigma)$ to $H^{-1/2}(\Sigma)$. We introduce the diagonal transmission operator defined as
$$\mathbf{T} := \begin{bmatrix} T & 0 \\ 0 & T \end{bmatrix} \; : \; \mathbb{M}_D \to \mathbb{M}_N, \tag{2.56}$$
which is by assumption also a self-adjoint positive isomorphism on $\mathbb{M}_D$.

Then $\mathbf{T}$ defines a norm on $\mathbb{M}_D$, induced by the scalar product
$$t_D(\mathbb{x}_D, \mathbb{y}_D) := \langle\!\langle \mathbf{T}\mathbb{x}_D, \overline{\mathbb{y}_D} \rangle\!\rangle_\Sigma, \qquad \forall \mathbb{x}_D, \mathbb{y}_D \in \mathbb{M}_D. \tag{2.57}$$

If we note for all elements of $\mathbb{M}_D$

$$\mathbb{x}_D = \begin{bmatrix} x_{1,D} \\ x_{2,D} \end{bmatrix}, \qquad \text{and} \qquad \mathbb{y}_D = \begin{bmatrix} y_{1,D} \\ y_{2,D} \end{bmatrix}, \tag{2.58}$$

then this scalar product can be written in full as

$$t_D(\mathbb{x}_D, \mathbb{y}_D) := \langle T x_{1,D}, \overline{y_{1,D}} \rangle_\Sigma + \langle T x_{2,D}, \overline{y_{2,D}} \rangle_\Sigma. \tag{2.59}$$

Similarly, the inverse operator

$$\mathbf{T}^{-1} := \begin{bmatrix} T^{-1} & 0 \\ 0 & T^{-1} \end{bmatrix} \; : \; \mathbb{M}_N \to \mathbb{M}_D, \tag{2.60}$$

is a self-adjoint positive isomorphism on $\mathbb{M}_N$ and it defines a norm on $\mathbb{M}_N$, induced by the scalar product

$$t_N(\mathbb{x}_N, \mathbb{y}_N) := \langle\!\langle \mathbb{x}_N, \mathbf{T}^{-1} \overline{\mathbb{y}_N} \rangle\!\rangle_\Sigma, \qquad \forall \mathbb{x}_N, \mathbb{y}_N \in \mathbb{M}_N. \tag{2.61}$$

Decomposition of the multi-trace spaces The Dirichlet multi-trace space $\mathbb{M}_D$ can be decomposed naturally as follows:

$$\forall \mathbb{x}_D = \begin{bmatrix} x_{1,D} \\ x_{2,D} \end{bmatrix} \in \mathbb{M}_D, \qquad \begin{bmatrix} x_{1,D} \\ x_{2,D} \end{bmatrix} = \begin{bmatrix} 1/2\,(x_{1,D} + x_{2,D}) \\ 1/2\,(x_{1,D} + x_{2,D}) \end{bmatrix} + \begin{bmatrix} 1/2\,(x_{1,D} - x_{2,D}) \\ -1/2\,(x_{1,D} - x_{2,D}) \end{bmatrix}. \tag{2.62}$$

Then, if we set (notice the introduction of the operator $\mathbf{T}$ in the definition of $\mathbb{z}_N$)

$$\mathbb{y}_D = \begin{bmatrix} 1/2\,(x_{1,D} + x_{2,D}) \\ 1/2\,(x_{1,D} + x_{2,D}) \end{bmatrix} \qquad \text{and} \qquad \mathbb{z}_N = \mathbf{T} \begin{bmatrix} 1/2\,(x_{1,D} - x_{2,D}) \\ -1/2\,(x_{1,D} - x_{2,D}) \end{bmatrix}, \tag{2.63}$$

we have the decomposition

$$\mathbb{x}_D = \mathbb{y}_D + \mathbf{T}^{-1} \mathbb{z}_N, \qquad \text{where} \qquad \begin{cases} \mathbb{y}_D \in \mathbb{S}_D, \\ \mathbb{z}_N \in \mathbb{S}_N. \end{cases} \tag{2.64}$$

In fact, we can introduce the projector, defined on $\mathbb{M}_D$, by

$$\mathbf{P}_D := \begin{bmatrix} \mathrm{Id}/2 & \mathrm{Id}/2 \\ \mathrm{Id}/2 & \mathrm{Id}/2 \end{bmatrix}, \tag{2.65}$$

and we have

$$\mathrm{Rg}\, \mathbf{P}_D = \mathbb{S}_D, \qquad \mathrm{Ker}\, \mathbf{P}_D = \mathbf{T}\mathbb{S}_N. \tag{2.66}$$

Notice finally that this projector has an interesting relationship with the exchange operator

$$\mathbf{P}_D = 1/2\,(\mathrm{Id} + \mathbf{\Pi}). \tag{2.67}$$

Similarly, we can decompose the space $\mathbb{M}_N$:

$$\forall \mathbb{c}_N = \begin{bmatrix} x_{1,N} \\ x_{2,N} \end{bmatrix} \in \mathbb{M}_N, \qquad \begin{bmatrix} x_{1,N} \\ x_{2,N} \end{bmatrix} = \begin{bmatrix} 1/2\,(x_{1,N} + x_{2,N}) \\ 1/2\,(x_{1,N} + x_{2,N}) \end{bmatrix} + \begin{bmatrix} 1/2\,(x_{1,N} - x_{2,N}) \\ -1/2\,(x_{1,N} - x_{2,N}) \end{bmatrix}, \tag{2.68}$$

and we have the decomposition

$$\mathbb{c}_N = \mathbf{T}\mathbb{b}_D + \mathbb{c}_N, \qquad \text{where} \qquad \begin{cases} \mathbb{b}_D = \mathbf{T}^{-1} \begin{bmatrix} 1/2\,(x_{1,N} + x_{2,N}) \\ 1/2\,(x_{1,N} + x_{2,N}) \end{bmatrix} \in \mathbb{S}_D, \\ \mathbb{c}_N = \begin{bmatrix} 1/2\,(x_{1,N} - x_{2,N}) \\ -1/2\,(x_{1,N} - x_{2,N}) \end{bmatrix} \in \mathbb{S}_N. \end{cases} \tag{2.69}$$

This motivates the introduction of the projector, defined on $\mathbb{M}_N$, as

$$\mathbf{P}_N := \begin{bmatrix} \mathrm{Id}/2 & -\mathrm{Id}/2 \\ -\mathrm{Id}/2 & \mathrm{Id}/2 \end{bmatrix} = 1/2\,(\mathrm{Id} - \mathbf{\Pi})\,. \tag{2.70}$$

These decompositions are written in the more compact forms

$$\begin{aligned} \mathbb{M}_D &= \mathbb{S}_D \oplus \mathbf{T}^{-1}\mathbb{S}_N, \\ \mathbb{M}_N &= \mathbf{T}\mathbb{S}_D \oplus \mathbb{S}_N. \end{aligned} \tag{2.71}$$

Orthogonality of the decompositions We point out that these decompositions are respectively orthogonal for the scalar products t_D and t_N. Indeed, we have for the two cases

$$\begin{aligned} t_D(\mathbb{y}_D, \mathbf{T}^{-1}\mathbb{z}_N) &= \langle\!\langle \mathbf{T}\mathbb{y}_D, \mathbf{T}^{-1}\overline{\mathbb{z}_N} \rangle\!\rangle_\Sigma = \langle\!\langle \mathbb{y}_D, \overline{\mathbb{z}_N} \rangle\!\rangle_\Sigma = 0, \\ t_N(\mathbf{T}\mathbb{b}_D, \mathbb{c}_N) &= \langle\!\langle \mathbf{T}\mathbb{b}_D, \mathbf{T}^{-1}\overline{\mathbb{c}_N} \rangle\!\rangle_\Sigma = \langle\!\langle \mathbb{b}_D, \overline{\mathbb{c}_N} \rangle\!\rangle_\Sigma = 0, \end{aligned} \tag{2.72}$$

since $\mathbb{y}_D, \mathbb{b}_D \in \mathbb{S}_D$ and $\mathbb{z}_N, \mathbb{c}_N \in \mathbb{S}_N$.

This also means that the projector $\mathbf{P}_D$ onto $\mathbb{S}_D$ (respectively the projector $\mathbf{P}_N$ onto $\mathbb{S}_N$) is orthogonal for the scalar product t_D induced by $\mathbf{T}$ (respectively for the scalar product t_N induced by $\mathbf{T}^{-1}$).

Finally, let us point out that these orthogonal decompositions holds regardless of the transmission operator T that is chosen (provided of course that this operator is a self-adjoint positive isomorphism between the trace spaces).

2.3.3 New derivation of the characterization of the single-trace space

We provide below an alternative route to get to the characterization (2.39) with the important additional benefit that this new way will be fairly easily amenable to generalization to a geometrical configuration allowing junction points.

Let us consider a couple of local solutions

$$\mathbb{u} := \begin{bmatrix} u_1 \\ u_2 \end{bmatrix} \in H^1(\Delta;\Omega_1) \times H^1(\Delta;\Omega_2). \tag{2.73}$$

Our goal here is to retrieve the usual transmission conditions. The couple $\mathbb{u}$ viewed as a global element of $L^2(\Omega)$ is an element of $H^1(\Omega)$ if, and only if, its Dirichlet multi-trace belongs to the Dirichlet single-trace space

$$\boldsymbol{\gamma}_D \mathbb{u} \in \mathbb{S}_D. \tag{2.74}$$

Besides, it is an element of $H^1(\Delta;\Omega)$ if, and only if, its Neumann multi-trace also belongs to the Neumann single-trace space

$$\boldsymbol{\gamma}_N \mathbb{u} \in \mathbb{S}_N. \tag{2.75}$$

Using the orthogonal projectors $\mathbf{P}_D$ and $\mathbf{P}_N$ defined respectively in (2.65) and (2.70), we have the equivalence

$$\begin{cases} \boldsymbol{\gamma}_D \mathbb{u} \in \mathbb{S}_D, \\ \boldsymbol{\gamma}_N \mathbb{u} \in \mathbb{S}_N, \end{cases} \quad \Leftrightarrow \quad \begin{cases} (\mathrm{Id} - \mathbf{P}_D)\,\boldsymbol{\gamma}_D \mathbb{u} = 0, \\ (\mathrm{Id} - \mathbf{P}_N)\,\boldsymbol{\gamma}_N \mathbb{u} = 0. \end{cases} \tag{2.76}$$

The idea is to introduce the Robin quantities (2.32) and the exchange operator $\mathbf{\Pi}$ using the relations with the projectors (2.67) and (2.70). To introduce the Robin quantities, we need to

multiply $\boldsymbol{\gamma}_D \mathbb{u}$ with the transmission operator $\mathbf{T}$. This is why, from the decompositions (2.71) of the multi-trace spaces, it is actually more relevant to write

$$\begin{cases} \boldsymbol{\gamma}_D \mathbb{u} \in \mathbb{S}_D, \\ \boldsymbol{\gamma}_N \mathbb{u} \in \mathbb{S}_N, \end{cases} \qquad \Leftrightarrow \qquad \begin{cases} \mathbf{P}_N \mathbf{T} \boldsymbol{\gamma}_D \mathbb{u} = 0, \\ (\mathrm{Id} - \mathbf{P}_N)\, \boldsymbol{\gamma}_N \mathbb{u} = 0. \end{cases} \tag{2.77}$$

On a side note, we point out that one can also get to the same point using the following identity, valid in $\mathbb{M}_D$

$$\mathbf{T}\,(\mathrm{Id} - \mathbf{P}_D) = \mathbf{P}_N \mathbf{T}, \tag{2.78}$$

but this will not be true for more general partitions. Using simple properties of the projection operator $\mathbf{P}_N$, namely $\mathbf{P}_N^2 = \mathbf{P}_N$, we obtain the equivalence

$$\begin{cases} \boldsymbol{\gamma}_D \mathbb{u} \in \mathbb{S}_D, \\ \boldsymbol{\gamma}_N \mathbb{u} \in \mathbb{S}_N, \end{cases} \qquad \Leftrightarrow \qquad (\mathrm{Id} - \mathbf{P}_N)\, \boldsymbol{\gamma}_N \mathbb{u} - \mathrm{i}\kappa \mathbf{P}_N \mathbf{T} \boldsymbol{\gamma}_D \mathbb{u} = 0. \tag{2.79}$$

From $\mathbf{P}_N = {}^1\!/_2\,(\mathrm{Id} + \boldsymbol{\Pi})$ we readily obtain

$$\begin{array}{ll} & (\mathrm{Id} - \mathbf{P}_N)\, \boldsymbol{\gamma}_N \mathbb{u} - \mathrm{i}\kappa \mathbf{P}_N \mathbf{T} \boldsymbol{\gamma}_D \mathbb{u} = 0, \\ \Leftrightarrow & {}^1\!/_2\ (\mathrm{Id} + \boldsymbol{\Pi})\, \boldsymbol{\gamma}_N \mathbb{u} - {}^1\!/_2\, \mathrm{i}\kappa\, (\mathrm{Id} - \boldsymbol{\Pi})\, \mathbf{T} \boldsymbol{\gamma}_D \mathbb{u} = 0, \\ \Leftrightarrow & [\boldsymbol{\gamma}_N \mathbb{u} - \mathrm{i}\kappa \mathbf{T} \boldsymbol{\gamma}_D \mathbb{u}] - \boldsymbol{\Pi}\, [-\boldsymbol{\gamma}_N \mathbb{u} - \mathrm{i}\kappa \mathbf{T} \boldsymbol{\gamma}_D \mathbb{u}] = 0, \\ \Leftrightarrow & \left(\mathbf{R}^+ - \boldsymbol{\Pi} \mathbf{R}^-\right) \boldsymbol{\gamma} \mathbb{u} = 0. \end{array} \tag{2.80}$$

In fact, to summarize, we proved again the characterization (2.39)

$$\begin{array}{l} \forall \mathbb{u} = (u_1, u_2) \in H^1(\Delta; \Omega_1) \times H^1(\Delta; \Omega_2), \\ \left(\mathbb{u} \in H^1(\Delta; \Omega) \qquad \Leftrightarrow \qquad \boldsymbol{\gamma} \mathbb{u} \in \mathbb{S} = \mathrm{Ker}\left(\mathbf{R}^+ - \boldsymbol{\Pi} \mathbf{R}^-\right) \right). \end{array} \tag{2.81}$$

The main difference with the previous proof lies in the fact that the matching conditions (or continuity requirements) at the interface Σ are completely hidden. It follows that the method of proof actually generalizes to geometrical configurations allowing junction points.

2.4 Generalizations

Subsequent chapters will cover the generalization of the previously described ideas in several directions.

2.4.1 Generalization to configurations without junction points

In Part I of this manuscript, we exclude the presence of junctions points in the partition.

Generalization to J sub-domains The first obvious generalization concerns partitions with more than two sub-domains, that are of particular interest for applications. The generalization is pretty straightforward in geometrical configurations that excludes cross-points, which is what we are going to consider first in Part I. This assumption simplifies in particular the functional analysis since all interfaces are closed manifolds.

Generalization to Maxwell's equations Another generalization of interest that motivated this work concerns the extension to Maxwell's equations. We do this by introducing an abstract formalism for a sub-class of wave propagation problems that covers both the acoustic and electromagnetic settings.

Note that the extension to Maxwell equation is (as usual) complicated by some theoretical difficulties. We think in particular to the loss of compacity of the embedding of the natural solution space $\mathbf{H}(\mathbf{curl})$ in $\mathbf{L}^2$, which was a theoretical obstacle to prove the well-posedness of the local sub-problems. This is usually tackled by using so-called Helmholtz-Hodge decompositions, but it was somehow insufficient for our particular configuration as we shall see. In addition, the construction of suitable transmission operators is more intricate and this is due to the nature of the two tangential trace spaces.

Several spaces in which to set the interface problem It shall be noted that the interface problem (2.15) can be set in different spaces. We presented here the most natural derivation for which the space is $H^{-1/2}(\Sigma) \times H^{-1/2}(\Sigma)$ as was done for instance in [91, 44]. In contrast, in [42], the authors use $L^2(\Sigma) \times L^2(\Sigma)$. Following some symmetry, a third choice, which was not used in the literature to the best of our knowledge, is to set the interface problem in $H^{1/2}(\Sigma) \times H^{1/2}(\Sigma)$. We shall consider all three cases (and their corresponding counterparts in the electromagnetic setting) by indexing the operators that we will introduce with a parameter σ in $\{0, 1/2, 1\}$.

2.4.2 Generalization to configurations with junction points

A more difficult generalization concerns the analysis with junction points, which is the main subject of Part III. This is made possible by exploiting the ideas presented in Section 2.3. Still, one key idea, borrowed from the multi-trace formalism, was not present in this simple two-domain configuration. This idea is to consider traces of local solutions at the whole boundary of the corresponding sub-domains (which are closed manifolds) instead of traces at interfaces (which may not be closed). This is especially important to keep a more pleasant functional setting to work with.

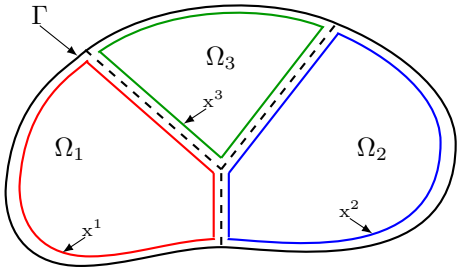

Figure 2.2: Visual representation of the three components of an element of the multi-trace spaces, for instance $(\mathrm{x}_1, \mathrm{x}_2, \mathrm{x}_3) \in \mathbb{M}_D$.

2.4.2.1 An obstacle of geometrical nature

However, if the traces are taken on the whole boundary of the sub-domains, they will include a part on the physical boundary and the generalization of the above discussion is not straightforward. To explain the difficulty, let us take the example of the configuration of Figure 2.2. We

have three sub-domains Ω_j, with $j \in \{1,2,3\}$, the multi-trace spaces become (we use the same notations as in the two-domain configuration)

$$\begin{aligned} \mathbb{M}_D &:= H^{1/2}(\partial\Omega_1) \times H^{1/2}(\partial\Omega_2) \times H^{1/2}(\partial\Omega_3), \\ \mathbb{M}_N &:= H^{-1/2}(\partial\Omega_1) \times H^{-1/2}(\partial\Omega_2) \times H^{-1/2}(\partial\Omega_3). \end{aligned} \tag{2.82}$$

We can then define the trace operators (the outward unit normal to Ω_j is ν_j)

$$\begin{aligned} \boldsymbol{\gamma}_D \ &: H^1(\Omega_1) \times H^1(\Omega_2) \times H^1(\Omega_3) \to \mathbb{M}_D, \\ \mathbb{u} = \begin{bmatrix} u_1 \\ u_2 \\ u_3 \end{bmatrix} &\mapsto \begin{bmatrix} u_1|_{\partial\Omega_1} \\ u_2|_{\partial\Omega_2} \\ u_3|_{\partial\Omega_3} \end{bmatrix}, \end{aligned} \tag{2.83}$$

and

$$\begin{aligned} \boldsymbol{\gamma}_n \ &: \mathbf{H}(\mathrm{div};\Omega_1) \times \mathbf{H}(\mathrm{div};\Omega_2) \times \mathbf{H}(\mathrm{div};\Omega_3) \to \mathbb{M}_N, \\ \mathbb{u} := \begin{bmatrix} \mathbf{u}_1 \\ \mathbf{u}_2 \\ \mathbf{u}_3 \end{bmatrix} &\mapsto \begin{bmatrix} (\nu_1 \cdot \mathbf{u}_1)|_{\partial\Omega_1} \\ (\nu_2 \cdot \mathbf{u}_2)|_{\partial\Omega_2} \\ (\nu_3 \cdot \mathbf{u}_3)|_{\partial\Omega_3} \end{bmatrix}. \end{aligned} \tag{2.84}$$

The single-trace spaces are

$$\begin{aligned} \mathbb{S}_D &= \boldsymbol{\gamma}_D \, H^1(\Omega), \\ \mathbb{S}_N &= \boldsymbol{\gamma}_n \, \mathbf{H}(\mathrm{div};\Omega). \end{aligned} \tag{2.85}$$

The duality pairing becomes

$$\begin{aligned} \langle\!\langle \cdot,\cdot \rangle\!\rangle_\Sigma \ &: \mathbb{M}_N \times \mathbb{M}_{\mathbb{D}} \to \mathbb{C}, \\ \left(\begin{bmatrix} x_{1,N} \\ x_{2,N} \\ x_{3,N} \end{bmatrix}, \begin{bmatrix} x_{1,D} \\ x_{2,D} \\ x_{3,D} \end{bmatrix} \right) &\mapsto \langle x_{1,N}, x_{1,D} \rangle_{\partial\Omega_1} + \langle x_{2,N}, x_{2,D} \rangle_{\partial\Omega_2} + \langle x_{3,N}, x_{3,D} \rangle_{\partial\Omega_3}. \end{aligned} \tag{2.86}$$

The issue comes from the fact that the orthogonality between the Dirichlet and Neumann single-trace spaces (see (2.54)), which is a key ingredient in the new derivation (see (2.72)), is lost:

$$\forall \mathbb{x}_N \in \mathbb{S}_N, \ \mathbb{x}_D \in \mathbb{S}_D, \qquad \langle\!\langle \mathbb{x}_N, \mathbb{x}_D \rangle\!\rangle_\Sigma \neq 0. \tag{2.87}$$

To see this, it is enough to consider elements

$$\begin{aligned} \mathbb{x}_N &\in L^2(\partial\Omega_1) \times L^2(\partial\Omega_2) \times L^2(\partial\Omega_3) \cap \mathbb{S}_N, \\ \mathbb{x}_D &\in L^2(\partial\Omega_1) \times L^2(\partial\Omega_2) \times L^2(\partial\Omega_3) \cap \mathbb{S}_D, \end{aligned} \tag{2.88}$$

we can then formally split the duality products. The parts on the interfaces cancel and it remains the parts on the physical boundary Γ only, which have no reason to cancel

$$\langle\!\langle \mathbb{x}_N, \mathbb{x}_D \rangle\!\rangle_\Sigma = \langle x_{1,N}, x_{1,D} \rangle_{\partial\Omega_1 \cap \Gamma} + \langle x_{2,N}, x_{2,D} \rangle_{\partial\Omega_2 \cap \Gamma} + \langle x_{3,N}, x_{3,D} \rangle_{\partial\Omega_3 \cap \Gamma} \neq 0. \tag{2.89}$$

An easy solution It is clear that the above problem disappears altogether if we exclude the presence of *boundary* junction points, i.e. cross-points between a transmission interface and the physical boundary, as illustrated in Figure 2.3a. One then considers traces on the whole boundary of the sub-domains, except for the part on the physical boundary. However, we are able to deal with *interior* junction points. This approach is the one adopted in Chapter 9, where the ideas presented in Section 2.3 are generalized in the abstract setting we introduced. This approach has the benefit of being an exact generalization of the more standard method described in Chapter 3, in absence of junctions.

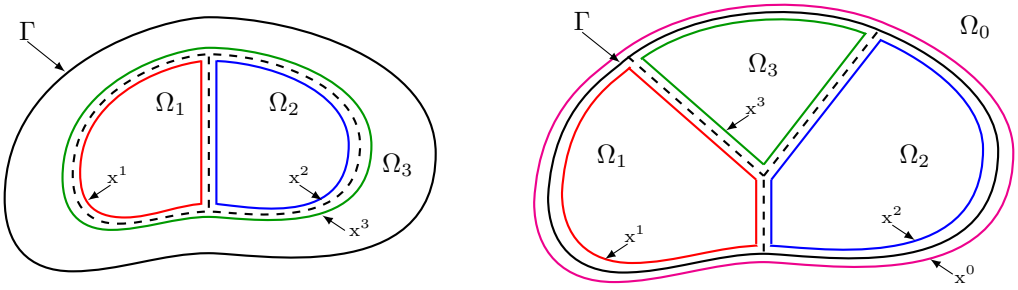

(a) Interior junctions only.

(b) Interior and boundary junctions.

Figure 2.3: Visual representation of the components of an element of the multi-trace spaces, for two configurations.

2.4.2.2 Generalization to arbitrary partitions

Nevertheless, it is not satisfactory to impose that the partition does not contain boundary junction points. Two approaches can be considered, that we discuss below.

Introducing the complementary unbounded domain To deal with boundary junctions, one idea is to introduce a fictitious domain Ω_0 defined as the unbounded complementary of the physical domain

$$\Omega_0 := \mathbb{R}^2 \setminus \left(\cup_{i=1}^3 \overline{\Omega_i}\right). \tag{2.90}$$

As a result, an additional component is added in the multi-trace space in a natural manner, as illustrated in Figure 2.3b. Since traces are defined on both sides of all boundaries, the orthogonality can be recovered.

For wave propagation problems, this approach can be very sensible. Indeed, in many problems, an absorbing boundary condition is imposed on Γ in an attempt to model an unbounded domain. This can be taken into account exactly by using integral equations. This point of view is the one adopted in [29] for instance, but will not be further developed here.

Orthogonality by construction The second approach that allows to deal with general configurations is to bake the orthogonality into the definition of the single-trace spaces. The multi-trace spaces are still defined as in (2.82), which is illustrated on Figure 2.2. The Dirichlet single-trace space is also defined as $\mathbb{S}_D = \boldsymbol{\gamma}_D \; H^1(\Omega)$. However, the Neumann single-trace space will be defined as

$$\mathbb{S}_N := \{\mathbb{x}_N \in \mathbb{M}_N \mid \langle\!\langle \mathbb{x}_N, \mathbb{x}_D \rangle\!\rangle_\Sigma = 0, \; \forall \mathbb{x}_D \in \mathbb{S}_D\}. \tag{2.91}$$

Of course the two definitions coincide in the two-domain configuration, but this is not true in general.

To see why this is the right approach, we need to consider variational formulations. Let us resume the discussion with the two-domain configuration. The model problem (2.1) is written equivalently in variational form as

$$\begin{cases} \text{Find } u \in H^1(\Omega) \text{ such that,} \\ a(u,v) = l(v), \qquad \forall v \in H^1(\Omega), \end{cases} \tag{2.92}$$

where we introduced for $u, v \in H^1(\Omega)$

$$\begin{aligned} a(u,v) &:= (\mathbf{grad}\, u, \mathbf{grad}\, v)_{L^2(\Omega)^2} - \kappa^2\, (u,v)_{L^2(\Omega)} - \mathrm{i}\kappa (u|_\Gamma, v|_\Gamma)_{L^2(\Gamma)}, \\ l(v) &:= (f,v)_{L^2(\Omega)} + (g, v|_\Gamma)_{L^2(\Gamma)}. \end{aligned} \tag{2.93}$$

Let us introduce in addition the local versions for $u_j, v_j \in H^1(\Omega_j)$, $j \in \{1,2\}$,

$$\begin{aligned} a_1(u_1,v_1) &:= (\mathbf{grad}\, u_1, \mathbf{grad}\, v_1)_{L^2(\Omega_1)^2} - \kappa^2\, (u_1,v_1)_{L^2(\Omega_1)}, \\ a_2(u_2,v_2) &:= (\mathbf{grad}\, u_2, \mathbf{grad}\, v_2)_{L^2(\Omega_2)^2} - \kappa^2\, (u_2,v_2)_{L^2(\Omega_2)} - \mathrm{i}\kappa (u_2|_\Gamma, v_2|_\Gamma)_{L^2(\Gamma)}, \\ l_1(v_1) &:= (f|_{\Omega_1}, v_1)_{L^2(\Omega_1)}, \\ l_2(v_2) &:= (f|_{\Omega_2}, v_2)_{L^2(\Omega_2)} + (g, v_2|_\Gamma)_{L^2(\Gamma)}. \end{aligned} \tag{2.94}$$

It is a standard result that the problem (2.92) is equivalent to

$$\begin{cases} \text{Find } (u_1,u_2) \in H^1(\Omega_1) \times H^1(\Omega_2),\ \lambda \in H^{-1/2}(\Sigma) \text{ such that,} \\ a_1(u_1,v_1) - \langle \lambda, v_1|_\Sigma \rangle_\Sigma = l_1(v_1), \qquad \forall v_1 \in H^1(\Omega_1), \\ a_2(u_2,v_2) + \langle \lambda, v_2|_\Sigma \rangle_\Sigma = l_2(v_2), \qquad \forall v_2 \in H^1(\Omega_2), \\ u_1|_\Sigma = u_2|_\Sigma, \qquad \text{on } \Sigma. \end{cases} \tag{2.95}$$

Interestingly, the multi-trace formalism allows to reformulate the above problem (2.95) as

$$\begin{cases} \text{Find } (u_1,u_2) \in H^1(\Omega_1) \times H^1(\Omega_2),\ \aleph_N = (x_{1,N}, x_{2,N}) \in \mathbb{S}_N \text{ such that,} \\ a_1(u_1,v_1) - \langle x_{1,N}, v_1|_\Sigma \rangle_\Sigma = l_1(v_1), \qquad \forall v_1 \in H^1(\Omega_1), \\ a_2(u_2,v_2) - \langle x_{2,N}, v_2|_\Sigma \rangle_\Sigma = l_2(v_2), \qquad \forall v_2 \in H^1(\Omega_2), \\ \boldsymbol{\gamma}_D(u_1,u_2) \in \mathbb{S}_D. \end{cases} \tag{2.96}$$

Note that the single-trace $\aleph_N$ identifies as the couple of Neumann traces $\boldsymbol{\gamma}_N(u_1,u_2)$ of the broken solution (u_1,u_2). This can be further reformulated as

$$\begin{cases} \text{Find } (u_1,u_2) \in H^1(\Omega_1) \times H^1(\Omega_2),\ \aleph_N \in \mathbb{S}_N \text{ such that,} \\ [a_1(u_1,v_1) + a_2(u_2,v_2)] - [l_1(v_1) + l_2(v_2)] \\ \qquad\qquad = \langle\!\langle \aleph_N, \boldsymbol{\gamma}_D(v_1,v_2) \rangle\!\rangle_\Sigma, \qquad \forall (v_1,v_2) \in H^1(\Omega_1) \times H^1(\Omega_2), \\ \boldsymbol{\gamma}_D(u_1,u_2) \in \mathbb{S}_D. \end{cases} \tag{2.97}$$

We will resume this discussion with more detail in the following, but it is readily seen that the existence of such a $\aleph_N$ in $\mathbb{M}_N$ exists by the Riesz representation theorem. Moreover, the model problem is recovered provided $\aleph_N$ is an element of $\mathbb{S}_N$ as defined in (2.91). These arguments will carry over to more general partitions with the definitions of the multi-trace spaces as in (2.82). However, in general the element $\aleph_N$ of $\mathbb{S}_N$ will not represent the Neumann trace anymore.

This approach is considered in more detail in Chapter 10, in the discrete setting only (but the approach can be conducted in the continuous setting without difficulties).

Part I

Onion-like DDM

Chapter 3

Continuous setting

Contents

In this chapter, we describe in the continuous setting a class of domain decomposition methods we consider in this work. We chose to describe the domain decomposition method in an abstract framework, valid for our main applications, which are mainly second order systems of equations, which are compact perturbations of elliptic systems. In particular, the typical instances of systems we have in mind are Helmholtz and Maxwell equations, which will serve as illustrative examples as we describe the general theory. While the abstract formalism might obfuscate the presentation a little, we believe that it has the great benefit of highlighting the main ideas pertaining to the method while allowing in the meantime to stress the main differences between acoustics and electromagnetism.

Influenced by the work of Xavier Claeys [29], a novelty of the approach we adopt in the following, compared to previous descriptions of similar ideas [42, 91, 44], is to view everything from the perspective of traces (see Section 3.2.2). The motivation for this comes from the fact that the iterative algorithm is actually written at the interfaces (this is not new). As a result, the main objects that the solver manipulates are not collections of local solutions but rather collections of traces, elements of a space which we refer to as the *multi-trace space* (see Definition 3.16). Both zeroth and first order traces (as well as couples of the two) will be manipulated in this work. The goal of the domain decomposition procedure is then to select the unique element of the multi-trace space which corresponds to the actual solution of our original problem. It is then natural to try to characterize this element. We do that by introducing two subspaces of the multi-trace space. The first one is the so-called *Cauchy trace space* (see Definition 3.18), which is the space of couples of zeroth and first order traces that represent functions satisfying the original physical equation locally in each sub-domain. The second subspace we introduce is the so-called *single-trace space* (see Definition 3.20), whose elements match in some sense at an interface (expressing the transmission conditions between sub-domains), hence imposing the global regularity required by the solution of the original problem. Matching conditions for both the zeroth and first order traces should be satisfied. Roughly speaking (see Proposition 3.24 for the details), it is then possible to characterize the solution as the intersection between the two subspaces.

To devise the domain decomposition method, we introduce the so-called *transmission or impedance operator* which is a boundary operator used to combined the two traces together, constituting a generalized Robin trace. As we shall show, the transmission operator is the keystone of the method and should be designed carefully as its properties will have a tremendous impact on the efficiency of the approach. The analysis is conducted for a class of transmission operators having some general properties. The construction of some suitable operators is addressed in Part II of this manuscript. We then show in Section 3.2.4 that the Robin trace of the solution of the model problem is a fixed point of a boundary operator defined on the skeleton (see Proposition 3.38). This boundary operator involves a *scattering operator* (see (3.176)) whose graph is linked to the Cauchy trace space (Proposition 3.30) and the *exchange operator* (see (3.184)) whose graph is linked to the single-trace space (Proposition 3.37). The scattering operator takes an incoming Robin trace and computes an outgoing Robin trace after solving a local problem in the sub-domain. As a result, its properties (and well-posedness) are heavily influenced by the choice of the transmission operator. On the contrary, the exchange operator is, in this chapter, independent of the transmission operator. This feature is a key difference with the method described in Chapter 9.

Two algorithms to solve the interface problem are then introduced. The first one is a fixed point iteration algorithm, the relaxed Jacobi algorithm, for which we analyze in detail the con-

vergence. The analysis is performed in a particular norm induced by a suitable inner-product built from the transmission operator. The second algorithm we consider is the GMRES algorithm and is seen as an improvement of the previous algorithm.

3.1 Abstract definitions

3.1.1 Generic definitions and tools

To set some definitions, we consider a generic open bounded Lipschitz domain $\mathcal{O}$ subset of $\mathbb{R}^d$, with $d = 1, 2, 3$, intended to be either our model domain or a sub-domain of the partition. Its boundary is denoted by $\partial\mathcal{O}$ with outward normal unit vector ν.

Unknowns and differential operators The complex-valued unknowns of our model problem, considered as a first order system of equation, will be denoted

$$\begin{aligned} u &: \mathcal{O} \to \mathbb{C}^{m_0}, \\ v &: \mathcal{O} \to \mathbb{C}^{m_1}, \end{aligned} \tag{3.1}$$

where $m_0\,, m_1 \in \{1, d, d \times d\}$, depending on the type of wave propagation problem we wish to solve. However, since we will write our model problem as a second order equation, v will not appear explicitly but in the form $v = \mathrm{D}u$, where D is a first-order differential operator defined as

$$\mathrm{D} := \sum_{j=1}^{d} \mathcal{D}_j \partial_{x_j}, \tag{3.2}$$

such that $\mathcal{D}_j \in \mathbb{R}^{m_1 \times m_0}$, for all $j = 1, \ldots, d$. We denote by D^* the formal adjoint of D defined as

$$\mathrm{D}^* := -\sum_{j=1}^{d} \mathcal{D}_j^* \partial_{x_j}. \tag{3.3}$$

We readily provide two examples of systems that fit in this rather general setting, namely the (time harmonic) Helmholtz and Maxwell equations.

Example 1: Helmholtz. *In the acoustic setting, the unknowns are the pressure p, hence a scalar field, so that $m_0 \equiv 1$, and the velocity field $\mathbf{u}$, proportional to $\mathbf{grad}\, p$, so that $m_1 \equiv d$. The differential operators are then identified as*

$$\mathrm{D} \equiv \mathbf{grad} \quad \textit{and} \quad \mathrm{D}^* \equiv -\operatorname{div}. \tag{3.4}$$

Besides, one can check that

$$\mathcal{D}_j := (\delta_{1j}, \ldots, \delta_{dj})^t, \qquad \forall j \in \{1, \ldots, d\}. \tag{3.5}$$

Example 2: Maxwell. *In the electromagnetic setting (we will only consider in what follows 3D Maxwell equations, so that $d \equiv 3$), the unknowns are the electric field $\mathbf{E}$, hence a vector field, so that $m_0 \equiv 3$, and the magnetic field $\mathbf{H}$, proportional to $\mathbf{curl}\,\mathbf{E}$, so that $m_1 \equiv 3$. The differential operators are then identified as*

$$\mathrm{D} \equiv \mathbf{curl} \quad \textit{and} \quad \mathrm{D}^* \equiv \mathbf{curl}. \tag{3.6}$$

Besides, one can check that

$$\mathcal{D}_1 = \begin{pmatrix} 0 & 0 & 0 \\ 0 & 0 & -1 \\ 0 & 1 & 0 \end{pmatrix}, \qquad \mathcal{D}_2 = \begin{pmatrix} 0 & 0 & 1 \\ 0 & 0 & 0 \\ -1 & 0 & 0 \end{pmatrix}, \qquad \mathcal{D}_3 = \begin{pmatrix} 0 & -1 & 0 \\ 1 & 0 & 0 \\ 0 & 0 & 0 \end{pmatrix} \tag{3.7}$$

Volume spaces We introduce the following (solution) spaces

$$\begin{aligned} \mathrm{U}(\mathrm{D};\mathcal{O}) &:= \left\{ u \in L^2(\mathcal{O})^{m_0} \mid \mathrm{D}u \in L^2(\mathcal{O})^{m_1} \right\}, \\ \mathrm{U}(\mathrm{D}^*;\mathcal{O}) &:= \left\{ u \in L^2(\mathcal{O})^{m_1} \mid \mathrm{D}^*u \in L^2(\mathcal{O})^{m_0} \right\}. \end{aligned} \tag{3.8}$$

Let κ_0 be a scalar, supposed to be the inverse of a characteristic length of our problem. In practice, it can be the wavenumber of the medium of propagation, or of a reference medium in the heterogeneous case. We equip our solution space $\mathrm{U}(\mathrm{D};\mathcal{O})$ with the following κ_0-dependent scalar product and (energy) norm

$$\begin{aligned} &(u,v)_{\mathrm{U}(\mathrm{D};\mathcal{O})} := \kappa_0 \, (u,v)_{L^2(\mathcal{O})^{m_0}} + {\kappa_0}^{-1} \, (\mathrm{D}u, \mathrm{D}v)_{L^2(\mathcal{O})^{m_1}}, \qquad \forall u, v \in \mathrm{U}(\mathrm{D};\mathcal{O}), \\ &\|u\|^2_{\mathrm{U}(\mathrm{D};\mathcal{O})} := (u, \overline{u})_{\mathrm{U}(\mathrm{D};\mathcal{O})}, \qquad \forall u \in \mathrm{U}(\mathrm{D};\mathcal{O}). \end{aligned} \tag{3.9}$$

Notice that we introduced κ_0 in order to have two terms with the same homogeneity in the definition of the scalar product.

Example 1: Helmholtz. *Let us set*

$$\mathbf{L}^2(\mathcal{O}) := L^2(\mathcal{O})^3. \tag{3.10}$$

In the acoustic setting, the natural functional spaces are

$$\begin{aligned} \mathrm{U}(\mathrm{D};\mathcal{O}) \equiv H^1(\mathcal{O}) &:= \left\{ p \in L^2(\mathcal{O}) \mid \mathbf{grad}\, p \in \mathbf{L}^2(\mathcal{O}) \right\}, \\ \mathrm{U}(\mathrm{D}^*;\mathcal{O}) \equiv \mathbf{H}(\mathrm{div};\mathcal{O}) &:= \left\{ \mathbf{u} \in \mathbf{L}^2(\mathcal{O}) \mid \mathrm{div}\, \mathbf{u} \in L^2(\mathcal{O}) \right\}, \end{aligned} \tag{3.11}$$

Example 2: Maxwell. *In the electromagnetic setting, the natural functional spaces are*

$$\begin{aligned} \mathrm{U}(\mathrm{D};\mathcal{O}) \equiv \mathbf{H}(\mathbf{curl};\mathcal{O}) &:= \left\{ \mathbf{E} \in \mathbf{L}^2(\mathcal{O}) \mid \mathbf{curl}\, \mathbf{E} \in \mathbf{L}^2(\mathcal{O}) \right\}, \\ \mathrm{U}(\mathrm{D}^*;\mathcal{O}) &\equiv \mathbf{H}(\mathbf{curl};\mathcal{O}). \end{aligned} \tag{3.12}$$

We will require in the following the following density assumption.

Assumption 3.1. *We suppose that*

$$\begin{aligned} &\text{the space } \mathcal{D}(\overline{\mathcal{O}})^{m_0} \text{ is dense in } \mathrm{U}(\mathrm{D};\mathcal{O}), \\ &\text{the space } \mathcal{D}(\overline{\mathcal{O}})^{m_1} \text{ is dense in } \mathrm{U}(\mathrm{D}^*;\mathcal{O}). \end{aligned} \tag{3.13}$$

Example 1: Helmholtz. *In the acoustic setting, we have the following density results [79, Th. 1.2 and Th. 2.4]*

$$\begin{aligned} &\text{the space } \mathcal{D}(\overline{\mathcal{O}}) \text{ is dense in } H^1(\mathcal{O}), \\ &\text{the space } \mathcal{D}(\overline{\mathcal{O}})^d \text{ is dense in } \mathbf{H}(\mathrm{div};\mathcal{O}). \end{aligned} \tag{3.14}$$

Example 2: Maxwell. *In the electromagnetic setting, we have the following density result [79, Th. 2.10]*

$$\text{the space } \mathcal{D}(\overline{\mathcal{O}})^3 \text{ is dense in } \mathbf{H}(\mathbf{curl};\mathcal{O}). \tag{3.15}$$

Integration by parts formula We shall make the (reasonable) assumption that $C^1(\overline{\mathcal{O}})$ is dense in both $\mathrm{U}(\mathrm{D};\mathcal{O})$ and $\mathrm{U}(\mathrm{D}^*;\mathcal{O})$.

We introduce the following (matrix-valued) fields over the boundary $\partial\mathcal{O}$

$$\begin{aligned} \mathcal{D}_\nu \ &: \partial\mathcal{O} \to \mathbb{R}^{m_1\times m_0}, \qquad \text{with adjoint} \qquad \mathcal{D}_\nu^* \ : \partial\mathcal{O} \to \mathbb{R}^{m_1\times m_0}, \\ x &\mapsto \sum_{j=1}^d \nu_j(x)\mathcal{D}_j, \qquad\qquad\qquad\qquad x \mapsto \sum_{j=1}^d \nu_j(x)\mathcal{D}_j^*. \end{aligned} \tag{3.16}$$

For any (complex-valued) $u \in C^1\left(\overline{\mathcal{O}}\right)^{m_0}$ and $v \in C^1\left(\overline{\mathcal{O}}\right)^{m_1}$, the following integration by parts formula holds

$$(v, \mathrm{D}u)_{L^2(\mathcal{O})^{m_1}} - (\mathrm{D}^*v, u)_{L^2(\mathcal{O})^{m_0}} = (\mathcal{D}_\nu^* v, u)_{L^2(\partial\mathcal{O})^{m_0}} \equiv (v, \mathcal{D}_\nu u)_{L^2(\partial\mathcal{O})^{m_1}}. \tag{3.17}$$

Example 1: Helmholtz. *In the acoustic setting, we set $\mathcal{D}_\nu := \nu$ so that, for any $\mathbf{u} \in C^1\left(\overline{\mathcal{O}}\right)^3$ and $p \in C^1\left(\overline{\mathcal{O}}\right)$,*

$$\mathcal{D}_\nu p = p\nu \qquad \text{and} \qquad \mathcal{D}_\nu^* \mathbf{u} = \nu \cdot \mathbf{u}, \tag{3.18}$$

and we recover the usual integration by parts formula

$$(\mathbf{u}, \mathbf{grad}\, p)_{\mathbf{L}^2(\mathcal{O})} + (\operatorname{div}\mathbf{u}, p)_{L^2(\mathcal{O})} = (\nu\cdot\mathbf{u}, p)_{L^2(\partial\mathcal{O})}. \equiv (\mathbf{u}, p\nu)_{\mathbf{L}^2(\partial\mathcal{O})} \tag{3.19}$$

Example 2: Maxwell. *In the electromagnetic setting, we set*

$$\mathcal{D}_\nu := \begin{pmatrix} 0 & -\nu_3 & \nu_2 \\ \nu_3 & 0 & -\nu_1 \\ -\nu_2 & \nu_1 & 0 \end{pmatrix} \qquad \text{and} \qquad \mathcal{D}_\nu^* := \begin{pmatrix} 0 & \nu_3 & -\nu_2 \\ -\nu_3 & 0 & \nu_1 \\ \nu_2 & -\nu_1 & 0 \end{pmatrix} \tag{3.20}$$

so that, for any $\mathbf{H} \in C^1\left(\overline{\mathcal{O}}\right)^3$ and $\mathbf{E} \in C^1\left(\overline{\mathcal{O}}\right)^3$,

$$\mathcal{D}_\nu \mathbf{E} = \nu \times \mathbf{E} \qquad \text{and} \qquad \mathcal{D}_\nu^* \mathbf{H} = -\nu\times\mathbf{H} \equiv \mathbf{H}\times\nu. \tag{3.21}$$

and we recover the usual integration by parts formula

$$(\mathbf{H}, \mathbf{curl}\,\mathbf{E})_{\mathbf{L}^2(\mathcal{O})} - (\mathbf{curl}\,\mathbf{H}, \mathbf{E})_{\mathbf{L}^2(\mathcal{O})} = (\mathbf{H}\times\nu, \mathbf{E})_{\mathbf{L}^2(\partial\mathcal{O})} \equiv (\mathbf{H}, \nu\times\mathbf{E})_{\mathbf{L}^2(\partial\mathcal{O})}. \tag{3.22}$$

Trace spaces and operators The definition of trace operators and trace spaces is delicate in this general setting, as it depends heavily on the coefficients involved in the differential operators. This is the reason why we suppose that the following assumption holds true in what follows.

Assumption 3.2 (Continuous and surjective trace operators). *We assume that there exists two bounded (matrix-valued) functions defined on the boundary $\partial\mathcal{O}$*

$$\mathcal{A}_0 \ : \ \partial\mathcal{O} \to \mathbb{R}^{m_0\times m_0}, \qquad \text{and} \qquad \mathcal{A}_1 \ : \ \partial\mathcal{O} \to \mathbb{R}^{m_1\times m_0}, \tag{3.23}$$

such that, for any (complex-valued) $u \in C^1\left(\overline{\mathcal{O}}\right)^{m_0}$ and $v \in C^1\left(\overline{\mathcal{O}}\right)^{m_1}$,

$$(\mathcal{A}_1 v, \mathcal{A}_0 u)_{L^2(\partial\mathcal{O})^{m_0}} = (\mathcal{D}_\nu^* v, u)_{L^2(\partial\mathcal{O})^{m_0}} \equiv (v, \mathcal{D}_\nu u)_{L^2(\partial\mathcal{O})^{m_1}}. \tag{3.24}$$

Besides, we will suppose that $\mathcal{A}_0$ is independent of the orientation of the normal vector ν, while $\mathcal{A}_1$ is anti-symmetric with respect to its orientation so that $\mathcal{A}_1$ is changed into $-\mathcal{A}_1$ if the orientation of ν is flipped.

In addition, we suppose that there exists two Hilbert spaces, the trace spaces*, denoted by*

$$\mathrm{X}_0(\partial\mathcal{O}) \qquad \textit{and} \qquad \mathrm{X}_1(\partial\mathcal{O}), \tag{3.25}$$

such that we have the continuous embeddings

$$\begin{aligned} H^{1/2}(\partial\mathcal{O})^{m_0} &\subset \mathrm{X}_0(\partial\mathcal{O}), \\ \mathrm{X}_1(\partial\mathcal{O}) &\subset H^{-1/2}(\partial\mathcal{O})^{m_0}. \end{aligned} \tag{3.26}$$

These trace spaces are assumed to be dual *to each other*

$$\mathrm{X}_0(\partial\mathcal{O})' = \mathrm{X}_1(\partial\mathcal{O}), \tag{3.27}$$

with duality pairing

$$\langle\cdot,\cdot\rangle_{\partial\mathcal{O}} \ : \ \mathrm{X}_1(\partial\mathcal{O}) \times \mathrm{X}_0(\partial\mathcal{O}) \to \mathbb{C}, \tag{3.28}$$

and such that the (interior) trace maps

$$\begin{aligned} \gamma_{\mathrm{D},\partial\mathcal{O}} \ &: \ u \mapsto \mathcal{A}_0 u|_{\partial\mathcal{O}}, \qquad \forall u \in C^1\left(\overline{\mathcal{O}}\right)^{m_0}, \\ \gamma_{\mathrm{D}^*,\partial\mathcal{O}} \ &: \ v \mapsto \mathcal{A}_1 v|_{\partial\mathcal{O}}, \qquad \forall v \in C^1\left(\overline{\mathcal{O}}\right)^{m_1}, \end{aligned} \tag{3.29}$$

can be uniquely extended into linear continuous and surjective trace mappings*, still denoted* $\gamma_{\mathrm{D},\partial\mathcal{O}}$ *and* $\gamma_{\mathrm{D}^*,\partial\mathcal{O}}$*, such that*

$$\begin{aligned} \gamma_{\mathrm{D},\partial\mathcal{O}} \ &\mathrm{U}(\mathrm{D};\mathcal{O}) \to \mathrm{X}_0(\partial\mathcal{O}), \\ \gamma_{\mathrm{D}^*,\partial\mathcal{O}} \ &\mathrm{U}(\mathrm{D}^*;\mathcal{O}) \to \mathrm{X}_1(\partial\mathcal{O}). \end{aligned} \tag{3.30}$$

Finally, we assume that the trace space $\mathrm{X}_0(\partial\mathcal{O})$ *can be equipped with the graph norm*

$$\|\mathrm{x}_0\|_{\mathrm{X}_0(\partial\mathcal{O})} := \inf_{\substack{u\in\mathrm{U}(\mathrm{D};\mathcal{O}) \\ \gamma_{0,\partial\mathcal{O}}\, u=\mathrm{x}_0}} \|u\|_{\mathrm{U}_\Gamma(\mathrm{D};\mathcal{O})}, \qquad \forall \mathrm{x}_0 \in \mathrm{X}_0(\partial\mathcal{O}), \tag{3.31}$$

which, by construction, satisfies

$$\|\gamma_{\mathrm{D},\partial\mathcal{O}}\, u\|_{\mathrm{X}_0(\partial\mathcal{O})} \leq \|u\|_{\mathrm{U}(\mathrm{D};\mathcal{O})}, \qquad \forall u \in \mathrm{U}(\mathrm{D};\mathcal{O}), \tag{3.32}$$

and the space $\mathrm{X}_1(\partial\mathcal{O})$ *can be equipped with the corresponding canonical dual norm, namely*

$$\|\mathrm{x}_1\|_{\mathrm{X}_1(\partial\mathcal{O})} := \sup_{\substack{\mathrm{x}_0\in\mathrm{X}_0(\partial\mathcal{O}) \\ \mathrm{x}_0\neq 0}} \frac{\langle \mathrm{x}_1, \mathrm{x}_0\rangle_{\partial\mathcal{O}}}{\|\mathrm{x}_0\|_{\mathrm{X}_0(\partial\mathcal{O})}}, \qquad \forall \mathrm{x}_1 \in \mathrm{X}_1(\partial\mathcal{O}). \tag{3.33}$$

Example 1: Helmholtz. *In the acoustic setting, Assumption 3.2 holds if one simply takes*

$$\mathcal{A}_0 := \mathrm{Id}_{\mathbb{R}^d} \qquad \textit{and} \qquad \mathcal{A}_1 := \mathcal{D}_\nu^* \equiv \nu\,\cdot\,. \tag{3.34}$$

The associated natural trace spaces, respective images of $H^1(\mathcal{O})$ *and* $\mathbf{H}(\mathrm{div};\mathcal{O})$ *for the trace operators* $\gamma_{\mathrm{D},\partial\mathcal{O}}$ *(in this case the restriction operator) and* $\gamma_{\mathrm{D}^*,\partial\mathcal{O}}$ *(in this case the normal trace operator) are then*

$$\mathrm{X}_0(\partial\mathcal{O}) \equiv H^{1/2}(\partial\mathcal{O}), \qquad \textit{and} \qquad \mathrm{X}_1(\partial\mathcal{O}) \equiv H^{-1/2}(\partial\mathcal{O}). \tag{3.35}$$

Example 2: Maxwell. *In the electromagnetic setting, notice that, for any* $\mathbf{H} \in C^1\left(\overline{\mathcal{O}}\right)^3$ *and* $\mathbf{E} \in C^1\left(\overline{\mathcal{O}}\right)^3$,

$$(\mathbf{H} \times \nu, \mathbf{E})_{\mathbf{L}^2(\partial\mathcal{O})} = (\mathbf{H} \times \nu, \nu \times (\mathbf{E} \times \nu))_{\mathbf{L}^2(\partial\mathcal{O})}. \tag{3.36}$$

One can show that Assumption 3.2 holds if one takes

$$\mathcal{A}_0 := \mathcal{D}_\nu \mathcal{D}_\nu^* \equiv \nu \times (\cdot \times \nu) \qquad \text{and} \qquad \mathcal{A}_1 := \mathcal{D}_\nu^* \equiv -\nu \times \cdot. \tag{3.37}$$

For a regular enough boundary $\partial\mathcal{O}$*, the associated natural trace spaces, respective images of* $\mathbf{H}(\mathbf{curl}; \mathcal{O})$ *for the trace operators* $\gamma_{\mathrm{D},\partial\mathcal{O}}$ *(in this case the tangential trace operator) and* $\gamma_{\mathrm{D}^*,\partial\mathcal{O}}$ *(in this case the rotated tangential trace operator) are then*

$$\begin{aligned} \mathrm{X}_0(\partial\mathcal{O}) \equiv \mathbf{H}^{-1/2}(\mathrm{curl}; \partial\mathcal{O}) &:= \left\{ \mathbf{x} \in H^{-1/2}(\partial\mathcal{O})^3 \mid \mathrm{curl}\, \mathbf{x} \in H^{-1/2}(\partial\mathcal{O}) \right\}, \\ \mathrm{X}_1(\partial\mathcal{O}) \equiv \mathbf{H}^{-1/2}(\mathrm{div}; \partial\mathcal{O}) &:= \left\{ \mathbf{x} \in H^{-1/2}(\partial\mathcal{O})^3 \mid \mathrm{div}\, \mathbf{x} \in H^{-1/2}(\partial\mathcal{O}) \right\}. \end{aligned} \tag{3.38}$$

When the boundary is not regular enough the proper definition of the trace spaces is more involved, see [20, 21].

An immediate consequence of the above assumption is the following generalized integration by parts formula, for any $u \in \mathrm{U}(\mathrm{D}; \mathcal{O})$ and $v \in \mathrm{U}(\mathrm{D}^*; \mathcal{O})$, we have

$$(v, \mathrm{D}u)_{L^2(\mathcal{O})^{m_1}} - (\mathrm{D}^* v, u)_{L^2(\mathcal{O})^{m_0}} = \langle \gamma_{\mathrm{D}^*,\partial\mathcal{O}}\, v, \gamma_{\mathrm{D},\partial\mathcal{O}}\, u \rangle_{\partial\mathcal{O}}. \tag{3.39}$$

If the boundary $\partial\mathcal{O}$ consists of K connected closed components $(\partial\mathcal{O}_k)_{k=1}^K$ so that

$$\begin{aligned} &\partial\mathcal{O} := \bigcup_{k=1}^K \partial\mathcal{O}_k, \\ &\overline{\partial\mathcal{O}}_k \cap \overline{\partial\mathcal{O}}_l = \emptyset, \qquad \forall k, l \in \{1, \ldots, K\},\ k \neq l, \end{aligned} \tag{3.40}$$

then it is obvious that we can define the restrictions of the two traces to any specific component $\partial\mathcal{O}_k$, $k \in \{1, \ldots, K\}$, and still define trace spaces and trace operators which are continuous and surjective mappings as follows

$$\begin{aligned} \gamma_{\mathrm{D},\partial\mathcal{O}_k} &\ \mathrm{U}(\mathrm{D}; \mathcal{O}) \to \mathrm{X}_0(\partial\mathcal{O}_k), \\ \gamma_{\mathrm{D}^*,\partial\mathcal{O}_k} &\ \mathrm{U}(\mathrm{D}^*; \mathcal{O}) \to \mathrm{X}_1(\partial\mathcal{O}_k). \end{aligned} \tag{3.41}$$

Furthermore, the duality pairing between the trace spaces can be split as follows: for any $\mathrm{x}_0 \in \mathrm{X}_0(\partial\mathcal{O})$ and $\mathrm{x}_1 \in \mathrm{X}_1(\partial\mathcal{O})$, we have

$$\langle \mathrm{x}_1, \mathrm{x}_0 \rangle_{\partial\mathcal{O}} = \sum_{k=1}^K \langle \mathrm{x}_1|_{\partial\mathcal{O}_k}, \mathrm{x}_0|_{\partial\mathcal{O}_k} \rangle_{\partial\mathcal{O}_k}. \tag{3.42}$$

We will also need at some point the following assumption.

Assumption 3.3. *We suppose that*

$$\begin{aligned} \mathrm{Ker}\, \gamma_{\mathrm{D},\partial\mathcal{O}} &= \overline{\mathcal{D}(\mathcal{O})^{m_0}}^{\|\cdot\|_{\mathrm{U}(\mathrm{D};\mathcal{O})}}, \\ \mathrm{Ker}\, \gamma_{\mathrm{D}^*,\partial\mathcal{O}} &= \overline{\mathcal{D}(\mathcal{O})^{m_1}}^{\|\cdot\|_{\mathrm{U}(\mathrm{D}^*;\mathcal{O})}}. \end{aligned} \tag{3.43}$$

Example 1: Helmholtz. *In the acoustic setting, we have the results [79, Th. 1.5 and Th. 2.6]*

$$\begin{aligned} &\operatorname{Ker}\gamma_{\mathrm{D},\partial\mathcal{O}} = H^1_0(\mathcal{O}), \qquad \textit{where} \qquad H^1_0(\mathcal{O}) = \overline{\mathcal{D}(\mathcal{O})}^{\|\cdot\|_{H^1(\mathcal{O})}}, \\ &\operatorname{Ker}\gamma_{\mathrm{D}^*,\partial\mathcal{O}} = \mathbf{H}_0(\mathrm{div},\mathcal{O}), \qquad \textit{where} \qquad \mathbf{H}_0(\mathrm{div},\mathcal{O}) = \overline{\mathcal{D}(\mathcal{O})^d}^{\|\cdot\|_{\mathbf{H}(\mathrm{div};\mathcal{O})}}. \end{aligned} \tag{3.44}$$

Example 2: Maxwell. *In the electromagnetic setting, we have the result [79, Th. 2.12]*

$$\operatorname{Ker}\gamma_{\mathrm{D},\partial\mathcal{O}} = \operatorname{Ker}\gamma_{\mathrm{D}^*,\partial\mathcal{O}} = \mathbf{H}_0(\mathbf{curl},\mathcal{O}), \qquad \textit{where} \qquad \mathbf{H}_0(\mathbf{curl},\mathcal{O}) = \overline{\mathcal{D}(\mathcal{O})^3}^{\|\cdot\|_{\mathbf{H}(\mathbf{curl};\mathcal{O})}}. \tag{3.45}$$

Pivot space In addition to Assumption 3.2 we shall make the following additional hypothesis.

Assumption 3.4. *We assume that there exists a third Hilbert (trace) space, denoted by* $\mathrm{X}_{1/2}(\partial\mathcal{O})$*, such that*

$$\mathrm{X}_{1/2}(\partial\mathcal{O}) \subset L^2(\partial\mathcal{O})^{m_0}, \tag{3.46}$$

so that we can adopt the identification

$$\mathrm{X}_{1/2}(\partial\mathcal{O})' \equiv \mathrm{X}_{1/2}(\partial\mathcal{O}). \tag{3.47}$$

We suppose that this space acts as a pivot space *between the trace spaces* $\mathrm{X}_0(\partial\mathcal{O})$ *and* $\mathrm{X}_1(\partial\mathcal{O})$*, by which we mean that there exists linear operator* $\mathrm{t}_{1/2}$ *satisfying*

$$\begin{aligned} &\mathrm{t}_{1/2} \textit{ is an } \text{isomorphim } \textit{from } \mathrm{X}_0(\partial\mathcal{O}) \textit{ to } \mathrm{X}_{1/2}(\partial\mathcal{O}), \\ \textit{and} \qquad &\mathrm{t}^*_{1/2} \textit{ is an } \text{isomorphim } \textit{from } \mathrm{X}_{1/2}(\partial\mathcal{O}) \textit{ to } \mathrm{X}_1(\partial\mathcal{O}). \end{aligned} \tag{3.48}$$

Note that the pivot space does not necessarily occupy a position that is midway between the trace spaces in terms of regularity.

The pivot trace space is endowed with the natural inner product (and associated norm) which we denote by

$$(\cdot,\cdot)_{\partial\mathcal{O}} := (\cdot,\cdot)_{L^2(\partial\mathcal{O})^{m_0}}, \tag{3.49}$$

and

$$\|\mathrm{x}_{1/2}\|^2_{\partial\mathcal{O}} := (\mathrm{x}_{1/2}, \overline{\mathrm{x}_{1/2}})_{\partial\mathcal{O}}, \qquad \mathrm{x}_{1/2} \in \mathbb{M}_{1/2,\|}. \tag{3.50}$$

Example 1: Helmholtz. *In the acoustic setting, the (only possible) pivot space is*

$$\mathrm{X}_{1/2}(\partial\mathcal{O}) \equiv L^2(\partial\mathcal{O}). \tag{3.51}$$

A possible realization of the isomorphism $\mathrm{t}_{1/2}$ *is* $(\mathrm{Id} - \Delta_{\partial\mathcal{O}})^{\frac{1}{4}}$ *where* $\Delta_{\partial\mathcal{O}}$ *is the Laplace-Beltrami operator.*

Example 2: Maxwell. *In the electromagnetic setting, the pivot space is*

$$\mathrm{X}_{1/2}(\partial\mathcal{O}) \equiv \mathbf{L}^2(\partial\mathcal{O}). \tag{3.52}$$

In this case, the construction of a possible isomorphism $\mathrm{t}_{1/2}$ *is more involved than for acoustics and requires the used of the so-called Hodge (or Helmholtz) decomposition of tangential vector fields on* $\partial\mathcal{O}$*.*

Model equation Let a be a bounded and Lipschitz (symmetric matrix valued) field over the domain

$$\mathsf{a} \ : \ \mathcal{O} \to \mathbb{C}^{m_1 \times m_1}, \tag{3.53}$$

we introduce the second order differential operator L_a defined on

$$\mathrm{U}(\mathrm{D}, \mathrm{L}_\mathsf{a}; \mathcal{O}) := \left\{ u \in \mathrm{U}(\mathrm{D}; \mathcal{O}) \mid \mathrm{L}_\mathsf{a} u \in L^2(\mathcal{O})^{m_0} \right\}. \tag{3.54}$$

such that

$$\mathrm{L}_\mathsf{a} := \mathrm{D}^* \, \mathsf{a} \, \mathrm{D}. \tag{3.55}$$

In addition, let n be another bounded and Lipschitz (matrix-valued) field over the domain

$$\mathsf{n} \ : \ \mathcal{O} \to \mathbb{C}^{m_1 \times m_1}, \tag{3.56}$$

The model equation we are going to consider can be written (here in its homogeneous form)

$$(\mathrm{L}_\mathsf{a} - {\kappa_0}^2 \, \mathsf{n}) u = 0, \qquad \text{in } \mathcal{O}. \tag{3.57}$$

Example 1: Helmholtz. *The time harmonic Helmholtz equation in heterogeneous media and at frequency ω can be written, for the pressure p, as*

$$\left(-\operatorname{div} \frac{1}{\rho} \, \mathbf{grad} - \frac{\omega^2}{\lambda} \right) p = 0, \qquad \text{in } \mathcal{O}, \tag{3.58}$$

where ρ is the mass density and λ is the incompressibility of the medium under consideration. The velocity field is computed from the pressure as $\mathbf{u} = (\omega\rho)^{-1} \, \mathbf{grad}\, p$. The speed c and wavenumber k of the medium are then defined respectively as

$$c := \sqrt{\frac{\lambda}{\rho}}, \qquad k := \frac{\omega}{c} = \omega \sqrt{\frac{\rho}{\lambda}}. \tag{3.59}$$

This PDE fits in the abstract framework that was previously presented provided we set

$$\mathsf{a} \equiv \rho_r^{-1}, \qquad \mathsf{n} \equiv \lambda_r^{-1} \qquad \textit{and} \qquad \kappa_0 \equiv \omega \sqrt{\frac{\rho_0}{\lambda_0}}, \tag{3.60}$$

where ρ_0 and λ_0 are reference (constant) scalar coefficients of the medium of propagation, and $\rho_r := \rho/\rho_0$ and $\lambda_r := \lambda/\lambda_0$ are the (variable) relative coefficients.

Example 2: Maxwell. *The (one-field) time harmonic Maxwell equation in (isotrope) heterogeneous media and at frequency ω can be written, for the electric field $\mathbf{E}$, as*

$$\left(\mathbf{curl} \, \frac{1}{\mu} \, \mathbf{curl} - \omega^2 \epsilon \right) \mathbf{E} = 0, \qquad \text{in } \mathcal{O}, \tag{3.61}$$

where μ is the permeability and ϵ is the permittivity of the medium under consideration. The magnetic field can be computed from the electric field as $\mathbf{H} = (\mathrm{i}\omega\mu)^{-1} \, \mathbf{curl}\, \mathbf{E}$. The speed c and wavenumber k of the medium are then defined respectively as

$$c := \sqrt{\frac{1}{\epsilon\mu}}, \qquad k := \frac{\omega}{c} = \omega\sqrt{\epsilon\mu}. \tag{3.62}$$

This PDE fits in the abstract framework that was previously presented provided we set

$$\mathsf{a} \equiv \mu_r^{-1}, \qquad \mathsf{n} \equiv \epsilon_r \qquad \textit{and} \qquad \kappa_0 \equiv \omega\sqrt{\mu_0\epsilon_0}, \tag{3.63}$$

where μ_0 and ϵ_0 are reference (constant) scalar coefficients of the medium of propagation and $\mu_r := \mu/\mu_0$ and $\epsilon_r := \epsilon/\epsilon_0$ are the relative (variable) coefficients.

Physical trace operators Using Assumption 3.2, we now introduce the following (physical) trace operators

$$\begin{aligned} \gamma_{0,\partial\mathcal{O}} &:= \gamma_{\mathrm{D},\partial\mathcal{O}}\,, \\ \gamma_{1,\partial\mathcal{O}} &:= {\kappa_0}^{-1}\,\gamma_{\mathrm{D}^*,\partial\mathcal{O}}\,\mathsf{aD}. \end{aligned} \tag{3.64}$$

Note that we chose to rescale $\gamma_{1,\partial\mathcal{O}}$ by the constant factor κ_0 in order to have two traces with the same dimension.

It follows from the generalized integration by parts formula (3.39) that we have the following classical result.

Lemma 3.5 (**First Green identity**). *We have, for all* $u \in \mathrm{U}(\mathrm{D},\mathrm{L}_{\mathsf{a}};\mathcal{O})$, $v \in \mathrm{U}(\mathrm{D};\mathcal{O})$,

$$(\mathrm{L}_{\mathsf{a}}u, v)_{L^2(\mathcal{O})^{m_0}} - (\mathsf{aD}u, \mathrm{D}v)_{L^2(\mathcal{O})^{m_1}} = -\kappa_0\,\langle \gamma_{1,\partial\mathcal{O}}\,u, \gamma_{0,\partial\mathcal{O}}\,v\rangle_{\partial\mathcal{O}}. \tag{3.65}$$

Example 1: Helmholtz. *In the acoustic setting, we have the following explicit expressions for the Dirichlet trace operator* $\gamma_{0,\partial\mathcal{O}}$ *and the Neumann trace operator* $\gamma_{1,\partial\mathcal{O}}$*, for sufficiently regular functions*

$$\gamma_{0,\partial\mathcal{O}} := \cdot|_{\partial\mathcal{O}} \qquad \textit{and} \qquad \gamma_{1,\partial\mathcal{O}} := {\kappa_0}^{-1}\,\nu\cdot(\rho_r^{-1}\,\mathbf{grad}\,\cdot|_{\partial\mathcal{O}}) \equiv {\kappa_0}^{-1}\,\rho_r^{-1}\,\partial_\nu\,\cdot|_{\partial\mathcal{O}}. \tag{3.66}$$

Example 2: Maxwell. *In the electromagnetic setting, we have the following explicit expressions for the tangential trace operator* $\gamma_{0,\partial\mathcal{O}}$ *and the rotated tangential trace operator* $\gamma_{1,\partial\mathcal{O}}$*, for sufficiently regular functions*

$$\gamma_{0,\partial\mathcal{O}} := \nu\times(\cdot|_{\partial\mathcal{O}}\times\nu) \qquad \textit{and} \qquad \gamma_{1,\partial\mathcal{O}} := -\,{\kappa_0}^{-1}\,\nu\times(\mu_r^{-1}\,\mathbf{curl}\,\cdot|_{\partial\mathcal{O}}). \tag{3.67}$$

Robin boundary condition In this general setting, the analysis of variational formulations stemming from problems with (standard) Robin boundary condition, which are linear combinations of the two traces γ_0 and γ_1, require to introduce another volume Hilbert space with additional regularity.

In order to define this more regular space, we shall suppose that the boundary $\partial\mathcal{O}$ is composed of a first connected component denoted $\partial\mathcal{O}_R$, intended to be the boundary on which the Robin boundary condition is imposed, and additional components, disconnected from $\partial\mathcal{O}_R$. The definitions we set below can be easily adapted if either $\partial\mathcal{O}_R$ or $\partial\mathcal{O}\setminus\partial\mathcal{O}_R$ are empty.

We introduce,

$$\begin{aligned} &\mathrm{U}_{\partial\mathcal{O}_R}(\mathrm{D};\mathcal{O}) := \left\{u\in\mathrm{U}(\mathrm{D};\mathcal{O}) \mid \gamma_{0,\partial\mathcal{O}_R}\,u\in\mathrm{X}_{1/2}(\partial\mathcal{O}_R)\right\}, \\ &\mathrm{U}_{\partial\mathcal{O}_R}(\mathrm{D}^*;\mathcal{O}) := \left\{u\in\mathrm{U}(\mathrm{D}^*;\mathcal{O}) \mid \gamma_{0,\partial\mathcal{O}_R}\,u\in\mathrm{X}_{1/2}(\partial\mathcal{O}_R)\right\}, \\ &\mathrm{U}_{\partial\mathcal{O}_R}(\mathrm{D},\mathrm{L}_{\mathsf{a}};\mathcal{O}) := \left\{u\in\mathrm{U}(\mathrm{D},\mathrm{L}_{\mathsf{a}};\mathcal{O}) \mid \gamma_{0,\partial\mathcal{O}_R}\,u\in\mathrm{X}_{1/2}(\partial\mathcal{O}_R)\right\}. \end{aligned} \tag{3.68}$$

The space $\mathrm{U}_{\partial\mathcal{O}_R}(\mathrm{D};\mathcal{O})$ is made into an Hilbert space with the help of the following scalar product and associated norm, defined for all $u,v\in\mathrm{U}_{\partial\mathcal{O}_R}(\mathrm{D};\mathcal{O})$, as

$$\begin{aligned} (u,v)_{\mathrm{U}_{\partial\mathcal{O}_R}(\mathrm{D};\mathcal{O})} &:= (u,v)_{\mathrm{U}(\mathrm{D};\mathcal{O})} + (\gamma_{0,\partial\mathcal{O}_R}\,u, \gamma_{0,\partial\mathcal{O}_R}\,v)_{L^2(\partial\mathcal{O}_R)^{m_0}}, \\ \|u\|^2_{\mathrm{U}_{\partial\mathcal{O}_R}(\mathrm{D};\mathcal{O})} &:= (u,\overline{u})_{\mathrm{U}_{\partial\mathcal{O}_R}(\mathrm{D};\mathcal{O})}. \end{aligned} \tag{3.69}$$

Example 1: Helmholtz. *In the acoustic setting, the space* $H^{1/2}(\partial\mathcal{O})$ *is included in* $L^2(\partial\mathcal{O})$*, hence* $\mathrm{U}_{\partial\mathcal{O}}(\mathrm{D};\mathcal{O}) = \mathrm{U}(\mathrm{D};\mathcal{O}) \equiv H^1(\mathcal{O})$.

Example 2: Maxwell. *In the electromagnetic setting, because* $\mathbf{H}^{-1/2}(\mathrm{curl};\partial\mathcal{O})$ *is not included in* $\mathbf{L}^2(\partial\mathcal{O})^3$*, we need to introduce the following space as our solution space for our model problem to be able to study properly Robin boundary conditions*

$$\mathrm{U}_\Gamma(\mathrm{D};\mathcal{O}) \equiv \mathbf{H}_{\partial\mathcal{O}}(\mathbf{curl};\mathcal{O}) := \left\{\mathbf{E}\in\mathbf{H}(\mathbf{curl},\mathcal{O}) \mid \gamma_{0,\partial\mathcal{O}}\,\mathbf{E}\in\mathbf{L}^2(\partial\mathcal{O})\right\}. \tag{3.70}$$

Combined trace operator We also introduce the Cartesian product of the trace spaces as

$$\mathrm{X}(\partial\mathcal{O}) := \mathrm{X}_0(\partial\mathcal{O}) \times \mathrm{X}_1(\partial\mathcal{O}), \tag{3.71}$$

and define the following (continuous but not surjective) combined trace operator

$$\begin{aligned} \gamma_{\partial\mathcal{O}} \quad & \mathrm{U}(\mathrm{D}, \mathrm{L}_{\mathsf{a}}; \mathcal{O}) \to \mathrm{X}(\partial\mathcal{O}), \\ & u \mapsto (\gamma_{0,\partial\mathcal{O}}\, u, \gamma_{1,\partial\mathcal{O}}\, u). \end{aligned} \tag{3.72}$$

We introduce the following bilinear form

$$[\cdot,\cdot]_{\partial\mathcal{O}} \ : \ \mathrm{X}(\partial\mathcal{O}) \times \mathrm{X}(\partial\mathcal{O}) \to \mathbb{C}, \tag{3.73}$$

such that, for all $\mathrm{x} = (\mathrm{x}_0, \mathrm{x}_1) \in \mathrm{X}(\partial\mathcal{O})$ and $\mathrm{y} = (\mathrm{y}_0, \mathrm{y}_1) \in \mathrm{X}(\partial\mathcal{O})$,

$$[\mathrm{x}, \mathrm{y}]_{\partial\mathcal{O}} := \langle \mathrm{y}_1, \mathrm{x}_0 \rangle_{\partial\mathcal{O}} - \langle \mathrm{x}_1, \mathrm{y}_0 \rangle_{\partial\mathcal{O}}. \tag{3.74}$$

It is a simple computation to show the following lemma.

Lemma 3.6.

$$\mathrm{i}[\mathrm{x}, \overline{\mathrm{x}}]_{\partial\mathcal{O}} = 2\,\Im\langle \mathrm{x}_1, \overline{\mathrm{x}_0} \rangle_{\partial\mathcal{O}}, \qquad \forall \mathrm{x} \equiv (\mathrm{x}_0, \mathrm{x}_1) \in \mathrm{X}(\partial\mathcal{O}). \tag{3.75}$$

Proof. Let $\mathrm{x} \equiv (\mathrm{x}_0, \mathrm{x}_1) \in \mathrm{X}(\partial\mathcal{O})$, we have

$$[\mathrm{x}, \overline{\mathrm{x}}]_{\partial\mathcal{O}} = \langle \overline{\mathrm{x}_1}, \mathrm{x}_0 \rangle_{\partial\mathcal{O}} - \langle \mathrm{x}_1, \overline{\mathrm{x}_0} \rangle_{\partial\mathcal{O}} = \overline{\langle \mathrm{x}_1, \overline{\mathrm{x}_0} \rangle_{\partial\mathcal{O}}} - \langle \mathrm{x}_1, \overline{\mathrm{x}_0} \rangle_{\partial\mathcal{O}} = -2\mathrm{i}\Im\langle \mathrm{x}_1, \overline{\mathrm{x}_0} \rangle_{\partial\mathcal{O}}. \tag{3.76}$$

■

3.1.2 Model problem

We consider an open, bounded, simply connected, Lipschitz domain Ω subset of $\mathbb{R}^d$, with $d = 1, 2, 3$. Its boundary is denoted by $\Gamma := \partial\Omega$ with outward unit normal vector ν, and consists in one single connected component. We wish to solve a time-harmonic wave propagation problem on Ω. We denote by $\omega \in \mathbb{R}^+$ the pulsation of the problem and by $\kappa_0 \in \mathbb{R}^+$ the wavenumber of a reference medium (for instance, the air in the acoustic setting, or the vacuum in the electromagnetic setting). We adopt the following convention.

Convention 3.7. *The sign convention of the harmonic regime (hence of the Fourier transform) is chosen to be* $e^{-\mathrm{i}\omega t}$.

The propagative medium is characterized relatively to the reference medium by two (dimensionless) bounded Lipschitz functions

$$\begin{aligned} \mathsf{a} \ &: \ \Omega \to \mathbb{C}^{m_1 \times m_1}, \\ \mathsf{n} \ &: \ \Omega \to \mathbb{C}^{m_0 \times m_0}, \end{aligned} \tag{3.77}$$

such that there exist $\mathsf{a}_- > 0$, $\mathsf{a}_+ > 0$, $\mathsf{n}_- > 0$ and $\mathsf{n}_+ > 0$,

$$\begin{aligned} & \mathsf{a}_- < |\mathsf{a}| < \mathsf{a}_+, && \Im\, \mathsf{a} \le 0, \\ & \mathsf{n}_- < |\mathsf{n}| < \mathsf{n}_+, && \Im\, \mathsf{n} \ge 0. \end{aligned} \tag{3.78}$$

From Convention 3.7 these conditions mean in particular that the medium can only propagate or absorb energy. We are particularly interested in the case where these coefficients are real, which is actually the more challenging situation.

Strong formulation Let $f \in \mathrm{U}_\Gamma(\mathrm{D};\Omega)'$ and $g \in L^2(\Gamma)^{m_0}$. The archetype of a propagative model problem we will consider in the following is given by the following problem

$$\begin{cases} \text{Find } u \in \mathrm{U}_\Gamma(\mathrm{D};\Omega) \text{ such that} & \\ (\mathsf{L_a} - {\kappa_0}^2 \mathsf{n}) u = f, & \text{in } \Omega, \\ (\gamma_{1,\Gamma} - \mathrm{i}\gamma_{0,\Gamma}) u = g, & \text{on } \Gamma. \end{cases} \tag{3.79}$$

Remark 3.8. *It follows from Convention 3.7 that the equation on Γ models a first order (crude) absorbing boundary condition, which expression is formally very close to the transmission conditions we will consider later.*

Example 1: Helmholtz. *In the acoustic setting, our model problem is written*

$$\begin{cases} \textit{Find } p \in H^1(\Omega) \textit{ such that} & \\ \left(-\operatorname{div} \rho_r^{-1} \mathbf{grad} - {\kappa_0}^2 \lambda_r^{-1}\right) p = f, & \textit{in } \Omega, \\ \left(\rho_r^{-1}\, \partial_\nu - \mathrm{i}\kappa_0\right) p = \kappa_0 g, & \textit{on } \Gamma. \end{cases} \tag{3.80}$$

Example 2: Maxwell. *In the electromagnetic setting, our model problem is written*

$$\begin{cases} \textit{Find } \mathbf{E} \in \mathbf{H}_\Gamma(\mathbf{curl};\Omega) \textit{ such that} & \\ \left(\mathbf{curl}\, \mu_r^{-1}\, \mathbf{curl} - {\kappa_0}^2 \epsilon_r\right) \mathbf{E} = f, & \textit{in } \Omega, \\ \mu_r^{-1}\, \mathbf{curl}\, \mathbf{E} \times \nu - \mathrm{i}\kappa_0\, \nu \times (\mathbf{E} \times \nu) = \kappa_0 g, & \textit{on } \Gamma. \end{cases} \tag{3.81}$$

Weak formulation The variational formulation of (3.79) is written

$$\begin{cases} \text{Find } u \in \mathrm{U}_\Gamma(\mathrm{D};\Omega) \text{ such that} \\ a(u,v) = l(v), \qquad \forall v \in \mathrm{U}_\Gamma(\mathrm{D};\Omega), \end{cases} \tag{3.82}$$

where, for all $u, v \in \mathrm{U}_\Gamma(\mathrm{D};\Omega)$, we have the definitions,

$$\begin{cases} a(u,v) := {\kappa_0}^{-1} (\mathsf{a}\, \mathrm{D}u, \mathrm{D}v)_{L^2(\Omega)^{m_1}} - \kappa_0\, (\mathsf{n}u, v)_{L^2(\Omega)^{m_0}} - \mathrm{i}(\gamma_{0,\Gamma}\, u, \gamma_{0,\Gamma}\, v)_{L^2(\Gamma)^{m_0}}, \\ l(v) := {\kappa_0}^{-1} \langle f, v \rangle_\Omega + (g, \gamma_{0,\Gamma}\, v)_{L^2(\Gamma)^{m_0}}. \end{cases} \tag{3.83}$$

Because of the abstract framework, we shall make the following assumption, which will be justified in Section 3.4 when we consider actual wave propagation problems.

Assumption 3.9 (**Well-posedness of the model problem**). *For all $f \in \mathrm{U}_\Gamma(\mathrm{D};\Omega)'$ and $g \in L^2(\Gamma)^{m_0}$ the model problem* (3.79)*, or equivalently its weak formulation* (3.82)*, is well-posed. Namely, there exists a unique solution $u \in \mathrm{U}_\Gamma(\mathrm{D};\Omega)$ and we have the following stability result*

$$\|u\|_{\mathrm{U}_\Gamma(\mathrm{D};\Omega)} \leq \alpha \left(\|f\|_{\mathrm{U}_\Gamma(\mathrm{D};\Omega)'} + \|g\|_{L^2(\Gamma)^{m_0}} \right), \tag{3.84}$$

for a positive constant $\alpha > 0$.

3.1.3 Geometric domain partitioning

After describing the geometric partition of the domain Ω, we introduce the space of broken solutions which consists in collections of solutions local to each sub-domain.

Partition into non-overlapping domains We introduce a domain partitioning of Ω, denoted $\mathcal{P}_\Omega$, into J non-overlapping, Lipschitz, open sub-domains Ω_j, $j \in \{1, \dots, J\}$,

$$\mathcal{P}_\Omega \equiv (\Omega_j)_{j=1}^J, \tag{3.85}$$

such that

$$\overline{\Omega} = \bigcup_{j=1}^J \overline{\Omega}_j, \qquad \text{with} \qquad \Omega_j \cap \Omega_k = \emptyset, \quad \text{if } j \neq k. \tag{3.86}$$

We define the following boundaries and skeleton Σ

$$\begin{aligned} &\Gamma_j := \partial\Omega_j, && j \in \{1, \dots, J\}, \\ &\Gamma_{jk} := \partial\Omega_j \cap \partial\Omega_k, && (j,k) \in \{1, \dots, J\}^2, \quad j \neq k, \\ &\Sigma := \bigcup_{j=1}^J \Gamma_j, \end{aligned} \tag{3.87}$$

and

$$\begin{aligned} &\tilde{\Gamma}_j := \Gamma_j \setminus \Gamma, && j \in \{1, \dots, J\}, \\ &\tilde{\Sigma} := \Sigma \setminus \Gamma. \end{aligned} \tag{3.88}$$

Of course, some of the boundaries Γ_{jk} are empty. We insist on the fact that, *a priori*, the boundaries Γ_j are (unions of) closed surfaces ($\partial\Gamma_j = \emptyset$) while the subsets Γ_{jk} may be open ($\partial\Gamma_{jk} \neq \emptyset$).

For convenience, we introduce the (ordered) index sets

$$\mathbb{K}_j := \left\{ k \in \{1, \dots, J\} \setminus \{j\} \;\middle|\; \Gamma_{jk} \neq \emptyset \right\}, \qquad \forall j \in \{1, \dots, J\}, \tag{3.89}$$

and

$$\mathbb{J} := \bigcup_{j=1}^J \left\{ (j,k) \in \{1, \dots, J\}^2 \;\middle|\; k \in \mathbb{K}_j \right\}. \tag{3.90}$$

The cardinal of this set is equal to twice the number of non-empty interfaces between two distinct sub-domains. An element of the set $\mathbb{J}$ represent the two distinct sub-domain indices that share a (non-empty) common interface. Besides, note that by symmetry

$$\forall (j,k) \in \{1, \dots, J\}^2, \qquad \Big((j,k) \in \mathbb{J} \quad \Leftrightarrow \quad (k,j) \in \mathbb{J} \Big). \tag{3.91}$$

Broken solution spaces In a domain decomposition framework one works with collections of local solutions that satisfies the PDE and physical boundary conditions in each sub-domain. The full (Sobolev) regularity of the true solution is imposed by the transmission conditions at interfaces between sub-domains. This motivates the introduction of the following broken solution spaces,

$$\begin{aligned} \mathbb{U}(\mathrm{D}; \mathcal{P}_\Omega) &:= \left\{ \mathfrak{u} \in L^2(\Omega)^{m_0} \mid \mathfrak{u}|_{\Omega_j} \in \mathrm{U}(\mathrm{D}; \Omega_j), \ \forall j \in \{1, \dots, J\} \right\}, \\ \mathbb{U}(\mathrm{D}^*; \mathcal{P}_\Omega) &:= \left\{ \mathfrak{u} \in L^2(\Omega)^{m_0} \mid \mathfrak{u}|_{\Omega_j} \in \mathrm{U}(\mathrm{D}^*; \Omega_j), \ \forall j \in \{1, \dots, J\} \right\}, \\ \mathbb{U}(\mathrm{D}, \mathrm{L}_\mathsf{a}; \mathcal{P}_\Omega) &:= \left\{ \mathfrak{u} \in L^2(\Omega)^{m_0} \mid \mathfrak{u}|_{\Omega_j} \in \mathrm{U}(\mathrm{D}, \mathrm{L}_\mathsf{a}; \Omega_j), \ \forall j \in \{1, \dots, J\} \right\}. \end{aligned} \tag{3.92}$$

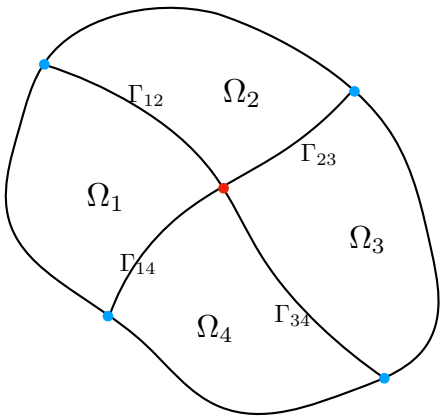

(a) Example of a general partition with interior and boundary cross points (card $\mathbb{J} = 8$).

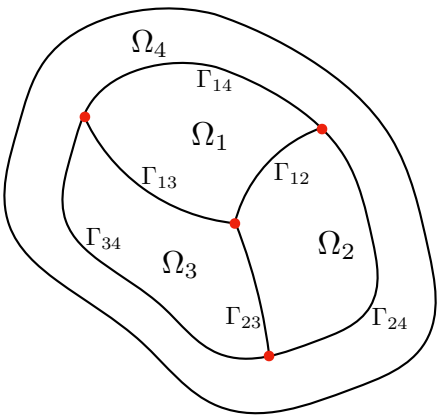

(b) Example of partition with interior cross points but without boundary cross points (card $\mathbb{J} = 12$).

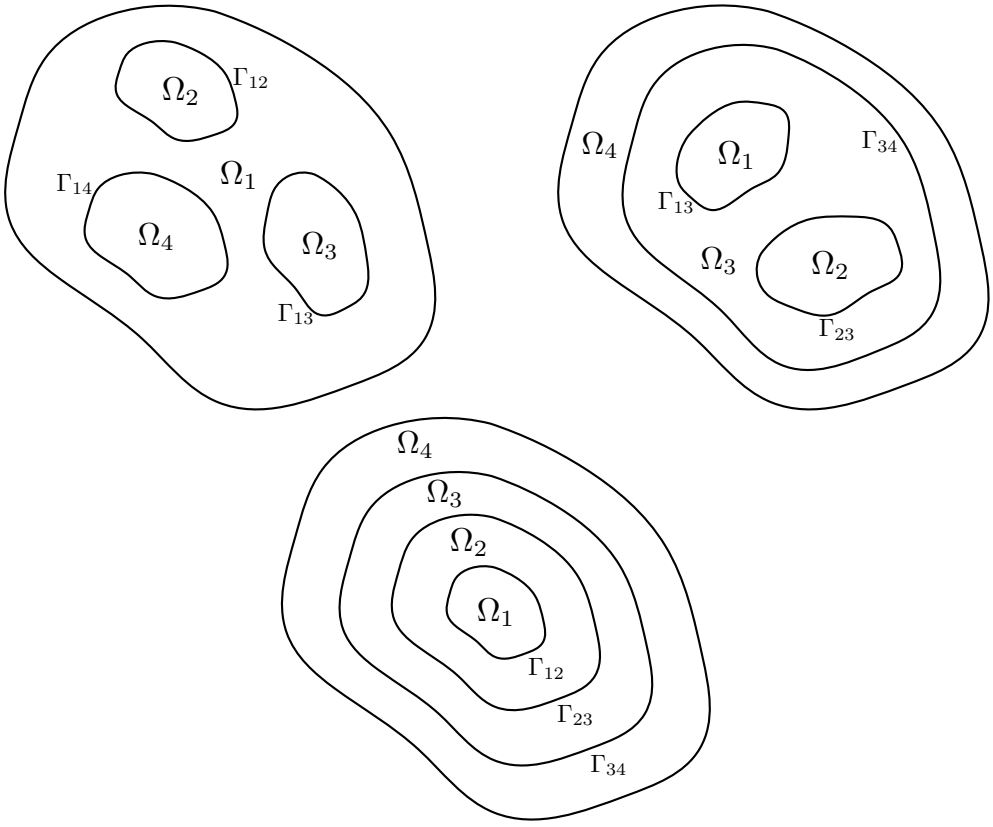

(c) Examples of partitions without any cross points (card $\mathbb{J} = 6$).

Figure 3.1: Different approaches for partitioning the computational domain.

Besides, recalling our previous discussion about Robin boundary condition on Γ we set,

$$\begin{aligned}
\mathbb{U}_\Gamma(\mathrm{D};\mathcal{P}_\Omega) &:= \left\{ \mathbb{u} \in L^2(\Omega)^{m_0} \mid \mathbb{u}|_{\Omega_j} \in \mathrm{U}_\Gamma(\mathrm{D};\Omega_j),\ \forall j \in \{1,\dots,J\} \right\},\\
\mathbb{U}_\Gamma(\mathrm{D}^*;\mathcal{P}_\Omega) &:= \left\{ \mathbb{u} \in L^2(\Omega)^{m_0} \mid \mathbb{u}|_{\Omega_j} \in \mathrm{U}_\Gamma(\mathrm{D}^*;\Omega_j),\ \forall j \in \{1,\dots,J\} \right\},\\
\mathbb{U}_\Gamma(\mathrm{D},\mathrm{L}_\mathsf{a};\mathcal{P}_\Omega) &:= \left\{ \mathbb{u} \in L^2(\Omega)^{m_0} \mid \mathbb{u}|_{\Omega_j} \in \mathrm{U}_\Gamma(\mathrm{D},\mathrm{L}_\mathsf{a};\Omega_j),\ \forall j \in \{1,\dots,J\} \right\}.
\end{aligned} \tag{3.93}$$

We equip the broken space $\mathbb{U}_\Gamma(\mathrm{D};\mathcal{P}_\Omega)$ by the following scalar product (and associated norm)

$$(\mathbb{u},\mathbb{v})_{\mathbb{U}_\Gamma(\mathrm{D};\mathcal{P}_\Omega)} := \sum_{j=1}^{J} (\mathbb{u}|_{\Omega_j},\mathbb{v}|_{\Omega_j})_{\mathrm{U}_\Gamma(\mathrm{D};\Omega_j)}, \qquad \forall \mathbb{u},\mathbb{v} \in \mathbb{U}_\Gamma(\mathrm{D};\mathcal{P}_\Omega). \tag{3.94}$$

Note that we have, for $\mathrm{op} \in \{\mathrm{D},\mathrm{D}^*,\mathrm{L}_\mathsf{a}\}$,

$$\begin{aligned}
\mathrm{U}(\mathrm{op};\Omega) \ &\subsetneq\ \mathbb{U}(\mathrm{op};\mathcal{P}_\Omega) \ \subsetneq\ L^2(\Omega)^{m_0},\\
\mathrm{U}_\Gamma(\mathrm{op};\Omega) \ &\subsetneq\ \mathbb{U}_\Gamma(\mathrm{op};\mathcal{P}_\Omega) \ \subsetneq\ L^2(\Omega)^{m_0},
\end{aligned} \tag{3.95}$$

and that the scalar products and norms on the broken spaces agree with the continuous ones.

Elements of the broken space $\mathbb{U}(\mathrm{D};\mathcal{P}_\Omega)$ may admit jumps (for both trace operators) along interfaces between sub-domains. In a domain decomposition algorithm, one construct sequences of broken solutions in $\mathbb{U}_\Gamma(\mathrm{D};\mathcal{P}_\Omega)$ which (hopefully) converges to the actual regular solution of the original undecomposed problem, which lives in $\mathrm{U}_\Gamma(\mathrm{D};\Omega)$.

Splittings of the variational problem Note that we have a natural splitting of the sesquilinear form a as follows

$$a(u,v) := \sum_{j=1}^{J} a_j(u|_{\Omega_j}, v|_{\Omega_j}), \qquad \forall u,v \in \mathrm{U}_\Gamma(\mathrm{D};\Omega), \tag{3.96}$$

where, for all $j \in \{1,\dots,J\}$, $u_j, v_j \in \mathrm{U}_\Gamma(\mathrm{D};\Omega_j)$,

$$a_j(u_j,v_j) := {\kappa_0}^{-1}(\mathsf{a}\,\mathrm{D}u_j,\mathrm{D}v_j)_{L^2(\Omega_j)^{m_1}} - \kappa_0\,(\mathsf{n}u_j,v_j)_{L^2(\Omega_j)^{m_0}} - \mathrm{i}(\gamma_{0,\Gamma}\,u_j,\gamma_{0,\Gamma}\,v_j)_{L^2(\Gamma)^{m_0}}. \tag{3.97}$$

This motivates the introduction of the (broken) version $\mathbb{a}$ of the above sesquilinear form a, defined on the (larger) broken solution space $\mathbb{U}_\Gamma(\mathrm{D};\mathcal{P}_\Omega)$:

$$\mathbb{a}(u,v) := \sum_{j=1}^{J} a_j(u|_{\Omega_j}, v|_{\Omega_j}), \qquad \forall u,v \in \mathbb{U}_\Gamma(\mathrm{D};\mathcal{P}_\Omega). \tag{3.98}$$

We require more regularity on the source terms that could be assumed on the model problem to avoid any difficulties after decomposition, in particular in the definition of the co-normal derivative. Assuming $f \in \mathrm{U}(\mathrm{D};\Omega)'$ for instance would possibly induce non-zero distributions with support at transmission interfaces later on. Therefore, when we consider our domain decomposition method, we make the following assumption.

Assumption 3.10. *The source of the model problem is such that $f \in L^2(\Omega)^{m_0}$.*

Since both source terms are regular enough, namely $f \in L^2(\Omega)^{m_0}$ and $g \in L^2(\Gamma)^{m_0}$, we also have a natural splitting of the linear form l as follows

$$l(v) := \sum_{j=1}^{J} l_j(v|_{\Omega_j}), \qquad \forall v \in \mathrm{U}_\Gamma(\mathrm{D};\Omega), \tag{3.99}$$

where, for all $j \in \{1,\dots,J\}$, $v_j \in \mathrm{U}_\Gamma(\mathrm{D};\Omega_j)$,

$$l_j(v_j) := {\kappa_0}^{-1}(f|_{\Omega_j}, v_j)_{L^2(\Omega_j)^{m_0}} + (g, \gamma_{0,\Gamma}\, v_j)_{L^2(\Gamma)^{m_0}}. \tag{3.100}$$

This motivates the introduction of the (broken) version $\mathbb{l}$ of the above linear form l, defined on the (larger) broken solution space $\mathbb{U}_\Gamma(\mathrm{D};\mathcal{P}_\Omega)$:

$$\mathbb{l}(v) := \sum_{j=1}^{J} l_j(v|_{\Omega_j}), \qquad \forall v \in \mathbb{U}_\Gamma(\mathrm{D};\mathcal{P}_\Omega). \tag{3.101}$$

3.2 Abstract domain decomposition method

3.2.1 Free junction assumptions

Some results in the first part (Part I) of this manuscript require the following assumptions on the geometric partition. Unless stated otherwise, from this point onwards in Part I we suppose that these assumptions hold. We shall however point out precisely where these assumptions are necessary. In fact, we shall provide a generalization of the theory in Part III of this manuscript.

Assumption 3.11 (**Absence of interior junction points**). *We suppose that*

$$\Gamma_j \cap \Gamma_k \cap \Gamma_l = \emptyset, \qquad \forall (j,k,l) \in \{1,\dots,J\}^3, \quad j \neq k,\ k \neq l,\ l \neq j. \tag{3.102}$$

This assumption can be further extended as follows:

Assumption 3.12 (**Absence of boundary junction points**). *We suppose that*

$$\Gamma_j \cap \Gamma_k \cap \Gamma = \emptyset, \qquad \forall (j,k) \in \{1,\dots,J\}^2, \quad j \neq k. \tag{3.103}$$

An important implication of these assumptions is that all the interfaces Γ_{jk} are closed manifolds of $\mathbb{R}^d$. The definitions of functional spaces and operators of the previous section for a general domain Ω extend naturally to the local sub-domains Ω_j, for $j = 1,\dots,J$. In particular, under Assumptions 3.11 and 3.12 there will be no definition issues for the trace operators and the trace spaces. As a result, in each sub-domain we have the following first Green identity for all $u_j \in \mathrm{U}_\Gamma(\mathrm{D},\mathrm{L}_{\mathsf{a}};\Omega_j)$ and $v_j \in \mathrm{U}_\Gamma(\mathrm{D};\Omega_j)$,

$$\begin{aligned}(\mathrm{L}_{\mathsf{a}} u_j, v_j)_{L^2(\Omega_j)^{m_0}} - (\mathsf{a}\,\mathrm{D}u_j, \mathrm{D}v_j)_{L^2(\Omega_j)^{m_1}} \\ = -\kappa_0 \langle \gamma_{1,\Gamma}\, u_j, \gamma_{0,\Gamma}\, v_j\rangle_\Gamma - \kappa_0 \sum_{k\in\mathbb{K}_j} \langle \gamma_{1,\Gamma_{jk}}\, u_j, \gamma_{0,\Gamma_{jk}}\, v_j\rangle_{\Gamma_{jk}}.\end{aligned} \tag{3.104}$$

It follows from Assumption 3.12 that we can choose the numbering of the sub-domains so that there is exactly one sub-domain, by convention with number $j = 1$, for which part of its boundary is Γ, the physical boundary of Ω. For the sake of simplicity, we always mention in the following the boundary condition $(\gamma_{1,\Gamma} - \mathrm{i}\gamma_{0,\Gamma})u|_{\Omega_j} = 0$ on Γ for all $j \in \{1,\dots,J\}$, but it is obvious that when $j > 1$, this condition is meaningless and should be discarded. For the same reason, it should be noted that $\mathrm{U}_\Gamma(\mathrm{D};\Omega_j) \equiv \mathrm{U}(\mathrm{D};\Omega_j)$ for $j > 1$ and the first term on the right-hand-side in (3.104) is actually present only if $j = 1$.

3.2.2 A first equivalent transmission problem

We then specify which (physical) transmissions conditions these solutions shall satisfy (in addition to the PDE) to be solution of the original (undecomposed) problem.

3.2.2.1 Transmission conditions

The following lemma makes clear the difference between the U (regular) and the $\mathbb{U}$ (broken) versions of the solution spaces.

Lemma 3.13. *An element u in $\mathbb{U}(\mathrm{D};\mathcal{P}_\Omega)$ is an element of $\mathrm{U}(\mathrm{D};\Omega)$ if, and only if,*

$$\gamma_{\mathrm{D},\Gamma_{jk}}\left(u|_{\Omega_j}\right) = \gamma_{\mathrm{D},\Gamma_{kj}}\left(u|_{\Omega_k}\right), \qquad \forall (j,k) \in \mathbb{J}. \tag{3.105}$$

An element u in $\mathbb{U}(\mathrm{D}^*;\mathcal{P}_\Omega)$ is an element of $\mathrm{U}(\mathrm{D}^*;\Omega)$ if, and only if,

$$\gamma_{\mathrm{D}^*,\Gamma_{jk}}\left(u|_{\Omega_j}\right) = -\gamma_{\mathrm{D}^*,\Gamma_{kj}}\left(u|_{\Omega_k}\right), \qquad \forall (j,k) \in \mathbb{J}. \tag{3.106}$$

Proof. Let $\mathfrak{u} \in \mathbb{U}(\mathrm{D};\mathcal{P}_\Omega)$ and a test function $\phi \in \mathcal{D}(\Omega)^{m_0}$, the quantity $\mathrm{D}u$ is defined in a distributional sense as

$$\langle \mathrm{D}u, \phi\rangle_\Omega = \langle u, \mathrm{D}^*\phi\rangle_\Omega, \tag{3.107}$$

where $\langle\cdot,\cdot\rangle_\Omega$ denotes the usual duality pairing between a distribution and a test function. Now, we can split the right hand side into local contributions and using integration by parts (3.39), in each of the sub-domains we get

$$\begin{aligned}
\langle \mathrm{D}u, \phi\rangle_\Omega &= \sum_{j=1}^{J}\Big(\langle \mathrm{D}u_j, \phi_j\rangle_{\Omega_j} - \langle \gamma_{\mathrm{D}^*,\Gamma}\,\phi_j, \gamma_{\mathrm{D},\Gamma}\,u_j\rangle_{\Gamma\cap\Gamma_j} - \sum_{k\in\mathbb{K}_j}\langle \gamma_{\mathrm{D}^*,\Gamma_{jk}}\,\phi_j, \gamma_{\mathrm{D},\Gamma_{jk}}\,u_j\rangle_{\Gamma_{jk}}\Big),\\
&= \sum_{j=1}^{J}\Big(\langle \mathrm{D}u_j, \phi_j\rangle_{\Omega_j} - \sum_{k\in\mathbb{K}_j}\langle \gamma_{\mathrm{D}^*,\Gamma_{jk}}\,\phi_j, \gamma_{\mathrm{D},\Gamma_{jk}}\,u_j\rangle_{\Gamma_{jk}}\Big),
\end{aligned} \tag{3.108}$$

where we used as a short hand $u_j := u|_{\Omega_j}$, $\phi_j := \phi|_{\Omega_j}$ and the (exterior) boundary term vanish because of the compact support of ϕ. By definition of the trace operators (3.29) (see also Assumption 3.2) and the regularity of the test function ϕ, we have $\gamma_{\mathrm{D}^*,\Gamma_{jk}}\,\phi_j = -\gamma_{\mathrm{D}^*,\Gamma_{kj}}\,\phi_k$. We deduce that

$$\langle \mathrm{D}u, \phi\rangle_\Omega = \Big(\sum_{j=1}^{J}\langle \mathrm{D}u_j, \phi_j\rangle_{\Omega_j}\Big) - \Big(\sum_{\substack{(j,k)\in\mathbb{J}\\ j<k}}\langle \gamma_{\mathrm{D}^*,\Gamma_{jk}}\,\phi_j, \gamma_{\mathrm{D},\Gamma_{jk}}\,u_j - \gamma_{\mathrm{D},\Gamma_{kj}}\,u_k\rangle_{\Gamma_{jk}}\Big), \tag{3.109}$$

hence, u in $\mathbb{U}(\mathrm{D};\mathcal{P}_\Omega)$ is an element of $\mathrm{U}(\mathrm{D};\Omega)$ if, and only if, for all $(j,k)\in\mathbb{J}$,

$$\langle \gamma_{\mathrm{D}^*,\Gamma_{jk}}\,\phi_j, \gamma_{\mathrm{D},\Gamma_{jk}}\,u_j - \gamma_{\mathrm{D},\Gamma_{kj}}\,u_k\rangle_{\Gamma_{jk}} = 0. \tag{3.110}$$

From Assumption 3.1, $\mathcal{D}(\overline{\Omega})^{m_0}$ is dense in $\mathrm{U}(\mathrm{D}^*;\Omega)$. It follows that for each interface Γ_{jk}, the image of $\mathcal{D}(\overline{\Omega})^{m_0}$ by the (continuous) trace operator $\gamma_{\mathrm{D}^*,\Gamma_{jk}}$ is dense into $\mathrm{X}_1(\Gamma_{jk})$ the image of $\mathrm{U}(\mathrm{D}^*;\Omega)$ by the (continuous) trace operator $\gamma_{\mathrm{D}^*,\Gamma_{jk}}$. As a result, we have

$$\gamma_{\mathrm{D},\Gamma_{jk}}\,u_j = \gamma_{\mathrm{D},\Gamma_{kj}}\,u_k, \qquad \text{in } \mathrm{X}_0(\Gamma_{jk}), \qquad \forall (j,k)\in\mathbb{J}. \tag{3.111}$$

The proof of the other result is similar and omitted for the sake of brevity, we just remark that for a test function ϕ we will have in this case $\gamma_{\mathrm{D},\Gamma_{jk}}\,\phi_j = \gamma_{\mathrm{D},\Gamma_{kj}}\,\phi_k$ (notice the sign change, hence the change of sign in the corresponding result). ■

From the previous lemma, and by definition of the physical trace operators (3.64), we have the following result.

Corollary 3.14. *An element u in $\mathbb{U}(\mathrm{D};\mathcal{P}_\Omega)$ (respectively in $\mathbb{U}_\Gamma(\mathrm{D};\mathcal{P}_\Omega)$) is an element of $\mathrm{U}(\mathrm{D};\Omega)$ (respectively in $\mathrm{U}_\Gamma(\mathrm{D};\Omega)$) if, and only if,*

$$\gamma_{0,\Gamma_{jk}}\left(u|_{\Omega_j}\right) = \gamma_{0,\Gamma_{kj}}\left(u|_{\Omega_k}\right), \qquad \forall (j,k) \in \mathbb{J}. \tag{3.112}$$

An element u in $\mathbb{U}(\mathrm{D},\mathrm{L_a};\mathcal{P}_\Omega)$ (respectively in $\mathbb{U}_\Gamma(\mathrm{D},\mathrm{L_a};\mathcal{P}_\Omega)$) is an element of $\mathrm{U}(\mathrm{D},\mathrm{L_a};\Omega)$ (respectively in $\mathrm{U}_\Gamma(\mathrm{D},\mathrm{L_a};\Omega)$) if, and only if,

$$\begin{cases} \gamma_{0,\Gamma_{jk}}\left(u|_{\Omega_j}\right) = \gamma_{0,\Gamma_{kj}}\left(u|_{\Omega_k}\right), \\ \gamma_{1,\Gamma_{jk}}\left(u|_{\Omega_j}\right) = -\gamma_{1,\Gamma_{kj}}\left(u|_{\Omega_k}\right), \end{cases} \qquad \forall (j,k) \in \mathbb{J}. \tag{3.113}$$

3.2.2.2 Equivalent transmission problem

The following proposition is an immediate consequence of Corollary 3.14.

Proposition 3.15. *The model problem* (3.79) *is equivalent to the following transmission problem:*

$$\begin{cases} \textit{Find } \mathfrak{u} \in \mathbb{U}_\Gamma(\mathrm{D};\mathcal{P}_\Omega) \textit{ such that}: \\ \forall j \in \{1,\dots,J\}, & \begin{cases} (\mathrm{L_a} - {\kappa_0}^2\mathsf{n})u|_{\Omega_j} = f|_{\Omega_j}, & \textit{in } \Omega_j, \\ (\gamma_{1,\Gamma} - \mathrm{i}\gamma_{0,\Gamma})u|_{\Omega_j} = g, & \textit{on } \Gamma \cap \Gamma_j, \end{cases} \\ \forall (j,k) \in \mathbb{J}, & \begin{cases} \gamma_{0,\Gamma_{jk}}\left(u|_{\Omega_j}\right) = \gamma_{0,\Gamma_{kj}}\left(u|_{\Omega_k}\right), \\ \gamma_{1,\Gamma_{jk}}\left(u|_{\Omega_j}\right) = -\gamma_{1,\Gamma_{kj}}\left(u|_{\Omega_k}\right), \end{cases} & \textit{on } \Gamma_{jk}. \end{cases} \tag{3.114}$$

Proof. ($\Rightarrow$) Let u be a solution of the model problem (3.79):

$$\begin{cases} \text{Find } u \in \mathrm{U}_\Gamma(\mathrm{D};\Omega) \text{ such that} & \\ (\mathrm{L_a} - {\kappa_0}^2\mathsf{n})u = f, & \text{in } \Omega, \\ (\gamma_{1,\Gamma} - \mathrm{i}\gamma_{0,\Gamma})u = g, & \text{on } \Gamma. \end{cases} \tag{3.115}$$

Since u satisfies the PDE in Ω in a distributional sense, by testing for each $j \in \{1,\dots,J\}$ with a test function in $C_0^\infty(\Omega_j)$ (extended by zero outside Ω_j), the restriction $u|_{\Omega_j}$, which ought to be in $\mathrm{U}_\Gamma(\mathrm{D};\Omega j)$, satisfies the PDE in each sub-domain Ω_j. The physical boundary condition on Γ is not affected by the decomposition since we exclude the case of boundary junction points (Assumption 3.12). We get

$$\begin{cases} (\mathrm{L_a} - {\kappa_0}^2\mathsf{n})u|_{\Omega_j} = f|_{\Omega_j}, & \text{in } \Omega_j,\ \forall j \in \{0,\dots,J\}, \\ (\gamma_{1,\Gamma} - \mathrm{i}\gamma_{0,\Gamma})u = g, & \text{on } \Gamma. \end{cases} \tag{3.116}$$

Besides u is explicitly sought as an element of $\mathrm{U}_\Gamma(\mathrm{D};\Omega)$ so that according to Corollary 3.14 the trace γ_0 should match across each interface. Since in addition u satisfy the PDE in the whole of Ω and by Assumption 3.10 necessarily $u \in \mathrm{U}_\Gamma(\mathrm{D},\mathrm{L_a};\Omega)$ and Corollary 3.14 then yields the continuity of both traces γ_0 and γ_1. Finally, u is solution of (3.114).

($\Leftarrow$) Conversely, suppose that u is a solution of (3.114). From the continuity of the traces γ_0 and γ_1, Corollary 3.14 yields that $u \in \mathrm{U}_\Gamma(\mathrm{D},\mathrm{L_a};\Omega)$. It follows that $(\mathrm{L_a} - {\kappa_0}^2\mathsf{n})u$ makes sense in

$L^2(\Omega)^{m_0}$ and we can write for any test function $\phi \in C_0^\infty(\Omega)$

$$\begin{aligned}((\mathrm{L_a} - {\kappa_0}^2\mathsf{n})u, \phi)_{L^2(\Omega)^{m_0}} &= \sum_{j=1}^{J} ((\mathrm{L_a} - {\kappa_0}^2\mathsf{n})u|_{\Omega_j}, \phi|_{\Omega_j})_{L^2(\Omega_j)^{m_0}}, \\ &= \sum_{j=1}^{J} (f|_{\Omega_j}, \phi|_{\Omega_j})_{L^2(\Omega_j)^{m_0}} = (f, \phi)_{L^2(\Omega)^{m_0}},\end{aligned} \tag{3.117}$$

where we could write the last equality thanks to Assumption 3.10. Finally, using the same argument for the physical boundary condition on Γ, u is solution of the model problem (3.79). ■

Example 1: Helmholtz. *In the acoustic setting, the equivalent transmission problem is written*

$$\begin{cases} \textit{Find } p \in L^2(\Omega) \textit{ such that}: & \\ \forall j \in \{1, \dots, J\}, & \begin{cases} p_j := p|_{\Omega_j} \in H^1(\Omega_j), & \\ \left(-\operatorname{div} \rho_r^{-1} \mathbf{grad} - {\kappa_0}^2 \lambda_r^{-1}\right) p_j = f|_{\Omega_j}, & \textit{in } \Omega_j, \\ \left(\rho_r^{-1}\, \partial_\nu - \mathrm{i}\kappa_0\right) p_j = \kappa_0 g|_{\Gamma_j}, & \textit{on } \Gamma \cap \Gamma_j. \end{cases} \\ \forall (j,k) \in \mathbb{J}, & \begin{cases} p_j|_{\Gamma_{jk}} = p_k|_{\Gamma_{kj}}, & \\ \rho_r^{-1}\, \partial_{\nu_{jk}} p_j = -\rho_r^{-1}\, \partial_{\nu_{kj}} p_k. & \textit{on } \Gamma_{jk}. \end{cases} \end{cases} \tag{3.118}$$

In the system above we introduced ν_{jk} the unit normal vector on the interface Γ_{jk}, for any $(j,k) \in \mathbb{J}$, and defined to be outward to the domain Ω_j, so that by definition $\nu_{jk} = -\nu_{kj}$.

Example 2: Maxwell. *In the electromagnetic setting, the equivalent transmission problem is written*

$$\begin{cases} \textit{Find } \mathbf{E} \in \mathbf{L}^2(\Omega) \textit{ such that}: & \\ \forall j \in \{1, \dots, J\}, & \begin{cases} \mathbf{E}_j := \mathbf{E}|_{\Omega_j} \in \mathbf{H}_\Gamma(\mathbf{curl}; \Omega_j), & \\ \left(\mathbf{curl}\, \mu_r^{-1}\, \mathbf{curl} - {\kappa_0}^2 \epsilon_r\right) \mathbf{E}_j = f|_{\Omega_j}, & \textit{in } \Omega_j, \\ \mu_r^{-1}\, \mathbf{curl}\, \mathbf{E}_j \times \nu - \mathrm{i}\kappa_0\, \nu \times (\mathbf{E}_j \times \nu) = \kappa_0 g|_{\Gamma_j}, & \textit{on } \Gamma \cap \Gamma_j. \end{cases} \\ \forall (j,k) \in \mathbb{J}, & \begin{cases} \nu_{jk} \times (\mathbf{E}_j \times \nu_{jk}) = \nu_{kj} \times (\mathbf{E}_k \times \nu_{kj}), & \\ \mu_r^{-1}\, \mathbf{curl}\, \mathbf{E}_j \times \nu_{jk} = -\mu_r^{-1}\, \mathbf{curl}\, \mathbf{E}_k \times \nu_{kj}. & \textit{on } \Gamma_{jk}. \end{cases} \end{cases} \tag{3.119}$$

3.2.3 Multi-trace formalism

We introduce now a set of definitions to provide a characterization of the solution of the original problem entirely through its trace. The framework described below is inspired by the work of Xavier Claeys [29] and the so-called Multi-Trace Formalism (MTF). This formalism (which — we concede — might be disconcerting, especially in this very abstract setting) allows for very concise formulations. Besides, it is very rewarding as it will turn out to be a fertile ground to relax the somewhat penalizing no cross-point assumption (see Chapter 9). We present this framework in this simplified free junction setting to be able to draw a parallel between the classical approach described in this section and the more general method described later. We refer the reader to [42, 44, 78, 91] for a more standard approach of the same DD method in the acoustic setting. Note that there already exists some literature making connections between the MTF and domain decomposition methods [7, 35, 31, 39, 55]. The MTF comes in two main flavors, the *local* [83,

84] and the *non-local* versions [32, 38]. In this chapter we will rely on the former version while we will exploit the latter version in Part III of this manuscript.

With this aim, we introduce the *multi-trace space* $\mathbb{M}_{\shortparallel}$ whose elements are collections of couples of zeroth and first order traces at each interface, and from both sides of it. We then introduce two important subspaces of $\mathbb{M}_{\shortparallel}$. The first one is the so-called *Cauchy trace space* $\mathbb{C}_{\shortparallel}$, which is the space of couples of zeroth and first order traces that are compatible in the sense that they represent a (broken) function satisfying the homogeneous physical equation locally in each sub-domain. The second subspace is the so-called *single-trace space* $\mathbb{S}_{\shortparallel}$, whose elements match in some sense at an interface (expressing the transmission conditions between sub-domains), hence imposing the global regularity required by the solution of the original problem. Roughly speaking (up to a contribution of the source of the problem) the trace of the solution belongs to the intersection between the two subspaces.

A remark on our notations We shall use when necessary the symbol $\shortparallel$ as an index to denote a space or an operator whose definition relies on the free junction assumption. In contrast in Part III, we shall replace it with the symbol $\times$ to indicate a definition that is valid even in presence of junctions.

3.2.3.1 Multi-trace spaces

We introduce global trace spaces whose elements are collection of traces on all interfaces (from both sides) between two sub-domains.

Definition 3.16 (**Multi-trace spaces**). *The global multi-trace spaces are defined as*

$$\begin{aligned}
\mathbb{M}_{0,\shortparallel}\left(\tilde{\Sigma}\right) &:= \bigtimes_{(j,k)\in\mathbb{J}} \mathrm{X}_0(\Gamma_{jk}),\\
\mathbb{M}_{1,\shortparallel}\left(\tilde{\Sigma}\right) &:= \bigtimes_{(j,k)\in\mathbb{J}} \mathrm{X}_1(\Gamma_{jk}),\\
\mathbb{M}_{1/2,\shortparallel}\left(\tilde{\Sigma}\right) &:= \bigtimes_{(j,k)\in\mathbb{J}} \mathrm{X}_{1/2}(\Gamma_{jk}),\\
\mathbb{M}_{\shortparallel}\left(\tilde{\Sigma}\right) &:= \bigtimes_{(j,k)\in\mathbb{J}} \mathrm{X}(\Gamma_{jk}) \equiv \mathbb{M}_{0,\shortparallel}\left(\tilde{\Sigma}\right) \times \mathbb{M}_{1,\shortparallel}\left(\tilde{\Sigma}\right).
\end{aligned} \tag{3.120}$$

Note that because Assumption 3.11 and Assumption 3.12 hold, each manifold Γ_{jk} is necessarily closed.

The multi-trace space $\mathbb{M}_{0,\shortparallel}\left(\tilde{\Sigma}\right)$ (respectively, $\mathbb{M}_{1,\shortparallel}\left(\tilde{\Sigma}\right)$) is composed of collections of traces of order 0 (respectively, 1) on each interface and from both sides of it. The term *multi-trace* refers to the fact that at a single interface between two distinct sub-domains, two (interior) traces from each of the two sub-domains appear in such collections. Indeed, for each interface Γ_{jk} with $(j,k) \in \mathbb{J}$ (hence not empty), there also exists Γ_{kj} which actually refers to the same manifold. Therefore, the two traces from the sub-domains Ω_j and Ω_k are present in the collections. Importantly, these two traces need *not* be compatible, in the sense that they are not necessarily traces of solutions that are globally regular across the said interface.

The multi-trace space $\mathbb{M}_{1/2,\shortparallel}\left(\tilde{\Sigma}\right)$ will acts as a pivot space between $\mathbb{M}_{0,\shortparallel}\left(\tilde{\Sigma}\right)$ and $\mathbb{M}_{1,\shortparallel}\left(\tilde{\Sigma}\right)$ for the duality induced by $\langle\!\langle \cdot,\cdot \rangle\!\rangle_{\shortparallel}$ (see (3.127)).

The multi-trace space $\mathbb{M}_{\shortparallel}\left(\tilde{\Sigma}\right)$ is defined as the collections of couples of traces of order 0 and 1 on each interface. Note that this space could also be defined as the Cartesian product of the two previous multi-trace spaces, which differs only by a reordering of the components. We shall make

the natural identification between the two definitions and use them interchangeably depending on the context.

For the sake of simplicity, we omit the dependence to the skeleton domain and simply write $\mathbb{M}_{\|} := \mathbb{M}_{\|}\left(\tilde{\Sigma}\right)$ and so on, unless it is not clear from the context.

We provide below the particularization of the above abstract definition to our main target applications.

Example 1: Helmholtz. *In the acoustic setting, the multi-trace spaces are*

$$\begin{aligned}
\mathbb{M}_{0,\|}\left(\tilde{\Sigma}\right) &\equiv \bigtimes_{(j,k)\in\mathbb{J}} H^{1/2}(\Gamma_{jk}),\\
\mathbb{M}_{1,\|}\left(\tilde{\Sigma}\right) &\equiv \bigtimes_{(j,k)\in\mathbb{J}} H^{-1/2}(\Gamma_{jk}),\\
\mathbb{M}_{1/2,\|}\left(\tilde{\Sigma}\right) &\equiv \bigtimes_{(j,k)\in\mathbb{J}} L^2(\Gamma_{jk}).
\end{aligned} \tag{3.121}$$

Example 2: Maxwell. *In the electromagnetic setting, the multi-trace spaces are*

$$\begin{aligned}
\mathbb{M}_{0,\|}\left(\tilde{\Sigma}\right) &\equiv \bigtimes_{(j,k)\in\mathbb{J}} \mathbf{H}^{-1/2}(\mathrm{curl};\Gamma_{jk}),\\
\mathbb{M}_{1,\|}\left(\tilde{\Sigma}\right) &\equiv \bigtimes_{(j,k)\in\mathbb{J}} \mathbf{H}^{-1/2}(\mathrm{div};\Gamma_{jk}),\\
\mathbb{M}_{1/2,\|}\left(\tilde{\Sigma}\right) &\equiv \bigtimes_{(j,k)\in\mathbb{J}} \mathbf{L}^2_t(\Gamma_{jk}).
\end{aligned} \tag{3.122}$$

Trace operators By construction, the following global trace operators are continuous mappings from the broken solution spaces into the multi-trace spaces

$$\begin{aligned}
\boldsymbol{\gamma}_{0,\|} &: \mathbb{U}(\mathrm{D};\mathcal{P}_\Omega) \to \mathbb{M}_{0,\|},\\
&\quad u \mapsto \left(\gamma_{0,\Gamma_{jk}}\, u|_{\Omega_j}\right)_{(j,k)\in\mathbb{J}},\\
\boldsymbol{\gamma}_{1,\|} &: \mathbb{U}(\mathrm{D},\mathrm{L}_{\mathsf{a}};\mathcal{P}_\Omega) \to \mathbb{M}_{1,\|},\\
&\quad u \mapsto \left(\gamma_{1,\Gamma_{jk}}\, u|_{\Omega_j}\right)_{(j,k)\in\mathbb{J}},\\
\boldsymbol{\gamma}_{\|} &: \mathbb{U}(\mathrm{D},\mathrm{L}_{\mathsf{a}};\mathcal{P}_\Omega) \to \mathbb{M}_{\|},\\
&\quad u \mapsto \left(\gamma_{\Gamma_{jk}}\, u|_{\Omega_j}\right)_{(j,k)\in\mathbb{J}}.
\end{aligned} \tag{3.123}$$

In addition, from Assumption 3.2, the mappings $\boldsymbol{\gamma}_{0,\|}$ and $\boldsymbol{\gamma}_{1,\|}$ are surjective. It is clear that, up to a re-ordering of the elements, we can make the identification $\boldsymbol{\gamma}_{\|} \equiv (\boldsymbol{\gamma}_{0,\|}, \boldsymbol{\gamma}_{1,\|})$.

Remark 3.17. *Without Assumptions 3.11 and 3.12 the range of these trace operators could not necessarily be these trace spaces (but rather larger spaces).*

Norms and duality pairings In the definitions below, and systematically in the remainder of this document, we shall use the following notations for elements of the multi-trace spaces

$$\begin{aligned}
&\mathbb{x}_0 = \left(\mathrm{x}_0^{jk}\right)_{(j,k)\in\mathbb{J}}, && \mathbb{y}_0 = \left(\mathrm{y}_0^{jk}\right)_{(j,k)\in\mathbb{J}} && \in \mathbb{M}_{0,\|},\\
&\mathbb{x}_1 = \left(\mathrm{x}_1^{jk}\right)_{(j,k)\in\mathbb{J}}, && \mathbb{y}_1 = \left(\mathrm{y}_1^{jk}\right)_{(j,k)\in\mathbb{J}} && \in \mathbb{M}_{1,\|},\\
&\mathbb{x}_{1/2} = \left(\mathrm{x}_{1/2}^{jk}\right)_{(j,k)\in\mathbb{J}}, && \mathbb{y}_{1/2} = \left(\mathrm{y}_{1/2}^{jk}\right)_{(j,k)\in\mathbb{J}} && \in \mathbb{M}_{1/2,\|},\\
&\mathbb{x} = \left(\mathrm{x}^{jk}\right)_{(j,k)\in\mathbb{J}} \equiv (\mathbb{x}_0, \mathbb{x}_1), && \mathbb{y} = \left(\mathrm{y}^{jk}\right)_{(j,k)\in\mathbb{J}} \equiv (\mathbb{y}_0, \mathbb{y}_1) && \in \mathbb{M}_{\|}.
\end{aligned} \tag{3.124}$$

The multi-trace spaces can be endowed with the norms stemming from their Cartesian product structure. Recalling the definitions of the norms on a single domain given in (3.31), (3.33) and (3.50), we set, for each $\sigma \in \{0, 1/2, 1\}$,

$$\|\mathbb{x}_\sigma\|^2_{\mathbb{M}_{\sigma,\|}} := \sum_{(j,k)\in\mathbb{J}} \|\mathrm{x}_\sigma^{jk}\|^2_{\mathrm{X}_\sigma(\Gamma_{jk,h})}. \tag{3.125}$$

Besides, we introduce the natural norm on $\mathbb{M}_\|$ as follows

$$\|\mathbb{x}\|^2_{\mathbb{M}_\|} := \|\mathbb{x}_0\|^2_{\mathbb{M}_{0,\|}} + \|\mathbb{x}_1\|^2_{\mathbb{M}_{1,\|}}, \qquad \forall \mathbb{x} \equiv (\mathbb{x}_0, \mathbb{x}_1) \in \mathbb{M}_\|. \tag{3.126}$$

Recalling the local duality pairing $\langle\cdot,\cdot\rangle_{\partial\mathcal{O}}$ between the two dual trace spaces (3.28) on a single boundary $\partial\mathcal{O}$, we introduce the duality pairing between multi-trace spaces (which does not involve any complex conjugation operation)

$$\begin{aligned} \langle\!\langle \cdot,\cdot \rangle\!\rangle_\| \; &: \mathbb{M}_{1,\|} \times \mathbb{M}_{0,\|} \to \mathbb{C}, \\ &(\mathbb{x}_1,\, \mathbb{x}_0) \mapsto \sum_{(j,k)\in\mathbb{J}} \langle \mathrm{x}_1^{jk}, \mathrm{x}_0^{jk} \rangle_{\Gamma_{jk}}. \end{aligned} \tag{3.127}$$

Recalling our definition (3.49) of the inner product $(\cdot,\cdot)_{\partial\mathcal{O}}$ on the pivot trace space $\mathrm{X}_{1/2}(\partial\mathcal{O})$ on a single boundary $\partial\mathcal{O}$, we also equip the (pivot) multi-trace space with its natural scalar product (and associated norm) which reads

$$\begin{aligned} (\!(\cdot,\cdot)\!)_\| \; &: \mathbb{M}_{1/2,\|} \times \mathbb{M}_{1/2,\|} \to \mathbb{C}, \\ &(\mathbb{x}_{1/2},\, \mathbb{x}_{1/2}) \mapsto \sum_{(j,k)\in\mathbb{J}} (\mathrm{x}_{1/2}^{jk}, \mathrm{y}_{1/2}^{jk})_{\mathrm{X}_{1/2}(\Gamma_{jk})}. \end{aligned} \tag{3.128}$$

Recalling the definition (3.73) of the bilinear form $[\cdot,\cdot]_{\partial\mathcal{O}}$ on $\mathrm{X}(\partial\mathcal{O})$ for a single boundary $\partial\mathcal{O}$, we finally define the skew symmetric bilinear form

$$\begin{aligned} [\![\cdot,\cdot]\!]_\| \; &: \mathbb{M}_\| \times \mathbb{M}_\| \to \mathbb{C}, \\ &(\mathbb{x},\, \mathbb{y}) \mapsto \sum_{(j,k)\in\mathbb{J}} [\mathrm{x}^{jk}, \mathrm{y}^{jk}]_{\Gamma_{jk}} = \langle\!\langle \mathbb{y}_1, \mathbb{x}_0 \rangle\!\rangle_\| - \langle\!\langle \mathbb{x}_1, \mathbb{y}_0 \rangle\!\rangle_\|. \end{aligned} \tag{3.129}$$

3.2.3.2 Cauchy-trace spaces

We define a first subset of the space of multi-trace spaces which is the space of traces of a function whose restriction in each sub-domain satisfies the *homogeneous* PDE and physical boundary conditions on Γ (see (3.130)). In particular, note that no boundary condition on the transmission interface is imposed in the following definition and that the two traces associated to the two sides of a single interface between two sub-domains need not satisfy a matching condition.

Definition 3.18 (**Cauchy-trace space**). *For each $j = 1, \ldots, J$, define the subspace of solutions of the homogeneous PDE in Ω_j as*

$$S(\Omega_j) := \left\{ u_j \in \mathrm{U}_\Gamma(\mathrm{D};\Omega_j) \text{ such that } \begin{cases} (\mathrm{L}_\mathsf{a} - \kappa_0{}^2\mathsf{n})u_j = 0, & \text{in } \Omega_j, \\ (\gamma_{1,\Gamma} - \mathrm{i}\gamma_{0,\Gamma})u_j = 0, & \text{on } \Gamma \cap \Gamma_j. \end{cases} \right\}. \tag{3.130}$$

For each $j = 1, \ldots, J$, the local space of Cauchy traces is defined as

$$\mathrm{C}_\|(\Gamma_j) := \left\{ \left(\mathrm{x}^{jk}\right)_{k\in\mathbb{K}_j} \in \bigtimes_{k\in\mathbb{K}_j} \mathrm{X}(\Gamma_{jk}) \;\middle|\; \exists u_j \in S(\Omega_j),\ \mathrm{x}^{jk} := \gamma_{\Gamma_{jk}} u_j,\ \forall k \in \mathbb{K}_j \right\}. \tag{3.131}$$

The global Cauchy trace space is defined as

$$\mathbb{C}_{\shortparallel}\left(\tilde{\Sigma}\right) := \bigtimes_{j=1}^{J} \mathrm{C}_{\shortparallel}\left(\Gamma_j\right), \tag{3.132}$$

which we identify as a subspace of $\mathbb{M}_{\shortparallel}$ *in a straightforward manner.*

Because elements of the Cauchy trace space $\mathbb{C}_{\shortparallel}$ are traces of local solutions $u|_{\Omega_j}$ that satisfy the original equation locally in each sub-domain Ω_j, it is natural that they satisfy some sort of energy conservation result, as stated in the following proposition. Since we are interested in harmonic wave propagation problems, the notion of energy balance is not properly defined. When we say that the energy decreases we mean that there is a dissipation phenomenon in the problem either by dissipation through the boundary or by absorption from the medium (coefficients a and n in the PDE with non vanishing imaginary parts). If neither of this two dissipation phenomenon are present (which is possible in a single sub-domain), we say that the energy is conserved. A similar result in a more general setting (in the whole space and with junctions) can be found in [29, Lem. 6.1].

Proposition 3.19 (**Energy balance interpretation**). *The energy decreases globally in* Ω*, which translates as*

$$\mathrm{i}\left[\!\left[\mathbb{x}, \overline{\mathbb{x}}\right]\!\right]_{\shortparallel} < 0, \qquad \forall \mathbb{x} \in \mathbb{C}_{\shortparallel}. \tag{3.133}$$

Proof. Let

$$\mathbb{x} = \left(\mathrm{x}^{jk}\right)_{(j,k)\in\mathbb{J}} \in \mathbb{C}_{\shortparallel}, \qquad \mathrm{x}^{jk} = (\mathrm{x}_0^{jk}, \mathrm{x}_1^{jk}), \quad \forall (j,k) \in \mathbb{J}. \tag{3.134}$$

For each $j \in \{1, \dots, J\}$, by definition of the local Cauchy trace space $\mathrm{C}_{\shortparallel}$ given in (3.131), there exists $u_j \in \mathrm{U}_{\Gamma}(\mathrm{D}; \Omega_j)$ such that

$$\begin{cases} \left(\mathrm{L}_{\mathsf{a}} - {\kappa_0}^2 \mathsf{n}\right) u_j = 0, & \text{in } \Omega_j, \\ (\gamma_{1,\Gamma} - \mathrm{i}\gamma_{0,\Gamma}) u_j = 0, & \text{on } \Gamma, \\ \gamma_{\Gamma_{jk}} u_j = \mathrm{x}^{jk}, & \text{on } \Gamma_{jk},\ \forall k \in \mathbb{K}_j. \end{cases} \tag{3.135}$$

We have, using Lemma 3.6 and the first Green identity (3.104)

$$\begin{aligned} \mathrm{i}\frac{1}{2}\sum_{k\in\mathbb{K}_j} [\mathrm{x}^{jk}, \overline{\mathrm{x}^{jk}}]_{\Gamma_{jk}} &= \Im \sum_{k\in\mathbb{K}_j} \langle \gamma_{1,\Gamma_{jk}} u_j, \gamma_{0,\Gamma_{jk}} \overline{u_j} \rangle_{\Gamma_{jk}}, \\ &= \Im \Big[-{\kappa_0}^{-1} (\mathrm{L}_{\mathsf{a}} u_j, \overline{u_j})_{L^2(\Omega_j)^{m_0}} + {\kappa_0}^{-1} (\mathsf{a}\, \mathrm{D}u_j, \mathrm{D}\overline{u_j})_{L^2(\Omega_j)^{m_1}} \\ &\qquad - \langle \gamma_{1,\Gamma} u_j, \gamma_{0,\Gamma} \overline{u_j} \rangle_{\Gamma} \Big]. \end{aligned} \tag{3.136}$$

From (3.135), we obtain

$$\begin{aligned} \mathrm{i}\frac{1}{2}\sum_{k\in\mathbb{K}_j} [\mathrm{x}^{jk}, \overline{\mathrm{x}^{jk}}]_{\Gamma_{jk}} = \Big[&-\kappa_0 (\Im(\mathsf{n}) u_j, \overline{u_j})_{L^2(\Omega_j)^{m_0}} + {\kappa_0}^{-1} (\Im(\mathsf{a})\, \mathrm{D}u_j, \mathrm{D}\overline{u_j})_{L^2(\Omega_j)^{m_1}} \\ &- \|\gamma_{0,\Gamma} u_j\|^2_{L^2(\Gamma)^{m_0}} \Big] \le 0, \end{aligned} \tag{3.137}$$

from the assumption (3.78). This proves that the energy is conserved or diminished locally in each sub-domain, the global result follows by summing over all sub-domains. ∎

In each sub-domain Ω_j, we are therefore in either of the following two situations

1. If the imaginary parts of the coefficients a and n in the PDE are identically zero and the boundary of the sub-domain Ω_j does not include part of the physical boundary Γ, we have

$$\mathrm{i}\frac{1}{2}\sum_{k\in\mathbb{K}_j}[\mathrm{x}^{jk},\overline{\mathrm{x}^{jk}}]_{\Gamma_{jk}}=0,\qquad\forall(\mathrm{x}^{jk})_{k\in\mathbb{K}_j}\in\mathrm{C}_{\shortparallel}\left(\Gamma_j\right),\tag{3.138}$$

   and we say that the energy is conserved in the sub-domain.

2. On the contrary, if the imaginary parts of the coefficients do not vanish everywhere in the sub-domain, or its boundary includes part of the physical boundary we have

$$\mathrm{i}\frac{1}{2}\sum_{k\in\mathbb{K}_j}[\mathrm{x}^{jk},\overline{\mathrm{x}^{jk}}]_{\Gamma_{jk}}<0,\qquad\forall(\mathrm{x}^{jk})_{k\in\mathbb{K}_j}\in\mathrm{C}_{\shortparallel}\left(\Gamma_j\right),\tag{3.139}$$

   and we say that the energy decreases in the sub-domain.

3.2.3.3 Single-trace spaces

It is clear that the transmission conditions that we shall impose on our local solutions should be equivalent to (3.112) and (3.113) (sometimes referred to as physical coupling conditions). This is the motivation to introduce a second subspace $\mathbb{S}_{\shortparallel}$ of the multi-trace space $\mathbb{M}_{\shortparallel}$, which is the space of traces that match across all interfaces, hence deserving to be named *single-trace*, in contrast to a general *multi-trace*.

Definition 3.20 (**Single-trace spaces**). *The global single-trace spaces are defined as*

$$\begin{aligned}
\mathbb{S}_{0,\shortparallel}\left(\tilde{\Sigma}\right)&:=\left\{\mathbb{x}_0=(\mathrm{x}_0^{jk})_{(j,k)\in\mathbb{J}}\in\mathbb{M}_{0,\shortparallel}\quad|\quad\mathrm{x}_0^{jk}=\mathrm{x}_0^{kj},\ \forall(j,k)\in\mathbb{J}\right\},\\
\mathbb{S}_{1,\shortparallel}\left(\tilde{\Sigma}\right)&:=\left\{\mathbb{x}_1=(\mathrm{x}_1^{jk})_{(j,k)\in\mathbb{J}}\in\mathbb{M}_{1,\shortparallel}\quad|\quad\mathrm{x}_1^{jk}=-\mathrm{x}_1^{kj},\ \forall(j,k)\in\mathbb{J}\right\},\\
\mathbb{S}_{\shortparallel}\left(\tilde{\Sigma}\right)&:=\mathbb{S}_{0,\shortparallel}\left(\tilde{\Sigma}\right)\times\mathbb{S}_{1,\shortparallel}\left(\tilde{\Sigma}\right).
\end{aligned}\tag{3.140}$$

It is enlightening to state a few properties of these single-traces spaces. To do so, let us define the following global trace operators (see in particular Assumption 3.2 for the definition of the local traces)

$$\begin{aligned}
\boldsymbol{\gamma}_{\mathrm{D},\shortparallel}\ &:\ \mathbb{U}(\mathrm{D};\mathcal{P}_\Omega)\to\mathbb{M}_{0,\shortparallel},\\
&\qquad u\mapsto\left(\gamma_{\mathrm{D},\tilde{\Gamma}_{jk}}\,u|_{\Omega_j}\right)_{(j,k)\in\mathbb{J}},\\
\boldsymbol{\gamma}_{\mathrm{D}^*,\shortparallel}\ &:\mathbb{U}(\mathrm{D}^*;\mathcal{P}_\Omega)\to\mathbb{M}_{1,\shortparallel},\\
&\qquad u\mapsto\left(\gamma_{\mathrm{D}^*,\tilde{\Gamma}_{jk}}\,u|_{\Omega_j}\right)_{(j,k)\in\mathbb{J}}.
\end{aligned}\tag{3.141}$$

Of course from (3.64), we have $\boldsymbol{\gamma}_{\mathrm{D},\shortparallel}=\boldsymbol{\gamma}_{0,\shortparallel}$. However, we introduced the operator $\boldsymbol{\gamma}_{\mathrm{D},\shortparallel}$ to respect the symmetry in our notations.

Elements of the single-trace spaces are traces of functions that have some "global regularity" property, in a Sobolev sense, as stated by the following proposition which is based on Lemma 3.13.

Proposition 3.21. *Under Assumptions 3.11 and 3.12, we have*

$$\begin{aligned}
\mathbb{S}_{0,\shortparallel}&=\boldsymbol{\gamma}_{\mathrm{D},\shortparallel}\,\mathrm{U}(\mathrm{D};\Omega)&&\Big(=\boldsymbol{\gamma}_{\mathrm{D},\shortparallel}\,\mathrm{U}_\Gamma(\mathrm{D};\Omega)\Big),\\
\mathbb{S}_{1,\shortparallel}&=\boldsymbol{\gamma}_{\mathrm{D}^*,\shortparallel}\,\mathrm{U}(\mathrm{D}^*;\Omega)&&\Big(=\boldsymbol{\gamma}_{\mathrm{D}^*,\shortparallel}\,\mathrm{U}_\Gamma(\mathrm{D}^*;\Omega)\Big).
\end{aligned}\tag{3.142}$$

Proof. The surjectivity properties of the global trace operators which follow from the one of the local trace operators stated in Assumption 3.2 provide us with the inclusions

$$\begin{aligned} &\mathbb{S}_{0,\|} \subset \boldsymbol{\gamma}_{\mathrm{D},\|}\,\mathrm{U}(\mathrm{D};\Omega), \\ &\mathbb{S}_{1,\|} \subset \boldsymbol{\gamma}_{\mathrm{D}^*,\|}\,\mathrm{U}(\mathrm{D}^*;\Omega). \end{aligned} \tag{3.143}$$

The regularity result from Lemma 3.13 provides us with the reverse inclusions

$$\begin{aligned} &\mathbb{S}_{0,\|} \supset \boldsymbol{\gamma}_{\mathrm{D},\|}\,\mathrm{U}(\mathrm{D};\Omega), \\ &\mathbb{S}_{1,\|} \supset \boldsymbol{\gamma}_{\mathrm{D}^*,\|}\,\mathrm{U}(\mathrm{D}^*;\Omega). \end{aligned} \tag{3.144}$$

The substitution from $\mathrm{U}(\mathrm{D};\Omega)$ to $\mathrm{U}_\Gamma(\mathrm{D};\Omega)$ and $\mathrm{U}(\mathrm{D}^*;\Omega)$ to $\mathrm{U}_\Gamma(\mathrm{D}^*;\Omega)$ is ■

We deduce the following corollary, which in some sense is a rewriting of Lemma 3.13. It is a characterization of the difference between the U (regular) and the $\mathbb{U}$ (broken) versions of the solution spaces using the single-trace spaces.

Corollary 3.22. *We have*

$$\begin{array}{lllll} \text{(i)} & \forall u \in \mathbb{U}_\Gamma(\mathrm{D};\mathcal{P}_\Omega), & \boldsymbol{\gamma}_{\mathrm{D},\|}u = \boldsymbol{\gamma}_{0,\|}u \in \mathbb{S}_{0,\|} & \Leftrightarrow & u \in \mathrm{U}_\Gamma(\mathrm{D};\Omega), \\ \text{(ii)} & \forall u \in \mathbb{U}_\Gamma(\mathrm{D}^*;\mathcal{P}_\Omega), & \boldsymbol{\gamma}_{\mathrm{D}^*,\|}u \in \mathbb{S}_{1,\|} & \Leftrightarrow & u \in \mathrm{U}_\Gamma(\mathrm{D}^*;\Omega), \\ \text{(iii)} & \forall u \in \mathbb{U}_\Gamma(\mathrm{D},\mathrm{L}_{\mathsf{a}};\mathcal{P}_\Omega), & \boldsymbol{\gamma}_{\|}u \in \mathbb{S}_{\|} & \Leftrightarrow & u \in \mathrm{U}_\Gamma(\mathrm{D},\mathrm{L}_{\mathsf{a}};\Omega). \end{array} \tag{3.145}$$

Proof. It is clear that one implication ($\Leftarrow$) stems from Proposition 3.21. We need only to prove the reverse implication ($\Rightarrow$).

(i) Let $u \in \mathbb{U}_\Gamma(\mathrm{D};\mathcal{P}_\Omega)$ such that $\boldsymbol{\gamma}_{0,\|}u \in \mathbb{S}_{0,\|}$. By Proposition 3.21 of $\mathbb{S}_{0,\|}$, there exists $v \in \mathrm{U}_\Gamma(\mathrm{D};\Omega)$ such that $\boldsymbol{\gamma}_{0,\|}(v-u) = 0$. It follows that $w := v - u \in \operatorname{Ker}\boldsymbol{\gamma}_{0,\|} = \operatorname{Ker}\boldsymbol{\gamma}_{\mathrm{D},\|}$ and by Lemma 3.13 we get $w \in \mathrm{U}_\Gamma(\mathrm{D};\Omega)$ so that finally $u = v + w$ does belong to $\mathrm{U}_\Gamma(\mathrm{D};\Omega)$.

(ii) Let $u \in \mathbb{U}_\Gamma(\mathrm{D}^*;\mathcal{P}_\Omega)$ such that $\boldsymbol{\gamma}_{1,\|}u \in \mathbb{S}_{1,\|}$. By Proposition 3.21 of $\mathbb{S}_{1,\|}$, there exists $v \in \mathrm{U}_\Gamma(\mathrm{D}^*;\Omega)$ such that $\boldsymbol{\gamma}_{1,\|}(v-u) = 0$. It follows that $w := v - u \in \operatorname{Ker}\boldsymbol{\gamma}_{1,\|} = \operatorname{Ker}\boldsymbol{\gamma}_{\mathrm{D}^*,\|}$ and by Lemma 3.13 we get $w \in \mathrm{U}_\Gamma(\mathrm{D}^*;\Omega)$ so that finally $u = v + w$ does belong to $\mathrm{U}_\Gamma(\mathrm{D}^*;\Omega)$.

(iii) Let $u \in \mathbb{U}_\Gamma(\mathrm{D},\mathrm{L}_{\mathsf{a}};\mathcal{P}_\Omega)$ such that $\boldsymbol{\gamma}_{\|}u \in \mathbb{S}_{\|}$, which rewrites from Definition 3.20 as $\boldsymbol{\gamma}_{0,\|}u \in \mathbb{S}_{0,\|}$ and $\boldsymbol{\gamma}_{1,\|}u \in \mathbb{S}_{1,\|}$. We just proved in (i) that from $\boldsymbol{\gamma}_{0,\|}u \in \mathbb{S}_{0,\|}$ we have $u \in \mathrm{U}_\Gamma(\mathrm{D};\Omega)$. If we let $v \in L^2(\Omega)^{m_1}$ such that for each $j \in \{1,\dots,J\}$, $v|_{\Omega_j} = \mathsf{a}\mathrm{D}u|_{\Omega_j}$, we have $\boldsymbol{\gamma}_{1,\|}v \in \mathbb{S}_{1,\|}$ and we just proved in (ii) that then $v \in \mathrm{U}_\Gamma(\mathrm{D}^*;\Omega)$. Hence we get $\mathsf{a}\mathrm{D}u \in \mathrm{U}_\Gamma(\mathrm{D}^*;\Omega)$ and we have $u \in \mathrm{U}_\Gamma(\mathrm{D},\mathrm{L}_{\mathsf{a}};\Omega)$. ■

The following proposition states that the single trace spaces are orthogonal in some sense. It provides as a result a characterization of these spaces, which will prove useful when we consider the discretization of the method. Besides, such a result is an easy particular case of more general results, for instance in [28, Prop. 2.1], [36, Prop. 2.1] and [29, Prop. 4.1] for the acoustic setting and in [37, Prop. 3.1] for the electromagnetic setting. In fact, as we shall see, a result of this type is the corner stone of the theory that allows the presence of junction points.

Proposition 3.23. *The single trace spaces are such that*

$$\begin{array}{lllll} \forall \mathbb{x}_0 \in \mathbb{M}_{0,\|}, & \Big(\mathbb{x}_0 \in \mathbb{S}_{0,\|} & \Leftrightarrow & \langle\!\langle \mathbb{y}_1, \mathbb{x}_0 \rangle\!\rangle_{\|} = 0, & \forall \mathbb{y}_1 \in \mathbb{S}_{1,\|}\Big), \\ \forall \mathbb{x}_1 \in \mathbb{M}_{1,\|}, & \Big(\mathbb{x}_1 \in \mathbb{S}_{1,\|} & \Leftrightarrow & \langle\!\langle \mathbb{x}_1, \mathbb{y}_0 \rangle\!\rangle_{\|} = 0, & \forall \mathbb{y}_0 \in \mathbb{S}_{0,\|}\Big), \\ \forall \mathbb{x} \in \mathbb{M}_{\|}, & \Big(\mathbb{x} \in \mathbb{S}_{\|} & \Leftrightarrow & [\![\mathbb{x}, \mathbb{y}]\!]_{\|} = 0, & \forall \mathbb{y} \in \mathbb{S}_{\|}\Big). \end{array} \tag{3.146}$$

Proof. Let $\mathrm{x}_0 \equiv (\mathrm{x}_0^{jk})_{(j,k)\in\mathbb{J}} \in \mathbb{M}_{0,\|}$ and $\mathrm{x}_1 \equiv (\mathrm{x}_1^{jk})_{(j,k)\in\mathbb{J}} \in \mathbb{M}_{1,\|}$, we first establish the identity

$$\left\langle\!\left\langle \mathbb{x}_1, \mathbb{x}_0 \right\rangle\!\right\rangle_{\|} = \sum_{(j,k)\in\mathbb{J}} \langle \mathrm{x}_1^{jk}, \mathrm{x}_0^{jk} \rangle_{\Gamma_{jk}} = \sum_{\substack{(j,k)\in\mathbb{J} \\ j<k}} \left[\langle \mathrm{x}_1^{jk}, \mathrm{x}_0^{jk} \rangle_{\Gamma_{jk}} + \langle \mathrm{x}_1^{kj}, \mathrm{x}_0^{kj} \rangle_{\Gamma_{jk}} \right]. \tag{3.147}$$

Now, if $\mathrm{x}_0 \in \mathbb{S}_{0,\|}$ and $\mathrm{x}_1 \in \mathbb{S}_{1,\|}$, it follows from Definition 3.20 that $\left\langle\!\left\langle \mathbb{x}_1, \mathbb{x}_0 \right\rangle\!\right\rangle_{\|} = 0$. Reciprocally, let $\mathrm{x}_0 \in \mathbb{M}_{0,\|}$ such that for any $\mathrm{x}_1 \in \mathbb{S}_{1,\|}$, we have $\left\langle\!\left\langle \mathbb{x}_1, \mathbb{x}_0 \right\rangle\!\right\rangle_{\|} = 0$. We obtain

$$\left\langle\!\left\langle \mathbb{x}_1, \mathbb{x}_0 \right\rangle\!\right\rangle_{\|} = \sum_{\substack{(j,k)\in\mathbb{J} \\ j<k}} \langle \mathrm{x}_1^{jk}, \mathrm{x}_0^{jk} - \mathrm{x}_0^{kj} \rangle_{\Gamma_{jk}} = 0, \tag{3.148}$$

which holds for any x_1, so that $\mathrm{x}_0^{jk} = \mathrm{x}_0^{kj}$ for any $(j,k) \in \mathbb{J}$ and finally $\mathrm{x}_0 \in \mathbb{S}_{0,\|}$.

The other results stated by the proposition can be obtained analogously. ■

3.2.3.4 Characterization of the trace of the solution

We are now ready to characterize the solution of the model problem (3.79) (or equivalently of the transmission problem (3.114)) entirely through its trace. This is the purpose of the following proposition.

Proposition 3.24. *Let $F \in \mathbb{U}_\Gamma(\mathrm{D}; \mathcal{P}_\Omega)$ be any source lifting such that (the choice is not unique)*

$$\begin{cases} (\mathrm{L}_{\mathsf{a}} - {\kappa_0}^2 \mathsf{n}) F|_{\Omega_j} = f|_{\Omega_j}, & \text{in } \Omega_j,\ \forall j \in \{1,\dots,J\}, \\ (\gamma_{1,\Gamma} - \mathrm{i}\gamma_{0,\Gamma}) F = g, & \text{on } \Gamma. \end{cases} \tag{3.149}$$

Let $\mathbb{u} \in \mathbb{U}_\Gamma(\mathrm{D}, \mathrm{L}_{\mathsf{a}}; \mathcal{P}_\Omega)$. Then, u is solution of the model problem (3.79) if, and only if,

$$\boldsymbol{\gamma}_{\|} u \in (\mathbb{C}_{\|} + \boldsymbol{\gamma}_{\|} F) \cap \mathbb{S}_{\|}. \tag{3.150}$$

Proof. Given any $F \in \mathbb{U}_\Gamma(\mathrm{D}; \mathcal{P}_\Omega)$ satisfying (3.149), from Proposition 3.15, $\mathbb{u} \in \mathbb{U}_\Gamma(\mathrm{D}; \mathcal{P}_\Omega)$ is solution of the model problem (3.79) if, and only if,

$$\begin{cases} \text{Find } \mathbb{u} \in \mathbb{U}_\Gamma(\mathrm{D}; \mathcal{P}_\Omega) \text{ such that :} \\ \forall j \in \{1,\dots,J\}, & \begin{cases} (\mathrm{L}_{\mathsf{a}} - {\kappa_0}^2 \mathsf{n})(u - F)|_{\Omega_j} = 0, & \text{in } \Omega_j, \\ (\gamma_{1,\Gamma} - \mathrm{i}\gamma_{0,\Gamma})(u - F)|_{\Omega_j} = 0, & \text{on } \Gamma \cap \Gamma_j, \end{cases} \\ \forall (j,k) \in \mathbb{J}, & \begin{cases} \gamma_{0,\Gamma_{jk}}\left(u|_{\Omega_j}\right) = \gamma_{0,\Gamma_{kj}}\left(u|_{\Omega_k}\right), \\ \gamma_{1,\Gamma_{jk}}\left(u|_{\Omega_j}\right) = -\gamma_{1,\Gamma_{kj}}\left(u|_{\Omega_k}\right), \end{cases} & \text{on } \Gamma_{jk}. \end{cases} \tag{3.151}$$

By Definition 3.18 of the Cauchy trace space $\mathbb{C}_{\|}$ and from Proposition 3.21 on the single trace space $\mathbb{S}_{\|}$, $\mathbb{u} \in \mathbb{U}_\Gamma(\mathrm{D}; \mathcal{P}_\Omega)$ is solution of the model problem (3.79) if, and only if,

$$\begin{cases} \boldsymbol{\gamma}_{\|}(u - F) \in \mathbb{C}_{\|}, & (u \text{ satisfies the PDE in each sub-domain}), \\ \boldsymbol{\gamma}_{\|} u \in \mathbb{S}_{\|}, & (\text{the transmission conditions are satisfied}). \end{cases} \tag{3.152}$$

■

The above characterization of the trace of the unique solution of the model problem (3.79) as the intersection of a vector space and an affine space entails necessarily that this intersection

is reduced to a singleton. This fact is corroborated and completed by the following proposition. A similar result in a more general setting (in the whole space and with junctions) was proven in the case of constant coefficients for instance in [32, Prop. 6.1] for the acoustic setting and in [37, Prop. 6.1] for the electromagnetic setting. The extension to variable coefficients for the acoustic setting is available in [29, Prop. 6.1].

Proposition 3.25. *We have the direct sum*

$$\mathbb{M}_{\shortparallel} = \mathbb{C}_{\shortparallel} \oplus \mathbb{S}_{\shortparallel}. \tag{3.153}$$

Proof.

Null intersection $\mathbb{C}_{\shortparallel} \cap \mathbb{S}_{\shortparallel} = \{0\}$. Let $\mathbb{x} \equiv (\mathrm{x}^{jk})_{(j,k)\in\mathbb{J}} \in \mathbb{C}_{\shortparallel} \cap \mathbb{S}_{\shortparallel}$. First, since $\mathbb{x} \in \mathbb{C}_{\shortparallel}$, from Definition 3.18 of the Cauchy trace space $\mathbb{C}_{\shortparallel}$, for all $j \in \{1, \dots, J\}$, we can find a lifting $u_j \in \mathrm{U}_\Gamma(\mathrm{D}; \Omega_j)$ such that

$$\begin{cases} (\mathrm{L}_{\mathsf{a}} - {\kappa_0}^2 \mathsf{n}) u_j = 0, & \text{in } \Omega_j, \\ (\gamma_{1,\Gamma} - \mathrm{i}\gamma_{0,\Gamma}) u_j = 0, & \text{on } \Gamma, \end{cases} \tag{3.154}$$

and

$$\gamma_{\Gamma_{jk}} u_j = \mathrm{x}^{jk}, \qquad \text{on } \Gamma_{jk},\ \forall k \in \mathbb{K}_j. \tag{3.155}$$

Now let $\mathbb{u} \in \mathbb{U}_\Gamma(\mathrm{D}; \mathcal{P}_\Omega)$ such that

$$u|_{\Omega_j} = u_j, \qquad \forall j \in \{1, \dots, J\}, \tag{3.156}$$

we remark that u belongs in fact to $\mathbb{U}_\Gamma(\mathrm{D}, \mathrm{L}_{\mathsf{a}}; \mathcal{P}_\Omega)$ (so that its trace $\boldsymbol{\gamma}_{\shortparallel}$ is well defined) and by construction it is such that

$$\boldsymbol{\gamma}_{\shortparallel} u = \mathbb{x} \in \mathbb{C}_{\shortparallel} \cap \mathbb{S}_{\shortparallel}. \tag{3.157}$$

From Proposition 3.24, it follows that u actually satisfies the homogeneous model problem (3.79) in the whole of Ω

$$\boldsymbol{\gamma}_{\shortparallel} u \in \mathbb{C}_{\shortparallel} \cap \mathbb{S}_{\shortparallel} \qquad \Leftrightarrow \qquad \begin{cases} u \in \mathrm{U}_\Gamma(\mathrm{D}; \Omega), & \\ (\mathrm{L}_{\mathsf{a}} - {\kappa_0}^2 \mathsf{n}) u = 0, & \text{in } \Omega, \\ (\gamma_{1,\Gamma} - \mathrm{i}\gamma_{0,\Gamma}) u = 0, & \text{on } \Gamma. \end{cases} \tag{3.158}$$

The well-posedness of this problem (Assumption 3.9) yields $u = 0$, hence $\mathbb{x} = \boldsymbol{\gamma}_{\shortparallel} u = 0$.

Decomposition. Let $\mathbb{x} \equiv (\mathbb{x}_0, \mathbb{x}_1) \in \mathbb{M}_{\shortparallel}$ with $\mathbb{x}_0 \equiv (\mathrm{x}_0^{jk})_{(j,k)\in\mathbb{J}}$ and $\mathbb{x}_1 \equiv (\mathrm{x}_1^{jk})_{(j,k)\in\mathbb{J}}$. We wish to construct $\mathbb{y} \in \mathbb{C}_{\shortparallel}$ and $\mathbb{z} \in \mathbb{S}_{\shortparallel}$ such that $\mathbb{x} = \mathbb{y} + \mathbb{z}$. The proof performs explicitly the projection of $\mathbb{x}$ on the subspace $\mathbb{C}_{\shortparallel}$ in parallel to the subspace $\mathbb{S}_{\shortparallel}$. To construct $\mathbb{y}$, we consider the following transmission problem

$$\begin{cases} \mathbb{u} \in \mathbb{U}_\Gamma(\mathrm{D}; \mathcal{P}_\Omega) \text{ such that}, & \\ (\mathrm{L}_{\mathsf{a}} - {\kappa_0}^2 \mathsf{n}) u|_{\Omega_j} = 0, & \text{in } \Omega_j,\ \forall j \in \{1, \dots, J\} \\ (\gamma_{1,\Gamma} - \mathrm{i}\gamma_{0,\Gamma}) u = 0, & \text{on } \Gamma, \\ \gamma_{0,\Gamma_{jk}} u|_{\Omega_j} - \gamma_{0,\Gamma_{kj}} u|_{\Omega_k} = \mathrm{x}_0^{jk} - \mathrm{x}_0^{kj}, & \text{on } \Gamma_{jk},\ \forall (j,k) \in \mathbb{J}, \\ \gamma_{1,\Gamma_{jk}} u|_{\Omega_j} + \gamma_{1,\Gamma_{kj}} u|_{\Omega_k} = \mathrm{x}_1^{jk} + \mathrm{x}_1^{kj}, & \text{on } \Gamma_{jk},\ \forall (j,k) \in \mathbb{J}. \end{cases} \tag{3.159}$$

To solve the above problem, we proceed in two steps

1. Lifting of $\mathbb{x}_0$: define

$$\begin{cases} v \in \mathbb{U}_\Gamma(\mathrm{D}, \mathrm{L}_\mathsf{a}; \mathcal{P}_\Omega) \text{ such that,} \\ \gamma_{0,\Gamma_{jk}} v|_{\Omega_j} - \gamma_{0,\Gamma_{kj}} v|_{\Omega_k} = \mathrm{x}_0^{jk} - \mathrm{x}_0^{kj}, \qquad \text{on } \Gamma_{jk},\ \forall k \in \mathbb{K}_j. \end{cases} \tag{3.160}$$

Any such lifting will work, a particular lifting can be constructed for instance by solving coercive (note the change of sign in the equation and the real parts of the coefficients) local problems (which are well-posed):

$$\forall j \in \{1, \dots, J\}, \qquad \begin{cases} v|_{\Omega_j} \in \mathrm{U}_\Gamma(\mathrm{D}; \Omega_j) \text{ such that,} & \\ (\mathrm{L}_{\Re(\mathsf{a})} + {\kappa_0}^2 \Re(\mathsf{n})) v|_{\Omega_j} = 0, & \text{in } \Omega_j, \\ (\gamma_{1,\Gamma} - \mathrm{i}\gamma_{0,\Gamma}) v|_{\Omega_j} = 0, & \text{on } \Gamma_j \cap \Gamma, \\ \gamma_{0,\Gamma_{jk}} v|_{\Omega_j} = \mathrm{x}_0^{jk}, & \text{on } \Gamma_{jk},\ \forall k \in \mathbb{K}_j. \end{cases} \tag{3.161}$$

2. Lifting of $\mathbb{x}_1$: define

$$\begin{cases} w \in \mathrm{U}_\Gamma(\mathrm{D}; \Omega) \text{ such that,} & \\ (\mathrm{L}_\mathsf{a} - {\kappa_0}^2 \mathsf{n})(v - w)|_{\Omega_j} = 0, & \text{in } \Omega_j,\ \forall j \in \{1, \dots, J\} \\ (\gamma_{1,\Gamma} - \mathrm{i}\gamma_{0,\Gamma})(v - w) = 0, & \text{on } \Gamma, \\ \gamma_{1,\Gamma_{jk}} (v - w)|_{\Omega_j} + \gamma_{1,\Gamma_{kj}} (v - w)|_{\Omega_k} = \mathrm{x}_1^{jk} + \mathrm{x}_1^{kj}, & \text{on } \Gamma_{jk},\ \forall (j,k) \in \mathbb{J}. \end{cases} \tag{3.162}$$

Such a solution $w \in \mathrm{U}_\Gamma(\mathrm{D}; \Omega)$ exists from the well-posedness of the model problem (3.79) (Assumption 3.9).

Set

$$u := v - w \in \mathbb{U}_\Gamma(\mathrm{D}; \mathcal{P}_\Omega). \tag{3.163}$$

From (3.160)

$$\gamma_{0,\Gamma_{jk}} v|_{\Omega_j} - \gamma_{0,\Gamma_{kj}} v|_{\Omega_k} = \mathrm{x}_0^{jk} - \mathrm{x}_0^{kj}, \qquad \text{on } \Gamma_{jk},\ \forall (j,k) \in \mathbb{J}, \tag{3.164}$$

and since $w \in \mathrm{U}_\Gamma(\mathrm{D}; \Omega)$, using Proposition 3.21, we have

$$\gamma_{0,\Gamma_{jk}} w|_{\Omega_j} - \gamma_{0,\Gamma_{kj}} w|_{\Omega_k} = 0, \qquad \text{on } \Gamma_{jk},\ \forall (j,k) \in \mathbb{J}, \tag{3.165}$$

so that

$$\gamma_{0,\Gamma_{jk}} u|_{\Omega_j} - \gamma_{0,\Gamma_{kj}} u|_{\Omega_k} = \mathrm{x}_0^{jk} - \mathrm{x}_0^{kj}, \qquad \text{on } \Gamma_{jk},\ \forall (j,k) \in \mathbb{J}, \tag{3.166}$$

It is therefore clear from (3.162) that u solves the transmission problem (3.159).

Set

$$\mathbb{y} \equiv (\mathbb{y}_0, \mathbb{y}_1) := \boldsymbol{\gamma}_\parallel u \equiv (\boldsymbol{\gamma}_{0,\parallel} u, \boldsymbol{\gamma}_{1,\parallel} u). \tag{3.167}$$

By construction u satisfies the PDE in each sub-domain Ω_j (and the physical boundary condition) and Definition 3.18 of the Cauchy trace space $\mathbb{C}_\parallel$ yields $\mathbb{y} \in \mathbb{C}_\parallel$.

Now, set

$$\mathbb{z} \equiv (\mathbb{z}_0, \mathbb{z}_1) := \mathbb{x} - \mathbb{y}. \tag{3.168}$$

Introducing

$$\begin{aligned} \mathbb{y}_0 &\equiv (\mathrm{y}_0^{jk})_{(j,k)\in\mathbb{J}}, \qquad & \mathbb{y}_1 &\equiv (\mathrm{y}_1^{jk})_{(j,k)\in\mathbb{J}}, \\ \mathbb{z}_0 &\equiv (\mathrm{z}_0^{jk})_{(j,k)\in\mathbb{J}}, \qquad & \mathbb{z}_1 &\equiv (\mathrm{z}_1^{jk})_{(j,k)\in\mathbb{J}}, \end{aligned} \tag{3.169}$$

the last two equations of (3.159) are rewritten as

$$\begin{cases} \mathrm{x}_0^{jk} - \mathrm{y}_0^{jk} = \mathrm{x}_0^{kj} - \mathrm{y}_0^{kj}, \\ \mathrm{x}_1^{jk} - \mathrm{y}_1^{jk} = -\mathrm{x}_1^{kj} + \mathrm{y}_1^{kj}, \end{cases} \quad \forall (j,k) \in \mathbb{J}, \quad \Leftrightarrow \quad \begin{cases} \mathrm{z}_0^{kj} = \mathrm{z}_0^{kj}, \\ \mathrm{z}_1^{kj} = -\mathrm{z}_1^{kj}, \end{cases} \quad \forall (j,k) \in \mathbb{J}, \tag{3.170}$$

which, by Definition 3.20 of the single trace space $\mathbb{S}_\shortparallel$, proves that $\mathbb{z} \in \mathbb{S}_\shortparallel$.

Finally we have constructed the decomposition

$$\mathbb{x} = \mathbb{y} + \mathbb{z}, \qquad \text{with} \qquad \begin{cases} \mathbb{y} \in \mathbb{C}_\shortparallel, \\ \mathbb{z} \in \mathbb{S}_\shortparallel. \end{cases} \tag{3.171}$$

■

3.2.4 Reformulation as an interface problem

The previous characterization (see Proposition 3.24) of the trace of the (unique) solution of the original problem (3.79) using the two subsets $\mathbb{C}_\shortparallel$ and $\mathbb{S}_\shortparallel$ of the multi-trace space $\mathbb{M}_\shortparallel$ is admittedly elegant but not very practical. In this section, we exploit the above characterization to equivalently recast the original problem (3.79) as a problem posed on the skeleton $\tilde{\Sigma}$ of the partition (see (3.200)).

3.2.4.1 Transmission operators

We start by introducing a key ingredient of our formulation, the transmission operators. The choice of a transmission operator completely characterizes the domain decomposition method and its property will greatly influence the efficiency of the method.

Definition 3.26 (**Transmission operators**). *We call* transmission *operators any* continuous *and* injective *mappings such that*

$$\begin{aligned} &\mathbf{T}_{0,\shortparallel} \ : \ \mathbb{M}_{0,\shortparallel} \to \mathbb{M}_{1,\shortparallel}, && \mathbf{T}_{1/2,\shortparallel} \ : \ \mathbb{M}_{0,\shortparallel} \to \mathbb{M}_{1/2,\shortparallel}, \\ &\mathbf{T}_{1,\shortparallel} \ : \ \mathbb{M}_{1,\shortparallel} \to \mathbb{M}_{0,\shortparallel}, && \mathbf{T}_{-1/2,\shortparallel} \ : \ \mathbb{M}_{1,\shortparallel} \to \mathbb{M}_{1/2,\shortparallel}. \end{aligned} \tag{3.172}$$

Note that the assumptions on the transmission operators given in the above definition are the bare minimum we shall require. They will need to satisfy additional assumptions as we proceed with the theory, see Assumptions 3.28, 3.36 and 3.47.

Besides, we also introduce an additional *continuous* mapping

$$\mathbf{Z} \ : \ \mathbb{M}_{0,\shortparallel} \to \mathbb{M}_{1,\shortparallel}. \tag{3.173}$$

This operator $\mathbf{Z}$ is less important to the domain decomposition method and shall rather be seen as an additional parameter that is available to tune the method in order to improve its efficiency. In fact, all what follows still stands if one considers this operator to be identically equal to zero.

From the Cartesian nature of multi-trace spaces on which they are defined, the transmission operators have a special block structure as either an operator matrix of size $\operatorname{card} \mathbb{J} \times \operatorname{card} \mathbb{J}$ (if we adopt the interface point of view) or an operator matrix of size $J \times J$ (if we adopt the sub-domain point of view). We provide two examples of the transmission operators structure in Figure 3.2. These sketches correspond to the bottom and top-right geometrical configurations that are given in Figure 3.1c.

The transmission operators (together with the operator $\mathbf{Z}$) are used to combine the two types of traces into so-called generalized Robin multi-traces.

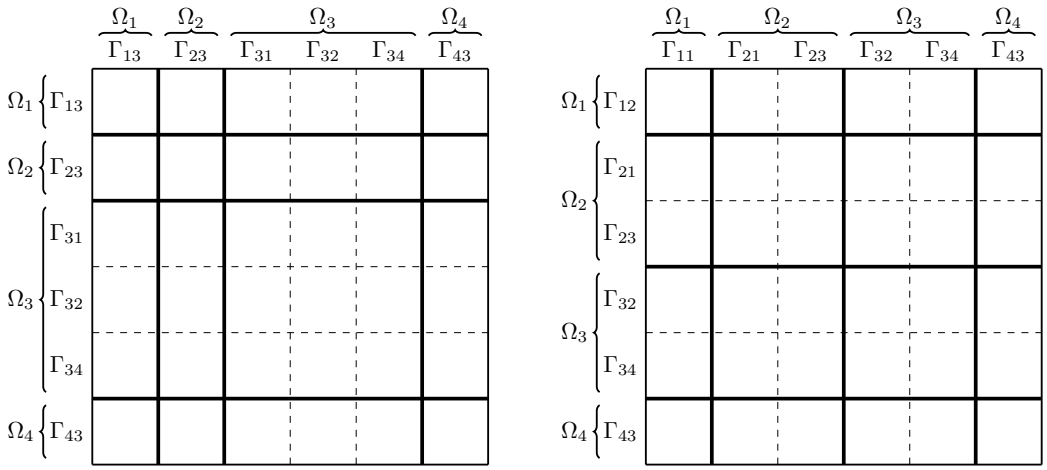

(a) Top right geometric partition in Figure 3.1c. (b) Bottom geometric partition in Figure 3.1c.

Figure 3.2: Sketch of the operator matrix of transmission operators.

Definition 3.27 (**Generalized Robin operators**). *For each $\sigma \in \{0, 1/2, 1\}$, we introduce the global operators,*

$$\begin{aligned}\mathbf{R}^{\pm}_{\sigma,\|} \ &: \mathbb{M}_{\|} \equiv (\mathbb{M}_{0,\|}, \mathbb{M}_{1,\|}) \to \mathbb{M}_{\sigma,\|},\\ &\mathbb{x} \equiv (\mathbb{x}_0, \mathbb{x}_1) \mapsto \begin{cases} \pm\mathbf{T}_{1,\|}\left(\mathbb{x}_1 + \mathbf{Z}\mathbb{x}_0\right) - \mathrm{i}\mathbb{x}_0, & \text{if } \sigma = 0,\\ \pm\mathbf{T}_{-1/2,\|}\left(\mathbb{x}_1 + \mathbf{Z}\mathbb{x}_0\right) - \mathrm{i}\mathbf{T}_{1/2,\|}\mathbb{x}_0, & \text{if } \sigma = 1/2,\\ \pm\left(\mathbb{x}_1 + \mathbf{Z}\mathbb{x}_0\right) - \mathrm{i}\mathbf{T}_{0,\|}\mathbb{x}_0, & \text{if } \sigma = 1,\end{cases}\end{aligned} \tag{3.174}$$

Again, for the same reasons, the generalized Robin operators $\mathbf{R}^{\pm}_{\sigma,\|}$, $\sigma \in \{0, 1/2, 1\}$, have a special block structure. However they are this time (block) "*rectangular*" since they map a couple of zeroth and first order multi-traces (element of $\mathbb{M}_{\|} \equiv \mathbb{M}_{0,\|} \times \mathbb{M}_{1,\|}$) to an element of $\mathbb{M}_{\sigma,\|}$.

It is clear from the mapping properties of the transmission operators (see equation (3.173) and Definition 3.26), that these quantities are well-balanced in a functional sense: all three terms that appear in their definition naturally belong to the same multi-trace space.

If $\mathbb{u} \in \mathbb{U}_{\Gamma}(\mathrm{D}, \mathrm{L}_{\mathsf{a}}; \mathcal{P}_{\Omega})$, for any $\sigma \in \{0, 1/2, 1\}$, the quantity $\mathbf{R}^{+}_{\sigma,\|}\boldsymbol{\gamma}_{\|}u$ will be referred to as an *incoming* Robin trace while the quantity $\mathbf{R}^{-}_{\sigma,\|}\boldsymbol{\gamma}_{\|}u$ will be referred to as an *outgoing* Robin trace, according to standard practice in [42, 44, 91].

3.2.4.2 Scattering operators

Another key ingredient in the reformulation of the problem at the interface is the so-called scattering operator which takes an incoming Robin trace, solves the PDE in each sub-domain and computes an outgoing Robin trace.

Because of the abstract setting, we make the following assumption (which puts constraints on the transmission operators) before proceeding. Of course, we shall get back to this and justify it in what follows, but we emphasize that it is not trivial to satisfy.

Assumption 3.28. *For each $\sigma \in \{0, 1/2, 1\}$ and for any $\mathbb{x}_\sigma \in \mathbb{M}_{\sigma,\|}$, $f \in L^2(\Omega)^{m_0}$, $g \in L^2(\Gamma)^{m_0}$,*

the transmission operators are such that the following problem is well-defined:

$$\begin{cases} \textit{Find } u_\sigma \in \mathbb{U}_\Gamma(\mathrm{D};\mathcal{P}_\Omega) \textit{ such that} & \\ (\mathrm{L}_{\mathsf{a}} - \kappa_0{}^2\mathsf{n})u_\sigma|_{\Omega_j} = f|_{\Omega_j}, & \textit{in } \Omega_j,\ \forall j \in \{1,\dots,J\}, \\ (\gamma_{1,\Gamma} - \mathrm{i}\gamma_{0,\Gamma})u_\sigma = g, & \textit{on } \Gamma, \\ \mathbf{R}^+_{\sigma,\|}\boldsymbol{\gamma}_\| u_\sigma = \mathbb{x}_\sigma, & \textit{on } \tilde{\Sigma}. \end{cases} \tag{3.175}$$

The problem (3.175) consists in local sub-problems which are coupled through the last equation. In practice though, the transmission operators will be chosen in order to decouple those sub-problems, leading to some possible parallelization of the algorithm, see Section 3.2.4.5 for further discussion on this matter.

Upon satisfying the above assumption, we can now safely define the scattering operators.

Definition 3.29 (**Scattering operator**). *For each $\sigma \in \{0, 1/2, 1\}$, we define the global scattering operators,*

$$\begin{aligned} \mathbf{S}_{\sigma,\|} \ &: \mathbb{M}_{\sigma,\|} \to \mathbb{M}_{\sigma,\|}, \\ &\mathbb{x}_\sigma \mapsto \mathbf{R}^-_{\sigma,\|}\boldsymbol{\gamma}_\| u_\sigma, \end{aligned} \tag{3.176}$$

where $u_\sigma \in \mathbb{U}_\Gamma(\mathrm{D};\mathcal{P}_\Omega)$ is such that

$$\begin{cases} (\mathrm{L}_{\mathsf{a}} - \kappa_0{}^2\mathsf{n})u_\sigma|_{\Omega_j} = 0, & \textit{in } \Omega_j,\ \forall j \in \{1,\dots,J\}, \\ (\gamma_{1,\Gamma} - \mathrm{i}\gamma_{0,\Gamma})u_\sigma = 0, & \textit{on } \Gamma, \\ \mathbf{R}^+_{\sigma,\|}\boldsymbol{\gamma}_\| u_\sigma = \mathbb{x}_\sigma, & \textit{on } \tilde{\Sigma}. \end{cases} \tag{3.177}$$

From the above definition, we readily obtain a characterization of the Cauchy trace space $\mathbb{C}_\|$ (Definition 3.18) as the kernel of an operator involving the generalized Robin operators $\mathbf{R}^\sigma_{\pm,\|}$ and the scattering operator $\mathbf{S}_{\sigma,\|}$. The main ingredient of the proof is the injectivity assumption on the transmission operators (see Definition 3.26).

Proposition 3.30 (**Characterization of the Cauchy trace space**). *For each $\sigma \in \{0, 1/2, 1\}$, we have the following characterization of the Cauchy-trace space:*

$$\mathbb{C}_\| = \mathrm{Ker}\left(\mathbf{R}^-_{\sigma,\|} - \mathbf{S}_{\sigma,\|}\mathbf{R}^+_{\sigma,\|}\right). \tag{3.178}$$

Proof. ($\Rightarrow$) Let $\mathbb{x} \in \mathbb{C}_\|$. From Definition 3.18 of the Cauchy trace space $\mathbb{C}_\|$, there exists $u \in \mathrm{U}_\Gamma(\mathrm{D};\Omega_j)$ such that $\boldsymbol{\gamma}_\| u = \mathbb{x}$ and

$$\begin{cases} (\mathrm{L}_{\mathsf{a}} - \kappa_0{}^2\mathsf{n})u|_{\Omega_j} = 0, & \text{in } \Omega_j,\ \forall j \in \{1,\dots,J\} \\ (\gamma_{1,\Gamma} - \mathrm{i}\gamma_{0,\Gamma})|_{\Omega_j} = 0, & \text{on } \Gamma \cap \Gamma_j. \end{cases} \tag{3.179}$$

If, for any $\sigma \in \{0, 1/2, 1\}$, we let $\mathbb{y} := \mathbf{R}^+_{\sigma,\|}\boldsymbol{\gamma}_\| u = \mathbf{R}^+_{\sigma,\|}\mathbb{x}$, by Definition 3.29 of the scattering operator $\mathbf{S}_{\sigma,\|}$, we have $\mathbf{R}^-_{\sigma,\|}\boldsymbol{\gamma}_\| u := \mathbf{S}_{\sigma,\|}\mathbb{y}$ which are rewritten as $\mathbf{R}^-_{\sigma,\|}\mathbb{x} = \mathbf{S}_{\sigma,\|}\mathbf{R}^+_{\sigma,\|}\mathbb{x}$.

($\Leftarrow$) Let $\sigma \in \{0, 1/2, 1\}$ and $\mathbb{x} \in \mathbb{M}_\|$ be such that $\mathbf{R}^-_{\sigma,\|}\mathbb{x} = \mathbf{S}_{\sigma,\|}\mathbf{R}^+_{\sigma,\|}\mathbb{x}$. By Assumption 3.28, there exists $u_\sigma \in \mathrm{U}_\Gamma(\mathrm{D};\Omega_j)$ such that

$$\begin{cases} (\mathrm{L}_{\mathsf{a}} - \kappa_0{}^2\mathsf{n})u_\sigma|_{\Omega_j} = 0, & \text{in } \Omega_j,\ \forall j \in \{1,\dots,J\}, \\ (\gamma_{1,\Gamma} - \mathrm{i}\gamma_{0,\Gamma})u_\sigma = 0, & \text{on } \Gamma, \\ \mathbf{R}^+_{\sigma,\|}\boldsymbol{\gamma}_\| u_\sigma = \mathbf{R}^+_{\sigma,\|}\mathbb{x}, & \text{on } \tilde{\Sigma}, \end{cases} \tag{3.180}$$

and from Definition 3.29 of the scattering operator $\mathbf{S}_{\sigma,\|}$ we have $\mathbf{R}^-_{\sigma,\|}\boldsymbol{\gamma}_\| u_\sigma := \mathbf{S}_{\sigma,\|}\mathbf{R}^+_{\sigma,\|}\mathbb{x}$. It follows that

$$\begin{cases} \mathbf{R}^+_{\sigma,\|}\boldsymbol{\gamma}_\| u_\sigma = \mathbf{R}^+_{\sigma,\|}\mathbb{x}, \\ \mathbf{R}^-_{\sigma,\|}\boldsymbol{\gamma}_\| u_\sigma = \mathbf{R}^-_{\sigma,\|}\mathbb{x}. \end{cases} \tag{3.181}$$

It remains to prove that $\boldsymbol{\gamma}_\| u_\sigma = \mathbb{x}$. We give the proof for $\sigma = 1$, the other proofs follow the same lines. By Definition 3.27 of the generalized Robin operators $\mathbf{R}^\pm_{\sigma,\|}$, the system (3.180) is rewritten as

$$\begin{cases} (\boldsymbol{\gamma}_{1,\|} u_1 + \mathbf{Z}\boldsymbol{\gamma}_{0,\|} u_1) - \mathrm{i}\mathbf{T}_{0,\|}\boldsymbol{\gamma}_{0,\|} u_1 = (\mathbb{x}_1 + \mathbf{Z}\mathbb{x}_0) - \mathrm{i}\mathbf{T}_{0,\|}\mathbb{x}_0, \\ -(\boldsymbol{\gamma}_{1,\|} u_1 + \mathbf{Z}\boldsymbol{\gamma}_{0,\|} u_1) - \mathrm{i}\mathbf{T}_{0,\|}\boldsymbol{\gamma}_{0,\|} u_1 = -(\mathbb{x}_1 + \mathbf{Z}\mathbb{x}_0) - \mathrm{i}\mathbf{T}_{0,\|}\mathbb{x}_0, \end{cases} \tag{3.182}$$

so that taking linear combinations we get

$$\begin{cases} \mathbf{T}_{0,\|}\left(\boldsymbol{\gamma}_{0,\|} u_1 - \mathbb{x}_0\right) = 0, \\ \left(\boldsymbol{\gamma}_{1,\|} u_1 - \mathbb{x}_1\right) + \mathbf{Z}\left(\boldsymbol{\gamma}_{0,\|} u_1 - \mathbb{x}_0\right) = 0, \end{cases} \quad \Rightarrow \quad \begin{cases} \boldsymbol{\gamma}_{0,\|} u_1 = \mathbb{x}_0, \\ \boldsymbol{\gamma}_{1,\|} u_1 = \mathbb{x}_1, \end{cases} \quad \Rightarrow \quad \boldsymbol{\gamma}_\| u_1 = \mathbb{x}, \tag{3.183}$$

using the injectivity assumption on the transmission operator $\mathbf{T}_{0,\|}$ (Definition 3.26). ■

3.2.4.3 Exchange operator

The last key ingredient in the reformulation of the original problem as a problem on the skeleton $\tilde{\Sigma}$ is the so-called exchange operator $\boldsymbol{\Pi}_\|$. The role of this operator is to couple all sub-domains by exchanging information through all interfaces.

Definition 3.31 (Exchange operator). *We introduce the exchange operator, denoted $\boldsymbol{\Pi}_\|$, such that, for any $\sigma \in \{0, 1/2, 1\}$,*

$$\forall \mathbb{x}_\sigma, \mathbb{y}_\sigma \in \mathbb{M}_{\sigma,\|}, \qquad \left(\mathbb{y}_\sigma = \boldsymbol{\Pi}_\| \mathbb{x}_\sigma \qquad \Leftrightarrow \qquad \mathrm{x}_\sigma^{jk} = \mathrm{y}_\sigma^{kj}, \quad \forall (j,k) \in \mathbb{J}\right), \tag{3.184}$$

with the convention that $\mathbb{x}_\sigma \equiv (\mathrm{x}_\sigma^{jk})_{(j,k)\in\mathbb{J}}$ and $\mathbb{y}_\sigma \equiv (\mathrm{y}_\sigma^{jk})_{(j,k)\in\mathbb{J}}$.

Remark 3.32. *Because this operator is very simple, we do not introduce different operators $\boldsymbol{\Pi}_{\sigma,\|}$, $\sigma \in \{0, 1/2, 1\}$. Strictly speaking, because its definition does not depend on σ, we could define this operator on the largest trace space that includes both $\mathbb{M}_{0,\|}$ and $\mathbb{M}_{1,\|}$, namely*

$$\bigtimes_{(j,k)\in\mathbb{J}} H^{-1/2}(\Gamma_{jk})^{m_0}. \tag{3.185}$$

From the Cartesian nature of multi-trace spaces, the exchange operator has a special block structure. We provide two examples of the exchange operator structure in Figure 3.3. These sketches correspond to the bottom and top-right geometrical configurations that are given in Figure 3.1c.

The following two propositions are immediate consequences of the above definition.

Proposition 3.33. *For each $\sigma \in \{0, 1/2, 1\}$, the exchange operator $\boldsymbol{\Pi}_\|$ is an involution of $\mathbb{M}_{\sigma,\|}$,*

$$\boldsymbol{\Pi}_\|^2 = \mathrm{Id} \qquad \text{in } \mathbb{M}_{\sigma,\|}. \tag{3.186}$$

Proposition 3.34. *For each $\sigma \in \{0, 1/2, 1\}$, the two operators $1/2\,(\mathrm{Id} \pm \boldsymbol{\Pi}_\|)$ are two* complementary projectors *in $\mathbb{M}_{\sigma,\|}$,*

$$\begin{aligned} &1/4[\mathrm{Id} \pm \boldsymbol{\Pi}_\|]^2 = 1/2\,[\mathrm{Id} \pm \boldsymbol{\Pi}_\|], \\ &[\mathrm{Id} + \boldsymbol{\Pi}_\|]\,[\mathrm{Id} - \boldsymbol{\Pi}_\|] = [\mathrm{Id} - \boldsymbol{\Pi}_\|]\,[\mathrm{Id} + \boldsymbol{\Pi}_\|] = 0. \end{aligned} \tag{3.187}$$

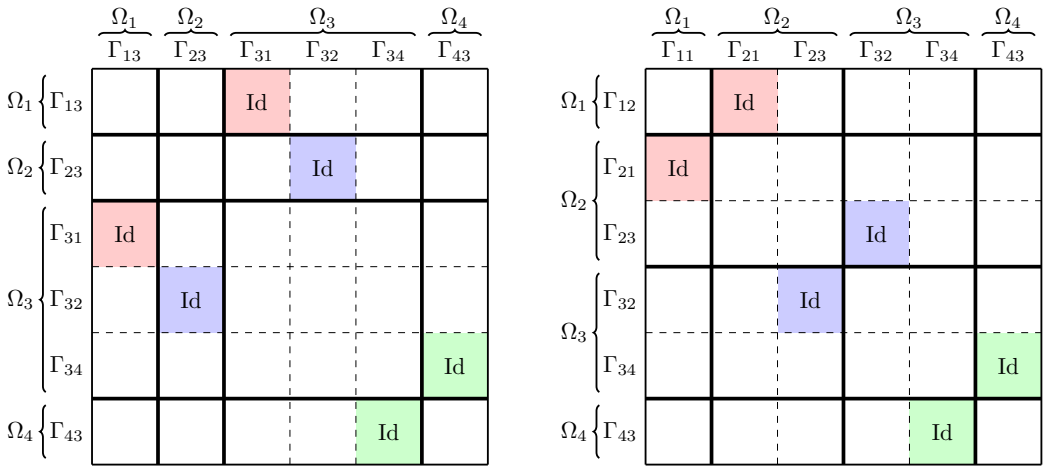

(a) Top right geometric partition in Figure 3.1c. (b) Bottom geometric partition in Figure 3.1c.

Figure 3.3: Sketch of the operator matrix of the exchange operator. The non-zero operators are the Id blocks featured by the shaded areas.

Using Definition 3.31 of the exchange operator $\mathbf{\Pi}_{\shuffle}$, we are able to characterize the kernel of the above projectors and rephrase Definition 3.20 of the single trace space $\mathbb{S}_{\shuffle}$. This is the subject of the following proposition.

Proposition 3.35. *We have*

$$\mathbb{x} \equiv (\mathbb{x}_0, \mathbb{x}_1) \in \mathbb{S}_{\shuffle} \quad \Leftrightarrow \quad \begin{cases} \mathbb{x}_0 \in \mathbb{S}_{0,\shuffle}, \\ \mathbb{x}_1 \in \mathbb{S}_{1,\shuffle}, \end{cases} \quad \Leftrightarrow \quad \begin{cases} \mathbb{x}_0 \in \operatorname{Ker}\left(\mathrm{Id} - \mathbf{\Pi}_{\shuffle}\right), \\ \mathbb{x}_1 \in \operatorname{Ker}\left(\mathrm{Id} + \mathbf{\Pi}_{\shuffle}\right). \end{cases} \tag{3.188}$$

Before proceeding, we impose some additional requirements on the transmission operators.

Assumption 3.36. *The transmission operators are such that*

- $\mathbf{Z}$ *is* symmetric *with respect to* $\langle\!\langle \cdot, \cdot \rangle\!\rangle_{\shuffle}$

$$\langle\!\langle \overline{\mathbf{Z}\mathbb{x}_0}, \mathbb{y}_0 \rangle\!\rangle_{\shuffle} = \langle\!\langle \mathbf{Z}\mathbb{y}_0, \overline{\mathbb{x}_0} \rangle\!\rangle_{\shuffle}, \qquad \forall \mathbb{x}_0, \mathbb{y}_0 \in \mathbb{M}_{0,\shuffle}. \tag{3.189}$$

  and anti-commutes *with* $\mathbf{\Pi}_{\shuffle}$

$$\mathbf{Z}\mathbf{\Pi}_{\shuffle} = -\mathbf{\Pi}_{\shuffle}\mathbf{Z}; \tag{3.190}$$

- $\mathbf{T}_{\sigma,\shuffle}$ commutes *with* $\mathbf{\Pi}_{\shuffle}$ *for all* $\sigma \in \{0, 1/2, 1\}$,

$$\mathbf{T}_{\sigma,\shuffle}\mathbf{\Pi}_{\shuffle} = \mathbf{\Pi}_{\shuffle}\mathbf{T}_{\sigma,\shuffle}. \tag{3.191}$$

Upon making the above assumption, which we assume to hold in what follows, we can characterize the single-trace space $\mathbb{S}_{\shuffle}$ (Definition 3.20) as the kernel of an operator involving the generalized Robin operators $\mathbf{R}^{\pm}_{\sigma,\shuffle}$ and the exchange operator $\mathbf{\Pi}_{\shuffle}$. A similar result in a more general setting (in the whole space and with junctions) was proven for instance in [29, Prop. 5.4] for the acoustic setting.

Proposition 3.37 (**Characterization of the single-trace space**). *For each* $\sigma \in \{0, 1/2, 1\}$, *we have the following characterization of the single-trace space* (3.140)*:*

$$\mathbb{S}_{\shortparallel} = \operatorname{Ker}\left(\mathbf{R}^{\pm}_{\sigma,\shortparallel} - \mathbf{\Pi}_{\shortparallel}\mathbf{R}^{\mp}_{\sigma,\shortparallel}\right). \tag{3.192}$$

Proof. First note that, for any $\sigma \in \{0, 1/2, 1\}$ and any $\mathbb{x} \in \mathbb{M}_{\shortparallel}$, $\mathbf{R}^{+}_{\sigma,\shortparallel}\mathbb{x} = \mathbf{\Pi}_{\shortparallel}\mathbf{R}^{-}_{\sigma,\shortparallel}\mathbb{x}$ is equivalent to $\mathbf{R}^{-}_{\sigma,\shortparallel}\mathbb{x} = \mathbf{\Pi}_{\shortparallel}\mathbf{R}^{+}_{\sigma,\shortparallel}\mathbb{x}$ since the exchange operator $\mathbf{\Pi}_{\shortparallel}$ is an involution according to Proposition 3.33.

We prove the equivalence for $\sigma = 1$, the proofs for the other two cases formally take the same route.

($\Leftarrow$) Let $\mathbb{x} \equiv (\mathbb{x}_0, \mathbb{x}_1) \in \mathbb{M}_{\shortparallel}$ such that $\mathbf{R}^{+}_{1,\shortparallel}\mathbb{x} = \mathbf{\Pi}_{\shortparallel}\mathbf{R}^{-}_{1,\shortparallel}\mathbb{x}$. From Definition 3.27 of the generalized Robin operators $\mathbf{R}^{\pm}_{1,\shortparallel}$, we get

$$\begin{aligned} \mathbf{R}^{+}_{1,\shortparallel}\mathbb{x} = \mathbf{\Pi}_{\shortparallel}\mathbf{R}^{-}_{1,\shortparallel}\mathbb{x} \quad &\Rightarrow \quad +(\mathbb{x}_1 + \mathbf{Z}\mathbb{x}_0) - \mathrm{i}\mathbf{T}_{0,\shortparallel}\mathbb{x}_0 = \mathbf{\Pi}_{\shortparallel}\left[-(\mathbb{x}_1 + \mathbf{Z}\mathbb{x}_0) - \mathrm{i}\mathbf{T}_{0,\shortparallel}\mathbb{x}_0\right], \\ &\Rightarrow \quad \left[\mathrm{Id} + \mathbf{\Pi}_{\shortparallel}\right](\mathbb{x}_1 + \mathbf{Z}\mathbb{x}_0) - \mathrm{i}\left[\mathrm{Id} - \mathbf{\Pi}_{\shortparallel}\right]\mathbf{T}_{0,\shortparallel}\mathbb{x}_0 = 0. \end{aligned} \tag{3.193}$$

Using the projection properties of $\mathrm{Id} \pm \mathbf{\Pi}_{\shortparallel}$ given in Proposition 3.34 we deduce

$$\begin{cases} \left[\mathrm{Id} + \mathbf{\Pi}_{\shortparallel}\right](\mathbb{x}_1 + \mathbf{Z}\mathbb{x}_0) = 0, \\ \left[\mathrm{Id} - \mathbf{\Pi}_{\shortparallel}\right]\mathbf{T}_{0,\shortparallel}\mathbb{x}_0 = 0, \end{cases} \tag{3.194}$$

so that using the commutativity properties of Assumption 3.36 we have

$$\begin{cases} \mathbf{T}_{0,\shortparallel}\left[\mathrm{Id} - \mathbf{\Pi}_{\shortparallel}\right]\mathbb{x}_0 = 0, \\ \left[\mathrm{Id} + \mathbf{\Pi}_{\shortparallel}\right]\mathbb{x}_1 + \mathbf{Z}\left[\mathrm{Id} - \mathbf{\Pi}_{\shortparallel}\right]\mathbb{x}_0 = 0. \end{cases} \tag{3.195}$$

Hence, using the injectivity of $\mathbf{T}_{0,\shortparallel}$, we get

$$\begin{cases} \left[\mathrm{Id} - \mathbf{\Pi}_{\shortparallel}\right]\mathbb{x}_0 = 0, \\ \left[\mathrm{Id} + \mathbf{\Pi}_{\shortparallel}\right]\mathbb{x}_1 = 0. \end{cases} \tag{3.196}$$

We finally use the characterization of the single trace space $\mathbb{S}_{\shortparallel}$ given in Proposition 3.35 to obtain $\mathbb{x} \equiv (\mathbb{x}_0, \mathbb{x}_1) \in \mathbb{S}_{\shortparallel}$.

($\Rightarrow$) Reciprocally, let $\mathbb{x} \equiv (\mathbb{x}_0, \mathbb{x}_1) \in \mathbb{S}_{\shortparallel}$. Using again the characterization of the single trace space given in Proposition 3.35 together with the commutation relations of Assumption 3.36 we obtain successively

$$\begin{cases} \left[\mathrm{Id} - \mathbf{\Pi}_{\shortparallel}\right]\mathbb{x}_0 = 0, \\ \left[\mathrm{Id} + \mathbf{\Pi}_{\shortparallel}\right]\mathbb{x}_1 = 0, \end{cases} \quad \Rightarrow \quad \begin{cases} \mathbf{T}_{0,\shortparallel}\left(\mathrm{Id} - \mathbf{\Pi}_{\shortparallel}\right)\mathbb{x}_0 = 0, \\ \mathbf{Z}\left(\mathrm{Id} - \mathbf{\Pi}_{\shortparallel}\right)\mathbb{x}_0 = 0, \\ \left(\mathrm{Id} + \mathbf{\Pi}_{\shortparallel}\right)\mathbb{x}_1 = 0, \end{cases} \quad \Rightarrow \quad \begin{cases} \left(\mathrm{Id} - \mathbf{\Pi}_{\shortparallel}\right)\mathbf{T}_{0,\shortparallel}\mathbb{x}_0 = 0, \\ \left(\mathrm{Id} + \mathbf{\Pi}_{\shortparallel}\right)\mathbf{Z}\mathbb{x}_0 = 0, \\ \left(\mathrm{Id} + \mathbf{\Pi}_{\shortparallel}\right)\mathbb{x}_1 = 0, \end{cases} \tag{3.197}$$

so that taking an adequate linear combination we get

$$\begin{aligned} &\left[\mathrm{Id} + \mathbf{\Pi}_{\shortparallel}\right](\mathbb{x}_1 + \mathbf{Z}\mathbb{x}_0) - \mathrm{i}\left[\mathrm{Id} - \mathbf{\Pi}_{\shortparallel}\right]\mathbf{T}_{0,\shortparallel}\mathbb{x}_0 = 0, \\ \Rightarrow \quad &+(\mathbb{x}_1 + \mathbf{Z}\mathbb{x}_0) - \mathrm{i}\mathbf{T}_{0,\shortparallel}\mathbb{x}_0 = \mathbf{\Pi}_{\shortparallel}\left[-(\mathbb{x}_1 + \mathbf{Z}\mathbb{x}_0) - \mathrm{i}\mathbf{T}_{0,\shortparallel}\mathbb{x}_0\right], \\ \Rightarrow \quad &\mathbf{R}^{+}_{1,\shortparallel}\mathbb{x} = \mathbf{\Pi}_{\shortparallel}\mathbf{R}^{-}_{1,\shortparallel}\mathbb{x} \end{aligned} \tag{3.198}$$

from Definition 3.27 of the generalized Robin operators $\mathbf{R}^{\pm}_{1,\shortparallel}$. ∎

3.2.4.4 Equivalent interface problem

With the help of the scattering operators $\mathbf{S}_{\sigma,\|}$ and exchange operator $\mathbf{\Pi}_{\|}$ we are now in a position to recast the original problem (3.79) (or equivalently the transmission problem (3.114)) as a problem for the trace of the solution posed on the skeleton $\tilde{\Sigma}$.

Proposition 3.38 (**Equivalent interface problem**). *Let $\sigma \in \{0, 1/2, 1\}$. Let $F_\sigma \in \mathbb{U}_\Gamma(\mathrm{D}; \mathcal{P}_\Omega)$ be the (unique) source lifting such that*

$$\begin{cases} (\mathrm{L}_{\mathsf{a}} - {\kappa_0}^2 \mathsf{n}) F_\sigma|_{\Omega_j} = f|_{\Omega_j}, & \text{in } \Omega_j,\ \forall j \in \{1, \dots, J\}, \\ (\gamma_{1,\Gamma} - \mathrm{i}\gamma_{0,\Gamma}) F_\sigma = g, & \text{on } \Gamma, \\ \mathbf{R}^+_{\sigma,\|} \boldsymbol{\gamma}_{\|} F_\sigma = 0, & \text{on } \tilde{\Sigma}. \end{cases} \tag{3.199}$$

Consider the problem

$$\begin{cases} \text{Find } \mathbb{x}_\sigma \in \mathbb{M}_{\sigma,\|}, \\ (\mathrm{Id} - \mathbf{\Pi}_{\|} \mathbf{S}_{\sigma,\|})\, \mathbb{x}_\sigma = \mathbf{\Pi}_{\|} \mathbf{R}^-_{\sigma,\|} \boldsymbol{\gamma}_{\|} F_\sigma. \end{cases} \tag{3.200}$$

If $u \in \mathrm{U}_\Gamma(\mathrm{D}; \Omega)$ is solution of the model problem (3.79), then its trace $\mathbb{x}_\sigma := \mathbf{R}^+_{\sigma,\|} \boldsymbol{\gamma}_{\|} u$ satisfies the interface problem (3.200).

Reciprocally, if $\mathbb{x}_\sigma \in \mathbb{M}_{\sigma,\|}$ is solution of the interface problem (3.200) and if $v_\sigma \in \mathbb{U}_\Gamma(\mathrm{D}; \mathcal{P}_\Omega)$ is the (unique) solution of

$$\begin{cases} (\mathrm{L}_{\mathsf{a}} - {\kappa_0}^2 \mathsf{n}) v_\sigma|_{\Omega_j} = 0, & \text{in } \Omega_j,\ \forall j \in \{1, \dots, J\}, \\ (\gamma_{1,\Gamma} - \mathrm{i}\gamma_{0,\Gamma}) v_\sigma = 0, & \text{on } \Gamma, \\ \mathbf{R}^+_{\sigma,\|} \boldsymbol{\gamma}_{\|} v_\sigma = \mathbb{x}_\sigma, & \text{on } \tilde{\Sigma}, \end{cases} \tag{3.201}$$

then $\mathbb{u} \in \mathbb{U}_\Gamma(\mathrm{D}; \mathcal{P}_\Omega)$ defined as $u_\sigma := v_\sigma + F_\sigma$ is solution of the model problem (3.79).

Proof. Let F_σ be the unique solution (by Assumption 3.28) of (3.199), then it satisfies (3.149). We will rely on the characterization given by Proposition 3.24, which states that $u \in \mathrm{U}_\Gamma(\mathrm{D}, \mathrm{L}_{\mathsf{a}}; \Omega)$ is solution of the model problem (3.79) if, and only if,

$$\boldsymbol{\gamma}_{\|} u \in (\mathbb{C}_{\|} + \boldsymbol{\gamma}_{\|} F_\sigma) \cap \mathbb{S}_{\|}. \tag{3.202}$$

($\Rightarrow$) Let $u \in \mathrm{U}_\Gamma(\mathrm{D}; \Omega)$ be the solution of the model problem (3.79), then $\boldsymbol{\gamma}_{\|} u \in (\mathbb{C}_{\|} + \boldsymbol{\gamma}_{\|} F_\sigma) \cap \mathbb{S}_{\|}$. From Propositions 3.30 and 3.37 we have

$$\begin{cases} \boldsymbol{\gamma}_{\|}(u - F_\sigma) \in \mathbb{C}_{\|}, \\ \boldsymbol{\gamma}_{\|} u \in \mathbb{S}_{\|}, \end{cases} \quad \Leftrightarrow \quad \begin{cases} \mathbf{R}^-_{\sigma,\|} \boldsymbol{\gamma}_{\|}(u - F_\sigma) = \mathbf{S}_{\sigma,\|} \mathbf{R}^+_{\sigma,\|} \boldsymbol{\gamma}_{\|}(u - F_\sigma), \\ \mathbf{R}^+_{\sigma,\|} \boldsymbol{\gamma}_{\|} u = \mathbf{\Pi}_{\|} \mathbf{R}^-_{\sigma,\|} \boldsymbol{\gamma}_{\|} u. \end{cases} \tag{3.203}$$

Hence using $\mathbf{R}^+_{\sigma,\|} \boldsymbol{\gamma}_{\|} F_\sigma = 0$ from (3.199) we deduce

$$\begin{cases} \mathbf{R}^-_{\sigma,\|} \boldsymbol{\gamma}_{\|} u = \mathbf{S}_{\sigma,\|} \mathbf{R}^+_{\sigma,\|} \boldsymbol{\gamma}_{\|} u + \mathbf{R}^-_{\sigma,\|} \boldsymbol{\gamma}_{\|} F_\sigma, \\ \mathbf{R}^+_{\sigma,\|} \boldsymbol{\gamma}_{\|} u = \mathbf{\Pi}_{\|} \mathbf{R}^-_{\sigma,\|} \boldsymbol{\gamma}_{\|} u. \end{cases} \tag{3.204}$$

Eliminating $\mathbf{R}^-_{\sigma,\|} \boldsymbol{\gamma}_{\|} u$ it is then immediate that

$$\mathbf{R}^+_{\sigma,\|} \boldsymbol{\gamma}_{\|} u = \mathbf{\Pi}_{\|} \mathbf{S}_{\sigma,\|} \mathbf{R}^+_{\sigma,\|} \boldsymbol{\gamma}_{\|} u + \mathbf{\Pi}_{\|} \mathbf{R}^-_{\sigma,\|} \boldsymbol{\gamma}_{\|} F_\sigma, \tag{3.205}$$

hence its trace $\mathbb{x}_\sigma := \mathbf{R}^+_{\sigma,\|} \boldsymbol{\gamma}_{\|} u$ satisfies the interface problem (3.200).

($\Leftarrow$) Reciprocally, let $\mathbb{x}_\sigma \in \mathbb{M}_{\sigma,\|}$ be solution of the interface problem (3.200) and let $v_\sigma \in \mathbb{U}_\Gamma(\mathrm{D};\mathcal{P}_\Omega)$ be the unique solution (by Assumption 3.28) to (3.201). Then, by definition of the Cauchy trace space $\mathbb{C}_\|$ (Definition 3.18), its trace $\boldsymbol{\gamma}_\| v_\sigma \in \mathbb{C}_\|$. If we set $u_\sigma := v_\sigma + F_\sigma$, we readily obtain $\boldsymbol{\gamma}_\|(u_\sigma - F_\sigma) \in \mathbb{C}_\|$. Besides, using $\mathbb{x}_\sigma = \mathbf{R}^+_{\sigma,\|}\boldsymbol{\gamma}_\| v_\sigma$ from (3.201), we rewrite (3.200) as

$$(\mathrm{Id} - \boldsymbol{\Pi}_\| \mathbf{S}_{\sigma,\|})\,\mathbb{x}_\sigma = \boldsymbol{\Pi}_\| \mathbf{R}^-_{\sigma,\|}\boldsymbol{\gamma}_\| F_\sigma, \qquad \Leftrightarrow \qquad (\mathrm{Id} - \boldsymbol{\Pi}_\| \mathbf{S}_{\sigma,\|})\,\mathbf{R}^+_{\sigma,\|}\boldsymbol{\gamma}_\| v_\sigma = \boldsymbol{\Pi}_\| \mathbf{R}^-_{\sigma,\|}\boldsymbol{\gamma}_\| F_\sigma. \tag{3.206}$$

Using Proposition 3.30 we get

$$\mathbf{R}^+_{\sigma,\|}\boldsymbol{\gamma}_\| v_\sigma - \boldsymbol{\Pi}_\| \mathbf{R}^-_{\sigma,\|}\boldsymbol{\gamma}_\| v_\sigma = \boldsymbol{\Pi}_\| \mathbf{R}^-_{\sigma,\|}\boldsymbol{\gamma}_\| F_\sigma. \tag{3.207}$$

Finally, using the fact that $\mathbf{R}^+_{\sigma,\|}\boldsymbol{\gamma}_\| F_\sigma = 0$ from (3.199) and the definition of u_σ yield

$$\mathbf{R}^+_{\sigma,\|}\boldsymbol{\gamma}_\| u_\sigma = \boldsymbol{\Pi}_\| \mathbf{R}^-_{\sigma,\|}\boldsymbol{\gamma}_\| u_\sigma. \tag{3.208}$$

Proposition 3.37 then gives $\boldsymbol{\gamma}_\| u_\sigma \in \mathbb{S}_\|$. Finally we indeed have $\boldsymbol{\gamma}_\| u_\sigma \in (\mathbb{C}_\| + \boldsymbol{\gamma}_\| F_\sigma) \cap \mathbb{S}_\|$. ■

Remark 3.39. *It is perhaps worth mentioning an alternative equivalent interface problem, exchanging the order of composition of* $\mathbf{S}_{\sigma,\|}$ *and* $\boldsymbol{\Pi}_\|$*. Let* $\sigma \in \{0, 1/2, 1\}$ *and consider instead the alternative interface problem*

$$\begin{cases} \text{Find } \mathbb{x}_\sigma \in \mathbb{M}_{\sigma,\|}, \\ (\mathrm{Id} - \mathbf{S}_{\sigma,\|}\boldsymbol{\Pi}_\|)\,\mathbb{x}_\sigma = \mathbf{R}^-_{\sigma,\|}\boldsymbol{\gamma}_\| F_\sigma. \end{cases} \tag{3.209}$$

If $u \in \mathrm{U}_\Gamma(\mathrm{D};\Omega)$ *is solution of the model problem* (3.79)*, then its trace* $\mathbb{x}_\sigma := \mathbf{R}^-_{\sigma,\|}\boldsymbol{\gamma}_\| u$ *satisfies the interface problem* (3.209)*. Reciprocally, if* $\mathbb{x}_\sigma \in \mathbb{M}_{\sigma,\|}$ *is solution of the interface problem* (3.209) *and if* $v_\sigma \in \mathbb{U}_\Gamma(\mathrm{D};\mathcal{P}_\Omega)$ *is the (unique) solution of* (3.201) *then* $\mathbb{u} \in \mathbb{U}_\Gamma(\mathrm{D};\mathcal{P}_\Omega)$ *defined as* $u_\sigma := v_\sigma + F_\sigma$ *is solution of the model problem* (3.79)*.*

While the choice of using (3.200) *or* (3.209) *in a practical implementation is not really important, taking* $\sigma = 1$ *rather than* $\sigma = 0$ *or* $\sigma = 1/2$ *has important impacts that we shall discuss in the following.*

3.2.4.5 Block diagonal transmission operators

We now investigate the particular case of *block diagonal* transmission operators. We emphasize that this sub-case is in fact the *only case of practical interest* as any other alternative would prevent us to get any parallelization of the domain decomposition algorithm. It is interesting to note though that the theory does not rest on this assumption. As a result one would typically imposes the following additional requirement (which is not restrictive) on the transmission operators.

Assumption 3.40 (Block diagonal transmission operators). *The operators* $\mathbf{Z}$ *and* $\mathbf{T}_{\sigma,\|}$*,* $\sigma \in \{-1/2, 0, 1/2, 1\}$*, viewed as operator matrices of size* $\operatorname{card}\mathbb{J} \times \operatorname{card}\mathbb{J}$*, are diagonal*

$$\begin{aligned} \mathbf{Z} &= \mathit{diag}_{(j,k)\in\mathbb{J}}\left(\mathbf{Z}^{jk}\right), \\ \mathbf{T}_{\sigma,\|} &= \mathit{diag}_{(j,k)\in\mathbb{J}}\left(\mathbf{T}^{jk}_{\sigma,\|}\right), \end{aligned} \tag{3.210}$$

where, for all $(j,k) \in \mathbb{J}$*, we have*

$$\begin{aligned} \mathbf{T}^{jk}_{0,\|} &: \mathrm{X}_0(\Gamma_{jk}) \to \mathrm{X}_1(\Gamma_{jk}), & \mathbf{T}^{jk}_{1/2,\|} &: \mathrm{X}_0(\Gamma_{jk}) \to \mathrm{X}_{1/2}(\Gamma_{jk}), \\ \mathbf{T}^{jk}_{1,\|} &: \mathrm{X}_1(\Gamma_{jk}) \to \mathrm{X}_0(\Gamma_{jk}), & \mathbf{T}^{jk}_{-1/2,\|} &: \mathrm{X}_1(\Gamma_{jk}) \to \mathrm{X}_{1/2}(\Gamma_{jk}), \end{aligned} \tag{3.211}$$

and

$$\mathbf{Z}^{jk} : \mathrm{X}_0(\Gamma_{jk}) \to \mathrm{X}_1(\Gamma_{jk}). \tag{3.212}$$

We provide two examples of a (block) diagonal transmission operator in Figure 3.4. These sketches correspond to the bottom and top-right geometrical configurations that are given in Figure 3.1c. The non-zero operators are represented by the hatched areas.

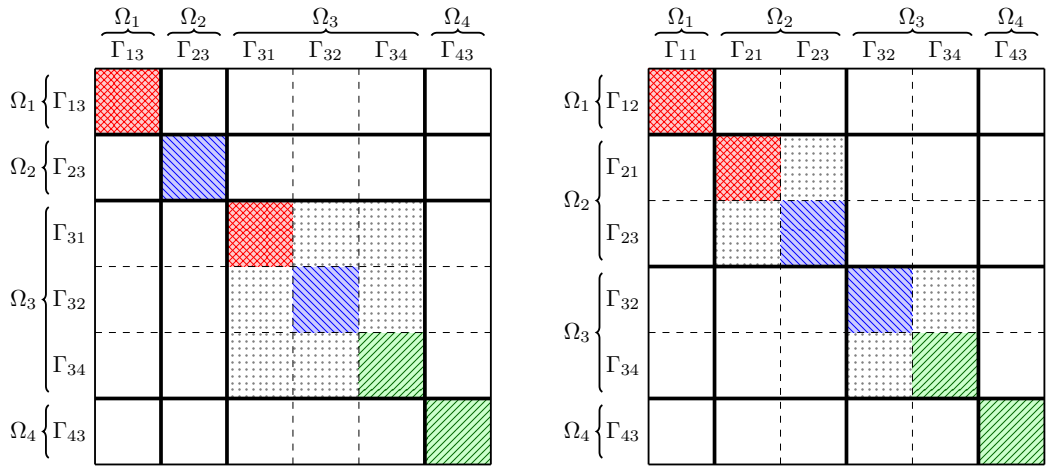

(a) Top right geometric partition in Figure 3.1c. (b) Bottom geometric partition in Figure 3.1c.

Figure 3.4: Sketch of the operator matrix of diagonal transmission operators. The non-zero operators are featured by the hatched areas. When the hatching pattern and color match, the operators are equal in order to satisfy Assumption 3.36 as stated in Proposition 3.41.

We can then give a sufficient condition on the elements of the transmission operators in order to satisfy Assumption 3.36.

Proposition 3.41. *Suppose that Assumption 3.40 holds. If each diagonal elements of* $\mathbf{Z}$ *and* $\mathbf{T}_{\sigma,\|}$, $\sigma \in \{0, 1/2, 1\}$, *satisfy*

$$\begin{aligned} \mathbf{Z}^{jk} &= -\mathbf{Z}^{kj}, \qquad \forall (j,k) \in \mathbb{J}, \qquad j < k, \\ \mathbf{T}^{jk}_{\sigma,\|} &= \mathbf{T}^{kj}_{\sigma,\|}, \qquad \forall (j,k) \in \mathbb{J}, \qquad j < k, \end{aligned} \tag{3.213}$$

and for all $(j,k) \in \mathbb{J}$, $\mathbf{Z}^{jk}$ *is symmetric, then Assumption 3.36 is satisfied.*

To represent (block) operators that shall be equal in order to satisfy Assumption 3.36, we used identical hatching patterns and colors in the sketch of the transmission operator given in Figure 3.4.

Remark 3.42. *One could argue that considering diagonal operators of the form of* (3.210)*, is too restrictive. Indeed, we could instead consider each* $\mathbf{Z}$ *and* $\mathbf{T}_{\sigma,\|}$, $\sigma \in \{-1/2, 0, 1/2, 1\}$ *to be* block *diagonal, with* J *blocks, where each non-zero block would be local to a single sub-domain and of size* $\operatorname{card} \mathbb{K}_j \times \operatorname{card} \mathbb{K}_j$, *for each* $j \in \{1, \dots, J\}$. *Such an operator would increase the filling in the transmission matrix. This is represented in Figure 3.4 in the example configuration by the dotted area. It is then possible to show that the algorithm remains with the same parallel structure (albeit with a possible extra computational cost). However, to satisfy Assumption 3.36, one must have*

$$\begin{aligned} (\mathbf{Z})_{(j,k),\,(m,n)} &= -(\mathbf{Z})_{(k,j),\,(n,m)}, \qquad \forall (j,k),(m,n) \in \mathbb{J}^2, \\ (\mathbf{T}_{\sigma,\|})_{(j,k),\,(m,n)} &= (\mathbf{T}_{\sigma,\|})_{(k,j),\,(n,m)}, \qquad \forall (j,k),(m,n) \in \mathbb{J}^2. \end{aligned} \tag{3.214}$$

The condition (3.213) *written for a block diagonal operator, then shows that only the pure diagonal elements,* $(\mathbf{Z})_{(j,k),\,(j,k)}$ *and* $(\mathbf{T}_{\sigma,\parallel})_{(j,k),\,(j,k)}$ *for* $(j,k) \in \mathbb{J}$*, can be non-zero. In the illustration of Figure 3.4 this means that the dotted area needs to be identically zero.*

Furthermore, the diagonal structure of the transmission operators implies a diagonal structure for the scattering operator. To see that we first introduce local versions of the Robin operators at an interface.

Definition 3.43 (Local generalized Robin operators). *For each* $\sigma \in \{0, 1/2, 1\}$ *and* $(j,k) \in \mathbb{J}$*, we introduce the local operators,*

$$\mathbf{R}^{jk,\pm}_{\sigma,\parallel} : \mathrm{X}(\Gamma_{jk}) \to \mathrm{X}_\sigma(\Gamma_{jk}),$$
$$\mathrm{x} \equiv (\mathrm{x}_0, \mathrm{x}_1) \mapsto \begin{cases} \pm\mathbf{T}^{jk}_{1,\parallel}\left(\mathrm{x}_1 + \mathbf{Z}^{jk}\mathrm{x}_0\right) - \mathrm{i}\mathrm{x}_0, & \text{if } \sigma = 0, \\ \pm\mathbf{T}^{jk}_{-1/2,\parallel}\left(\mathrm{x}_1 + \mathbf{Z}^{jk}\mathrm{x}_0\right) - \mathrm{i}\mathbf{T}^{jk}_{1/2,\parallel}\mathrm{x}_0, & \text{if } \sigma = 1/2, \\ \pm\left(\mathrm{x}_1 + \mathbf{Z}^{jk}\mathrm{x}_0\right) - \mathrm{i}\mathbf{T}^{jk}_{0,\parallel}\mathrm{x}_0, & \text{if } \sigma = 1, \end{cases} \tag{3.215}$$

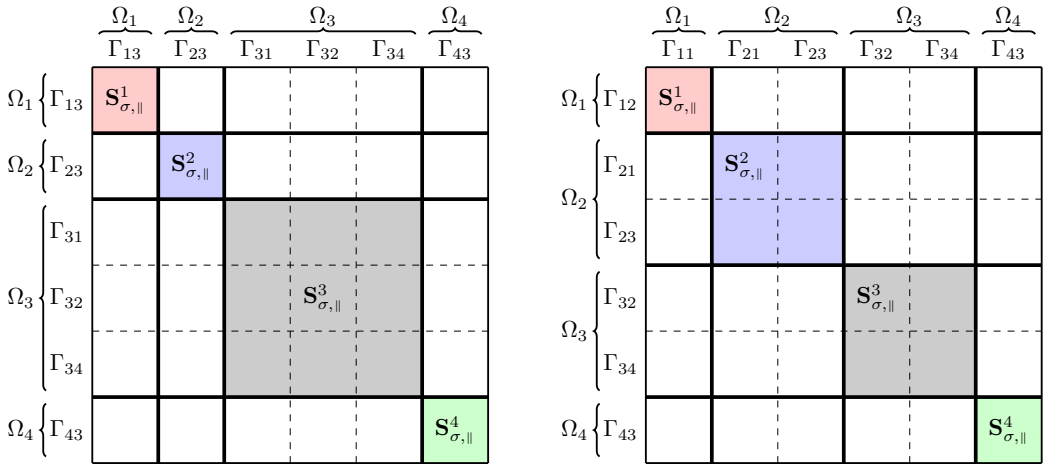

(a) Top right geometric partition in Figure 3.1c. (b) Bottom geometric partition in Figure 3.1c.

Figure 3.5: Sketch of the operator matrix of diagonal scattering operators. The non-zero operators are featured by the shaded areas.

Then, for each $\sigma \in \{0, 1/2, 1\}$, we have

$$\mathbf{S}_{\sigma,\parallel} = \mathrm{diag}_{j\in\{1,\ldots,J\}}\left(\mathbf{S}^j_{\sigma,\parallel}\right), \tag{3.216}$$

where the local scattering operators are given in the following definition.

Note that the level of element granularity for the scattering operator viewed as an operator matrix is not the same as for the transmission operators. There are $\mathrm{card}\,\mathbb{J}$ elements on the diagonal of the transmission operators, while there are J elements on the diagonal of the scattering operator. Each diagonal element $\mathbf{S}^j_{\sigma,\parallel}$, $j \in \{1,\ldots,J\}$ is itself of size $\mathrm{card}\,\mathbb{K}_j \times \mathrm{card}\,\mathbb{K}_j$.

Definition 3.44 (**Local scattering operator**). *For each $\sigma \in \{0, 1/2, 1\}$ and $j \in \{1, \dots, J\}$, we define the local scattering operators,*

$$\begin{aligned} \mathbf{S}^j_{\sigma,\|} \ : \ & \bigtimes_{k\in\mathbb{K}_j} \mathrm{X}_\sigma(\Gamma_{jk}) \to \bigtimes_{k\in\mathbb{K}_j} \mathrm{X}_\sigma(\Gamma_{jk}), \\ & \big(\mathrm{x}^{jk}_\sigma\big)_{k\in\mathbb{K}_j} \mapsto \Big(\mathbf{R}^{jk,-}_{\sigma,\|}\ \gamma_{\Gamma_{jk}}\, u_{\sigma,j}\Big)_{k\in\mathbb{K}_j}, \end{aligned} \tag{3.217}$$

where, for all $j \in \{1, \dots, J\}$, $u_{\sigma,j} \in \mathrm{U}_\Gamma(\mathrm{D}; \Omega_j)$ is such that

$$\begin{cases} (\mathrm{L}_{\mathsf{a}} - {\kappa_0}^2 \mathsf{n}) u_{\sigma,j} = 0, & \text{in } \Omega_j, \\ (\gamma_{1,\Gamma} - \mathrm{i}\gamma_{0,\Gamma}) u_{\sigma,j} = 0, & \text{on } \Gamma, \\ \mathbf{R}^{jk,+}_{\sigma,\|}\ \gamma_{\Gamma_{jk}}\, u_{\sigma,j} = \mathrm{x}^{jk}_\sigma, & \text{on } \Gamma_{jk},\ \forall k \in \mathbb{K}_j. \end{cases} \tag{3.218}$$

It is now clear that applying the scattering operator consists in solving local problems locally in each sub-domain (hence hopefully in parallel), thereby insuring that the PDE is satisfied locally. It is the exchange operator that couples all sub-domains together by exchanging information, thereby insuring the global continuity of the solution.

Besides, we note that satisfying Assumption 3.28 now amounts to satisfy the following assumption, and we shall provide in Section 3.4 sufficient conditions to satisfy it.

Assumption 3.45 (**Well-posedness of local sub-problems**). *For each $\sigma \in \{0, 1/2, 1\}$, $j \in \{1, \dots, J\}$ and for any $\big(\mathrm{x}^{jk}_\sigma\big)_{k\in\mathbb{K}_j} \in \bigtimes_{k\in\mathbb{K}_j} \mathrm{X}_\sigma(\Gamma_{jk})$, $f \in L^2(\Omega)^{m_0}$, $g \in L^2(\Gamma)^{m_0}$, the transmission operators are such that the following local sub-problems are well-defined:*

$$\begin{cases} \text{Find } u_{\sigma,j} \in \mathrm{U}_\Gamma(\mathrm{D}; \Omega_j) \text{ such that} & \\ (\mathrm{L}_{\mathsf{a}} - {\kappa_0}^2 \mathsf{n}) u_{\sigma,j} = f|_{\Omega_j}, & \text{in } \Omega_j, \\ (\gamma_{1,\Gamma} - \mathrm{i}\gamma_{0,\Gamma}) u_{\sigma,j} = g, & \text{on } \Gamma_j \cap \Gamma, \\ \mathbf{R}^{jk,+}_{\sigma,\|}\ \gamma_{\Gamma_{jk}}\, u_{\sigma,j} = \mathrm{x}^{jk}_\sigma, & \text{on } \Gamma_{jk},\ \forall k \in \mathbb{K}_j. \end{cases} \tag{3.219}$$

If the transmission operator is diagonal, one can rewrite the equation (3.200), for $\sigma = 1$ for instance, in the more usual form of the following transmission problem

$$\begin{cases} \text{Find } \mathfrak{u} \in \mathbb{U}_\Gamma(\mathrm{D}; \mathcal{P}_\Omega) \text{ such that :} & \\ (\mathrm{L}_{\mathsf{a}} - {\kappa_0}^2 \mathsf{n}) u|_{\Omega_j} = f|_{\Omega_j}, & \text{in } \Omega_j,\ \forall j \in \{1, \dots, J\}, \\ (\gamma_{1,\Gamma} - \mathrm{i}\gamma_{0,\Gamma}) u = g, & \text{on } \Gamma, \\ \Big(+ \gamma_{1,\Gamma_{jk}} + (\mathbf{Z}^{jk} - \mathrm{i}\mathbf{T}^{jk}_{0,\|}) \gamma_{0,\Gamma_{jk}} \Big) u|_{\Omega_j} & \\ \qquad = \Big(- \gamma_{1,\Gamma_{kj}} + (\mathbf{Z}^{jk} - \mathrm{i}\mathbf{T}^{jk}_{0,\|}) \gamma_{0,\Gamma_{kj}} \Big) u|_{\Omega_k} & \text{on } \Gamma_{jk},\ \forall (j,k) \in \mathbb{J}. \end{cases} \tag{3.220}$$

3.3 Iterative domain decomposition methods

Our reformulation of the model problem (3.79) in the form of the interface problem (3.200) would be pointless if it was not easier to solve. Provided the transmission operators are diagonal, multiple local sub-problems are hidden behind the problem (3.200), which are however still coupled. This is why to provide an actual practical way of computing a solution, we need to resort to iterative solvers. Such solvers will involve solving independently (hence hopefully in parallel) the local sub-problems at each iteration (using the information of the previous iteration). The update of the source terms of the local sub-problems will happen in between each iteration with an actual exchange or communication of information between sub-domains.

3.3.1 Iterative algorithm

Let $\sigma \in \{0, 1/2, 1\}$, F_σ be the solution of (3.199), and define

$$\mathbb{b}_\sigma := \mathbf{\Pi}_\shortparallel \mathbf{R}^-_{\sigma,\shortparallel} \boldsymbol{\gamma}_\shortparallel F_\sigma. \tag{3.221}$$

In this section, we want to devise (and study the convergence of) an algorithm to solve

$$\begin{cases} \text{Find } \mathbb{x}_\sigma \in \mathbb{M}_{\sigma,\shortparallel} \text{ such that,} \\ (\mathrm{Id} - \mathbf{\Pi}_\shortparallel \mathbf{S}_{\sigma,\shortparallel})\, \mathbb{x}_\sigma = \mathbb{b}_\sigma. \end{cases} \tag{3.222}$$

Recall that, according to Proposition 3.24, having found such a $\mathbb{x}_\sigma$ solution of (3.222), the global volume solution of the model problem (3.79) can be computed as

$$u_\sigma := v_\sigma + F_\sigma, \tag{3.223}$$

where $v_\sigma \in \mathbb{U}_\Gamma(\mathrm{D}; \mathcal{P}_\Omega)$ is such that

$$\begin{cases} (\mathrm{L}_\mathsf{a} - {\kappa_0}^2 \mathsf{n}) v_\sigma|_{\Omega_j} = 0, & \text{in } \Omega_j,\ \forall j \in \{1, \dots, J\}, \\ (\gamma_{1,\Gamma} - \mathrm{i}\gamma_{0,\Gamma}) v_\sigma = 0, & \text{on } \Gamma, \\ \mathbf{R}^+_{\sigma,\shortparallel} \boldsymbol{\gamma}_\shortparallel v_\sigma = \mathbb{x}_\sigma, & \text{on } \tilde{\Sigma}, \end{cases} \tag{3.224}$$

which is well-posed according to Assumption 3.28.

Relaxed Jacobi algorithm One of the simplest iterative method to solve (3.222) is the (relaxed) Jacobi algorithm. Let $\mathbb{x}^0_\sigma \in \mathbb{M}_{\sigma,\shortparallel}$ and a relaxation parameter $0 < r \leq 1$ be given, a sequence $(\mathbb{x}^n_\sigma)_{n\in\mathbb{N}}$ in $\mathbb{M}_{\sigma,\shortparallel}$ is constructed using the (relaxed) Jacobi algorithm as follows

$$\mathbb{x}^{n+1}_\sigma = [(1-r)\mathrm{Id} + r\mathbf{\Pi}_\shortparallel \mathbf{S}_{\sigma,\shortparallel}]\, \mathbb{x}^n_\sigma + r\, \mathbb{b}_\sigma, \qquad n \in \mathbb{N}. \tag{3.225}$$

The standard Jacobi algorithm can be recovered by setting $r = 1$. Constructing this sequence of traces also constructs a sequence of broken solutions $(v^n_\sigma)_{n\in\mathbb{N}}$ in $\mathbb{U}_\Gamma(\mathrm{D}; \mathcal{P}_\Omega)$ when the action of $\mathbf{S}_{\sigma,\shortparallel}$ is computed. For each $n \in \mathbb{N}$ the broken solution v^n_σ satisfy

$$\begin{cases} (\mathrm{L}_\mathsf{a} - {\kappa_0}^2 \mathsf{n}) v^n_\sigma|_{\Omega_j} = 0, & \text{in } \Omega_j,\ \forall j \in \{1, \dots, J\}, \\ (\gamma_{1,\Gamma} - \mathrm{i}\gamma_{0,\Gamma}) v^n_\sigma = 0, & \text{on } \Gamma, \\ \mathbf{R}^+_{\sigma,\shortparallel} \boldsymbol{\gamma}_\shortparallel v^n_\sigma = \mathbb{x}^n_\sigma, & \text{on } \tilde{\Sigma}. \end{cases} \tag{3.226}$$

The true solution of the original problem is then (hopefully, if convergence occurs) the limit of the broken solutions $(u^n_\sigma := v^n_\sigma + F_\sigma)_{n\in\mathbb{N}}$ in $\mathbb{U}_\Gamma(\mathrm{D}; \mathcal{P}_\Omega)$.

Remark 3.46. *While it might not be immediate to see, the algorithm* (3.225) *deserves to be referred to as a (relaxed) Jacobi algorithm — in the parlance of iterative solvers for linear systems — when the operators are viewed as operator matrices of size $J \times J$. Indeed,* Id *and $\mathbf{\Pi}_\shortparallel \mathbf{S}_{\sigma,\shortparallel}$ are respectively the diagonal and off-diagonal parts of the full operator* $\mathrm{Id} - \mathbf{\Pi}_\shortparallel \mathbf{S}_{\sigma,\shortparallel}$. *To see why, recall that $\mathbf{S}_{\sigma,\shortparallel}$ is diagonal (independent solves in each sub-domains) and $\mathbf{\Pi}_\shortparallel$ has only off-diagonal elements (a sub-domain does not exchange with itself).*

3.3.2 Convergence analysis

We now turn to the convergence analysis of the previously described iterative method.

3.3.2.1 A particular choice of scalar product

We have equipped our multi-trace spaces with the norm stemming from the Cartesian product structure of the multi-trace space. In this sub-section, we introduce different, albeit equivalent, norms.

Scalar products Unless stated otherwise, we shall assume in the following that Assumption 3.47 holds.

Assumption 3.47. *We suppose that the transmission operators are* positive definite isomorphisms *between the multi-trace spaces. In addition, we suppose to have the following relations*

$$\mathbf{T}_{0,\|} = \mathbf{T}^*_{1/2,\|}\mathbf{T}_{1/2,\|}, \qquad \mathbf{T}^*_{1/2,\|} = \left(\mathbf{T}_{-1/2,\|}\right)^{-1}, \qquad \textit{and} \qquad \mathbf{T}_{1,\|} = \left(\mathbf{T}_{0,\|}\right)^{-1}. \tag{3.227}$$

It is implicit from Assumption 3.47 that the operators $\mathbf{T}_{0,\|}$ and $\mathbf{T}_{1,\|}$ are supposed to be *self-adjoint*.

We can equip the multi-trace spaces $\mathbb{M}_{0,\|}$, $\mathbb{M}_{1,\|}$ and $\mathbb{M}_{1/2,\|}$ and $\mathbb{M}_{\|}$ respectively with the following scalar products

$$\begin{aligned}
&\mathrm{t}_{0,\|}(\mathbb{x}_0, \mathbb{y}_0) := \langle\!\langle \mathbf{T}_{0,\|}\mathbb{x}_0, \overline{\mathbb{y}_0} \rangle\!\rangle_{\|}, && \forall \mathbb{x}_0, \mathbb{y}_0 \in \mathbb{M}_{0,\|},\\
&\mathrm{t}_{1,\|}(\mathbb{x}_1, \mathbb{y}_1) := \langle\!\langle \mathbb{y}_1, \mathbf{T}_{1,\|}\overline{\mathbb{x}_1} \rangle\!\rangle_{\|}, && \forall \mathbb{x}_1, \mathbb{y}_1 \in \mathbb{M}_{1,\|},\\
&\mathrm{t}_{1/2,\|}(\mathbb{x}_{1/2}, \mathbb{y}_{1/2}) = \langle\!\langle (\mathbf{T}_{-1/2,\|})^{-1}\mathbb{x}_{1/2},\ (\mathbf{T}_{1/2,\|})^{-1}\overline{\mathbb{y}_{1/2}} \rangle\!\rangle_{\|}, && \forall \mathbb{x}_{1/2}, \mathbb{y}_{1/2} \in \mathbb{M}_{1/2,\|}.
\end{aligned} \tag{3.228}$$

Norms We can then endow the multi-trace spaces $\mathbb{M}_{0,\|}$, $\mathbb{M}_{1,\|}$ and $\mathbb{M}_{1/2,\|}$with the norms induced by the previous scalar products. Hence we define

$$\begin{aligned}
&\|\mathbb{x}_0\|^2_{\mathbf{T}_{0,\|}} := \mathrm{t}_{0,\|}(\mathbb{x}_0, \mathbb{x}_0), && \forall \mathbb{x}_0 \in \mathbb{M}_{0,\|},\\
&\|\mathbb{x}_1\|^2_{\mathbf{T}_{1,\|}} := \mathrm{t}_{1,\|}(\mathbb{x}_1, \mathbb{x}_1), && \forall \mathbb{x}_1 \in \mathbb{M}_{1,\|},\\
&\|\mathbb{x}_{1/2}\|^2_{\mathbf{T}_{1/2,\|}} := \mathrm{t}_{1/2,\|}(\mathbb{x}_{1/2}, \mathbb{x}_{1/2}), && \forall \mathbb{x}_{1/2} \in \mathbb{M}_{1/2,\|}.
\end{aligned} \tag{3.229}$$

Remark 3.48. *Since the transmission operators are supposed to be continuous and coercive (by assumption 3.47), the norms defined in* (3.229) *are equivalent to the ones previously defined in* (3.125)*.*

3.3.2.2 A sufficient condition for convergence

The previous problem can be recast in the following abstract framework. Let V be a Hilbert space, $A : V \to V$ and $b \in V$. We are set to solve

$$(\mathrm{Id} - A)x = b. \tag{3.230}$$

The problem is formally related to the convergence of the following Neumann series

$$x = (\mathrm{Id} - A)^{-1}b = \sum_{n=0}^{+\infty} A^n b, \tag{3.231}$$

which is known to converge provided A is bounded and a *strict* contraction $\|A\|_V < 1$ in V. The following proposition, adapted from [42, Th. 6], provides weaker sufficient conditions for the convergence of the abstract interface problem (3.230).

Proposition 3.49. *Let V be a Hilbert space endowed with a norm $\|\cdot\|_V$. Let $x^0 \in V \setminus \{0\}$, $0 < r < 1$ and define the sequence*

$$x^{n+1} = ((1-r)\mathrm{Id} + rA)\, x^n, \qquad n \in \mathbb{N}. \tag{3.232}$$

If the following two assumptions hold true

- $\mathrm{Id} - A$ *is* injective *in V;*
- A *is a* contraction *in V;*

then the relaxed Jacobi algorithm (3.232) *converges to 0 in V.*

Proof. The convexity of $x \mapsto \|x\|_V^2$ yields the identity for any $x, y \in V$, with $0 \le r \le 1$,

$$\|(1-r)x + ry\|_V^2 = (1-r)\|x\|_V^2 + r\|y\|_V^2 - r(1-r)\|x-y\|_V^2. \tag{3.233}$$

Let $n \in \mathbb{N}$, using the above identity with $x = x^n$ and $y = Ax^n$ we get

$$\|x^{n+1}\|_V^2 = (1-r)\|x^n\|_V^2 + r\|Ax^n\|_V^2 - r(1-r)\|x^n - Ax^n\|_V^2. \tag{3.234}$$

Since A is a contraction in V we have for all $x \in V$,

$$\|Ax\|_V \le \|x\|_V. \tag{3.235}$$

It follows that

$$\|x^{n+1}\|_V^2 \le \|x^n\|_V^2 - r(1-r)\|x^n - Ax^n\|_V^2, \tag{3.236}$$

so that the sequence $(x^n)_{n\in\mathbb{N}}$ is non-increasing. Furthermore,

$$r(1-r)\|x^n - Ax^n\|_V^2 \le \|x^n\|_V^2 - \|x^{n+1}\|_V^2, \tag{3.237}$$

and we deduce that for any $N \in \mathbb{N}$,

$$r(1-r)\sum_{n=0}^{N} \|(\mathrm{Id} - A)x^n\|_V^2 \le \|x^0\|_V^2 - \|x^{N+1}\|_V^2 \le \|x^0\|_V^2, \tag{3.238}$$

and (since in addition $0 < r < 1$) the series

$$\sum_{n=0}^{\infty} \|(\mathrm{Id} - A)x^n\|_V^2 < +\infty, \tag{3.239}$$

is finite. We therefore conclude to the strong convergence of $((\mathrm{Id} - A)x^n)_{n\in\mathbb{N}}$ to 0, and thereby to its weak convergence: for any $y \in V$,

$$((\mathrm{Id} - A)x^n, y)_V \to 0, \qquad \text{as } n \to \infty. \tag{3.240}$$

Besides, from the boundedness of the sequence $(x^n)_{n\in\mathbb{N}}$ we also deduce that it admits a sub-sequence, still denoted $(x^n)_{n\in\mathbb{N}}$, that converges weakly, say to an element x of V. For any $y \in V$, we get

$$((\mathrm{Id} - A)x^n, y)_V = (x^n, (\mathrm{Id} - A)^* y)_V \to (x, (\mathrm{Id} - A)^* y)_V, \qquad \text{as } n \to \infty. \tag{3.241}$$

Finally, from (3.240) and (3.241), we have for any $y \in V$,

$$(x, (\mathrm{Id} - A)^* y)_V = ((\mathrm{Id} - A)x, y)_V = 0, \tag{3.242}$$

and the injectivity of $\mathrm{Id} - A$ yields $x = 0$. Since the limit is independent of the sub-sequence, the whole sequence converges (to 0). ∎

If we set $A = \mathbf{\Pi}_{\shortparallel}\mathbf{S}_{\sigma,\shortparallel}$ and $V = \mathbb{M}_{\sigma,\shortparallel}$, the purpose of the next few results is to verify that the assumptions of the previous abstract proposition are satisfied in our particular case. We start with the injectivity assumption which is a direct consequence of the following lemma.

Lemma 3.50. *Let $\sigma \in \{0, 1/2, 1\}$ and $\mathbb{b}_\sigma \in \mathbb{M}_{\sigma,\shortparallel}$. Consider the two problems*

$$\begin{cases} \text{Find } \mathbb{x}_\sigma \in \mathbb{M}_{\sigma,\shortparallel} \text{ such that}: \\ (\mathrm{Id} - \mathbf{\Pi}_{\shortparallel}\mathbf{S}_{\sigma,\shortparallel})\,\mathbb{x}_\sigma = \mathbb{b}_\sigma, \end{cases} \tag{3.243}$$

and

$$\begin{cases} \text{Find } \mathbb{y} \in \mathbb{C}_{\shortparallel} \text{ such that}: \\ \left(\mathbf{R}^+_{\sigma,\shortparallel} - \mathbf{\Pi}_{\shortparallel}\mathbf{R}^-_{\sigma,\shortparallel}\right)\mathbb{y} = \mathbb{b}_\sigma. \end{cases} \tag{3.244}$$

If $\mathbb{x}_\sigma \in \mathbb{M}_{\sigma,\shortparallel}$ is solution to the problem (3.243)*, then there exists $\mathbb{y} \in \mathbb{C}_{\shortparallel}$ solution to the problem* (3.244) *such that $\mathbb{x}_\sigma = \mathbf{R}^+_{\sigma,\shortparallel}\mathbb{y}$.*

Reciprocally, if $\mathbb{y} \in \mathbb{C}_{\shortparallel}$ is solution to the problem (3.244) *then $\mathbb{x}_\sigma = \mathbf{R}^+_{\sigma,\shortparallel}\mathbb{y} \in \mathbb{M}_{\sigma,\shortparallel}$ is solution to the problem* (3.243)*.*

Proof. Let $\sigma \in \{0, 1/2, 1\}$ and $\mathbb{b}_\sigma \in \mathbb{M}_{\sigma,\shortparallel}$.

($\Rightarrow$) Suppose to have $\mathbb{x}_\sigma \in \mathbb{M}_{\sigma,\shortparallel}$ a solution to the problem (3.243) and let $u_\sigma \in \mathbb{U}_\Gamma(\mathrm{D};\mathcal{P}_\Omega)$ be such that

$$\begin{cases} (\mathsf{L_a} - \kappa_0{}^2\mathsf{n})u_\sigma|_{\Omega_j} = 0, & \text{in } \Omega_j,\ \forall j \in \{1,\dots,J\}, \\ (\gamma_{1,\Gamma} - \mathrm{i}\gamma_{0,\Gamma})u_\sigma = 0, & \text{on } \Gamma, \\ \mathbf{R}^+_{\sigma,\shortparallel}\boldsymbol{\gamma}_{\shortparallel}u_\sigma = \mathbb{x}_\sigma, & \text{on } \tilde{\Sigma}, \end{cases} \tag{3.245}$$

which is well defined thanks to Assumption 3.28 and set

$$\mathbb{y} := \boldsymbol{\gamma}_{\shortparallel}u_\sigma \in \mathbb{M}_{\shortparallel}, \qquad \text{so that by construction} \qquad \mathbb{x}_\sigma = \mathbf{R}^+_{\sigma,\shortparallel}\mathbb{y}. \tag{3.246}$$

By Definition 3.18 of the Cauchy trace space $\mathbb{C}_{\shortparallel}$ we also have $\mathbb{y} \in \mathbb{C}_{\shortparallel}$ and the characterization of this space given in Proposition 3.30 yields

$$\left(\mathbf{R}^-_{\sigma,\shortparallel} - \mathbf{S}_{\sigma,\shortparallel}\mathbf{R}^+_{\sigma,\shortparallel}\right)\mathbb{y} = 0. \tag{3.247}$$

Finally, equation (3.243) is rewritten as

$$\left(\mathbf{R}^+_{\sigma,\shortparallel} - \mathbf{\Pi}_{\shortparallel}\mathbf{R}^-_{\sigma,\shortparallel}\right)\mathbb{y} = \mathbb{b}_\sigma, \tag{3.248}$$

which finally proves that $\mathbb{y} \in \mathbb{C}_{\shortparallel}$ solves (3.244).

($\Leftarrow$) Suppose to have $\mathbb{y} \in \mathbb{C}_{\shortparallel}$ a solution to the problem (3.244) and set $\mathbb{x}_\sigma := \mathbf{R}^+_{\sigma,\shortparallel}\mathbb{y}$. Using the characterization of the Cauchy trace space $\mathbb{C}_{\shortparallel}$ given in Proposition 3.30 we have

$$\left(\mathbf{R}^-_{\sigma,\shortparallel} - \mathbf{S}_{\sigma,\shortparallel}\mathbf{R}^+_{\sigma,\shortparallel}\right)\mathbb{y} = 0. \tag{3.249}$$

Then, equation (3.244) is readily rewritten

$$(\mathrm{Id} - \mathbf{\Pi}_{\shortparallel}\mathbf{S}_{\sigma,\shortparallel})\,\mathbb{x}_\sigma = \mathbb{b}_\sigma, \tag{3.250}$$

■

From the previous lemma we immediately obtain the following result.

Proposition 3.51. *Let $\sigma \in \{0, 1/2, 1\}$, the operator $(\mathrm{Id} - \mathbf{\Pi}_{\shortparallel}\mathbf{S}_{\sigma,\shortparallel})$ is injective on $\mathbb{M}_{\sigma,\shortparallel}$.*

Proof. Let $\sigma \in \{0, 1/2, 1\}$ and $\mathbb{x}_\sigma \in \mathbb{M}_{\sigma,\|}$ be such that

$$(\mathrm{Id} - \mathbf{\Pi}_\| \mathbf{S}_{\sigma,\|})\, \mathbb{x}_\sigma = 0. \tag{3.251}$$

Using Lemma 3.50, there exists necessarily a $\mathbb{y} \in \mathbb{C}_\|$ such that $\mathbb{x}_\sigma = \mathbf{R}^+_{\sigma,\|}\mathbb{y}$ and

$$\left(\mathbf{R}^+_{\sigma,\|} - \mathbf{\Pi}_\| \mathbf{R}^-_{\sigma,\|}\right) \mathbb{y} = 0. \tag{3.252}$$

Using the characterization of $\mathbb{S}_\|$ given in Proposition 3.37 we get from this last equation that $\mathbb{y} \in \mathbb{S}_\|$ so that in fact $\mathbb{y} \in \mathbb{C}_\| \cap \mathbb{S}_\|$, which is reduced to the singleton $\{0\}$ from Proposition 3.25. Finally from $\mathbb{y} = 0$ we obtain $\mathbb{x}_\sigma = \mathbf{R}^+_{\sigma,\|}\mathbb{y} = 0$. ∎

To prove the property of contraction of $\mathbf{\Pi}_\| \mathbf{S}_{\sigma,\|}$, we first need to establish the following lemma. Crucially, the result is established in the norms induced by the transmission operators, and rests in particular on Assumption 3.47.

Lemma 3.52. *For each $\sigma \in \{0, 1/2, 1\}$, we have,*

$$\|\mathbf{R}^-_{\sigma,\|}\mathbb{x}\|^2_{\mathbf{T}_{\sigma,\|}} - \|\mathbf{R}^+_{\sigma,\|}\mathbb{x}\|^2_{\mathbf{T}_{\sigma,\|}} = 2\mathrm{i}[\![\mathbb{x}, \overline{\mathbb{x}}]\!]_\|, \qquad \forall \mathbb{x} \in \mathbb{M}_\|. \tag{3.253}$$

Proof. We prove the equality for $\sigma = 1$, the two other proofs are similar. Let $\mathbb{x} \equiv (\mathbb{x}_0, \mathbb{x}_1) \in \mathbb{M}_\|$. By definition of the norms (3.229) and the Robin operators (3.174), we have

$$\begin{aligned} \|\mathbf{R}^+_{1,\|}\mathbb{x}\|^2_{\mathbf{T}_{1,\|}} &= \|\mathbb{x}_1 + \mathbf{Z}\mathbb{z}_0 - \mathrm{i}\mathbf{T}_{0,\|}\mathbb{x}_0\|^2_{\mathbf{T}_{1,\|}}, \\ &= \langle\!\langle \mathbb{x}_1 + \mathbf{Z}\mathbb{z}_0 - \mathrm{i}\mathbf{T}_{0,\|}\mathbb{x}_0,\ \mathbf{T}_{1,\|}\overline{(\mathbb{x}_1 + \mathbf{Z}\mathbb{z}_0 - \mathrm{i}\mathbf{T}_{0,\|}\mathbb{x}_0)} \rangle\!\rangle_\|. \end{aligned} \tag{3.254}$$

Now using the self-adjointness of $\mathbf{T}_{0,\|}$ and Assumption 3.47, this yields

$$\begin{aligned} \|\mathbf{R}^+_{1,\|}\mathbb{x}\|^2_{\mathbf{T}_{1,\|}} &= \langle\!\langle (\mathbb{x}_1 + \mathbf{Z}\mathbb{x}_0) - \mathrm{i}\mathbf{T}_{0,\|}\mathbb{x}_0,\ \mathbf{T}_{1,\|}\overline{(\mathbb{x}_1 + \mathbf{Z}\mathbb{x}_0)} + \mathrm{i}\overline{\mathbb{x}_0} \rangle\!\rangle_\|, \\ &= \|\mathbb{x}_1 + \mathbf{Z}\mathbb{x}_0\|^2_{\mathbf{T}_{1,\|}} + \|\mathbb{x}_0\|^2_{\mathbf{T}_{0,\|}} - \mathrm{i}\langle\!\langle \overline{\mathbb{x}_1 + \mathbf{Z}\mathbb{x}_0},\ \mathbb{x}_0 \rangle\!\rangle_\| + \mathrm{i}\langle\!\langle \mathbb{x}_1 + \mathbf{Z}\mathbb{x}_0,\ \overline{\mathbb{x}_0} \rangle\!\rangle_\|, \\ &= \|\mathbb{x}_1 + \mathbf{Z}\mathbb{x}_0\|^2_{\mathbf{T}_{1,\|}} + \|\mathbb{x}_0\|^2_{\mathbf{T}_{0,\|}} - \mathrm{i}\langle\!\langle \overline{\mathbb{x}_1}, \mathbb{x}_0 \rangle\!\rangle_\| + \mathrm{i}\langle\!\langle \mathbb{x}_1, \overline{\mathbb{x}_0} \rangle\!\rangle_\| \\ &\quad - \mathrm{i}\langle\!\langle \overline{\mathbf{Z}\mathbb{x}_0},\ \mathbb{x}_0 \rangle\!\rangle_\| + \mathrm{i}\langle\!\langle \mathbf{Z}\mathbb{x}_0, \overline{\mathbb{x}_0} \rangle\!\rangle_\|. \end{aligned} \tag{3.255}$$

Using the symmetry of $\mathbf{Z}$ (Assumption 3.36), the last two terms simplify and we get

$$\begin{aligned} \|\mathbf{R}^+_{1,\|}\mathbb{x}\|^2_{\mathbf{T}_{1,\|}} &= \|\mathbb{x}_1 + \mathbf{Z}\mathbb{x}_0\|^2_{\mathbf{T}_{1,\|}} + \|\mathbb{x}_0\|^2_{\mathbf{T}_{0,\|}} - 2\Im\langle\!\langle \mathbb{x}_1, \overline{\mathbb{x}_0} \rangle\!\rangle_\|, \\ &= \|\mathbb{x}_1 + \mathbf{Z}\mathbb{x}_0\|^2_{\mathbf{T}_{1,\|}} + \|\mathbb{x}_0\|^2_{\mathbf{T}_{0,\|}} - \mathrm{i}[\![\mathbb{x}, \overline{\mathbb{x}}]\!]_\|, \end{aligned} \tag{3.256}$$

using Lemma 3.6 to get the last result. Similarly,

$$\|\mathbf{R}^-_{1,\|}\mathbb{x}\|^2_{\mathbf{T}_{1,\|}} = \|\mathbb{x}_1 + \mathbf{Z}\mathbb{x}_0\|^2_{\mathbf{T}_{1,\|}} + \|\mathbb{x}_0\|^2_{\mathbf{T}_{0,\|}} + \mathrm{i}[\![\mathbb{x}, \overline{\mathbb{x}}]\!]_\|. \tag{3.257}$$

∎

We are now able to prove the property of contraction of the scattering operator $\mathbf{S}_{\sigma,\|}$ (Definition 3.29). Such a result was already proven in the acoustic setting in [42, Th. 3] or [91, Lem. 3], but with only two sub-domains in this latter reference. A similar result in a more general setting (in the whole space and in presence of junctions, but for the scalar equation) can also be found in [29, Lem. 7.1].

Proposition 3.53 (**Contraction property of the scattering operator**). *Let $\sigma \in \{0, 1/2, 1\}$, the scattering operator $\mathbf{S}_{\sigma,\|}$ is a contraction of $\mathbb{M}_{\sigma,\|}$, for our particular choice of norm* (3.229)*,*

$$\|\mathbf{S}_{\sigma,\|}\mathbb{x}_\sigma\|_{\mathbf{T}_{\sigma,\|}} \leq \|\mathbb{x}_\sigma\|_{\mathbf{T}_{\sigma,\|}}, \qquad \forall \mathbb{x}_\sigma \in \mathbb{M}_{\sigma,\|}. \tag{3.258}$$

Proof. Let $\sigma \in \{0, 1/2, 1\}$ and $\mathbb{x}_\sigma \in \mathbb{M}_{\sigma,\times}$. Let us introduce $u_\sigma \in \mathbb{U}_\Gamma(\mathrm{D}; \mathcal{P}_\Omega)$ be such that

$$\begin{cases} (\mathrm{L_a} - \kappa_0{}^2\mathsf{n})u_\sigma|_{\Omega_j} = 0, & \text{in } \Omega_j,\ \forall j \in \{1, \dots, J\}, \\ (\gamma_{1,\Gamma} - \mathrm{i}\gamma_{0,\Gamma})u_\sigma = 0, & \text{on } \Gamma, \\ \mathbf{R}^+_{\sigma,\|}\boldsymbol{\gamma}_\| u_\sigma = \mathbb{x}_\sigma, & \text{on } \tilde{\Sigma}, \end{cases} \tag{3.259}$$

which is well defined thanks to Assumption 3.28. Set $\mathbb{y} = \boldsymbol{\gamma}_\| u_\sigma$, by Definition 3.29 of the scattering operator $\mathbf{S}_{\sigma,\|}$ we have

$$\mathbf{R}^-_{\sigma,\|}\mathbb{y} = \mathbf{S}_{\sigma,\|}\mathbb{x}_\sigma, \tag{3.260}$$

and we also have by construction

$$\mathbb{x}_\sigma = \mathbf{R}^+_{\sigma,\|}\mathbb{y}. \tag{3.261}$$

It follows that

$$\|\mathbf{S}_{\sigma,\|}\mathbb{x}_\sigma\|_{\mathbf{T}_{\sigma,\|}} - \|\mathbb{x}_\sigma\|_{\mathbf{T}_{\sigma,\|}} = \|\mathbf{R}^-_{\sigma,\|}\mathbb{y}\|_{\mathbf{T}_{\sigma,\|}} - \|\mathbf{R}^+_{\sigma,\|}\mathbb{y}\|_{\mathbf{T}_{\sigma,\|}} \tag{3.262}$$

Using Lemma 3.52, we obtain

$$\|\mathbf{S}_{\sigma,\|}\mathbb{x}_\sigma\|_{\mathbf{T}_{\sigma,\|}} - \|\mathbb{x}_\sigma\|_{\mathbf{T}_{\sigma,\|}} = 2\mathrm{i}[\![\mathbb{x}, \overline{\mathbb{x}}]\!]_\|. \tag{3.263}$$

Applying the energy conservation results of Proposition 3.19 we finally get

$$\|\mathbf{S}_{\sigma,\|}\mathbb{x}_\sigma\|_{\mathbf{T}_{\sigma,\|}} - \|\mathbb{x}_\sigma\|_{\mathbf{T}_{\sigma,\|}} \leq 0. \tag{3.264}$$

■

From the definition of the exchange operator (3.184), we readily have the following result.

Proposition 3.54 (**Properties of the exchange operator**). *Let $\sigma \in \{0, 1/2, 1\}$, the exchange operator $\mathbf{\Pi}_\|$ is self-adjoint with respect to the duality product $\langle\!\langle \cdot, \cdot \rangle\!\rangle_\|$,*

$$\langle\!\langle \mathbf{\Pi}_\|\mathbb{x}_1, \mathbb{y}_0 \rangle\!\rangle_\| = \langle\!\langle \mathbb{x}_1, \mathbf{\Pi}_\|\mathbb{y}_0 \rangle\!\rangle_\|, \qquad \forall (\mathbb{x}_1, \mathbb{y}_0) \in \mathbb{M}_\|, \tag{3.265}$$

and an isometry of $\mathbb{M}_{\sigma,\|}$, for our particular choice of norm (3.229)*,*

$$\|\mathbf{\Pi}_\|\mathbb{x}_\sigma\|_{\mathbf{T}_{\sigma,\|}} = \|\mathbb{x}_\sigma\|_{\mathbf{T}_{\sigma,\|}}, \qquad \forall \mathbb{x}_\sigma \in \mathbb{M}_{\sigma,\|}. \tag{3.266}$$

Proof. The self-adjointness follows, for any $\mathbb{x}_0 = (\mathrm{x}_0^{jk})_{(j,k)\in\mathbb{J}} \in \mathbb{M}_{0,\|}$ and $\mathbb{x}_1 = (\mathrm{x}_1^{jk})_{(j,k)\in\mathbb{J}} \in \mathbb{M}_{1,\|}$, from

$$\langle\!\langle \mathbf{\Pi}_\|\mathbb{x}_1, \mathbb{x}_0 \rangle\!\rangle_\| = \sum_{(j,k)\in\mathbb{J}} \langle \mathrm{x}_1^{kj}, \mathrm{x}_0^{jk} \rangle_{\Gamma_{jk}} = \langle\!\langle \mathbb{x}_1, \mathbf{\Pi}_\|\mathbb{x}_0 \rangle\!\rangle_\|. \tag{3.267}$$

Finally, using Assumption 3.36 and Proposition 3.33, we obtain, for all $\mathbb{x}_1 \in \mathbb{M}_{1,\|}$,

$$\|\mathbf{\Pi}_\|\mathbb{x}_1\|_{\mathbf{T}_{1,\|}} = \langle\!\langle \mathbf{\Pi}_\|\mathbb{x}_1, \mathbf{T}_{1,\|}\overline{\mathbf{\Pi}_\|\mathbb{x}_1} \rangle\!\rangle_\| = \langle\!\langle \mathbf{\Pi}_\|\mathbb{x}_1, \mathbf{\Pi}_\|\mathbf{T}_{1,\|}\overline{\mathbb{x}_1} \rangle\!\rangle_\| = \langle\!\langle \mathbb{x}_1, \mathbf{T}_{1,\|}\overline{\mathbb{x}_1} \rangle\!\rangle_\| = \|\mathbb{x}_1\|_{\mathbf{T}_{1,\|}}, \tag{3.268}$$

which proves (3.266) for the case $\sigma = 1$, the other two proofs follow the same route. ■

Combining both Proposition 3.53 and Proposition 3.54 we get the contraction property we were looking for.

Corollary 3.55 (**Contraction property**). *Let $\sigma \in \{0, 1/2, 1\}$, we have*

$$\|\mathbf{\Pi}_{\shortparallel}\mathbf{S}_{\sigma,\shortparallel}\mathbb{x}_\sigma\|_{\mathbf{T}_{\sigma,\shortparallel}} \leq \|\mathbb{x}_\sigma\|_{\mathbf{T}_{\sigma,\shortparallel}}, \qquad \forall \mathbb{x}_\sigma \in \mathbb{M}_{\sigma,\shortparallel}. \tag{3.269}$$

We are now ready to state our first important convergence result. A similar result was already stated in [42, Th. 6] for the acoustic setting only.

Theorem 3.56 (**Convergence of the relaxed Jacobi algorithm**). *The sequence of broken solutions $(u_\sigma^n)_{n\in\mathbb{N}}$ computed according to* (3.226)*, converges to u the solution of the model problem* (3.79)

$$\|u_\sigma^n - u\|_{\mathbb{U}_\Gamma(\mathrm{D};\mathcal{P}_\Omega)} \to 0, \qquad as \qquad n \to \infty. \tag{3.270}$$

Proof. At each iteration $n \in \mathbb{N}$, we can define an error on the trace $\epsilon_\sigma^n \in \mathbb{M}_{\sigma,\shortparallel}$ such that

$$\epsilon_\sigma^n = \mathbb{x}_\sigma^n - \mathbb{x}_\sigma, \tag{3.271}$$

where the sequence $(\mathbb{x}_\sigma^n)_{n\in\mathbb{N}}$ is computed through (3.225) and $\mathbb{x}_\sigma$ is the solution of (3.222). By the well-posedness of the problem (3.226), there exists a strictly positive constant C such that

$$\|u_\sigma^n - u\|_{\mathbb{U}_\Gamma(\mathrm{D};\mathcal{P}_\Omega)} \leq C\|\epsilon_\sigma^n\|_{\mathbf{T}_{\sigma,\shortparallel}}. \tag{3.272}$$

We can readily show that the error ϵ_σ^n satisfies

$$\epsilon_\sigma^{n+1} = [(1-r)\mathrm{Id} + r\mathbf{\Pi}_{\shortparallel}\mathbf{S}_{\sigma,\shortparallel}]\,\epsilon_\sigma^n, \qquad n \in \mathbb{N}. \tag{3.273}$$

The end of the proof is then a direct application to the sequence $(\epsilon_\sigma^n)_{n\in\mathbb{N}}$ of the abstract result given in Proposition 3.49 whose two assumptions are verified in Proposition 3.51 and Proposition 3.55. ■

3.3.2.3 A sufficient condition for geometric convergence

The following proposition, adapted from [42, Th. 7], supplements Proposition 3.49 and makes clear what additional assumption is required to obtain geometric convergence.

Proposition 3.57. *If, in addition to the assumptions of Proposition 3.49,*

- $\mathrm{Id} - A$ *is an* isomorphism *in V,*

then the relaxed Jacobi algorithm (3.273) *converges* geometrically *to 0 in V. Specifically, there exist $C > 0$ and $0 < \tau < 1$ such that*

$$\|x^n\|_V \leq C\tau^n. \tag{3.274}$$

Proof. Let $n \in \mathbb{N}$, we use again the convexity identity (3.233) from the proof of Theorem 3.49 and we get

$$\|x^{n+1}\|_V^2 = (1-r)\|x^n\|_V^2 + r\|Ax^n\|_V^2 - r(1-r)\|x^n - Ax^n\|_V^2. \tag{3.275}$$

Since A is a contraction in V from the assumptions of Proposition 3.49, we have for all $x \in V$,

$$\|Ax\|_V \leq \|x\|_V. \tag{3.276}$$

Since $\mathrm{Id} - A$ is an isomorphism in V, there exists $\delta > 0$ such that, for all $x \in V$

$$\|x\|_V \leq \delta \|(\mathrm{Id} - A)x\|_V. \tag{3.277}$$

From (3.275) we get

$$\|x^{n+1}\|_V \leq \sqrt{1 - r(1-r)\delta^{-2}}\ \|x^n\|_V. \tag{3.278}$$

Besides, using again the contraction property of A, we have for all $x \in V$,

$$\|x\|_V \leq \delta \|(\mathrm{Id} - A)x\|_V \leq \delta \left(\|x\|_V + \|Ax\|_V\right) \leq 2\delta \|x\|_V. \tag{3.279}$$

Hence $0 \leq \delta^{-1} \leq 2$ and it can be proven that for all $0 \leq r \leq 1$, we have $0 \leq r(1-r) \leq \frac{1}{4}$. It follows that

$$0 \leq \tau := \sqrt{1 - r(1-r)\delta^{-2}} \leq 1. \tag{3.280}$$

■

Remark 3.58. *Depending on the authors, the type of convergence given in Proposition 3.57 can be called* linear, exponential *[42, 44, 91, 30] or* geometric *[29, 33]. We chose to use the term* geometric *in this manuscript in contrast to the* algebraic *convergence proved for local transmission operators [49].*

To apply the previous proposition, we need only to prove that the operator $\mathrm{Id} - \mathbf{\Pi}_{\shortparallel} \mathbf{S}_{\sigma,\shortparallel}$ is surjective (its injectivity was the subject of Proposition 3.51). To do so we first need to establish additional preparatory results.

Recall that, according to Proposition 3.21, the operator $\mathbf{R}^{+}_{\sigma,\shortparallel} - \mathbf{\Pi}_{\shortparallel} \mathbf{R}^{-}_{\sigma,\shortparallel}$ (respectively the operator $\mathbf{R}^{-}_{\sigma,\shortparallel} - \mathbf{\Pi}_{\shortparallel} \mathbf{R}^{+}_{\sigma,\shortparallel}$) is not injective on $\mathbb{M}_{\sigma,\shortparallel}$, its kernel is $\mathbb{S}_{\shortparallel} \neq \{0\}$. It is however surjective, as stated in the following lemma which relies mainly on the assumption that the transmission operator $\mathbf{T}_{\sigma,\shortparallel}$ is invertible (which directly follows from Assumption 3.47).

Lemma 3.59. *For each $\sigma \in \{0, 1/2, 1\}$, the operator $\mathbf{R}^{+}_{\sigma,\shortparallel} - \mathbf{\Pi}_{\shortparallel} \mathbf{R}^{-}_{\sigma,\shortparallel}$ (respectively the operator $\mathbf{R}^{-}_{\sigma,\shortparallel} - \mathbf{\Pi}_{\shortparallel} \mathbf{R}^{+}_{\sigma,\shortparallel}$) is surjective from $\mathbb{M}_{\shortparallel} \equiv (\mathbb{M}_{0,\shortparallel}, \mathbb{M}_{1,\shortparallel})$ onto $\mathbb{M}_{\sigma,\shortparallel}$.*

Proof. First note that, for any $\sigma \in \{0, 1/2, 1\}$, the result for the operator $\mathbf{R}^{-}_{\sigma,\shortparallel} - \mathbf{\Pi}_{\shortparallel} \mathbf{R}^{+}_{\sigma,\shortparallel}$ is equivalent to the result for the operator $\mathbf{R}^{+}_{\sigma,\shortparallel} - \mathbf{\Pi}_{\shortparallel} \mathbf{R}^{-}_{\sigma,\shortparallel}$ since the exchange operator $\mathbf{\Pi}_{\shortparallel}$ is an involution according to Proposition 3.33.

We prove the results for $\sigma = 1$, the proofs for the other two cases formally take the same route.

Let $\mathbb{b}_1 \in \mathbb{M}_{1,\shortparallel}$. We seek $\mathbb{y} \equiv (\mathbb{y}_0, \mathbb{y}_1) \in \mathbb{M}_{\shortparallel}$ such that

$$\mathbf{R}^{+}_{1,\shortparallel} \mathbb{y} - \mathbf{\Pi}_{\shortparallel} \mathbf{R}^{-}_{1,\shortparallel} \mathbb{y} = \mathbb{b}_1 \tag{3.281}$$

which, by Definition 3.27 of the generalized Robin operators $\mathbf{R}^{\pm}_{1,\shortparallel}$, is equivalent to

$$(\mathbb{y}_1 + \mathbf{Z} - \mathrm{i}\mathbf{T}_{0,\shortparallel} \mathbb{y}_0) - \mathbf{\Pi}_{\shortparallel} \left(-\mathbb{y}_1 - \mathbf{Z} - \mathrm{i}\mathbf{T}_{0,\shortparallel} \mathbb{y}_0\right) = \mathbb{b}_1, \tag{3.282}$$

which is rewritten as

$$(\mathrm{Id} + \mathbf{\Pi}_{\shortparallel}) (\mathbb{y}_1 + \mathbf{Z}\mathbb{y}_0) + (\mathrm{Id} - \mathbf{\Pi}_{\shortparallel}) (-\mathrm{i}\mathbf{T}_{0,\shortparallel} \mathbb{y}_0) = \mathbb{b}_1. \tag{3.283}$$

Using the properties of the projectors $1/2(\mathrm{Id} \pm \mathbf{\Pi}_{\shortparallel})$ given in Proposition 3.34, it is then immediate to check that a solution is at hand if $\mathbb{y}_0$ and $\mathbb{y}_1$ satisfy

$$\begin{cases} -\mathrm{i}\mathbf{T}_{0,\shortparallel} \mathbb{y}_0 = \frac{1}{4} (\mathrm{Id} - \mathbf{\Pi}_{\shortparallel})\ \mathbb{b}_1, \\ \mathbb{y}_1 + \mathbf{Z}\mathbb{y}_0 = \frac{1}{4} (\mathrm{Id} + \mathbf{\Pi}_{\shortparallel})\ \mathbb{b}_1. \end{cases} \tag{3.284}$$

A solution $\mathbb{y} \equiv (\mathbb{y}_0, \mathbb{y}_1) \in \mathbb{M}_\parallel$ to (3.281) is then

$$\begin{cases} \mathbb{y}_0 = \frac{\mathrm{i}}{4}(\mathbf{T}_{0,\parallel})^{-1}\,(\mathrm{Id} - \mathbf{\Pi}_\parallel)\ \mathbb{b}_1, \\ \mathbb{y}_1 = \frac{1}{4}\,(\mathrm{Id} + \mathbf{\Pi}_\parallel)\ \mathbb{b}_1 - \frac{\mathrm{i}}{4}\mathbf{Z}(\mathbf{T}_{0,\parallel})^{-1}\,(\mathrm{Id} - \mathbf{\Pi}_\parallel)\ \mathbb{b}_1. \end{cases} \tag{3.285}$$

■

As a direct corollary to Propositions 3.25, 3.37 and Lemma 3.59 we have the following easy result. Notice that the cornerstone to establish this result is the decomposition $\mathbb{M}_\parallel = \mathbb{C}_\parallel \oplus \mathbb{S}_\parallel$ from Proposition 3.25.

Corollary 3.60. *For each $\sigma \in \{0, 1/2, 1\}$, the operator $\mathbf{R}^+_{\sigma,\parallel} - \mathbf{\Pi}_\parallel \mathbf{R}^-_{\sigma,\parallel}$ (respectively the operator $\mathbf{R}^-_{\sigma,\parallel} - \mathbf{\Pi}_\parallel \mathbf{R}^+_{\sigma,\parallel}$) is a bijection from $\mathbb{C}_\parallel$ to $\mathbb{M}_{\sigma,\parallel}$.*

Proof. Let $\sigma \in \{0, 1/2, 1\}$. Again, first note that the result for the operator $\mathbf{R}^-_{\sigma,\parallel} - \mathbf{\Pi}_\parallel \mathbf{R}^+_{\sigma,\parallel}$ is equivalent to the result for the operator $\mathbf{R}^+_{\sigma,\parallel} - \mathbf{\Pi}_\parallel \mathbf{R}^-_{\sigma,\parallel}$ since the exchange operator $\mathbf{\Pi}_\parallel$ is an involution according to Proposition 3.33.

From Lemma 3.59, the operator $\mathbf{R}^+_{\sigma,\parallel} - \mathbf{\Pi}_\parallel \mathbf{R}^-_{\sigma,\parallel}$ is surjective from $\mathbb{M}_\parallel$ onto $\mathbb{M}_{\sigma,\parallel}$. From Proposition 3.37 we know that its kernel is $\mathbb{S}_\parallel$. From Proposition 3.25 we have that $\mathbb{M}_\parallel = \mathbb{C}_\parallel \oplus \mathbb{S}_\parallel$. It follows that the operator $\mathbf{R}^+_{\sigma,\parallel} - \mathbf{\Pi}_\parallel \mathbf{R}^-_{\sigma,\parallel}$ is invertible on $\mathbb{C}_\parallel$. ■

We are finally able to verify that we satisfy in our particular setting the required additional assumption of the abstract result contain in Proposition 3.57.

Proposition 3.61. *For each $\sigma \in \{0, 1/2, 1\}$, the operator $\mathrm{Id} - \mathbf{\Pi}_\parallel \mathbf{S}_{\sigma,\parallel}$ is an isomorphism on $\mathbb{M}_{\sigma,\parallel}$.*

Proof. We proved the injectivity of this operator in Proposition 3.51, so we need to only to establish its surjectivity. Let $\sigma \in \{0, 1/2, 1\}$ and $\mathbb{b}_\sigma \in \mathbb{M}_{\sigma,\parallel}$. From Lemma 3.50 we know that to find a $\mathbb{x}_\sigma \in \mathbb{M}_{\sigma,\parallel}$ such that

$$(\mathrm{Id} - \mathbf{\Pi}_\parallel \mathbf{S}_{\sigma,\parallel})\,\mathbb{x}_\sigma = \mathbb{b}_\sigma, \tag{3.286}$$

it is enough to find a $\mathbb{y} \in \mathbb{C}_\parallel$ such that

$$\left(\mathbf{R}^+_{\sigma,\parallel} - \mathbf{\Pi}_\parallel \mathbf{R}^-_{\sigma,\parallel}\right)\mathbb{y} = \mathbb{b}_\sigma, \tag{3.287}$$

and set $\mathbb{x}_\sigma = \mathbf{R}^+_{\sigma,\parallel}\mathbb{y}$. The above problem in $\mathbb{y}$ is uniquely solvable by application of Corollary 3.60 and we are done. ■

Remark 3.62. *For any $\sigma \in \{0, 1/2, 1\}$, by inspecting the proofs, we can actually give an explicit construction of the solution $\mathbb{x}_\sigma$ of the interface problem:*

$$\begin{cases} \textit{Find } \mathbb{x}_\sigma \in \mathbb{M}_{\sigma,\parallel} \textit{ such that}: \\ (\mathrm{Id} - \mathbf{\Pi}_\parallel \mathbf{S}_{\sigma,\parallel})\,\mathbb{x}_\sigma = \mathbb{b}_\sigma. \end{cases} \tag{3.288}$$

The steps are as follows:

1. *Find any solution (there is no uniqueness) of*

$$\begin{cases} \textit{Find } \mathbb{y} \in \mathbb{M}_\parallel \textit{ such that}: \\ \left(\mathbf{R}^+_{\sigma,\parallel} - \mathbf{\Pi}_\parallel \mathbf{R}^-_{\sigma,\parallel}\right)\mathbb{y} = \mathbb{b}_\sigma. \end{cases} \tag{3.289}$$

   One particular solution can be computed according to (3.285) *from the proof of Lemma 3.59;*

2. *Project this solution onto* $\mathbb{C}_\shortparallel$ *in parallel to* $\mathbb{S}_\shortparallel$*: an explicit projection is performed in the proof of Proposition 3.25 for instance;*

3. *If we still denote by* $\mathbb{y}$ *the result of this projection, the solution is then* $\mathbb{x}_\sigma = \mathbf{R}^+_{\sigma,\shortparallel}\mathbb{y}$*, according to Lemma 3.50.*

This is not a surprise, but we emphasize however that this construction involves solving a global problem on Ω*, during the projection step, hence is of no use in practice.*

We are finally able to state the following important convergence result. For the acoustic setting, a similar result was already stated in [78, Th. 3.3], [42, Th. 7], [91, Th. 1], but for two sub-domains only, and in [29, Sec. 7.3], but for a more general partition with junctions.

Theorem 3.63 (**Geometric convergence of the relaxed Jacobi algorithm).** *The sequence of broken solutions* $(u_\sigma^n)_{n\in\mathbb{N}}$ *computed according to* (3.226)*, converges* geometrically *to* u *the solution of the model problem* (3.79)*. Specifically, there exist* $C > 0$ *and* $0 < \tau < 1$ *such that*

$$\|u_\sigma^n - u\|_{\mathbb{U}_\Gamma(\mathrm{D};\mathcal{P}_\Omega)} \leq C\tau^n, \qquad \forall n \in \mathbb{N}. \tag{3.290}$$

Proof. Arguing as in the proof of Theorem 3.56, this is a direct application of Proposition 3.57 whose essential assumption is verified by Proposition 3.61. ■

3.3.3 GMRES algorithm

While the theoretical analysis of the Jacobi algorithm allows to get some deep insight on the efficiency of the method, such an algorithm is rarely used in practice. Krylov methods are the preferred choice in real-life applications, in particular one will typically resort to the Gmres algorithm in our non-symmetric case. See [122, 123] for the definition of this algorithm.

Importantly, geometric convergence of the relaxed Jacobi algorithm guarantees geometric convergence of the Gmres counter-part, even the restarted version. This is the subject of the following lemma which uses again the notations and assumptions of Proposition 3.49 and Proposition 3.57.

Lemma 3.64. *Let* V *be a Hilbert space endowed with a norm* $\|\cdot\|_V$*. Suppose we are set to solve in* V*, for a given* $b \in V$*,*

$$(\mathrm{Id} - A)\, x = b. \tag{3.291}$$

Let $x_J^0 = 0$*,* $0 < r < 1$ *and define a sequence* $(x_J^n)_{n\in\mathbb{N}}$ *of solutions using the relaxed Jacobi algorithm*

$$x_J^{n+1} = ((1-r)\mathrm{Id} + rA)\, x_J^n + rb, \qquad n \in \mathbb{N}. \tag{3.292}$$

Similarly let $x_G^0 = 0$ *and define a sequence* $(x_G^n)_{n\in\mathbb{N}}$ *of solutions using the* Gmres *algorithm (using the scalar product in* V*). If the following two assumptions hold true*

- $\mathrm{Id} - A$ *is an* isomorphism *in* V*;*
- A *is a* contraction *in* V*;*

then both the sequence $(x_J^n)_{n\in\mathbb{N}}$ *computed using the relaxed Jacobi algorithm* (3.292) *and the sequence* $(x_G^n)_{n\in\mathbb{N}}$ *computed using the* Gmres *algorithm converge* geometrically *to* x *the (by assumption well-defined) solution of* (3.291) *in* V*. Specifically, there exist* $C_J > 0$*,* $C_G > 0$ *and* $0 < \tau < 1$ *such that*

$$\|x_J^n - x\|_V \leq C_J\, \tau^n, \qquad \textit{and} \qquad \|x_G^n - x\|_V \leq C_G\, \tau^n. \tag{3.293}$$

Proof. Let us defined the residual for the relaxed Jacobi algorithm

$$r_J^n := (\mathrm{Id} - A)\, x_J^n - b = (\mathrm{Id} - A)\,(x_J^n - x)\,, \qquad \forall n \in \mathbb{N}, \tag{3.294}$$

and similarly the residual for the GMRES algorithm

$$r_G^n := (\mathrm{Id} - A)\, x_G^n - b = (\mathrm{Id} - A)\,(x_G^n - x)\,, \qquad \forall n \in \mathbb{N}. \tag{3.295}$$

We will use the following characterization of the iterates of the GMRES algorithm [11, 45]: the iterates x_G^n for $n \geq 1$ are such that

$$\|r_G^n\|_V := \min\left\{\|p\,(\mathrm{Id} - A)\, r_G^0\|_V \mid p \in \mathcal{P}_n,\ p(0) = 1\right\}, \tag{3.296}$$

where $\mathcal{P}_n$ is the set of polynomials of degree at most n. It follows that x_G^n is the minimizer in the so-called Krylov sub-space $V_n \subset V$ defined for $n \geq 1$ such that

$$V_n := \mathrm{vect}\left\{b,\ (\mathrm{Id} - A)r,\ (\mathrm{Id} - A)^2 r, \ldots,\ (\mathrm{Id} - A)^n r\right\}. \tag{3.297}$$

Besides, it turns out that each x_J^n for $n \geq 1$ is also an element of V_n, which can be proved by induction. Indeed, we have trivially

$$x_J^1 = rb \in V_1, \tag{3.298}$$

and assuming that $x_J^n \in V_n$ is true for $n \geq 1$ we have

$$x_J^{n+1} = ((1 - r)\mathrm{Id} + rA)\, x_J^n + rb = x_J^n - r\,(\mathrm{Id} - A)\, x_J^n + rb, \tag{3.299}$$

so that $x_J^{n+1} \in V_{n+1}$. Using the characterization (3.296), we get

$$\|r_G^n\|_V \leq \|r_J^n\|_V, \qquad \forall n \in \mathbb{N}, \tag{3.300}$$

which is a first interesting result on the residuals.

Let us now prove the estimates on the errors $x_J^n - x$ and $x_G^n - x$. With the given assumptions, the existence of C_J and τ so that

$$\|x_J^n - x\|_V \leq C_J\, \tau^n, \tag{3.301}$$

is ensured by Proposition 3.57. It follows that, using the fact that A is a contraction in V

$$\|r_J^n\|_V = \|(\mathrm{Id} - A)\,(x_J^n - x)\,\|_V \leq \|x_J^n - x\|_V + \|A\,(x_J^n - x)\,\|_V \leq 2\|x_J^n - x\|_V \leq 2C_J\tau^n. \tag{3.302}$$

Now, from the fact that $\mathrm{Id} - A$ is an isomorphism in V hence have a bounded inverse, we have the existence of $\delta > 0$ such that

$$\|x_G^n - x\|_V = \|(\mathrm{Id} - A)^{-1} r_G^n\|_V \leq \delta \|r_G^n\|_V \leq \delta \|r_J^n\|_V \leq 2\delta C_J \tau^n, \tag{3.303}$$

which proves the (non optimal) estimate with $C_G = 2\delta C_J$. ∎

The derivation of better convergence estimates for the GMRES algorithm would be of considerable interest but was not further pursued in this work.

3.4 Well-posedness of some wave propagation problems

In this section we consider some wave propagation models of particular interest. We show how they fit in the abstract framework that was previously presented by proving the remaining main assumptions this framework required, namely the well-posedness of the model problem and the local sub-problems (Assumption 3.9 and Assumption 3.45).

3.4.1 Acoustics

We consider a generic bounded, simply connected, Lipschitz domain Ω with a closed Lipschitz boundary composed of two connected components: one component, denoted Γ, where we impose a first order absorbing boundary condition; and a second component, denoted Σ, where we impose a transmission-like boundary condition.

Let $f \in H^1(\Omega)'$, $g \in L^2(\Gamma)$ and $\mathrm{x} \in H^{-1/2}(\Sigma)$, we consider the following problem

$$\begin{cases} \text{Find } p \in H^1(\Omega) \text{ such that} & \\ \left(-\operatorname{div} \rho_r^{-1} \mathbf{grad} - {\kappa_0}^2 \lambda_r^{-1}\right) p = f, & \text{in } \Omega, \\ \left(\gamma_{1,\Gamma} - \mathrm{i}\gamma_{0,\Gamma}\right) p = g, & \text{on } \Gamma, \\ \left(\gamma_{1,\Sigma} + [\mathrm{Z} - \mathrm{i}\mathrm{T}]\, \gamma_{0,\Sigma}\right) p = \mathrm{x}, & \text{on } \Sigma. \end{cases} \tag{3.304}$$

Here T and Z respectively represent one diagonal block of the operators $\mathbf{T}_{0,\parallel}$ and $\mathbf{Z}$, corresponding to the boundary of one sub-domain.

This problem is representative of both the model problem (3.304) (for which the transmission boundary $\Sigma = \emptyset$) and the local sub-problems (3.218) (for which the physical boundary Γ may or may not be empty). We shall therefore prove that the above problem is well-posed without excluding the two exclusive cases $\Sigma = \emptyset$ or $\Gamma = \emptyset$.

We shall show in the remainder of this sub-section that the above problem is well-posed under the following assumption.

Assumption 3.65. *We suppose that the coefficients satisfy*

$$\begin{aligned} &0 < \Re\left(\rho_r\right) < +\infty, \qquad &&0 \leq \Im\left(\rho_r\right) < +\infty, \\ &0 < \Re\left(\lambda_r^{-1}\right) < +\infty, \qquad &&0 \leq \Im\left(\lambda_r^{-1}\right) < +\infty, \end{aligned} \qquad \text{in } \Omega_\Sigma. \tag{3.305}$$

In addition, we suppose that the transmission operators are such that

- T *is a* self-adjoint positive isomorphism *from* $H^{1/2}(\Gamma)$ *to* $H^{-1/2}(\Gamma)$*;*
- Z *is a* symmetric continuous operator *from* $H^{1/2}(\Gamma)$ *to* $H^{-1/2}(\Gamma)$*,*

with

$$\frac{\beta_{\mathrm{T}}}{\alpha_{\mathrm{Z}}} > \max\left(\frac{\inf_\Omega \Im\left(\rho_r\right)}{\inf_\Omega \Re\left(\rho_r\right)}, \frac{\inf_\Omega \Im\left(\lambda_r\right)}{\inf_\Omega \Re\left(\lambda_r\right)}\right), \tag{3.306}$$

where α_{Z} *is the continuity constant of* Z *and* β_{T} *is the coercivity constant of* T*.*

In particular, we do *not* assume that the imaginary parts of the coefficients are strictly positive almost everywhere in Ω, which would considerably simplify the analysis since that would mean that the medium is purely dissipative. We are rather interested in the case where they vanish in at least some subsets (of non zero measure) of Ω so that the medium is (at least partly) propagative.

We shall prove the well posedness of the above problem using a variational approach, hence consider the weak form of (3.304) which is written

$$\begin{cases} \text{Find } p \in H^1(\Omega) \text{ such that} & \\ a(p, p^t) + \langle [\mathrm{Z} - \mathrm{i}\mathrm{T}]\, \gamma_{0,\Sigma}\, p, \gamma_{0,\Sigma}\, p^t \rangle_\Sigma = l(p^t), & \forall p^t \in H^1(\Omega), \end{cases} \tag{3.307}$$

where, for all $p, q \in H^1(\Omega)$,

$$\begin{cases} a(p,q) := {\kappa_0}^{-1} (\rho_r^{-1} \mathbf{grad}\, p, \mathbf{grad}\, q)_{L^2(\Omega)} - \kappa_0 (\lambda_r^{-1} p, q)_{L^2(\Omega)} - \mathrm{i} (\gamma_{0,\Gamma}\, p, \gamma_{0,\Gamma}\, q)_{L^2(\Gamma)}, \\ l(q) := {\kappa_0}^{-1} \langle f, q \rangle_\Omega + \langle g, \gamma_{0,\Gamma}\, q \rangle_\Gamma. \end{cases} \tag{3.308}$$

Such well-posedness result is not new, similar results can be found for instance in [91, Lem. 1] or [44, Lem. 2.1]. The only difference is that the proof below allows the coefficient to have a non-vanishing imaginary part. The following two lemmas states that the sesquilinear form a can be decomposed in two parts: a coercive part and a compact part.

Lemma 3.66 (**Coercive form**). *Under Assumption 3.65, the sesquilinear form, defined for all $p, q \in H^1(\Omega)$, as*

$$\begin{aligned} a_+(p,q) :=& {\kappa_0}^{-1}(\rho_r^{-1}\,\mathbf{grad}\,p, \mathbf{grad}\,q)_{L^2(\Omega)} + \kappa_0(\lambda_r^{-1}p,q)_{L^2(\Omega)} \\ & - \mathrm{i}(\gamma_{0,\Gamma}\,p, \gamma_{0,\Gamma}\,q)_{L^2(\Gamma)} + \langle[\mathrm{Z}-\mathrm{i}\mathrm{T}]\,\gamma_{0,\Sigma}\,p, \gamma_{0,\Sigma}\,q\rangle_{\Sigma}, \end{aligned} \tag{3.309}$$

is continuous and coercive on $H^1(\Omega)$.

Proof. The continuity of the above sesquilinear form follows readily from the boundedness of the coefficient ρ_r and λ_r and the continuity property of Z and T contained in Assumption 3.65. To prove coercivity, let $p \in H^1(\Omega)$, we have for a $\lambda \in \mathbb{R}^+$,

$$\begin{aligned} \lambda\Re a_+(p,p) - \Im a_+(p,p) \geq & \left(\lambda \inf_\Omega \Re(\rho_r) - \inf_\Omega \Im(\rho_r)\right) |\rho_r|^{-2}\, {\kappa_0}^{-1} \|\,\mathbf{grad}\,p\|^2_{L^2(\Omega)} \\ & + \left(\lambda \inf_\Omega \Re(\lambda_r) - \inf_\Omega \Im(\lambda_r)\right) |\lambda_r|^{-2}\, \kappa_0 \|p\|^2_{L^2(\Omega)} \\ & + \|\gamma_{0,\Gamma}\,p\|^2_{L^2(\Gamma)} + (\beta_{\mathrm{T}} - \lambda\alpha_{\mathrm{Z}})\, \|\gamma_{0,\Sigma}\,p\|^2_{H^{1/2}(\Sigma)}. \end{aligned} \tag{3.310}$$

Hence, if λ is such that

$$\frac{\beta_{\mathrm{T}}}{\alpha_{\mathrm{Z}}} > \lambda > \max\left(0,\ \frac{\inf_\Omega \Im\,(\rho_r)}{\inf_\Omega \Re\,(\rho_r)},\ \frac{\inf_\Omega \Im\,(\lambda_r)}{\inf_\Omega \Re\,(\lambda_r)}\right), \tag{3.311}$$

for any $p \in H^1(\Omega)$, there exists $C > 0$ such that

$$\lambda\Re a_+(p,p) - \Im a_+(p,p) \geq C\|p\|^2_{H^1(\Omega)}. \tag{3.312}$$

■

Lemma 3.67 (**Compact operator**). *Under Assumption 3.65, the operator*

$$K\ :\ L^2(\Omega) \to L^2(\Omega) \tag{3.313}$$

such that $Kp \in H^1(\Omega) \subset L^2(\Omega)$ is defined, for all $p \in L^2(\Omega)$, as

$$a_+(Kp, q) = -2\kappa_0(\lambda_r^{-1}p, q)_{L^2(\Omega)}, \qquad \forall q \in H^1(\Omega). \tag{3.314}$$

is compact in $L^2(\Omega)$.

Proof. Lemma 3.66 ensures, via application of the Lax-Migram Lemma, that there exists a constant C such that, for all $p \in L^2(\Omega)$

$$\|Kp\|_{H^1(\Omega)} \leq C\|p\|_{L^2(\Omega)}. \tag{3.315}$$

Let $(u_n)_n^\infty$ be a bounded sequence in $L^2(\Omega)$. Using the above inequality $(Ku_n)_n^\infty$ is a bounded sequence in $H^1(\Omega) \subset L^2(\Omega)$. Using the compacity of the embedding $H^1(\Omega) \hookrightarrow L^2(\Omega)$ there is a subsequence converging strongly in $L^2(\Omega)$, which implies that K is compact. ■

We now have all the ingredients to establish the following proposition. A similar result was already stated in [78, Th. 3.1] in [42, Th. 3] and in [91, Lem. 1], but for two sub-domains only in the latter case.

Proposition 3.68 (**Well-posedness of the model problem**). *Under Assumption 3.65, the problem* (3.304) *is well-posed.*

Proof. Using the definitions of the coercive form a_+ (Lemma 3.66) and the operator K (Lemma 3.67), the problem in $p \in H^1(\Omega)$ is equivalent to finding $p \in L^2(\Omega)$ such that

$$(\mathrm{Id} + K)p = b, \tag{3.316}$$

where by application of the Lax-Milgram Lemma, $b \in H^1(\Omega) \subset L^2(\Omega)$, is the unique solution of

$$a_+(b, p_0^t) = l(p_0^t), \qquad \forall p_0^t \in H^1(\Omega). \tag{3.317}$$

From Lemma 3.67 the operator K is compact in $L^2(\Omega)$, the Fredholm alternative is applicable and the proof reduces to a uniqueness result.

For the proof of uniqueness, let p and q in $H^1(\Omega)$ be two solutions to (3.307). By linearity, the difference $e = q - p$ satisfy

$$a(e, e^t) + \langle [\mathrm{Z} - \mathrm{i}\mathrm{T}]\, \gamma_{0,\Sigma}\, e, \gamma_{0,\Sigma}\, e^t \rangle_\Sigma = 0, \qquad \forall e^t \in H^1(\Omega). \tag{3.318}$$

Choosing $e^t = e$ and taking the imaginary part yields

$$\begin{aligned} {\kappa_0}^{-1} (\Im\left(\rho_r^{-1}\right) \mathbf{grad}\, e, \mathbf{grad}\, e)_{L^2(\Omega)} - \kappa_0 (\Im\left(\lambda_r^{-1}\right) e, e)_{L^2(\Omega)} \\ - (\gamma_{0,\Gamma}\, e, \gamma_{0,\Gamma}\, e)_{L^2(\Gamma)} - \langle \mathrm{T} \gamma_{0,\Sigma}\, e, \gamma_{0,\Sigma}\, e \rangle_\Sigma = 0. \end{aligned} \tag{3.319}$$

We deduce that $\gamma_{0,\Gamma}\, e = 0$ on Γ on the one hand, and the positivity and injectivity of the transmission operator T from Assumption 3.65 gives that $\gamma_{0,\Sigma}\, e = 0$ on Σ on the other hand, so that the Dirichlet trace of e vanish on the whole boundary $\partial\Omega$. The proof then follows using a unique continuation result, see [8], and the connectivity of Ω. ■

3.4.2 Electromagnetism

We consider a generic bounded, simply connected, Lipschitz domain Ω with a closed Lipschitz boundary composed of two connected components: one component, denoted Γ, where we impose a first order absorbing boundary condition; and a second component, denoted Σ, where we impose a transmission-like boundary condition.

Let $\mathbf{F} \in \mathbf{H}_\Gamma(\mathbf{curl}; \Omega)'$ such that $\mathrm{div}\, \mathbf{F} = 0$ in a distributional sense (charge conservation equation), $\mathbf{g} \in \mathbf{L}^2(\Gamma)$ and $\mathbf{x} \in \mathbf{H}^{-1/2}(\mathrm{div}; \Sigma)$, we consider the following problem

$$\begin{cases} \text{Find } \mathbf{E} \in \mathbf{H}_\Gamma(\mathbf{curl}; \Omega) \text{ such that} & \\ \left(\mathbf{curl}\, \mu_r^{-1}\, \mathbf{curl} - {\kappa_0}^2 \epsilon_r\right) \mathbf{E} = \mathbf{F}, & \text{in } \Omega, \\ (\gamma_{1,\Gamma} - \mathrm{i}\gamma_{0,\Gamma})\, \mathbf{E} = \mathbf{g}, & \text{on } \Gamma, \\ (\gamma_{1,\Sigma} + [\mathbf{Z} - \mathrm{i}\mathbf{T}]\, \gamma_{0,\Sigma})\, \mathbf{E} = \mathbf{x}, & \text{on } \Sigma. \end{cases} \tag{3.320}$$

Here $\mathbf{T}$ and $\mathbf{Z}$ respectively represent one diagonal block of the operators $\mathbf{T}_{0,\|}$ and $\mathbf{Z}$, corresponding to the boundary of one sub-domain.

In the abstract domain decomposition method that was presented above, we made two main well-posedness assumptions. The first one (Assumption 3.9) is that the model problem (3.79) is

well-posed, which would correspond to the above model problem (3.321) with an empty transmission boundary $\Sigma = \emptyset$. The second assumption (Assumption 3.45) is that each of the local sub-problems (3.218) (appearing in the definition of the scattering operator) are well-posed. These problems would correspond to the above model problem (3.321) with a transmission boundary that is always not empty $\Sigma \neq \emptyset$ but the physical boundary Γ may (pure interior sub-domain) or may not (sub-domain with the exterior physical boundary) be empty. Therefore, when conducting the analysis, we shall pay attention that it is valid for all of the three following (exclusive) configurations: $\Sigma = \emptyset$; or $\Gamma = \emptyset$; or $\Sigma \neq \emptyset$ & $\Gamma \neq \emptyset$.

3.4.2.1 Well-posedness of the model problem

We first consider the easier case of the model problem, for which $\Sigma = \emptyset$. Let $\mathbf{F} \in \mathbf{H}_\Gamma(\mathbf{curl};\Omega)'$ such that $\operatorname{div}\mathbf{F} = 0$ in a distributional sense (charge conservation equation) and $\mathbf{g} \in \mathbf{L}^2(\Gamma)$, the model problem reads

$$\begin{cases} \text{Find } \mathbf{E} \in \mathbf{H}_\Gamma(\mathbf{curl};\Omega) \text{ such that} \\ \left(\mathbf{curl}\,\mu_r^{-1}\,\mathbf{curl} - {\kappa_0}^2\epsilon_r\right)\mathbf{E} = \mathbf{F}, & \text{in } \Omega, \\ \left(\gamma_{1,\Gamma} - \mathrm{i}\gamma_{0,\Gamma}\right)\mathbf{E} = \mathbf{g}, & \text{on } \Gamma. \end{cases} \tag{3.321}$$

We shall show in the remainder of this sub-section that the above problem is well-posed under the following assumption.

Assumption 3.69. *We suppose that the coefficients satisfy*

$$\begin{array}{ll} 0 < \Re(\mu_r) < +\infty, & 0 \leq \Im(\mu_r) < +\infty, \\ 0 < \Re(\epsilon_r) < +\infty, & 0 \leq \Im(\epsilon_r) < +\infty, \end{array} \quad \text{in } \Omega_\Sigma. \tag{3.322}$$

In particular, we do *not* assume that the imaginary parts of the coefficients are strictly positive almost everywhere in Ω, which would considerably simplify the analysis since that would mean that the medium is purely dissipative. We are rather interested in the case where they vanish in at least some subsets (of non zero measure) of Ω so that the medium is (at least partly) propagative.

As for acoustics, the first difficulty in the analysis of this problem is the fact that the sesquilinear form associated to the original problem is not coercive, hence typically requires the Fredholm alternative to provide conditions under which the problem has a solution. What makes the analysis even more technical is that we do not have the compacity of the embedding $\mathbf{H}(\mathbf{curl};\Omega) \hookrightarrow \mathbf{L}^2(\Omega)$. This comes from the fact that the **curl** operator has a large (infinite dimensional) null space (related to the divergence condition). This requires to use the Helmholtz decomposition to remove this null-space.

We follow the ideas presented in [6, Sec. 8.3.3], [107, Chap. 4 and 10] and [110, Sec. 5.4.2 and 5.4.3].

We shall prove the well posedness of the above problem using a variational approach, hence consider the weak form of (3.321) which is rewritten as

$$\begin{cases} \text{Find } \mathbf{E} \in \mathbf{H}_\Gamma(\mathbf{curl};\Omega) \text{ such that} \\ a(\mathbf{E},\mathbf{E}^t) = l(\mathbf{E}^t), \qquad \forall \mathbf{E}^t \in \mathbf{H}_\Gamma(\mathbf{curl};\Omega), \end{cases} \tag{3.323}$$

where, for all $\mathbf{u},\mathbf{v} \in \mathbf{H}_\Gamma(\mathbf{curl};\Omega)$,

$$\begin{cases} a(\mathbf{u},\mathbf{v}) := {\kappa_0}^{-1}(\mu_r^{-1}\,\mathbf{curl}\,\mathbf{u},\mathbf{curl}\,\mathbf{v})_{\mathbf{L}^2(\Omega)} - \kappa_0(\epsilon_r\mathbf{u},\mathbf{v})_{\mathbf{L}^2(\Omega)} - \mathrm{i}(\gamma_{0,\Gamma}\,\mathbf{u},\gamma_{0,\Gamma}\,\mathbf{v})_{\mathbf{L}^2(\Gamma)}, \\ l(\mathbf{v}) := {\kappa_0}^{-1}\langle\mathbf{F},\mathbf{v}\rangle_\Omega + \langle\mathbf{g},\gamma_{0,\Gamma}\,\mathbf{v}\rangle_\Gamma. \end{cases} \tag{3.324}$$

The space $\mathbf{H}_\Gamma(\mathbf{curl};\Omega)$ is made into a Hilbert space with the inner product $(\cdot,\cdot)_{\mathbf{H}_\Gamma(\mathbf{curl};\Omega)}$ defined, for all $\mathbf{u},\mathbf{v}\in\mathbf{H}_\Gamma(\mathbf{curl};\Omega)$, as

$$(\mathbf{u},\mathbf{v})_{\mathbf{H}_\Gamma(\mathbf{curl};\Omega)} := {\kappa_0}^{-1}(\mathbf{curl}\,\mathbf{u},\mathbf{curl}\,\mathbf{v})_{\mathbf{L}^2(\Omega)} + \kappa_0(\mathbf{u},\mathbf{v})_{\mathbf{L}^2(\Omega)} + (\gamma_{0,\Gamma}\,\mathbf{u},\gamma_{0,\Gamma}\,\mathbf{v})_{\mathbf{L}^2(\Gamma)}. \tag{3.325}$$

We shall need in what follows the following technical lemma, which we state without proof, see [6, Th. 3.3.1] and [107, Th. 3.37] for additional details. Note that this result rests in particular on the simply connected assumption on the domain Ω.

Lemma 3.70 (**Extraction of a scalar potential**). *For any* $\mathbf{E}$ *in* $\mathbf{L}^2(\Omega)$,

$$\mathbf{curl}\,\mathbf{E}=0,\ \textit{in}\ \Omega \qquad \Leftrightarrow \qquad \exists\, p\in H^1(\Omega):\ \mathbf{E}=\mathbf{grad}\,p. \tag{3.326}$$

We can then deduce the following lemma, providing a useful decomposition of elements of $\mathbf{H}_\Gamma(\mathbf{curl};\Omega)$, see [6, Eq. (8.29)] and [107, Lem 4.5]. Note that the dependence of the space $\mathbf{H}_\Gamma(\mathbf{curl},\operatorname{div}\epsilon_r\,0;\Omega)$ on the coefficient ϵ_r is required in the proof of Proposition 3.75.

Lemma 3.71 (**Helmholtz decomposition**). *Suppose that* ϵ_r *is uniformly bounded on* Ω, *we have*

$$\mathbf{H}_\Gamma(\mathbf{curl};\Omega)=\mathbf{H}_\Gamma(\mathbf{curl},\operatorname{div}\epsilon_r\,0;\Omega)\oplus\mathbf{grad}\,H^1_0(\Omega), \tag{3.327}$$

where

$$\mathbf{H}_\Gamma(\mathbf{curl},\operatorname{div}\epsilon_r\,0;\Omega) := \left\{\mathbf{E}\in\mathbf{H}_\Gamma(\mathbf{curl};\Omega)\mid(\epsilon_r\mathbf{E},\mathbf{grad}\,p)_{\mathbf{L}^2(\Omega)}=0,\ \forall p\in H^1_0(\Omega)\right\}. \tag{3.328}$$

Proof. Suppose $\mathbf{E}\in\mathbf{H}_\Gamma(\mathbf{curl};\Omega)$ such as $\mathbf{curl}\,\mathbf{E}=0$ in Ω with a vanishing tangential trace $\gamma_{0,\partial\Omega}\,\mathbf{E}=0$. Then from Lemma 3.70, there exists some $p\in H^1(\Omega)$ such that $\mathbf{E}=\mathbf{grad}\,p$. Since in addition $\gamma_{0,\partial\Omega}\,\mathbf{E}=0$ and p is defined up to a constant, we can find a $p\in H^1_0(\Omega)$. Hence the space $\mathbf{grad}\,H^1_0(\Omega)$ is a non empty subspace of $\mathbf{H}_\Gamma(\mathbf{curl};\Omega)$.

Since the space $\mathbf{grad}\,H^1_0(\Omega)$ is closed in $\mathbf{H}_\Gamma(\mathbf{curl};\Omega)$, for any $\mathbf{E}\in\mathbf{H}_\Gamma(\mathbf{curl};\Omega)$, we can construct its projection $\mathbf{E}_g$ onto $\mathbf{grad}\,H^1_0(\Omega)$ by solving

$$(\mathbf{E}_g,\mathbf{grad}\,p)_{\mathbf{H}_\Gamma(\mathbf{curl};\Omega)}=(\epsilon_r\mathbf{E},\mathbf{grad}\,p)_{\mathbf{L}^2(\Omega)},\qquad \forall p\in H^1_0(\Omega), \tag{3.329}$$

which satisfies the conditions of the Lax-Milgram Lemma (from the boundedness of ϵ). By simple properties of a projection we also have

$$(\mathbf{E}_g,\mathbf{grad}\,p)_{\mathbf{H}_\Gamma(\mathbf{curl};\Omega)}=(\epsilon_r\mathbf{E}_g,\mathbf{grad}\,p)_{\mathbf{L}^2(\Omega)},\qquad \forall p\in H^1_0(\Omega), \tag{3.330}$$

hence $\mathbf{E}_0:=\mathbf{E}-\mathbf{E}_g\in\mathbf{H}_\Gamma(\mathbf{curl},\operatorname{div}\epsilon_r\,0;\Omega)$ and the decomposition holds. ■

In addition, we have the following compact embedding result, which we state without proof, see [6, Th. 8.1.3] and [107, Th. 4.7] for more detail. Importantly, for this result to hold, $\Sigma=\emptyset$.

Lemma 3.72 (**Compact embedding**). *The space* $\mathbf{H}_\Gamma(\mathbf{curl},\operatorname{div}\epsilon_r\,0;\Omega)$ *is compactly embedded in* $\mathbf{L}^2(\Omega)$.

We show in the following two lemmas that the sesquilinear form a is composed of a coercive part a_+ and a compact perturbation.

Lemma 3.73 (**Coercive form**). *Under Assumption 3.69, the sesquilinear form* a_+ *defined, for all* $\mathbf{u},\mathbf{v}\in\mathbf{H}_\Gamma(\mathbf{curl};\Omega)$, *as*

$$a_+(\mathbf{u},\mathbf{v}) := {\kappa_0}^{-1}(\mu_r^{-1}\,\mathbf{curl}\,\mathbf{u},\mathbf{curl}\,\mathbf{v})_{\mathbf{L}^2(\Omega)} + \kappa_0(\epsilon_r\mathbf{u},\mathbf{v})_{\mathbf{L}^2(\Omega)} - \mathrm{i}(\gamma_{0,\Gamma}\,\mathbf{u},\gamma_{0,\Gamma}\,\mathbf{v})_{\mathbf{L}^2(\Gamma)}, \tag{3.331}$$

is continuous and coercive on $\mathbf{H}_\Gamma(\mathbf{curl};\Omega)$.

Proof. The continuity of a_+ follows readily from the boundedness of the coefficient μ_r and ϵ_r contained in Assumption 3.69. To prove coercivity, let $\mathbf{u} \in \mathbf{H}_\Gamma(\mathbf{curl};\Omega)$, we have for a $\lambda \in \mathbb{R}^+$,

$$\begin{aligned}\lambda \Re a_+(\mathbf{u},\mathbf{u}) - \Im a_+(\mathbf{u},\mathbf{u}) \geq \left(\lambda \inf_\Omega \Re(\mu_r) - \inf_\Omega \Im(\mu_r)\right) |\mu_r|^{-2}\, {\kappa_0}^{-1} \|\mathbf{curl}\,\mathbf{u}\|^2_{\mathbf{L}^2(\Omega)} \\ + \left(\lambda \inf_\Omega \Re(\epsilon_r) - \sup_\Omega \Im(\epsilon_r)\right)\, \kappa_0 \|\mathbf{u}\|^2_{\mathbf{L}^2(\Omega)} + \|\gamma_{0,\Gamma}\,\mathbf{u}\|^2_{\mathbf{L}^2(\Gamma)}.\end{aligned} \tag{3.332}$$

Hence, if Assumption 3.69 holds, we can take any λ such that

$$\lambda > \max\left(0,\ \frac{\inf_\Omega \Im\,(\mu_r)}{\inf_\Omega \Re\,(\mu_r)},\ \frac{\sup_\Omega \Im\,(\epsilon_r)}{\inf_\Omega \Re\,(\epsilon_r)}\right), \tag{3.333}$$

so that for any $\mathbf{u} \in \mathbf{H}_\Gamma(\mathbf{curl};\Omega)$, there exists $C > 0$ such that

$$\lambda \Re a_+(\mathbf{u},\mathbf{u}) - \Im a_+(\mathbf{u},\mathbf{u}) \geq C \|\mathbf{u}\|^2_{\mathbf{H}_\Gamma(\mathbf{curl};\Omega)}. \tag{3.334}$$

■

Lemma 3.74 (Compact operator). *Under Assumption 3.69, the operator*

$$K\ :\ \mathbf{L}^2(\Omega) \to \mathbf{L}^2(\Omega) \tag{3.335}$$

such that $K\mathbf{u} \in \mathbf{H}_\Gamma(\mathbf{curl}, \operatorname{div} \epsilon_r\, 0;\Omega) \subset \mathbf{L}^2(\Omega)$ *is defined, for all* $\mathbf{u} \in \mathbf{L}^2(\Omega)$*, as*

$$a_+(K\mathbf{u},\mathbf{v}) = -2\kappa_0(\epsilon_r\mathbf{u},\mathbf{v})_{\mathbf{L}^2(\Omega)}, \qquad \forall \mathbf{v} \in \mathbf{H}_\Gamma(\mathbf{curl}, \operatorname{div} \epsilon_r\, 0;\Omega). \tag{3.336}$$

is compact in $\mathbf{L}^2(\Omega)$*.*

Proof. Lemma 3.73 ensures, via application of the Lax-Migram Lemma, that there exists a constant C such that, for all $\mathbf{u} \in \mathbf{L}^2(\Omega)$

$$\|K\mathbf{u}\|_{\mathbf{H}_\Gamma(\mathbf{curl}, \operatorname{div} \epsilon_r\, 0;\Omega)} \leq C \|\mathbf{u}\|_{\mathbf{L}^2(\Omega)}. \tag{3.337}$$

Let $(u_n)_n^\infty$ be a bounded sequence in $\mathbf{L}^2(\Omega)$. Using the above inequality $(Ku_n)_n^\infty$ is a bounded sequence in $\mathbf{H}_\Gamma(\mathbf{curl}, \operatorname{div} \epsilon_r\, 0;\Omega) \subset \mathbf{L}^2(\Omega)$. Using Lemma 3.72, there is a subsequence converging strongly in $\mathbf{L}^2(\Omega)$, which implies that K is compact. ■

We now have all the ingredients to establish the following proposition.

Proposition 3.75 (Well-posedness of the model problem). *Under Assumption 3.69, the problem* (3.321) *is well-posed.*

Proof. We consider the variational form of the problem given in (3.323), namely

$$\begin{cases}\text{Find } \mathbf{E} \in \mathbf{H}_\Gamma(\mathbf{curl};\Omega) \text{ such that} \\ a(\mathbf{E},\mathbf{E}^t) = l(\mathbf{E}^t), & \forall \mathbf{E}^t \in \mathbf{H}_\Gamma(\mathbf{curl};\Omega).\end{cases} \tag{3.338}$$

By decomposing the unknown and test functions, elements of $\mathbf{H}_\Gamma(\mathbf{curl};\Omega)$, according to the decomposition stated in Lemma 3.71, we first show that the problem reduces to two uncoupled problems in $\mathbf{H}_\Gamma(\mathbf{curl}, \operatorname{div} \epsilon_r\, 0;\Omega)$ and $H^1_0(\Omega)$. Indeed, we have the basic properties

$$\begin{aligned}&\mathbf{curl}\,\mathbf{grad} \equiv 0, \\ &(\epsilon_r\mathbf{E}_0, \mathbf{grad}\, p)_{\mathbf{L}^2(\Omega)} = 0, \qquad \forall p \in H^1_0(\Omega),\ \mathbf{E}_0 \in \mathbf{H}_\Gamma(\mathbf{curl}, \operatorname{div} \epsilon_r\, 0;\Omega), \\ &\mathbf{grad}\ :\ H^1_0(\Omega) \to \{\mathbf{u} \in \mathbf{H}_\Gamma(\mathbf{curl};\Omega) \mid \gamma_{0,\partial\Omega}\,\mathbf{u} = 0\},\end{aligned} \tag{3.339}$$

and recalling the definitions of the sesquilinear forms a and a_+ given respectively in (3.324) and (3.331), the variational problem (3.323) is shown to be equivalent to:

$$\begin{cases} \text{Find } p \in H^1_0(\Omega) \text{ and } \mathbf{E}_0 \in \mathbf{H}_\Gamma(\mathbf{curl}, \operatorname{div} \epsilon_r\, 0; \Omega) \text{ such that} \\ -\kappa_0(\epsilon_r \,\mathbf{grad}\, p, \mathbf{grad}\, q)_{\mathbf{L}^2(\Omega)} = l(\mathbf{grad}\, q), & \forall q \in H^1_0(\Omega), \\ a_+(\mathbf{E}_0, \mathbf{E}_0^t) - 2\kappa_0(\epsilon_r \mathbf{E}_0, \mathbf{E}_0^t)_{\mathbf{L}^2(\Omega)} = l(\mathbf{E}_0^t), & \forall \mathbf{E}_0^t \in \mathbf{H}_\Gamma(\mathbf{curl}, \operatorname{div} \epsilon_r\, 0; \Omega). \end{cases} \tag{3.340}$$

Since ϵ_r has a bounded and strictly uniformly positive real part, by application of the Lax-Milgram Lemma, the problem in $p \in H^1_0(\Omega)$ is well-posed. Now, using the definitions of the coercive form a_+ (Lemma 3.73) and the operator K (Lemma 3.74), the problem in $\mathbf{E}_0 \in \mathbf{H}_\Gamma(\mathbf{curl}, \operatorname{div} \epsilon_r\, 0; \Omega)$ is equivalent to finding $\mathbf{E}_0 \in \mathbf{L}^2(\Omega)$ such that

$$(\mathrm{Id} + K)\mathbf{E}_0 = \mathbf{b}, \tag{3.341}$$

where by application of the Lax-Milgram Lemma, $\mathbf{b} \in \mathbf{H}_\Gamma(\mathbf{curl}, \operatorname{div} \epsilon_r\, 0; \Omega) \subset \mathbf{L}^2(\Omega)$, is the unique solution of

$$a_+(\mathbf{b}, \mathbf{E}_0^t) = l(\mathbf{E}_0^t), \qquad \forall \mathbf{E}_0^t \in \mathbf{H}_\Gamma(\mathbf{curl}, \operatorname{div} \epsilon_r\, 0; \Omega). \tag{3.342}$$

From Lemma 3.74 the operator K is compact in $\mathbf{L}^2(\Omega)$, the Fredholm alternative is applicable and the proof reduces to a uniqueness result.

For the proof of uniqueness, let $\mathbf{E}_1$ and $\mathbf{E}_2$ in $\mathbf{H}_\Gamma(\mathbf{curl}; \Omega)$ be two solutions to (3.323). By linearity, the difference $\mathbf{e} = \mathbf{E}_2 - \mathbf{E}_1$ satisfy

$$a(\mathbf{e}, \mathbf{E}^t) = 0, \qquad \forall \mathbf{E}^t \in \mathbf{H}_\Gamma(\mathbf{curl}; \Omega). \tag{3.343}$$

Choosing $\mathbf{E}^t = \mathbf{e}$ and taking the imaginary part yields

$$\kappa_0{}^{-1}(\Im\left(\mu_r^{-1}\right) \mathbf{curl}\, \mathbf{e}, \mathbf{curl}\, \mathbf{e})_{\mathbf{L}^2(\Omega)} - \kappa_0(\Im\left(\epsilon_r\right) \mathbf{e}, \mathbf{e})_{\mathbf{L}^2(\Omega)} - (\gamma_{0,\Gamma}\, \mathbf{e}, \gamma_{0,\Gamma}\, \mathbf{e})_{\mathbf{L}^2(\Gamma)} = 0. \tag{3.344}$$

We deduce that $\gamma_{0,\partial\Omega}\, \mathbf{e} = 0$ on $\partial\Omega = \Gamma$. The proof then follows using a unique continuation result, see Theorem 8.3.10 in [6] and the proof of Theorem 4.12 in [107]. ■

3.4.2.2 Well-posedness of local sub-problems

We now consider the case of local sub-problems where the transmission boundary $\Sigma \neq \emptyset$.

A first idea We now consider the weak form of (3.320) which is written as

$$\begin{cases} \text{Find } \mathbf{E} \in \mathbf{H}_\Gamma(\mathbf{curl}; \Omega) \text{ such that} \\ a(\mathbf{E}, \mathbf{E}^t) + \langle [\mathbf{Z} - \mathrm{i}\mathbf{T}]\, \gamma_{0,\Sigma}\, \mathbf{E}, \gamma_{0,\Sigma}\, \mathbf{E}^t \rangle_\Sigma = l(\mathbf{E}^t) + \langle \mathbf{x}, \gamma_{0,\Sigma}\, \mathbf{E}^t \rangle_\Sigma, \qquad \forall \mathbf{E}^t \in \mathbf{H}_\Gamma(\mathbf{curl}; \Omega), \end{cases} \tag{3.345}$$

where a and l where given in (3.324).

We can make the following assumption on the operators $\mathbf{T}$ and $\mathbf{Z}$, which is required anyway for the convergence analysis.

Assumption 3.76. *In addition to Assumption 3.69 we suppose that the transmission operators are such that*

- $\mathbf{T}$ *is a* self-adjoint positive isomorphism *from* $\mathbf{H}^{-1/2}(\mathrm{curl}; \Gamma)$ *to* $\mathbf{H}^{-1/2}(\mathrm{div}; \Gamma)$*;*
- $\mathbf{Z}$ *is a* symmetric continuous operator *from* $\mathbf{H}^{-1/2}(\mathrm{curl}; \Gamma)$ *to* $\mathbf{H}^{-1/2}(\mathrm{div}; \Gamma)$.

The first idea is to adapt the proof for the model problem above. It is clear that the Helmholtz decomposition from Lemma 3.71

$$\mathbf{H}_\Gamma(\mathbf{curl};\Omega) = \mathbf{H}_\Gamma(\mathbf{curl}, \operatorname{div} \epsilon_r\, 0;\Omega) \oplus \mathbf{grad}\, H_0^1(\Omega), \tag{3.346}$$

still holds in the case where $\Sigma \neq \emptyset$.

Besides, we can define a coercive sesquilinear form, as stated by the following lemma, which takes as a model Lemma 3.73.

Lemma 3.77 (**Coercive form**). *Under Assumption 3.69 and if*

$$\frac{\beta_{\mathbf{T}}}{\alpha_{\mathbf{Z}}} > \max\left(\frac{\inf_\Omega \Im\left(\mu_r\right)}{\inf_\Omega \Re\left(\mu_r\right)},\ \frac{\sup_\Omega \Im\left(\epsilon_r\right)}{\inf_\Omega \Re\left(\epsilon_r\right)}\right), \tag{3.347}$$

where $\alpha_{\mathbf{Z}}$ is the continuity constant of $\mathbf{Z}$ and $\beta_{\mathbf{T}}$ is the coercivity constant of $\mathbf{T}$, the sesquilinear form, defined for all $\mathbf{u},\mathbf{v} \in \mathbf{H}_\Gamma(\mathbf{curl};\Omega)$, as

$$\tilde{a}_+(\mathbf{u},\mathbf{v}) := a_+(\mathbf{u},\mathbf{v}) + \langle [\mathbf{Z} - \mathrm{i}\mathbf{T}]\, \gamma_{0,\Sigma}\, \mathbf{u}, \gamma_{0,\Sigma}\, \mathbf{v}\rangle_\Sigma, \tag{3.348}$$

where a_+ was defined in (3.331)*, is continuous and coercive on $\mathbf{H}_\Gamma(\mathbf{curl};\Omega)$.*

Proof. The continuity of the above sesquilinear form follows readily from the boundedness of the coefficient μ_r and ϵ_r and the continuity property of $\mathbf{Z}$ and $\mathbf{T}$ contained in Assumption 3.69 and Assumption 3.76. To prove coercivity, let $\mathbf{u} \in \mathbf{H}_\Gamma(\mathbf{curl};\Omega)$, we have for a $\lambda \in \mathbb{R}^+$,

$$\begin{aligned}\lambda \Re\tilde{a}_+(\mathbf{u},\mathbf{u}) - \Im\tilde{a}_+(\mathbf{u},\mathbf{u}) \geq &\left(\lambda \inf_\Omega \Re(\mu_r) - \inf_\Omega \Im(\mu_r)\right) |\mu_r|^{-2}\, {\kappa_0}^{-1} \|\,\mathbf{curl}\,\mathbf{u}\|^2_{\mathbf{L}^2(\Omega)} \\ &+ \left(\lambda \inf_\Omega \Re(\epsilon_r) - \sup_\Omega \Im(\epsilon_r)\right)\, \kappa_0 \|\mathbf{u}\|^2_{\mathbf{L}^2(\Omega)} \\ &+ \|\gamma_{0,\Gamma}\, \mathbf{u}\|^2_{\mathbf{L}^2(\Gamma)} + (\beta_{\mathbf{T}} - \lambda\alpha_{\mathbf{Z}})\, \|\gamma_{0,\Sigma}\, \mathbf{u}\|^2_{\mathbf{H}^{-1/2}(\mathrm{curl};\Sigma)}.\end{aligned} \tag{3.349}$$

Hence, if λ is such that

$$\frac{\beta_{\mathbf{T}}}{\alpha_{\mathbf{Z}}} > \lambda > \max\left(0,\ \frac{\inf_\Omega \Im\left(\mu_r\right)}{\inf_\Omega \Re\left(\mu_r\right)},\ \frac{\sup_\Omega \Im\left(\epsilon_r\right)}{\inf_\Omega \Re\left(\epsilon_r\right)}\right), \tag{3.350}$$

for any $\mathbf{u} \in \mathbf{H}_\Gamma(\mathbf{curl};\Omega)$, there exists $C > 0$ such that

$$\lambda \Re\tilde{a}_+(\mathbf{u},\mathbf{u}) - \Im\tilde{a}_+(\mathbf{u},\mathbf{u}) \geq C\|\mathbf{u}\|^2_{\mathbf{H}_\Gamma(\mathbf{curl};\Omega)}. \tag{3.351}$$

■

However, we were *not* able to state a compacity result such as Lemma 3.72 and as a result we are not able to define a compact operator K in the model of Lemma 3.74. Indeed, we no longer have an implicit control on the tangential or normal traces on the transmission interface Σ (as we do for simple first order absorbing boundary conditions such as the one imposed on Γ for instance) that is required for the standard compact embedding results to hold.

If we are then not able to prove the existence of a solution by application of the Fredholm alternative, we are nevertheless able to prove the unicity of the solution.

Proposition 3.78 (**Uniqueness result**). *Under Assumption 3.69 and Assumption 3.76 the problem* (3.320) *has a unique solution, if it exists.*

Proof. Let $\mathbf{E}_1$ and $\mathbf{E}_2$ in $\mathbf{H}_\Gamma(\mathbf{curl};\Omega)$ be two solutions to (3.323). By linearity, the difference $\mathbf{e} = \mathbf{E}_2 - \mathbf{E}_1$ satisfy

$$a(\mathbf{e}, \mathbf{E}^t) + \langle [\mathbf{Z} - \mathrm{i}\mathbf{T}]\, \gamma_{0,\Sigma}\, \mathbf{e}, \gamma_{0,\Sigma}\, \mathbf{E}^t \rangle_\Sigma = 0, \qquad \forall \mathbf{E}^t \in \mathbf{H}_\Gamma(\mathbf{curl};\Omega). \tag{3.352}$$

Choosing $\mathbf{E}^t = \mathbf{e}$ and taking the imaginary part yields

$$\begin{aligned} {\kappa_0}^{-1} (\Im\left(\mu_r^{-1}\right) \mathbf{curl}\, \mathbf{e}, \mathbf{curl}\, \mathbf{e})_{\mathbf{L}^2(\Omega)} - \kappa_0 (\Im\left(\epsilon_r\right) \mathbf{e}, \mathbf{e})_{\mathbf{L}^2(\Omega)} \\ - (\gamma_{0,\Gamma}\, \mathbf{e}, \gamma_{0,\Gamma}\, \mathbf{e})_{\mathbf{L}^2(\Gamma)} - \langle \mathbf{T} \gamma_{0,\Sigma}\, \mathbf{e}, \gamma_{0,\Sigma}\, \mathbf{e} \rangle_\Sigma = 0. \end{aligned} \tag{3.353}$$

We deduce that $\gamma_{0,\Gamma}\, \mathbf{e} = 0$ on Γ on the one hand, and the positivity and injectivity of the transmission operator $\mathbf{T}$ from Assumption 3.76 gives that $\gamma_{0,\Sigma}\, \mathbf{e} = 0$ on Σ on the other hand, so that the tangential trace of $\mathbf{e}$ vanish on the whole boundary $\partial\Omega$. The proof then follows using a unique continuation result, see Theorem 8.3.10 in [6] and the proof of Theorem 4.12 in [107]. ■

It follows from the previous proposition that it only remains to prove the existence of the solution to the local sub-problems. We provide below two (partial) results (Proposition 3.80 and Proposition 3.86) to bypass the previously identified difficulty posed by the lack of compacity. These results are not completely satisfactory in the sense that we do not prove that the local sub-problems are well-posed in full generality. They are nevertheless a strong indication that the well-posedness result holds true.

A first partial result The first approach we present rests on the following assumption.

Assumption 3.79. *Let* $\mathbf{F} \in \mathbf{H}_\Gamma(\mathbf{curl};\Omega)'$ *such that* $\operatorname{div} \mathbf{F} = 0$ *in a distributional sense (charge conservation equation),* $\mathbf{g} \in \mathbf{L}^2(\Gamma)$ *and* $\mathbf{x} \in \mathbf{H}^{-1/2}(\mathrm{curl};\Sigma)$*, we assume that the following (Dirichlet) problem*

$$\begin{cases} \textit{Find } \mathbf{E} \in \mathbf{H}_\Gamma(\mathbf{curl};\Omega) \textit{ such that} & \\ \left(\mathbf{curl}\, \mu_r^{-1}\, \mathbf{curl} - {\kappa_0}^2 \epsilon_r\right) \mathbf{E} = \mathbf{F}, & \textit{in } \Omega, \\ \left(\gamma_{1,\Gamma} - \mathrm{i}\gamma_{0,\Gamma}\right) \mathbf{E} = \mathbf{g}, & \textit{on } \Gamma, \\ \gamma_{0,\Sigma}\, \mathbf{E} = \mathbf{x}, & \textit{on } \Sigma, \end{cases} \tag{3.354}$$

is well-posed.

If Γ is not empty (or if the imaginary parts of the coefficients ϵ_r and μ_r do not vanish in the sub-domain Ω) the well-posedness of the above problem can be proven using standard results, see for instance [107, Chap. 4]. However it may happen that some (interior) sub-domains are such that $\Gamma = \emptyset$ (and in which the coefficients are real). The problem above can still be well-posed but in general one must exclude so called *interior eigenvalues* or *resonances*, which correspond to values of κ_0 such that there exist non-trivial $\mathbf{E}$ elements of

$$\mathbf{H}_0(\mathbf{curl};\Omega) := \{\mathbf{E} \in \mathbf{H}(\mathbf{curl};\Omega) \mid \gamma_{0,\Sigma}\, \mathbf{E} = 0\}, \tag{3.355}$$

such that

$$(\mu_r^{-1}\, \mathbf{curl}\, \mathbf{E}, \mathbf{curl}\, \mathbf{E}^t)_{\mathbf{L}^2(\Omega)} = {\kappa_0}^2 (\epsilon_r \mathbf{E}, \mathbf{E}^t)_{\mathbf{L}^2(\Omega)}, \qquad \forall \mathbf{E}^t \in \mathbf{H}_0(\mathbf{curl};\Omega). \tag{3.356}$$

Using Assumption 3.79, we can properly define the operator

$$\begin{aligned} \Lambda_i \ &: \mathbf{H}^{-1/2}(\mathrm{curl};\Sigma) \to \mathbf{H}^{-1/2}(\mathrm{div};\Sigma), \\ &\mathbf{x} \mapsto \gamma_{1,\Sigma}\, \mathbf{E}, \end{aligned} \tag{3.357}$$

where $\mathbf{E} \in \mathbf{H}_\Gamma(\mathbf{curl};\Omega)$ is such that

$$\begin{cases} \left(\mathbf{curl}\,\mu_r^{-1}\,\mathbf{curl} - {\kappa_0}^2\epsilon_r\right)\mathbf{E} = 0, & \text{in } \Omega, \\ \left(\gamma_{1,\Gamma} - \mathrm{i}\gamma_{0,\Gamma}\right)\mathbf{E} = 0, & \text{on } \Gamma, \\ \gamma_{0,\Sigma}\,\mathbf{E} = \mathbf{x}, & \text{on } \Sigma. \end{cases} \tag{3.358}$$

The following proposition states the well-posedness of the local sub-problems.

Proposition 3.80 (**Well-posedness of the local sub-problems**). *Under Assumption 3.69, Assumption 3.76 and Assumption 3.79, the problem* (3.320) *is well-posed.*

Proof. Let $\mathbf{E}_0 \in \mathbf{H}_\Gamma(\mathbf{curl};\Omega)$ be the source lifting such that

$$\begin{cases} \left(\mathbf{curl}\,\mu_r^{-1}\,\mathbf{curl} - {\kappa_0}^2\epsilon_r\right)\mathbf{E}_0 = \mathbf{F}, & \text{in } \Omega, \\ \left(\gamma_{1,\Gamma} - \mathrm{i}\gamma_{0,\Gamma}\right)\mathbf{E}_0 = \mathbf{g}, & \text{on } \Gamma, \\ \gamma_{0,\Sigma}\,\mathbf{E}_0 = 0, & \text{on } \Sigma, \end{cases} \tag{3.359}$$

which is uniquely defined from Assumption 3.79. Solving the problem (3.320) is then equivalent to solve

$$\begin{cases} \text{Find } \mathbf{E} \in \mathbf{H}_\Gamma(\mathbf{curl};\Omega) \text{ such that} & \\ \left(\mathbf{curl}\,\mu_r^{-1}\,\mathbf{curl} - {\kappa_0}^2\epsilon_r\right)\mathbf{E} = 0, & \text{in } \Omega, \\ \left(\gamma_{1,\Gamma} - \mathrm{i}\gamma_{0,\Gamma}\right)\mathbf{E} = 0, & \text{on } \Gamma, \\ \left(\gamma_{1,\Sigma} + [\mathbf{Z} - \mathrm{i}\mathbf{T}]\,\gamma_{0,\Sigma}\right)\mathbf{E} = \mathbf{x} - \gamma_{1,\Sigma}\,\mathbf{E}_0, & \text{on } \Sigma. \end{cases} \tag{3.360}$$

Using the operator Λ_i this problem is equivalent to the problem

$$\begin{cases} \text{Find } \mathbf{y} \in \mathbf{H}^{-1/2}(\mathrm{curl};\Sigma) \text{ such that} \\ (\Lambda_i + \mathbf{Z} - \mathrm{i}\mathbf{T})\mathbf{y} = \mathbf{x} - \gamma_{1,\Sigma}\,\mathbf{E}_0, \end{cases} \tag{3.361}$$

in the sense that having a solution to one problem immediately yields a solution for the other. Indeed, it is clear that if $\mathbf{E}$ is a solution to (3.360), then its trace $\gamma_{0,\Sigma}\,\mathbf{E}$ is solution to (3.361). Reciprocally, if $\mathbf{y}$ is solution to (3.361), then $\mathbf{E}$ solution to (3.360) is found by solving

$$\begin{cases} \left(\mathbf{curl}\,\mu_r^{-1}\,\mathbf{curl} - {\kappa_0}^2\epsilon_r\right)\mathbf{E} = 0, & \text{in } \Omega, \\ \left(\gamma_{1,\Gamma} - \mathrm{i}\gamma_{0,\Gamma}\right)\mathbf{E} = 0, & \text{on } \Gamma, \\ \gamma_{0,\Sigma}\,\mathbf{E} = \mathbf{y}, & \text{on } \Sigma, \end{cases} \tag{3.362}$$

which is well-posed thanks to Assumption 3.79.

It is therefore enough to prove that the problem (3.361) is well-posed, which stems from the coercivity of the operator $\Lambda_i + \mathbf{Z} - \mathrm{i}\mathbf{T}$ on $\mathbf{H}^{-1/2}(\mathrm{curl};\Sigma)$. Let us now prove this result. Let $\mathbf{y} \in \mathbf{H}^{-1/2}(\mathrm{curl};\Sigma)$ and $\mathbf{u} \in \mathbf{H}_\Gamma(\mathbf{curl};\Omega)$ such that

$$\begin{cases} \left(\mathbf{curl}\,\mu_r^{-1}\,\mathbf{curl} - {\kappa_0}^2\epsilon_r\right)\mathbf{u} = 0, & \text{in } \Omega, \\ \left(\gamma_{1,\Gamma} - \mathrm{i}\gamma_{0,\Gamma}\right)\mathbf{u} = 0, & \text{on } \Gamma, \\ \gamma_{0,\Sigma}\,\mathbf{u} = \mathbf{y}, & \text{on } \Sigma, \end{cases} \tag{3.363}$$

so that we have by definition

$$\langle \Lambda_i \mathbf{y}, \mathbf{y}\rangle_\Sigma = (\mu_r^{-1}\,\mathbf{curl}\,\mathbf{u}, \mathbf{curl}\,\mathbf{u})_{\mathbf{L}^2(\Omega)} - {\kappa_0}^2(\epsilon_r\mathbf{u},\mathbf{u})_{\mathbf{L}^2(\Omega)} - \|\gamma_{0,\Gamma}\,\mathbf{u}\|^2_{\mathbf{L}^2(\Gamma)}. \tag{3.364}$$

It follows that, using in particular the symmetry property of the operator $\mathbf{Z}$ from Assumption 3.76,

$$-\Im\left[\langle(\Lambda_i+\mathbf{Z}-\mathrm{i}\mathbf{T})\mathbf{y},\mathbf{y}\rangle_\Sigma\right]=-(\Im(\mu_r^{-1})\,\mathbf{curl}\,\mathbf{u},\mathbf{curl}\,\mathbf{u})_{\mathbf{L}^2(\Omega)}+{\kappa_0}^2(\Im(\epsilon_r)\mathbf{u},\mathbf{u})_{\mathbf{L}^2(\Omega)}+\langle\mathbf{T}\mathbf{y},\mathbf{y}\rangle_\Sigma, \tag{3.365}$$

so that using the positivity of the imaginary parts of the coefficients from Assumption 3.69 and the coercivity property of the operator $\mathbf{T}$ from Assumption 3.76,

$$-\Im\left[\langle(\Lambda_i+\mathbf{Z}-\mathrm{i}\mathbf{T})\mathbf{y},\mathbf{y}\rangle_\Sigma\right]\geq\langle\mathbf{T}\mathbf{y},\mathbf{y}\rangle_\Sigma\geq\beta_{\mathbf{T}}\|\mathbf{y}\|^2_{\mathbf{H}^{-1/2}(\mathrm{curl};\Sigma)}. \tag{3.366}$$

where we denoted by $\beta_{\mathbf{T}}$ the coercivity constant of $\mathbf{T}$. ■

Assumption 3.69 on the coefficients of the PDE is natural. Assumption 3.76 on the transmission operator is required by the convergence analysis. Assumption 3.79 on the well-posedness of the interior problem may not be satisfied in a general configuration. However, it seems that the assumption comes from the method of proof rather than being required for a true reason.

A second partial result For the sole purpose of simplifying the discussion, we suppose here that Γ is empty, so that the only boundary of Ω is Σ. Besides, we shall suppose that $\mathbf{Z}$ is identically zero.

Let us define the bounded open domain Ω_e as an exterior strip enclosing the domain Ω such that $\Omega\cap\Omega_e=\emptyset$ and $\partial\Omega_e=\Sigma\cup\Gamma_e$, see Figure 3.6. Then $\tilde{\Omega}:=\Omega\cup\Sigma\cup\Omega_e$ is a bounded, simply connected, Lipschitz domain with boundary Γ_e that admits a non-overlapping partition made up of two sub-domains Ω and Ω_e. The common interface of the two non-overlapping sub-domains being Σ.

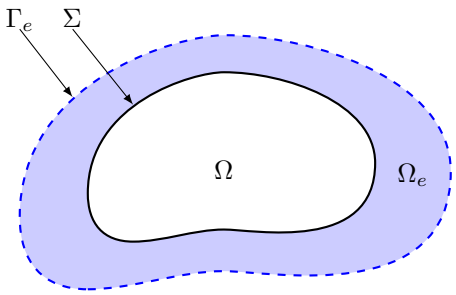

Figure 3.6: Sketch of the configuration with the exterior strip Ω_e.

In addition, let us introduce the real and strictly positive coefficients $\epsilon_{r,e}$ and $\mu_{r,e}$ as bounded functions of Ω_e

$$\begin{aligned}&0<\Re\left(\mu_{r,e}\right)<+\infty, \qquad \Im\left(\mu_{r,e}\right)=0,\\ &0<\Re\left(\epsilon_{r,e}\right)<+\infty, \qquad \Im\left(\epsilon_{r,e}\right)=0,\end{aligned} \qquad \text{in } \Omega_e. \tag{3.367}$$

We introduce a special type of transmission operator (the sign comes from the fact that the normal in the definition of $\gamma_{1,\Sigma}$ is inward with respect to Ω_e)

$$\begin{aligned}\mathbf{T}_e\ &:\mathbf{H}^{-1/2}(\mathrm{curl};\Sigma)\to\mathbf{H}^{-1/2}(\mathrm{div};\Sigma),\\ &\mathbf{x}\mapsto-\gamma_{1,\Sigma}\,\mathbf{E}_e,\end{aligned} \tag{3.368}$$

where $\mathbf{E}_e \in \mathbf{H}_\Gamma(\mathbf{curl};\Omega_e)$ is such that

$$\begin{cases} \left(\mathbf{curl}\,\mu_{r,e}^{-1}\,\mathbf{curl} + {\kappa_0}^2\epsilon_{r,e}\right)\mathbf{E}_e = 0, & \text{in } \Omega_e, \\ \gamma_{0,\Gamma_e}\,\mathbf{E}_e = 0, & \text{on } \Gamma_e, \\ \gamma_{0,\Sigma}\,\mathbf{E}_e = \mathbf{x}, & \text{on } \Sigma. \end{cases} \tag{3.369}$$

This operator is well defined since the above problem is coercive. Besides, it satisfies the Assumption 3.76 on the transmission operator for the convergence analysis. In fact this is a completely valid candidate to be used in a domain decomposition method. We shall actually study very similar operators in Chapter 8.

We claim that for this special type of operator the local sub-problems are well-posed. We will first prove this claim and then show that the well-posedness result carries over if any compact perturbation of this operator is used as a transmission operator.

Let $\mathbf{F} \in \mathbf{H}_\Gamma(\mathbf{curl};\Omega)'$ such that $\operatorname{div}\mathbf{F} = 0$ in a distributional sense (charge conservation equation), $\mathbf{g} \in \mathbf{L}^2(\Gamma)$ and $\mathbf{x} \in \mathbf{H}^{-1/2}(\operatorname{div};\Sigma)$, we consider the problem

$$\begin{cases} \text{Find } \mathbf{E} \in \mathbf{H}(\mathbf{curl};\Omega) \text{ such that} & \\ \left(\mathbf{curl}\,\mu_r^{-1}\,\mathbf{curl} - {\kappa_0}^2\epsilon_r\right)\mathbf{E} = \mathbf{F}, & \text{in } \Omega, \\ \left(\gamma_{1,\Sigma} - \mathrm{i}\mathbf{T}_e\gamma_{0,\Sigma}\right)\mathbf{E} = \mathbf{x}, & \text{on } \Sigma. \end{cases} \tag{3.370}$$

By definition of $\mathbf{T}_e$, the problem (3.370) is rewritten as as the following transmission problem

$$\begin{cases} \text{Find } \mathbf{E} \in \mathbf{H}(\mathbf{curl};\Omega) \text{ and } \mathbf{E}_e \in \mathbf{H}(\mathbf{curl};\Omega_e) \text{ such that} & \\ \left(\mathbf{curl}\,\mu_r^{-1}\,\mathbf{curl} - {\kappa_0}^2\epsilon_r\right)\mathbf{E} = \mathbf{F}, & \text{in } \Omega, \\ \left(\mathbf{curl}\,\mu_{r,e}^{-1}\,\mathbf{curl} + {\kappa_0}^2\epsilon_{r,e}\right)\mathbf{E}_e = 0, & \text{in } \Omega_e, \\ \gamma_{0,\Gamma_e}\,\mathbf{E}_e = 0, & \text{on } \Gamma_e, \\ \gamma_{1,\Sigma}\,\mathbf{E} + \mathrm{i}\gamma_{1,\Sigma}\,\mathbf{E}_e = \mathbf{x}, & \text{on } \Sigma, \\ \gamma_{0,\Sigma}\,\mathbf{E}_e = \gamma_{0,\Sigma}\,\mathbf{E}, & \text{on } \Sigma. \end{cases} \tag{3.371}$$

The last condition on Σ implies that in fact it is enough to look for an element $\tilde{\mathbf{E}}$ of $\mathbf{H}(\mathbf{curl};\tilde{\Omega})$ with $\mathbf{E} := \tilde{\mathbf{E}}|_\Omega$ and $\mathbf{E}_e := \tilde{\mathbf{E}}|_{\Omega_e}$. We shall prove the well posedness of the above problem using a variational approach, hence consider its the weak form which is written as

$$\begin{cases} \text{Find } \tilde{\mathbf{E}} \in \mathbf{H}_{\Gamma_e 0}(\mathbf{curl};\tilde{\Omega}) \text{ such that} \\ \tilde{a}(\tilde{\mathbf{E}},\tilde{\mathbf{E}}^t) = \tilde{l}(\tilde{\mathbf{E}}^t), \qquad \forall \tilde{\mathbf{E}}^t \in \mathbf{H}(\mathbf{curl};\tilde{\Omega}), \end{cases} \tag{3.372}$$

where we introduced the space

$$\mathbf{H}_{\Gamma_e 0}(\mathbf{curl};\tilde{\Omega}) := \left\{\mathbf{E} \in \mathbf{H}(\mathbf{curl};\tilde{\Omega}) \mid \gamma_{0,\Gamma_e}\,\mathbf{E} = 0\right\}, \tag{3.373}$$

and the sesquilinear forms

$$\begin{cases} a(\mathbf{u},\mathbf{v}) := {\kappa_0}^{-1}(\mu_r^{-1}\,\mathbf{curl}\,\mathbf{u},\mathbf{curl}\,\mathbf{v})_{\mathbf{L}^2(\Omega)} - \kappa_0(\epsilon_r\mathbf{u},\mathbf{v})_{\mathbf{L}^2(\Omega)}, & \forall \mathbf{u},\mathbf{v} \in \mathbf{H}(\mathbf{curl};\Omega), \\ a_e(\mathbf{u},\mathbf{v}) := {\kappa_0}^{-1}(\mu_{r,e}^{-1}\,\mathbf{curl}\,\mathbf{u},\mathbf{curl}\,\mathbf{v})_{\mathbf{L}^2(\Omega_e)} + \kappa_0(\epsilon_{r,e}\mathbf{u},\mathbf{v})_{\mathbf{L}^2(\Omega_e)}, & \forall \mathbf{u},\mathbf{v} \in \mathbf{H}(\mathbf{curl};\Omega_e), \\ \tilde{a}(\mathbf{u},\mathbf{v}) := a(\mathbf{u}|_\Omega,\mathbf{v}|_\Omega) - \mathrm{i}a_e(\mathbf{u}|_{\Omega_e},\mathbf{v}|_{\Omega_e}), & \forall \mathbf{u},\mathbf{v} \in \mathbf{H}(\mathbf{curl};\tilde{\Omega}). \end{cases} \tag{3.374}$$

and

$$\tilde{l}(\mathbf{v}) := {\kappa_0}^{-1}\langle \mathbf{F}, \mathbf{v}|_\Omega\rangle_\Omega, \qquad \forall \mathbf{v} \in \mathbf{H}(\mathbf{curl};\tilde{\Omega}). \tag{3.375}$$

Let us introduce the global coefficients $\tilde{\epsilon}_r$ and $\tilde{\mu}_r$ defined on $\tilde{\Omega}$ and such that

$$\begin{cases} \tilde{\epsilon}_r|_\Omega = \epsilon_r, \\ \tilde{\mu}_r|_\Omega^{-1} = \mu_r^{-1}, \end{cases} \quad \text{and} \quad \begin{cases} \tilde{\epsilon}_r|_{\Omega_e} = -\mathrm{i}\epsilon_{r,e}, \\ \tilde{\mu}_r|_{\Omega_e}^{-1} = -\mathrm{i}\mu_{r,e}^{-1}. \end{cases} \tag{3.376}$$

We can state a similar Helmholtz decomposition as in Lemma 3.71, whose proof is omitted for the sake of brevity.

Lemma 3.81 (**Helmholtz decomposition**). *We have*

$$\mathbf{H}_{\Gamma_e 0}(\mathbf{curl}; \tilde{\Omega}) = \mathbf{H}_{\Gamma_e 0}(\mathbf{curl}, \operatorname{div} \tilde{\epsilon}_r\, 0; \tilde{\Omega}) \oplus \mathbf{grad}\, H_0^1(\tilde{\Omega}), \tag{3.377}$$

where

$$\mathbf{H}_{\Gamma_e 0}(\mathbf{curl}, \operatorname{div} \tilde{\epsilon}_r\, 0; \tilde{\Omega}) := \left\{ \mathbf{E} \in \mathbf{H}_{\Gamma_e 0}(\mathbf{curl}; \tilde{\Omega}) \mid (\tilde{\epsilon}_r \mathbf{E}, \mathbf{grad}\, p)_{\mathbf{L}^2(\tilde{\Omega})} = 0,\ \forall p \in H_0^1(\tilde{\Omega}) \right\}. \tag{3.378}$$

By extending the domain Ω to $\tilde{\Omega}$ we have gained a control on the tangential trace on the boundary of the domain under consideration. We are therefore able to state the following compacity result, which stems for instance from [53, Th. 5.1].

Lemma 3.82 (**Compact embedding**). *The space* $\mathbf{H}_{\Gamma_e}(\mathbf{curl}, \operatorname{div} \tilde{\epsilon}_r\, 0; \tilde{\Omega})$ *is compactly embedded in* $\mathbf{L}^2(\tilde{\Omega})$.

We show in the following two lemmas that the sesquilinear form $\tilde{a}$ is composed of a coercive part $\tilde{a}_+$ and a compact perturbation.

Lemma 3.83 (**Coercive form**). *Under Assumption 3.69, the sesquilinear form* $\tilde{a}_+$ *defined, for all* $\mathbf{u}, \mathbf{v} \in \mathbf{H}_{\Gamma_e 0}(\mathbf{curl}; \tilde{\Omega})$, *as*

$$\begin{cases} \tilde{a}_+(\mathbf{u}, \mathbf{v}) := a_+(\mathbf{u}|_\Omega, \mathbf{v}|_\Omega) - \mathrm{i} a_e(\mathbf{u}|_{\Omega_e}, \mathbf{v}|_{\Omega_e}), & \forall \mathbf{u}, \mathbf{v} \in \mathbf{H}(\mathbf{curl}; \tilde{\Omega}), \\ a_+(\mathbf{u}, \mathbf{v}) := {\kappa_0}^{-1} (\mu_r^{-1}\, \mathbf{curl}\, \mathbf{u}, \mathbf{curl}\, \mathbf{v})_{\mathbf{L}^2(\Omega)} + \kappa_0 (\epsilon_r \mathbf{u}, \mathbf{v})_{\mathbf{L}^2(\Omega)}, & \forall \mathbf{u}, \mathbf{v} \in \mathbf{H}(\mathbf{curl}; \Omega), \end{cases} \tag{3.379}$$

is continuous and coercive on $\mathbf{H}_{\Gamma_e 0}(\mathbf{curl}; \tilde{\Omega})$.

Proof. The continuity of a_+ follows readily from the boundedness of the coefficient μ_r and ϵ_r contained in Assumption 3.69. To prove coercivity, let $\mathbf{u} \in \mathbf{H}_\Gamma(\mathbf{curl}; \Omega)$, we have for a $\lambda \in \mathbb{R}^+$,

$$\begin{aligned} \lambda \Re \tilde{a}_+(\mathbf{u}, \mathbf{u}) - \Im \tilde{a}_+(\mathbf{u}, \mathbf{u}) \geq & \left(\lambda \inf_\Omega \Re(\mu_r) - \inf_\Omega \Im(\mu_r) \right) |\mu_r|^{-2}\, {\kappa_0}^{-1} \| \mathbf{curl}\, \mathbf{u}|_\Omega \|^2_{\mathbf{L}^2(\Omega)} \\ & + |\mu_{r,e}|^{-2} \inf_{\Omega_e} \mu_{r,e}\, {\kappa_0}^{-1} \| \mathbf{curl}\, \mathbf{u}|_{\Omega_e} \|^2_{\mathbf{L}^2(\Omega_e)} \\ & + \left(\lambda \inf_\Omega \Re(\epsilon_r) - \sup_\Omega \Im(\epsilon_r) \right) \kappa_0 \|\mathbf{u}|_\Omega\|^2_{\mathbf{L}^2(\Omega)} \\ & + \sup_{\Omega_e} \epsilon_{r,e}\, \kappa_0 \|\mathbf{u}|_{\Omega_e}\|^2_{\mathbf{L}^2(\Omega_e)}. \end{aligned} \tag{3.380}$$

If Assumption 3.69 holds, we can take any λ such that

$$\lambda > \max\left(0,\ \frac{\inf_\Omega \Im(\mu_r)}{\inf_\Omega \Re(\mu_r)},\ \frac{\sup_\Omega \Im(\epsilon_r)}{\inf_\Omega \Re(\epsilon_r)}\right), \tag{3.381}$$

so that for any $\mathbf{u} \in \mathbf{H}_{\Gamma_e 0}(\mathbf{curl}; \tilde{\Omega})$, there exists $C > 0$ such that

$$\lambda \Re \tilde{a}_+(\mathbf{u}, \mathbf{u}) - \Im \tilde{a}_+(\mathbf{u}, \mathbf{u}) \geq C \|\mathbf{u}\|^2_{\mathbf{H}_{\Gamma_e 0}(\mathbf{curl}; \tilde{\Omega})}. \tag{3.382}$$

■

Lemma 3.84 (Compact operator). *Under Assumption 3.69, the operator*

$$\tilde{K} \,:\, \mathbf{L}^2(\tilde{\Omega}) \to \mathbf{L}^2(\tilde{\Omega}) \tag{3.383}$$

such that $\tilde{K}\mathbf{u} \in \mathbf{H}_{\Gamma_e 0}(\mathbf{curl}, \operatorname{div} \tilde{\epsilon}_r\, 0; \tilde{\Omega}) \subset \mathbf{L}^2(\tilde{\Omega})$ *is defined, for all* $\mathbf{u} \in \mathbf{L}^2(\tilde{\Omega})$*, as*

$$a_+(\tilde{K}\mathbf{u}, \mathbf{v}) = -2\kappa_0(\tilde{\epsilon}_r \mathbf{u}, \mathbf{v})_{\mathbf{L}^2(\tilde{\Omega})}, \qquad \forall \mathbf{v} \in \mathbf{H}_{\Gamma_e 0}(\mathbf{curl}, \operatorname{div} \tilde{\epsilon}_r\, 0; \tilde{\Omega}). \tag{3.384}$$

is compact in $\mathbf{L}^2(\tilde{\Omega})$*.*

Proof. It follows the lines of the proof of Lemma 3.74. ■

We now have all the ingredients to establish the following proposition.

Proposition 3.85 (Well-posedness of the local sub-problems with $\mathbf{T}_e$). *Under Assumption 3.69, the problem* (3.370) *is well-posed.*

Proof. We consider the variational form of the problem given in (3.372), namely

$$\begin{cases} \text{Find } \mathbf{E} \in \mathbf{H}_{\Gamma_e 0}(\mathbf{curl}; \tilde{\Omega}) \text{ such that} \\ \tilde{a}(\mathbf{E}, \mathbf{E}^t) = \tilde{l}(\mathbf{E}^t), & \forall \mathbf{E}^t \in \mathbf{H}_{\Gamma_e 0}(\mathbf{curl}; \tilde{\Omega}). \end{cases} \tag{3.385}$$

By decomposing the unknown and test functions, elements of $\mathbf{H}_{\Gamma_e 0}(\mathbf{curl}; \tilde{\Omega})$, according to the decomposition stated in Lemma 3.81, the problem (3.372) reduces to two uncoupled problems in $\mathbf{H}_{\Gamma_e 0}(\mathbf{curl}, \operatorname{div} \tilde{\epsilon}_r\, 0; \tilde{\Omega})$ and $H^1_0(\tilde{\Omega})$ which are

$$\begin{cases} \text{Find } p \in H^1_0(\tilde{\Omega}) \text{ and } \mathbf{E}_0 \in \mathbf{H}_{\Gamma_e 0}(\mathbf{curl}, \operatorname{div} \tilde{\epsilon}_r\, 0; \tilde{\Omega}) \text{ such that} \\ -\kappa_0(\tilde{\epsilon}_r \operatorname{\mathbf{grad}} p, \operatorname{\mathbf{grad}} q)_{\mathbf{L}^2(\tilde{\Omega})} = \tilde{l}(\operatorname{\mathbf{grad}} q), & \forall q \in H^1_0(\tilde{\Omega}), \\ \tilde{a}_+(\mathbf{E}_0, \mathbf{E}_0^t) - 2\kappa_0(\tilde{\epsilon}_r \mathbf{E}_0, \mathbf{E}_0^t)_{\mathbf{L}^2(\tilde{\Omega})} = \tilde{l}(\mathbf{E}_0^t), & \forall \mathbf{E}_0^t \in \mathbf{H}_{\Gamma_e 0}(\mathbf{curl}, \operatorname{div} \tilde{\epsilon}_r\, 0; \tilde{\Omega}). \end{cases} \tag{3.386}$$

The coefficient $\tilde{\epsilon}_r$ is such that the sesquilinear form defined on $H^1_0(\tilde{\Omega}) \times H^1_0(\tilde{\Omega})$ by

$$(p, q) \mapsto -\kappa_0(\tilde{\epsilon}_r \operatorname{\mathbf{grad}} p, \operatorname{\mathbf{grad}} q)_{\mathbf{L}^2(\tilde{\Omega})}, \tag{3.387}$$

is coercive. By application of the Lax-Milgram Lemma, it follows that the problem in $p \in H^1_0(\tilde{\Omega})$ is well-posed.

Using the definitions of the coercive form $\tilde{a}_+$ (Lemma 3.83) and the operator $\tilde{K}$ (Lemma 3.84), the problem in $\mathbf{E}_0 \in \mathbf{H}_{\Gamma_e 0}(\mathbf{curl}, \operatorname{div} \tilde{\epsilon}_r\, 0; \tilde{\Omega})$ is equivalent to finding $\mathbf{E}_0 \in \mathbf{L}^2(\tilde{\Omega})$ such that

$$(\mathrm{Id} + \tilde{K})\mathbf{E}_0 = \mathbf{b}, \tag{3.388}$$

where by application of the Lax-Milgram Lemma, $\mathbf{b} \in \mathbf{H}_{\Gamma_e 0}(\mathbf{curl}, \operatorname{div} \tilde{\epsilon}_r\, 0; \tilde{\Omega}) \subset \mathbf{L}^2(\tilde{\Omega})$, is the unique solution of

$$\tilde{a}_+(\mathbf{b}, \mathbf{E}_0^t) = \tilde{l}(\mathbf{E}_0^t), \qquad \forall \mathbf{E}_0^t \in \mathbf{H}_{\Gamma_e 0}(\mathbf{curl}, \operatorname{div} \tilde{\epsilon}_r\, 0; \tilde{\Omega}). \tag{3.389}$$

From Lemma 3.84 the operator $\tilde{K}$ is compact in $\mathbf{L}^2(\tilde{\Omega})$, the Fredholm alternative is applicable and the proof reduces to a uniqueness result, which was already established (Proposition 3.78). ■

To prove the well-posedness of the local sub-problems for a general transmission operator $\mathbf{T}$, we will again recast the problem on the transmission interface Σ, but instead of using a Dirichlet-like boundary condition, the idea is to switch to a Robin-like boundary condition based on the particular transmission operator $\mathbf{T}_e$.

Using Proposition 3.85, we can properly define the operator

$$\begin{aligned} \Lambda_{i,\mathbf{T}_e} \ &: \mathbf{H}^{-1/2}(\mathrm{curl};\Sigma) \to \mathbf{H}^{-1/2}(\mathrm{div};\Sigma), \\ &\mathbf{x} \mapsto \gamma_{1,\Sigma}\,\mathbf{E}, \end{aligned} \tag{3.390}$$

where $\mathbf{E} \in \mathbf{H}(\mathbf{curl};\Omega)$ is such that

$$\begin{cases} \left(\mathbf{curl}\,\mu_r^{-1}\,\mathbf{curl} - {\kappa_0}^2\epsilon_r\right)\mathbf{E} = 0, & \text{in } \Omega, \\ \left(\gamma_{1,\Sigma} - \mathrm{i}\mathbf{T}_e\gamma_{0,\Sigma}\right)\mathbf{E} = \mathbf{x}, & \text{on } \Sigma. \end{cases} \tag{3.391}$$

We are then able to state the well-posedness results for compact perturbations of the particular transmission operator $\mathbf{T}_e$.

Proposition 3.86 (Well-posedness of the local sub-problems). *Let $\mathbf{F} \in \mathbf{H}_\Gamma(\mathbf{curl};\Omega)'$ such that $\mathrm{div}\,\mathbf{F} = 0$ in a distributional sense (charge conservation equation) and $\mathbf{x} \in \mathbf{H}^{-1/2}(\mathrm{div};\Sigma)$. Under Assumption 3.69, Assumption 3.76 and if*

$$\mathbf{T} - \mathbf{T}_e \text{ is compact from } \mathbf{H}^{-1/2}(\mathrm{curl};\Sigma) \text{ to } \mathbf{H}^{-1/2}(\mathrm{div};\Sigma), \tag{3.392}$$

the problem

$$\begin{cases} \text{Find } \mathbf{E} \in \mathbf{H}(\mathbf{curl};\Omega) \text{ such that} \\ \left(\mathbf{curl}\,\mu_r^{-1}\,\mathbf{curl} - {\kappa_0}^2\epsilon_r\right)\mathbf{E} = \mathbf{F}, & \text{in } \Omega, \\ \left(\gamma_{1,\Sigma} - \mathrm{i}\mathbf{T}\gamma_{0,\Sigma}\right)\mathbf{E} = \mathbf{x}, & \text{on } \Sigma. \end{cases} \tag{3.393}$$

is well-posed.

Proof. Let $\mathbf{E}_0 \in \mathbf{H}(\mathbf{curl};\Omega)$ be the source lifting such that

$$\begin{cases} \left(\mathbf{curl}\,\mu_r^{-1}\,\mathbf{curl} - {\kappa_0}^2\epsilon_r\right)\mathbf{E}_0 = \mathbf{F}, & \text{in } \Omega, \\ \left(\gamma_{1,\Sigma} - \mathrm{i}\mathbf{T}_e\gamma_{0,\Sigma}\right)\mathbf{E}_0 = 0, & \text{on } \Sigma, \end{cases} \tag{3.394}$$

which is uniquely defined from Proposition 3.85. Solving the problem (3.393) is then equivalent to solve

$$\begin{cases} \text{Find } \mathbf{E} \in \mathbf{H}(\mathbf{curl};\Omega) \text{ such that} \\ \left(\mathbf{curl}\,\mu_r^{-1}\,\mathbf{curl} - {\kappa_0}^2\epsilon_r\right)\mathbf{E} = 0, & \text{in } \Omega, \\ \left(\gamma_{1,\Sigma} - \mathrm{i}\mathbf{T}\gamma_{0,\Sigma}\right)\mathbf{E} = \mathbf{y}, & \text{on } \Sigma, \end{cases} \tag{3.395}$$

where

$$\mathbf{y} = \mathbf{x} - \left(\gamma_{1,\Sigma} - \mathrm{i}\mathbf{T}\gamma_{0,\Sigma}\right)\mathbf{E}_0 \in \mathbf{H}^{-1/2}(\mathrm{div};\Sigma). \tag{3.396}$$

Using the operator $\Lambda_{i,\mathbf{T}_e}$ this problem is equivalent to the problem

$$\begin{cases} \text{Find } \mathbf{z} \in \mathbf{H}^{-1/2}(\mathrm{curl};\Sigma) \text{ such that} \\ (\Lambda_{i,\mathbf{T}_e}(\mathbf{T} - \mathbf{T}_e) - \mathbf{T})\mathbf{z} = \mathrm{i}\,(\Lambda_{i,\mathbf{T}_e} - \mathrm{Id})\mathbf{y}, \end{cases} \tag{3.397}$$

in the sense that having a solution to one problem immediately yields a solution for the other. Let us prove this equivalence.

($\Rightarrow$) Suppose that $\mathbf{E}$ is a solution to (3.395), by definition of $\Lambda_{i,\mathbf{T}_e}$ we have

$$\gamma_{1,\Sigma}\,\mathbf{E} = \Lambda_{i,\mathbf{T}_e}\left[\left(\gamma_{1,\Sigma} - \mathrm{i}\mathbf{T}_e\gamma_{0,\Sigma}\right)\mathbf{E}\right], \tag{3.398}$$

so that we have, using twice the equation on Σ from (3.395),

$$\begin{aligned} & \Lambda_{i,\mathbf{T}_e}\ [(\gamma_{1,\Sigma}\ - \mathrm{i}\mathbf{T}_e\gamma_{0,\Sigma}\,)\,\mathbf{E}] - \mathrm{i}\mathbf{T}\gamma_{0,\Sigma}\,\mathbf{E} = \mathbf{y}, \\ \Rightarrow \quad & \Lambda_{i,\mathbf{T}_e}\ [\mathrm{i}\,(\mathbf{T}-\mathbf{T}_e)\,\gamma_{0,\Sigma}\,\mathbf{E} + \mathbf{y}] - \mathrm{i}\mathbf{T}\gamma_{0,\Sigma}\,\mathbf{E} = \mathbf{y}, \end{aligned} \tag{3.399}$$

from which we readily find that the trace $\gamma_{0,\Sigma}\,\mathbf{E}$ is solution to (3.397).

($\Leftarrow$) Reciprocally, if $\mathbf{z}$ is solution to (3.397), then $\mathbf{E}$ solution to (3.395) is found by solving

$$\begin{cases} \left(\mathbf{curl}\,\mu_r^{-1}\,\mathbf{curl} - {\kappa_0}^2\epsilon_r\right)\mathbf{E} = 0, & \text{in } \Omega, \\ (\gamma_{1,\Gamma}\ - \mathrm{i}\gamma_{0,\Gamma}\,)\,\mathbf{E} = 0, & \text{on } \Gamma, \\ (\gamma_{1,\Sigma}\ - \mathrm{i}\mathbf{T}_e\gamma_{0,\Sigma}\,)\,\mathbf{E} = \mathrm{i}(\mathbf{T}-\mathbf{T}_e)\mathbf{z} + \mathbf{y}, & \text{on } \Sigma, \end{cases} \tag{3.400}$$

which is well-posed thanks to Proposition 3.85.

The operator involved in problem (3.397) is the sum of a compact operator $\Lambda_{i,\mathbf{T}_e}\,(\mathbf{T}-\mathbf{T}_e)$ and a coercive operator $\mathbf{T}$ in $\mathbf{H}^{-1/2}(\mathrm{div};\Sigma)$, hence by Fredholm alternative, the well-posedness of the associated problem is reduced to a uniqueness result, which was already established (Proposition 3.78). The compacity of the operator $\Lambda_{i,\mathbf{T}_e}\,(\mathbf{T}-\mathbf{T}_e)$ stems from the compacity of the operator $\mathbf{T}-\mathbf{T}_e$ from $\mathbf{H}^{-1/2}(\mathrm{curl};\Sigma)$ to $\mathbf{H}^{-1/2}(\mathrm{div};\Sigma)$ and the continuity of $\Lambda_{i,\mathbf{T}_e}$. The coercivity of $\mathbf{T}$ is contained in Assumption 3.76. ■

Chapter 4

Discrete setting

Contents

This chapter is devoted to the numerical analysis of the Galerkin approximation of the method presented in Chapter 3. This is *one* (our) choice of discretization, which we actually implemented and tested numerically (see Chapter 7 and Chapter 8 for numerical experiments). Of course, other discretization methods are possible, we mention in particular mixed-hybrid discretization, in the spirit of [49].

The structure of the presentation is similar to that of the continuous setting of the previous chapter and also makes use of the multi-trace formalism, which was firstly used in this domain decomposition context in [29, 33]. We introduce discrete variants of the spaces and operators that were previously defined. The only complication that arises from the discrete setting comes from the fact that the first order trace is only defined weakly. We therefore need to resort to variational definitions of the continuous operators so that they are amenable to discretization. The discrete Galerkin approximation of the model problem is then naturally recast in the form of a discrete counterpart of the interface problem (3.200).

We also address in this chapter the delicate question of *uniform stability* with respect to the discretization parameter of the (geometric) convergence of the iterative domain decomposition method, which was recognized before this work as an open question in [91, Rem. 3, Chap. 6]. Indeed, we prove for the case of the Helmholtz equation that the convergence rate of the discrete Jacobi algorithm is uniformly bounded above with respect to the discretization parameter, provided the transmission operator is itself stable. The more difficult case of Maxwell equations is not fully covered here, but we provide some elements laying the foundation for future work in this direction.

The method described in Chapter 3 could be written for any $\sigma \in \{0, 1/2, 1\}$, which sets respectively the interface problem in the trace spaces $\mathbb{M}_{0,\|}$, $\mathbb{M}_{1/2,\|}$ or $\mathbb{M}_{1,\|}$. If one can implement in practice the method for any of these three cases, we chose to use in this chapter and in our numerical experiments the formulation for $\sigma = 1$. This means that the Lagrange multiplier, solution of the interface problem on which the iterative algorithm is applied, can be identified as an element of the *dual* trace space (in this case $\mathbb{M}_{1,h,\|}$). This is a rather natural choice for the Galerkin method considered here and is slightly more efficient compared to the other choices $\sigma \in \{1/2, 1\}$, if carefully implemented.

For simplicity and because in practice we do not see any reasonable argument for not doing so, we only consider in this chapter diagonal transmission operators in the sense of Assumption 3.40.

4.1 Abstract definitions

4.1.1 Generic definitions and tools

To set some definitions, we consider an open, bounded, simply connected, polygonal/polyhedral, Lipschitz domain $\mathcal{O}$ subset of $\mathbb{R}^d$, with $d = 1, 2, 3$, intended to be either our model domain or a sub-domain of the partition.

Its (polygonal) boundary is denoted by $\partial\mathcal{O}$ with outward unit normal vector ν, and consists in one single connected component. We suppose that the boundary $\partial\mathcal{O}$ is composed of a first connected component denoted $\partial\mathcal{O}_R$, intended to be the boundary on which the Robin boundary condition is imposed, and several additional components, disconnected from $\partial\mathcal{O}_R$, denoted by $\partial\mathcal{O}_T$, intended to be transmission boundaries. The definitions we set below can be easily adapted if either $\partial\mathcal{O}_R$ or $\partial\mathcal{O}_T$ are empty.

Discrete functional space Our purpose is to consider Galerkin approximations of our model problem amenable to numerical computing. To this end, we will consider a discrete family $(\mathrm{V}_h(\mathcal{O}))_{h>0}$, indexed by the discretization parameter $h > 0$, of finite dimensional sub-sets of the solution space

$$\mathrm{V}_h(\mathcal{O}) \subset \mathrm{U}_{\partial\mathcal{O}_R}(\mathrm{D}; \mathcal{O}), \tag{4.1}$$

which we refer to as discrete approximation spaces, such that they satisfy an approximation property, namely

$$\forall u \in \mathrm{U}_{\partial\mathcal{O}_R}(\mathrm{D};\mathcal{O}), \qquad \liminf_{\substack{h\to 0,\\ u_h\in \mathrm{V}_h(\mathcal{O})}} \|u-u_h\|_{\mathrm{U}_{\partial\mathcal{O}_R}(\mathrm{D};\mathcal{O})} = 0. \tag{4.2}$$

Since these are finite dimensional spaces, they are closed subspaces of the Hilbert space $\mathrm{U}_{\partial\mathcal{O}_R}(\mathrm{D};\mathcal{O})$, hence Hilbert spaces as well, equipped with the inherited inner product and norm.

Remark 4.1 (**Finite element discretization**). *To construct the family of discrete finite dimensional spaces, we have in mind finite element conformal approximation spaces which are built upon a triangulation of the domain. To this end, one will typically consider a family, indexed by the mesh parameter $h > 0$, of* regular triangulations *$\mathcal{M}_h(\mathcal{O})$ of the domain $\mathcal{O}$ into (non-degenerate) closed* simplices*, generically denoted by K. For all $h > 0$, the mesh $\mathcal{M}_h(\mathcal{O})$ will be assumed to be* conformal*: the domain $\mathcal{O}$ is exactly resolved by the triangulation, namely*

$$\overline{\mathcal{O}} = \bigcup_{K\in\mathcal{M}_h(\mathcal{O})} \overline{K}, \tag{4.3}$$

and such that the intersection of two different elements is either empty, one edge, or one face of both elements. In addition, we shall require the family $(\mathcal{M}_h)_{h>0}$ to be h-uniformly shape regular*: if ρ_K is the diameter of the largest ball included in the simplex K and h_K is the diameter of the simplex K, we suppose*

$$\liminf_{\substack{h\to 0,\\ K\in\mathcal{M}_h(\Omega)}} \frac{\rho_K}{h_K} > 0. \tag{4.4}$$

Example 1: Helmholtz. *In the acoustic setting, the approximation spaces we consider (here and in our numerical experiments) are constructed as described in Remark 4.1, by first considering a family of simplicial triangulations of the domain $\mathcal{O}$. The discrete spaces are then generated by standard conforming $\mathbb{P}_k$ Lagrange functions ($k \geq 1$) defined on the mesh $\mathcal{M}_h(\mathcal{O})$, see [65] for a general reference.*

Example 2: Maxwell. *In the electromagnetic setting, the approximation spaces we consider (here and in our numerical experiments) are also constructed as described in Remark 4.1, by first considering a family of simplicial triangulations of the domain $\mathcal{O}$. The discrete spaces are then generated using standard conforming Nedelec edge elements of arbitrary order.*

Discrete trace spaces We introduce the natural (finite dimensional) discrete trace space as the image of $\mathrm{V}_h(\mathcal{O})$ by the trace operator $\gamma_{0,\partial\mathcal{O}}$ defined in (3.64), namely

$$\mathrm{X}_{0,h}(\partial\mathcal{O}) := \gamma_{0,\partial\mathcal{O}}\,\mathrm{V}_h(\mathcal{O}) \ \subset \mathrm{X}_0(\partial\mathcal{O}), \tag{4.5}$$

which is a subset of $\mathrm{X}_0(\partial\mathcal{O})$ by continuity of the trace operator. We equip this space with the graph norm

$$\|\mathrm{x}_0\|_{\mathrm{X}_{0,h}(\partial\mathcal{O})} := \inf_{\substack{u\in\mathrm{V}_h(\mathcal{O})\\ \gamma_{0,\partial\mathcal{O}}\,u=\mathrm{x}_0}} \|u\|_{\mathrm{U}_\Gamma(\mathrm{D};\mathcal{O})}, \qquad \forall \mathrm{x}_0 \in \mathrm{X}_{0,h}(\partial\mathcal{O}). \tag{4.6}$$

In addition, we set

$$\mathrm{X}_{1,h}(\partial\mathcal{O}) := \mathrm{X}_{0,h}(\partial\mathcal{O})'. \tag{4.7}$$

If follows that by construction

$$\mathrm{X}_{1,h}(\partial\mathcal{O}) \not\subset \mathrm{X}_1(\partial\mathcal{O}). \tag{4.8}$$

We nevertheless use the same notation as for the continuous setting, namely

$$\langle \cdot, \cdot \rangle_{\partial\mathcal{O}} \ : \ \mathrm{X}_{1,h}(\partial\mathcal{O}) \times \mathrm{X}_{0,h}(\partial\mathcal{O}) \to \mathbb{C}, \tag{4.9}$$

to denote the duality pairing between $\mathrm{X}_{1,h}(\partial\mathcal{O})$ and $\mathrm{X}_{0,h}(\partial\mathcal{O})$. The space $\mathrm{X}_{1,h}(\partial\mathcal{O})$ is equipped with the corresponding canonical dual norm, namely

$$\|\mathrm{x}_1\|_{\mathrm{X}_{1,h}(\partial\mathcal{O})} := \sup_{\substack{\mathrm{x}_0 \in \mathrm{X}_{0,h}(\partial\mathcal{O}) \\ \mathrm{x}_0 \neq 0}} \frac{\langle \mathrm{x}_1, \mathrm{x}_0 \rangle_{\partial\mathcal{O}}}{\|\mathrm{x}_0\|_{\mathrm{X}_{0,h}(\partial\mathcal{O})}}, \qquad \forall \mathrm{x}_1 \in \mathrm{X}_{1,h}(\partial\mathcal{O}). \tag{4.10}$$

Again, we introduce the Cartesian product of the trace spaces as

$$\mathrm{X}_h(\partial\mathcal{O}) := \mathrm{X}_{0,h}(\partial\mathcal{O}) \times \mathrm{X}_{1,h}(\partial\mathcal{O}). \tag{4.11}$$

Example 1: Helmholtz. *In the acoustic setting, the natural trace of the standard $\mathbb{P}_k$-Lagrange elements in the volume generates the associated $\mathbb{P}_k$-Lagrange elements on the embedded surface.*

Example 2: Maxwell. *The natural tangential trace of Nedelec edge elements in the volume generates the associated Nedelec edge elements on the embedded surface.*

Trace preserving and h-uniform continuous discrete lifting We assume that we can construct a particular type of lifting operator, which will be a crucial ingredient in the analysis.

Assumption 4.2. *There exist a* continuous lifting *of the natural trace*

$$\mathrm{E}_{h,\partial\mathcal{O}} \ : \ \mathrm{X}_{0,h}(\partial\mathcal{O}) \to \mathrm{V}_h(\mathcal{O}), \tag{4.12}$$

which is trace preserving*, namely*

$$\forall \mathrm{x}_0 \in \mathrm{X}_{0,h}(\partial\mathcal{O}), \qquad \gamma_{0,\partial\mathcal{O}} \, \mathrm{E}_{h,\partial\mathcal{O}} \, \mathrm{x}_0 = \mathrm{x}_0. \tag{4.13}$$

To prove h-uniform convergence results, we shall require in addition the following stronger assumption.

Assumption 4.3. *There exists a trace-preserving continuous lifting of the natural trace satisfying Assumption 4.2 which is* h-uniform*.*

Example 1: Helmholtz. *In the acoustic setting, a lifting satisfying the requirements of Assumption 4.2 and Assumption 4.3 can be constructed from the Scott-Zhang [126] interpolator.*

To construct a uniformly stable lifting which preserves the Dirichlet trace a natural idea is to compose any continuous right inverse of the Dirichlet trace operator with a discrete interpolator. The classical Lagrange interpolator [65, 5] fails to provide a practical answer because it lacks the continuity property for non-smooth functions since it requires point-wise function evaluations. The Clément interpolator [40] is continuous but fails to preserve the prescribed trace on the boundary. An interpolator featuring the suitable properties have been proposed by Scott and Zhang [126] for general conforming Lagrange finite elements of any order in $\mathbb{R}^d$, $d = 2, 3$. For the sake of illustration, we briefly recall below the construction of this operator for $\mathbb{P}_1$ Lagrange finite elements on triangles.

For each vertex M_i of the mesh, choose arbitrarily σ_i an edge connected to M_i. The application $v \in \mathbb{P}_1(\sigma_i) \mapsto v(M_i) \in \mathbb{R}$ is a continuous linear form on $\mathbb{P}_1(\sigma_i) \subset L^2(\sigma_i)$. From Riesz theorem, there exists a unique $\psi_i \in \mathbb{P}_1(\sigma_i)$ such that, for all $v \in \mathbb{P}_1(\sigma_i)$, we have $v(M_i) = (\psi_i, v)_{L^2(\sigma_i)}$. Let

w_i be the $\mathbb{P}_1$ Lagrange basis function associated to the vertex M_i. There is a natural definition of an interpolation operator P_h on $H^1(\Omega)$ such that: for all $v \in H^1(\Omega)$,

$$P_h v := \sum_i (\psi_i, v)_{L^2(\sigma_i)} w_i. \tag{4.14}$$

From the trace theorem, P_h is a continuous linear mapping from $H^1(\Omega)$ to $\mathrm{V}_h(\Omega)$ and is invariant on $\mathrm{V}_h(\Omega)$. To preserve the trace on the boundary, we require in addition that for all vertices M_i on the boundary of Ω, the edge σ_i is chosen to belong to the boundary. This operator P_h is the Scott-Zhang operator and satisfies our requirements, see [126, Th. 2.1 and Cor. 4.1] for more detail.

An extension of this interpolation operator to fractional Sobolev spaces has been given in [27]. For an extension to anisotropic meshes see [4].

Example 2: Maxwell. *In the electromagnetic setting, a lifting satisfying the requirements of Assumption 4.2 and Assumption 4.3 can be constructed implicitly.*

The construction of a uniformly stable lifting which preserves the tangential trace can also be obtained by composing any continuous right inverse of the tangential trace operator with a discrete interpolator. A discrete interpolator with the correct properties has been constructed implicitly in a recent paper by Ainsworth, Guzmán and Sayas, see [1]. Note that the construction is actually based on the Scott-Zhang interpolator.

4.1.2 Discrete approximation of the model problem

We consider again in this chapter an open, bounded, simply connected, polygonal/polyhedral, Lipschitz domain Ω subset of $\mathbb{R}^d$, with $d = 1, 2, 3$. Its (polygonal) boundary is denoted by $\Gamma := \partial\Omega$ with outward unit normal vector ν, and consists in one single connected component. Our aim is to construct (numerical) approximations of our model problem (3.79) of a wave propagation problem, for $f \in \mathrm{U}_\Gamma(\mathrm{D};\Omega)'$ and $g \in L^2(\Gamma)^{m_0}$. Recall that the equivalent variational formulation of the model problem (3.79), assumed to be well-posed, is written as

$$\begin{cases} \text{Find } u \in \mathrm{U}_\Gamma(\mathrm{D};\Omega) \text{ such that} \\ a(u,v) = l(v), \qquad \forall v \in \mathrm{U}_\Gamma(\mathrm{D};\Omega), \end{cases} \tag{4.15}$$

where, for all $u, v \in \mathrm{U}_\Gamma(\mathrm{D};\Omega)$, we recall the definitions,

$$\begin{cases} a(u,v) := {\kappa_0}^{-1}(\mathsf{a}\,\mathrm{D}u, \mathrm{D}v)_{L^2(\Omega)^{m_1}} - \kappa_0\,(\mathsf{n}u, v)_{L^2(\Omega)^{m_0}} - \mathsf{i}(\gamma_{0,\Gamma}\,u, \gamma_{0,\Gamma}\,v)_{L^2(\Gamma)^{m_0}}, \\ l(v) := {\kappa_0}^{-1}(f,v)_{L^2(\Omega)^{m_0}} + (g, \gamma_{0,\Gamma}\,v)_{L^2(\Gamma)^{m_0}}. \end{cases} \tag{4.16}$$

The above (bi)-linear forms are assumed continuous with respect to their arguments. In the forthcoming analysis, we shall require the continuity constant $|||a|||$ of a, such that

$$|a(u,v)| \le |||a|||\, \|u\|_{\mathrm{U}_\Gamma(\mathrm{D};\Omega)} \|v\|_{\mathrm{U}_\Gamma(\mathrm{D};\Omega)}. \qquad \forall u, v \in \mathrm{U}_\Gamma(\mathrm{D};\Omega). \tag{4.17}$$

We introduce a family of discrete approximation spaces $(\mathrm{V}_h(\Omega))_{h>0}$, indexed by the discretization parameter $h > 0$, of finite dimensional sub-sets of the solution space

$$\mathrm{V}_h(\Omega) \subset \mathrm{U}_\Gamma(\mathrm{D};\Omega), \tag{4.18}$$

and we are set to study the family of Galerkin approximations of (4.15),

$$\begin{cases} \text{Find } u_h \in \mathrm{V}_h(\Omega) \text{ such that} \\ a(u_h, v_h) = l(v_h), \qquad \forall v_h \in \mathrm{V}_h(\Omega). \end{cases} \tag{4.19}$$

For the sake of simplicity we will suppose that the integrals featured in the bilinear and linear forms can be evaluated exactly. Because of the abstract framework, we shall make the following assumption.

Assumption 4.4 (**Well-posedness of the discrete model problem**). *For any $h > 0$, $l \in \mathrm{U}_\Gamma(\mathrm{D};\Omega)'$ the discrete model problem (4.19) is well-posed: there exists a unique solution $u_h \in \mathrm{V}_h(\Omega)$ and a constant $0 < \alpha_{a,h} < +\infty$ such that*

$$\|u_h\|_{\mathrm{U}_\Gamma(\mathrm{D};\Omega)} \leq \alpha_{a,h} \|l\|_{\mathrm{U}_\Gamma(\mathrm{D};\Omega)'}. \tag{4.20}$$

Of course, the analysis of such problems often reveals that the above assumption is only valid for h small enough, which is a caveat that does not invalidate the following theory.

4.1.3 Geometric domain partitioning

Partition For each $h > 0$, we introduce a domain partitioning of Ω, denoted $\mathcal{P}_{\Omega,h}$, into J non-overlapping, simply connected, polygonal/polyhedral, Lipschitz, open sub-domains $\Omega_{j,h}$, $j \in \{1,\dots,J\}$,

$$\mathcal{P}_{\Omega,h} \equiv (\Omega_{j,h})_{j=1}^{J}, \tag{4.21}$$

such that

$$\overline{\Omega} = \bigcup_{j=1}^{J} \overline{\Omega}_{j,h}, \qquad \text{with} \qquad \Omega_{j,h} \cap \Omega_{k,h} = \emptyset, \quad \text{if } j \neq k. \tag{4.22}$$

We define the following boundaries and skeleton Σ_h

$$\begin{aligned} &\Gamma_{j,h} := \partial\Omega_{j,h}, && j \in \{1,\dots,J\}, \\ &\Gamma_{jk,h} := \partial\Omega_{j,h} \cap \partial\Omega_{k,h}, && (j,k) \in \{1,\dots,J\}^2, \quad j \neq k, \\ &\Sigma_h := \bigcup_{j=1}^{J} \Gamma_{j,h}, \end{aligned} \tag{4.23}$$

and

$$\begin{aligned} &\tilde{\Gamma}_{j,h} := \Gamma_{j,h} \setminus \Gamma_h, && j \in \{1,\dots,J\}, \\ &\tilde{\Sigma}_h := \Sigma_h \setminus \Gamma_h. \end{aligned} \tag{4.24}$$

When we study the question of h-uniform convergence, we shall require the following assumption.

Assumption 4.5 (h-**independent geometric partition**). *The partition is independent of h*

$$\begin{aligned} &\mathcal{P}_{\Omega,h} \equiv \mathcal{P}_\Omega, \\ &\Omega_{j,h} \equiv \Omega_j, \ \Gamma_{j,h} \equiv \Gamma_j, && j \in \{1,\dots,J\}, \\ &\Gamma_{jk,h} \equiv \Gamma_{jk}, && (j,k) \in \{1,\dots,J\}^2, \quad j \neq k, \\ &\Sigma_h \equiv \Sigma. \end{aligned} \tag{4.25}$$

However, we will *not* consider that Assumption 4.5 holds in general, because this partitioning approach is not the most convenient from a practical viewpoint, see Remark 4.6. We shall point out exactly when we require this assumption and emphasize that most of the analysis do not rely on it.

Remark 4.6 (**Conformal mesh and partition**). *In practice, as we already remarked, the discrete sequence of partition and solution spaces is constructed together with a discrete sequence of meshes and associated finite element approximation spaces. The partition is assumed to be* conformal *in the sense that all sub-domains are supposed to be resolved exactly by the triangulation, in the sense of* (4.3). *Besides, because each $\Omega_{j,h}$ is resolved by the triangulation, so is each boundary Γ_j^h as well as the skeleton Σ_h.*

Two different situations may occur:

1. *The first typical situation occurs when the partitioning is done prior to the discretization: the computational domain is decomposed as a first step in subdomains and, only afterwards, the mesh is generated in each subdomain separately. In this case the challenge is to obtain a conformal mesh globally: compatibility between subdomain triangulations has to be enforced at interfaces. Two examples of this situation are represented in Figure 4.1a and Figure 4.1b. Each subdomain $\Omega_{j,h}$, and the subdomain partition itself, then remains unchanged as $h \to 0$.*

2. *Another approach consists in generating a mesh on the whole computational domain Ω first, and then subdividing it in subdomains using for instance an automatic graph partitioner such as e.g.* METIS *[89]. In this manner, conformity of subdomain triangulations at interfaces is automatically satisfied. However the partition itself has no reason to stabilize for $h \to 0$, and there is no guarantee that each subdomain geometrically converges. Boundaries of subdomains may get rougher as $h \to 0$. This second situation is depicted in Figure 4.1a and Figure 4.1b. This is actually the most practical way of proceeding in real-life applications, however Assumption 4.5 is hardly ever satisfied in this case.*

The existence of both these situations, which can have a significant impact on the stability analysis, is the reason we introduced Assumption 4.5.

Figure 4.1 gives examples of the two types of partition we may consider, for partitions with and without junction points. The analysis we present here covers type of partitioning (before and after discretization), albeit the stability analysis will require to suppose that the partition is independent of the discretization parameter. In this chapter we assume in addition that no junction are present in the partition.

Discrete broken solution spaces We introduce the local discrete approximation spaces as the space of local restrictions to the subdomains of global functions

$$\mathrm{V}_h(\Omega_{j,h}) := \mathrm{V}_h(\Omega)|_{\Omega_{j,h}} \qquad \forall j \in \{1, \dots, J\},\ \forall h > 0, \tag{4.26}$$

from which we can define the following discrete broken solution spaces

$$\mathbb{V}_h(\mathcal{P}_{\Omega,h}) := \left\{ \mathbb{v} \in L^2(\Omega)^{m_0} \mid \mathbb{v}|_{\Omega_{j,h}} \in \mathrm{V}_h(\Omega_{j,h}),\ \forall j \in \{1, \dots, J\} \right\}, \qquad \forall h > 0. \tag{4.27}$$

We insist that our approach is based on an *internal approximation*: our approximation spaces are such that we have, for all $h > 0$,

$$\begin{aligned} &\mathrm{V}_h(\Omega) \subset \mathrm{U}_\Gamma(\mathrm{D}; \Omega), \\ &\mathrm{V}_h(\Omega_{j,h}) \subset \mathrm{U}_\Gamma(\mathrm{D}; \Omega_{j,h}), \qquad \forall j \in \{1, \dots, J\}, \\ &\mathbb{V}_h(\mathcal{P}_{\Omega,h}) \subset \mathbb{U}_\Gamma(\mathrm{D}; \mathcal{P}_{\Omega,h}). \end{aligned} \tag{4.28}$$

Besides, by construction, we necessarily have, for all $h > 0$,

$$\mathrm{V}_h(\Omega) \subset \mathbb{V}_h(\mathcal{P}_{\Omega,h}), \tag{4.29}$$

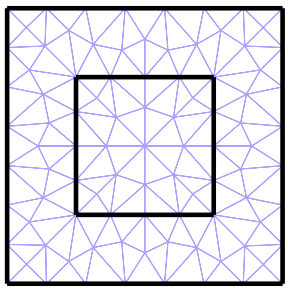

(a) Without junctions, before discretization.

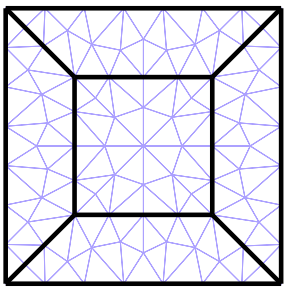

(b) With junctions, before discretization.

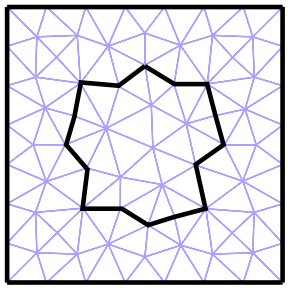

(c) Without junctions, after discretization.

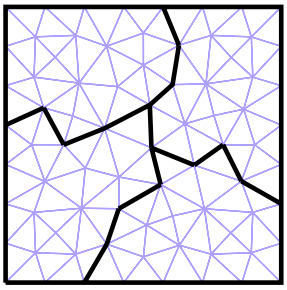

(d) With junctions, after discretization.

Figure 4.1: Two approaches for partitioning the computational domain: before and after discretization.

so that

$$\mathrm{V}_h(\Omega) \subset \mathrm{U}_\Gamma(\mathrm{D};\Omega) \cap \mathbb{V}_h(\mathcal{P}_{\Omega,h}), \tag{4.30}$$

but because of the abstract setting the reverse inclusion $\mathrm{U}_\Gamma(\mathrm{D};\Omega) \cap \mathbb{V}_h(\mathcal{P}_{\Omega,h}) \subset \mathrm{V}_h(\Omega)$ does not necessarily hold, which is the reason why we introduce the following assumption (not restrictive in practice).

Assumption 4.7 (**Partition-conformal discrete approximation space**). *For each $h > 0$, we suppose that the discrete approximation space $\mathrm{V}_h(\Omega)$ is such that*

$$\mathrm{V}_h(\Omega) = \mathrm{U}_\Gamma(\mathrm{D};\Omega) \cap \mathbb{V}_h(\mathcal{P}_{\Omega,h}). \tag{4.31}$$

Remark 4.8. *For our two target applications, namely Helmholtz and Maxwell equations, the approximations spaces are built using finite elements, hence will be partition-conformal if the mesh partition on which the finite elements spaces are built is itself conformal (see Remark 4.6).*

4.2 Abstract discrete domain decomposition

4.2.1 Multi-trace formalism

4.2.1.1 Multi-trace spaces

Similarly as in the continuous setting, we introduce discrete global trace spaces whose elements are collection of traces on all interfaces between two sub-domains.

Definition 4.9 (**Discrete multi-trace spaces**). *The discrete global multi-trace spaces are defined as*

$$\begin{aligned}
\mathbb{M}_{0,h,\|}\left(\tilde{\Sigma}_h\right) &:= \bigtimes_{(j,k)\in\mathbb{J}} \mathrm{X}_{0,h}(\Gamma_{jk,h}),\\
\mathbb{M}_{1,h,\|}\left(\tilde{\Sigma}_h\right) &:= \bigtimes_{(j,k)\in\mathbb{J}} \mathrm{X}_{1,h}(\Gamma_{jk,h}),\\
\mathbb{M}_{h,\|}\left(\tilde{\Sigma}_h\right) &:= \bigtimes_{(j,k)\in\mathbb{J}} \mathrm{X}_{h}(\Gamma_{jk,h}) \equiv \mathbb{M}_{0,h,\|}\left(\tilde{\Sigma}_h\right) \times \mathbb{M}_{1,h,\|}\left(\tilde{\Sigma}_h\right).
\end{aligned} \tag{4.32}$$

It is clear that we have

$$\mathbb{M}_{0,h,\|}\left(\tilde{\Sigma}_h\right) \subset \mathbb{M}_{0,\|}\left(\tilde{\Sigma}_h\right) := \bigtimes_{(j,k)\in\mathbb{J}} \mathrm{X}_{0}(\Gamma_{jk,h}), \tag{4.33}$$

where $\mathbb{M}_{0,\times}\left(\tilde{\Sigma}_h\right)$ is the continuous multi-trace space defined on the h dependent skeleton $\tilde{\Sigma}$. However, we shall keep in mind that

$$\mathbb{M}_{1,h,\|}\left(\tilde{\Sigma}_h\right) \not\subset \mathbb{M}_{1,\|}\left(\tilde{\Sigma}_h\right) := \bigtimes_{(j,k)\in\mathbb{J}} \mathrm{X}_{1}(\Gamma_{jk,h}). \tag{4.34}$$

We introduce the global trace operator

$$\boldsymbol{\gamma}_{0,h,\|} := \left(\gamma_{0,\Gamma_{jk,h}}\right)_{(j,k)\in\mathbb{J}} : \mathbb{V}_h(\mathcal{P}_{\Omega,h}) \to \mathbb{M}_{0,h,\|}, \tag{4.35}$$

which is by construction a continuous and surjective mapping from the broken solution space into the Dirichlet multi-trace space.

Norms and duality pairings The multi-trace space $\mathbb{M}_{0,h,\|}$ can be endowed with the norms stemming from its Cartesian product structure. Recalling the definition of the norm on a single domain given in (4.6), we set,

$$\|\mathbb{x}_0\|^2_{\mathbb{M}_{0,h,\|}} := \sum_{(j,k)\in\mathbb{J}} \|\mathrm{x}_0^{jk}\|^2_{\mathrm{X}_{0,h}(\Gamma_{jk,h})}, \qquad \forall \mathbb{x}_0 \equiv (\mathrm{x}_0^{jk})_{(j,k)\in\mathbb{J}} \in \mathbb{M}_{0,h,\|}. \tag{4.36}$$

Recalling the local duality pairing $\langle\cdot,\cdot\rangle_{\partial\mathcal{O}}$ between the two dual trace spaces (4.9) on a single boundary $\partial\mathcal{O}$, we introduce the duality pairing between multi-trace spaces (which does not involve any complex conjugation operation)

$$\begin{aligned}
\left\langle\!\left\langle\cdot,\cdot\right\rangle\!\right\rangle_{\|} &: \mathbb{M}_{1,h,\|} \times \mathbb{M}_{0,h,\|} \to \mathbb{C},\\
&(\mathbb{x}_1,\, \mathbb{x}_0) \mapsto \sum_{(j,k)\in\mathbb{J}} \langle \mathrm{x}_1^{jk}, \mathrm{x}_0^{jk}\rangle_{\Gamma_{jk,h}}.
\end{aligned} \tag{4.37}$$

The space $\mathbb{M}_{1,h,\|}$ is equipped with the corresponding canonical dual norm, namely

$$\|\mathbb{x}_1\|_{\mathbb{M}_{1,h,\|}} := \sup_{\substack{\mathbb{x}_0\in\mathbb{M}_{0,h,\|}\\ \mathbb{x}_0\neq 0}} \frac{\left\langle\!\left\langle \mathbb{x}_1, \mathbb{x}_0\right\rangle\!\right\rangle_{\|}}{\|\mathbb{x}_0\|_{\mathbb{M}_{0,h,\|}}}, \qquad \forall \mathbb{x}_1 \in \mathbb{M}_{1,h,\|}. \tag{4.38}$$

Besides, we introduce the natural norm on $\mathbb{M}_{h,\|}$ as follows

$$\|\mathbb{x}\|^2_{\mathbb{M}_{h,\|}} := \|\mathbb{x}_0\|^2_{\mathbb{M}_{0,h,\|}} + \|\mathbb{x}_1\|^2_{\mathbb{M}_{1,h,\|}}, \qquad \forall \mathbb{x} \equiv (\mathbb{x}_0, \mathbb{x}_1) \in \mathbb{M}_{h,\|}. \tag{4.39}$$

Lifting operators With the help of Assumption 4.2, it is clear that one can construct a (trace preserving) continuous lifting operator

$$\mathbb{E}_{h,\|} : \mathbb{M}_{0,h,\|} \to \mathbb{V}_h(\mathcal{P}_{\Omega,h}). \tag{4.40}$$

We shall require in the forthcoming analysis the continuity constant of this lifting operator, denoted $|||\mathbb{E}_{h,\|}|||$, and such that

$$\| \mathbb{E}_{h,\|} \mathbb{x}_0 \|_{\mathbb{U}_\Gamma(\mathrm{D};\mathcal{P}_{\Omega,h})} \leq |||\mathbb{E}_{h,\|}||| \, \|\mathbb{x}_0\|_{\mathbb{M}_{0,h,\|}}, \qquad \forall \mathbb{x}_0 \in \mathbb{M}_{0,h,\|}. \tag{4.41}$$

4.2.1.2 Cauchy-trace spaces

We define a first subset of the space of discrete multi-trace spaces which can also be reinterpreted as the space of traces of a function whose restriction in each sub-domain satisfies the PDE (and physical boundary conditions), very much like in the continuous setting (see Definition 3.18). However this time we resort to variational definitions, since the first order trace is only defined weakly here. The bilinear a_j was defined in (3.97) and the broken version $\mathfrak{a}$ was defined in (3.98).

Definition 4.10 (**Discrete Cauchy-trace space**). *For each $j = 1, \dots, J$, the space of local discrete Cauchy traces $\mathrm{C}_{h,\|}(\Gamma_{j,h})$ is defined as the subset of $\bigtimes_{k\in\mathbb{K}_j} \mathrm{X}_h(\Gamma_{jk,h})$ such that: for all $\mathrm{x} \in \bigtimes_{k\in\mathbb{K}_j} \mathrm{X}_h(\Gamma_{jk,h})$,*

$$\begin{aligned} & \mathrm{x} \equiv (\mathrm{x}_0^{jk}, \mathrm{x}_1^{jk})_{k\in\mathbb{K}_j} \in \mathrm{C}_{h,\|}(\Gamma_{j,h}) \\ \Leftrightarrow \quad & \exists u_j \in \mathrm{V}_h(\Omega_{j,h}) \text{ such that} \\ & \qquad \begin{cases} a_j(u_j, v_j) = \sum_{k\in\mathbb{K}_j} \langle \mathrm{x}_1^{jk}, \gamma_{0,\Gamma_{jk,h}} v_j \rangle_{\Gamma_{jk,h}}, & \forall v_j \in \mathrm{V}_h(\Omega_{j,h}), \\ \mathrm{x}_0^{jk} = \gamma_{0,\Gamma_{jk,h}} u_j, & \forall k \in \mathbb{K}_j. \end{cases} \end{aligned} \tag{4.42}$$

The global discrete Cauchy trace space is defined as

$$\mathbb{C}_{h,\|}(\tilde{\Sigma}_h) := \bigtimes_{j=1}^{J} \mathrm{C}_{h,\|}(\Gamma_{j,h}), \tag{4.43}$$

or, equivalently,

$$\begin{aligned} & \mathbb{x} \equiv (\mathbb{x}_0, \mathbb{x}_1) \in \mathbb{C}_{h,\|}(\tilde{\Sigma}_h) \\ \Leftrightarrow \quad & \exists \mathbb{u} \in \mathbb{V}_h(\mathcal{P}_{\Omega,h}) \text{ such that } \begin{cases} \mathfrak{a}(\mathbb{u}, \mathbb{v}) = \langle\!\langle \mathbb{x}_1, \boldsymbol{\gamma}_{0,h,\|} \mathbb{v} \rangle\!\rangle_{\|}, & \forall \mathbb{v} \in \mathbb{V}_h(\mathcal{P}_{\Omega,h}), \\ \mathbb{x}_0 = \boldsymbol{\gamma}_{0,h,\|} \mathbb{u}, \end{cases} \end{aligned} \tag{4.44}$$

which we identify as a subspace of $\mathbb{M}_{h,\|}$ in a straightforward manner.

4.2.1.3 Single-trace spaces

We introduce a second subspace of the multi-trace space, which is the space of traces that match across all interfaces. The definition in this discrete setting follows closely the one from the continuous setting (see Definition 3.20).

Definition 4.11 (**Discrete single-trace spaces**). *The global discrete single-trace spaces are defined as*

$$\begin{aligned} \mathbb{S}_{0,h,\|}(\tilde{\Sigma}_h) &:= \left\{ \mathbb{x}_0 = (\mathrm{x}_0^{jk})_{(j,k)\in\mathbb{J}} \in \mathbb{M}_{0,h,\|} \quad | \quad \mathrm{x}_0^{jk} = \mathrm{x}_0^{kj}, \ \forall (j,k) \in \mathbb{J} \right\}, \\ \mathbb{S}_{1,h,\|}(\tilde{\Sigma}_h) &:= \left\{ \mathbb{x}_1 = (\mathrm{x}_1^{jk})_{(j,k)\in\mathbb{J}} \in \mathbb{M}_{1,h,\|} \quad | \quad \mathrm{x}_1^{jk} = -\mathrm{x}_1^{kj}, \ \forall (j,k) \in \mathbb{J} \right\}, \\ \mathbb{S}_{h,\|}(\tilde{\Sigma}_h) &:= \mathbb{S}_{0,h,\|}(\tilde{\Sigma}_h) \times \mathbb{S}_{1,h,\|}(\tilde{\Sigma}_h). \end{aligned} \tag{4.45}$$

We have, by construction

$$\mathbb{S}_{0,h,\|} = \mathbb{M}_{0,h,\|} \cap \mathbb{S}_{0,\|}\left(\tilde{\Sigma}_h\right) \subset \mathbb{S}_{0,\|}\left(\tilde{\Sigma}_h\right), \tag{4.46}$$

where $\mathbb{S}_{0,\|}\left(\tilde{\Sigma}_h\right)$ is the continuous single-trace space defined on the h dependent skeleton $\tilde{\Sigma}$.

Again, we review some of the properties linked to the discrete single-trace spaces that will prove useful in what follows. Most of them are inherited from the continuous setting.

First, we have the following important result, which stems from Assumption 4.7 and Proposition 3.21.

Proposition 4.12. *Under Assumptions 3.11 and 3.12, we have*

$$\mathbb{S}_{0,h,\|} = \boldsymbol{\gamma}_{0,h,\|}\, \mathrm{V}_h(\Omega). \tag{4.47}$$

Proof. From Proposition 3.21, we have

$$\mathbb{S}_{0,\|} = \boldsymbol{\gamma}_{0,h,\|} \mathrm{U}_\Gamma(\mathrm{D};\Omega), \tag{4.48}$$

from the surjectivity of the trace operator, we have

$$\mathbb{M}_{0,h,\|} = \boldsymbol{\gamma}_{0,h,\|} \mathbb{V}_h(\mathcal{P}_{\Omega,h}), \tag{4.49}$$

and from Assumption 4.7, we have

$$\mathbb{V}_h(\mathcal{P}_{\Omega,h}) \cap \mathrm{U}_\Gamma(\mathrm{D};\Omega) = \mathrm{V}_h(\Omega), \tag{4.50}$$

Hence, the definition of $\mathbb{S}_{0,h,\|}$ is rewritten as

$$\mathbb{S}_{0,h,\|} = \mathbb{M}_{0,h,\|} \cap \mathbb{S}_{0,\|} = \boldsymbol{\gamma}_{0,h,\|} \left(\mathbb{V}_h(\mathcal{P}_{\Omega,h}) \cap \mathrm{U}_\Gamma(\mathrm{D};\Omega)\right) = \boldsymbol{\gamma}_{0,h,\|} \mathrm{V}_h(\Omega). \tag{4.51}$$

■

The following lemma, which stems directly from Assumption 4.7 and Corollary 3.14, will help make clear the difference between the $\mathrm{V}_h(\Omega)$ (regular) and the $\mathbb{V}_h(\mathcal{P}_{\Omega,h})$ (broken) versions of the solution spaces using the single-trace space. It is the discrete analogue of Corollary 3.14.

Lemma 4.13. *An element $\mathbb{u}$ in $\mathbb{V}_h(\mathcal{P}_{\Omega,h})$ is an element of $\mathrm{V}_h(\Omega)$ if, and only if,*

$$\gamma_{0,\Gamma_{jk,h}}\, \mathbb{u}|_{\Omega_{j,h}} = \gamma_{0,\Gamma_{kj,h}}\, \mathbb{u}|_{\Omega_{k,h}}, \qquad \forall (j,k) \in \mathbb{J}. \tag{4.52}$$

Proof. We have the trivial inclusion $\mathrm{V}_h(\Omega) \subset \mathbb{V}_h(\mathcal{P}_{\Omega,h})$. Besides, if $\mathbb{u}$ in $\mathbb{V}_h(\mathcal{P}_{\Omega,h})$ satisfies (4.52) then using Corollary 3.14, we get that $\mathbb{u} \in \mathrm{U}_\Gamma(\mathrm{D};\Omega) \cap \mathbb{V}_h(\mathcal{P}_{\Omega,h})$, which is nothing but $\mathrm{V}_h(\Omega)$ from Assumption 4.7. ■

We deduce the following corollary, which is a characterization of the difference between the $\mathrm{V}_h(\Omega)$ (regular) and the $\mathbb{V}_h(\mathcal{P}_{\Omega,h})$ (broken) versions of the solution spaces using the single-trace spaces.

Corollary 4.14. *We have*

$$\forall u \in \mathbb{V}_h(\mathcal{P}_{\Omega,h}), \qquad \boldsymbol{\gamma}_{0,h,\|} u \in \mathbb{S}_{0,h,\|} \quad \Leftrightarrow \quad u \in \mathrm{V}_h(\Omega). \tag{4.53}$$

Proof. It is clear that one implication ($\Leftarrow$) stems from Proposition 4.12. We need only to prove the reverse implication ($\Rightarrow$).

Let $u \in \mathbb{V}_h(\mathcal{P}_{\Omega,h})$ such that $\boldsymbol{\gamma}_{0,h,\|} u \in \mathbb{S}_{0,h,\|}$. By Proposition 4.12 of $\mathbb{S}_{0,h,\|}$, there exists $v \in \mathrm{V}_h(\Omega)$ such that $\boldsymbol{\gamma}_{0,h,\|}(v-u) = 0$. It follows that $w := v - u \in \operatorname{Ker} \boldsymbol{\gamma}_{0,h,\|}$ and by Lemma 4.13 we get $w \in \mathrm{V}_h(\Omega)$ so that finally $u = v + w$ does belong to $\mathrm{V}_h(\Omega)$. ■

In addition, we have the following result, analogue of Proposition 3.23, which will prove useful in this discrete context.

Proposition 4.15. *The discrete single trace spaces are such that*

$$\begin{aligned} &\forall \mathbb{x}_0 \in \mathbb{M}_{0,h,\|}, \quad \Big(\mathbb{x}_0 \in \mathbb{S}_{0,h,\|} \quad \Leftrightarrow \quad \langle\!\langle \mathbb{y}_1, \mathbb{x}_0 \rangle\!\rangle_{\|} = 0, \quad \forall \mathbb{y}_1 \in \mathbb{S}_{1,h,\|}\Big), \\ &\forall \mathbb{x}_1 \in \mathbb{M}_{1,h,\|}, \quad \Big(\mathbb{x}_1 \in \mathbb{S}_{1,h,\|} \quad \Leftrightarrow \quad \langle\!\langle \mathbb{x}_1, \mathbb{y}_0 \rangle\!\rangle_{\|} = 0, \quad \forall \mathbb{y}_0 \in \mathbb{S}_{0,h,\|}\Big). \end{aligned} \tag{4.54}$$

Proof. It is a trivial adaptation of the proof of Proposition 3.23. ∎

4.2.1.4 A first equivalent transmission problem

We are now ready to rewrite the (discrete) approximation (4.19) of the model problem (3.79) This is the purpose of the following proposition, analogue to Proposition 3.24. The broken sesquilinear and linear forms $\mathbb{o}$ and $\mathbb{l}$ were defined in (3.98) and (3.101).

Proposition 4.16 (**Equivalent discrete transmission problem**)**.** *If $u_h \in \mathrm{V}_h(\Omega)$ is solution of the discrete model problem* (4.19) *then there exists $\mathbb{x} \equiv (\mathbb{x}_0, \mathbb{x}_1) \in \mathbb{S}_{h,\|}$ such that*

$$\begin{cases} \mathbb{o}(u_h, \mathbb{v}) - \mathbb{l}(\mathbb{v}) = \langle\!\langle \mathbb{x}_1, \boldsymbol{\gamma}_{0,h,\|} \mathbb{v} \rangle\!\rangle_{\|}, & \forall \mathbb{v} \in \mathbb{V}_h(\mathcal{P}_{\Omega,h}), \\ \boldsymbol{\gamma}_{0,h,\|} u_h = \mathbb{x}_0. \end{cases} \tag{4.55}$$

Reciprocally, if $u_h \in \mathbb{V}_h(\mathcal{P}_{\Omega,h})$ and $\mathbb{x} \equiv (\mathbb{x}_0, \mathbb{x}_1) \in \mathbb{S}_{h,\|}$ are such that (4.55) *is satisfied then u_h is solution of the discrete model problem* (4.19)*.*

Proof. ($\Rightarrow$) Let $u_h \in \mathrm{V}_h(\Omega)$ be the solution of the (discrete) approximation (4.19) of the model problem (3.79). Since $u_h \in \mathrm{V}_h(\Omega)$, from Proposition 4.12 we immediately have

$$\mathbb{x}_0 := \boldsymbol{\gamma}_{0,h,\|} u_h \in \mathbb{S}_{0,h,\|}. \tag{4.56}$$

Now, by Riesz representation theorem, there exists $\mathbb{x}_1 \in \mathbb{M}_{1,h,\|}$ such that

$$\langle\!\langle \mathbb{x}_1, \mathbb{x}_0^t \rangle\!\rangle_{\|} = \mathbb{o}(u_h, \mathbb{E}_{h,\|}\, \mathbb{x}_0^t) - \mathbb{l}(\mathbb{E}_{h,\|}\, \mathbb{x}_0^t), \qquad \forall \mathbb{x}_0^t \in \mathbb{M}_{0,h,\|}. \tag{4.57}$$

Let us show that $\mathbb{x}_1$ is independent of the particular lifting $\mathbb{E}_{h,\|}$. Let $\mathbb{v} \in \mathbb{V}_h(\mathcal{P}_{\Omega,h})$, we have

$$\boldsymbol{\gamma}_{0,h,\|} \left(\mathbb{v} - \mathbb{E}_{h,\|}\, \boldsymbol{\gamma}_{0,h,\|} \mathbb{v}\right) = 0 \in \mathbb{S}_{0,h,\|}, \tag{4.58}$$

so that, by application of Corollary 4.14, we know that $\mathbb{v} - \mathbb{E}_{h,\|}\, \boldsymbol{\gamma}_{0,h,\|} \mathbb{v} \in \mathrm{V}_h(\Omega)$. It follows that

$$\mathbb{o}(u_h, \mathbb{v} - \mathbb{E}_{h,\|}\, \boldsymbol{\gamma}_{0,h,\|} \mathbb{v}) - \mathbb{l}(\mathbb{v} - \mathbb{E}_{h,\|}\, \boldsymbol{\gamma}_{0,h,\|} \mathbb{v}) = a(u_h, \mathbb{v} - \mathbb{E}_{h,\|}\, \boldsymbol{\gamma}_{0,h,\|} \mathbb{v}) - l(\mathbb{v} - \mathbb{E}_{h,\|}\, \boldsymbol{\gamma}_{0,h,\|} \mathbb{v}) = 0, \tag{4.59}$$

hence

$$\mathbb{o}(u_h, \mathbb{E}_{h,\|}\, \boldsymbol{\gamma}_{0,h,\|} \mathbb{v}) - \mathbb{l}(\mathbb{E}_{h,\|}\, \boldsymbol{\gamma}_{0,h,\|} \mathbb{v}) = \mathbb{o}(u_h, \mathbb{v}) - \mathbb{l}(\mathbb{v}), \tag{4.60}$$

and finally, using the surjectivity of the trace $\boldsymbol{\gamma}_{0,h,\|}$ from $\mathbb{V}_h(\mathcal{P}_{\Omega,h})$ into $\mathbb{M}_{0,h,\|}$,

$$\langle\!\langle \mathbb{x}_1, \boldsymbol{\gamma}_{0,h,\|} \mathbb{v} \rangle\!\rangle_{\|} = \mathbb{o}(u_h, \mathbb{v}) - \mathbb{l}(\mathbb{v}), \qquad \forall \mathbb{v} \in \mathbb{V}_h(\mathcal{P}_{\Omega,h}). \tag{4.61}$$

Let $\mathbb{z}_0 \in \mathbb{S}_{0,h,\|}$, using again Proposition 4.12, there exists $v^t \in \mathrm{V}_h(\Omega)$ such that $\mathbb{z}_0 = \boldsymbol{\gamma}_{0,h,\|} v^t$. Since $u_h \in \mathrm{V}_h(\Omega)$ satisfies the discrete model problem (4.19), we have

$$\langle\!\langle \mathbb{x}_1, \mathbb{z}_0 \rangle\!\rangle_{\|} = \mathbb{o}(u_h, v^t) - \mathbb{l}(v^t) = a(u_h, v^t) - l(v^t) = 0, \tag{4.62}$$

which means, from Proposition 4.15, that

$$\mathbb{x}_1 \in \mathbb{S}_{1,h,\|} \qquad \text{and hence} \qquad \mathbb{x} \equiv (\mathbb{x}_0, \mathbb{x}_1) \in \mathbb{S}_{h,\|}. \tag{4.63}$$

($\Leftarrow$) Reciprocally, suppose that there exists $u_h \in \mathbb{V}_h(\mathcal{P}_{\Omega,h})$ and $\mathbb{x} \equiv (\mathbb{x}_0, \mathbb{x}_1) \in \mathbb{S}_{h,\|}$ such that (4.55) holds. We immediately conclude from $\boldsymbol{\gamma}_{0,h,\|} u_h = \mathbb{x}_0 \in \mathbb{S}_{0,h,\|}$ and Corollary 4.14 that $u_h \in \mathrm{V}_h(\Omega)$. Now testing with elements of $\mathrm{V}_h(\Omega)$,

$$a(u_h, v_h) - l(v_h) = \mathbb{a}(u_h, v_h) - \mathbb{l}(v_h) = \left\langle\!\!\left\langle \mathbb{x}_1, \boldsymbol{\gamma}_{0,h,\|} v_h \right\rangle\!\!\right\rangle_{\|} = 0, \qquad \forall v_h \in \mathrm{V}_h(\Omega), \tag{4.64}$$

using Proposition 4.15 together with the fact that $\mathbb{x}_1 \in \mathbb{S}_{1,h,\|}$. Hence, $u_h \in \mathrm{V}_h(\Omega)$ is the solution of the discrete model problem (4.19). ■

We state now the result on the decomposition of the discrete multi-trace space in the sum of the discrete single-trace and Cauchy-trace spaces, analogue of Proposition 3.25. A similar result in a more general setting (with junctions) was already available for the scalar equation only, see [33, Prop. 7.1].

Proposition 4.17. *We have the direct sum*

$$\mathbb{M}_{h,\|} = \mathbb{C}_{h,\|} \oplus \mathbb{S}_{h,\|}. \tag{4.65}$$

In addition, if we denote by $\mathbf{P}_{\mathbb{C}_{h,\|}}$ *the projector from* $\mathbb{M}_{h,\|}$ *onto* $\mathbb{C}_{h,\|}$ *in parallel to* $\mathbb{S}_{h,\|}$*, then we have the following estimate*

$$\alpha_{\mathbf{P}_{\mathbb{C}_{h,\|}}} := \sup_{\substack{\mathbb{x} \in \mathbb{M}_{h,\|} \\ \mathbb{x} \neq 0}} \frac{\|\mathbf{P}_{\mathbb{C}_{h,\|}} \mathbb{x}\|_{\mathbb{M}_{h,\|}}}{\|\mathbb{x}\|_{\mathbb{M}_{h,\|}}} \leq \Big(1 + |||a|||^2 \, |||\mathbb{E}_{h,\|}|||^2\Big)^{1/2} \Big[\Big(1 + \alpha_{a,h}^{-1} \, |||a|||\Big) |||\mathbb{E}_{h,\|}||| + \alpha_{a,h}^{-1}\Big]. \tag{4.66}$$

Proof.

Null intersection $\mathbb{C}_{h,\|} \cap \mathbb{S}_{h,\|} = \{0\}$. Let $\mathbb{x} \in \mathbb{C}_{h,\|} \cap \mathbb{S}_{h,\|}$. Since $\mathbb{x} \in \mathbb{C}_{h,\|}$, we can find $\mathbb{u} \in \mathbb{V}_h(\mathcal{P}_{\Omega,h})$ such that

$$\begin{cases} \mathbb{a}(\mathbb{u}, v) = \left\langle\!\!\left\langle \mathbb{x}_1, \boldsymbol{\gamma}_{0,h,\|} v \right\rangle\!\!\right\rangle_{\|}, & \forall \mathbb{v} \in \mathbb{V}_h(\mathcal{P}_{\Omega,h}), \\ \mathbb{x}_0 = \boldsymbol{\gamma}_{0,h,\|} \mathbb{u}. \end{cases} \tag{4.67}$$

Then since $\mathbb{x} \in \mathbb{S}_{h,\|}$, from Proposition 4.16, it follows that $\mathbb{u}$ actually satisfies the homogeneous approximation of model problem (4.19) in the whole of Ω

$$\begin{cases} \mathbb{u} \in \mathrm{V}_h(\Omega), \\ a(\mathbb{u}, v) = 0, \qquad \forall v \in \mathrm{V}_h(\Omega). \end{cases} \tag{4.68}$$

The well-posedness of this problem (Assumption 4.4) yields $\mathbb{u} = 0$, hence $\mathbb{x} = 0$ by continuity of the trace operator $\boldsymbol{\gamma}_{0,h,\|}$.

Decomposition. Let $\mathbb{x} \equiv (\mathbb{x}_0, \mathbb{x}_1) \in \mathbb{M}_{h,\|}$. We wish to construct $\mathbb{y} \in \mathbb{C}_{h,\|}$ and $\mathbb{z} \in \mathbb{S}_{h,\|}$ such that $\mathbb{x} = \mathbb{y} + \mathbb{z}$. The proof performs explicitly the projection of $\mathbb{x}$ on the subspace $\mathbb{C}_{h,\|}$ in parallel to the subspace $\mathbb{S}_{h,\|}$. We define

$$\begin{cases} u \in \mathrm{V}_h(\Omega) \text{ such that,} \\ a(u, v) = \mathbb{a}(\mathbb{E}_{h,\|} \, \mathbb{x}_0, v) - \left\langle\!\!\left\langle \mathbb{x}_1, \boldsymbol{\gamma}_{0,h,\|} v \right\rangle\!\!\right\rangle_{\|}, & \forall v \in \mathrm{V}_h(\Omega), \end{cases} \tag{4.69}$$

Such a solution exists from the well-posedness of the model problem (4.19) (Assumption 4.4).

Set

$$\mathbb{y}_0 := \boldsymbol{\gamma}_{0,h,\|}(\mathbb{E}_{h,\|}\,\mathbb{x}_0 - u) = \mathbb{x}_0 - \boldsymbol{\gamma}_{0,h,\|}u, \tag{4.70}$$

and define $\mathbb{y}_1 \in \mathbb{M}_{1,h,\|}$ such that

$$\mathfrak{a}(u - \mathbb{E}_{h,\|}\,\mathbb{x}_0, \mathbb{E}_{h,\|}\,\mathbb{x}_0^t) = -\langle\!\langle \mathbb{y}_1, \mathbb{x}_0^t \rangle\!\rangle_{\|}, \qquad \forall \mathbb{x}_0^t \in \mathbb{M}_{0,h,\|}. \tag{4.71}$$

By construction, using Definition 4.10 of the discrete Cauchy space $\mathbb{C}_{h,\|}$, we have

$$\mathbb{y} := (\mathbb{y}_0, \mathbb{y}_1) \in \mathbb{C}_{h,\|}. \tag{4.72}$$

Now, set

$$\mathbb{z} \equiv (\mathbb{z}_0, \mathbb{z}_1) := \mathbb{x} - \mathbb{y}. \tag{4.73}$$

Using Proposition 4.12 together with the fact that $u \in \mathrm{V}_h(\Omega)$, we have

$$\mathbb{z}_0 := \mathbb{x}_0 - \mathbb{y}_0 = \boldsymbol{\gamma}_{0,h,\|}u \in \mathbb{S}_{0,h,\|}. \tag{4.74}$$

Besides, for any $\mathbb{s}_0 \in \mathbb{S}_{0,h,\|}$, we can test with $\mathbb{E}_{h,\|}\,\mathbb{s}_0 \in \mathrm{V}_h(\Omega)$ in (4.69) (note that $\mathbb{E}_{h,\|}\,\mathbb{s}_0$ does belong to $\mathrm{V}_h(\Omega)$ from Lemma 4.13) and with $\mathbb{s}_0$ in (4.71) to obtain

$$\langle\!\langle \mathbb{z}_1, \mathbb{s}_0 \rangle\!\rangle_{\|} = \langle\!\langle \mathbb{x}_1 - \mathbb{y}_1, \mathbb{s}_0 \rangle\!\rangle_{\|} = 0, \tag{4.75}$$

so that, using Proposition 4.15 we obtain $\mathbb{z}_1 \in \mathbb{S}_{1,h,\|}$ and hence:

$$\mathbb{z} \in \mathbb{S}_{h,\|}. \tag{4.76}$$

It is then straightforward to check that

$$\mathbb{x} = \mathbb{y} + \mathbb{z}, \qquad \text{with} \qquad \begin{cases} \mathbb{y} \in \mathbb{C}_{h,\|}, \\ \mathbb{z} \in \mathbb{S}_{h,\|}. \end{cases} \tag{4.77}$$

Explicit estimate. We adopt the same notations as for the proof of the decomposition. By definition of the projector $\mathbf{P}_{\mathbb{C}_{h,\|}}$, we have,

$$\mathbb{y} \equiv (\mathbb{y}_0, \mathbb{y}_1) := \mathbf{P}_{\mathbb{C}_{h,\|}}\mathbb{x}, \qquad \text{so that} \qquad \|\mathbf{P}_{\mathbb{C}_{h,\|}}\mathbb{x}\|^2_{\mathbb{M}_{h,\|}} = \|\mathbb{y}\|^2_{\mathbb{M}_{h,\|}} = \|\mathbb{y}_0\|^2_{\mathbb{M}_{0,h,\|}} + \|\mathbb{y}_1\|^2_{\mathbb{M}_{1,h,\|}}. \tag{4.78}$$

By definition of $\mathbb{y}$, we have

$$\begin{aligned} \|\mathbb{y}_0\|_{\mathbb{M}_{0,h,\|}} &\leq \|\,\mathbb{E}_{h,\|}\,\mathbb{x}_0 - u\|_{\mathrm{U}_\Gamma(\mathrm{D};\mathcal{P}_{\Omega,h})} \leq \left(|||\mathbb{E}_{\|}||| \, \|\mathbb{x}_0\|_{\mathbb{M}_{0,h,\|}} + \|u\|_{\mathrm{U}_\Gamma(\mathrm{D};\mathcal{P}_{\Omega,h})}\right), \\ \|\mathbb{y}_1\|_{\mathbb{M}_{1,h,\|}} &\leq |||a||| \, |||\mathbb{E}_{\|}||| \, \|\,\mathbb{E}_{h,\|}\,\mathbb{x}_0 - u\|_{\mathrm{U}_\Gamma(\mathrm{D};\mathcal{P}_{\Omega,h})} \leq |||a||| \, |||\mathbb{E}_{\|}||| \, \left(|||\mathbb{E}_{\|}||| \, \|\mathbb{x}_0\|_{\mathbb{M}_{0,h,\|}} + \|u\|_{\mathrm{U}_\Gamma(\mathrm{D};\mathcal{P}_{\Omega,h})}\right). \end{aligned} \tag{4.79}$$

Besides, by definition of u we have

$$\|u\|_{\mathrm{U}_\Gamma(\mathrm{D};\mathcal{P}_{\Omega,h})} \leq \alpha_{a,h}^{-1} \left(|||a||| \, |||\mathbb{E}_{h,\|}||| \, \|\mathbb{x}_0\|_{\mathbb{M}_{0,h,\|}} + \|\mathbb{x}_1\|_{\mathbb{M}_{1,h,\|}}\right). \tag{4.80}$$

We readily obtain the claimed estimate

$$\begin{aligned} \|\mathbf{P}_{\mathbb{C}_{h,\|}}\mathbb{x}\|^2_{\mathbb{M}_{h,\|}} &\leq \left(1 + |||a|||^2 \, |||\mathbb{E}_{h,\|}|||^2\right) \left[\left(1 + \alpha_{a,h}^{-1} \, |||a|||\right) |||\mathbb{E}_{h,\|}||| \, \|\mathbb{x}_0\|_{\mathbb{M}_{0,h,\|}} + \alpha_{a,h}^{-1} \, \|\mathbb{x}_1\|_{\mathbb{M}_{1,h,\|}}\right]^2, \\ &\leq \left(1 + |||a|||^2 \, |||\mathbb{E}_{h,\|}|||^2\right) \left[\left(1 + \alpha_{a,h}^{-1} \, |||a|||\right)|||\mathbb{E}_{h,\|}||| + \alpha_{a,h}^{-1}\right]^2 \, \|\mathbb{x}\|^2_{\mathbb{M}_{h,\|}}. \end{aligned} \tag{4.81}$$

■

4.2.2 Reformulation as an interface problem

In this section, repeating the steps of Chapter 3, we exploit the above characterization (see Proposition 4.16) of the trace of the solution to equivalently recast the discrete approximation of the original problem (4.19) as a problem (4.145) posed on the skeleton $\tilde{\Sigma}$ of the partition.

4.2.2.1 Transmission operators and associated scalar products

We start by introducing the key ingredient of our formulation, the transmission operator from Definition 3.26, this time as a bilinear form.

Definition 4.18 (**Transmission operator**). *We call* transmission *operator any* continuous *and* positive definite *bilinear form*

$$\mathrm{t}_{0,h,\|} \ : \ \mathbb{M}_{0,h,\|} \times \mathbb{M}_{0,h,\|} \to \mathbb{C}, \tag{4.82}$$

such that

$$\mathrm{t}_{0,h,\|}(\mathbb{x}_0, \overline{\mathbb{x}_0}) > 0, \qquad \forall \mathbb{x}_0 \in \mathbb{M}_{0,h,\|} \setminus \{0\}. \tag{4.83}$$

Besides, we also introduce the following additional *continuous* bilinear form, representation of the operator $\mathbf{Z}$ introduced in (3.173),

$$\mathrm{z}_h \ : \ \mathbb{M}_{0,h,\|} \times \mathbb{M}_{0,h,\|} \to \mathbb{C}, \tag{4.84}$$

such that

$$\forall \mathbb{x}_0 \in \mathbb{M}_{0,h,\|}, \qquad \mathrm{z}_h(\mathbb{x}_0, \overline{\mathbb{x}_0}) \in \mathbb{R}. \tag{4.85}$$

For the sake of simplicity, and because it will always be the case in practice, we suppose that these operators are diagonal.

Definition 4.19 (**Diagonal operators**). *The transmission operator* $\mathrm{t}_{0,h,\|}$ *and the operator* z_h *will be called* diagonal *if there exist, for each* $(j,k) \in \mathbb{J}$*, the following local continuous bilinear forms*

$$\begin{aligned} \mathrm{t}^{jk}_{0,h,\|} \ &: \ \mathrm{X}_{0,h}(\Gamma_{jk,h}) \times \mathrm{X}_{0,h}(\Gamma_{jk,h}) \to \mathbb{C}, \\ \mathrm{z}^{jk}_{h} \ &: \ \mathrm{X}_{0,h}(\Gamma_{jk,h}) \times \mathrm{X}_{0,h}(\Gamma_{jk,h}) \to \mathbb{C}, \end{aligned} \tag{4.86}$$

such that

$$\begin{aligned} \mathrm{t}_{0,h,\|}(\mathbb{x}_0, \mathbb{y}_0) &:= \sum_{(j,k)\in\mathbb{J}} \mathrm{t}^{jk}_{0,h,\|}(\mathrm{x}^{jk}_0, \mathrm{y}^{jk}_0), \qquad \forall \mathbb{x}_0, \mathbb{y}_0 \in \mathbb{M}_{0,h,\|}, \\ \mathrm{z}_h(\mathbb{x}_0, \mathbb{y}_0) &:= \sum_{(j,k)\in\mathbb{J}} \mathrm{z}^{jk}_{h}(\mathrm{x}^{jk}_0, \mathrm{y}^{jk}_0), \qquad \forall \mathbb{x}_0, \mathbb{y}_0 \in \mathbb{M}_{0,h,\|}. \end{aligned} \tag{4.87}$$

where we adopted the notation $\mathbb{x}_0 \equiv (\mathrm{x}^{jk}_0)_{(j,k)\in\mathbb{J}}$ *and* $\mathbb{y}_0 \equiv (\mathrm{y}^{jk}_0)_{(j,k)\in\mathbb{J}}$.

Scalar product and norm We can then endow the multi-trace space $\mathbb{M}_{0,h,\|}$ with the norm induced by the previous scalar product. Hence we define

$$\|\mathbb{x}_0\|^2_{\mathrm{t}_{0,h,\|}} := \mathrm{t}_{0,h,\|}(\mathbb{x}_0, \overline{\mathbb{x}_0}), \qquad \forall \mathbb{x}_0 \in \mathbb{M}_{0,h,\|}. \tag{4.88}$$

Because of the finite dimensional setting, the norms $\|\cdot\|_{\mathbb{M}_{0,h,\|}}$ (defined in (4.36)) and $\|\cdot\|_{\mathrm{t}_{0,h,\|}}$ are always equivalent on $\mathbb{M}_{0,h,\|}$. However, they are not necessarily h-uniformly equivalent. This is why we introduce the continuity constant

$$|||\mathrm{t}_{0,h,\|}||| := \sup_{\substack{\mathbb{x}_0,\mathbb{y}_0\in\mathbb{M}_{0,h,\|} \\ \mathbb{x}_0,\mathbb{y}_0\neq 0}} \frac{|\mathrm{t}_{0,h,\|}(\mathbb{x}_0, \mathbb{y}_0)|}{\|\mathbb{x}_0\|_{\mathbb{M}_{0,h,\|}} \|\mathbb{y}_0\|_{\mathbb{M}_{0,h,\|}}}, \tag{4.89}$$

and coercivity constant

$$\beta_{\mathrm{t}_{0,h,\|}} := \inf_{\substack{\mathbb{x}_0 \in \mathbb{M}_{0,h,\|} \\ \mathbb{x}_0 \neq 0}} \frac{\mathrm{t}_{0,h,\|}(\mathbb{x}_0,\, \overline{\mathbb{x}_0})}{\|\mathbb{x}_0\|^2_{\mathbb{M}_{0,h,\|}}}. \tag{4.90}$$

By definition, it follows that

$$\beta_{\mathrm{t}_{0,h,\|}} \, \|\mathbb{x}_0\|^2_{\mathbb{M}_{0,h,\|}} \leq \|\mathbb{x}_0\|^2_{\mathrm{t}_{0,h,\|}} \leq |||\mathrm{t}_{0,h,\|}||| \, \|\mathbb{x}_0\|^2_{\mathbb{M}_{0,h,\|}}, \qquad \forall \mathbb{x}_0 \in \mathbb{M}_{0,h,\|}. \tag{4.91}$$

We can define a norm on the multi-trace space $\mathbb{M}_{1,h,\|}$. To do so, using Riesz representation theorem, we first introduce the operator, $\mathbf{T}_{0,h,\|}$ from $\mathbb{M}_{0,h,\|}$ into its dual

$$\begin{aligned} \mathbf{T}_{0,h,\|} \; &: \mathbb{M}_{0,h,\|} \to \mathbb{M}_{0,h,\|}{}' = \mathbb{M}_{1,h,\|}, \\ &\mathbb{x}_0 \mapsto \mathbb{x}_1, \end{aligned} \tag{4.92}$$

where $\mathbb{x}_1 \in \mathbb{M}_{1,h,\|}$ is such that

$$\mathrm{t}_{0,h,\|}(\mathbb{x}_0,\, \mathbb{x}_0^t) = \langle\!\langle \mathbb{x}_1, \mathbb{x}_0^t \rangle\!\rangle_{\|}, \qquad \forall \mathbb{x}_0^t \in \mathbb{M}_{0,h,\|}. \tag{4.93}$$

From Definition 4.18, $\mathbf{T}_{0,h,\|}$ is clearly invertible and we can then define

$$\mathbf{T}_{1,h,\|} := \mathbf{T}^{-1}_{0,h,\|} \; : \mathbb{M}_{1,h,\|} \to \mathbb{M}_{0,h,\|}. \tag{4.94}$$

The norm on the discrete multi-trace space $\mathbb{M}_{1,h,\|}$ is then defined as

$$\|\mathbb{x}_1\|^2_{\mathrm{t}_{1,h,\|}} := \langle\!\langle \mathbb{x}_1, \overline{\mathbf{T}_{1,\|}\mathbb{x}_1} \rangle\!\rangle_{\|}, \qquad \forall \mathbb{x}_1 \in \mathbb{M}_{1,h,\|}. \tag{4.95}$$

The following easy lemma states that the norms $\|\cdot\|_{\mathbb{M}_{1,h,\|}}$ (defined in (4.38)) and $\|\cdot\|_{\mathrm{t}_{1,h,\|}}$ are equivalent (not necessarily h-uniformly equivalent though).

Lemma 4.20. *We have*

$$\beta_{\mathrm{t}_{0,h,\|}} \, |||\mathrm{t}_{0,h,\|}|||^{-2} \, \|\mathbb{x}_1\|^2_{\mathbb{M}_{1,h,\|}} \leq \|\mathbb{x}_1\|^2_{\mathrm{t}_{1,h,\|}} \leq \beta^{-1}_{\mathrm{t}_{0,h,\|}} \, \|\mathbb{x}_1\|^2_{\mathbb{M}_{1,h,\|}}, \qquad \forall \mathbb{x}_1 \in \mathbb{M}_{1,h,\|}. \tag{4.96}$$

Proof. Let $\mathbb{x}_1 \in \mathbb{M}_{1,h,\|}$, we have on the one hand

$$\|\mathbb{x}_1\|^2_{\mathrm{t}_{1,h,\|}} = \langle\!\langle \mathbb{x}_1, \overline{\mathbf{T}_{1,\|}\mathbb{x}_1} \rangle\!\rangle_{\|} \leq \|\mathbb{x}_1\|_{\mathbb{M}_{1,h,\|}} \|\mathbf{T}_{1,\|}\mathbb{x}_1\|_{\mathbb{M}_{0,h,\|}} \leq \beta^{-1}_{\mathrm{t}_{0,h,\|}} \, \|\mathbb{x}_1\|^2_{\mathbb{M}_{1,h,\|}}. \tag{4.97}$$

On the other hand

$$\begin{aligned} \|\mathbb{x}_1\|^2_{\mathrm{t}_{1,h,\|}} &= \mathrm{t}_{1/2,\|}(\mathbf{T}_{1,\|}\mathbb{x}_1, \overline{\mathbf{T}_{1,\|}\mathbb{x}_1}) = \|\mathbf{T}_{1,\|}\mathbb{x}_1\|^2_{\mathbf{T}_{0,\|}}, \\ &\geq \beta_{\mathrm{t}_{0,h,\|}} \|\mathbf{T}_{1,\|}\mathbb{x}_1\|^2_{\mathbb{M}_{0,h,\|}} \geq \beta_{\mathrm{t}_{0,h,\|}} \, |||\mathrm{t}_{0,h,\|}|||^{-2} \, \|\mathbb{x}_1\|^2_{\mathbb{M}_{1,h,\|}}. \end{aligned} \tag{4.98}$$

■

Generalized Robin operators The transmission operator $\mathrm{t}_{0,h,\|}$ together with the bilinear form z_h are used to combine the two types of traces into so-called generalized Robin multi-traces.

Definition 4.21 (**Discrete generalized Robin operators**). *We introduce the global operators,*

$$\mathbf{R}^{\pm}_{1,h,\|} \; : \mathbb{M}_{h,\|} \to \mathbb{M}_{1,h,\|}, \tag{4.99}$$

where, for any $\mathbb{x} \equiv (\mathbb{x}_0, \mathbb{x}_1) \in \mathbb{M}_{h,\|}$, we define $\mathbf{R}^{\pm}_{1,h,\|}$ as

$$\langle\!\langle \mathbf{R}^{\pm}_{1,h,\|}\mathbb{x}, \mathbb{x}_0^t \rangle\!\rangle_{\|} = \pm \left[\langle\!\langle \mathbb{x}_1, \mathbb{x}_0^t \rangle\!\rangle_{\|} + \mathrm{z}_h(\mathbb{x}_0,\, \mathbb{x}_0^t) \right] - \mathrm{it}_{0,h,\|}(\mathbb{x}_0,\, \mathbb{x}_0^t), \qquad \forall \mathbb{x}_0^t \in \mathbb{M}_{0,h,\|}. \tag{4.100}$$

If the transmission operators are diagonal we can define local Robin operators at a single interface: for each $(j,k) \in \mathbb{J}$ and any $\mathrm{x} \equiv (\mathrm{x}_0, \mathrm{x}_1) \in \mathrm{X}(\Gamma_{jk,h})$, we define $\mathbf{R}^{jk,\pm}_{1,h,\|}$ as

$$\langle \mathbf{R}^{jk,\pm}_{1,h,\|}\mathrm{x}, \mathrm{x}_0^t \rangle_{\Gamma_{jk,h}} = \pm \left[\langle \mathbb{x}_1, \mathrm{x}_0^t \rangle_{\Gamma_{jk,h}} + \mathrm{z}^{jk}_h(\mathrm{x}_0,\, \mathrm{x}_0^t) \right] - \mathrm{it}^{jk}_{0,h,\|}(\mathrm{x}_0,\, \mathrm{x}_0^t), \qquad \forall \mathrm{x}_0^t \in \mathrm{X}_0(\Gamma_{jk,h}). \tag{4.101}$$

4.2.2.2 Scattering operators

We recall that the scattering operators were introduced in Definition 3.29. We then showed that, under Assumption 3.40, which we suppose to hold in this chapter, they are diagonal operators in the form of (3.216), with diagonal components given in Definition 3.44. We are now going to introduce a discrete version of those scattering operators using only variational definitions, easily amenable to discretization.

Definition 4.22 (**Discrete scattering operator**). *We define the global scattering operators,*

$$\mathbf{S}_{1,h,\|} \ : \ \mathbb{M}_{1,h,\|} \to \mathbb{M}_{1,h,\|}, \tag{4.102}$$

where for any $\mathbb{x}_1 \in \mathbb{M}_{1,h,\|}$ *we define*

$$\left\langle\!\left\langle \mathbf{S}_{1,h,\|}\mathbb{x}_1, \mathbb{x}_0^t \right\rangle\!\right\rangle_{\|} = -\left\langle\!\left\langle \mathbb{x}_1, \mathbb{x}_0^t \right\rangle\!\right\rangle_{\|} - 2\mathrm{i}\mathrm{t}_{0,h,\|}(\boldsymbol{\gamma}_{0,h,\|}u_1,\, \mathbb{x}_0^t), \tag{4.103}$$

with $\mathbb{u} \in \mathbb{V}_h(\mathcal{P}_{\Omega,h})$ *such that: for all* $\mathbb{v} \in \mathbb{V}_h(\mathcal{P}_{\Omega,h})$

$$\mathbb{a}(\mathbb{u},\mathbb{v}) + [\mathrm{z}_h(\boldsymbol{\gamma}_{0,h,\|}\mathbb{u},\, \boldsymbol{\gamma}_{0,h,\|}\mathbb{v}) - \mathrm{i}\mathrm{t}_{0,h,\|}(\boldsymbol{\gamma}_{0,h,\|}\mathbb{u},\, \boldsymbol{\gamma}_{0,h,\|}\mathbb{v})] = \left\langle\!\left\langle \mathbb{x}_1, \boldsymbol{\gamma}_{0,h,\|}\mathbb{v} \right\rangle\!\right\rangle_{\|}. \tag{4.104}$$

If the transmission operators are diagonal, the scattering operators are themselves diagonal and we have,

$$\begin{aligned} &\mathbf{S}_{1,h,\|} = \mathit{diag}_{j\in\{1,\dots,J\}}\left(\mathbf{S}^j_{1,h,\|}\right), \\ &\mathbf{S}^j_{1,h,\|} \ : \ (\mathrm{X}_{1,h}(\Gamma_{jk,h}))_{k\in\mathbb{K}_j} \to (\mathrm{X}_{1,h}(\Gamma_{jk,h}))_{k\in\mathbb{K}_j}, \end{aligned} \tag{4.105}$$

where for any $\mathrm{x}_1 \equiv (\mathrm{x}_1^{jk})_{k\in\mathbb{K}_j} \in (\mathrm{X}_{1,h}(\Gamma_{jk,h}))_{k\in\mathbb{K}_j}$ *we define, for any* $k \in \mathbb{K}_j$,

$$\langle (\mathbf{S}^j_{1,h,\|}\mathrm{x}_1)|_{\Gamma_{jk,h}}, \mathrm{x}_0^t\rangle_{\Gamma_{jk,h}} = -\langle \mathrm{x}_1^{jk}, \mathrm{x}_0^t\rangle_{\Gamma_{jk,h}} - 2\mathrm{i}\mathrm{t}^{jk}_{0,h,\|}(\gamma_{0,\Gamma_{jk,h}}\, u_{j,h},\, \mathrm{x}_0^t), \qquad \forall \mathrm{x}_0^t \in \mathrm{X}_{0,h}(\Gamma_{jk,h}), \tag{4.106}$$

with $u_{j,h} \in \mathrm{V}_h(\Omega_{j,h})$, $j \in \{1,\dots,J\}$, *such that: for all* $v_{j,h} \in \mathrm{V}_h(\Omega_{j,h})$,

$$\begin{aligned} a_j(u_{j,h}, v_{j,h}) + \sum_{k\in\mathbb{K}_j} \Big[\mathrm{z}_h^{jk}(\gamma_{0,\Gamma_{jk,h}}\, u_{j,h},\, \gamma_{0,\Gamma_{jk,h}}\, v_{j,h}) \ -\mathrm{i}\mathrm{t}^{jk}_{0,h,\|}(\gamma_{0,\Gamma_{jk,h}}\, u_{j,h},\, \gamma_{0,\Gamma_{jk,h}}\, v_{j,h}) \Big] \\ = \sum_{k\in\mathbb{K}_j} \langle \mathrm{x}_1^{jk}, \gamma_{0,\Gamma_{jk,h}}\, v_{j,h}\rangle_{\Gamma_{jk,h}}. \end{aligned} \tag{4.107}$$

The following proposition shows that the above scattering operators are well-defined. Of course, the result relies on the properties of the transmission operator from Definition 4.18. This proposition is based on a similar result in a more general setting (with junctions) available for the scalar equation, see [33, Lem. 4.4].

Proposition 4.23 (**Well-posedness of local problems**). *Let*

$$\alpha_{s,h,\|} := \inf_{\substack{\mathbb{u}\in\mathbb{V}_h(\mathcal{P}_{\Omega,h}) \\ \mathbb{u}\neq 0}} \sup_{\substack{\mathbb{v}\in\mathbb{V}_h(\mathcal{P}_{\Omega,h}) \\ \mathbb{v}\neq 0}} \frac{|\mathbb{a}(\mathbb{u},\mathbb{v}) + \mathrm{z}_h(\boldsymbol{\gamma}_{0,h,\|}\mathbb{u},\, \boldsymbol{\gamma}_{0,h,\|}\mathbb{v}) - \mathrm{i}\mathrm{t}_{0,h,\|}(\boldsymbol{\gamma}_{0,h,\|}\mathbb{u},\, \boldsymbol{\gamma}_{0,h,\|}\mathbb{v})|}{\|\mathbb{u}\|_{\mathbb{U}_\Gamma(\mathrm{D};\mathcal{P}_\Omega)}\|\mathbb{v}\|_{\mathbb{U}_\Gamma(\mathrm{D};\mathcal{P}_\Omega)}}. \tag{4.108}$$

We have, for any h,

$$\alpha_{s,h,\|} > 0. \tag{4.109}$$

As a result, for any linear form $\mathbb{l}$ *on* $\mathbb{V}_h(\mathcal{P}_{\Omega,h})$, *the following problem is well-posed:*

$$\begin{cases} \textit{Find } \mathbb{u} \in \mathbb{V}_h(\mathcal{P}_{\Omega,h}) \textit{ such that}: \\ \mathbb{a}(\mathbb{u},\mathbb{v}) + [\mathrm{z}_h(\boldsymbol{\gamma}_{0,h,\|}\mathbb{u},\, \boldsymbol{\gamma}_{0,h,\|}\mathbb{v}) - \mathrm{i}\mathrm{t}_{0,h,\|}(\boldsymbol{\gamma}_{0,h,\|}\mathbb{u},\, \boldsymbol{\gamma}_{0,h,\|}\mathbb{v})] = \mathbb{l}(\mathbb{v}), \qquad \forall \mathbb{v} \in \mathbb{V}_h(\mathcal{P}_{\Omega,h}). \end{cases} \tag{4.110}$$

Proof. Suppose by contradiction that the above inf − sup constant vanishes for some $\mathfrak{u} \in \mathbb{V}_h(\mathcal{P}_{\Omega,h})$, then

$$\mathfrak{a}(\mathfrak{u},\mathfrak{v}) + \mathrm{z}_h(\boldsymbol{\gamma}_{0,h,\parallel}\mathfrak{u},\, \boldsymbol{\gamma}_{0,h,\parallel}\mathfrak{v}) - \mathrm{it}_{0,h,\parallel}(\boldsymbol{\gamma}_{0,h,\parallel}\mathfrak{u},\, \boldsymbol{\gamma}_{0,h,\parallel}\mathfrak{v}) = 0, \qquad \forall \mathfrak{v} \in \mathbb{V}_h(\mathcal{P}_{\Omega,h}). \tag{4.111}$$

Testing by $\overline{\mathfrak{u}}$ (see (3.98) for the definition of the sesquilinear form $\mathfrak{a}$), we get

$$\begin{aligned} &{\kappa_0}^{-1}(\mathsf{a}\,\mathrm{D}\mathfrak{u}, \mathrm{D}\overline{\mathfrak{u}})_{L^2(\Omega)^{m_1}} - \kappa_0\,(\mathsf{n}\mathfrak{u}, \overline{\mathfrak{u}})_{L^2(\Omega)^{m_0}} - \mathrm{i}(\gamma_{0,\Gamma}\,\mathfrak{u}, \gamma_{0,\Gamma}\,\overline{\mathfrak{u}})_{L^2(\Gamma)^{m_0}} \\ &\quad + \mathrm{z}_h(\boldsymbol{\gamma}_{0,h,\parallel}\mathfrak{u},\, \boldsymbol{\gamma}_{0,h,\parallel}\overline{\mathfrak{u}}) - \mathrm{it}_{0,h,\parallel}(\boldsymbol{\gamma}_{0,h,\parallel}\mathfrak{u},\, \boldsymbol{\gamma}_{0,h,\parallel}\overline{\mathfrak{u}}) = 0. \end{aligned} \tag{4.112}$$

Since the imaginary parts of the coefficients a and n are respectively supposed negative and positive (see (3.78)) and from the property of z_0 in (4.85), retaining only the imaginary part above implies necessarily that

$$\mathrm{t}_{0,h,\parallel}(\boldsymbol{\gamma}_{0,h,\parallel}\mathfrak{u},\, \boldsymbol{\gamma}_{0,h,\parallel}\overline{\mathfrak{u}}) = 0, \tag{4.113}$$

so that by the definiteness of $\mathrm{t}_{0,h,\parallel}$, we have $\boldsymbol{\gamma}_{0,h,\parallel}\mathfrak{u} = 0$. From Corollary 4.14, we deduce that $\mathfrak{u} \in \mathrm{V}_h(\Omega)$ and, testing by $v \in \mathrm{V}_h(\Omega)$ in (4.111) we get

$$\mathfrak{a}(\mathfrak{u}, v) + \mathrm{z}_h(\boldsymbol{\gamma}_{0,h,\parallel}\mathfrak{u},\, \boldsymbol{\gamma}_{0,h,\parallel}v) - \mathrm{it}_{0,h,\parallel}(\boldsymbol{\gamma}_{0,h,\parallel}\mathfrak{u},\, \boldsymbol{\gamma}_{0,h,\parallel}v) = a(\mathfrak{u}, v) = 0, \qquad \forall v \in \mathrm{V}_h(\Omega). \tag{4.114}$$

The well-posedness of the discrete model problem (4.19) stated in Assumption 4.4 gives that $\mathfrak{u} = 0$ which is a contradiction. ∎

Again, we point out that such a result is valid for our target applications for h small enough, but this is not an issue for the abstract analysis.

An important question we shall ask ourselves is the stability of the above constant $\alpha_{s,h,\parallel}$ with respect to the mesh parameter h. We can answer this question in the acoustic setting. The following statement is based on a similar result in a more general setting (with junctions) available for the scalar equation, see [33, Lem. 4.4].

Example 1: Helmholtz. *In the acoustic setting, if the partition is independent of h (see Assumption 4.5), as well as the transmission operator, the estimate $\alpha_{s,h,\parallel}$ defined in* (4.108) *is h-uniformly bounded*

$$\alpha^{\star}_{s,\parallel} := \liminf_{h\to 0} \alpha_{s,h,\parallel} > 0. \tag{4.115}$$

Proof. The proof proceeds by contradiction. Suppose there exists a sequence $(h_k)_k$ of mesh parameters converging to 0, associated to a sequence of $\mathfrak{u}_{h_k} \in \mathbb{V}_h(\mathcal{P}_{\Omega,h})$ such that $\|\mathfrak{u}_{h_k}\|_{\mathbb{U}(\mathrm{D};\mathcal{P}_\Omega)} = 1$ and

$$\sup_{\mathfrak{v}\in\mathbb{V}_h(\mathcal{P}_{\Omega,h})} |\mathfrak{a}(\mathfrak{u}_{h_k},\mathfrak{v}) + \mathrm{z}_h(\boldsymbol{\gamma}_{0,h,\parallel}\mathfrak{u}_{h_k},\, \boldsymbol{\gamma}_{0,h,\parallel}\mathfrak{v}) - \mathrm{it}_{0,h,\parallel}(\boldsymbol{\gamma}_{0,h,\parallel}\mathfrak{u}_{h_k},\, \boldsymbol{\gamma}_{0,h,\parallel}\mathfrak{v})| \to 0, \qquad \text{as } h_k \to 0. \tag{4.116}$$

Since the sequence $(\mathfrak{u}_{h_k})_k$ is bounded in $\mathbb{U}(\mathrm{D};\mathcal{P}_\Omega)$, we can assume that the sequence $(\mathfrak{u}_{h_k})_k$ converges towards some $\mathfrak{u}_\infty$ weakly in $\mathbb{U}(\mathrm{D};\mathcal{P}_\Omega)$, extracting a sub-sequence if necessary. Since in this setting $\mathbb{U}(\mathrm{D};\mathcal{P}_\Omega)$ is a cartesian product of H^1 spaces on each sub-domain, the sequence $(\mathfrak{u}_{h_k})_k$ converges strongly towards $\mathfrak{u}_\infty$ in the cartesian product of L^2 spaces in each sub-domain, hence in $L^2(\Omega)$. The weak convergence of the sequence $(\mathfrak{u}_{h_k})_k$ implies that, for any $\mathfrak{v} \in \mathbb{V}_h(\mathcal{P}_{\Omega,h})$,

$$\begin{aligned} &|\mathfrak{a}(\mathfrak{u}_{h_k},\mathfrak{v}) + \mathrm{z}_h(\boldsymbol{\gamma}_{0,h,\parallel}\mathfrak{u}_{h_k},\, \boldsymbol{\gamma}_{0,h,\parallel}\mathfrak{v}) - \mathrm{it}_{0,h,\parallel}(\boldsymbol{\gamma}_{0,h,\parallel}\mathfrak{u}_{h_k},\, \boldsymbol{\gamma}_{0,h,\parallel}\mathfrak{v})| \\ &\quad \to |\mathfrak{a}(\mathfrak{u}_\infty,\mathfrak{v}) + \mathrm{z}_h(\boldsymbol{\gamma}_{0,h,\parallel}\mathfrak{u}_\infty,\, \boldsymbol{\gamma}_{0,h,\parallel}\mathfrak{v}) - \mathrm{it}_{0,h,\parallel}(\boldsymbol{\gamma}_{0,h,\parallel}\mathfrak{u}_\infty,\, \boldsymbol{\gamma}_{0,h,\parallel}\mathfrak{v})| = 0, \qquad \text{as } h_k \to 0. \end{aligned} \tag{4.117}$$

Arguing as in the proof of Proposition 4.23, if follows that $\mathfrak{u}_\infty = 0$, and the sequence $(\mathfrak{u}_{h_k})_k$ converges strongly towards 0 in $L^2(\Omega)$. We write, by definition of the norm and of the sesquilinear form a,

$$\|\mathfrak{u}_{h_k}\|^2_{\mathbb{U}(\mathrm{D};\mathcal{P}_\Omega)} \leq \left(\inf_\Omega \Re(a)\right)^2 \left(\Re\, a(\mathfrak{u}_{h_k}, \mathfrak{u}_{h_k}) + \kappa_0\, (\mathfrak{n}\mathfrak{u}_{h_k}, \overline{\mathfrak{u}_{h_k}})_{L^2(\Omega)^{m_0}}\right) + \kappa_0 \|\mathfrak{u}_{h_k}\|^2_{L^2(\Omega)^{m_0}}. \quad (4.118)$$

From (4.116) we have that $\Re\, a(\mathfrak{u}_{h_k}, \mathfrak{u}_{h_k}) \to 0$ and since we proved that $\|\mathfrak{u}_{h_k}\|_{L^2(\Omega)^{m_0}} \to 0$, it follows that $\|\mathfrak{u}_{h_k}\|_{\mathbb{U}(\mathrm{D};\mathcal{P}_\Omega)} \to 0$, which a contradiction. ■

A direct consequence of the well-posedness of the above problem (4.104) is the well-posedness of the following local sub-problems in each sub-domain, for diagonal operators.

Corollary 4.24. *If the transmission operator* $\mathrm{t}_{0,h,\|}$ *and operator* z_0 *are diagonal, for all* $j \in \{1, \ldots, J\}$ *and any linear form* l_j *on* $\mathrm{V}_h(\Omega_{j,h})$*, the problem*

$$\begin{cases} \text{Find } u_j \in \mathrm{V}_h(\Omega_{j,h}) \text{ such that :} \\ a_j(u_j, v_j) + \sum_{k\in\mathbb{K}_j} \Big[\mathrm{z}_h^{jk}(\gamma_{0,\Gamma_{jk,h}}\, u_j,\, \gamma_{0,\Gamma_{jk,h}}\, v_j) \\ \qquad\qquad -\mathrm{it}^{jk}_{0,h,\|}(\gamma_{0,\Gamma_{jk,h}}\, u_j,\, \gamma_{0,\Gamma_{jk,h}}\, v_j)\Big] = l_j(v_j) \qquad \forall v_j \in \mathrm{V}_h(\Omega_{j,h}), \end{cases} \quad (4.119)$$

is well posed.

We are then able to provide an equivalent discrete characterization to the one from Proposition 3.30, which is similar to [33, Lem. 7.2].

Proposition 4.25 (**Characterization of the discrete Cauchy trace space**)**.** *We have the following characterization of the discrete Cauchy-trace space:*

$$\mathbb{C}_{h,\|} = \mathrm{Ker}\left(\mathbf{R}^-_{1,h,\|} - \mathbf{S}_{1,h,\|}\mathbf{R}^+_{1,h,\|}\right). \quad (4.120)$$

Proof. From Definition 4.21 and Definition 4.22, $\mathbb{x} \equiv (\mathbb{x}_0, \mathbb{x}_1) \in \mathbb{M}_{h,\|}$ satisfy

$$\mathbf{R}^-_{1,h,\|}\mathbb{x} = \mathbf{S}_{1,h,\|}\mathbf{R}^+_{1,h,\|}\mathbb{x}, \quad (4.121)$$

if, and only if, there exists $\mathbb{u} \in \mathbb{V}_h(\mathcal{P}_{\Omega,h})$ such that

$$\begin{aligned} &\begin{cases} \mathfrak{a}(\mathbb{u}, \mathbb{v}) + [\mathrm{z}_h(\boldsymbol{\gamma}_{0,h,\|}\mathbb{u},\, \boldsymbol{\gamma}_{0,h,\|}\mathbb{v}) - \mathrm{it}_{0,h,\|}(\boldsymbol{\gamma}_{0,h,\|}\mathbb{u},\, \boldsymbol{\gamma}_{0,h,\|}\mathbb{v})] \\ \qquad = \langle\!\langle \mathbb{x}_1, \boldsymbol{\gamma}_{0,h,\|}\mathbb{v}\rangle\!\rangle_\| + \mathrm{z}_h(\mathbb{x}_0,\, \boldsymbol{\gamma}_{0,h,\|}\mathbb{v}) - \mathrm{it}_{0,h,\|}(\mathbb{x}_0,\, \boldsymbol{\gamma}_{0,h,\|}\mathbb{v}), & \forall \mathbb{v} \in \mathbb{V}_h(\mathcal{P}_{\Omega,h}), \\ -\left[\langle\!\langle \mathbb{x}_1, \mathbb{x}_0^t\rangle\!\rangle_\| + \mathrm{z}_h(\mathbb{x}_0,\, \mathbb{x}_0^t)\right] - \mathrm{it}_{0,h,\|}(\mathbb{x}_0,\, \mathbb{x}_0^t) \\ \qquad = -\left[\langle\!\langle \mathbb{x}_1, \mathbb{x}_0^t\rangle\!\rangle_\| + \mathrm{z}_h(\mathbb{x}_0,\, \mathbb{x}_0^t)\right] + \mathrm{it}_{0,h,\|}(\mathbb{x}_0,\, \mathbb{x}_0^t) - 2\mathrm{it}_{0,h,\|}(\boldsymbol{\gamma}_{0,h,\|}\mathbb{u},\, \mathbb{x}_0^t), & \forall \mathbb{x}_0^t \in \mathbb{M}_{0,h,\|}. \end{cases} \\ \Leftrightarrow &\begin{cases} \mathfrak{a}(\mathbb{u}, \mathbb{v}) + \mathrm{z}_h(\boldsymbol{\gamma}_{0,h,\|}\mathbb{u} - \mathbb{x}_0,\, \boldsymbol{\gamma}_{0,h,\|}\mathbb{v}) - \mathrm{it}_{0,h,\|}(\boldsymbol{\gamma}_{0,h,\|}\mathbb{u} - \mathbb{x}_0,\, \boldsymbol{\gamma}_{0,h,\|}\mathbb{v}) \\ \qquad = \langle\!\langle \mathbb{x}_1, \boldsymbol{\gamma}_{0,h,\|}\mathbb{v}\rangle\!\rangle_\|, & \forall \mathbb{v} \in \mathbb{V}_h(\mathcal{P}_{\Omega,h}), \\ \mathrm{t}_{0,h,\|}(\mathbb{x}_0,\, \mathbb{x}_0^t) = \mathrm{t}_{0,h,\|}(\boldsymbol{\gamma}_{0,h,\|}\mathbb{u},\, \mathbb{x}_0^t), & \forall \mathbb{x}_0^t \in \mathbb{M}_{0,h,\|}, \end{cases} \\ \Leftrightarrow &\begin{cases} \mathfrak{a}(\mathbb{u}, \mathbb{v}) = \langle\!\langle \mathbb{x}_1, \boldsymbol{\gamma}_{0,h,\|}\mathbb{v}\rangle\!\rangle_\|, \qquad \forall \mathbb{v} \in \mathbb{V}_h(\mathcal{P}_{\Omega,h}), \\ \boldsymbol{\gamma}_{0,h,\|}\mathbb{u} = \mathbb{x}_0, \end{cases} \end{aligned} \quad (4.122)$$

which yields $\mathbb{x} \in \mathbb{C}_{h,\|}$ from Definition 4.10. Note that we used the injectivity property (see (4.83)) of $\mathrm{t}_{0,h,\|}$ to establish the last equivalence. ■

4.2.2.3 Exchange operator

We can extend without difficulty the definition of the exchange operator $\mathbf{\Pi}_{\shortparallel}$ to the discrete trace spaces. For each $\sigma \in \{0,1\}$, the exchange operator, denoted $\mathbf{\Pi}_{\shortparallel}$, is such that

$$\forall \mathbb{x}_\sigma, \mathbb{y}_\sigma \in \mathbb{M}_{\sigma,h,\shortparallel}, \qquad \left(\mathbb{y}_\sigma = \mathbf{\Pi}_{\shortparallel}\mathbb{x}_\sigma \qquad \Leftrightarrow \qquad \mathrm{x}_\sigma^{jk} = \mathrm{y}_\sigma^{kj}, \quad \forall (j,k) \in \mathbb{J}\right), \tag{4.123}$$

with the convention that $\mathbb{x}_\sigma \equiv (\mathrm{x}_\sigma^{jk})_{(j,k)\in\mathbb{J}}$ and $\mathbb{y}_\sigma \equiv (\mathrm{y}_\sigma^{jk})_{(j,k)\in\mathbb{J}}$.

Therefore, one can convince himself that the properties of the exchange operator carry over from the continuous setting to the discrete setting. We briefly recall below these properties for convenience.

Again, it follows from its definition that the exchange operator remains an involution of the discrete trace spaces (see Proposition 3.33) and defines two complementary projectors $\mathrm{Id} + \mathbf{\Pi}_{\shortparallel}$ and $\mathrm{Id} - \mathbf{\Pi}_{\shortparallel}$ (see Proposition 3.34).

Proposition 4.26. *For each $\sigma \in \{0,1\}$, the exchange operator $\mathbf{\Pi}_{\shortparallel}$ is an involution of $\mathbb{M}_{\sigma,h,\shortparallel}$,*

$$\mathbf{\Pi}_{\shortparallel}^2 = \mathrm{Id} \qquad \text{in } \mathbb{M}_{\sigma,h,\shortparallel}. \tag{4.124}$$

Proposition 4.27. *For each $\sigma \in \{0,1\}$, the two operators $1/2\,(\mathrm{Id} \pm \mathbf{\Pi}_{\shortparallel})$ are two* complementary projectors *in $\mathbb{M}_{\sigma,h,\shortparallel}$,*

$$\begin{aligned} &1/4[\mathrm{Id} \pm \mathbf{\Pi}_{\shortparallel}]^2 = 1/2\,[\mathrm{Id} \pm \mathbf{\Pi}_{\shortparallel}]\,, \\ &[\mathrm{Id} + \mathbf{\Pi}_{\shortparallel}]\,[\mathrm{Id} - \mathbf{\Pi}_{\shortparallel}] = [\mathrm{Id} - \mathbf{\Pi}_{\shortparallel}]\,[\mathrm{Id} + \mathbf{\Pi}_{\shortparallel}] = 0. \end{aligned} \tag{4.125}$$

It is then straightforward to establish the following result, counterpart of Proposition 4.28.

Proposition 4.28. *We have*

$$\mathbb{x} \equiv (\mathbb{x}_0, \mathbb{x}_1) \in \mathbb{S}_{h,\shortparallel} \quad \Leftrightarrow \quad \begin{cases} \mathbb{x}_0 \in \mathbb{S}_{0,h,\shortparallel}, \\ \mathbb{x}_1 \in \mathbb{S}_{1,h,\shortparallel}, \end{cases} \quad \Leftrightarrow \quad \begin{cases} \mathbb{x}_0 \in \mathrm{Ker}\,(\mathrm{Id} - \mathbf{\Pi}_{\shortparallel})\,, \\ \mathbb{x}_1 \in \mathrm{Ker}\,(\mathrm{Id} + \mathbf{\Pi}_{\shortparallel})\,. \end{cases} \tag{4.126}$$

Finally, we recall the self-adjointness property of $\mathbf{\Pi}_{\shortparallel}$ already stated in Proposition 3.54.

Proposition 4.29. *Let $\sigma \in \{0,1\}$, the exchange operator $\mathbf{\Pi}_{\shortparallel}$ is self-adjoint with respect to the duality product $\langle\!\langle \cdot, \cdot \rangle\!\rangle_{\shortparallel}$,*

$$\langle\!\langle \mathbf{\Pi}_{\shortparallel}\mathbb{x}_1, \mathbb{y}_0 \rangle\!\rangle_{\shortparallel} = \langle\!\langle \mathbb{x}_1, \mathbf{\Pi}_{\shortparallel}\mathbb{y}_0 \rangle\!\rangle_{\shortparallel}, \qquad \forall (\mathbb{x}_1, \mathbb{y}_0) \in \mathbb{M}_{0,h,\shortparallel} \times \mathbb{M}_{1,h,\shortparallel}. \tag{4.127}$$

Proof. For any $\mathbb{x}_0 = (\mathrm{x}_0^{jk})_{(j,k)\in\mathbb{J}} \in \mathbb{M}_{0,h,\shortparallel}$ and $\mathbb{x}_1 = (\mathrm{x}_1^{jk})_{(j,k)\in\mathbb{J}} \in \mathbb{M}_{1,h,\shortparallel}$, we have

$$\langle\!\langle \mathbf{\Pi}_{\shortparallel}\mathbb{x}_1, \mathbb{x}_0 \rangle\!\rangle_{\shortparallel} = \sum_{(j,k)\in\mathbb{J}} \langle \mathrm{x}_1^{kj}, \mathrm{x}_0^{jk} \rangle_{\Gamma_{jk,h}} = \langle\!\langle \mathbb{x}_1, \mathbf{\Pi}_{\shortparallel}\mathbb{x}_0 \rangle\!\rangle_{\shortparallel}. \tag{4.128}$$

■

Upon making the following assumption (akin to Assumption 3.36), which we assume to hold in what follows, we can again characterize the discrete single-trace space.

Assumption 4.30. *The bilinear form z_h is supposed* symmetric

$$\mathrm{z}_h(\mathbb{x}_0,\, \mathbb{y}_0) = \mathrm{z}_h(\mathbb{y}_0,\, \mathbb{x}_0), \qquad \forall \mathbb{x}_0, \mathbb{y}_0 \in \mathbb{M}_{0,h,\shortparallel}, \tag{4.129}$$

and such that

$$\mathrm{z}_h(\mathbb{x}_0,\, \mathbf{\Pi}_{\shortparallel}\mathbb{y}_0) = -\mathrm{z}_h(\mathbf{\Pi}_{\shortparallel}\mathbb{x}_0,\, \mathbb{y}_0), \qquad \forall \mathbb{x}_0, \mathbb{y}_0 \in \mathbb{M}_{0,h,\shortparallel}. \tag{4.130}$$

The transmission operator is such that

$$\mathrm{t}_{0,h,\shortparallel}(\mathbb{x}_0,\, \mathbf{\Pi}_{\shortparallel}\mathbb{y}_0) = \mathrm{t}_{0,h,\shortparallel}(\mathbf{\Pi}_{\shortparallel}\mathbb{x}_0,\, \mathbb{y}_0), \qquad \forall \mathbb{x}_0, \mathbb{y}_0 \in \mathbb{M}_{0,h,\shortparallel}. \tag{4.131}$$

Simple sufficient conditions on diagonal operators to satisfy the above assumption are provided in the following proposition (see Proposition 3.41 for its counterpart in the continuous setting).

Proposition 4.31. *Suppose that the transmission operators are diagonal in the sense of Definition 4.19. If each diagonal elements of* z_h *and* $\mathrm{t}_{0,h,\|}$ *satisfy*

$$\begin{aligned} &\mathrm{z}_h^{jk} = -\mathrm{z}_h^{kj}, \qquad \forall (j,k) \in \mathbb{J}, \qquad j<k, \\ &\mathrm{t}_{0,h,\|}^{jk} = \mathrm{t}_{0,h,\|}^{kj}, \qquad \forall (j,k) \in \mathbb{J}, \qquad j<k, \end{aligned} \tag{4.132}$$

and for all $(j,k) \in \mathbb{J}$, z_h^{jk} *is symmetric, then Assumption 4.30 is satisfied.*

We are now able to characterize the discrete single-trace space $\mathbb{S}_{h,\|}$ (Definition 4.11) as the kernel of an operator involving the discrete generalized Robin operators $\mathbf{R}_{1,h,\|}^{\pm}$ and the exchange operator $\mathbf{\Pi}_{\|}$. Albeit in a less general setting (without junctions), this result is similar to [33, Lem. 4.3] which is derived for the scalar equation.

Proposition 4.32 (Characterization of the discrete single-trace space). *We have the following characterization of the single-trace space* (4.45)*:*

$$\mathbb{S}_{h,\|} = \operatorname{Ker}\left(\mathbf{R}_{1,h,\|}^{\pm} - \mathbf{\Pi}_{\|}\mathbf{R}_{1,h,\|}^{\mp}\right). \tag{4.133}$$

Proof. First note that, for any $\mathbb{x} \in \mathbb{M}_{\|}$, $\mathbf{R}_{1,\|}^{+}\mathbb{x} = \mathbf{\Pi}_{\|}\mathbf{R}_{1,\|}^{-}\mathbb{x}$ is equivalent to $\mathbf{R}_{1,\|}^{-}\mathbb{x} = \mathbf{\Pi}_{\|}\mathbf{R}_{1,\|}^{+}\mathbb{x}$ since the exchange operator $\mathbf{\Pi}_{\|}$ is an involution according to Proposition 4.26.

($\Rightarrow$) Let $\mathbb{x} \equiv (\mathbb{x}_0, \mathbb{x}_1) \in \mathbb{S}_{\|}$. Using again the characterization of the single trace space given in Proposition 4.28 together with the properties of Assumption 4.30 we obtain successively

$$\begin{cases} [\mathrm{Id} - \mathbf{\Pi}_{\|}]\,\mathbb{x}_0 = 0, \\ [\mathrm{Id} + \mathbf{\Pi}_{\|}]\,\mathbb{x}_1 = 0, \end{cases} \quad \Rightarrow \quad \begin{cases} \langle\!\langle (\mathrm{Id} + \mathbf{\Pi}_{\|})\,\mathbb{x}_1, \mathbb{x}_0^t \rangle\!\rangle_{\|} = 0, & \forall \mathbb{x}_0^t \in \mathbb{M}_{0,h,\|}, \\ \mathrm{z}_h((\mathrm{Id} - \mathbf{\Pi}_{\|})\,\mathbb{x}_0,\, \mathbb{x}_0^t) = 0, & \forall \mathbb{x}_0^t \in \mathbb{M}_{0,h,\|}, \\ \mathrm{t}_{0,h,\|}((\mathrm{Id} - \mathbf{\Pi}_{\|})\,\mathbb{x}_0,\, \mathbb{x}_0^t) = 0, & \forall \mathbb{x}_0^t \in \mathbb{M}_{0,h,\|}, \end{cases} \tag{4.134}$$

so that taking an adequate linear combination we get

$$\langle\!\langle (\mathrm{Id} + \mathbf{\Pi}_{\|})\,\mathbb{x}_1, \mathbb{x}_0^t \rangle\!\rangle_{\|} + \mathrm{z}_h((\mathrm{Id} - \mathbf{\Pi}_{\|})\,\mathbb{x}_0,\, \mathbb{x}_0^t) - \mathrm{it}_{0,h,\|}((\mathrm{Id} - \mathbf{\Pi}_{\|})\,\mathbb{x}_0,\, \mathbb{x}_0^t) = 0, \qquad \forall \mathbb{x}_0^t \in \mathbb{M}_{0,h,\|}. \tag{4.135}$$

This is rewritten as

$$\begin{aligned} &\langle\!\langle \mathbb{x}_1, \mathbb{x}_0^t \rangle\!\rangle_{\|} + \mathrm{z}_h(\mathbb{x}_0,\, \mathbb{x}_0^t) - \mathrm{it}_{0,h,\|}(\mathbb{x}_0,\, \mathbb{x}_0^t) \\ &\qquad = -\langle\!\langle \mathbf{\Pi}_{\|}\mathbb{x}_1, \mathbb{x}_0^t \rangle\!\rangle_{\|} + \mathrm{z}_h(\mathbf{\Pi}_{\|}\mathbb{x}_0,\, \mathbb{x}_0^t) - \mathrm{it}_{0,h,\|}(\mathbf{\Pi}_{\|}\mathbb{x}_0,\, \mathbb{x}_0^t), \qquad \forall \mathbb{x}_0^t \in \mathbb{M}_{0,h,\|}. \end{aligned} \tag{4.136}$$

Hence, using the properties from Assumption 4.30 it follows that

$$\begin{aligned} &\langle\!\langle \mathbb{x}_1, \mathbb{x}_0^t \rangle\!\rangle_{\|} + \mathrm{z}_h(\mathbb{x}_0,\, \mathbb{x}_0^t) - \mathrm{it}_{0,h,\|}(\mathbb{x}_0,\, \mathbb{x}_0^t) \\ &\qquad = -\langle\!\langle \mathbb{x}_1, \mathbf{\Pi}_{\|}\mathbb{x}_0^t \rangle\!\rangle_{\|} - \mathrm{z}_h(\mathbb{x}_0,\, \mathbf{\Pi}_{\|}\mathbb{x}_0^t) - \mathrm{it}_{0,h,\|}(\mathbb{x}_0,\, \mathbf{\Pi}_{\|}\mathbb{x}_0^t), \qquad \forall \mathbb{x}_0^t \in \mathbb{M}_{0,h,\|}. \end{aligned} \tag{4.137}$$

Using Definition 4.21 of the generalized Robin operators $\mathbf{R}_{1,h,\|}^{\pm}$ we obtain

$$\begin{aligned} &\langle\!\langle \mathbb{x}_1, \mathbb{x}_0^t \rangle\!\rangle_{\|} + \mathrm{z}_h(\mathbb{x}_0,\, \mathbb{x}_0^t) - \mathrm{it}_{0,h,\|}(\mathbb{x}_0,\, \mathbb{x}_0^t) \\ &\qquad = \langle\!\langle \mathbf{R}_{1,h,\|}^{-}\mathbb{x}_1, \mathbf{\Pi}_{\|}\mathbb{x}_0^t \rangle\!\rangle_{\|} = \langle\!\langle \mathbf{\Pi}_{\|}\mathbf{R}_{1,h,\|}^{-}\mathbb{x}_1, \mathbb{x}_0^t \rangle\!\rangle_{\|}, \qquad \forall \mathbb{x}_0^t \in \mathbb{M}_{0,h,\|}. \end{aligned} \tag{4.138}$$

Finally, using the self-adjointness of $\mathbf{\Pi}_{\shortparallel}$ (Proposition 3.54), we get

$$\langle\!\langle \mathbb{x}_1, \mathbb{x}_0^t \rangle\!\rangle_{\shortparallel} + \mathrm{z}_h(\mathbb{x}_0, \mathbb{x}_0^t) - \mathrm{it}_{0,h,\shortparallel}(\mathbb{x}_0, \mathbb{x}_0^t) = \langle\!\langle \mathbf{\Pi}_{\shortparallel} \mathbf{R}^-_{1,h,\shortparallel} \mathbb{x}_1, \mathbb{x}_0^t \rangle\!\rangle_{\shortparallel}, \qquad \forall \mathbb{x}_0^t \in \mathbb{M}_{0,h,\shortparallel}, \tag{4.139}$$

which is rewritten as $\mathbf{R}^+_{1,h,\shortparallel} \mathbb{x} = \mathbf{\Pi}_{\shortparallel} \mathbf{R}^-_{1,h,\shortparallel} \mathbb{x}$.

($\Leftarrow$) Reciprocally, let $\mathbb{x} \equiv (\mathbb{x}_0, \mathbb{x}_1) \in \mathbb{M}_{h,\shortparallel}$ such that $\mathbf{R}^+_{1,h,\shortparallel} \mathbb{x} = \mathbf{\Pi}_{\shortparallel} \mathbf{R}^-_{1,h,\shortparallel} \mathbb{x}$. It is easy to see that we can repeat the steps above, in reverse order, up to equation (4.135). By testing respectively by $(\mathrm{Id} - \mathbf{\Pi}_{\shortparallel}) \mathbb{x}_0^t$ and $(\mathrm{Id} + \mathbf{\Pi}_{\shortparallel}) \mathbb{x}_0^t$ in (4.135) we get, for any $\mathbb{x}_0^t \in \mathbb{M}_{0,h,\shortparallel}$,

$$\begin{cases} \langle\!\langle (\mathrm{Id} + \mathbf{\Pi}_{\shortparallel})\, \mathbb{x}_1, (\mathrm{Id} - \mathbf{\Pi}_{\shortparallel}) \mathbb{x}_0^t \rangle\!\rangle_{\shortparallel} + \mathrm{z}_h((\mathrm{Id} - \mathbf{\Pi}_{\shortparallel})\, \mathbb{x}_0,\, (\mathrm{Id} - \mathbf{\Pi}_{\shortparallel}) \mathbb{x}_0^t) \\ \qquad\qquad -\mathrm{it}_{0,h,\shortparallel}((\mathrm{Id} - \mathbf{\Pi}_{\shortparallel})\, \mathbb{x}_0,\, (\mathrm{Id} - \mathbf{\Pi}_{\shortparallel}) \mathbb{x}_0^t) = 0, \\ \langle\!\langle (\mathrm{Id} + \mathbf{\Pi}_{\shortparallel})\, \mathbb{x}_1, (\mathrm{Id} + \mathbf{\Pi}_{\shortparallel}) \mathbb{x}_0^t \rangle\!\rangle_{\shortparallel} + \mathrm{z}_h((\mathrm{Id} - \mathbf{\Pi}_{\shortparallel})\, \mathbb{x}_0,\, (\mathrm{Id} + \mathbf{\Pi}_{\shortparallel}) \mathbb{x}_0^t) \\ \qquad\qquad -\mathrm{it}_{0,h,\shortparallel}((\mathrm{Id} - \mathbf{\Pi}_{\shortparallel})\, \mathbb{x}_0,\, (\mathrm{Id} + \mathbf{\Pi}_{\shortparallel}) \mathbb{x}_0^t) = 0. \end{cases} \tag{4.140}$$

Using the properties of Assumption 4.30 and the self-adjointness of $\mathbf{\Pi}_{\shortparallel}$ from Proposition 4.29 this is rewritten as

$$\begin{cases} \langle\!\langle (\mathrm{Id} - \mathbf{\Pi}_{\shortparallel})\, (\mathrm{Id} + \mathbf{\Pi}_{\shortparallel})\, \mathbb{x}_1, \mathbb{x}_0^t \rangle\!\rangle_{\shortparallel} + \mathrm{z}_h((\mathrm{Id} + \mathbf{\Pi}_{\shortparallel})\, (\mathrm{Id} - \mathbf{\Pi}_{\shortparallel})\, \mathbb{x}_0,\, \mathbb{x}_0^t) - \mathrm{it}_{0,h,\shortparallel}((\mathrm{Id} - \mathbf{\Pi}_{\shortparallel})^2 \mathbb{x}_0,\, \mathbb{x}_0^t) = 0, \\ \langle\!\langle (\mathrm{Id} + \mathbf{\Pi}_{\shortparallel})^2 \mathbb{x}_1, \mathbb{x}_0^t \rangle\!\rangle_{\shortparallel} + \mathrm{z}_h((\mathrm{Id} - \mathbf{\Pi}_{\shortparallel})^2 \mathbb{x}_0,\, \mathbb{x}_0^t) - \mathrm{it}_{0,h,\shortparallel}((\mathrm{Id} + \mathbf{\Pi}_{\shortparallel})(\mathrm{Id} - \mathbf{\Pi}_{\shortparallel}) \mathbb{x}_0,\, \mathbb{x}_0^t) = 0. \end{cases} \tag{4.141}$$

Using the properties of the projectors from Proposition 4.27, we obtain

$$\begin{cases} \mathrm{t}_{0,h,\shortparallel}((\mathrm{Id} - \mathbf{\Pi}_{\shortparallel}) \mathbb{x}_0,\, \mathbb{x}_0^t) = 0, \\ \langle\!\langle (\mathrm{Id} + \mathbf{\Pi}_{\shortparallel}) \mathbb{x}_1, \mathbb{x}_0^t \rangle\!\rangle_{\shortparallel} + \mathrm{z}_h((\mathrm{Id} - \mathbf{\Pi}_{\shortparallel}) \mathbb{x}_0,\, \mathbb{x}_0^t) = 0, \end{cases} \qquad \forall \mathbb{x}_0^t \in \mathbb{M}_{0,h,\shortparallel}, \tag{4.142}$$

hence, using the injectivity property (see (4.83)) of the transmission operator $\mathrm{t}_{0,h,\shortparallel}$, yields (4.126). ■

4.2.2.4 Equivalent interface problem

With the help of the discrete scattering operators $\mathbf{S}_{1,h,\shortparallel}$ and exchange operator $\mathbf{\Pi}_{\shortparallel}$ we are now in a position to recast the discrete approximation of the original problem (4.19) as a problem posed on the skeleton $\tilde{\Sigma}_h$.

Proposition 4.33 (**Equivalent discrete interface problem**). *Let $\mathbb{F}_h \in \mathbb{V}_h(\mathcal{P}_{\Omega,h})$ be the (unique) source lifting such that*

$$\mathfrak{a}(\mathbb{F}_h, v) + \mathrm{z}_h(\boldsymbol{\gamma}_{0,h,\shortparallel} \mathbb{F}_h,\, \boldsymbol{\gamma}_{0,h,\shortparallel} v) - \mathrm{it}_{0,h,\shortparallel}(\boldsymbol{\gamma}_{0,h,\shortparallel} \mathbb{F}_h,\, \boldsymbol{\gamma}_{0,h,\shortparallel} v) = \mathbb{l}(v), \qquad \forall \mathbb{v} \in \mathbb{V}_h(\mathcal{P}_{\Omega,h}), \tag{4.143}$$

and define $\mathbb{f} \equiv (\mathbb{f}_0, \mathbb{f}_1) \in \mathbb{M}_{h,\shortparallel}$ such that

$$\begin{cases} \langle\!\langle \mathbb{f}_1, \mathbb{x}_0^t \rangle\!\rangle_{\shortparallel} = -\mathrm{z}_h(\boldsymbol{\gamma}_{0,h,\shortparallel} \mathbb{F}_h,\, \mathbb{x}_0^t) + \mathrm{it}_{0,h,\shortparallel}(\boldsymbol{\gamma}_{0,h,\shortparallel} \mathbb{F}_h,\, \mathbb{x}_0^t), \qquad \forall \mathbb{x}_0^t \in \mathbb{M}_{0,h,\shortparallel}, \\ \mathbb{f}_0 := \boldsymbol{\gamma}_{0,h,\shortparallel} \mathbb{F}_h. \end{cases} \tag{4.144}$$

Consider the problem

$$\begin{cases} \text{Find } \mathbb{x}_1 \in \mathbb{M}_{1,h,\shortparallel}, \\ (\mathrm{Id} - \mathbf{\Pi}_{\shortparallel} \mathbf{S}_{1,h,\shortparallel}) \mathbb{x}_1 = \mathbf{\Pi}_{\shortparallel} \mathbf{R}^-_{1,h,\shortparallel} \mathbb{f}. \end{cases} \tag{4.145}$$

If $u_h \in \mathrm{V}_h(\Omega)$ is solution of the (discrete) approximation (4.19) *of the model problem* (3.79) *then $\mathbb{x}_1 = \mathbf{R}^+_{1,h,\|}\mathbb{y} \in \mathbb{M}_{1,h,\|}$ where $\mathbb{y} \equiv (\mathrm{y}_0, \mathbb{y}_1) \in \mathbb{M}_{h,\|}$ is defined as*

$$\begin{cases} \mathfrak{a}(u_h, \mathbb{v}_h) - \mathbb{l}(\mathbb{v}_h) = \langle\!\langle \mathbb{y}_1, \boldsymbol{\gamma}_{0,h,\|}\mathbb{v}_h \rangle\!\rangle_{\|}, & \forall \mathbb{v}_h \in \mathbb{V}_h(\mathcal{P}_{\Omega,h}), \\ \boldsymbol{\gamma}_{0,h,\|} u_h = \mathbb{y}_0, \end{cases} \tag{4.146}$$

solves problem (4.145).

Reciprocally, if $\mathbb{x}_1 \in \mathbb{M}_{1,h,\|}$ is solution of the interface problem (4.145) *and if $\mathbb{v} \in \mathbb{V}_h(\mathcal{P}_{\Omega,h})$ is the (unique) solution of*

$$\mathfrak{a}(\mathbb{v}_h, \mathbb{v}_h^t) + \mathrm{z}_h(\boldsymbol{\gamma}_{0,h,\|}\mathbb{v}_h,\, \boldsymbol{\gamma}_{0,h,\|}\mathbb{v}_h^t) - \mathrm{it}_{0,h,\|}(\boldsymbol{\gamma}_{0,h,\|}\mathbb{v}_h,\, \boldsymbol{\gamma}_{0,h,\|}\mathbb{v}_h^t) = \langle\!\langle \mathbb{x}_1, \boldsymbol{\gamma}_{0,h,\|}\mathbb{v}_h^t \rangle\!\rangle_{\|}, \quad \forall \mathbb{v}_h^t \in \mathbb{V}_h(\mathcal{P}_{\Omega,h}), \tag{4.147}$$

then $u_h \in \mathbb{V}_h(\mathcal{P}_{\Omega,h})$ defined as $u_h := \mathbb{v}_h + \mathbb{F}_h$ is solution of the (discrete) approximation (4.19) *of the model problem* (3.79).

Proof. Let $\mathbb{F}_h$ and $\mathbb{f} \equiv (\mathbb{f}_0, \mathbb{f}_1) \in \mathbb{M}_{h,\|}$ satisfy (4.143) (which are uniquely defined by Proposition 4.23). Note that by construction, it holds that

$$\begin{aligned} & + \Big(\langle\!\langle \mathbb{f}_1, \mathbb{x}_0^t \rangle\!\rangle_{\|} + \mathrm{z}_h(\mathbb{f}_0,\, \mathbb{x}_0^t) \Big) - \mathrm{it}_{0,h,\|}(\mathbb{f}_0,\, \mathbb{x}_0^t) = 0, \qquad \forall \mathbb{x}_0^t \in \mathbb{M}_{0,h,\|}, \\ \Leftrightarrow \quad & \mathbf{R}^+_{1,h,\|}\mathbb{f} = 0, \end{aligned} \tag{4.148}$$

and $\mathbb{F}_h \in \mathbb{V}_h(\mathcal{P}_{\Omega,h})$ is such that

$$\begin{cases} \mathfrak{a}(\mathbb{F}_h, \mathbb{v}_h) - \mathbb{l}(\mathbb{v}_h) = \langle\!\langle \mathbb{f}_1, \boldsymbol{\gamma}_{0,h,\|}\mathbb{v}_h \rangle\!\rangle_{\|}, & \forall \mathbb{v}_h \in \mathbb{V}_h(\mathcal{P}_{\Omega,h}), \\ \boldsymbol{\gamma}_{0,h,\|}\mathbb{F}_h = \mathbb{f}_0. \end{cases} \tag{4.149}$$

($\Rightarrow$) If $u_h \in \mathrm{V}_h(\Omega)$ is solution of the (discrete) approximation (4.19) of the model problem (3.79), then by Proposition 4.16, we know that $\mathbb{y} \equiv (\mathrm{y}_0, \mathbb{y}_1)$ defined in (4.146) above belongs to $\mathbb{S}_{h,\|}$. Besides, from both (4.146) and (4.149), we get

$$\begin{cases} \mathfrak{a}(u_h - \mathbb{F}_h, \mathbb{v}_h) = \langle\!\langle \mathbb{y}_1 - \mathbb{f}_1, \boldsymbol{\gamma}_{0,h,\|}\mathbb{v}_h \rangle\!\rangle_{\|}, & \forall \mathbb{v}_h \in \mathbb{V}_h(\mathcal{P}_{\Omega,h}), \\ \boldsymbol{\gamma}_{0,h,\|}(u_h - \mathbb{F}_h) = \mathbb{y}_0 - \mathbb{f}_0, \end{cases} \tag{4.150}$$

so that by Definition 4.10 of $\mathbb{C}_{h,\|}$, we have $\mathbb{y} - \mathbb{f} \in \mathbb{C}_{h,\|}$. From the characterizations of both the Cauchy trace space stated in Proposition 4.25 and the single trace space stated in Proposition 4.32 we have

$$\begin{cases} \mathbb{y} - \mathbb{f} \in \mathbb{C}_{h,\|}, \\ \mathbb{y} \in \mathbb{S}_{h,\|}, \end{cases} \quad \Leftrightarrow \quad \begin{cases} \mathbf{R}^-_{1,h,\|}(\mathbb{y} - \mathbb{f}) = \mathbf{S}_{1,h,\|}\mathbf{R}^+_{1,h,\|}(\mathbb{y} - \mathbb{f}), \\ \mathbf{R}^+_{1,h,\|}\mathbb{y} = \boldsymbol{\Pi}_{\|}\mathbf{R}^-_{1,h,\|}\mathbb{y}. \end{cases} \tag{4.151}$$

Hence using $\mathbf{R}^+_{1,h,\|}\mathbb{f} = 0$ we deduce

$$\begin{cases} \mathbf{R}^-_{1,h,\|}\mathbb{y} = \mathbf{S}_{1,h,\|}\mathbf{R}^+_{1,h,\|}\mathbb{y} + \mathbf{R}^-_{1,h,\|}\mathbb{f}, \\ \mathbf{R}^+_{1,h,\|}\mathbb{y} = \boldsymbol{\Pi}_{\|}\mathbf{R}^-_{1,h,\|}\mathbb{y}. \end{cases} \tag{4.152}$$

Eliminating $\mathbf{R}^-_{1,h,\|}\mathbb{y}$ it is then immediate that

$$\mathbf{R}^+_{1,h,\|}\mathbb{y} = \boldsymbol{\Pi}_{\|}\mathbf{S}_{1,h,\|}\mathbf{R}^+_{1,h,\|}\mathbb{y} + \boldsymbol{\Pi}_{\|}\mathbf{R}^-_{1,h,\|}\mathbb{f}. \tag{4.153}$$

hence the quantity $\mathbb{x}_1 := \mathbf{R}^+_{1,h,\|}\mathbb{y}$ satisfies the interface problem (4.145).

($\Leftarrow$) Reciprocally, let $\mathbb{x}_1 \in \mathbb{M}_{1,h,\|}$ be solution of the interface problem (4.145) and let $\mathbb{v}_h \in \mathbb{V}_h(\mathcal{P}_{\Omega,h})$ be the unique solution (by Proposition 4.23) to (4.147). Then, define $\mathbb{z} \equiv (\mathbb{z}_0, \mathbb{z}_1) \in \mathbb{M}_{h,\|}$ such that

$$\begin{cases} \mathbb{a}(\mathbb{v}_h, \mathbb{v}_h^t) = \langle\!\langle \mathbb{z}_1, \boldsymbol{\gamma}_{0,h,\|}\mathbb{v}_h^t \rangle\!\rangle_\|, & \forall \mathbb{v}_h^t \in \mathbb{V}_h(\mathcal{P}_{\Omega,h}), \\ \boldsymbol{\gamma}_{0,h,\|}\mathbb{v}_h = \mathbb{z}_0, \end{cases} \tag{4.154}$$

so that using (4.149), we get

$$\begin{cases} \mathbb{a}(\mathbb{v}_h + \mathbb{F}_h, \mathbb{v}_h^t) - \mathbb{l}(\mathbb{v}_h) = \langle\!\langle \mathbb{z}_1 + \mathbb{f}_1, \boldsymbol{\gamma}_{0,h,\|}\mathbb{v}_h \rangle\!\rangle_\|, & \forall \mathbb{v}_h^t \in \mathbb{V}_h(\mathcal{P}_{\Omega,h}), \\ \boldsymbol{\gamma}_{0,h,\|}(\mathbb{v}_h + \mathbb{F}_h) = \mathbb{z}_0 + \mathbb{f}_0. \end{cases} \tag{4.155}$$

If we set

$$\begin{aligned} u_h &:= \mathbb{v}_h + \mathbb{F}_h, \\ \mathbb{y} \equiv (\mathbb{y}_0, \mathbb{y}_1) &:= \mathbb{z} + \mathbb{f} \equiv (\mathbb{z}_0 + \mathbb{f}_0, \mathbb{z}_1 + \mathbb{f}_1), \end{aligned} \tag{4.156}$$

we obtain

$$\begin{cases} \mathbb{a}(u_h, \mathbb{v}^t) - \mathbb{l}(\mathbb{v}^t) = \langle\!\langle \mathbb{y}_1, \boldsymbol{\gamma}_{0,h,\|}\mathbb{v}^t \rangle\!\rangle_\|, & \forall \mathbb{v}^t \in \mathbb{V}_h(\mathcal{P}_{\Omega,h}), \\ \boldsymbol{\gamma}_{0,h,\|}u_h = \mathbb{y}_0. \end{cases} \tag{4.157}$$

Using Proposition 4.16 all that remains to prove is that $\mathbb{y} \in \mathbb{S}_{h,\|}$. We have, combining (4.147) and (4.154)

$$\langle\!\langle \mathbb{x}_1, \mathbb{x}_0^t \rangle\!\rangle_\| = + \left[\langle\!\langle \mathbb{z}_1, \mathbb{x}_0^t \rangle\!\rangle_\| + \mathrm{z}_h(\mathbb{z}_0, \mathbb{x}_0^t) \right] - \mathrm{it}_{0,h,\|}(\mathbb{z}_0, \mathbb{x}_0^t), \qquad \forall \mathbb{x}_0^t \in \mathbb{M}_{0,h,\|}, \tag{4.158}$$

so that $\mathbb{x}_1 = \mathbf{R}^+_{1,h,\|}\mathbb{z}$ by Definition 4.21 of the generalized Robin operator. We can rewrite (3.200) as

$$\begin{aligned} & (\mathrm{Id} - \boldsymbol{\Pi}_\| \mathbf{S}_{1,h,\|})\, \mathbb{x}_1 = \boldsymbol{\Pi}_\| \mathbf{R}^-_{1,h,\|} \mathbb{f}, \\ \Leftrightarrow \quad & (\mathrm{Id} - \boldsymbol{\Pi}_\| \mathbf{S}_{1,h,\|})\, \mathbf{R}^+_{1,h,\|} \mathbb{z} = \boldsymbol{\Pi}_\| \mathbf{R}^-_{1,h,\|} \mathbb{f}. \end{aligned} \tag{4.159}$$

Using Proposition 4.25 we get

$$\mathbf{R}^+_{1,h,\|}\mathbb{z} - \boldsymbol{\Pi}_\| \mathbf{R}^-_{1,h,\|}\mathbb{z} = \boldsymbol{\Pi}_\| \mathbf{R}^-_{1,h,\|}\mathbb{f}. \tag{4.160}$$

Hence using $\mathbf{R}^+_{1,h,\|}\mathbb{f} = 0$ together with the definition of $\mathbb{y}$ we obtain that

$$\mathbf{R}^+_{1,h,\|}\mathbb{y} = \boldsymbol{\Pi}_\| \mathbf{R}^-_{1,h,\|}\mathbb{y}. \tag{4.161}$$

Proposition 4.32 then gives $\mathbb{y} \in \mathbb{S}_{h,\|}$. ■

4.3 Iterative discrete domain decomposition methods

4.3.1 Iterative algorithm

Let $\mathbb{F}_h$ be the solution of (4.143) with $\mathbb{f} \equiv (\mathbb{f}_0, \mathbb{f}_1) \in \mathbb{M}_{h,\|}$ defined in (4.144) and set

$$\mathbb{b}_1 := \boldsymbol{\Pi}_\| \mathbf{R}^-_{1,h,\|}\mathbb{f}. \tag{4.162}$$

In this section, we want to devise (and study the convergence of) an algorithm to solve

$$\begin{cases} \text{Find } \mathbb{x}_1 \in \mathbb{M}_{1,h,\|} \text{ such that,} \\ (\mathrm{Id} - \boldsymbol{\Pi}_\| \mathbf{S}_{1,h,\|})\, \mathbb{x}_1 = \mathbb{b}_1. \end{cases} \tag{4.163}$$

Having found such a $\mathbb{x}_1$ solution of (4.163), a global volume solution u_h can be computed by solving

$$\begin{cases} \text{Find } \mathbb{v}_h \in \mathbb{V}_h(\mathcal{P}_{\Omega,h}) \text{ such that,} \\ a(\mathbb{v}_h, \mathbb{v}_h^t) + \mathrm{z}_h(\boldsymbol{\gamma}_{0,h,\parallel}\mathbb{v}_h, \boldsymbol{\gamma}_{0,h,\parallel}\mathbb{v}_h^t) \\ \qquad -\mathrm{it}_{0,h,\parallel}(\boldsymbol{\gamma}_{0,h,\parallel}\mathbb{v}_h, \boldsymbol{\gamma}_{0,h,\parallel}\mathbb{v}_h^t) = \langle\!\langle \mathbb{x}_1, \boldsymbol{\gamma}_{0,h,\parallel}\mathbb{v}_h^t \rangle\!\rangle_{\parallel}, \qquad \forall \mathbb{v}_h^t \in \mathbb{V}_h(\mathcal{P}_{\Omega,h}). \end{cases} \tag{4.164}$$

Then the global solution of the discrete model problem (4.19) is $u_h := \mathbb{v}_h + \mathbb{F}_h$.

Relaxed Jacobi algorithm We consider again here the (relaxed) Jacobi algorithm to solve the interface problem (4.163) on the skeleton. Let $\mathbb{x}_1^0 \in \mathbb{M}_{1,h,\parallel}$ and a relaxation parameter $0 < r \leq 1$ be given, a sequence $(\mathbb{x}_1^n)_{n\in\mathbb{N}}$ in $\mathbb{M}_{1,h,\parallel}$ is constructed using the (relaxed) Jacobi algorithm as follows

$$\mathbb{x}_1^{n+1} = [(1-r)\mathrm{Id} + r\boldsymbol{\Pi}_{\parallel}\mathbf{S}_{1,h,\parallel}]\,\mathbb{x}_1^n + r\,\mathbb{b}_1, \qquad n \in \mathbb{N}. \tag{4.165}$$

Constructing this sequence of traces also constructs a sequence of broken solutions $(\mathbb{v}_h^n)_{n\in\mathbb{N}}$ in $\mathbb{V}_h(\mathcal{P}_{\Omega,h})$ when the action of $\mathbf{S}_{1,h,\parallel}$ is computed. For each $n \in \mathbb{N}$ the broken solution $\mathbb{v}_h^n$ satisfy

$$a(\mathbb{v}_h^n, \mathbb{v}_h^t) + \mathrm{z}_h(\boldsymbol{\gamma}_{0,h,\parallel}\mathbb{v}_h^n, \boldsymbol{\gamma}_{0,h,\parallel}\mathbb{v}_h^t) - \mathrm{it}_{0,h,\parallel}(\boldsymbol{\gamma}_{0,h,\parallel}\mathbb{v}_h^n, \boldsymbol{\gamma}_{0,h,\parallel}\mathbb{v}_h^t) = \langle\!\langle \mathbb{x}_1^n, \boldsymbol{\gamma}_{0,h,\parallel}\mathbb{v}_h^t \rangle\!\rangle_{\parallel}, \quad \forall \mathbb{v}_h^t \in \mathbb{V}_h(\mathcal{P}_{\Omega,h}). \tag{4.166}$$

The true solution u_h of the discrete model problem (4.19) is then (hopefully, if convergence occurs) the limit as $n \to \infty$ of the broken solutions $(\mathbb{u}_h^n := \mathbb{v}_h^n + \mathbb{F}_h)_{n\in\mathbb{N}}$ in $\mathbb{V}_h(\mathcal{P}_{\Omega,h})$.

4.3.2 Discrete convergence analysis

We now turn to the convergence analysis of the previously described iterative method. In this discrete setting there are two independent convergence processes. We study here the convergence with respect to increasing n, the iteration number, of the iterative discrete solution $\mathbb{u}_h^n \in \mathbb{V}_h(\mathcal{P}_{\Omega,h})$ towards the discrete solution $u_h \in \mathrm{V}_h(\Omega)$ of (4.19). The convergence with respect to decreasing h, the discretization parameter, of the discrete solution $u_h \in \mathrm{V}_h(\Omega)$ of (4.19) towards the continuous solution $u \in \mathrm{U}_\Gamma(\mathrm{D};\Omega)$ of (3.79), although a legitimate question, is not addressed here. However, we shall study the behaviour of the convergence rate as h goes to 0.

The discrete convergence analysis of the relaxed Jacobi algorithm follows closely the one from the continuous setting in Section 3.3.2. It is clear that the new interface problem (4.163) takes the form of the abstract problem (3.230). To prove the geometric convergence of the above fixed point algorithm, we simply need to check that the assumptions of Proposition 3.57 are satisfied in our particular case where $V = \mathbb{M}_{1,h,\parallel}$ and $A = \boldsymbol{\Pi}_{1,\times}\mathbf{S}_{1,h,\parallel}$.

We first state the contraction property of the discrete scattering operator, analogue of Proposition 3.53. A similar result in a slightly different setting (with junctions) but for the scalar equation only can be found in [33, Lem. 5.1].

Proposition 4.34 (**Contraction property of the scattering operator**). *The scattering operator $\mathbf{S}_{1,h,\parallel}$ is a contraction of $\mathbb{M}_{1,h,\parallel}$, for our particular choices of norm* (4.95)*,*

$$\|\mathbf{S}_{1,h,\parallel}\mathbb{x}_1\|_{\mathrm{t}_{1,h,\parallel}} \leq \|\mathbb{x}_1\|_{\mathrm{t}_{1,h,\parallel}}, \qquad \forall \mathbb{x}_1 \in \mathbb{M}_{1,h,\parallel}. \tag{4.167}$$

Proof. Let $\mathbb{x}_1 \in \mathbb{M}_{1,h,\parallel}$, we have by definition of $\mathbf{T}_{0,\parallel}$ (see (4.92)) and $\mathbf{S}_{1,h,\parallel}$ (see (4.22))

$$\mathbf{S}_{1,h,\parallel}\mathbb{x}_1 = -\mathbb{x}_1 - 2\mathrm{i}\mathbf{T}_{0,h,\parallel}\boldsymbol{\gamma}_{0,h,\parallel}\mathbb{u}, \tag{4.168}$$

where $\mathfrak{u} \in \mathbb{V}_h(\mathcal{P}_{\Omega,h})$ is such that

$$\mathfrak{c}(\mathfrak{u}, \mathfrak{v}_h) + \mathrm{z}_h(\boldsymbol{\gamma}_{0,h,\|}\mathfrak{u}, \boldsymbol{\gamma}_{0,h,\|}\mathfrak{v}_h) - \mathrm{i}\mathrm{t}_{0,h,\|}(\boldsymbol{\gamma}_{0,h,\|}\mathfrak{u}, \boldsymbol{\gamma}_{0,h,\|}\mathfrak{v}_h) = \langle\!\langle \mathfrak{x}_1, \boldsymbol{\gamma}_{0,h,\|}\mathfrak{v}_h \rangle\!\rangle_{\|}, \qquad \forall \mathfrak{v}_h \in \mathbb{V}_h(\mathcal{P}_{\Omega,h}). \tag{4.169}$$

We have, from the definitions of the norm (4.95) and of $\mathbf{T}_{1,\|}$, see (4.94),

$$\begin{aligned}
\|\mathbf{S}_{1,h,\|}\mathfrak{x}_1\|^2_{\mathrm{t}_{1,h,\|}} &= \langle\!\langle -\mathfrak{x}_1 - 2\mathrm{i}\mathbf{T}_{0,h,\|}\boldsymbol{\gamma}_{0,h,\|}\mathfrak{u},\, \mathbf{T}_{1,\|}\left(\overline{-\mathfrak{x}_1 - 2\mathrm{i}\mathbf{T}_{0,h,\|}\boldsymbol{\gamma}_{0,h,\|}\mathfrak{u}}\right)\rangle\!\rangle_{\|} \\
&= \langle\!\langle \mathfrak{x}_1, \mathbf{T}_{1,\|}\overline{\mathfrak{x}_1}\rangle\!\rangle_{\|} + 4\mathrm{t}_{0,h,\|}(\boldsymbol{\gamma}_{0,h,\|}\mathfrak{u},\, \overline{\boldsymbol{\gamma}_{0,h,\|}\mathfrak{u}}) \\
&\quad + 2\mathrm{i}\langle\!\langle \mathbf{T}_{0,\|}\boldsymbol{\gamma}_{0,h,\|}\mathfrak{u}, \overline{\mathbf{T}_{1,\|}\mathfrak{x}_1}\rangle\!\rangle_{\|} - 2\mathrm{i}\langle\!\langle \mathfrak{x}_1, \overline{\boldsymbol{\gamma}_{0,h,\|}\mathfrak{u}}\rangle\!\rangle_{\|}, \\
&= \langle\!\langle \mathfrak{x}_1, \mathbf{T}_{1,\|}\overline{\mathfrak{x}_1}\rangle\!\rangle_{\|} + 4\|\boldsymbol{\gamma}_{0,h,\|}\mathfrak{u}\|^2_{\mathrm{t}_{0,h,\|}} + 2\mathrm{i}\langle\!\langle \overline{\mathfrak{x}_1}, \boldsymbol{\gamma}_{0,h,\|}\mathfrak{u}\rangle\!\rangle_{\|} - 2\mathrm{i}\langle\!\langle \mathfrak{x}_1, \overline{\boldsymbol{\gamma}_{0,h,\|}\mathfrak{u}}\rangle\!\rangle_{\|}, \\
&= \|\mathfrak{x}_1\|^2_{\mathrm{t}_{1,h,\|}} + 4\|\boldsymbol{\gamma}_{0,h,\|}\mathfrak{u}\|^2_{\mathrm{t}_{0,h,\|}} + 4\Im\langle\!\langle \mathfrak{x}_1, \overline{\boldsymbol{\gamma}_{0,h,\|}\mathfrak{u}}\rangle\!\rangle_{\|}.
\end{aligned} \tag{4.170}$$

Besides, by definition of $\mathfrak{u}$ (testing by $\mathfrak{u}$ in (4.169)), and the bilinear form $\mathfrak{c}$ (see (3.98)) we have

$$\begin{aligned}
\Im\langle\!\langle \mathfrak{x}_1, \overline{\boldsymbol{\gamma}_{0,h,\|}\mathfrak{u}}\rangle\!\rangle_{\|} = \kappa_0{}^{-1}(\Im(\mathsf{a})\,\mathrm{D}\mathfrak{u}, \mathrm{D}\overline{\mathfrak{u}})_{L^2(\Omega)^{m_1}} - \kappa_0\,(\Im(\mathsf{n})\mathfrak{u}, \overline{\mathfrak{u}})_{L^2(\Omega)^{m_0}} \\
- \|\gamma_{0,\Gamma}\,\mathfrak{u}\|^2_{L^2(\Gamma)^{m_0}} - \|\boldsymbol{\gamma}_{0,h,\|}\mathfrak{u}\|^2_{\mathrm{t}_{0,h,\|}},
\end{aligned} \tag{4.171}$$

which yields since the imaginary parts of the coefficients a and n are respectively supposed negative and positive (see (3.78)),

$$\begin{aligned}
\|\mathbf{S}_{1,h,\|}\mathfrak{x}_1\|^2_{\mathrm{t}_{1,h,\|}} - \|\mathfrak{x}_1\|^2_{\mathrm{t}_{1,h,\|}} = \kappa_0{}^{-1}(\Im(\mathsf{a})\,\mathrm{D}\mathfrak{u}, \mathrm{D}\overline{\mathfrak{u}})_{L^2(\Omega)^{m_1}} \\
- \kappa_0\,(\Im(\mathsf{n})\mathfrak{u}, \overline{\mathfrak{u}})_{L^2(\Omega)^{m_0}} - \|\gamma_{0,\Gamma}\,\mathfrak{u}\|^2_{L^2(\Gamma)^{m_0}} \leq 0.
\end{aligned} \tag{4.172}$$

■

Besides, we readily check that the exchange operator $\boldsymbol{\Pi}_{\|}$ is an isometry of $\mathbb{M}_{1,h,\|}$, see Proposition 3.54 for the corresponding result in the continuous setting. A similar result valid in the acoustic setting only (but with junctions) can be found in [33, Lem. 4.3].

Proposition 4.35. *The exchange operator $\boldsymbol{\Pi}_{\|}$ is an isometry of $\mathbb{M}_{1,h,\|}$, for our particular choice of norm* (4.95)*,*

$$\|\boldsymbol{\Pi}_{\|}\mathfrak{x}_1\|_{\mathrm{t}_{1,h,\|}} = \|\mathfrak{x}_1\|_{\mathrm{t}_{1,h,\|}}, \qquad \forall \mathfrak{x}_1 \in \mathbb{M}_{1,h,\|}. \tag{4.173}$$

Proof. Using Assumption 4.30 we have

$$\mathbf{T}_{0,h,\|}\boldsymbol{\Pi}_{\|} = \boldsymbol{\Pi}_{\|}\mathbf{T}_{0,h,\|}, \tag{4.174}$$

so that, since $\mathbf{T}_{1,h,\|} = \mathbf{T}_{0,h,\|}^{-1}$,

$$\mathbf{T}_{1,h,\|}\boldsymbol{\Pi}_{\|} = \boldsymbol{\Pi}_{\|}\mathbf{T}_{1,h,\|}. \tag{4.175}$$

Using the self-adjointness of $\boldsymbol{\Pi}_{\|}$ from Proposition 4.35 and the involution property of $\boldsymbol{\Pi}_{\|}$ from Proposition 4.26, we obtain, for all $\mathfrak{x}_1 \in \mathbb{M}_{1,h,\|}$,

$$\|\boldsymbol{\Pi}_{\|}\mathfrak{x}_1\|^2_{\mathrm{t}_{1,h,\|}} = \langle\!\langle \boldsymbol{\Pi}_{\|}\mathfrak{x}_1, \mathbf{T}_{1,h,\|}\overline{\boldsymbol{\Pi}_{\|}\mathfrak{x}_1}\rangle\!\rangle_{\|} = \langle\!\langle \boldsymbol{\Pi}_{\|}\mathfrak{x}_1, \boldsymbol{\Pi}_{\|}\mathbf{T}_{1,h,\|}\overline{\mathfrak{x}_1}\rangle\!\rangle_{\|} = \langle\!\langle \mathfrak{x}_1, \mathbf{T}_{1,h,\|}\overline{\mathfrak{x}_1}\rangle\!\rangle_{\|} = \|\mathfrak{x}_1\|^2_{\mathrm{t}_{1,h,\|}}. \tag{4.176}$$

■

Combining both Proposition 4.34 and Proposition 4.35 we get the contraction property we were looking for. Again, a similar result valid in the acoustic setting only (but with junctions) can be found in [33, Lem. 5.1].

Corollary 4.36 (**Contraction property**). *We have*

$$\left\|\boldsymbol{\Pi}_{\shortparallel}\mathbf{S}_{1,h,\shortparallel}\mathbb{x}_1\right\|_{\mathbb{t}_{1,h,\shortparallel}} \leq \left\|\mathbb{x}_1\right\|_{\mathbb{t}_{1,h,\shortparallel}}, \qquad \forall \mathbb{x}_1 \in \mathbb{M}_{1,h,\shortparallel}. \tag{4.177}$$

The second requirement of Proposition 3.57 to obtain geometric convergence is verified next. Similar results, valid in the acoustic setting only, can be found in [30, Th. 3] and in [33, Prop. 5.2], for a more general geometric configuration.

Proposition 4.37. *The operator* $\mathrm{Id} - \boldsymbol{\Pi}_{\shortparallel}\mathbf{S}_{1,h,\shortparallel}$ *is an isomorphism on* $\mathbb{M}_{1,h,\shortparallel}$.

Proof. Since $\mathbb{M}_{1,h,\shortparallel}$ is finite dimensional, we only need to prove injectivity. Let $\mathbb{x}_1 \in \mathbb{M}_{1,h,\shortparallel}$ be such that

$$(\mathrm{Id} - \boldsymbol{\Pi}_{\shortparallel}\mathbf{S}_{1,h,\shortparallel})\,\mathbb{x}_1 = 0. \tag{4.178}$$

Define (which exists from Proposition 4.23)

$$\begin{cases} \mathbb{u} \in \mathbb{V}_h(\mathcal{P}_{\Omega,h}) \text{ such that} \\ \mathbb{a}(\mathbb{u},\mathbb{v}) + \mathrm{z}_h(\boldsymbol{\gamma}_{0,h,\shortparallel}\mathbb{u},\, \boldsymbol{\gamma}_{0,h,\shortparallel}\mathbb{v}) - \mathrm{it}_{0,h,\shortparallel}(\boldsymbol{\gamma}_{0,h,\shortparallel}\mathbb{u},\, \boldsymbol{\gamma}_{0,h,\shortparallel}\mathbb{v}) = \left\langle\!\left\langle \mathbb{x}_1, \boldsymbol{\gamma}_{0,h,\shortparallel}\mathbb{v}\right\rangle\!\right\rangle_{\shortparallel}, \qquad \forall \mathbb{v} \in \mathbb{V}_h(\mathcal{P}_{\Omega,h}). \end{cases} \tag{4.179}$$

Then let $\mathbb{y} \equiv (\mathbb{y}_0, \mathbb{y}_1) \in \mathbb{M}_{h,\shortparallel}$ such that

$$\begin{cases} \left\langle\!\left\langle \mathbb{y}_1, \mathbb{x}_0^t\right\rangle\!\right\rangle_{\shortparallel} = -\mathrm{z}_h(\boldsymbol{\gamma}_{0,h,\shortparallel}\mathbb{u},\, \mathbb{x}_0^t) + \mathrm{it}_{0,h,\shortparallel}(\boldsymbol{\gamma}_{0,h,\shortparallel}\mathbb{u},\, \mathbb{x}_0^t) + \left\langle\!\left\langle \mathbb{x}_1, \mathbb{x}_0^t\right\rangle\!\right\rangle_{\shortparallel}, & \forall \mathbb{x}_0^t \in \mathbb{M}_{0,h,\shortparallel}, \\ \mathbb{y}_0 = \boldsymbol{\gamma}_{0,h,\shortparallel}\mathbb{u}. \end{cases} \tag{4.180}$$

By construction

$$\begin{cases} \mathbb{a}(\mathbb{u},\mathbb{v}) = \left\langle\!\left\langle \mathbb{y}_1, \boldsymbol{\gamma}_{0,h,\shortparallel}\mathbb{v}\right\rangle\!\right\rangle_{\shortparallel}, & \forall \mathbb{v} \in \mathbb{V}_h(\mathcal{P}_{\Omega,h}), \\ \boldsymbol{\gamma}_{0,h,\shortparallel}\mathbb{u} = \mathbb{y}_0, \end{cases} \tag{4.181}$$

so that $\mathbb{y} \in \mathbb{C}_{h,\shortparallel}$ and Proposition 4.25 yields

$$\left(\mathbf{R}^-_{1,h,\shortparallel} - \mathbf{S}_{1,h,\shortparallel}\mathbf{R}^+_{1,h,\shortparallel}\right)\mathbb{y} = 0. \tag{4.182}$$

Besides,

$$\left\langle\!\left\langle \mathbb{y}_1, \mathbb{x}_0^t\right\rangle\!\right\rangle_{\shortparallel} + \mathrm{z}_h(\mathbb{y}_0,\, \mathbb{x}_0^t) - \mathrm{it}_{0,h,\shortparallel}(\mathbb{y}_0,\, \mathbb{x}_0^t) = \left\langle\!\left\langle \mathbb{x}_1, \mathbb{x}_0^t\right\rangle\!\right\rangle_{\shortparallel}, \qquad \forall \mathbb{x}_0^t \in \mathbb{M}_{0,h,\shortparallel}, \tag{4.183}$$

so that by Definition 4.21 of the generalized Robin operators

$$\mathbf{R}^+_{1,h,\shortparallel}\mathbb{y} = \mathbb{x}_1. \tag{4.184}$$

Now (4.178) is rewritten as

$$\left(\mathbf{R}^+_{1,h,\shortparallel} - \boldsymbol{\Pi}_{\shortparallel}\mathbf{R}^-_{1,h,\shortparallel}\right)\mathbb{y} = 0, \tag{4.185}$$

and Proposition 4.32 yields $\mathbb{y} \in \mathbb{S}_{h,\shortparallel}$. Finally $\mathbb{y} \in \mathbb{C}_{h,\shortparallel} \cap \mathbb{S}_{h,\shortparallel}$, hence from Proposition 4.17, $\mathbb{y} = 0$ and $\mathbb{x}_1 = \mathbf{R}^+_{1,h,\shortparallel}\mathbb{y} = 0$. ∎

We are now ready to state our discrete convergence result, analogue of Theorem 3.63. Similar results, valid in the acoustic setting only, can be found in [30, Th. 2] and in [33, Th. 6.1], for a more general geometric configuration.

Theorem 4.38 (**Geometric convergence of the discrete relaxed Jacobi algorithm**). *The sequence of broken solutions* $(\mathfrak{u}_h^n)_{n\in\mathbb{N}}$ *computed according to* (4.166)*, converges* geometrically *to* u_h *the solution of the discrete approximation of the model problem* (4.19)*. Specifically, there exist* $C > 0$ *and* $0 < \tau < 1$*, which might depend on* h*, such that*

$$\|\mathfrak{u}_h^n - u_h\|_{\mathbb{U}_\Gamma(\mathrm{D};\mathcal{P}_{\Omega,h})} \leq C\,\tau^n, \qquad \forall n \in \mathbb{N}. \tag{4.186}$$

Proof. Arguing as in the proof of Theorem 3.56, this is direct application of the abstract result in Proposition 3.57. The assumptions of the latter result are systematically checked in Proposition 4.36 and Proposition 4.37. ■

Of course this theorem is less important than its counterpart in the continuous setting. Indeed, if one uses an iterative algorithm applied to a finite dimensional system of equations, one will always get geometric convergence (or no convergence at all). This is why the forthcoming discrete stability analysis, which addresses the question of the behaviour of the geometric convergence rate as h goes to 0, is particularly relevant.

4.3.3 Discrete stability

We have seen that in the discrete setting, the relaxed Jacobi algorithm is (geometrically) convergent provided that the transmission operator defines a scalar product on the multi-trace space. The important question of discrete stability remains, namely can we get h-uniform (geometric) convergence.

Explicit bounds To provide answers to this question we need explicit bounds with respect to the discretization parameter h on the convergence rate.

A careful inspection of the proof of Theorem 3.63 (or of the abstract result in Proposition 3.57) will reveal that the main ingredient we need is an estimate on the continuity constant of the inverse of the operator $\mathrm{Id} - \boldsymbol{\Pi}_{\shortparallel}\mathbf{S}_{1,h,\shortparallel}$. From Proposition 4.37 we already know that the following quantity is strictly positive,

$$\zeta_{h,\shortparallel} := \inf_{\substack{\mathbb{x}_1 \in \mathbb{M}_{1,h,\shortparallel} \\ \mathbb{x}_1 \neq 0}} \frac{\|(\mathrm{Id} - \boldsymbol{\Pi}_{\shortparallel}\mathbf{S}_{1,h,\shortparallel})\mathbb{x}_1\|_{\mathbb{M}_{1,h,\shortparallel}}}{\|\mathbb{x}_1\|_{\mathbb{M}_{1,h,\shortparallel}}} > 0. \tag{4.187}$$

The estimate is provided by the following proposition, similar to [33, Prop. 7.1 and 7.3].

Proposition 4.39 (**Explicit discrete estimate**). *We have*

$$\begin{aligned}\zeta_{h,\shortparallel} \geq 2\frac{\beta_{\mathrm{t}_{0,h,\shortparallel}}}{|||\mathrm{t}_{0,h,\shortparallel}|||}\,(1 + |||\mathrm{z}_h||| + |||\mathrm{t}_{0,h,\shortparallel}|||)^{-1}\Big(1 + (1 + |||\mathrm{z}_h|||)\;\beta_{\mathrm{t}_{0,h,\shortparallel}}^{-1/2}\Big)^{-1} \\ \Big(1 + |||a|||^2\;|||\mathbb{E}_{h,\shortparallel}|||^2\Big)^{-1/2}\Big[\Big(1 + \alpha_{a,h}^{-1}\;|||a|||\Big)|||\mathbb{E}_{h,\shortparallel}||| + \alpha_{a,h}^{-1}\Big]^{-1} > 0.\end{aligned} \tag{4.188}$$

Proof. Let $\mathbb{b}_1 \in \mathbb{M}_{1,h,\shortparallel}$. We need to provide an explicit construction of $\mathbb{a}_1 \in \mathbb{M}_{1,h,\shortparallel}$ such that

$$(\mathrm{Id} - \boldsymbol{\Pi}_{\shortparallel}\mathbf{S}_{1,h,\shortparallel})\,\mathbb{a}_1 = \mathbb{b}_1, \tag{4.189}$$

in order to estimate its norm. The construction below follows closely the steps taken in the proof of the surjectivity of the operator $\mathrm{Id} - \boldsymbol{\Pi}_{\shortparallel}\mathbf{S}_{1,\shortparallel}$ that was conducted in the continuous setting and summed up in Remark 3.62.

1. First we look for a solution to

$$\begin{cases} \text{Find } \mathbb{y} \in \mathbb{M}_{h,\|} \text{ such that :} \\ \left(\mathbf{R}^{+}_{1,h,\|} - \mathbf{\Pi}_{\|}\mathbf{R}^{-}_{1,h,\|}\right)\mathbb{y} = \mathbb{b}_1. \end{cases} \tag{4.190}$$

Inspired by (3.285) from the proof of Lemma 3.59, we construct first $\mathbb{x}_0 \in \mathbb{M}_{0,h,\|}$ such that

$$\mathrm{t}_{0,h,\|}(\mathbb{x}_0, \mathbb{x}_0^t) = \frac{\mathrm{i}}{4}\langle\!\langle (\mathrm{Id} - \mathbf{\Pi}_{\|})\mathbb{b}_1, \mathbb{x}_0^t\rangle\!\rangle_{\|}, \qquad \forall \mathbb{x}_0^t \in \mathbb{M}_{0,h,\|}, \tag{4.191}$$

and we have, using the fact that $1/2\,(\mathrm{Id} - \mathbf{\Pi}_{\|})$ is a projector,

$$\|\mathbb{x}_0\|_{\mathbb{M}_{0,h,\|}} \leq \frac{1}{2}\beta^{-1/2}_{\mathrm{t}_{0,h,\|}}\ \|\mathbb{b}_1\|_{\mathbb{M}_{1,h,\|}}. \tag{4.192}$$

Then we construct $\mathbb{x}_1 \in \mathbb{M}_{1,h,\|}$ such that

$$\langle\!\langle \mathbb{x}_1, \mathbb{x}_0^t\rangle\!\rangle_{\|} = \frac{1}{4}\langle\!\langle (\mathrm{Id} + \mathbf{\Pi}_{\|})\mathbb{b}_1, \mathbb{x}_0^t\rangle\!\rangle_{\|} - \mathrm{z}_h(\mathbb{x}_0, \mathbb{x}_0^t), \qquad \forall \mathbb{x}_0^t \in \mathbb{M}_{0,h,\|}, \tag{4.193}$$

and we have, using the fact that $1/2\,(\mathrm{Id} + \mathbf{\Pi}_{\|})$ is also a projector,

$$\|\mathbb{x}_1\|_{\mathbb{M}_{1,h,\|}} \leq \frac{1}{2}\|\mathbb{b}_1\|_{\mathbb{M}_{1,h,\|}} + |||\mathrm{z}_h|||\ \|\mathbb{x}_0\|_{\mathbb{M}_{0,h,\|}} \leq \frac{1}{2}\left(1 + |||\mathrm{z}_h|||\ \beta^{-1/2}_{\mathrm{t}_{0,h,\|}}\right)\|\mathbb{b}_1\|_{\mathbb{M}_{1,h,\|}}. \tag{4.194}$$

Now, set $\mathbb{x} := (\mathbb{x}_0, \mathbb{x}_1) \in \mathbb{M}_{h,\|}$, so that

$$\begin{aligned} \|\mathbb{x}\|_{\mathbb{M}_{\|}} &\leq \frac{1}{2}\left[\beta^{-1}_{\mathrm{t}_{0,h,\|}} + \left(1 + |||\mathrm{z}_h|||\ \beta^{-1/2}_{\mathrm{t}_{0,h,\|}}\right)^2\right]^{1/2}\|\mathbb{b}_1\|_{\mathbb{M}_{1,h,\|}}, \\ &\leq \frac{1}{2}\left(1 + (1 + |||\mathrm{z}_h|||)\ \beta^{-1/2}_{\mathrm{t}_{0,h,\|}}\right)\|\mathbb{b}_1\|_{\mathbb{M}_{1,h,\|}}. \end{aligned} \tag{4.195}$$

Now let us check that it is a solution to (4.190): by definition, we have, for any $\mathbb{x}_0^t \in \mathbb{M}_{0,h,\|}$

$$\begin{aligned} \langle\!\langle \mathbf{R}^{+}_{1,h,\|}\mathbb{x}, \mathbb{x}_0^t\rangle\!\rangle_{\|} &= \langle\!\langle \mathbb{x}_1, \mathbb{x}_0^t\rangle\!\rangle_{\|} + \mathrm{z}_h(\mathbb{x}_0, \mathbb{x}_0^t) - \mathrm{it}_{0,h,\|}(\mathbb{x}_0, \mathbb{x}_0^t) = \langle\!\langle \frac{1}{2}\mathbb{b}_1, \mathbb{x}_0^t\rangle\!\rangle_{\|}, \\ \langle\!\langle \mathbf{R}^{-}_{1,h,\|}\mathbb{x}, \mathbb{x}_0^t\rangle\!\rangle_{\|} &= -\langle\!\langle \mathbb{x}_1, \mathbb{x}_0^t\rangle\!\rangle_{\|} - \mathrm{z}_h(\mathbb{x}_0, \mathbb{x}_0^t) - \mathrm{it}_{0,h,\|}(\mathbb{x}_0, \mathbb{x}_0^t) = -\langle\!\langle \frac{1}{2}\mathbf{\Pi}_{\|}\mathbb{b}_1, \mathbb{x}_0^t\rangle\!\rangle_{\|}, \end{aligned} \tag{4.196}$$

from which we deduce, using the involution property of the exchange operator $\mathbf{\Pi}_{\|}$ (Proposition 4.26),

$$\left(\mathbf{R}^{+}_{1,h,\|} - \mathbf{\Pi}_{\|}\mathbf{R}^{-}_{1,h,\|}\right)\mathbb{x} = \mathbb{b}_1. \tag{4.197}$$

2. From the previous solution $\mathbb{x} \in \mathbb{M}_{h,\|}$, Proposition 4.17 yields the existence of $\mathbb{y} \in \mathbb{C}_{h,\|}$ and $\mathbb{z} \in \mathbb{S}_{h,\|}$ such that

$$\mathbb{x} = \mathbb{y} + \mathbb{z}, \tag{4.198}$$

and we have

$$\|\mathbb{y}\|_{\mathbb{M}_{\|}} \leq\ \alpha_{\mathbb{P}_{\mathbb{C}_{h,\|}}}\ \|\mathbb{x}\|_{\mathbb{M}_{\|}} \leq \frac{1}{2}\ \alpha_{\mathbb{P}_{\mathbb{C}_{h,\|}}}\ \left(1 + (1 + |||\mathrm{z}_h|||)\ \beta^{-1/2}_{\mathrm{t}_{0,h,\|}}\right)\|\mathbb{b}_1\|_{\mathbb{M}_{1,h,\|}}. \tag{4.199}$$

Using the characterization of the single-trace space $\mathbb{S}_{h,\|}$ provided by Proposition 4.32, we have

$$\left(\mathbf{R}^{+}_{1,h,\|} - \mathbf{\Pi}_{\|}\mathbf{R}^{-}_{1,h,\|}\right)\mathbb{z} = 0, \tag{4.200}$$

so that the projection $\mathbb{y} \in \mathbb{C}_{h,\|}$ of $\mathbb{x}$ satisfies the same equation:

$$\left(\mathbf{R}^{+}_{1,h,\|} - \mathbf{\Pi}_{\|}\mathbf{R}^{-}_{1,h,\|}\right)\mathbb{y} = \mathbb{b}_1. \tag{4.201}$$

3. Set
$$\mathbb{o}_1 = \mathbf{R}^+_{1,h,\|}\mathbb{y}, \tag{4.202}$$
we have
$$\begin{aligned}\|\mathbb{o}_1\|_{\mathbb{M}_{1,h,\|}} &\leq \left(\|\mathbb{y}_1\|_{\mathbb{M}_{1,h,\|}} + (|||\mathbb{z}_h||| + |||\mathrm{t}_{0,h,\|}|||)\ \|\mathbb{y}_0\|_{\mathbb{M}_{0,h,\|}}\right),\\ &\leq (1 + |||\mathbb{z}_h||| + |||\mathrm{t}_{0,h,\|}|||)\ \|\mathbb{y}\|_{\mathbb{M}_\|},\\ &\leq \frac{1}{2}\alpha_{\mathbb{P}_{\mathbb{C}_{h,\|}}}\ (1 + |||\mathbb{z}_h||| + |||\mathrm{t}_{0,h,\|}|||)\left(1 + (1 + |||\mathbb{z}_h|||)\ \beta^{-1/2}_{\mathrm{t}_{0,h,\|}}\right)\|\mathbb{b}_1\|_{\mathbb{M}_{1,h,\|}}.\end{aligned} \tag{4.203}$$
Using the characterization of the Cauchy trace space $\mathbb{C}_{h,\|}$ provided by Proposition 4.32, we obtain from $\mathbb{y} \in \mathbb{C}_{h,\|}$,
$$\mathbf{R}^-_{1,h,\|}\mathbb{y} = \mathbf{S}_{1,h,\|}\mathbf{R}^+_{1,h,\|}\mathbb{y}. \tag{4.204}$$
Therefore, we get
$$(\mathrm{Id} - \mathbf{\Pi}_\|\mathbf{S}_{1,h,\|})\,\mathbb{o}_1 = (\mathrm{Id} - \mathbf{\Pi}_\|\mathbf{S}_{1,h,\|})\,\mathbf{R}^+_{1,h,\|}\mathbb{y} = \left(\mathbf{R}^+_{1,h,\|} - \mathbf{\Pi}_\|\mathbf{R}^-_{1,h,\|}\right)\mathbb{y} = \mathbb{b}_1, \tag{4.205}$$
and $\mathbb{o}_1$ is the (unique, by Proposition 4.37) solution of the original problem.

We obtained above an estimate using the norm $\|\cdot\|_{\mathbb{M}_{1,h,\|}}$ however we wish to establish a bound in the norm induced by $\mathrm{t}_{0,h,\|}$. From (4.96) we have
$$\|\mathbb{o}_1\|_{\mathrm{t}_{1,h,\|}} \leq \frac{1}{2}\alpha_{\mathbb{P}_{\mathbb{C}_{h,\|}}}\ \frac{|||\mathrm{t}_{0,h,\|}|||}{\beta_{\mathrm{t}_{0,h,\|}}}\ (1 + |||\mathbb{z}_h||| + |||\mathrm{t}_{0,h,\|}|||)\left(1 + (1 + |||\mathbb{z}_h|||)\ \beta^{-1/2}_{\mathrm{t}_{0,h,\|}}\right)\|\mathbb{b}_1\|_{\mathrm{t}_{1,h,\|}}. \tag{4.206}$$
The claimed estimate can then readily obtained from the expression of $\alpha_{\mathbb{P}_{\mathbb{C}_{h,\|}}}$ provided in Proposition 4.17. ■

h-uniform convergence The question of h-uniform stability is settled by the following proposition, similar to [33, Cor. 8.2].

Proposition 4.40. *If the partition is independent of h, see Assumption 4.5, and under the following additional assumptions:*

1. *In addition to Assumption 4.4, we suppose that the stability constant $\alpha_{a,h}$ of the original problem is h-uniform, namely*
$$\alpha^\star_a := \liminf_{h\to 0} \alpha_{a,h} > 0, \tag{4.207}$$

2. *In addition to the requirements of Definition 4.18, we suppose that the transmission operators are h-uniformly stable, namely*
$$|||\mathrm{t}_{0,\|}||| := \limsup_{h\to 0} |||\mathrm{t}_{0,h,\|}||| < +\infty, \qquad \textit{and} \qquad \beta^\star_{\mathrm{t}_{0,h,\|}} := \liminf_{h\to 0} \beta_{\mathrm{t}_0} > 0, \tag{4.208}$$

3. *We suppose that the stability constant $\alpha_{s,h,\|}$ of the decomposed problem, defined in Proposition 4.23, is h-uniform, namely*
$$\alpha^\star_{s,\|} := \liminf_{h\to 0} \alpha_{s,h,\|} > 0, \tag{4.209}$$

4. In addition to Assumption 4.2, we suppose that the discrete lifting is h-uniformly stable, namely

$$|||\mathbb{E}_{\shortparallel}||| := \limsup_{h\to 0} |||\mathbb{E}_{h,\shortparallel}||| < +\infty, \tag{4.210}$$

the sequence of broken solutions $(\mathfrak{u}_h^n)_{n\in\mathbb{N}}$ computed according to (4.166)*, converges geometrically and* h-uniformly *to u_h the solution of the discrete model problem* (4.19)*. Specifically, there exist $C > 0$ and $0 < \tau < 1$, independent of h, such that*

$$\|\mathfrak{u}_h^n - u_h\|_{\mathbb{U}_\Gamma(\mathrm{D};\mathcal{P}_{\Omega,h})} \leq C\tau^n, \qquad \forall n \in \mathbb{N}. \tag{4.211}$$

Proof. At each iteration $n \in \mathbb{N}$, we can define an error on the trace $\epsilon_1^n \in \mathbb{M}_{1,h,\shortparallel}$ such that

$$\epsilon_1^n = \mathfrak{x}_1^n - \mathfrak{x}_1, \tag{4.212}$$

where the sequence $(\mathfrak{x}_1^n)_{n\in\mathbb{N}}$ is computed through (4.165) and $\mathfrak{x}_1$ is the solution of (4.163). It follows that, the sequence $(\epsilon_1^n)_n$ satisfies the recurrence relation

$$\epsilon_1^{n+1} = \left[(1-r)\mathrm{Id} + r\mathbf{\Pi}_{\shortparallel}\mathbf{S}_{1,h,\shortparallel}\right]\epsilon_1^n, \qquad n \in \mathbb{N}, \tag{4.213}$$

and is such that, for all $\mathbb{v}^t \in \mathbb{V}_h(\mathcal{P}_{\Omega,h})$,

$$\mathfrak{a}(\mathfrak{u}_h^n - u_h, \mathbb{v}^t) + \mathrm{z}_h(\boldsymbol{\gamma}_{0,h,\shortparallel}(\mathfrak{u}_h^n - u_h), \boldsymbol{\gamma}_{0,h,\shortparallel}\mathbb{v}^t) - \mathrm{it}_{0,h,\shortparallel}(\boldsymbol{\gamma}_{0,h,\shortparallel}(\mathfrak{u}_h^n - u_h), \boldsymbol{\gamma}_{0,h,\shortparallel}\mathbb{v}^t) = \langle\!\langle \epsilon_1^n, \boldsymbol{\gamma}_{0,h,\shortparallel}\mathbb{v}^t \rangle\!\rangle_{\shortparallel}. \tag{4.214}$$

We use again the convexity identity (3.233) from the proof of Theorem 3.49 and we get

$$\|\epsilon_1^{n+1}\|_{\mathrm{t}_{1,h,\shortparallel}}^2 = (1-r)\|\epsilon_1^n\|_{\mathrm{t}_{1,h,\shortparallel}}^2 + r\|\mathbf{\Pi}_{\shortparallel}\mathbf{S}_{1,h,\shortparallel}\epsilon_1^n\|_{\mathrm{t}_{1,h,\shortparallel}}^2 - r(1-r)\|\left(\mathrm{Id} - \mathbf{\Pi}_{\shortparallel}\mathbf{S}_{1,h,\shortparallel}\right)\epsilon_1^n\|_{\mathrm{t}_{1,h,\shortparallel}}^2. \tag{4.215}$$

Since $\mathbf{\Pi}_{\shortparallel}\mathbf{S}_{1,h,\shortparallel}$ is a contraction in $\mathbb{M}_{1,h,\shortparallel}$ from Corollary 4.36, we have

$$\|\mathbf{\Pi}_{\shortparallel}\mathbf{S}_{1,h,\shortparallel}\epsilon_1^n\|_{\mathrm{t}_{1,h,\shortparallel}} \leq \|\epsilon_1^n\|_{\mathrm{t}_{1,h,\shortparallel}}, \tag{4.216}$$

and from Proposition 4.39 we have

$$\|\epsilon_1^n\|_{\mathrm{t}_{1,h,\shortparallel}} \leq \zeta_{h,\shortparallel}\, \|\left(\mathrm{Id} - \mathbf{\Pi}_{\shortparallel}\mathbf{S}_{1,h,\shortparallel}\right)\epsilon_1^n\|_{\mathrm{t}_{1,h,\shortparallel}}, \tag{4.217}$$

hence

$$\|\epsilon_1^n\|_{\mathrm{t}_{1,h,\shortparallel}} \leq \tau^n\|\epsilon_1^0\|_{\mathrm{t}_{1,h,\shortparallel}}, \tag{4.218}$$

where $\tau = \sqrt{1 - r(1-r)\zeta_{h,\shortparallel}^2}$ with $\zeta_{h,\shortparallel}$ defined in (4.187). By the stability of the problem (4.214), we have

$$\|\mathfrak{u}_h^n - u_h\|_{\mathbb{U}_\Gamma(\mathrm{D};\mathcal{P}_{\Omega,h})} \leq \left(\alpha_{s,\shortparallel}^\star\right)^{-1}\|\epsilon_1^n\|_{\mathrm{t}_{1,h,\shortparallel}} \leq \left(\alpha_{s,\shortparallel}^\star\right)^{-1}\tau^n\|\epsilon_1^0\|_{\mathrm{t}_{1,h,\shortparallel}}, \tag{4.219}$$

From problem (4.214) with $n = 0$, we also get

$$\|\epsilon_1^0\|_{\mathrm{t}_{1,h,\shortparallel}} \leq \left(|||a||| + |||\mathrm{z}_h||| + |||\mathrm{t}_{0,h,\shortparallel}|||\right)\|\mathfrak{u}_h^0 - u_h\|_{\mathbb{U}_\Gamma(\mathrm{D};\mathcal{P}_{\Omega,h})}. \tag{4.220}$$

Finally, we have the estimate

$$\frac{\|\mathfrak{u}_h^n - u_h\|_{\mathbb{U}_\Gamma(\mathrm{D};\mathcal{P}_{\Omega,h})}}{\|\mathfrak{u}_h^0 - u_h\|_{\mathbb{U}_\Gamma(\mathrm{D};\mathcal{P}_{\Omega,h})}} \leq \left(\alpha_{s,\shortparallel}^\star\right)^{-1}\left(|||a||| + |||\mathrm{z}_h||| + |||\mathrm{t}_{0,h,\shortparallel}|||\right)\left(1 - r(1-r)\zeta_{h,\shortparallel}^2\right)^{n/2}, \tag{4.221}$$

and the bound is h-uniform from all the above assumptions. ∎

Remark 4.41. *It should be noted that the stable lifting $\mathbb{E}_{h,\|}$ is a purely theoretical tool, whose existence (and stability) are solely required for the purposes of analysis. In particular, the implementation of the method does* not *require in general the actual implementation of $\mathbb{E}_{h,\|}$.*

The assumptions of the previous proposition deserves some discussion. The independence of the partition with respect to h is natural, although it is not observed in general in the numerical experiments if a graph partitioner is used.

In this abstract setting, the assumption (1) on the h-uniformity of the stability constant $\alpha_{a,h}$ is also natural, and is in fact independent of the domain decomposition method. In the acoustic setting, the assumption (1) follows from standard results, for a sufficiently refined mesh, we refer the reader to [86, Chap. 2] for instance. In the electromagnetic setting, the assumption (1) is also satisfied, although the analysis is slightly more involved, we refer the reader to [107, Chap. 7].

Assumption (2) on the stability of the transmission operators will not be satisfied by local operators, which will not be either h-uniformly bounded or $\inf - \sup$ stable. In contrast, suitable non-local operators will satisfy such bounds.

The assumption (3) was proved for the acoustic setting in a remark following Proposition 4.23, for transmission operators independent of h. However, the question of obtaining a proof of a corresponding result for the electromagnetic setting is yet to be addressed.

Finally, we note that the assumption (4) is valid for standard discretization strategies, such as standard Lagrange finite elements for the acoustic setting and Nedelec finite elements for the electromagnetic setting. We refer the reader to the remarks that were made following Assumption 4.3.

Remark 4.42. *Arguing as in Section 3.3.3, we remark that h-uniform geometric convergence of the relaxed Jacobi algorithm guarantees h-uniform geometric convergence of the* GMRES *counterpart.*

4.4 Matrix and vector representation

In this section we will describe in more concrete terms the implementation of the iterative scheme, writing all equations in matrix form. This will help gain a real insight on the implementation details underlying the solution strategy we propose. In this section, we assume that the finite dimensional spaces are constructed using standard finite element spaces defined on simplicial mesh triangulations.

Approximation spaces First of all, we set a few matrix notations. Let $j \in \{1, \ldots, J\}$, we assume to have a finite dimensional basis of $\mathrm{V}_h(\Omega_{j,h})$ consisting of $N(\Omega_{j,h}) := \dim\ \mathrm{V}_h(\Omega_{j,h})$ shape functions denoted $\varphi_{l,\Omega_{j,h}}$, $l \in \{1, \ldots, N(\Omega_{j,h})\}$. In practice, each $\varphi_{l,\Omega_{j,h}}$ will refer to the usual $\mathbb{P}_k$ Lagrange shape functions [65, Sec. 1.2.3] in the acoustic setting or to the volume Nedelec edge functions [65, Sec. 1.2.8] in the electromagnetic setting.

According to our assumptions, this also defines a basis of $\mathrm{X}_{0,h}(\tilde{\Gamma}_{j,h})$ consisting of $N(\tilde{\Gamma}_{j,h}) := \dim\ \mathrm{X}_{0,h}(\tilde{\Gamma}_{j,h})$ shape functions denoted $\varphi_{l,\tilde{\Gamma}_{j,h}}$, $l \in 1, \ldots, N(\tilde{\Gamma}_{j,h})$. Note that we assume that each shape function on $\tilde{\Gamma}_{j,h}$ is obtained by taking the natural trace (i.e. the Dirichlet or tangential trace) of some shape function on $\Omega_{j,h}$ so that for any $m \in \{1, \ldots, N(\tilde{\Gamma}_{j,h})\}$ there exists a $n \in \{1, \ldots, N(\Omega_{j,h})\}$ such that $\varphi_{m,\tilde{\Gamma}_{j,h}} = \varphi_{n,\Omega_{j,h}}|_{\tilde{\Gamma}_{j,h}}$.

With the previous notations, the dimension of the multi-trace space $\mathbb{M}_{0,h,\|}$ will be

$$M(\Sigma_h) := \dim \mathbb{M}_{0,h,\|} = \sum_{j=1}^{J} N(\tilde{\Gamma}_{j,h}). \tag{4.222}$$

Let us denote by ψ_m, $m \in \{1, \ldots, M(\Sigma_h)\}$ the basis functions of the multi-trace space $\mathbb{M}_{0,h,\|}$. The single-trace space $\mathbb{S}_{0,h,\times}$ is a sub-space of $\mathbb{M}_{0,h,\|}$ whose dimension will be denoted $N(\Sigma_h) := \dim \mathbb{S}_{0,h,\times}$. Note that by construction, $2N(\Sigma_h) = M(\Sigma_h)$.

Let us denote by $\widetilde{\psi}_n$, $n \in \{1, \ldots, N(\Sigma_h)\}$ the basis functions of the single-trace space $\mathbb{S}_{0,h,\times}$. We introduce in addition the (surjective) mapping Φ which associates to each index $m \in \{1, \ldots, M(\Sigma_h)\}$ the (unique) index $n := \Phi(m) \in \{1, \ldots, N(\Sigma_h)\}$ so that the two basis functions ψ_m and $\widetilde{\psi}_n$ are associated to the same geometrical element (a node in the acoustic setting, an edge in the electromagnetic setting).

Matrices For each sub-domain $\Omega_{j,h}$, $j \in \{1, \ldots, J\}$, we introduce the local matrices $\mathbf{A}_j$ of size $N(\Omega_{j,h}) \times N(\Omega_{j,h})$, such that

$$(\mathbf{A}_j)_{m,n} := a_j(\varphi_{n,\Omega_{j,h}}, \varphi_{m,\Omega_{j,h}}), \qquad \forall m, n \in \{1, \ldots, N(\Omega_{j,h})\}, \tag{4.223}$$

where the local sesquilinear form a_j is defined in (3.97). The local contributions of the right-hand side are represented by vectors $\mathbf{f}_j$ of size $N(\Omega_{j,h})$ defined by

$$(\mathbf{f}_j)_m := l_j(\varphi_{m,\Omega_{j,h}}), \qquad \forall m \in \{1, \ldots, N(\Omega_{j,h})\}, \tag{4.224}$$

where the local linear form l_j is defined in (3.100). We also introduce the local impedance matrices $\mathbf{T}_j$, of size $N(\tilde{\Gamma}_{j,h}) \times N(\tilde{\Gamma}_{j,h})$, such that

$$(\mathbf{T}_j)_{m,n} := \sum_{k \in \mathbb{K}_j} \mathrm{t}^{jk}_{0,h,\|}(\varphi_{n,\tilde{\Gamma}_{j,h}}|_{\tilde{\Gamma}_{k,h}}, \varphi_{m,\tilde{\Gamma}_{j,h}}|_{\tilde{\Gamma}_{k,h}}), \qquad \forall m, n \in \{1, \ldots, N(\tilde{\Gamma}_{j,h})\}, \tag{4.225}$$

and similarly the local matrices $\mathbf{Z}_j$, of size $N(\tilde{\Gamma}_{j,h}) \times N(\tilde{\Gamma}_{j,h})$, such that

$$(\mathbf{Z}_j)_{m,n} := \sum_{k \in \mathbb{K}_j} \mathrm{z}^{jk}_h(\varphi_{n,\tilde{\Gamma}_{j,h}}|_{\tilde{\Gamma}_{k,h}}, \varphi_{m,\tilde{\Gamma}_{j,h}}|_{\tilde{\Gamma}_{k,h}}), \qquad \forall m, n \in \{1, \ldots, N(\tilde{\Gamma}_{j,h})\}. \tag{4.226}$$

It will be convenient also to define boolean local trace matrices $\mathbf{B}_j$ of size $N(\tilde{\Gamma}_{j,h}) \times N(\Omega_{j,h})$, which restrict a vector representing a local solution to the vector representing its trace on the boundary of the local sub-domain. The entries of these matrices are defined by

$$(\mathbf{B}_j)_{m,n} := \begin{cases} 1, & \text{if } \varphi_{m,\tilde{\Gamma}_{j,h}} = \varphi_{n,\Omega_{j,h}}|_{\tilde{\Gamma}_{j,h}}, \\ 0, & \text{otherwise,} \end{cases} \quad \forall m \in \{1, \ldots, N(\tilde{\Gamma}_{j,h})\},\ n \in \{1, \ldots, N(\Omega_{j,h})\}. \tag{4.227}$$

Besides, let us define for each $j \in \{1, \ldots, J\}$, the boolean matrix $\mathbf{R}_j$ of size $N(\tilde{\Gamma}_{j,h}) \times M(\Sigma_h)$, which restricts a vector representing a global multi-trace to the vector representing the local trace contribution on the boundary of the local sub-domain $\Omega_{j,h}$. The entries of these matrices are defined by

$$(\mathbf{R}_j)_{m,n} := \begin{cases} 1, & \text{if } m = n - \sum_{k<j} N(\Omega_{k,h}), \\ 0, & \text{otherwise,} \end{cases} \quad \forall m \in \{1, \ldots, N(\tilde{\Gamma}_{j,h})\},\ n \in \{1, \ldots, M(\Sigma_h)\}. \tag{4.228}$$

Let us also define the matrix $\mathbf{Q}$ of size $M(\Sigma_h) \times N(\Sigma_h)$ which constructs a multi-trace vector from a single-trace vector. The entries of this matrix are defined by

$$(\mathbf{Q})_{m,n} := \begin{cases} 1, & \text{if } n = \Phi(m), \\ 0, & \text{otherwise,} \end{cases} \qquad \forall m \in \{1, \dots, M(\Sigma_h)\},\ n \in \{1, \dots, N(\Sigma_h)\}. \tag{4.229}$$

The local contributions

$$\mathbf{Q}_j := \mathbf{R}_j \mathbf{Q}, \qquad \forall j \in \{1, \dots, J\}, \tag{4.230}$$

will also prove useful.

One can then define the matrices of the local sub-problems

$$\mathbf{K}_j := \mathbf{A}_j + \mathbf{B}_j^* \mathbf{Z}_j \mathbf{B}_j - \mathrm{i}\mathbf{B}_j^* \mathbf{T}_j \mathbf{B}_j, \qquad \forall j \in \{1, \dots, J\}. \tag{4.231}$$

From Proposition 4.23, these matrices are invertible.

4.4.1 Scattering operator

Assuming that the above local matrices are assembled for each sub-domain, the evaluation of the scattering operator $\mathbf{S}_{1,h,\|}$ takes the form of Algorithm 4.1. Note that everything is parallel, the global multi-trace vectors $\mathbf{x}$ and $\mathbf{s}$ respectively input and output of the algorithm can be distributed on the cluster nodes on a distributed-memory architecture.

Algorithm 4.1 Evaluation of the scattering operator $\mathbf{S}_{1,h,\|}$

function GLOBALSCATTERING($\mathbf{x}$) ▷ Input size: $M(\Sigma_h)$
  $\mathbf{s} \leftarrow 0$ ▷ size: $M(\Sigma_h)$
  for $j = 1, \dots, J$ **do** ▷ Parallel loop
    $\mathbf{x}_j \leftarrow \mathbf{R}_j \mathbf{x}$ ▷ Local contribution of the multi-trace (size: $M(\tilde{\Gamma}_{j,h})$)
    $\mathbf{u}_j \leftarrow \mathbf{K}_j^{-1} \mathbf{B}_j^* \mathbf{x}_j$ ▷ Local solve (size: $N(\Omega_{j,h})$)
    $\mathbf{s}_j \leftarrow -\mathbf{x}_j - 2\mathrm{i}\mathbf{T}_j \mathbf{B}_j \mathbf{u}_j$ ▷ Local scattering (size: $N(\tilde{\Gamma}_{j,h})$)
    $\mathbf{s} \leftarrow \mathbf{s} + \mathbf{R}_j^* \mathbf{s}_j$
  end for
  return s ▷ Output size: $M(\Sigma_h)$
end function

4.4.2 Exchange operator

The definition of the exchange operator $\mathbf{\Pi}_\|$ is rather straightforward because of our assumption that no junctions are present. To formalize it with our notations, we define

$$\mathbf{\Pi}_{jk} := \mathbf{R}_k^* \mathbf{Q}_k \mathbf{Q}_j^* \mathbf{R}_j. \tag{4.232}$$

The corresponding definition of the exchange operator is then provided in matrix form by Algorithm 4.2.

4.4.3 Relaxed Jacobi algorithm

The assembly of the local matrices $\mathbf{A}_j$, $\mathbf{T}_j$ and the source terms $\mathbf{f}_j$ can be pre-computed before starting the iterative algorithm. In addition, the factorization of $\mathbf{K}_j$ (LU) shall also be performed. The last pre-computations possible are provided by Algorithm 4.3 which describes the

Algorithm 4.2 Evaluation of the exchange operator $\mathbf{\Pi}_{\|}$

function GLOBALEXCHANGE($\mathbf{x}$) ▷ Input size: $M(\Sigma_h)$
  $\mathbf{y} \leftarrow 0$ ▷ size: $M(\Sigma_h)$
  for $j = 1, \ldots, J$ **do**
    for $k \in \mathbb{K}_j$ **do** ▷ Loop on adjacent sub-domains
      $\mathbf{y} \leftarrow \mathbf{y} + \mathbf{\Pi}_{jk}\mathbf{x}$ ▷ Transfer of data from sub-domain Ω_j to sub-domain Ω_k
    end for
  end for
  return $\mathbf{y}$ ▷ Output size: $M(\Sigma_h)$
end function

computation of the lifting of the source terms represented by the local vectors $\mathbf{v}_j$ and the computation of the right-hand-side $\mathbb{b}_1$ represented by the vector $\mathbf{b}$ of the skeleton problem (4.163). Except for the application of the exchange operator, all the computations are independent and can be performed in parallel.

Algorithm 4.3 Lifting of the source

$\mathbf{b} \leftarrow 0$ ▷ size: $M(\Sigma_h)$
for $j = 1, \ldots, J$ **do** ▷ Parallel loop
  $\mathbf{v}_j \leftarrow \mathbf{K}_j^{-1}\mathbf{f}_j$ ▷ Local solve (size: $N(\Omega_{j,h})$)
  $\mathbf{b} \leftarrow \mathbf{b} - 2\mathrm{i}\,\mathbf{R}_j^*\mathbf{T}_j\mathbf{B}_j\mathbf{v}_j$ ▷ Skeleton problem right-hand-side $\mathbb{b}_1$
end for
$\mathbf{b} \leftarrow$ GLOBALEXCHANGE($\mathbf{b}$) ▷ Application of $\mathbf{\Pi}_{\|}$

After choosing a relaxation parameter $r \in (0, 1)$ and maximum number of iterations $n_{\max} \in \mathbb{N}^*$, the iterative relaxed Jacobi algorithm (4.165) takes the form of Algorithm 4.4 below. The only place where communications occurs are in the global exchange step. Of course, this basic algorithm can be completed by the computation of the residual for instance, and the iterations can be stopped if it is below a certain tolerance for some norm.

Algorithm 4.4 Relaxed Jacobi algorithm

$\mathbf{x} \leftarrow 0$ ▷ Initialization (size: $M(\Sigma_h)$)
for $n = 1, \ldots, n_{\max}$ **do**
  $\mathbf{s} \leftarrow$ GLOBALSCATTERING($\mathbf{x}$) ▷ Application of $\mathbf{S}_{1,h,\|}$ (size: $M(\Sigma_h)$)
  $\mathbf{p} \leftarrow$ GLOBALEXCHANGE($\mathbf{s}$) ▷ Application of $\mathbf{\Pi}_{\|}$ (size: $M(\Sigma_h)$)
  $\mathbf{x} \leftarrow (1 - r)\mathbf{x} + r\mathbf{p} + r\mathbf{b}$ ▷ Iteration (size: $M(\Sigma_h)$)
end for

Having found an approximation $\mathbf{x}$ of the solution of the skeleton problem (4.163) *via* the relaxed Jacobi algorithm, the global (broken) solution, represented by local vectors $\mathbf{u}_j$, can then be computed thanks to Algorithm 4.5. The local liftings of the source $\mathbf{v}_j$ have been computed thanks to Algorithm 4.3.

4.4.4 GMRES algorithm

We can also solve the linear system given by (4.163) iteratively using the GMRES algorithm. To define the algorithm, it suffices to provide a definition for a right-hand-side and a matrix-vector

Algorithm 4.5 Evaluation of the global broken solution

for $j = 1, \dots, J$ **do** ▷ Parallel loop
  $\mathbf{w}_j \leftarrow \mathbf{K}_j^{-1} \mathbf{B}_j^* \mathbf{R}_j \mathbf{x}$ ▷ Local solve (size: $N(\Omega_{j,h})$)
  $\mathbf{u}_j \leftarrow \mathbf{v}_j + \mathbf{w}_j$ ▷ Local solution (size: $N(\Omega_{j,h})$)
end for

product routine. The right-hand-side is denoted by $\mathbf{b}$ and can be computed (offline) according to Algorithm 4.3. The matrix-vector product procedure, which takes as input a global multi-trace vector $\mathbf{x}$, is given in Algorithm 4.6.

Algorithm 4.6 Matrix-vector product for the GMRES algorithm

function MATVEC($\mathbf{x}$) ▷ Input size: $M(\Sigma_h)$
  $\mathbf{s} \leftarrow$ GLOBALSCATTERING($\mathbf{x}$) ▷ Application of $\mathbf{S}_{1,h,\|}$ (size: $M(\Sigma_h)$)
  $\mathbf{p} \leftarrow$ GLOBALEXCHANGE($\mathbf{s}$) ▷ Application of $\mathbf{\Pi}_{\|}$ (size: $M(\Sigma_h)$)
  return $\mathbf{x} - \mathbf{p}$ ▷ Output size: $M(\Sigma_h)$
end function

Notice again here that apart from the computation of the global exchange step which ensures coupling between subdomains, all operations are local to the sub-domains. Having found an approximation $\mathbf{x}$ of the solution of the skeleton problem (4.163) *via* the GMRES algorithm, the global (broken) solution, represented by local vectors $\mathbf{u}_j$, can then be computed thanks to Algorithm 4.5.

Part II

Impedance operators

Chapter 5

Integral impedance operators

Contents

In this section we propose several transmission operators with suitable properties that could be used in the domain decomposition strategy that was previously described. All the operators we consider in this section are *integral* operators of convolution type with a singular kernel at the origin. Roughly speaking, the strength of the singularity is linked to the order of the operator and should be chosen wisely according the analysis previously developed.

In the domain decomposition method that has been previously described, the interface problem could be written in any of the three trace spaces: namely in $\mathbb{M}_{0,\|}$, $\mathbb{M}_{1/2,\|}$ or $\mathbb{M}_{1,\|}$, which correspond to taking respectively $\sigma = 0$, $1/2$ or 1. It is clear that, depending on this choice we need different transmission operators, namely respectively $\mathbf{T}_{1,\|}$ for $\sigma = 0$, $\mathbf{T}_{1/2,\|}$ or $\mathbf{T}_{-1/2,\|}$ for $\sigma = 1/2$ and $\mathbf{T}_{0,\|}$ for $\sigma = 1$. However, to implement a domain decomposition method in practice, one needs to implement *only one* type of transmission operator. The question that arises is then: which type of (non-local) transmission operator should one use?

This choice typically first depends on the type of discretization method at hand, for instance:

- for standard Galerkin discretization, it is more natural to implement either a $\mathbf{T}_{0,\|}$-type operator or a $\mathbf{T}_{1/2,\|}$-type operator;

- for some other types of discretization strategies (for instance using a mixed-hybrid approach), it may be more natural to implement either a $\mathbf{T}_{1,\parallel}$-type operator or a $\mathbf{T}_{-1/2,\parallel}$-type operator.

Then, there are two main routes:

- either construct directly a $\mathbf{T}_{0,\parallel}$ or a $\mathbf{T}_{1,\parallel}$-type operator (first strategy): in addition to being isomorphisms between the adequate trace spaces, such operators must also be self-adjoint and positive (to be able to define a scalar product on the trace space, see Assumption 3.47). As we shall see, such operators can be constructed from (almost standard) potential theory;

- or construct a $\mathbf{T}_{1/2,\parallel}$ or a $\mathbf{T}_{-1/2,\parallel}$-type operator (second strategy): in addition to being isomorphisms between the adequate trace spaces, such operators must be respectively such that
$$\mathbf{T}_{0,\parallel} = \mathbf{T}_{1/2,\parallel}{}^{*}\mathbf{T}_{1/2,\parallel}, \qquad \text{and} \qquad \mathbf{T}_{1,\parallel} = \mathbf{T}^{*}_{-1/2,\parallel}\mathbf{T}_{-1/2,\parallel}, \tag{5.1}$$
are posivite (the self-adjointness is guaranteed by construction). As we shall see, the construction of such operators is slightly more involved than for the previous ones. Besides, this type of operator requires the use of auxiliary variables (increasing as a result the size of the local sub-problem matrices), but can be worth the additional effort.

The operators $\mathbf{T}_{0,\parallel}$, $\mathbf{T}_{1,\parallel}$, $\mathbf{T}_{1/2,\parallel}$ and $\mathbf{T}_{-1/2,\parallel}$ are *global* operators *a priori* defined on the whole skeleton. However, as we have seen in previous chapters, practical implementations will always use *diagonal* operators, where a diagonal element is defined on a single interface between two adjacent sub-domains. It is therefore enough to describe the construction of a single diagonal element, since the definition of the global operator from a diagonal element is then straightforward. This is why in this chapter, we define operators on only one interface, assumed to be closed and denoted Σ. The diagonal element operator defined on this interface Σ is denoted T_α, with $\alpha \in \{-1/2, 0, 1/2, 1\}$.

An integral operator is by nature computationally heavy, mainly because of its convolution type. In a finite element discretization an integral operator typically appear in the form of a dense matrix which could make either the computational cost or the memory requirement of the method prohibitive. Besides, the dense matrix will appear in a larger linear system (of the local sub-problems), which is sparse. The resulting matrix, with the unusual sparse-dense structure, is less favorable to numerical computations. In particular the efficiency of state-of-the-art direct solvers may be severely damaged.

When comparing several options we must therefore not only take into account theoretical properties, but also assess the ease of implementation and the computational cost associated to the choice of operator. The main goal, in order to reduce the computational footprint of the method, is to try to sparsify in some sense the dense operator. Several different strategies can be considered, for instance compression techniques using the fast multipole method (FMM) or $\mathcal{H}$-matrices. However, we note that all those techniques could harm the properties of the operators and as a result the convergence of the algorithms.

The main strategy that was considered in previous works [91, 44] to circumvent this issue is to truncate the kernel (by a cut-off function). Using compact perturbation arguments, one could prove that the isomorphism property of the transmission operators outlives the truncation process. We are however (most of the time) unable to prove that the property of positivity is kept intact after truncation. As a result, for efficiency reasons, there is a strong interest in considering a $\mathbf{T}_{1/2,\parallel}$ or a $\mathbf{T}_{-1/2,\parallel}$-type operator (second strategy), for which the positivity is not required, over a $\mathbf{T}_{0,\parallel}$ or a $\mathbf{T}_{1,\parallel}$-type operator (first strategy).

The chapter is organized in two parts. In the first part, because they form our starting point for our attempted constructions in the electromagnetic setting, we recall what operators

have already been proposed in the acoustic case in previous works on the subject (namely [42, 91, 44]). Our treatment is however slightly more systematic than those references and can be seen as a complement to those works. In the second part, we discuss how these operators can be adapted to the electromagnetic setting. In particular, we explain why the construction of suitable operators is a much more difficult task. This work in the electromagnetic setting, mainly carried out together with Francis Collino, extends the first ideas presented in [34] where a first integral operator was presented.

Our presentation in this chapter builds upon some standard results of potential theory. However, we acknowledge that our discussion is in some places rather formal and lacks a rigorous treatment in order to justify properly our claims. The main reason we did not pursue in this direction is that, as we shall see in Chapter 7, the numerical results obtained using the integral operators described in this chapter are rather disappointing. Nevertheless, we believe that the ideas presented in this chapter are worth presenting in their own right.

5.1 Acoustic setting

We recall now the non-local operators that have been proposed to be used in the previously described domain decomposition method for acoustic wave propagation.

In this section, we consider the boundary Σ of a bounded Lipschitz domain Ω^- subset of $\mathbb{R}^d$, $d \in \{2, 3\}$ and we set $\Omega^+ := \mathbb{R}^d \setminus \overline{\Omega^-}$. We assume that the domain Ω_- is connected and simply connected (all its Betti numbers are zero) so that Σ is also connected and simply connected. We denote by ν the unit outward normal vector defined on Σ from Ω_- to Ω_+.

5.1.1 First strategy

In this section, we are set to construct a self-adjoint positive isomorphism so that

$$\begin{aligned} & \mathrm{T}_0 \ : \ H^{1/2}(\Sigma) \to H^{-1/2}(\Sigma), \\ \text{or} \quad & \mathrm{T}_1 \ : \ H^{-1/2}(\Sigma) \to H^{1/2}(\Sigma). \end{aligned} \tag{5.2}$$

5.1.1.1 Gagliardo or Sobolev-Slobodetskii semi-norms

In the acoustic setting, following an original idea proposed by Xavier Claeys, a possible choice that have been studied [91, Chap. 5] and [44, Sec. 3.1.1], is to use the integral representation of the Gagliardo or Sobolev-Slobodetskii semi-norms, which defines a semi-norm on $H^{1/2}(\Sigma)$. Given any (dimensionless) positive parameters α and β, a first possible choice is then (the semi-norm is the second term), for any $\phi, \psi \in H^{1/2}(\Sigma)$

$$\langle \mathrm{T}_0\phi, \psi\rangle_\Sigma := \alpha \int_\Sigma \phi(\mathbf{x})\overline{\psi}(\mathbf{x})\, \mathrm{d}\sigma(\mathbf{x}) + \frac{\beta}{k} \int_\Sigma \int_\Sigma \frac{(\phi(\mathbf{x}) - \phi(\mathbf{y}))\left(\overline{\psi}(\mathbf{x}) - \overline{\psi}(\mathbf{y})\right)}{|\mathbf{x}-\mathbf{y}|^d}\, \mathrm{d}\sigma(\mathbf{x})\mathrm{d}\sigma(\mathbf{y}). \tag{5.3}$$

A great interest of this operator rests in the fact that it can be quasi-localized while retaining its essential features for this domain decomposition context. By quasi-localization we mean here that it is possible to restrain its long range action in an attempt to decrease the associated computational cost. To do so, we can introduce a cut-off function $\chi \in L^\infty(\mathbb{R}^+)$ which is identically 1 on $(0, \frac{1}{2})$ and identically 0 on $(1, +\infty)$. We can then consider, given a characteristic length L,

the truncated operator defined for any $\phi, \psi \in H^{1/2}(\Sigma)$ by

$$\begin{aligned}\langle \mathrm{T}_{0,L}\phi, \psi\rangle_\Sigma :=& \alpha \int_\Sigma \phi(\mathbf{x})\overline{\psi}(\mathbf{x})\, \mathrm{d}\sigma(\mathbf{x}) \\ &+ \frac{\beta}{k}\int_\Sigma\int_\Sigma \chi\left(\frac{|\mathbf{x}-\mathbf{y}|}{L}\right) \frac{(\phi(\mathbf{x})-\phi(\mathbf{y}))\left(\overline{\psi}(\mathbf{x})-\overline{\psi}(\mathbf{y})\right)}{|\mathbf{x}-\mathbf{y}|^d}\, \mathrm{d}\sigma(\mathbf{x})\mathrm{d}\sigma(\mathbf{y}).\end{aligned} \tag{5.4}$$

The quasi-locality of the operator can be seen by considering ϕ and ψ with disjoint supports, separated by a distance greater than L (in the sense of the Euclidian distance in $\mathbb{R}^d$), and noticing that the above quantity is zero.

Interestingly, the truncated operator retains all its essential properties, in particular its positivity and isomorphism property [44, Th. 3.1]. Roughly speaking, the proof of this result rests on the fact that the truncated operator is a compact perturbation of the original operator, thanks to the compactness of the embedding of $H^{1/2}(\Sigma)$ in $L^2(\Sigma)$.

5.1.1.2 Potential theory

A different approach that was also considered is to built upon potential theory. In fact, to the best of our knowledge, only Riesz potentials where studied in this context [91, Chap. 4] and [44, Sec. 3]. We shall widen slightly the discussion by also considering Bessel potentials that have a kernel with better decaying properties at infinity.

Green kernel Let us define, for any positive real parameter $\sigma > 0$, the *Green kernel* or fundamental solution $\mathrm{G}_{d,\sigma}$ of the *Yukawa equation* (also known as the modified Helmholtz equation) as follows

$$\begin{cases} \left(-\Delta + \sigma^2\right)\mathrm{G}_{d,\sigma} = \delta_0, & \text{in } \mathbb{R}^d, \\ \lim_{|\mathbf{x}|\to+\infty} \mathrm{G}_{d,\sigma}(\mathbf{x}) = 0, \end{cases} \tag{5.5}$$

where δ_0 is the Dirac measure centered at the origin.

For $\sigma = 0$ the equation becomes the standard *Laplace equation* and we define similarly, the *Green kernel* or fundamental solution $\mathrm{G}_{d,0}$ as follows

$$\begin{cases} -\Delta \mathrm{G}_{d,0} = \delta_0, & \text{in } \mathbb{R}^d, \\ \lim_{|\mathbf{x}|\to+\infty} \mathrm{G}_{d,0}(\mathbf{x}) = 0. \end{cases} \tag{5.6}$$

These kernels admit the following expressions in the cases of interest

$$\begin{aligned} \sigma > 0, \quad & \begin{cases} \mathrm{G}_{2,\sigma}(\mathbf{x}) := \mathrm{K}_0(\sigma|\mathbf{x}|), & \mathbf{x} \in \mathbb{R}^2 \setminus \{0\}, \quad \text{if } d = 2, \\ \mathrm{G}_{3,\sigma}(\mathbf{x}) := \dfrac{\exp(-\sigma|\mathbf{x}|)}{4\pi|\mathbf{x}|}, & \mathbf{x} \in \mathbb{R}^3 \setminus \{0\}, \quad \text{if } d = 3, \end{cases} \\ \sigma = 0, \quad & \begin{cases} \mathrm{G}_{2,0}(\mathbf{x}) := -\dfrac{1}{2\pi}\ln|\mathbf{x}|, & \mathbf{x} \in \mathbb{R}^2 \setminus \{0\}, \quad \text{if } d = 2, \\ \mathrm{G}_{3,0}(\mathbf{x}) := \dfrac{1}{4\pi|\mathbf{x}|}, & \mathbf{x} \in \mathbb{R}^3 \setminus \{0\}, \quad \text{if } d = 3, \end{cases} \end{aligned} \tag{5.7}$$

where K_0 denotes the modified Bessel function of the second kind of order 0 [54, Sec. 10.25].

Volume potential From this fundamental solution, we are able to define the following volume potential, for any $f \in C_0^{+\infty}(\mathbb{R}^d)$ as an improper integral as follows

$$\mathcal{G}_{d,\sigma} f(\mathbf{x}) := \int_{\mathbb{R}^d} \mathrm{G}_{d,\sigma}(|\mathbf{x}-\mathbf{y}|) f(\mathbf{y})\, \mathrm{d}y, \qquad \forall \mathbf{x} \in \mathbb{R}^d. \tag{5.8}$$

The above potential is often referred to as a *Bessel potential* in the case $\sigma > 0$ and as a *Riesz potential* in the case $\sigma = 0$.

This potential can be extended to elements of $H^{-1}_{\mathrm{comp}}(\mathbb{R}^d)$ and defines then a continuous mapping so that [101, Sec. 6.1] [124, Th. 3.1.2]

$$\mathcal{G}_{d,\sigma} \ : \ H^{-1}_{\mathrm{comp}}(\mathbb{R}^d) \to H^1_{\mathrm{loc}}(\mathbb{R}^d). \tag{5.9}$$

Trace operators As we want to establish results on the boundary Σ we will need to make a short detour and define some notations.

We first define the Dirichlet trace operator γ_D^- (respectively γ_D^+) as the interior (respectively exterior) trace operator which is the natural extension to elements of $H^1(\Omega_-)$ (respectively $H^1(\Omega_+)$) of the restriction operator

$$u \mapsto u|_\Sigma, \tag{5.10}$$

for regular fields.

We also introduce the Neumann trace operator γ_N^- (respectively γ_N^+) as the interior (respectively exterior) trace operator which is the natural extension to elements of $H^1(\Delta;\Omega_-)$ (respectively $H^1(\Delta;\Omega_+)$) of the operator

$$\begin{aligned} & u \mapsto \nu \cdot (\mathbf{grad}\, u)|_\Sigma, \\ \text{(respectively} \qquad & u \mapsto -\nu \cdot (\mathbf{grad}\, u)|_\Sigma), \end{aligned} \tag{5.11}$$

for regular fields.

In addition, let us denote by $\{\gamma_D\}$ and $\{\gamma_N\}$ the two-sided trace operators defined respectively as

$$\{\gamma_D\} := \frac{1}{2}\left(\gamma_D^- + \gamma_D^+\right), \qquad \{\gamma_N\} := \frac{1}{2}\left(\gamma_N^- - \gamma_N^+\right). \tag{5.12}$$

We then introduce $\{\gamma_D^*\}$ and $\{\gamma_N^*\}$ as the respective formal adjoint operators of $\{\gamma_D\}$ and $\{\gamma_N\}$ (see [101, Eq. (6.14)] for a precise definition).

Besides, let us denote by $[\gamma_D]$ and $[\gamma_N]$ the jump of the trace operators defined respectively as

$$[\gamma_D] := \gamma_D^+ - \gamma_D^-, \qquad [\gamma_N] := \gamma_N^+ + \gamma_N^-. \tag{5.13}$$

Surface potentials Having defined the above volume potential, we can therefore define the so-called *single-layer* $\mathcal{S}_{d,\sigma}$ and *double-layer* $\mathcal{D}_{d,\sigma}$ potentials as

$$\mathcal{S}_{d,\sigma} := \mathcal{G}_{d,\sigma}\{\gamma_D^*\}, \qquad \mathcal{D}_{d,\sigma} := \mathcal{G}_{d,\sigma}\{\gamma_N^*\}. \tag{5.14}$$

One can give explicit representation of these operators, for any $\phi \in L^1(\Sigma)$, we have

$$\begin{aligned} \mathcal{S}_{d,\sigma}\phi(\mathbf{x}) &= \int_\Sigma \mathrm{G}_{d,\sigma}(|\mathbf{x}-\mathbf{y}|)\phi(\mathbf{y})\, \mathrm{d}\sigma(\mathbf{y}), \qquad \mathbf{x} \notin \Sigma \\ \mathcal{D}_{d,\sigma}\phi(\mathbf{x}) &= \int_\Sigma \nu(\mathbf{y}) \cdot \mathbf{grad}\, \mathrm{G}_{d,\sigma}(|\mathbf{x}-\mathbf{y}|)\phi(\mathbf{y})\, \mathrm{d}\sigma(\mathbf{y}), \qquad \mathbf{x} \notin \Sigma. \end{aligned} \tag{5.15}$$

The surface potentials enjoy the following *jump relations* [124, Th. 3.3.1]

$$\begin{aligned} [\gamma_D]\,\mathcal{S}_{d,\sigma} &= 0, \qquad [\gamma_D]\,\mathcal{D}_{d,\sigma} = \mathrm{Id}, \qquad \text{in } H^{1/2}(\Sigma), \\ [\gamma_N]\,\mathcal{S}_{d,\sigma} &= -\mathrm{Id}, \qquad [\gamma_N]\,\mathcal{D}_{d,\sigma} = 0, \qquad \text{in } H^{-1/2}(\Sigma). \end{aligned} \tag{5.16}$$

Let $u \in H^1(\Delta;\Omega_-) \times H^1_{\mathrm{loc}}(\Delta;\Omega_+)$ satisfying the homogeneous equation

$$\left(-\Delta + \sigma^2\right) u = 0, \qquad \text{in } \Omega_- \cup \Omega_+, \tag{5.17}$$

then we have the *representation formula* [124, Th. 3.1.8]

$$u = -\mathcal{S}_{d,\sigma}[\gamma_N]u + \mathcal{D}_{d,\sigma}[\gamma_D]u, \qquad \text{in } \Omega_- \cup \Omega_+. \tag{5.18}$$

In light of these results, one sees that the single layer and double layer potentials can be used as *ansatz* for the solution of some elliptic boundary value problem. In fact, this forms the basis of the so called *indirect* method to devise boundary integral equations as a reformulation of some boundary value problems.

Boundary integral operators We introduce the associated *single-layer* $V_{d,\sigma}$ and *hypersingular* $W_{d,\sigma}$ boundary integral operators

$$\begin{aligned} V_{d,\sigma} &:= \{\gamma_D\}\mathcal{S}_{d,\sigma} = \{\gamma_D\}\mathcal{G}_{d,\sigma}\{\gamma_D^*\}, \\ W_{d,\sigma} &:= \{\gamma_N\}\mathcal{D}_{d,\sigma} = \{\gamma_N\}\mathcal{G}_{d,\sigma}\{\gamma_N^*\}. \end{aligned} \tag{5.19}$$

Explicit integral representation of these operators are available. For $V_{d,\sigma}$ the integral representation is simply, as [124, Eq. (3.32)]

$$\langle V_{d,\sigma}\phi, \psi\rangle_\Sigma = \int_\Sigma \int_\Sigma \mathrm{G}_{d,\sigma}(|\mathbf{x}-\mathbf{y}|)\phi(\mathbf{y})\psi(\mathbf{x})\,\mathrm{d}\sigma(\mathbf{x})\mathrm{d}\sigma(\mathbf{y}). \tag{5.20}$$

The integral representation of $W_{d,\sigma}$ is more involved, we have [124, Cor. 3.324],

$$\begin{aligned} \langle W_{d,\sigma}\phi, \psi\rangle_\Sigma = \int_\Sigma \int_\Sigma \mathrm{G}_{d,\sigma}(|\mathbf{x}-\mathbf{y}|)\,[&\mathbf{curl}_\Sigma\,\phi(\mathbf{y})\cdot\mathbf{curl}_\Sigma\,\psi(\mathbf{x}) \\ &+\sigma^2(\nu(\mathbf{x})\cdot\nu(\mathbf{y}))\phi(\mathbf{y})\psi(\mathbf{x})]\;\mathrm{d}\sigma(\mathbf{x})\mathrm{d}\sigma(\mathbf{y}). \end{aligned} \tag{5.21}$$

The above integral representations make clear that the underlying operators are self-adjoint.

One can then prove that the boundary integral operators we introduced enjoy the following mapping properties [101, Th. 6.11] [124, Th. 3.1.16]

$$\begin{aligned} V_{d,\sigma} &: H^{-1/2}(\Sigma) \to H^{1/2}(\Sigma), \\ W_{d,\sigma} &: H^{1/2}(\Sigma) \to H^{-1/2}(\Sigma). \end{aligned} \tag{5.22}$$

These mapping properties can be understood, at least formally, from the definition (5.19). The operator $V_{d,\sigma}$ is the composition of, first the adjoint trace operator $\{\gamma_D^*\}$, which takes a trace in $H^{-1/2}(\Sigma)$ and lifts it in $H^{-1}_{\mathrm{comp}}(\mathbb{R}^d)$ losing half a degree of Sobolev regularity; then the volume potential $\mathcal{G}_{d,\sigma}$, which is a regularizing operator of order 2; and finally the trace operator $\{\gamma_D\}$, which takes an element of $H^1_{\mathrm{loc}}(\mathbb{R}^d)$ and computes its trace in $H^{1/2}(\Sigma)$ losing another half degree of regularity. For the operator $W_{d,\sigma}$, the reasoning is similar but now the trace operator $\{\gamma_N\}$ and its formal adjoint $\{\gamma_N^*\}$ are deregularizing of order $3/2$.

Moreover, we have the following coercivity results: the bilinear forms ($\sigma > 0$)

$$\begin{aligned} &\langle V_{d,\sigma}\cdot,\cdot\rangle \ : \ H^{1/2}(\Sigma)\times H^{1/2}(\Sigma)\to\mathbb{C},\\ &\langle W_{d,\sigma}\cdot,\cdot\rangle \ : \ H^{-1/2}(\Sigma)\times H^{-1/2}(\Sigma)\to\mathbb{C}, \end{aligned} \tag{5.23}$$

are coercive [124, Th. 3.5.4]. Besides, the bilinear forms ($\sigma = 0$)

$$\begin{aligned} &\langle V_{d,0}\cdot,\cdot\rangle \ : \ H^{1/2}(\Sigma)\times H^{1/2}(\Sigma)\to\mathbb{C},\\ &\langle W_{d,0}\cdot,\cdot\rangle \ : \ H^{-1/2}(\Sigma)/\mathbb{C}\times H^{-1/2}(\Sigma)/\mathbb{C}\to\mathbb{C}, \end{aligned} \tag{5.24}$$

are coercive [124, Th. 3.5.3]. The necessity to remove the constants for the operator $W_{d,0}$ is a manifestation of the non-uniqueness of solutions to the Neumann interior problem for the Laplace operator.

Equivalent transmission problems It is very instructive to see that the boundary integral operators $V_{d,\sigma}$ and $W_{d,\sigma}$ can be reinterpreted as (elliptic) transmission problems in the domain. Such results are obtained by exploiting the representation formula and the jump relations satisfied by the surface potentials.

Let $\mathrm{x}_0 \in H^{1/2}(\Sigma)$ and $\mathrm{x}_1 \in H^{-1/2}(\Sigma)$, we have for the boundary integral operator $V_{d,\sigma}$

$$\begin{aligned} &\mathrm{x}_0 = V_{d,\sigma}\mathrm{x}_1,\\ \Leftrightarrow\quad &\mathrm{x}_1 = \{\gamma_D\}u_0, \quad \text{where} \quad \begin{cases} u_0 \in H^1(\Omega_-)\times H^1(\Omega_+),\\ \left(-\Delta+\sigma^2\right)u_0 = 0, & \text{in } \Omega_-\cup\Omega_+,\\ [\gamma_D]u_0 = 0, & \text{on } \Sigma,\\ [\gamma_N]u_0 = -\mathrm{x}_1, & \text{on } \Sigma, \end{cases} \end{aligned} \tag{5.25}$$

and the boundary integral operator $W_{d,\sigma}$

$$\begin{aligned} &\mathrm{x}_1 = W_{d,\sigma}\mathrm{x}_0,\\ \Leftrightarrow\quad &\mathrm{x}_1 = \{\gamma_N\}u_1, \quad \text{where} \quad \begin{cases} u_1 \in H^1(\Omega_-)\times H^1(\Omega_+),\\ \left(-\Delta+\sigma^2\right)u_1 = 0, & \text{in } \Omega_-\cup\Omega_+,\\ [\gamma_D]u_1 = \mathrm{x}_0, & \text{on } \Sigma,\\ [\gamma_N]u_1 = 0, & \text{on } \Sigma. \end{cases} \end{aligned} \tag{5.26}$$

Transmission operators From the above discussion, we see that we have whole families of possible transmission operators at our disposal. The first two families of operators are the ones stemming from Bessel potentials ($\sigma > 0$), namely the following positive self-adjoint isomorphisms

$$\begin{aligned} &2\sigma\, V_{d,\sigma} \ : \ H^{-1/2}(\Sigma)\to H^{1/2}(\Sigma),\\ &\frac{2}{\sigma}\, W_{d,\sigma} \ : \ H^{1/2}(\Sigma)\to H^{-1/2}(\Sigma), \end{aligned} \tag{5.27}$$

respectively as a T_1 and a T_0-type operators. Note that we chose to rescale the operators by suitable constants (in part to make them dimensionless) and in fact we will often take in our numerical experiments $\sigma = \kappa_0$ where κ_0 is the wavenumber of the propagative problem we are trying to solve. It is clear by the above theory that any positive constant would work and we do not claim that this choice is optimal. However, this rescaling appears to be somehow sensible in

our numerical experiments and will be further motivated by the forthcoming modal analysis in spherical geometries.

Besides, one can consider the following positive self-adjoint isomorphisms resulting from Riesz potentials ($\sigma = 0$)

$$\begin{aligned} &2\kappa_0\, V_{d,0} \;:\; H^{-1/2}(\Sigma) \to H^{1/2}(\Sigma), \\ &\mathrm{Id} + \frac{2}{\kappa_0}\, W_{d,0} \;:\; H^{1/2}(\Sigma) \to H^{-1/2}(\Sigma), \end{aligned} \tag{5.28}$$

respectively as a T_1 and a T_0-type operators. Note that we had to add an identity term to ensure the injectivity of the operator constructed from $W_{d,0}$ (this is related to the kernel of the Laplace operator with Neumann boundary conditions). Again any other positive linear combinations of the two terms can be considered. To make the operators dimensionless, we chose to rescale them by the only characteristic length at our disposal, namely the wavenumber κ_0 of our original problem.

In previous works, only the operator which corresponds with our notations to $\sigma = 0$ and $\alpha\ \mathrm{Id} + \frac{4\beta}{\kappa_0}\, W_{d,0}$, α and β being two positive real parameters, is mentioned [44, Sec. 3.1.2]. We see that a larger class of operators is in fact available (in particular the choice $W_{d,\sigma}$, $\sigma > 0$ is interesting).

Comparison of Riesz and Bessel potentials The two kernels possess the same asymptotic behaviour at the origin $|\mathbf{x}| \sim 0$. Roughly speaking, this is because the strength of the associated singularity at $|\mathbf{x}| \sim 0$ is linked to the principal part of the differential operator, which is the same. As a result, the order of the corresponding pseudo-differential operator (behaviour at infinity $|\xi| \to +\infty$ in Fourier space) will be the same and the integral operators will have the mapping properties we are looking for.

The main difference between Bessel and Riesz potentials will come from the asymptotic behaviour at infinity $|\mathbf{x}| \to +\infty$. In the later case, we no longer have the exponential decay as $|\mathbf{x}|$ goes to $+\infty$. Qualitatively, this will entail a change of behaviour at the origin ($|\xi| \sim 0$ in Fourier space) of the associated pseudo-differential operator which will affect the propagative modes when we solve our boundary value problem. We shall see the implications of this more quantitatively when we will conduct a modal analysis on simple geometries. In particular, it will make things more complicated when trying to generalize this to the Maxwell setting.

Notice however that the analytical expressions of the Riesz kernels are somewhat simpler compared to their respective Bessel counterparts, in particular in view of numerical computations. Indeed, in practice during the actual assembly of the matrices associated to the integral operators, a substantial time is spent in the evaluation of the special functions of the kernels. In this respect, the Riesz potentials have a (slight) advantage.

Discussion of the practical use of these operators Using the above operators in a practical implementation of the domain decomposition method can be somehow advantageous since actual libraries to compute the boundary integral operators are already available, for instance BemTool[1]. Indeed, they are only a minor modifications (from the propagative to the dissipative version) of standard operators classically used to solve (mainly) unbounded scattering problems by means of integral equations.

The major drawback of these operators constructed from potential theory is their non-locality. To circumvent this issue, the operators built upon the Gagliardo semi-norms can be quasi-localized by truncation of the kernel so as to reduce the computational cost. Importantly this process retains the required properties of positivity and bijectivity. We could let the above

[1] https://github.com/xclaeys/BemTool

operator undergo the same kind of treatment and hope for the same result. However, we are then unfortunately unable to prove that the operator remains positive (the isomorphism property can be derived in the same manner as before). Other strategies could be considered, for instance the use of compression techniques such as $\mathcal{H}$-matrices. Still, on the analysis point of view, it remains to prove that the procedure does not damage the positivity (and bijectivity) of the operator. This difficulty motivates the next section.

5.1.2 Second strategy

In this section, we are set to construct an isomorphism so that

$$\begin{aligned} & \mathrm{T}_{1/2} \ : \ H^{1/2}(\Sigma) \to L^2(\Sigma), \\ \text{or} \quad & \mathrm{T}_{-1/2} \ : \ L^2(\Sigma) \to H^{-1/2}(\Sigma). \end{aligned} \tag{5.29}$$

A transmission operator T_0 or T_1 can then be constructed as

$$\begin{aligned} \mathrm{T}_0 &:= \mathrm{T}^*_{1/2}\mathrm{T}_{1/2} \ : \ H^{1/2}(\Sigma) \stackrel{\mathrm{T}_{1/2}}{\longrightarrow} L^2(\Sigma) \stackrel{\mathrm{T}^*_{1/2}}{\longrightarrow} H^{-1/2}(\Sigma), \\ \mathrm{T}_1 &:= \mathrm{T}^*_{-1/2}\mathrm{T}_{-1/2} \ : \ H^{-1/2}(\Sigma) \stackrel{\mathrm{T}_{-1/2}}{\longrightarrow} L^2(\Sigma) \stackrel{\mathrm{T}^*_{-1/2}}{\longrightarrow} H^{1/2}(\Sigma). \end{aligned} \tag{5.30}$$

By construction, these operators T_0 and T_1 will be self-adjoint and positive.

5.1.2.1 Gagliardo or Sobolev-Slobodetskii semi-norms

We mention briefly that it is again possible to use the integral representation of the Gagliardo or Sobolev-Slobodetskii semi-norms, this time on $H^{1/4}(\Sigma)$ [91, Chap. 5] and [44, Sec. 3.2.1] to provide a suitable transmission operator. Given any (dimensionless) positive parameters α and β, a possible operator is then,

$$(\mathrm{T}_{1/2}\phi,\psi)_\Sigma := \alpha \int_\Sigma \phi(\mathbf{x})\overline{\psi}(\mathbf{x})\,\mathrm{d}\sigma(\mathbf{x}) + \frac{\beta}{\sqrt{k}} \int_\Sigma \int_\Sigma \frac{\left(\phi(\mathbf{x})-\phi(\mathbf{y})\right)\left(\overline{\psi}(\mathbf{x})-\overline{\psi}(\mathbf{y})\right)}{|\mathbf{x}-\mathbf{y}|^{d-1/2}}\,\mathrm{d}\sigma(\mathbf{x})\mathrm{d}\sigma(\mathbf{y}). \tag{5.31}$$

For the case $d = 2$, it can be proven that this operator is indeed and isomorphism from $H^{1/2}(\Sigma)$ into $L^2(\Sigma)$, see [44, Lem. 3.3]. The result of the case $d = 3$ remains to be rigorously given.

We can again consider the truncated version of the above operator, defined by

$$\begin{aligned} (\mathrm{T}_{1/2,L}\phi,\psi)_\Sigma :=& \alpha \int_\Sigma \phi(\mathbf{x})\overline{\psi}(\mathbf{x})\,\mathrm{d}\sigma(\mathbf{x}) \\ &+ \frac{\beta}{\sqrt{k}} \int_\Sigma \int_\Sigma \chi\left(\frac{|\mathbf{x}-\mathbf{y}|}{L/2}\right) \frac{\left(\phi(\mathbf{x})-\phi(\mathbf{y})\right)\left(\overline{\psi}(\mathbf{x})-\overline{\psi}(\mathbf{y})\right)}{|\mathbf{x}-\mathbf{y}|^{d-1/2}}\,\mathrm{d}\sigma(\mathbf{x})\mathrm{d}\sigma(\mathbf{y}). \end{aligned} \tag{5.32}$$

The fact that this truncated operator (for $d = 2$) satisfies the requirement of the theory is given in [44, Th. 3.4].

5.1.2.2 Potential theory

The idea is to construct operators from potentials of fractional powers of the positive operator $(\sigma^2 - \Delta)^{s/2}$, $\sigma \geq 0$. The real s will be considered in the open interval $(1, 3)$. Indeed, there

actually exists an analytic expression of the associated fundamental solution [112, Ex. 2.2], for $s \neq d$,

$$\begin{aligned} \sigma > 0, \qquad & \mathrm{G}_{d,s,\sigma}(\mathbf{x}) := \frac{2^{1-s/2}}{(2\pi)^{d/2}\Gamma(\frac{s}{2})} \left(\frac{|\mathbf{x}|}{\sigma}\right)^{(s-d)/2} K_{|(s-d)/2|}(\sigma|\mathbf{x}|), \\ \sigma = 0, \qquad & \mathrm{G}_{d,s,0}(\mathbf{x}) := \frac{\Gamma(\frac{d-s}{2})}{2^s \pi^{d/2}\Gamma(\frac{s}{2})} \frac{1}{|\mathbf{x}|^{d-s}}, \end{aligned} \tag{5.33}$$

where K_ν is the modified Bessel function of the second kind [54, Sec. 10.25]. For the special case $s = d = 2$, the expressions were given in (5.7). At the origin these functions have the same asymptotic behaviour

$$\mathrm{G}_{d,s,\sigma} \sim \mathrm{G}_{d,s,0}, \qquad \text{as } r \to 0^+. \tag{5.34}$$

Besides, we have the following asymptotic behaviour at infinity

$$\mathrm{G}_{d,s,\sigma}(r) \ \sim \ \frac{1}{(2\pi)^{\frac{d-1}{2}} 2^{\frac{s}{2}}} \sigma^{-1} \left(\frac{\sigma}{r}\right)^{\frac{d-s+1}{2}} e^{-\sigma r}, \qquad \text{as } r \to +\infty. \tag{5.35}$$

It follows that $\mathrm{G}_{d,s,\sigma}$ is a locally integrable function and we can define the volume potential for any $f \in C_0^{+\infty}(\mathbb{R}^d)$ as

$$\mathcal{G}_{d,s,\sigma} f(\mathbf{x}) = \int_{\mathbb{R}^d} \mathrm{G}_{d,s,\sigma}(|\mathbf{x}-\mathbf{y}|) f(\mathbf{y}) \, \mathrm{d}y. \tag{5.36}$$

As far as we know, there does not exist a potential theory for fractional powers of the Yukawa (or Laplace) operator. Nevertheless, in view of the results that we already presented (which correspond to the case $s = 2$), we are led to define, at least formally, for $\sigma > 0$,

$$(V_{d,s,\sigma}\phi, \psi)_\Sigma = \sigma^{s-1} \int_\Sigma \int_\Sigma C_s \mathrm{G}_{d,s,\sigma}(|\mathbf{x}-\mathbf{y}|) \phi(\mathbf{y}) \psi(\mathbf{x}) \, \mathrm{d}\sigma(\mathbf{x}) \mathrm{d}\sigma(\mathbf{y}). \tag{5.37}$$

and

$$\begin{aligned} (W_{d,s,\sigma}\phi, \psi)_\Sigma = \sigma^{s-3} \int_\Sigma \int_\Sigma C_s \mathrm{G}_{d,s,\sigma}(|\mathbf{x}-\mathbf{y}|) \, [&\mathbf{curl}_\Sigma \, \phi(\mathbf{y}) \cdot \mathbf{curl}_\Sigma \, \psi(\mathbf{x}) \\ &+ \sigma^2 (\nu(\mathbf{x}) \cdot \nu(\mathbf{y})) \phi(\mathbf{y}) \psi(\mathbf{x})] \, \mathrm{d}\sigma(\mathbf{x}) \mathrm{d}\sigma(\mathbf{y}), \end{aligned} \tag{5.38}$$

with the renormalization constant

$$C_s = \frac{2\sqrt{\pi}\Gamma(\frac{s}{2})}{\Gamma(\frac{s-1}{2})}, \tag{5.39}$$

which is strictly positive if $s > 1$.

Remark 5.1. *The choice of this renormalization constant deserves some comments. It stems from the fact that the singularity of the kernel at the origin depends only on the difference $d - s$ and as a matter of fact we have*

$$\mathrm{G}_{d-1,s-1,\sigma} = C_s \mathrm{G}_{d,s,\sigma}. \tag{5.40}$$

It is therefore possible to provide an alternative interpretation of the above potentials. For $d = 3$, if we consider the case where Σ is a 2D plane, then the operator $V_{3,s,\sigma}$ defined above can be reinterpreted as exactly the potential associated to $(\sigma^2 - \Delta)^{(s-1)/2}$ on this plane. In Fourier space, we are then assured to have the correct scaling of the principal symbol of the integral operator, hence the desired asymptotic behavior, at least for this particular geometry. The modal

analysis for the sphere in 3D in the next chapter will actually prove that it is also the correct asymptotic for the spherical geometry, see in particular Proposition 6.36.

Besides, the renormalization includes the constants introduced in (5.27)*, so that we have*

$$V_{d,2,\sigma} = 2\sigma V_{d,\sigma}, \qquad \textit{and} \qquad W_{d,2,\sigma} = \frac{2}{\sigma} W_{d,\sigma}. \tag{5.41}$$

We expect the operator $V_{d,s,\sigma}$ (respectively $W_{d,s,\sigma}$) to be a pseudo differential operator of order $s-1$ (respectively $s-3$) for some real s. This suggests (but remains to be proved rigorously) that, for $\sigma > 0$,

$$\begin{aligned} &W_{d,5/2,\sigma} \ \text{ map continuously } H^{1/2}(\Sigma) \text{ into } L^2(\Sigma), \\ &V_{d,3/2,\sigma} \text{ map continuously } H^{-1/2}(\Sigma) \text{ into } L^2(\Sigma), \end{aligned} \tag{5.42}$$

so that they respectively make potential candidates for $\mathrm{T}_{1/2}$ or $\mathrm{T}_{-1/2}$-type transmission operators.

Static case For reasons previously exposed, we main be interested to consider the limit case $\sigma = 0$. Since the kernel $\mathrm{G}_{d,s,\sigma}$ is still defined for $\sigma = 0$, we can extend the definition of the previous operators as follows:

$$(V_{d,s,0}\phi, \psi)_\Sigma = {\kappa_0}^{s-1} \int_\Sigma \int_\Sigma C_s \mathrm{G}_{d,s,0}(|\mathbf{x}-\mathbf{y}|)\phi(\mathbf{y})\psi(\mathbf{x})\, \mathrm{d}\sigma(\mathbf{x})\mathrm{d}\sigma(\mathbf{y}). \tag{5.43}$$

and

$$(W_{d,s,0}\phi, \psi)_\Sigma = {\kappa_0}^{s-3} \int_\Sigma \int_\Sigma C_s \mathrm{G}_{d,s,0}(|\mathbf{x}-\mathbf{y}|)\, \mathbf{curl}_\Sigma\, \phi(\mathbf{y}) \cdot \mathbf{curl}_\Sigma\, \psi(\mathbf{x})\, \mathrm{d}\sigma(\mathbf{x})\mathrm{d}\sigma(\mathbf{y}). \tag{5.44}$$

Again, we expect the operator $V_{d,s,0}$ (respectively $W_{d,s,0}$) to be a pseudo differential operator of order $s-1$ (respectively $s-3$) for some real s. This suggests (but remains to be proved rigorously) that

$$\begin{aligned} &\mathrm{Id} + W_{d,5/2,0} \ \text{ map continuously } H^{1/2}(\Sigma) \text{ into } L^2(\Sigma), \\ &V_{d,3/2,0} \text{ map continuously } H^{-1/2}(\Sigma) \text{ into } L^2(\Sigma), \end{aligned} \tag{5.45}$$

so that they respectively make potential candidates for $\mathrm{T}_{1/2}$ or $\mathrm{T}_{-1/2}$-type transmission operators.

In [44, Sec. 3.1.2], the $\mathrm{T}_{1/2}$-type operator

$$\mathrm{Id} + \beta \mathrm{i}\, W_{d,5/2,0}, \tag{5.46}$$

is considered, where β is a real parameter, so that the T_0-type operator

$$\big(\mathrm{Id} + \mathrm{i}\beta\, W_{d,5/2,0}\big)^* \big(\mathrm{Id} + \mathrm{i}\beta\, W_{d,5/2,0}\big) = \mathrm{Id} + \beta^2\, W^*_{d,5/2,0} W_{d,5/2,0}, \tag{5.47}$$

is indeed a self-adjoint and positive operator, since $W^*_{d,5/2,0} - W_{d,5/2,0} = 0$ from the symmetry of $W_{d,5/2,0}$. For Σ smooth enough and in 2D only ($d = 2$), a proof that the operator

$$\alpha\, \mathrm{Id} + \tilde{\beta}\, W_{2,5/2,0} \ : \ H^{1/2}(\Sigma) \ \to \ L^2(\Sigma), \tag{5.48}$$

for two parameters $\alpha \in \mathbb{R}^*_+$ and $\tilde{\beta} \in \mathbb{C} \setminus \mathbb{R}_-$, is an isomorphism is given in [44, Lem. 3.7]. The proof assumes that Σ is $C^{1,\alpha}$ regular, $\alpha > 0$. The result is first proven for the circle, and then extended for a general curve using a compact perturbation technique.

5.1.3 Conclusion on possible transmission operators for Helmholtz

Because we considered many different candidate operators in our discussion above, we quickly sum up below which are the ones we find the most interesting.

The use of Gagliardo or Sobolev-Slobodetskii semi-norms was proposed in previous works, see the T_0-type operator in (5.4) and the $\mathrm{T}_{1/2}$-type operator in (5.32). The main interest of those operators is that we can prove that they retain their positivity and essential properties required for the convergence analysis even after truncation of their kernel. However, these operators are not commonly implemented and were as a result not considered in our numerical experiments.

Standard potential theory for the Helmholtz equation led us to suggest to use (for $\sigma > 0$)

$$\begin{array}{lll} 2\sigma\, V_{d,\sigma} & \text{or} \quad 2\kappa_0\, V_{d,0} & \text{as a } \mathrm{T}_1 \text{ operator,} \\ \dfrac{2}{\sigma}\, W_{d,\sigma} & \text{or} \quad \mathrm{Id} + \dfrac{2}{\kappa_0}\, W_{d,0} & \text{as a } \mathrm{T}_0 \text{ operator.} \end{array} \tag{5.49}$$

The operators $V_{d,\sigma}$ and $W_{d,\sigma}$ have integral representations given in (5.20) and (5.21) and are (or are close to operators) implemented in standard boundary element codes. However, we were not able to prove that they retain their properties if localization strategies or other compression techniques are applied to reduce their computational cost.

We will report several numerical results obtained using the operator ($d \in \{2, 3\}$)

$$\mathrm{T}_0^{\mathrm{Bessel}} = \frac{2}{\kappa_0}\, W_{d,\kappa_0} \tag{5.50}$$

in what follows.

Fractional powers of the Yukawa operator led us to suggest to use (for $\sigma > 0$)

$$\begin{array}{lll} W_{d,5/2,\sigma} & \text{or} \quad \mathrm{Id} + W_{d,5/2,0} & \text{as a } \mathrm{T}_{1/2} \text{ operator,} \\ V_{d,3/2,\sigma} & \text{or} \quad V_{d,3/2,0} & \text{as a } \mathrm{T}_{-1/2} \text{ operator.} \end{array} \tag{5.51}$$

See (5.37), (5.38), (5.43) and (5.44) for the variational definitions. These operators are in contrast less standard. Their kernels involve special functions that are costly to evaluate numerically and present non-classical (strong) singularities that require dedicated care in practical implementations. On the other hand, their are amenable to quasi-localization by truncation while retaining the required properties for the theory to apply.

Following [91], we tested in our numerical experiments in two-dimensions the operator

$$\mathrm{T}_0^{\mathrm{Riesz}} = \big(\mathrm{Id} + \mathrm{i}\, W_{2,5/2,0}\big)^* \big(\mathrm{Id} + \mathrm{i}\, W_{2,5/2,0}\big) = \mathrm{Id} + W_{2,5/2,0}^* W_{2,5/2,0}, \tag{5.52}$$

It is amenable to localization by truncation, while retaining the important properties required by the convergence analysis. This is why we tested this operator in our numerical experiments.

5.2 Electromagnetic setting

We now turn to the construction of suitable transmission operators for the (three-dimensional: $d = 3$) electromagnetic setting. The main idea is to try to generalize the operators that have been devised in the acoustic setting.

Unfortunately there is no obvious generalization of the operators constructed previously from the Gagliardo semi-norms. In fact, we are not aware of explicit integral representations for a semi-norm on $H^{-1/2}(\Sigma)$ to begin with. As a result, the integral operators that we are about to present are all built upon potential theory.

The main impediment we are faced with is that the transmission operator we wish to construct is not a (somewhat simple) pseudo differential operator of order 1 as it was the case in the acoustic setting. On the contrary, a suitable operator should be at the same time a pseudo differential of order 1 and -1 respectively for the two distinct components that make up a trace quantity. In fact, during our construction process we will need to keep in mind at all times the Helmholtz decomposition of trace fields and construct an operator whose action is opposite (in some sense) on the two components.

To explain this process in more detail, we first consider the simpler case of the half-space, for which we are able to understand more precisely what we need to do. In a second part, we will use standard potential theory for Maxwell's equations to provide a first class of possible transmission operators, for which we are unfortunately unable to provide a (quasi) localisation process that provably preserve positivity. In the last remaining section, we will construct an alternative that should be amenable to (quasi) localization with preserved positivity.

5.2.1 Fourier analysis on the half-space case

In this section we compute the Fourier symbol of a simple operator which has all the characteristics of the transmission operators we wish to construct: namely, self-adjointness, positivity and isomorphism. The simple geometrical setting allows for explicit computations which we found very instructive. Similar computations as the ones presented below can be found in [80, 87] for instance.

We consider the interface $\Sigma = \mathbb{R}^2 \times \{0\}$ separating the two half-spaces of $\mathbb{R}^3$ and we set $\Omega_+ := \mathbb{R}_2 \times \mathbb{R}^*_+$. The unit normal vector pointing outward of Ω is denoted ν. Let $\sigma > 0$ be a fixed positive real parameter. We then define the (dimensionless) positive self-adjoint isomorphism

$$\begin{aligned} \Lambda \ &: \mathbf{H}^{-1/2}(\mathrm{curl};\Sigma) \to \mathbf{H}^{-1/2}(\mathrm{div};\Sigma), \\ &\phi \mapsto \sigma^{-1}\gamma_\tau \, \mathbf{curl}\, \mathbf{u} \end{aligned} \tag{5.53}$$

where $\mathbf{u} \in \mathbf{H}(\mathbf{curl};\Omega_+)$ is the unique solution of

$$\begin{cases} \mathbf{curl}\,\mathbf{curl}\,\mathbf{u} + \sigma^2 \mathbf{u} = 0, & \text{in } \Omega_+, \\ \gamma_t \mathbf{u} = \phi, & \text{on } \Sigma. \end{cases} \tag{5.54}$$

The trace operators γ_τ and γ_t used above are to be understood as the continuous extensions to the space $\mathbf{H}(\mathbf{curl};\Omega_+)$ of the respective trace mappings defined for regular fields as $\mathbf{u} \mapsto \mathbf{u} \times \nu$ and $\mathbf{u} \mapsto \nu \times (\mathbf{u} \times \nu)$.

Let ϕ be any element of $\mathbf{H}^{-1/2}(\mathrm{curl};\Sigma)$ and $\mathbf{u} \in \mathbf{H}(\mathbf{curl};\Omega_+)$ be the solution of (5.54). First notice that $\mathbf{u}$ is equivalently solution of

$$\begin{cases} -\boldsymbol{\Delta}\mathbf{u} + \sigma^2 \mathbf{u} = 0, & \text{in } \Omega_+, \\ \mathrm{div}\,\mathbf{u} = 0, & \text{in } \Omega_+, \\ \gamma_t \mathbf{u} = \phi, & \text{on } \Sigma, \end{cases} \tag{5.55}$$

where $\boldsymbol{\Delta}$ is the (vectorial) Hodge-Laplacian operator.

To solve the above system, we perform a partial Fourier transform in the x_1 and x_2 directions. The Fourier transform of $\mathbf{u}$ (respectively ϕ) is denoted $\hat{\mathbf{u}} \equiv (\hat{u}_1, \hat{u}_2, \hat{u}_3)$ (respectively $\hat{\phi} \equiv (\hat{\phi}_1, \hat{\phi}_2)$). We find that

$$\begin{cases} -\frac{\mathrm{d}^2}{\mathrm{d}x_3^2}\hat{\mathbf{u}} + (\sigma^2 + |\mathbf{k}|^2)\,\hat{\mathbf{u}} = 0, \\ \mathrm{i}k_1\hat{u}_1 + \mathrm{i}k_2\hat{u}_2 + \frac{\mathrm{d}}{\mathrm{d}x_3}\hat{u}_3 = 0, \\ \hat{u}_1 = \hat{\phi}_1, \qquad \text{and} \qquad \hat{u}_2 = \hat{\phi}_2, \qquad \text{at} \qquad x_3 = 0, \end{cases} \tag{5.56}$$

where $\mathbf{k} \equiv (k_1, k_2)$ denotes the Fourier variable. It follows that

$$\begin{cases} \hat{u}_1 = \hat{\phi}_1 e^{-(\sigma^2+|\mathbf{k}|^2)^{1/2} x_3}, \\ \hat{u}_2 = \hat{\phi}_2 e^{-(\sigma^2+|\mathbf{k}|^2)^{1/2} x_3}, \\ \hat{u}_3 = (\sigma^2 + |\mathbf{k}|^2)^{-1/2} \left(\mathrm{i} k_1 \hat{\phi}_1 + \mathrm{i} k_2 \hat{\phi}_2 \right) e^{-(\sigma^2+|\mathbf{k}|^2)^{1/2} x_3}. \end{cases} \tag{5.57}$$

It is then a simple computation to show that the Fourier transform $\widehat{\Lambda\phi} \equiv ((\widehat{\Lambda\phi})_1, (\widehat{\Lambda\phi})_2)$ of $\Lambda\phi$ reads

$$\begin{cases} (\widehat{\Lambda\phi})_1 = \sigma^{-1}(\sigma^2 + |\mathbf{k}|^2)^{-1/2} \left[(\sigma^2 + k_2^2)\hat{\phi}_1 - k_1 k_2 \hat{\phi}_2 \right], \\ (\widehat{\Lambda\phi})_2 = \sigma^{-1}(\sigma^2 + |\mathbf{k}|^2)^{-1/2} \left[-k_1 k_2 \hat{\phi}_1 + (\sigma^2 + k_1^2)\hat{\phi}_2 \right]. \end{cases} \tag{5.58}$$

This yields the Fourier symbol of Λ which can be written in matrix form

$$\hat{\Lambda} = \sigma^{-1}(\sigma^2 + |\mathbf{k}|^2)^{-1/2} \begin{bmatrix} \sigma^2 + k_2^2 & -k_1 k_2 \\ -k_1 k_2 & \sigma^2 + k_1^2 \end{bmatrix} \tag{5.59}$$

It is possible to diagonalize the symbol on the basis given by the following normalised eigenvectors

$$\mathbf{e_{curl}} = |\mathbf{k}|^{-1} \begin{bmatrix} k_2 \\ -k_1 \end{bmatrix}, \qquad \mathbf{e_{grad}} = |\mathbf{k}|^{-1} \begin{bmatrix} k_1 \\ k_2 \end{bmatrix}, \tag{5.60}$$

with respective eigenvalues

$$\lambda_{\mathbf{curl}} = \sqrt{1 + \frac{|\mathbf{k}|^2}{\sigma^2}}, \qquad \lambda_{\mathbf{grad}} = \frac{1}{\sqrt{1 + \frac{|\mathbf{k}|^2}{\sigma^2}}}. \tag{5.61}$$

If we define the change of basis matrix

$$P = |\mathbf{k}|^{-1} \begin{bmatrix} -k_2 & k_1 \\ k_1 & k_2 \end{bmatrix} \tag{5.62}$$

we obtain the Fourier symbol of Λ in diagonalized form

$$\hat{\Lambda} = P \begin{bmatrix} \sqrt{1 + \frac{|\mathbf{k}|^2}{\sigma^2}} & \\ & \frac{1}{\sqrt{1 + \frac{|\mathbf{k}|^2}{\sigma^2}}} \end{bmatrix} P^T. \tag{5.63}$$

This simple computation on this simple geometry leads to make two crucial remarks, that remains true in a more general configuration:

- A natural decomposition of tangential fields, the so-called Helmholtz-Hodge decomposition, as a sum of a curl and a gradient should be considered;
- An isomorphism between the trace spaces $\mathbf{H}^{-1/2}(\mathrm{curl}; \Sigma)$ and $\mathbf{H}^{-1/2}(\mathrm{div}; \Sigma)$ should de-regularize (respectively regularize) the curl (respectively grad) part of the tangential field by exactly one order of Sobolev regularity.

Notice also that this operator behaves similarly as the identity operator for the low frequencies $|\mathbf{k}| \sim 0$ in Fourier space.

One readily sees from these remarks that the generalization to the electromagnetic setting of the previous work for the Helmholtz equation is a fairly delicate task.

5.2.2 Helmholtz-Hodge decomposition of trace spaces

For a simply connected and regular enough interface Σ, we have the following Helmholtz-Hodge decomposition

$$\begin{aligned} \mathbf{H}^{-1/2}(\mathrm{curl};\Sigma) &= \mathbf{grad}_\Sigma\, H^{1/2}(\Sigma) + \mathbf{curl}_\Sigma\, H^{3/2}(\Sigma), \\ \mathbf{H}^{-1/2}(\mathrm{div};\Sigma) &= \mathbf{grad}_\Sigma\, H^{3/2}(\Sigma) + \mathbf{curl}_\Sigma\, H^{1/2}(\Sigma). \end{aligned} \tag{5.64}$$

As we already hinted, this decomposition will play a central role in the construction of suitable transmission operators for Maxwell equations.

As we already mentioned, for a less regular interface Σ (in particular for polyhedra surfaces that we are naturally led to consider in this work), such a decomposition still holds but requires more involved concepts that we do not wish to introduce in this manuscript. We refer the interested reader to [22, Th. 2], [23, Th. 3.4], [85, Th. 2.2] and the references therein for more detail.

5.2.3 First strategy: using standard potential theory

In this section and the next one, we consider the boundary Σ of a bounded Lipschitz domain Ω^- subset of $\mathbb{R}^3$ (we are only interested in the three-dimensional case) and we set $\Omega^+ := \mathbb{R}^3 \setminus \overline{\Omega^-}$. We assume that the domain Ω is connected and simply connected (all its Betti numbers are zero) so that Σ is also connected and simply connected.

We are set to construct a self-adjoint positive isomorphism so that

$$\begin{aligned} & \mathrm{T}_0 \ : \ \mathbf{H}^{-1/2}(\mathrm{curl};\Sigma) \to \mathbf{H}^{-1/2}(\mathrm{div};\Sigma), \\ \text{or} \quad & \mathrm{T}_1 \ : \ \mathbf{H}^{-1/2}(\mathrm{div};\Sigma) \to \mathbf{H}^{-1/2}(\mathrm{curl};\Sigma). \end{aligned} \tag{5.65}$$

The above results on Helmholtz-Hodge decompositions of the trace spaces (and the simple computation in the half-space case) reveals that (at least formally) such an operator should de-regularize (respectively regularize) the curl (respectively grad) part of the tangential field by exactly one order of Sobolev regularity. We can write, schematically,

$$\begin{array}{ccc} \mathbf{H}^{-1/2}(\mathrm{curl};\Sigma) & = \mathbf{grad}_\Sigma\, H^{\frac{1}{2}} & + \mathbf{curl}_\Sigma\, H^{\frac{3}{2}} \\ \mathrm{T}_0 \big\downarrow & \overset{+1}{\searrow} & \overset{-1}{\searrow} \\ \mathbf{H}^{-1/2}(\mathrm{div};\Sigma) & = \mathbf{grad}_\Sigma\, H^{\frac{3}{2}} & + \mathbf{curl}_\Sigma\, H^{\frac{1}{2}} \end{array}$$

Again for Maxwell equations we will rely on potential theory. This idea was already investigated in a work prior to this thesis which can be found in [34]. Note that in this latter work the operator that was proposed was continuous from $\mathbf{H}^{-1/2}(\mathrm{div};\Sigma)$ to $\mathbf{H}^{-1/2}(\mathrm{curl};\Sigma)$ which therefore corresponds in our parlance to an operator T_1.

The potential theory for Maxwell's equation rests on the one established for the scalar case. Indeed, the Cartesian components of Maxwell solutions satisfy the scalar Helmholtz equation with Sommerfeld radiation condition [46, Th. 6.4 and 6.7]. We are interested by a coercive version of this theory but the main principles are the same.

Volume potential From the fundamental solution of Yukawa equation, we are able to define the following *vectorial* volume potential, for any $\mathbf{f} \in C_0^{+\infty}(\mathbb{R}^3)^3$ as an improper integral as follows

$$\boldsymbol{\mathcal{G}}_{3,\sigma} f(\mathbf{x}) := \int_{\mathbb{R}^3} \mathrm{G}_{3,\sigma}(|\mathbf{x}-\mathbf{y}|)\mathbf{f}(\mathbf{y})\,\mathrm{d}y, \qquad \forall \mathbf{x} \in \mathbb{R}^3. \tag{5.66}$$

This potential can be extended to elements of $H^{-1}_{\rm comp}(\mathbb{R}^3)^3$ and defines then a continuous mapping so that [25, Lem. 4]

$$\boldsymbol{\mathcal{G}}_{3,\sigma} \ : \ H^{-1}_{\rm comp}(\mathbb{R}^3)^3 \to H^{1}_{\rm loc}(\mathbb{R}^3)^3. \tag{5.67}$$

Trace operators We first define the tangential trace operator γ_t^- (respectively γ_t^+) as the interior (respectively exterior) trace operator which is the natural extension to elements of $\mathbf{H}(\mathbf{curl};\Omega_-)$ (respectively $\mathbf{H}(\mathbf{curl};\Omega_+)$) of the operator

$$u \mapsto \nu \times (u|_\Sigma \times \nu), \tag{5.68}$$

for regular fields.

We also introduce the trace operator γ_τ^- (respectively γ_τ^+) as the interior (respectively exterior) trace operator which is the natural extension to elements of $\mathbf{H}(\mathbf{curl}^2;\Omega_-)$ (respectively $\mathbf{H}(\mathbf{curl}^2;\Omega_+)$) of the operator

$$\begin{aligned} & u \mapsto (\mathbf{curl}\, u)|_\Sigma \times \nu, \\ (\text{respectively} \qquad & u \mapsto -(\mathbf{curl}\, u)|_\Sigma \times \nu), \end{aligned} \tag{5.69}$$

for regular fields.

In addition, let us denote by $\{\boldsymbol{\gamma}_t\}$ and $\{\boldsymbol{\gamma}_\tau\}$ the two-sided trace operators defined respectively as

$$\{\boldsymbol{\gamma}_t\} := \frac{1}{2}\left(\gamma_t^- + \gamma_t^+\right), \qquad \{\boldsymbol{\gamma}_\tau\} := \frac{1}{2}\left(\gamma_\tau^- - \gamma_\tau^+\right). \tag{5.70}$$

Besides, let us denote by $[\boldsymbol{\gamma}_t]$ and $[\boldsymbol{\gamma}_\tau]$ the jump of the trace operators defined respectively as

$$[\boldsymbol{\gamma}_t] := \gamma_t^+ - \gamma_t^-, \qquad [\boldsymbol{\gamma}_N] := \gamma_\tau^+ + \gamma_\tau^-. \tag{5.71}$$

Surface potentials We introduce the *vectorial* single-layer potential $\boldsymbol{\mathcal{S}}_{3,\sigma}$, extension to vectorial fields of the scalar single-layer potential $\mathcal{S}_\sigma$ acting on each of the Cartesian components so that

$$\boldsymbol{\Delta}\boldsymbol{\mathcal{S}}_{3,\sigma} = \sigma^2 \boldsymbol{\mathcal{S}}_{3,\sigma}. \tag{5.72}$$

It follows that this surface potential admits the following explicit representation, for any $\boldsymbol{\phi} \in L^1(\Sigma)^3$,

$$\boldsymbol{\mathcal{S}}_{3,\sigma}\boldsymbol{\phi}(\mathbf{x}) = \int_\Sigma \mathrm{G}_{3,\sigma}(|\mathbf{x}-\mathbf{y}|)\boldsymbol{\phi}(\mathbf{y})\, \mathrm{d}\sigma(\mathbf{y}), \qquad \mathbf{x} \notin \Sigma. \tag{5.73}$$

Besides, we introduce the two vectorial potentials

$$\begin{aligned} &\boldsymbol{\mathcal{T}}_{3,\sigma} := \sigma\, \boldsymbol{\mathcal{S}}_{3,\sigma} - \sigma^{-1}\ \mathbf{grad}\,\mathrm{div}\ \boldsymbol{\mathcal{S}}_{3,\sigma}, \\ &\boldsymbol{\mathcal{K}}_{3,\sigma} := \mathbf{curl}\ \boldsymbol{\mathcal{S}}_{3,\sigma}\ (\nu\times). \end{aligned} \tag{5.74}$$

Using the relation [25, Lem. 5]

$$\mathrm{div}\, \boldsymbol{\mathcal{S}}_{3,\sigma} = \mathcal{S}_\sigma\, \mathrm{div}_\Sigma, \tag{5.75}$$

we obtain an alternative expression for $\boldsymbol{\mathcal{T}}_{3,\sigma}$

$$\boldsymbol{\mathcal{T}}_{3,\sigma} = \sigma\, \boldsymbol{\mathcal{S}}_{3,\sigma} - \sigma^{-1}\ \mathbf{grad}\ \mathcal{S}_\sigma\ \mathrm{div}_\Sigma\,. \tag{5.76}$$

The surface potentials enjoy the following *jump relations* [25, Th. 7]

$$\begin{aligned} &[\boldsymbol{\gamma}_t]\, \boldsymbol{\mathcal{T}}_{3,\sigma} = 0, && [\boldsymbol{\gamma}_t]\, \boldsymbol{\mathcal{K}}_{3,\sigma} = -\mathrm{Id}, && \text{in } \mathbf{H}^{-1/2}(\mathrm{curl};\Sigma), \\ &[\boldsymbol{\gamma}_\tau]\, \boldsymbol{\mathcal{T}}_{3,\sigma} = -\sigma\,\mathrm{Id}, && [\boldsymbol{\gamma}_\tau]\, \boldsymbol{\mathcal{K}}_{3,\sigma} = 0, && \text{in } \mathbf{H}^{-1/2}(\mathrm{div};\Sigma). \end{aligned} \tag{5.77}$$

Let $u \in \mathbf{H}(\mathbf{curl}^2;\Omega_-)\times\mathbf{H}_{\rm loc}(\mathbf{curl}^2;\Omega_+)$ satisfying the homogeneous equation (and Silver-Müller radiation condition at infinity)

$$\left(\mathbf{curl}\,\mathbf{curl}+\sigma^2\right)u=0, \qquad \text{in } \Omega_-\cup\Omega_+, \tag{5.78}$$

then we have the Stratton-Chu *representation formula* [25, Th. 6]

$$u=-\sigma^{-1}\,\boldsymbol{\mathcal{T}}_{3,\sigma}[\boldsymbol{\gamma}_\tau]u-\boldsymbol{\mathcal{K}}_{3,\sigma}[\boldsymbol{\gamma}_t]u, \qquad \text{in } \Omega_-\cup\Omega_+. \tag{5.79}$$

Boundary integral operators From the potential $\boldsymbol{\mathcal{S}}_{3,\sigma}$ we can define the vectorial single-layer $\mathbf{V}_{3,\sigma}$ boundary integral operator

$$\mathbf{V}_{3,\sigma}:=\{\boldsymbol{\gamma}_t\}\,\boldsymbol{\mathcal{S}}_{3,\sigma}. \tag{5.80}$$

An explicit integral representation of the operator $\mathbf{V}_{3,\sigma}$ is available: we have

$$\langle\mathbf{V}_{3,\sigma}\boldsymbol{\phi},\boldsymbol{\psi}\rangle_\Sigma=\int_\Sigma\int_\Sigma \mathrm{G}_{3,\sigma}(|\mathbf{x}-\mathbf{y}|)\boldsymbol{\phi}(\mathbf{y})\cdot\boldsymbol{\psi}(\mathbf{x})\,\mathrm{d}\sigma(\mathbf{x})\mathrm{d}\sigma(\mathbf{y}). \tag{5.81}$$

From the potentials $\boldsymbol{\mathcal{T}}_{3,\sigma}$ and $\boldsymbol{\mathcal{K}}_{3,\sigma}$, we introduce the boundary integral operators

$$\begin{aligned}\mathbf{U}_{3,\sigma}&:=\{\boldsymbol{\gamma}_t\}\,\boldsymbol{\mathcal{T}}_{3,\sigma},\\ \mathbf{K}_{3,\sigma}&:=\sigma^{-1}\,\{\boldsymbol{\gamma}_\tau\}\,\boldsymbol{\mathcal{K}}_{3,\sigma}.\end{aligned} \tag{5.82}$$

Using the relation $\gamma_t\,\mathbf{grad}=\mathbf{grad}_\Sigma\,\gamma_D$ we obtain

$$\begin{aligned}\mathbf{U}_{3,\sigma}&:=\sigma\,\mathbf{V}_{3,\sigma}-\sigma^{-1}\,\mathbf{grad}_\Sigma\,V_\sigma\,\mathrm{div}_\Sigma,\\ \mathbf{K}_{3,\sigma}&:=\sigma\,(\nu\times)\,\mathbf{V}_{3,\sigma}\,(\nu\times)-\sigma^{-1}\,\mathbf{curl}_\Sigma\,V_\sigma\,\mathrm{curl}_\Sigma\end{aligned} \tag{5.83}$$

and in fact these two operators are linked by the relation

$$\mathbf{K}_{3,\sigma}=(\nu\times)\,\mathbf{U}_{3,\sigma}\,(\nu\times). \tag{5.84}$$

Explicit integral representations of the boundary integral operators are available (although not trivial to establish). For the operator $\mathbf{U}_{3,\sigma}$, we have

$$\begin{aligned}\langle\mathbf{U}_{3,\sigma}\boldsymbol{\phi},\boldsymbol{\psi}\rangle_\Sigma=\sigma&\int_\Sigma\int_\Sigma \mathrm{G}_{3,\sigma}(|\mathbf{x}-\mathbf{y}|)\,\boldsymbol{\phi}(\mathbf{y})\cdot\boldsymbol{\psi}(\mathbf{x})\,\mathrm{d}\sigma(\mathbf{x})\mathrm{d}\sigma(\mathbf{y})\\ &+\sigma^{-1}\int_\Sigma\int_\Sigma \mathrm{G}_{3,\sigma}(|\mathbf{x}-\mathbf{y}|)\,\mathrm{div}_\Sigma\,\boldsymbol{\phi}(\mathbf{y})\,\mathrm{div}_\Sigma\,\boldsymbol{\psi}(\mathbf{x})\,\mathrm{d}\sigma(\mathbf{x})\mathrm{d}\sigma(\mathbf{y}).\end{aligned} \tag{5.85}$$

And for the operator $\mathbf{K}_{3,\sigma}$ we have

$$\begin{aligned}\langle\mathbf{K}_{3,\sigma}\boldsymbol{\phi},\boldsymbol{\psi}\rangle_\Sigma=\sigma&\int_\Sigma\int_\Sigma \mathrm{G}_{3,\sigma}(|\mathbf{x}-\mathbf{y}|)\,(\nu(\mathbf{y})\times\boldsymbol{\phi}(\mathbf{y}))\cdot(\nu(\mathbf{x})\times\boldsymbol{\psi}(\mathbf{x}))\,\mathrm{d}\sigma(\mathbf{x})\mathrm{d}\sigma(\mathbf{y})\\ &+\sigma^{-1}\int_\Sigma\int_\Sigma \mathrm{G}_{3,\sigma}(|\mathbf{x}-\mathbf{y}|)\,\mathrm{curl}_\Sigma\,\boldsymbol{\phi}(\mathbf{y})\,\mathrm{curl}_\Sigma\,\boldsymbol{\psi}(\mathbf{x})\,\mathrm{d}\sigma(\mathbf{x})\mathrm{d}\sigma(\mathbf{y}).\end{aligned} \tag{5.86}$$

The above integral representations make clear that the operators $\mathbf{U}_{3,\sigma}$ and $\mathbf{K}_{3,\sigma}$ are self-adjoint. Besides, one can prove that they are positive isomorphisms between the trace spaces

$$\begin{aligned}\mathbf{U}_{3,\sigma}&:\mathbf{H}^{-1/2}(\mathrm{div};\Sigma)\to\mathbf{H}^{-1/2}(\mathrm{curl};\Sigma),\\ \mathbf{K}_{3,\sigma}&:\mathbf{H}^{-1/2}(\mathrm{curl};\Sigma)\to\mathbf{H}^{-1/2}(\mathrm{div};\Sigma),\end{aligned} \tag{5.87}$$

which follows from the coerciveness of the bilinear form ($\sigma > 0$)

$$\begin{aligned} &\langle \mathbf{U}_{3,\sigma}\cdot,\cdot\rangle \;:\; \mathbf{H}^{-1/2}(\mathrm{div};\Sigma)\times\mathbf{H}^{-1/2}(\mathrm{div};\Sigma)\to\mathbb{C},\\ &\langle \mathbf{K}_{3,\sigma}\cdot,\cdot\rangle \;:\; \mathbf{H}^{-1/2}(\mathrm{curl};\Sigma)\times\mathbf{H}^{-1/2}(\mathrm{curl};\Sigma)\to\mathbb{C}. \end{aligned} \tag{5.88}$$

Roughly speaking, one can see the operator $\mathbf{U}_{3,\sigma}$ as a dissipative (or coercive) counterpart of the boundary integral operator classically referred to as the EFIE operator. On the other hand, the operator $\mathbf{K}_{3,\sigma}$ (or rather its propagative version) is the basis of operator (or Calderón) preconditioning of the previous EFIE operator, even though the discretization of the preconditioner is a rather tricky task. We mention this to point out that such operators are therefore already well-known in the integral equation community. Besides, similarly as for the scalar case, several libraries are available to compute matrix representation of these operators using standard boundary elements.

Note that because of the relation (5.84), the matrix representations in the basis given respectively by standard (low order) Raviart-Thomas and Nedelec boundary elements of the two operators $\mathbf{U}_{3,\sigma}$ and $\mathbf{K}_{3,\sigma}$ are the same. We shall comment more on this when we consider discretization strategies.

Equivalent transmission problems Exploiting the representation formula and the jump relations satisfied by the surface potentials we can again reinterpret the action of the boundary integral operator $\mathbf{U}_{3,\sigma}$ as (elliptic) transmission problems in the domain.

Let $\mathrm{x}_0 \in \mathbf{H}^{-1/2}(\mathrm{curl};\Sigma)$ and $\mathrm{x}_1 \in \mathbf{H}^{-1/2}(\mathrm{div};\Sigma)$, we have for the boundary integral operator $V_{3,\sigma}$

$$\begin{aligned} &\mathrm{x}_0 = \mathbf{U}_{3,\sigma}\mathrm{x}_1,\\ \Leftrightarrow\quad &\mathrm{x}_0 = \{\boldsymbol{\gamma}_t\}u_0, \quad \text{where} \quad \begin{cases} u_0 \in \mathbf{H}(\mathbf{curl};\Omega_-)\times\mathbf{H}(\mathbf{curl};\Omega_+),\\ \left(\mathbf{curl}\,\mathbf{curl} + \sigma^2\right) u_0 = 0, & \text{in } \Omega_-\cup\Omega_+,\\ [\boldsymbol{\gamma}_t]u_0 = 0, & \text{on } \Sigma,\\ \sigma^{-1}[\boldsymbol{\gamma}_\tau]u_0 = -\mathrm{x}_1, & \text{on } \Sigma, \end{cases} \end{aligned} \tag{5.89}$$

and the boundary integral operator $\mathbf{K}_{3,\sigma}$

$$\begin{aligned} &\mathrm{x}_1 = \mathbf{K}_{3,\sigma}\mathrm{x}_0,\\ \Leftrightarrow\quad &\mathrm{x}_1 = \sigma^{-1}\{\boldsymbol{\gamma}_\tau\}u_1, \quad \text{where} \quad \begin{cases} u_1 \in \mathbf{H}(\mathbf{curl};\Omega_-)\times\mathbf{H}(\mathbf{curl};\Omega_+),\\ \left(\mathbf{curl}\,\mathbf{curl} + \sigma^2\right) u_1 = 0, & \text{in } \Omega_-\cup\Omega_+,\\ [\boldsymbol{\gamma}_t]u_1 = -\mathrm{x}_0, & \text{on } \Sigma,\\ [\boldsymbol{\gamma}_\tau]u_1 = 0, & \text{on } \Sigma. \end{cases} \end{aligned} \tag{5.90}$$

Transmission operators The above results encourage us to propose the following (rescaled) operators

$$\begin{aligned} &2\,\mathbf{U}_{3,\sigma} \;:\; \mathbf{H}^{-1/2}(\mathrm{div};\Sigma)\to\mathbf{H}^{-1/2}(\mathrm{curl};\Sigma),\\ &2\,\mathbf{K}_{3,\sigma} \;:\; \mathbf{H}^{-1/2}(\mathrm{curl};\Sigma)\to\mathbf{H}^{-1/2}(\mathrm{div};\Sigma), \end{aligned} \tag{5.91}$$

respectively as a T_1 and a T_0-type operators. This last operator is the one that we used in our numerical experiments.

It is easy to see that yet another operator could be a suitable candidate, which is the operator admitting the following explicit integral representation,

$$\begin{aligned}\langle \check{\mathbf{K}}_\sigma \boldsymbol{\phi}, \boldsymbol{\psi} \rangle_\Sigma = 2\sigma \int_\Sigma \int_\Sigma \mathrm{G}_{3,\sigma}(|\mathbf{x}-\mathbf{y}|)\ \boldsymbol{\phi}(\mathbf{y}) \cdot \boldsymbol{\psi}(\mathbf{x})\ \mathrm{d}\sigma(\mathbf{x})\mathrm{d}\sigma(\mathbf{y}) \\ + 2\sigma^{-1} \int_\Sigma \int_\Sigma \mathrm{G}_{3,\sigma}(|\mathbf{x}-\mathbf{y}|)\ \mathrm{curl}_\Sigma\, \boldsymbol{\phi}(\mathbf{y})\, \mathrm{curl}_\Sigma\, \boldsymbol{\psi}(\mathbf{x})\ \mathrm{d}\sigma(\mathbf{x})\mathrm{d}\sigma(\mathbf{y}).\end{aligned} \tag{5.92}$$

This operator is slightly less common than the previous ones, which is the only reason why we did not use it in our numerical experiments.

We mentioned previously that a domain decomposition method based on similar non-local operators for electromagnetic scattering was already proposed in [34] (in the simple spherical geometry which allows explicit calculus by means of separation of variables). Since their formulation involved an operator from $\mathbf{H}^{-1/2}(\mathrm{div};\Sigma)$ to $\mathbf{H}^{-1/2}(\mathrm{curl};\Sigma)$, the authors suggested to use the transmission operator $2\,\mathbf{U}_{3,\sigma}$.

Static case By mimicking what has been done in the scalar setting, we could be tempted to propose the operator arising from the limit case $\sigma = 0$. However, it is clear from the above explicit integral representations that the operators are simply not defined for $\sigma = 0$. Nevertheless, since the kernel $\mathrm{G}_{3,0}$ still makes sense, we could consider (slightly abusing notation),

$$\begin{aligned}\langle 2\,\mathbf{K}_{3,0} \boldsymbol{\phi}, \boldsymbol{\psi} \rangle_\Sigma = 2\kappa_0 \int_\Sigma \int_\Sigma \mathrm{G}_{3,0}(|\mathbf{x}-\mathbf{y}|)\ (\nu(\mathbf{y}) \times \boldsymbol{\phi}(\mathbf{y})) \cdot (\nu(\mathbf{x}) \times \boldsymbol{\psi}(\mathbf{x}))\ \mathrm{d}\sigma(\mathbf{x})\mathrm{d}\sigma(\mathbf{y}) \\ + 2{\kappa_0}^{-1} \int_\Sigma \int_\Sigma \mathrm{G}_{3,0}(|\mathbf{x}-\mathbf{y}|)\ \mathrm{curl}_\Sigma\, \boldsymbol{\phi}(\mathbf{y})\, \mathrm{curl}_\Sigma\, \boldsymbol{\psi}(\mathbf{x})\ \mathrm{d}\sigma(\mathbf{x})\mathrm{d}\sigma(\mathbf{y}).\end{aligned} \tag{5.93}$$

Of course, the other variants discussed above could be considered, as well as other (positive) linear combinations.

As we shall understand from the modal analysis presented in the next chapter, the above operator does not have an adequate behaviour for propagative modes, even tough it is perfectly sound choice as far as the theoretical requirements are concerned.

5.2.4 Second strategy: quasi-localizable operators

In this section, we are set to construct an isomorphism so that

$$\begin{aligned} & \mathrm{T}_{1/2} \ :\ \mathbf{H}^{-1/2}(\mathrm{curl};\Sigma) \to \mathbf{L}^2_t(\Sigma), \\ \text{or} \quad & \mathrm{T}_{-1/2} \ :\ \mathbf{L}^2_t(\Sigma) \to \mathbf{H}^{-1/2}(\mathrm{div};\Sigma). \end{aligned} \tag{5.94}$$

A transmission operator T_0 or T_1 can then be constructed as

$$\begin{aligned} & \mathrm{T}_0 := \mathrm{T}^*_{1/2}\mathrm{T}_{1/2} \ :\ \mathbf{H}^{-1/2}(\mathrm{curl};\Sigma) \xrightarrow{\mathrm{T}_{1/2}} \mathbf{L}^2_t(\Sigma) \xrightarrow{\mathrm{T}^*_{1/2}} \mathbf{H}^{-1/2}(\mathrm{div};\Sigma), \\ & \mathrm{T}_1 := \mathrm{T}^*_{-1/2}\mathrm{T}_{-1/2} \ :\ \mathbf{H}^{-1/2}(\mathrm{div};\Sigma) \xrightarrow{\mathrm{T}_{-1/2}} \mathbf{L}^2_t(\Sigma) \xrightarrow{\mathrm{T}^*_{-1/2}} \mathbf{H}^{-1/2}(\mathrm{curl};\Sigma). \end{aligned} \tag{5.95}$$

By construction, these operators T_0 and T_1 will be self-adjoint and positive. The main interest in considering this alternative route is to be able to apply the quasi-localization process by truncation of the kernel that was described previously.

According to the Helmholtz-Hodge decomposition we can write, schematically,

$$
\mathrm{T}_0 = \mathrm{T}^*_{1/2}\mathrm{T}_{1/2}
\left(\begin{array}{lcl}
\mathbf{H}^{-1/2}(\mathrm{curl};\Sigma) & = & \mathbf{grad}_\Sigma\, H^{\frac{1}{2}} + \mathbf{curl}_\Sigma\, H^{\frac{3}{2}} \\
\mathrm{T}_{1/2}\downarrow & & \searrow^{+\frac{1}{2}} \qquad \searrow^{-\frac{1}{2}} \\
\mathbf{L}^2_t(\Sigma) & = & \mathbf{grad}_\Sigma\, H^{1} + \mathbf{curl}_\Sigma\, H^{1} \\
\mathrm{T}^*_{1/2}\downarrow & & \searrow^{+\frac{1}{2}} \qquad \searrow^{-\frac{1}{2}} \\
\mathbf{H}^{-1/2}(\mathrm{div};\Sigma) & = & \mathbf{grad}_\Sigma\, H^{\frac{3}{2}} + \mathbf{curl}_\Sigma\, H^{\frac{1}{2}}
\end{array}\right)
$$

Vector potentials of the fractional Yukawa operator The construction of candidate transmission operators $\mathrm{T}_{1/2}$ will be based again on potentials of the fractional powers of the Yukawa positive operator $(\sigma^2 - \Delta)^{s/2}$, $\sigma \geq 0$ and $s \in (1,3)$.

The previous analysis led us to introduce three potentials, all based on the fundamental solution $\mathrm{G}_{d,s,\sigma}$ defined in (5.33). We define, for $\sigma > 0$

$$
\begin{aligned}
\langle \mathbf{V}_{3,s,\sigma}\boldsymbol{\phi}, \boldsymbol{\psi}\rangle_\Sigma &:= {\kappa_0}^{s-1} \int_\Sigma\int_\Sigma C_s \mathrm{G}_{3,s,\sigma}(|\mathbf{x}-\mathbf{y}|)\boldsymbol{\phi}(\mathbf{y})\cdot\boldsymbol{\psi}(\mathbf{x})\ \mathrm{d}\sigma(\mathbf{x})\mathrm{d}\sigma(\mathbf{y}), \\
\langle \mathbf{Q}^G_{3,s,\sigma}\boldsymbol{\phi}, \boldsymbol{\psi}\rangle_\Sigma &:= {\kappa_0}^{s-3} \int_\Sigma\int_\Sigma C_s \mathrm{G}_{3,s,\sigma}(|\mathbf{x}-\mathbf{y}|)\,\mathrm{div}_\Sigma\,\boldsymbol{\phi}(\mathbf{y})\,\mathrm{div}_\Sigma\,\boldsymbol{\psi}(\mathbf{x})\ \mathrm{d}\sigma(\mathbf{x})\mathrm{d}\sigma(\mathbf{y}), \\
\langle \mathbf{Q}^C_{3,s,\sigma}\boldsymbol{\phi}, \boldsymbol{\psi}\rangle_\Sigma &:= {\kappa_0}^{s-3} \int_\Sigma\int_\Sigma C_s \mathrm{G}_{3,s,\sigma}(|\mathbf{x}-\mathbf{y}|)\,\mathrm{curl}_\Sigma\,\boldsymbol{\phi}(\mathbf{y})\,\mathrm{curl}_\Sigma\,\boldsymbol{\psi}(\mathbf{x})\ \mathrm{d}\sigma(\mathbf{x})\mathrm{d}\sigma(\mathbf{y}),
\end{aligned}
\tag{5.96}
$$

with the renormalization constant (see Remark 5.1),

$$
C_s = \frac{2\sqrt{\pi}\Gamma(\frac{s}{2})}{\Gamma(\frac{s-1}{2})}, \tag{5.97}
$$

which is strictly positive if $s > 1$.

Because of the positivity of the operator from which they are built, these potentials will remain positive. We expect (but it remains to prove it rigorously) that, for some real s

$$
\begin{aligned}
&\mathbf{V}_{3,s,\sigma} \text{ is an operator or order } 1-s, \\
&\mathbf{Q}^G_{3,s,\sigma} \text{ is an operator or order } 3-s, \text{ selectively acting on the } \mathbf{grad}_\Sigma \text{ part}, \\
&\mathbf{Q}^C_{3,s,\sigma} \text{ is an operator or order } 3-s, \text{ selectively acting on the } \mathbf{curl}_\Sigma \text{ part}.
\end{aligned}
\tag{5.98}
$$

Of course, since we want to deal with fields that are not particularly regular, we will not be able to choose too large values for s. To continue the discussion below, we assume that the above conjecture holds true.

5.2.4.1 First ideas

Many different operators can be constructed from these ingredients and we have considered many variants.

Perhaps the first operator that comes to mind is $\sigma > 0$

$$
\mathbf{V}_{3,3/2,\sigma} + \mathbf{Q}^C_{3,5/2,\sigma}. \tag{5.99}
$$

To see why this could be a valid candidate, notice that the first term is regularising of half an order $(-\frac{1}{2})$ while the second term is de-regularising of half an order $(+\frac{1}{2})$, but acts only on the $\mathbf{curl}_\Sigma$ part of the tangential fields. The principal term for the $\mathbf{grad}_\Sigma$ part will be the first one, while for the $\mathbf{curl}_\Sigma$ part it will be the second term. Notice that any other linear combination

could be considered in (5.99), which would give two (strictly positive) additional parameters to tweak. We do not feature such parameters explicitly here and in the following for the sake of simplicity.

In the same spirit, if we were to construct an operator $\mathrm{T}_{-1/2}$, one could propose

$$\mathbf{V}_{3,5/2,\sigma} + \mathbf{Q}^G_{3,3/2,\sigma}. \tag{5.100}$$

The operators from (5.99) or (5.100) could be used in practice. However, they have two main drawbacks. The first one comes from the special function of the kernel of $\mathrm{G}_{d,s,\sigma}$ which is expensive to evaluate numerically. The second issue comes from the singularity of the two kernels involved, which are (in three dimensions) of strength $\frac{3}{2}$ and $\frac{1}{2}$. These types of singularities are not-standard and require special quadrature rules. Besides, a singularity of order $\frac{3}{2}$ is quite severe and would require very special care to be evaluated numerically with accuracy.

Riesz potentials To address the first issue it was proposed in the scalar setting to consider the limit case $\sigma = 0$, hence another candidate is

$$\mathbf{V}_{3,3/2,0} + \mathbf{Q}^C_{3,5/2,0}. \tag{5.101}$$

We recover then the Riesz potentials, for which the kernel does not involve any special function but only the singularity of the correct order. However, as we already mentioned the potential $\mathbf{V}_{3,3/2,0}$ suffers from a bad behaviour for low order, propagative modes. This issue will become blatant when we will conduct our modal analysis in the next chapter. We believe that such a matter is unacceptable if one would like to have some efficiency.

One needs a replacement for the operator $\mathbf{V}_{3,3/2,0}$. Remember that the role of this operator is to regularise the $\mathbf{grad}_\Sigma$ part of the tangential field. The idea is then to propose an operator that is the composition of a (positive) regularizing operator and a (positive) de-regularizing operator of adequate orders but acting specifically on the $\mathbf{grad}_\Sigma$ part of the fields. This is the reason why we propose

$$\left(\mathrm{Id} - {\kappa_0}^{-2}\,\mathbf{grad}_\Sigma\,\mathrm{div}_\Sigma\right)^{-1}\mathbf{Q}^G_{3,3/2,0} + \mathbf{Q}^C_{3,5/2,0}. \tag{5.102}$$

To see why this is a valid candidate operator, notice that the first term is composed of two positive operators of orders $+2$ and $-\frac{3}{2}$ which makes an operator of order $+\frac{1}{2}$ acting only on the $\mathbf{grad}_\Sigma$ part of tangential fields. The second term $\mathbf{Q}^C_{3,5/2,0}$ is retained from (5.101) since it already has the correct action on the $\mathbf{curl}_\Sigma$ part of tangential fields.

The operator in (5.102) is valid from a theoretical point of view, however it also suffers from two issues. The first one is the strong singularity of order $\frac{3}{2}$ that is still present in the first term. The second one will appear if one tries to discretize it with standard boundary elements. Indeed, the usual elements are the Raviart-Thomas and Nedelec elements which are respectively div_Σ and curl_Σ conforming (but not both). Therefore, we forecast that careless discretization of the operator may lead to trouble because of the presence at the same time of the operators $\mathbf{Q}^G_{3,3/2,0}$ and $\mathbf{Q}^C_{3,5/2,0}$. All-in-all, the operator in (5.102) does not appear to be a valuable improvement over the operator in (5.99). However, the ideas behind the construction of this operator are similar to the ones used in the next section.

5.2.4.2 A viable candidate?

We discuss briefly here the reasons that led us to propose a possible candidate which is the one that we actually implemented and tested numerically.

Definition The idea is to replace the term $\left(\mathrm{Id} - {\kappa_0}^{-2}\,\mathbf{grad}_\Sigma\,\mathrm{div}_\Sigma\right)^{-1}\mathbf{Q}^G_{3,3/2,0}$ in (5.102) with a better behaved operator (with a weaker singularity). Consider

$$\left(\mathrm{Id} - {\kappa_0}^{-2}\,\mathbf{grad}_\Sigma\,\mathrm{div}_\Sigma\right)^{-1/2}\mathbf{Q}^G_{3,5/2,0} + \mathbf{Q}^C_{3,5/2,0}. \tag{5.103}$$

The first term has again the required behaviour and only involves kernels with a singularity of order $\frac{1}{2}$. However, it now involves a square root operator which is, at first sight, difficult to evaluate.

The trick is then to let

$$\begin{aligned} \mathrm{T}^G_{1/2} &:= \left(\mathrm{Id} - {\kappa_0}^{-2}\,\mathbf{grad}_\Sigma\,\mathrm{div}_\Sigma\right)^{-1/2}\mathbf{Q}^G_{3,5/2,0}, \\ \mathrm{T}^C_{1/2} &:= \mathbf{Q}^C_{3,5/2,0}, \end{aligned} \tag{5.104}$$

so that we can define T_0 as

$$\mathrm{T}_0 = \left(\mathrm{T}^G_{1/2}\right)^* \mathrm{T}^G_{1/2} + \left(\mathrm{T}^C_{1/2}\right)^* \mathrm{T}^C_{1/2}. \tag{5.105}$$

It follows that, T_0 can be evaluated as

$$\mathrm{T}_0 = \left(\mathbf{Q}^G_{3,5/2,0}\right)^* \left(\mathrm{Id} - {\kappa_0}^{-2}\,\mathbf{grad}_\Sigma\,\mathrm{div}_\Sigma\right)^{-1} \mathbf{Q}^G_{3,5/2,0} + \left(\mathbf{Q}^C_{3,5/2,0}\right)^* \mathbf{Q}^C_{3,5/2,0}, \tag{5.106}$$

which no longer involves square root operators.

Truncation After truncation of the kernels, which is the main reason that pushes us to construct this operator, we may loose the injectivity property. To avoid this pitfall, a possible workaround is to add a (positive) compact operator to restore the desired behaviour. In the scalar setting, it was enough to simply add an identity term. It is however no longer an option in the electromagnetism case because it is not a compact operator and we would loose the isomorphism property (recall that we need an operator that is of order $-1/2$, i.e. regularizing, for the $\mathbf{grad}_\Sigma$ part of the field). A better option is to add a (positive) regularizing operator such as

$$\left(1 - {\kappa_0}^{-2}\,\mathbf{grad}_\Sigma\,\mathrm{div}_\Sigma\right)^{-1}, \tag{5.107}$$

which has the required properties and is only a compact perturbation. Finally, the operator that we considered reads

$$\begin{aligned} \mathrm{T}^{\mathrm{Riesz}}_0 =& \left(\mathrm{Id} - {\kappa_0}^{-2}\,\mathbf{grad}_\Sigma\,\mathrm{div}_\Sigma\right)^{-1} \\ &+ \left(\mathbf{Q}^G_{3,5/2,0}\right)^* \left(\mathrm{Id} - {\kappa_0}^{-2}\,\mathbf{grad}_\Sigma\,\mathrm{div}_\Sigma\right)^{-1} \mathbf{Q}^G_{3,5/2,0} \\ &+ \left(\mathbf{Q}^C_{3,5/2,0}\right)^* \mathbf{Q}^C_{3,5/2,0}. \end{aligned} \tag{5.108}$$

5.2.5 Conclusion on possible transmission operators for Maxwell

Because we considered many different candidate operators in our discussion above, we quickly sum up below which are the ones we find the most interesting.

Standard potential theory for Maxwell equations led us to suggest to use (for $\sigma > 0$)

$$\begin{aligned} &2\mathbf{U}_{3,\sigma} && \text{as a } \mathrm{T}_1 \text{ operator,} \\ &2\mathbf{K}_{3,\sigma} && \text{as a } \mathrm{T}_0 \text{ operator.} \end{aligned} \tag{5.109}$$

See (5.83) for the definitions of the operators $\mathbf{U}_{3,\sigma}$ and $\mathbf{K}_{3,\sigma}$. These operators have integral representations given in (5.85) and (5.86) and are (or are close to operators) implemented in standard boundary element codes. However, we were not able to prove that they retain their properties if localization strategies or other compression techniques are applied to reduce their computational cost.

We will report several numerical results obtained using the operator

$$\mathrm{T}_0^{\mathrm{Bessel}} = 2\mathbf{K}_{3,\kappa_0} \tag{5.110}$$

in what follows. The choice $\sigma = \kappa_0$ is motivated in particular by the modal analysis conducted in the next chapter.

Fractional powers of the Yukawa operator led us to suggest to use (for $\sigma > 0$)

$$\begin{aligned} &\mathbf{V}_{3,3/2,\sigma} + \mathbf{Q}^C_{3,5/2,\sigma} \qquad \text{as a } \mathrm{T}_{1/2} \text{ operator,} \\ &\mathbf{V}_{3,5/2,\sigma} + \mathbf{Q}^G_{3,3/2,\sigma} \qquad \text{as a } \mathrm{T}_{-1/2} \text{ operator.} \end{aligned} \tag{5.111}$$

See (5.96) for the definitions of these operators. These operators are in contrast less standard. Their kernels involve special functions that are costly to evaluate numerically and present non-classical (strong) singularities that require dedicated care in practical implementations. For both these reasons, we did not test these operators in our numerical experiments. On the other hand, their are amenable to quasi-localization by truncation while retaining the required properties for the theory to apply.

Finally, we proposed an operator constructed from Riesz potentials which reads

$$\mathrm{T}_0^{\mathrm{Riesz}} = \Theta^{-1} + \left(\mathbf{Q}^G_{3,5/2,0}\right)^* \Theta^{-1}\, \mathbf{Q}^G_{3,5/2,0} + \left(\mathbf{Q}^C_{3,5/2,0}\right)^* \mathbf{Q}^C_{3,5/2,0}, \tag{5.112}$$

where we used as a short-hand, the notation

$$\Theta = \mathrm{Id} - {\kappa_0}^{-2}\, \mathbf{grad}_\Sigma \,\mathrm{div}_\Sigma. \tag{5.113}$$

This operator involves weaker (albeit non-standard) singularities and the kernels do not involve special functions. It is amenable to localization by truncation, while retaining the important properties required by the convergence analysis. This is why we tested this operator in our numerical experiments. However, its discretization will prove to be somehow troublesome and computationally costly.

Chapter 6

Modal analysis in spherical geometries

Contents

The purpose of this chapter is to study more precisely some of the integral operators that were described in the previous chapter in a particular configuration allowing for explicit computations. We chose to study the spherical geometry that allows for analytical expressions of tangential fields using the Hilbert basis built upon (scalar and vector) spherical harmonics.

Modal analysis provides valuable insights on the convergence of domain decomposition algorithms and its main mechanisms. As we shall see in the following, all the operators involved are diagonalized in the aforementioned Hilbert basis — including the integral operators, this is one of the main tasks we are tackling in this chapter — and this decoupling allows for a fine understanding of their different contribution. One can essentially infer the convergence rate of the (relaxed) Jacobi algorithm from these decompositions (unfortunately, understanding the

convergence of the GMRES algorithm is less straightforward). In particular, following standard practice, we are brought to distinguish three main group of modes, namely, by increasing mode number: the propagative modes, the grazing modes and the evanescent modes. Depending on the transmission operator that is chosen, one of these groups will be the culprit for the slowing of the convergence. One then understands that we can also use modal analysis as a tool to design suitable transmission operators. For instance, some of the operators with adequate theoretical properties that we first considered turned out to be poorly designed after their modal decomposition was performed. Besides, since the definition of the candidate transmission operators often involve parameters that are available for tuning, one can use the modal analysis to try to optimize in some sense the operators to make them more efficient.

The results presented in this chapter mainly comes from a joint work with Francis Collino. We mention that modal analysis was used in the acoustic setting in [44, Sec. 4 and 5] and [91, Chap. 3] to analyse and improve (through parameter optimization) the performance of several transmission operators in the context of domain decomposition but for a circular geometry (in 2D). Similar techniques were also already used in the electromagnetic setting in [34] to study a dissipative version of the EFIE operator and in [59, Sec. 3.3], [61, Sec. 4] for their special, Padé-based, transmission operator. We also refer the interested reader to [110, Sec. 2.4 and 5.4.1] and finally to [128] which provides some interesting results on layer potentials in the spherical harmonic basis.

For the sake of clarity, we restrict the discussion to three transmission operators. These operators are all T_0-type operators and were all implemented and used in our numerical experiments (see next chapter). The first one is the identity operator of Després; the second one is $\mathrm{T}_0^{\mathrm{Bessel}} = 2\mathbf{K}_{3,\sigma}$ defined in (5.82) and stems from classical potential theory; and the third one is $\mathrm{T}_0^{\mathrm{Riesz}}$ defined in (5.112) and stems from (less standard) Riesz potentials. As we shall see, the last two operators are positive self-adjoint isomorphisms from $\mathbf{H}^{-1/2}(\mathrm{curl}; S_R)$ to $\mathbf{H}^{-1/2}(\mathrm{div}; S_R)$ so that the analysis of Chapter 3 is applicable. The first operator, the identity, is the simplest choice one could make and is used as a point of comparison. If the convergence analysis we performed in Chapter 3 is not directly applicable for this choice of transmission operator (Assumption 3.47 does not hold) other methods of proof can be used to obtain the convergence of the iterative methods considered, see [49] for instance.

This chapter contains two sections. In the first section we conduct the modal analysis of the domain decomposition method and show that the use of non local operators with suitable properties is mandatory for achieving geometric convergence of the relaxed Jacobi algorithm. Numerical results are provided to illustrate the analysis. All the technical proofs regarding the diagonalization results are gathered in the second section. We are in particular able to prove in the spherical setting that the operators proposed in the preceding chapter enjoy the required properties to obtain the geometric convergence.

A note on our notations In this chapter, we consider $\Sigma = S_R$ the sphere of radius R in $\mathbb{R}^3$ ($d = 3$), and we note

$$\Omega_+ = \left\{ \mathbf{x} \in \mathbb{R}^3 \;\middle|\; |\mathbf{x}| > 1 \right\}, \qquad \text{and} \qquad \Omega_- = \left\{ \mathbf{x} \in \mathbb{R}^3 \;\middle|\; |\mathbf{x}| < 1 \right\}. \tag{6.1}$$

The domain Ω_+ (respectively Ω_-) will be referred to as the exterior (respectively interior) domain. Besides, we denote by S^2 the unit sphere and by $\hat{\mathbf{r}}$ the outward unit normal vector.

The results of this chapter are established for a uniform and homogeneous medium characterized by its wavenumber $\kappa = \omega\sqrt{\mu\epsilon}$ (see (3.63) for the definitions of these quantities). Besides, we shall use from time to time Maxwell's equations in the form of a first order system for which some of the proofs of the following results are slightly easier. This will requires the use of the

impedance parameter Z defined as

$$Z := \sqrt{\frac{\mu}{\epsilon}}. \tag{6.2}$$

6.1 Modal analysis of the domain decomposition method

In this section we analyse the domain decomposition method in the non-overlapping two-domain decomposition of the whole of $\mathbb{R}^3$ into $\Omega_- \cup S_R \cup \Omega_+$. The particular geometry allows to perform a rather acute analysis of the convergence rate of the relaxed Jacobi algorithm.

6.1.1 Algorithm under study

We consider, in this particular two-domain partition, the interface problem (3.222) and the associated relaxed Jacobi algorithm (3.225) (for $\sigma = 1$) from Chapter 3. We specify below our notations for this particular setting.

Interface problem By linearity it is enough to study the homogeneous problem, which corresponds to study the convergence of the error. We therefore consider the interface problem

$$\begin{cases} \text{Find } \mathscr{x} \in \mathbf{H}^{-1/2}(\mathrm{div}; S_R)^2 \text{ such that,} \\ (\mathrm{Id} - \boldsymbol{\Pi}\mathbf{S})\,\mathscr{x} = 0, \end{cases} \tag{6.3}$$

where the exchange operator $\boldsymbol{\Pi}$ and the scattering operator $\mathbf{S}$ have the block representation in $\mathbf{H}^{-1/2}(\mathrm{div}; S_R)^2$

$$\boldsymbol{\Pi} := \begin{bmatrix} 0 & \mathrm{Id} \\ \mathrm{Id} & 0 \end{bmatrix}, \qquad \text{and} \qquad \mathbf{S} := \begin{bmatrix} \mathbf{S}_- & 0 \\ 0 & \mathbf{S}_+ \end{bmatrix}, \tag{6.4}$$

with the local scattering operators $\mathbf{S}_-$ and $\mathbf{S}_+$ such that ($\hat{\mathbf{r}}$ is the outward unit normal vector to S_R)

$$\mathbf{S}_\mp \ : \ \mathbf{J} \mapsto \pm(\kappa\mu)^{-1} \left(\mathbf{curl}\, \mathbf{E}_\pm \times \hat{\mathbf{r}}\right)|_{r=R} - \mathrm{i}\mathrm{T}_0\, \hat{\mathbf{r}} \times \left(\mathbf{curl}\, \mathbf{E}_\pm \times \hat{\mathbf{r}}\right)|_{r=R}, \tag{6.5}$$

where $\mathbf{E}_\pm$ is solution to

$$\begin{cases} (\mathbf{curl}\,\mathbf{curl} - \kappa^2)\mathbf{E}_\pm = 0, & \text{in } \Omega_\pm, \\ \mp(\kappa\mu)^{-1} \left(\mathbf{curl}\, \mathbf{E}_\pm \times \hat{\mathbf{r}}\right)|_{r=R} - \mathrm{i}\mathrm{T}_0\, \hat{\mathbf{r}} \times \left(\mathbf{curl}\, \mathbf{E}_\pm \times \hat{\mathbf{r}}\right)|_{r=R} = \mathbf{J}, & \text{on } S_R, \end{cases} \tag{6.6}$$

and

$$\lim_{r\to\infty} \ r\left((\kappa\mu)^{-1}\ \mathbf{curl}\, \mathbf{E}_+ \times \hat{\mathbf{r}} - \mathrm{i}\ \hat{\mathbf{r}} \times (\mathbf{E}_+ \times \hat{\mathbf{r}})\right) = 0. \tag{6.7}$$

Here T_0 is supposed to be a generic transmission operator intended to represent either the identity Id, $\mathrm{T}_0^{\mathrm{Bessel}} = 2\mathbf{K}_{3,\kappa}$ or $\mathrm{T}_0^{\mathrm{Riesz}}$ (see (5.112)).

Iterative algorithm Given a couple of traces $\mathscr{x}^0$ in $\mathbf{H}^{-1/2}(\mathrm{div}; S_R)^2$ (the initial error) and a relaxation parameter $r \in (0, 1)$ the relaxed Jacobi algorithm is,

$$\mathscr{x}^{n+1} = [(1-r)\mathrm{Id} + r\boldsymbol{\Pi}\mathbf{S}]\,\mathscr{x}^n, \qquad n \in \mathbb{N}. \tag{6.8}$$

We denote by

$$\mathbf{A}_r = (1-r)\mathrm{Id} + r\boldsymbol{\Pi}\mathbf{S}, \tag{6.9}$$

the iteration operator.

6.1.2 Diagonalization of the transmission operators

The modal analysis that we conduct below rests on the existence of an Hilbertian basis of $\mathbf{L}^2_t(S_R)$ given by the vector spherical harmonics. The family of vector spherical harmonics $\{\mathbf{\Psi}_{\ell,m}, \mathbf{\Phi}_{\ell,m}\}_{\ell,m}$, with $\ell \in \mathbb{N}^*$ and $-\ell \leq m \leq \ell$ (see Definition 6.12) forms a complete orthonormal system for the hermitian inner product in $\mathbf{L}^2_t(S^2)$.

We assume that the transmission operator T_0 is diagonalized by the vector spherical harmonics so that

$$\begin{cases} \mathrm{T}_0 \mathbf{\Psi}_{\ell,m} = \hat{T}^{\mathbf{\Psi}}_\ell \ \mathbf{\Psi}_{\ell,m}, \\ \mathrm{T}_0 \mathbf{\Phi}_{\ell,m} = \hat{T}^{\mathbf{\Phi}}_\ell \ \mathbf{\Phi}_{\ell,m}, \end{cases} \qquad \forall \ell \in \mathbb{N}^*, \ -\ell \leq m \leq \ell. \tag{6.10}$$

Note that the eigenvalues $\hat{T}^{\mathbf{\Psi}}_\ell$ and $\hat{T}^{\mathbf{\Phi}}_\ell$ do not depend on m and have therefore $2\ell+1$ multiplicity. This holds true for the transmission operators we are interested in, as stated by the two proposition below.

Operator stemming from potential theory We have the following diagonalization result for the transmission operator $\mathrm{T}_0^{\mathrm{Bessel}} = 2\mathbf{K}_{3,\kappa}$ defined in (6.92). The proof of this result can be found in Section 6.2.3, see in particular Proposition 6.22.

Proposition 6.1. *The transmission operator $\mathrm{T}_0^{\mathrm{Bessel}} = 2\mathbf{K}_{3,\kappa}$ is a continuous mapping from $\mathbf{H}^{-1/2}(\mathrm{curl}; S_R)$ to $\mathbf{H}^{-1/2}(\mathrm{div}; S_R)$ and is diagonalized by $\mathbf{\Psi}_{\ell,m}$ and $\mathbf{\Phi}_{\ell,m}$. The respective eigenvalues, with $2\ell+1$ multiplicity, read*

$$\begin{cases} t^{\mathrm{Bessel},\mathbf{\Psi}}(\ell) = 2\psi_\ell(\mathrm{i}\kappa R)\xi_\ell(\mathrm{i}\kappa R), \\ t^{\mathrm{Bessel},\mathbf{\Psi}}(\ell) = 2\psi'_\ell(\mathrm{i}\kappa R)\xi'_\ell(\mathrm{i}\kappa R), \end{cases} \qquad \forall \ell \in \mathbb{N}^*, \tag{6.11}$$

where ψ_ℓ and ξ_ℓ are the spherical Ricatti-Bessel functions (see Section 6.2). These eigenvalues are all real and strictly positive

$$t^{\mathrm{Bessel},\mathbf{\Psi}}(\ell) > 0, \qquad t^{\mathrm{Bessel},\mathbf{\Phi}}(\ell) > 0, \qquad \forall \ell \in \mathbb{N}^*, \tag{6.12}$$

and satisfy the following asymptotic behaviour at infinity

$$t^{\mathrm{Bessel},\mathbf{\Psi}}(\ell) \ \sim \ \left(\frac{\ell}{\kappa R}\right)^{-1}, \qquad t^{\mathrm{Bessel},\mathbf{\Phi}}(\ell) \ \sim \ \frac{\ell}{\kappa R}, \qquad \text{as } \ell \to \infty. \tag{6.13}$$

Operator based on Riesz potentials We have the following diagonalization result for the transmission operator $\mathrm{T}_0^{\mathrm{Riesz}}$ defined in (5.112). The proof of this result can be found in Section 6.2.4, see in particular Corollary 6.33.

Proposition 6.2. *The transmission operator $\mathrm{T}_0^{\mathrm{Riesz}}$ is a continuous mapping from $\mathbf{H}^{-1/2}(\mathrm{curl}; S_R)$ to $\mathbf{H}^{-1/2}(\mathrm{div}; S_R)$ and is diagonalized by $\mathbf{\Psi}_{\ell,m}$ and $\mathbf{\Phi}_{\ell,m}$. The respective eigenvalues, with $2\ell+1$ multiplicity, read*

$$\begin{cases} t^{,\mathrm{Riesz},\mathbf{\Psi}}(\ell) = \left(1 + \dfrac{\ell(\ell+1)}{(\kappa R)^2}\right)^{-1} + \left(1 + \dfrac{\ell(\ell+1)}{(\kappa R)^2}\right)^{-1} \left(\dfrac{\ell(\ell+1)}{(\kappa R)^{1/2}} \dfrac{\Gamma(\frac{1}{4}+\ell)}{\Gamma(\frac{7}{4}+\ell)}\right)^2, \\ t^{\mathrm{Riesz},\mathbf{\Phi}}(\ell) = 1 + \left(\dfrac{\ell(\ell+1)}{(\kappa R)^{1/2}} \dfrac{\Gamma(\frac{1}{4}+\ell)}{\Gamma(\frac{7}{4}+\ell)}\right)^2, \end{cases} \qquad \forall \ell \in \mathbb{N}^*. \tag{6.14}$$

These eigenvalues are all real and strictly positive

$$t^{\mathrm{Riesz},\mathbf{\Psi}}(\ell) > 0, \qquad t^{\mathrm{Riesz},\mathbf{\Phi}}(\ell) > 0, \qquad \forall \ell \in \mathbb{N}^*, \tag{6.15}$$

and satisfy the following asymptotic behaviour at infinity

$$t^{\mathrm{Riesz},\mathbf{\Psi}}(\ell) \ \sim \ \left(\frac{\ell}{\kappa R}\right)^{-1}, \qquad t^{\mathrm{Riesz},\mathbf{\Phi}}(\ell) \ \sim \ \frac{\ell}{\kappa R}, \qquad \text{as } \ell \to \infty. \tag{6.16}$$

6.1.3 Diagonalization of the scattering operators

For any $\mathbf{J} \in \mathbf{H}^{-1/2}(\mathrm{curl}; S_R)$, we define the operator $\mathbf{\Lambda}_+$ as

$$\mathbf{\Lambda}_+ \ : \ \mathbf{J} \mapsto -\kappa^{-1} \left(\mathbf{curl}\, \mathbf{E} \times \hat{\mathbf{r}}\right)|_{r=R}, \tag{6.17}$$

such that

$$\begin{cases} (\mathbf{curl}\,\mathbf{curl} - \kappa^2)\mathbf{E} = 0, & \text{in } \Omega_+, \\ \hat{\mathbf{r}} \times (\mathbf{E} \times \hat{\mathbf{r}})\,|_{r=R} = \mathbf{J}, & \text{on } S_R, \\ \lim_{r\to\infty} \ r\left(\mathbf{curl}\,\mathbf{E} \times \hat{\mathbf{r}} - \mathrm{i}\kappa \hat{\mathbf{r}} \times (\mathbf{E} \times \hat{\mathbf{r}})\right) = 0. \end{cases} \tag{6.18}$$

Similarly, for any $\mathbf{J} \in \mathbf{H}^{-1/2}(\mathrm{curl}; S_R)$, we define the operator $\mathbf{\Lambda}_-$ as

$$\mathbf{\Lambda}_- \ : \ \mathbf{J} \mapsto \kappa^{-1} \left(\mathbf{curl}\, \mathbf{E} \times \hat{\mathbf{r}}\right)|_{r=R}, \tag{6.19}$$

such that

$$\begin{cases} (\mathbf{curl}\,\mathbf{curl} - \kappa^2)\mathbf{E} = 0, & \text{in } \Omega_-, \\ \hat{\mathbf{r}} \times (\mathbf{E} \times \hat{\mathbf{r}})\,|_{r=R} = \mathbf{J}, & \text{on } S_R. \end{cases} \tag{6.20}$$

Remark 6.3 (**Eigenvalues of the interior Maxwell problem**). *It is worth noting that while the operator $\mathbf{\Lambda}_+$ is well-defined for any wavenumber κ, one must exclude a countable set of values of the wavenumber κ to be ensured of the well-posedness of the operator $\mathbf{\Lambda}_-$ (see [110, Th. 5.3.2] and the discussion thereafter). These values of the wavenumber κ correspond to the eigenvalues of the interior Maxwell problem inside S_R for which the problem* (6.20) *becomes ill-posed. For simplicity, we suppose in the remainder of this chapter that κ lies outside this set of eigenvalues.*

We have the following diagonalization result for these operators. The proof of this result can be found in Section 6.2.2, see in particular Proposition 6.19.

Proposition 6.4. *The operators $\mathbf{\Lambda}_\pm$ are diagonalized by $\mathbf{\Psi}_{\ell,m}$ and $\mathbf{\Phi}_{\ell,m}$. The respective eigenvalues $\widehat{\Lambda}^{\mathbf{\Psi}}_{\pm,\ell}$ and $\widehat{\Lambda}^{\mathbf{\Phi}}_{\pm,\ell}$, with $2\ell+1$ multiplicity, read*

$$\begin{cases} \widehat{\Lambda}^{\mathbf{\Psi}}_{-,\ell} = -\dfrac{\psi_\ell(\kappa R)}{\psi'_\ell(\kappa R)}, \\ \widehat{\Lambda}^{\mathbf{\Phi}}_{-,\ell} = +\dfrac{\psi'_\ell(\kappa R)}{\psi_\ell(\kappa R)}, \end{cases} \qquad \textit{and} \qquad \begin{cases} \widehat{\Lambda}^{\mathbf{\Psi}}_{+,\ell} = +\dfrac{\xi_\ell(\kappa R)}{\xi'_\ell(\kappa R)}, \\ \widehat{\Lambda}^{\mathbf{\Phi}}_{+,\ell} = -\dfrac{\xi'_\ell(\kappa R)}{\xi_\ell(\kappa R)}. \end{cases} \qquad \forall \ell \in \mathbb{N}^*. \tag{6.21}$$

These eigenvalues are such that

$$\Im(\widehat{\Lambda}^{\mathbf{\Psi}}_{-,\ell}) = \Im(\widehat{\Lambda}^{\mathbf{\Phi}}_{-,\ell}) = 0 \qquad \textit{and} \qquad \Im(\widehat{\Lambda}^{\mathbf{\Psi}}_{+,\ell}) < 0, \quad \Im(\widehat{\Lambda}^{\mathbf{\Phi}}_{+,\ell}) < 0, \qquad \forall \ell \in \mathbb{N}^*, \tag{6.22}$$

and satisfy the following asymptotic behaviour at infinity

$$\widehat{\Lambda}^{\mathbf{\Psi}}_{\pm,\ell} \ \sim \ -\frac{\kappa R}{\ell}, \qquad \widehat{\Lambda}^{\mathbf{\Phi}}_{\pm,\ell} \ \sim \ +\frac{\ell}{\kappa R}, \qquad \ell \to +\infty. \tag{6.23}$$

From the definitions of the operators $\mathbf{\Lambda}_\pm$ and the scattering operators $\mathbf{S}_\pm$, we formally have

$$\mathbf{S}_\pm = -(\mathbf{\Lambda}_\pm + \mathrm{i}\mathrm{T}_0)(\mathbf{\Lambda}_\pm - \mathrm{i}\mathrm{T}_0)^{-1}, \tag{6.24}$$

so that the eigenvalues of the local scattering operators $\mathbf{S}_-$ and $\mathbf{S}_+$ are, for $\alpha \in \{\mathbf{\Psi}, \mathbf{\Phi}\}$,

$$\hat{S}^\alpha_{\pm,\ell} = \frac{-\hat{\Lambda}^\alpha_{\pm,\ell} - \mathrm{i}\hat{T}^\alpha_\ell}{\hat{\Lambda}^\alpha_{\pm,\ell} - \mathrm{i}\hat{T}^\alpha_\ell}, \qquad \forall \ell \in \mathbb{N}^*. \tag{6.25}$$

Note that neither $\hat{T}^\alpha_\ell$ nor $\widehat{\Lambda}^\alpha_{\pm,\ell}$ vanish (we actually need to suppose that κ is not an eigenvalue of the interior problem so that it is true for the operator $\mathbf{\Lambda}_-$). We introduce the ratio (well-defined since by assumption $\hat{T}^\alpha_\ell > 0$)

$$\hat{Z}^\alpha_{\pm,\ell} = -\frac{\hat{\Lambda}^\alpha_{\pm,\ell}}{\hat{T}^\alpha_\ell}, \qquad \forall \ell \in \mathbb{N}^*. \tag{6.26}$$

and we can rewrite

$$\hat{S}^\alpha_{\pm,\ell} = -\frac{\hat{Z}^\alpha_{\pm,\ell} - \mathrm{i}}{\hat{Z}^\alpha_{\pm,\ell} + \mathrm{i}}, \qquad \forall \ell \in \mathbb{N}^*. \tag{6.27}$$

We recall now some simple properties of the Cayley transform from complex analysis.

Lemma 6.5 (**Cayley transform**). *The complex transform*

$$z \mapsto \frac{z - \mathrm{i}}{z + \mathrm{i}}, \tag{6.28}$$

has the following properties

1. *the upper half-plane, i.e.* $\{z = x + \mathrm{i}y \in \mathbb{C}$ *with* $x \in \mathbb{R}$ *and* $y > 0\}$*, is mapped to the open unit disk, i.e.* $\{z \in \mathbb{C}$ *with* $|z| < 1\}$*;*
2. *the real line is mapped to the unit circle minus the point* 1*, i.e.* $\{z \in \mathbb{C}$ *with* $|z| = 1,\ z \neq 1\}$*;*
3. *the point* 1 *is mapped to the point* $-\mathrm{i}$ *and the point* -1 *is mapped to the point* i*;*
4. *the origin* 0 *is mapped to the point* -1 *and the 'infinity' is formally mapped to the point* 1*.*

We stress that, ultimately, much of the analysis boils down to the above lemma and the properties of the Cayley transform, allowing to get a rather deep understanding of the convergence of the relaxed Jacobi algorithm. For instance, from this lemma we recover in this particular setting the contraction property of the scattering operators.

Corollary 6.6 (**Contraction property of local scattering operators**). *Let* $\alpha \in \{\mathbf{\Psi}, \mathbf{\Phi}\}$ *and* $\ell \in \mathbb{N}^*$*. If* $\hat{T}^\alpha_\ell$ *is real and strictly positive,*

$$\hat{T}^\alpha_\ell > 0, \tag{6.29}$$

then we have

$$|\hat{S}^\alpha_{-,\ell}| = 1, \qquad \textit{and} \qquad |\hat{S}^\alpha_{+,\ell}| < 1. \tag{6.30}$$

Proof. Let $\alpha \in \{\mathbf{\Psi}, \mathbf{\Phi}\}$. From energy conservation results, see Proposition 6.20, we know that $\hat{\Lambda}^\alpha_\ell$ has a non-positive imaginary part. Since by assumption $\hat{T}^\alpha_\ell$ is real and strictly positive, $\hat{Z}^\alpha_\ell$ does belong to the upper half-plane. It follows from Lemma 6.5 that $\hat{S}^\alpha_{\pm,\ell}$ does belong to the unit disk and we recover that the scattering operators are contraction operators. ■

Of course the assumption that $\hat{T}^\alpha_\ell$ is real and strictly positive is a direct consequence of Assumption 3.47. It is trivially satisfied by the identity operator and was verified for the other two transmission operators in Proposition 6.23 and Corollary 6.35.

6.1.4 Modal convergence analysis

We now arrive to the main purpose of this chapter which is to study the modal behaviour of the iteration operator involved in our domain decomposition method.

From the above diagonalization results of the scattering operators by the vector spherical harmonics, it is clear that the iteration operator $\mathbf{A}_r$ is completely represented by the countable family of two-by-two matrices

$$\mathbf{A}_{r,\ell}^{\alpha} = \begin{bmatrix} 1-r & r\,\hat{S}_{-,\ell}^{\alpha} \\ r\,\hat{S}_{+,\ell}^{\alpha} & 1-r \end{bmatrix}, \qquad \forall \ell \in \mathbb{N}^*,\ \alpha \in \{\mathbf{\Psi}, \mathbf{\Phi}\}. \tag{6.31}$$

The derivation of a meaningful estimate for the convergence factor of the relaxed Jacobi algorithm is not completely straightforward. We only cite the main result below and we refer the reader to [91, Sec. 3.1.3] and [44, Sec. 4.1.2] for a more comprehensive discussion.

If n is the iteration number, the approach consists in using an estimate for the norm

$$\|\big(\mathbf{A}_{r,\ell}^{\alpha}\big)^n\| := \sup_{\ell} |\big(\mathbf{A}_{r,\ell}^{\alpha}\big)^n|_2, \qquad \text{where} \qquad |\big(\mathbf{A}_{r,\ell}^{\alpha}\big)^n|_2 := \sup_{|\mathbb{x}|=1} |\big(\mathbf{A}_{r,\ell}^{\alpha}\big)^n \mathbb{x}|, \tag{6.32}$$

where $|\cdot|_2$ is the matrix norm subordinate to the euclidian norm $|\cdot|$ in $\mathbb{C}^2$.

Lemma 6.7. *If we set (using the standard convention regarding the definition of the square root in $\mathbb{C}$)*

$$\tau_{r,\ell} := \max_{\pm,\alpha} \left| (1-r) \pm r\sqrt{\hat{S}_{+,\ell}^{\alpha}\hat{S}_{-,\ell}^{\alpha}} \right|, \qquad \forall \ell \in \mathbb{N}^*, \tag{6.33}$$

we have the estimate

$$\tau_{r,\ell}^n \ \le\ |\big(\mathbf{A}_{r,\ell}^{\alpha}\big)^n|_2 \ \le\ (\tau_{r,\ell} + rn)\tau_{r,\ell}^{n-1}, \qquad \forall \ell \in \mathbb{N}^*. \tag{6.34}$$

Proof. See [91, Lem. 5] and [44, Lem. 4.1]. ■

We point out that the quantity $\tau_{r,\ell}$ is the maximum eigenvalue of $\mathbf{A}_{r,\ell}^{\mathbf{\Psi}}$ and $\mathbf{A}_{r,\ell}^{\mathbf{\Phi}}$.

The above lemma states that the computation of the quantity $\tau_{r,\ell}$ is enough to analyse the convergence of the relaxed Jacobi algorithm. From this point we understand that it all boils down to study the product $\hat{S}_{+,\ell}^{\alpha}\hat{S}_{-,\ell}^{\alpha}$.

Lemma 6.8. *If the eigenvalues of the transmission operators have the correct asymptotic behaviour*

$$\hat{T}_{\ell}^{\mathbf{\Psi}} \ \sim\ \left(\frac{\ell}{\kappa R}\right)^{-1}, \qquad \hat{T}_{\ell}^{\mathbf{\Phi}} \ \sim\ \frac{\ell}{\kappa R}, \qquad \textit{as } \ell \to \infty. \tag{6.35}$$

then there exists a positive constant δ such that

$$\lim_{\ell\to\infty} \hat{S}_{+,\ell}^{\mathbf{\Psi}}\hat{S}_{-,\ell}^{\mathbf{\Psi}} = \lim_{\ell\to\infty} \hat{S}_{+,\ell}^{\mathbf{\Phi}}\hat{S}_{-,\ell}^{\mathbf{\Phi}} = -1, \qquad \textit{and} \qquad \sup_{\ell,\alpha} |\hat{S}_{+,\ell}^{\alpha}\hat{S}_{-,\ell}^{\alpha} - 1| > \delta. \tag{6.36}$$

Proof. From Proposition 6.21, the eigenvalues of the Electric-to-Magnetic operators $\mathbf{\Lambda}_{\pm}$ satisfy, at infinity

$$\widehat{\Lambda}_{\pm,\ell}^{\mathbf{\Psi}} \ \sim\ -\frac{\kappa R}{\ell}, \qquad \text{and} \qquad \widehat{\Lambda}_{\pm,\ell}^{\mathbf{\Phi}} \ \sim\ +\frac{\ell}{\kappa R}, \qquad \ell \to +\infty. \tag{6.37}$$

Using the assumption (6.35), it follows that

$$\lim_{\ell\to\infty} \widehat{Z}_{\pm,\ell}^{\mathbf{\Psi}} = 1, \qquad \text{and} \qquad \lim_{\ell\to\infty} \widehat{Z}_{\pm,\ell}^{\mathbf{\Phi}} = -1, \tag{6.38}$$

so that, using Lemma 6.5,

$$\lim_{\ell\to\infty} \widehat{S}^{\boldsymbol{\Psi}}_{\pm,\ell} = \mathrm{i}, \qquad \text{and} \qquad \lim_{\ell\to\infty} \widehat{S}^{\boldsymbol{\Phi}}_{\pm,\ell} = -\mathrm{i}, \tag{6.39}$$

hence $\lim_{\ell\to\infty} \hat{S}^{\boldsymbol{\Psi}}_{+,\ell}\hat{S}^{\boldsymbol{\Psi}}_{-,\ell} = \lim_{\ell\to\infty} \hat{S}^{\boldsymbol{\Phi}}_{+,\ell}\hat{S}^{\boldsymbol{\Phi}}_{-,\ell} = -1$. Besides, there exists a $L \geq 0$, such that for all $\ell \geq L$ and $\alpha \in \{\boldsymbol{\Psi}, \boldsymbol{\Phi}\}$, $|\hat{S}^{\alpha}_{+,\ell}\hat{S}^{\alpha}_{-,\ell} - 1| > 1$. An appropriate δ is then

$$\delta = \min\left(1, \min_{\substack{1\leq\ell\leq L,\\ \alpha\in\{\boldsymbol{\Psi},\boldsymbol{\Phi}\}}} |\hat{S}^{\alpha}_{+,\ell}\hat{S}^{\alpha}_{-,\ell} - 1|\right) > 0. \tag{6.40}$$

■

We could actually relax the assumption (6.35), and only require the existence of two positive real constants C_α, $\alpha \in \{\boldsymbol{\Psi}, \boldsymbol{\Phi}\}$, such that

$$\hat{T}^{\boldsymbol{\Psi}}_{\ell} \sim C_{\boldsymbol{\Psi}} \left(\frac{\ell}{\kappa R}\right)^{-1}, \qquad \hat{T}^{\boldsymbol{\Phi}}_{\ell} \sim C_{\boldsymbol{\Phi}} \frac{\ell}{\kappa R}, \qquad \text{as } \ell \to \infty. \tag{6.41}$$

The limits $\lim_{\ell\to\infty} \hat{S}^{\boldsymbol{\Psi}}_{+,\ell}\hat{S}^{\boldsymbol{\Psi}}_{-,\ell}$ and $\lim_{\ell\to\infty} \hat{S}^{\boldsymbol{\Phi}}_{+,\ell}\hat{S}^{\boldsymbol{\Phi}}_{-,\ell}$ would then belong to the unit circle minus the point 1 and the rest of the discussion, including the next theorem, would follow without much additional difficulties.

Again the assumption that $\hat{T}^{\alpha}_{\ell}$ has the correct asymptotic behaviour is a direct consequence of Assumption 3.47. It is trivially *not* satisfied by the identity operator and was verified for the other two transmission operators in Proposition 6.24 and Proposition 6.37 with $C_\alpha = 1$, $\alpha \in \{\boldsymbol{\Psi}, \boldsymbol{\Phi}\}$, in both cases.

Theorem 6.9 (**Geometric convergence of the relaxed Jacobi algorithm**). *If*

$$\begin{aligned} &\hat{T}^{\boldsymbol{\Psi}}_{\ell} > 0, && \hat{T}^{\boldsymbol{\Phi}}_{\ell} > 0, && \forall \ell \in \mathbb{N}^*, \\ &\hat{T}^{\boldsymbol{\Psi}}_{\ell} \sim \left(\frac{\ell}{\kappa R}\right)^{-1}, && \hat{T}^{\boldsymbol{\Phi}}_{\ell} \sim \frac{\ell}{\kappa R}, && \textit{as } \ell \to \infty. \end{aligned} \tag{6.42}$$

then the estimate (6.33) *satisfies*

$$\sup_{\ell} \tau_{r,\ell} < 1, \tag{6.43}$$

and the relaxed Jacobi algorithm given in (6.8) *converges geometrically.*

Proof. The two assumptions on the spectrum of the transmission operator yield, according to both Lemma 6.6 and Lemma 6.8, the existence of $\epsilon > 0$ such that for $\ell \in \mathbb{N}^*$ and $\alpha \in \{\boldsymbol{\Psi}, \boldsymbol{\Phi}\}$

$$\left|\sqrt{\hat{S}^{\alpha}_{+,\ell}\hat{S}^{\alpha}_{-,\ell}}\right| < 1, \qquad \text{and} \qquad \sup_{\ell,\alpha} \left|\sqrt{\hat{S}^{\alpha}_{+,\ell}\hat{S}^{\alpha}_{-,\ell}} - 1\right| > \epsilon. \tag{6.44}$$

Using again the identity (3.233), we get for $\ell \in \mathbb{N}^*$ and $\alpha \in \{\boldsymbol{\Psi}, \boldsymbol{\Phi}\}$,

$$\begin{aligned} \left|(1-r) + r\sqrt{\hat{S}^{\alpha}_{+,\ell}\hat{S}^{\alpha}_{-,\ell}}\right|^2 &\leq (1-r) + r\left|\sqrt{\hat{S}^{\alpha}_{+,\ell}\hat{S}^{\alpha}_{-,\ell}}\right|^2 - r(1-r)\left|1 - \sqrt{\hat{S}^{\alpha}_{+,\ell}\hat{S}^{\alpha}_{-,\ell}}\right|^2 \\ &\leq 1 - r(1-r)\epsilon^2 < 1. \end{aligned} \tag{6.45}$$

We deduce that the estimate (6.33) satisfies

$$\sup_{\ell} \tau_{r,\ell} < 1, \tag{6.46}$$

and Lemma 6.7 yields the geometric convergence of the relaxed Jacobi algorithm. ■

Note that the condition is only sufficient to ensure the geometric convergence. While it is not *a priori* necessary, it is possible to show, for this particular geometry, negative results such as the impossibility of a geometric convergence for the relaxed Jacobi algorithm if the symbol of the transmission operator does not have an adequate asymptotic behaviour for large ℓ. We refer the reader to [91, Prop. 4] and [44, Th. 4.6] where such results are established in the acoustic setting in 2D (see also [91, Rem. 1]).

6.1.5 Numerical illustration

We consider now the particular case of a sphere S_R of radius $R = 2$ and a wavenumber $\kappa = 5$ (used in the definition of $\mathrm{T}_0^{\mathrm{Riesz}}$), this value being also used for the parameter $\sigma = 5$ of the operator $\mathrm{T}_0^{\mathrm{Bessel}} = 2\mathbf{K}_{3,\sigma}$.

Eigenvalues of the transmission operators We report in Figure 6.1 the eigenvalues of all these three candidate transmission operators. Beware that we represented the *inverse* of the eigenvalues associated to $\mathbf{\Psi}_{\ell,m}$ to showcase the asymptotic rate as ℓ grows. We observe numerically that these asymptotic rates for both non-local operators are the ones we were looking for. Notice in addition how all these operators have their eigenvalues close to 1 for small values of ℓ.

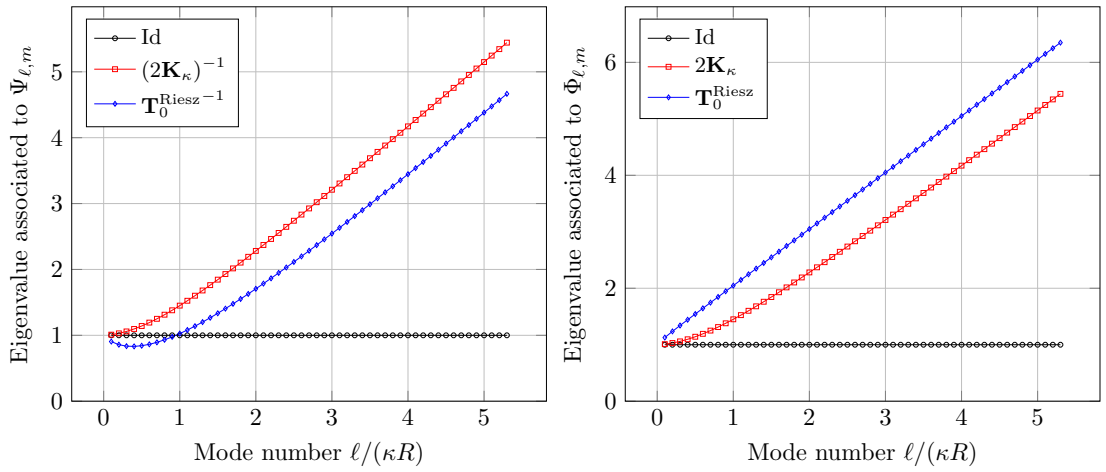

(a) $\mathbf{\Psi}_{\ell,m}$. (b) $\mathbf{\Phi}_{\ell,m}$.

Figure 6.1: Eigenvalues associated to each $\mathbf{\Psi}_{\ell,m}$ (left) and $\mathbf{\Phi}_{\ell,m}$ (right) of some transmission operators with respect to the mode number ℓ. Fixed parameters $\kappa = \sigma = 5$, $R = 2$.

Eigenvalues of the iteration operator Figure 6.2 reports the eigenvalues of the iteration operator $\mathbf{A}_r$ in the complex plane for the three transmission operators Id, $\mathrm{T}_0^{\mathrm{Bessel}} = 2\mathbf{K}_{3,\sigma}$ and $\mathrm{T}_0^{\mathrm{Riesz}}$.

For the case $r = 1$ (left column), we visualize that all the eigenvalues are inside the unit circle (featured with a dashed line). Note also that the accumulation points (which correspond to large mode numbers ℓ) are close to the points i and $-$i for the two non-local operator but seem to be -1 and 1 for the identity operator.

For the case $r = 0.5$ (right column), we visualize the effect of the relaxation. For the non-local operators, the accumulation points of the eigenvalues of the iteration operator are now strictly inside the unit circle, while the eigenvalues associated to the identity operator still accumulate near 1.

This is numerical evidence that the eigenvalues are ℓ-uniformly bounded away from the critical point 1 for the two non-local operators $\mathrm{T}_0^{\mathrm{Bessel}}$ and $\mathrm{T}_0^{\mathrm{Riesz}}$. This indicates in particular that the convergence factor of the relaxed Jacobi algorithm is strictly below one for these two operators. One understands however that the relaxation is mandatory to obtain the geometric convergence. In contrast, for the identity operator the eigenvalues are arbitrarily close to the critical point 1, even with the relaxation.

Modal convergence factor We report in Figure 6.3 the modal convergence factor $\tau_{r,\ell}$ of the relaxed Jacobi algorithm for a relaxation parameter $r = 0.5$.

For low mode number ℓ the convergence factor is very small (in fact close to r) which stems from the fact that all these transmission operators act as the identity for these (propagative) modes.

Notice that the asymptotic behaviour as ℓ increases is very different for the identity operator compared to the two others. This is a feature of any local transmission operator, or an operator with not the adequate order: the evanescent modes are not adequately taken into account and we have $\sup_\ell \tau_{r,\ell} = 1$ in this case. In contrast for the two non-local operators that we advocate, the asymptotic convergence factor is very good. This is of course due to the correct order of the transmission operator, in fact they were designed exactly for this purpose.

Finally, we note that the behaviour of all these operators is not so good for the grazing modes $\ell \sim \kappa R$. If for the non-local operators the maximum convergence factor is obtained for those modes, even for the identity operator we observe a local maximum. This is a general observation for propagative problems that is actually true in more generality than this particular setting. This is especially troublesome since these modes often carry a non negligible part of energy. To some extent, one can mitigate the effect of those modes as we describe in the next paragraph.

6.1.6 Optimization

As we already mentioned the operator $\mathrm{T}_0^{\mathrm{Riesz}}$ defined (5.112) can be parametrized:

$$\mathrm{T}_0^{\mathrm{Riesz}}[\alpha, \beta, \gamma] := \alpha\, \Theta^{-1} + \beta \left(\mathbf{Q}^G_{0,5/2}\right)^* \Theta^{-1}\, \mathbf{Q}^G_{0,5/2} + \gamma \left(\mathbf{Q}^C_{0,5/2}\right)^* \mathbf{Q}^C_{0,5/2}, \tag{6.47}$$

where α, β and γ are three strictly positive constants and still remain in the validity range of the theory. One can expect that choosing judiciously the values of these parameters could improve the convergence factor of the domain decomposition algorithm.

Direct optimization is difficult, but from the analytical expression of the eigenvalues we can apply optimization algorithms[1] to try to obtain those values. The result of this process in the case $R = 2$ and $\kappa = 5$ is provided in Figure 6.4. The optimized values of the above parameters in this particular case are $\alpha = 0.57$, $\beta = 1.5$ and $\gamma = 0.42$. Note that these values greatly varies with respect to κR.

Compare Figure 6.2e with Figure 6.4a, the eigenvalues are more 'condensed' and far away from the critical point $(1, 0)$. In Figure 6.4b the enhancement is well indicated by the decrease of the maximum convergence rate. Notice that the convergence factors for the lowest order mode ($\ell = 1$), the grazing modes ($\ell \sim \kappa R$) and the asymptotic convergence factor ($\ell \to \infty$) are very similar. This situation reminds of similar observations in [91, Sec. 3.2.3].

[1] We used the *Optim.jl* package in Julia, see [106].

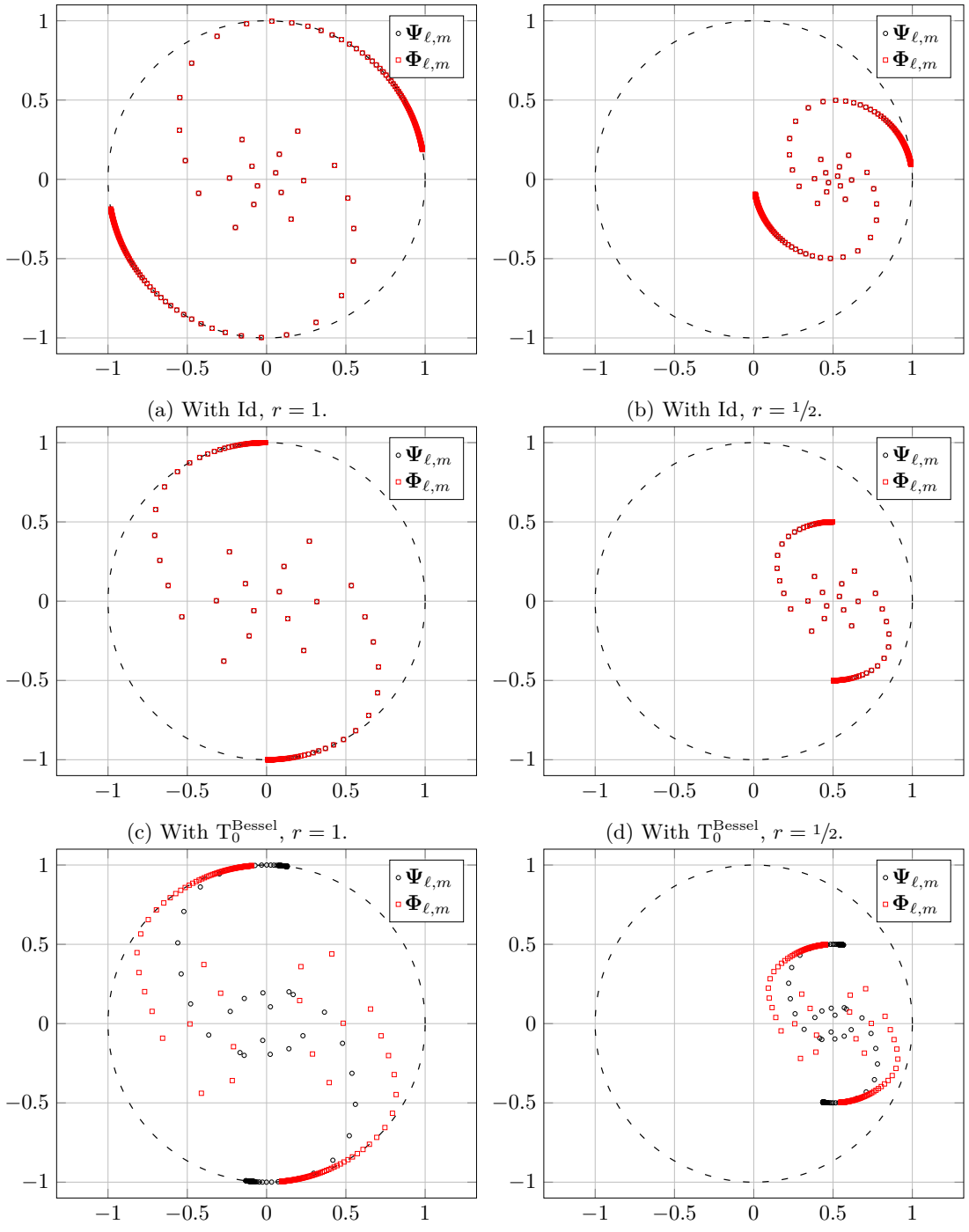

(a) With Id, $r = 1$. (b) With Id, $r = 1/2$.

(c) With $\mathrm{T}_0^{\mathrm{Bessel}}$, $r = 1$. (d) With $\mathrm{T}_0^{\mathrm{Bessel}}$, $r = 1/2$.

(e) With $\mathrm{T}_0^{\mathrm{Riesz}}$, $r = 1$. (f) With $\mathrm{T}_0^{\mathrm{Riesz}}$, $r = 1/2$.

Figure 6.2: Eigenvalues of the (iteration) operator $\mathbf{A}_r$ associated to each $\boldsymbol{\Psi}_{\ell,m}$ and $\boldsymbol{\Phi}_{\ell,m}$ in the complex plane for some transmission operators and for two values of the relaxation parameters $r = 1$ (left column) and $r = 1/2$ (right column). Fixed parameters $\kappa = \sigma = 5$, $R = 2$.

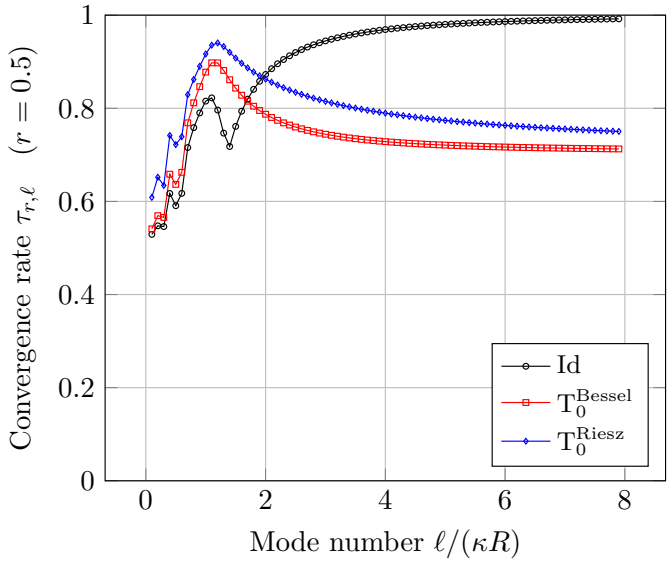

Figure 6.3: Modal convergence factor $\tau_{r,\ell}$ for some transmission operators. Fixed parameters $\kappa = \sigma = 5$, $R = 2$, $r = 0.5$.

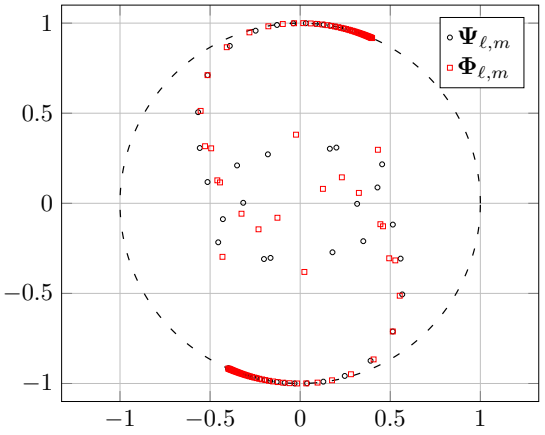

(a) Eigenvalues of the iteration operator for the optimized operator.

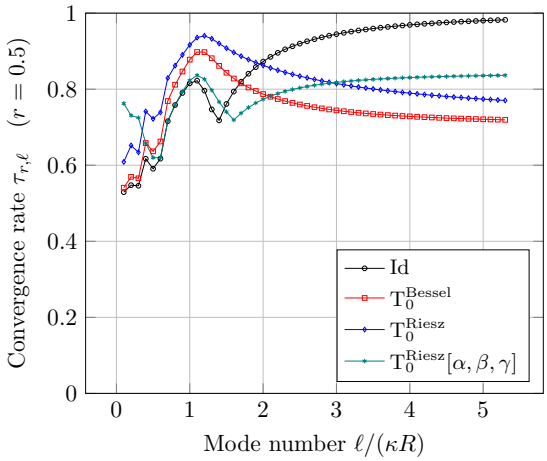

(b) Modal convergence factor.

Figure 6.4: Result of a possible optimization process on $T_0^{\text{Riesz}}[\alpha, \beta, \gamma]$. Fixed parameters $\kappa = \sigma = 5$, $R = 2$, $r = 0.5$.

We remark that it is also possible to parametrize in some sense the operator $\mathrm{T}_0^{\mathrm{Bessel}}$, since, for this particular spherical geometry, we have

$$\mathrm{T}_0^{\mathrm{Bessel}} = \mathrm{T}_0^{\mathrm{Bessel}}[1, 1, \sigma], \tag{6.48}$$

where ($d = 3$ and $s = 2$)

$$\mathrm{T}_0^{\mathrm{Bessel}}[\alpha, \beta, \sigma] := \alpha\, \mathbf{V}_{3,2,\sigma} + \beta\, \mathbf{Q}^C_{3,2,\sigma}, \tag{6.49}$$

with α and β two strictly positive constants, that could be tuned. We would get some similar improvements.

Of course the optimization is conducted in this particular ideal geometry and there are no guarantees that these optimized parameters are sensible values when the geometry changes (see also [91, Sec. 3.2.3.3] on this matter). Besides this optimization is only valid for the (relaxed) Jacobi algorithm. To simplify the discussion in what follows, we will only use the operator $\mathrm{T}_0^{\mathrm{Riesz}}$ defined in (5.112), i.e. keep $\alpha = \beta = \gamma = 1$ and the operator $\mathrm{T}_0^{\mathrm{Bessel}} = 2\mathbf{K}_{3,\sigma}$. In some sense, one could argue that this choice consists in choosing the optimal *asymptotic* convergence factor for large ℓ.

6.2 Diagonalization results

We show in this section that some boundary operators defined on the sphere S_R of radius R are diagonalized by the basis of spherical harmonics and we provide analytic expressions of the corresponding eigenvalues. We consider three different operators: the so-called Electric-to-Magnetic maps which take the tangential trace of the electric field and compute the (rotated) tangential trace of the corresponding magnetic field; the operator from standard potential theory $\mathrm{T}_0^{\mathrm{Bessel}} = 2\mathbf{K}_{3,\sigma}$ that we used as a transmission operator; and a class of integral operators which includes Riesz potentials that are involved in the definition of the other transmission operator we are considering $\mathrm{T}_0^{\mathrm{Riesz}}$.

6.2.1 Modal decompositions in spherical coordinates

In this sub-section, we gather some standard definitions and set some notations regarding Hilbert basis in spherical geometries. We only cite important properties that will be used in what follows. We then give classical results stating that solutions to Maxwell equations admit special convergent expansions in spherical coordinates.

6.2.1.1 Scalar spherical harmonics

We first recall the definition of Legendre polynomials P_ℓ, for $\ell \in \mathbb{N}$, power series solution of Legendre differential equation, defined on $[-1, 1]$ by

$$\frac{\mathrm{d}}{\mathrm{d}x}\left[(1-x^2)\frac{\mathrm{d}}{\mathrm{d}x}P_\ell(x)\right] + \ell(\ell+1)P_\ell(x) = 0, \qquad P_0(x) = 1. \tag{6.50}$$

One then defines the associated Legendre functions P_ℓ^m, for $-\ell \leq m \leq \ell$, defined on $[-1, 1]$ as [54, p. 14.2],

$$P_\ell^m(x) = (-1)^m (1-x^2)^{m/2} \frac{\mathrm{d}^m}{\mathrm{d}x^m} P_\ell(x). \tag{6.51}$$

Our definition of the (scalar) spherical harmonic $Y_{\ell,m}$ is as follows.

Definition 6.10 ([54, p. 14.30])**.** *The scalar spherical harmonics are defined for $\ell \in \mathbb{N}$, $-\ell \leq m \leq \ell$, $0 \leq \theta \leq \pi$ and $0 \leq \phi \leq 2\pi$ as*

$$Y_{\ell,m}(\theta,\phi) = \left(\frac{2\ell+1}{4\pi}\frac{(\ell-|m|)!}{(\ell+|m|)!}\right)^{1/2} P_\ell^{|m|}(\cos\theta)e^{im\phi}. \tag{6.52}$$

The interest in such objects becomes clear in light of the following proposition.

Proposition 6.11 ([110, Th. 2.4.1 and 2.4.4] and [46, Th. 2.7])**.** *The scalar spherical harmonic $Y_{\ell,m}$ of order ℓ is the eigenfunction of the Laplace-Beltrami operator associated with the eigenvalue $-\ell(\ell+1)$ with $2\ell+1$ multiplicity*

$$\Delta_{S^2} Y_{\ell,m} + \ell(\ell+1)Y_{\ell,m} = 0. \tag{6.53}$$

The family $(Y_{\ell,m})_{\ell,m}$ forms a complete orthonormal system for the hermitian inner product in $L^2(S^2)$ (orthogonal system also in $H^1(S^2)$).

In fact, for any real s, the hermitian product and the associated norm in $H^s(S^2)$ are given by [110, Eq. (2.5.5)]

$$\begin{aligned}(u,v)_{H^s(S^2)} &= \sum_{\ell=0}^{+\infty}\sum_{m=-\ell}^{\ell}(\ell(\ell+1))^s u_{\ell,m}\overline{v_{\ell,m}},\\ \|u\|^2_{H^s(S^2)} &= \sum_{\ell=0}^{+\infty}\sum_{m=-\ell}^{\ell}(\ell(\ell+1))^s |u_{\ell,m}|^2.\end{aligned} \tag{6.54}$$

for any u and v in $H^s(S^2)$ represented by their respective coefficients $(u_{\ell,m})_{\ell,m}$ and $(v_{\ell,m})_{\ell,m}$ in the basis of the spherical harmonics.

6.2.1.2 Vector spherical harmonics

Our definition of the *vector* spherical harmonics $\mathbf{\Psi}_{\ell,m}$ and $\mathbf{\Phi}_{\ell,m}$ is as follows — notice our choice of rescaling, which is not completely standard but is somewhat more pleasant to handle when computing norms of tangential fields.

Definition 6.12. *The vector spherical harmonics are defined for $\ell \in \mathbb{N}^*$, $-\ell \leq m \leq \ell$ as*

$$\begin{aligned}\mathbf{\Psi}_{\ell,m} &= (\ell(\ell+1))^{-1/2}\ \mathbf{grad}_{S^2}\, Y_{\ell,m},\\ \mathbf{\Phi}_{\ell,m} &= (\ell(\ell+1))^{-1/2}\ \mathbf{curl}_{S^2}\, Y_{\ell,m}.\end{aligned} \tag{6.55}$$

These two quantities are related through the simple identity

$$\mathbf{\Phi}_{\ell,m} = \mathbf{\Psi}_{\ell,m} \times \hat{\mathbf{r}}, \tag{6.56}$$

where $\hat{\mathbf{r}}$ is the outward unit normal vector to the unit sphere S^2.

The following proposition establishes in particular the Helmholtz-Hodge decomposition for tangential fields on the unit sphere.

Proposition 6.13 ([110, Th. 2.4.8] and [46, Th. 6.23])**.** *The family $\{\mathbf{\Psi}_{\ell,m}, \mathbf{\Phi}_{\ell,m}\}_{\ell,m}$ forms a complete orthonormal system for the hermitian inner product in $\mathbf{L}^2_t(S^2)$.*

Given two vectors $\mathbf{f}$ and $\mathbf{g}$ in $\mathbf{L}^2_t(S^2)$ represented by their respective coefficients $\{f^G_{\ell,m}, f^C_{\ell,m}\}_{\ell,m}$ and $\{g^G_{\ell,m}, g^C_{\ell,m}\}_{\ell,m}$, we can compute their hermitian products or norms in some spaces as follows. The hermitian product and the associated norm in $\mathbf{L}^2_t(S^2)$ are given by [110, Eq. (5.3.43) and (5.3.43)]

$$\begin{aligned}(\mathbf{f},\mathbf{g})_{\mathbf{L}^2_t(S^2)} &= \sum_{\ell=1}^{+\infty}\sum_{m=-\ell}^{\ell}\left(f^G_{\ell,m}\overline{g^G_{\ell,m}} + f^C_{\ell,m}\overline{g^C_{\ell,m}}\right),\\ \|\mathbf{f}\|^2_{\mathbf{L}^2_t(S^2)} &= \sum_{\ell=1}^{+\infty}\sum_{m=-\ell}^{\ell}\left(|f^G_{\ell,m}|^2 + |f^C_{\ell,m}|^2\right).\end{aligned} \tag{6.57}$$

The hermitian product and the associated norm in $\mathbf{H}^{-1/2}(\mathrm{div}; S^2)$ are given by [110, Eq. (5.3.52)]

$$\begin{aligned}(\mathbf{f},\mathbf{g})_{\mathbf{H}^{-1/2}(\mathrm{div};S^2)} &= \sum_{\ell=1}^{+\infty}\sum_{m=-\ell}^{\ell}\left((\ell(\ell+1))^{1/2} f^G_{\ell,m}\overline{g^G_{\ell,m}} + (\ell(\ell+1))^{-1/2} f^C_{\ell,m}\overline{g^C_{\ell,m}}\right),\\ \|\mathbf{f}\|^2_{\mathbf{H}^{-1/2}(\mathrm{div};S^2)} &= \sum_{\ell=1}^{+\infty}\sum_{m=-\ell}^{\ell}\left((\ell(\ell+1))^{1/2}|f^G_{\ell,m}|^2 + (\ell(\ell+1))^{-1/2}|f^C_{\ell,m}|^2\right).\end{aligned} \tag{6.58}$$

The hermitian product and the associated norm in $\mathbf{H}^{-1/2}(\mathrm{curl}; S^2)$ are given by [110, Eq. (5.3.53)]

$$\begin{aligned}(\mathbf{f},\mathbf{g})_{\mathbf{H}^{-1/2}(\mathrm{curl};S^2)} &= \sum_{\ell=1}^{+\infty}\sum_{m=-\ell}^{\ell}\left((\ell(\ell+1))^{-1/2} f^G_{\ell,m}\overline{g^G_{\ell,m}} + (\ell(\ell+1))^{1/2} f^C_{\ell,m}\overline{g^C_{\ell,m}}\right),\\ \|\mathbf{f}\|^2_{\mathbf{H}^{-1/2}(\mathrm{curl};S^2)} &= \sum_{\ell=1}^{+\infty}\sum_{m=-\ell}^{\ell}\left((\ell(\ell+1))^{-1/2}|f^G_{\ell,m}|^2 + (\ell(\ell+1))^{1/2}|f^C_{\ell,m}|^2\right).\end{aligned} \tag{6.59}$$

6.2.1.3 Spherical Bessel functions

We recall below several definitions of spherical Bessel functions, to avoid any possible confusion with existing literature in the choice of notations.

Definition 6.14. *The spherical Bessel functions are defined, for $\ell \in \mathbb{N}$ and complex arguments $z \in \mathbb{C}$, as ([54, p. 10.47])*

$$\begin{aligned} j_\ell(z) &= \sqrt{\frac{\pi}{2z}} J_{n+1/2}(z), & h^{(1)}_\ell(z) &= \sqrt{\frac{\pi}{2z}} H^{(1)}_{n+1/2}(z),\\ y_\ell(z) &= \sqrt{\frac{\pi}{2z}} Y_{n+1/2}(z), & h^{(2)}_\ell(z) &= \sqrt{\frac{\pi}{2z}} H^{(2)}_{n+1/2}(z).\end{aligned} \tag{6.60}$$

Definition 6.15. *The Riccati-Bessel functions are defined, for $\ell \in \mathbb{N}$ and complex arguments $z \in \mathbb{C}$, as*

$$\begin{aligned} \psi_\ell(z) &= z j_\ell(z), & \xi_\ell(z) &= z h^{(1)}_\ell(z),\\ \chi_\ell(z) &= z y_\ell(z), & \zeta_\ell(z) &= z h^{(2)}_\ell(z).\end{aligned} \tag{6.61}$$

6.2.1.4 Modal decomposition of solutions of Maxwell equations

The following proposition states that solutions of Maxwell equations in spherical coordinates can be written as expansions of spherical wave functions.

Proposition 6.16 ([46, Th. 6.24 and Th. 6.25])**.** *A divergence-free solution of the vector Maxwell equation in the domain delimited by two spheres of radius R_i and R_e with $R_i < R_e$ admits a convergent expansion representation in spherical coordinates as*

$$\begin{aligned}\mathbf{f}(r,\theta,\phi) = &\sum_{\ell=1}^{+\infty}\sum_{m=-\ell}^{\ell} \mathbf{curl}\left(\left(f_{\ell,m}^{C,\psi}\psi_\ell(\kappa r) + f_{\ell,m}^{C,\chi}\chi_\ell(\kappa r)\right) Y_{\ell,m}(\theta,\phi)\hat{\mathbf{r}}\right) \\ &+ \sum_{\ell=1}^{+\infty}\sum_{m=-\ell}^{\ell} \kappa^{-1}\,\mathbf{curl}\,\mathbf{curl}\left(\left(f_{\ell,m}^{G,\psi}\psi_\ell(\kappa r) + f_{\ell,m}^{G,\chi}\chi_\ell(\kappa r)\right) Y_{\ell,m}(\theta,\phi)\hat{\mathbf{r}}\right).\end{aligned} \tag{6.62}$$

A divergence-free solution of the vector Maxwell equation in the interior of the sphere S_R of radius R admits a convergent expansion representation in spherical coordinates as

$$\begin{aligned}\mathbf{f}(r,\theta,\phi) = &\sum_{\ell=1}^{+\infty}\sum_{m=-\ell}^{\ell} f_{\ell,m}^{C}\,\mathbf{curl}\left(\psi_\ell(\kappa r)Y_{\ell,m}(\theta,\phi)\hat{\mathbf{r}}\right) \\ &+ \sum_{\ell=1}^{+\infty}\sum_{m=-\ell}^{\ell} f_{\ell,m}^{G}\kappa^{-1}\,\mathbf{curl}\,\mathbf{curl}\left(\psi_\ell(\kappa r)Y_{\ell,m}(\theta,\phi)\hat{\mathbf{r}}\right).\end{aligned} \tag{6.63}$$

A divergence-free solution of the vector Maxwell equation in the exterior of the sphere S_R of radius R satisfying the Silver-Müller radiation condition at infinity admits a convergent expansion representation in spherical coordinates (with a correct time-dependence) as

$$\begin{aligned}\mathbf{f}(r,\theta,\phi) = &\sum_{\ell=1}^{+\infty}\sum_{m=-\ell}^{\ell} f_{\ell,m}^{C}\,\mathbf{curl}\left(\xi_\ell(\kappa r)Y_{\ell,m}(\theta,\phi)\hat{\mathbf{r}}\right) \\ &+ \sum_{\ell=1}^{+\infty}\sum_{m=-\ell}^{\ell} f_{\ell,m}^{G}\kappa^{-1}\,\mathbf{curl}\,\mathbf{curl}\left(\xi_\ell(\kappa r)Y_{\ell,m}(\theta,\phi)\hat{\mathbf{r}}\right).\end{aligned} \tag{6.64}$$

It will be convenient to compute the curl of such expansions, which is the purpose of the following lemma.

Lemma 6.17. *Let $\mathbf{f}$ be a vector field admitting a convergent expansion representation in spherical coordinates in the form of*

$$\begin{aligned}\mathbf{f}(r,\theta,\phi) = &\sum_{\ell=1}^{+\infty}\sum_{m=-\ell}^{\ell} f_{\ell,m}^{C}\,\mathbf{curl}\left(f_\ell(\kappa r)Y_{\ell,m}(\theta,\phi)\hat{\mathbf{r}}\right) \\ &+ \sum_{\ell=1}^{+\infty}\sum_{m=-\ell}^{\ell} f_{\ell,m}^{G}\kappa^{-1}\,\mathbf{curl}\,\mathbf{curl}\left(f_\ell(\kappa r)Y_{\ell,m}(\theta,\phi)\hat{\mathbf{r}}\right),\end{aligned} \tag{6.65}$$

where f_ℓ is any of the Ricatti-Bessel functions ψ_ℓ, χ_ℓ, ξ_ℓ or ζ_ℓ. Then we have

$$\begin{aligned}\mathbf{curl}\,\mathbf{f}(r,\theta,\phi) = &\sum_{\ell=1}^{+\infty}\sum_{m=-\ell}^{\ell} f_{\ell,m}^{C}\,\mathbf{curl}\,\mathbf{curl}\left(f_\ell(\kappa r)Y_{\ell,m}(\theta,\phi)\hat{\mathbf{r}}\right) \\ &+ \sum_{\ell=1}^{+\infty}\sum_{m=-\ell}^{\ell} f_{\ell,m}^{G}\kappa\,\mathbf{curl}\left(f_\ell(\kappa r)Y_{\ell,m}(\theta,\phi)\hat{\mathbf{r}}\right),\end{aligned} \tag{6.66}$$

Proof. We need only to prove that

$$\kappa^{-1}\,\mathbf{curl}\,\mathbf{curl}\,\mathbf{curl}\,(f_\ell(\kappa r)Y_{\ell,m}(\theta,\phi)\hat{\mathbf{r}}) = \kappa\,\mathbf{curl}\,(f_\ell(\kappa r)Y_{\ell,m}(\theta,\phi)\hat{\mathbf{r}})\,. \tag{6.67}$$

Let us introduce g_ℓ such that $f_\ell(z) = zg_\ell(z)$, so that g_ℓ is any of the spherical Bessel functions j_ℓ, y_ℓ, $h_\ell^{(1)}$ or $h_\ell^{(2)}$. Then $w_{\ell,m} := g_\ell(\kappa r)Y_{\ell,m}(\theta,\phi)$ satisfies the Helmholtz equation [46, Th. 2.9]

$$-(\Delta+\kappa^2)w_{\ell,m} = 0. \tag{6.68}$$

From $\mathbf{curl}\,\mathbf{grad} \equiv 0$, we have

$$\mathbf{curl}\left[r(\Delta+\kappa^2)w_{\ell,m}\hat{\mathbf{r}} + \mathbf{grad}\,w_{\ell,m}\right] = 0, \tag{6.69}$$

hence

$$\mathbf{curl}\left[\kappa^2\, rw_{\ell,m}\hat{\mathbf{r}} + \boldsymbol{\Delta}(rw_{\ell,m}\hat{\mathbf{r}})\right] = 0, \tag{6.70}$$

or again, since $\boldsymbol{\Delta} = \mathbf{grad}\,\mathrm{div} - \mathbf{curl}\,\mathbf{curl}$,

$$\mathbf{curl}\left[\kappa^2\, rw_{\ell,m}\hat{\mathbf{r}} + \mathbf{curl}\,\mathbf{curl}(rw_{\ell,m}\hat{\mathbf{r}})\right] = 0, \tag{6.71}$$

which are finally rewritten

$$\mathbf{curl}\left[\kappa^2\ (f_\ell(\kappa r)Y_{\ell,m}(\theta,\phi)\hat{\mathbf{r}}) + \mathbf{curl}\,\mathbf{curl}\,(f_\ell(\kappa r)Y_{\ell,m}(\theta,\phi)\hat{\mathbf{r}})\right] = 0. \tag{6.72}$$

■

We will also need in what follows the expression of the tangential trace of such decompositions, which can be easily deduced from the following proposition.

Proposition 6.18. *Let* $\mathbf{f}$ *be a vector field admitting a convergent expansion representation in spherical coordinates in the form of*

$$\begin{aligned}\mathbf{f}(r,\theta,\phi) = &\sum_{\ell=1}^{+\infty}\sum_{m=-\ell}^{\ell} f^C_{\ell,m}\,\mathbf{curl}\,(f_\ell(r)Y_{\ell,m}(\theta,\phi)\hat{\mathbf{r}}) \\ &+\sum_{\ell=1}^{+\infty}\sum_{m=-\ell}^{\ell} f^G_{\ell,m}\kappa^{-1}\,\mathbf{curl}\,\mathbf{curl}\,(f_\ell(r)Y_{\ell,m}(\theta,\phi)\hat{\mathbf{r}})\,.\end{aligned} \tag{6.73}$$

The tangential trace $\hat{\mathbf{r}}\times(\mathbf{f}\times\hat{\mathbf{r}})|_{S_R}$ *of* $\mathbf{f}$ *on the sphere* S_R *with radius* R *admits the following convergent expansion*

$$\hat{\mathbf{r}}\times(\mathbf{f}\times\hat{\mathbf{r}})|_{S_R} = \sum_{\ell=1}^{+\infty}\sum_{m=-\ell}^{\ell} R^{-1}(\ell(\ell+1))^{1/2}\left(f^C_{\ell,m}f_\ell(R)\boldsymbol{\Phi}_{\ell,m} + f^G_{\ell,m}\kappa^{-1}f'_\ell(R)\boldsymbol{\Psi}_{\ell,m}\right). \tag{6.74}$$

Proof. If $\mathbf{u} = u_r\hat{\mathbf{r}} + u_\theta\hat{\boldsymbol{\theta}} + u_\phi\hat{\boldsymbol{\phi}}$ denotes a vector vector field in $\mathbb{R}^3$ in spherical coordinates $(\hat{\mathbf{r}},\hat{\boldsymbol{\theta}},\hat{\boldsymbol{\phi}})$, we have

$$\begin{aligned}\mathbf{curl}\,\mathbf{u} = &\frac{1}{r\sin\theta}\left(\frac{\partial(\sin\theta u_\phi)}{\partial\theta} - \frac{\partial u_\theta}{\partial\phi}\right)\hat{\mathbf{r}} \\ &+\frac{1}{r}\left(-\frac{\partial(ru_\phi)}{\partial r} + \frac{1}{\sin\theta}\frac{\partial u_r}{\partial\phi}\right)\hat{\boldsymbol{\theta}} + \frac{1}{r}\left(\frac{\partial(ru_\theta)}{\partial r} - \frac{\partial u_r}{\partial\theta}\right)\hat{\boldsymbol{\phi}}.\end{aligned} \tag{6.75}$$

Besides, if u denotes a scalar field on the sphere S_R, the two following surface differential operators admit the expressions [110, Eq. (2.4.181) and (2.4.182)]

$$\begin{aligned} \mathbf{grad}_{S_R} u &= \frac{\partial u}{\partial \theta}\hat{\boldsymbol{\theta}} + \frac{1}{\sin\theta}\frac{\partial u}{\partial \phi}\hat{\boldsymbol{\phi}}, \\ \mathbf{curl}_{S_R} u &= \frac{1}{\sin\theta}\frac{\partial u}{\partial \phi}\hat{\boldsymbol{\theta}} - \frac{\partial u}{\partial \theta}\hat{\boldsymbol{\phi}}. \end{aligned} \tag{6.76}$$

From (6.75) and (6.76) we compute

$$\begin{aligned} \mathbf{curl}\,(f_r Y_{\ell,m}\hat{\mathbf{r}}) &= \frac{1}{r}\frac{1}{\sin\theta} f_\ell \frac{\partial Y_{\ell,m}}{\partial \phi}\hat{\boldsymbol{\theta}} - \frac{1}{r} f_\ell \frac{\partial Y_{\ell,m}}{\partial \theta}\hat{\boldsymbol{\phi}}, \\ &= r^{-1} f_\ell\, \mathbf{curl}_{S_R} Y_{\ell,m}, \end{aligned} \tag{6.77}$$

and

$$\begin{aligned} \hat{\mathbf{r}} \times [\mathbf{curl}\,\mathbf{curl}\,(f_r Y_{\ell,m}\hat{\mathbf{r}}) \times \hat{\mathbf{r}}] &= \frac{1}{r}\frac{\partial f_\ell}{\partial r}\frac{\partial Y_{\ell,m}}{\partial \theta}\hat{\boldsymbol{\theta}} + \frac{1}{r}\frac{1}{\sin\theta}\frac{\partial f_\ell}{\partial r}\frac{\partial Y_{\ell,m}}{\partial \phi}\hat{\boldsymbol{\phi}}, \\ &= r^{-1} f'_\ell\, \mathbf{grad}_{S_R} Y_{\ell,m}. \end{aligned} \tag{6.78}$$

The result then follows readily by definition of the spherical harmonics. ■

6.2.2 Electric-to-Magnetic operators

We first study the so-called Electric-to-Magnetic maps, akin to Dirichlet-to-Neumann maps but for the electromagnetic setting.

For any $\mathbf{J} \in \mathbf{H}^{-1/2}(\mathrm{curl}; S_R)$, we define the exterior Electric-to-Magnetic operator $\boldsymbol{\Lambda}_+$ as

$$\boldsymbol{\Lambda}_+ \;:\; \mathbf{J} \mapsto -\mathrm{i}Z\,(\mathbf{H} \times \hat{\mathbf{r}})\,|_{r=R}, \tag{6.79}$$

such that

$$\begin{cases} \mathbf{curl}\,\mathbf{E} - \mathrm{i}\kappa Z\mathbf{H} = 0, & \text{in } \Omega_+, \\ \mathbf{curl}\,\mathbf{H} + \mathrm{i}\kappa Z^{-1}\mathbf{E} = 0, & \text{in } \Omega_+, \\ \hat{\mathbf{r}} \times (\mathbf{E} \times \hat{\mathbf{r}})\,|_{r=R} = \mathbf{J}, & \text{on } S_R, \\ \lim_{r\to\infty}\; r\,(Z\mathbf{H} \times \hat{\mathbf{r}} - \hat{\mathbf{r}} \times (\mathbf{E} \times \hat{\mathbf{r}})) = 0. \end{cases} \tag{6.80}$$

Similarly, for any $\mathbf{J} \in \mathbf{H}^{-1/2}(\mathrm{curl}; S_R)$, we define the interior Electric-to-Magnetic operator $\boldsymbol{\Lambda}_-$ as

$$\boldsymbol{\Lambda}_- \;:\; \mathbf{J} \mapsto \mathrm{i}Z\,(\mathbf{H} \times \hat{\mathbf{r}})\,|_{r=R}, \tag{6.81}$$

such that

$$\begin{cases} \mathbf{curl}\,\mathbf{E} - \mathrm{i}\kappa Z\mathbf{H} = 0, & \text{in } \Omega_-, \\ \mathbf{curl}\,\mathbf{H} + \mathrm{i}\kappa Z^{-1}\mathbf{E} = 0, & \text{in } \Omega_-, \\ \hat{\mathbf{r}} \times (\mathbf{E} \times \hat{\mathbf{r}})\,|_{r=R} = \mathbf{J}, & \text{on } S_R. \end{cases} \tag{6.82}$$

Note that the denomination 'Electric-to-Magnetic' is convenient but slightly abusive since we included the factor $\mathrm{i}Z$ in the above definitions.

We suppose that these operators are well-defined, see Remark 6.3.

We are now able to state our first diagonalization result.

Proposition 6.19 ([110, Eq. (5.3.88)])**.** *The Electric-to-Magnetic operators $\mathbf{\Lambda}_\pm$ are diagonalized by $\mathbf{\Psi}_{\ell,m}$ and $\mathbf{\Phi}_{\ell,m}$. The respective eigenvalues $\widehat{\Lambda}^{\mathbf{\Psi}}_{\pm,\ell}$ and $\widehat{\Lambda}^{\mathbf{\Phi}}_{\pm,\ell}$, with $2\ell+1$ multiplicity, read*

$$\begin{cases} \widehat{\Lambda}^{\mathbf{\Psi}}_{-,\ell} = -\dfrac{\psi_\ell(\kappa R)}{\psi'_\ell(\kappa R)}, \\ \widehat{\Lambda}^{\mathbf{\Phi}}_{-,\ell} = +\dfrac{\psi'_\ell(\kappa R)}{\psi_\ell(\kappa R)}, \end{cases} \quad \textit{and} \quad \begin{cases} \widehat{\Lambda}^{\mathbf{\Psi}}_{+,\ell} = +\dfrac{\xi_\ell(\kappa R)}{\xi'_\ell(\kappa R)}, \\ \widehat{\Lambda}^{\mathbf{\Phi}}_{+,\ell} = -\dfrac{\xi'_\ell(\kappa R)}{\xi_\ell(\kappa R)}, \end{cases} \quad \forall \ell \in \mathbb{N}^*. \tag{6.83}$$

Proof. By Proposition 6.16, the fields $(\mathbf{E}_+, \mathbf{H}_+)$ solutions of (6.80) and $(\mathbf{E}_-, \mathbf{H}_-)$ solutions of (6.82) are necessary of the form of (6.64) and (6.63) respectively. We denote by $\{E^{\mathbf{\Psi}}_{\pm,\ell,m}, E^{\mathbf{\Phi}}_{\pm,\ell,m}\}_{\ell,m}$ and $\{H^{\mathbf{\Psi}}_{\pm,\ell,m}, H^{\mathbf{\Phi}}_{\pm,\ell,m}\}_{\ell,m}$ the corresponding coefficients with obvious convention and we have from the equations inside the domain and Lemma 6.17

$$\begin{cases} E^{\mathbf{\Phi}}_{\pm,\ell,m} - \mathrm{i}ZH^{\mathbf{\Psi}}_{\pm,\ell,m} = 0, \\ H^{\mathbf{\Phi}}_{\pm,\ell,m} + \mathrm{i}Z^{-1}E^{\mathbf{\Psi}}_{\pm,\ell,m} = 0. \end{cases} \tag{6.84}$$

From Proposition 6.18 we have

$$\begin{cases} \hat{\mathbf{r}} \times (\mathbf{E}_- \times \hat{\mathbf{r}})\,|_{S_R} = \displaystyle\sum_{\ell=1}^{+\infty} \sum_{m=-\ell}^{\ell} R^{-1}(\ell(\ell+1))^{1/2} \left(E^{\mathbf{\Phi}}_{-,\ell,m}\psi_\ell(\kappa R)\mathbf{\Phi}_{\ell,m} + E^{\mathbf{\Psi}}_{-,\ell,m}\psi'_\ell(\kappa R)\mathbf{\Psi}_{\ell,m} \right), \\ \hat{\mathbf{r}} \times (\mathbf{E}_+ \times \hat{\mathbf{r}})\,|_{S_R} = \displaystyle\sum_{\ell=1}^{+\infty} \sum_{m=-\ell}^{\ell} R^{-1}(\ell(\ell+1))^{1/2} \left(E^{\mathbf{\Phi}}_{+,\ell,m}\xi_\ell(\kappa R)\mathbf{\Phi}_{\ell,m} + E^{\mathbf{\Psi}}_{+,\ell,m}\xi'_\ell(\kappa R)\mathbf{\Psi}_{\ell,m} \right), \end{cases} \tag{6.85}$$

and, similarly, using the relation $\mathbf{\Phi}_{\ell,m} = \mathbf{\Psi}_{\ell,m} \times \hat{\mathbf{r}}$,

$$\begin{cases} \mathbf{H}_- \times \hat{\mathbf{r}}|_{S_R} = \displaystyle\sum_{\ell=1}^{+\infty} \sum_{m=-\ell}^{\ell} R^{-1}(\ell(\ell+1))^{1/2} \left(-H^{\mathbf{\Phi}}_{-,\ell,m}\psi_\ell(\kappa R)\mathbf{\Psi}_{\ell,m} + H^{\mathbf{\Psi}}_{-,\ell,m}\psi'_\ell(\kappa R)\mathbf{\Phi}_{\ell,m} \right), \\ -\mathbf{H}_+ \times \hat{\mathbf{r}}|_{S_R} = \displaystyle\sum_{\ell=1}^{+\infty} \sum_{m=-\ell}^{\ell} R^{-1}(\ell(\ell+1))^{1/2} \left(+H^{\mathbf{\Phi}}_{+,\ell,m}\xi_\ell(\kappa R)\mathbf{\Psi}_{\ell,m} - H^{\mathbf{\Psi}}_{+,\ell,m}\xi'_\ell(\kappa R)\mathbf{\Phi}_{\ell,m} \right). \end{cases} \tag{6.86}$$

Using the relations between the coefficients, we can rewrite

$$\begin{cases} \mathbf{H}_- \times \hat{\mathbf{r}}|_{S_R} = \displaystyle\sum_{\ell=1}^{+\infty} \sum_{m=-\ell}^{\ell} R^{-1}(\ell(\ell+1))^{1/2} Z^{-1} \left(\mathrm{i}E^{\mathbf{\Psi}}_{-,\ell,m}\psi_\ell(\kappa R)\mathbf{\Psi}_{\ell,m} - \mathrm{i}E^{\mathbf{\Phi}}_{-,\ell,m}\psi'_\ell(\kappa R)\mathbf{\Phi}_{\ell,m} \right), \\ -\mathbf{H}_+ \times \hat{\mathbf{r}}|_{S_R} = \displaystyle\sum_{\ell=1}^{+\infty} \sum_{m=-\ell}^{\ell} R^{-1}(\ell(\ell+1))^{1/2} Z^{-1} \left(-\mathrm{i}E^{\mathbf{\Psi}}_{+,\ell,m}\xi_\ell(\kappa R)\mathbf{\Psi}_{\ell,m} + \mathrm{i}E^{\mathbf{\Phi}}_{+,\ell,m}\xi'_\ell(\kappa R)\mathbf{\Phi}_{\ell,m} \right). \end{cases} \tag{6.87}$$

The above expressions for the eigenvalues are readily obtained by identification. ∎

We immediately deduce from the analytic expressions of the eigenvalues the following proposition. This result can be interpreted as expressing energy conservation, see also [110, Th. 5.3.5].

Proposition 6.20. *The eigenvalues of the Electric-to-Magnetic operators $\mathbf{\Lambda}_\pm$ satisfy*

$$\Im(\widehat{\Lambda}^{\mathbf{\Psi}}_{-,\ell}) = \Im(\widehat{\Lambda}^{\mathbf{\Phi}}_{-,\ell}) = 0 \qquad \textit{and} \qquad \Im(\widehat{\Lambda}^{\mathbf{\Psi}}_{+,\ell}) < 0, \quad \Im(\widehat{\Lambda}^{\mathbf{\Phi}}_{+,\ell}) < 0. \tag{6.88}$$

Proof. Since ψ_ℓ is real valued, the result for $\mathbf{\Lambda}_-$ is immediate. As for $\mathbf{\Lambda}_+$, the result follows from (see for instance [110, Th. 2.6.1]):

$$\Im\left(\frac{\xi'_\ell(\kappa R)}{\xi_\ell(\kappa R)}\right) = \frac{1}{|\xi_\ell(\kappa R)|^2} > 0. \tag{6.89}$$

■

From the expression of the eigenvalues, we also deduce the asymptotic behaviour for large ℓ of the Electric-to-Magnetic operators, as stated in the following proposition.

Proposition 6.21. *The eigenvalues of the Electric-to-Magnetic operators $\mathbf{\Lambda}_\pm$ satisfy, at infinity*

$$\begin{cases} \widehat{\Lambda}^{\mathbf{\Psi}}_{\pm,\ell} \;\sim\; -\frac{\kappa R}{\ell}, \\ \widehat{\Lambda}^{\mathbf{\Phi}}_{\pm,\ell} \;\sim\; +\frac{\ell}{\kappa R}, \end{cases} \qquad \ell \to +\infty. \tag{6.90}$$

Proof. From [46, Eq. (2.37) and (2.38)] we have, for $z \in \mathbb{C}$,

$$\begin{cases} \psi_\ell(z) \;\sim\; \frac{z^{\ell+1}}{(2\ell+1)!!}, \\ \psi_\ell(z) \;\sim\; (\ell+1)\frac{z^\ell}{(2\ell+1)!!}, \end{cases} \quad \text{and} \quad \begin{cases} \xi_\ell(z) \;\sim\; -\mathrm{i}\frac{(2\ell-1)!!}{z^\ell}, \\ \xi_\ell(z) \;\sim\; \mathrm{i}\ell\frac{(2\ell-1)!!}{z^{\ell+1}}, \end{cases} \qquad \ell \to +\infty, \tag{6.91}$$

with the notation $(2\ell+1)!! = 1\cdot 3\cdots(2\ell+1)$. The result is then readily established. ■

Numerical illustration We represent the eigenvalues of the operators $\mathbf{\Lambda}_\pm$ for $\kappa = 5$ in Figure 6.5 for a sphere S_R of radius $R = 2$. The range on the y-axis was purposely restricted and leaves some eigenvalues out of scope to better serve readability.

We recover numerically the result that the imaginary part of the interior Magnetic-to-Electric operator is identically zero, while it is negative for the exterior one. The regularizing (respectively de-regularizing) action of the operators $\mathbf{\Lambda}_\pm$ on $\mathbf{\Psi}_{\ell,m}$ (respectively $\mathbf{\Phi}_{\ell,m}$) is clear from the asymptotic behaviour for large ℓ of the real parts (or modulus) of their eigenvalues that one can infer from the graph. Note also that the eigenvalues in modulus are close to 1 for low mode numbers ℓ.

6.2.3 Operator stemming from potential theory

In this section we consider the operator $\mathrm{T}_0^{\mathrm{Bessel}} = 2\mathbf{K}_{3,\sigma}$, which is one of the transmission operator stemming from potential theory that we presented in the preceding chapter (and one of the operators we tested numerically). Notice that a modal analysis of a similar operator was already conducted in [34].

We recall the variational definition of $\mathbf{K}_{3,\sigma}$, valid for $\sigma \in \mathbb{C}$:

$$\begin{aligned} \langle \mathbf{K}_{3,\sigma}\boldsymbol{\phi}, \boldsymbol{\psi}\rangle_{S_R} =& \sigma \int_{S_R}\int_{S_R} \mathrm{G}_\sigma(|\mathbf{x}-\mathbf{y}|)\,(\nu(\mathbf{y})\times\boldsymbol{\phi}(\mathbf{y}))\cdot(\nu(\mathbf{x})\times\boldsymbol{\psi}(\mathbf{x}))\,\mathrm{d}\sigma(\mathbf{x})\mathrm{d}\sigma(\mathbf{y}) \\ &+ \sigma^{-1}\int_{S_R}\int_{S_R} \mathrm{G}_\sigma(|\mathbf{x}-\mathbf{y}|)\;\mathrm{curl}_{S_R}\boldsymbol{\phi}(\mathbf{y})\,\mathrm{curl}_{S_R}\boldsymbol{\psi}(\mathbf{x})\,\mathrm{d}\sigma(\mathbf{x})\mathrm{d}\sigma(\mathbf{y}). \end{aligned} \tag{6.92}$$

Proposition 6.22. *The operator $\mathbf{K}_{3,\sigma}$ given in* (6.92) *is diagonalized by $\mathbf{\Psi}_{\ell,m}$ and $\mathbf{\Phi}_{\ell,m}$. The respective eigenvalues, with $2\ell+1$ multiplicity, read*

$$\begin{cases} k_\ell^{\mathbf{\Psi}} = \psi_\ell(\mathrm{i}\sigma R)\xi_\ell(\mathrm{i}\sigma R), \\ k_\ell^{\mathbf{\Phi}} = \psi'_\ell(\mathrm{i}\sigma R)\xi'_\ell(\mathrm{i}\sigma R), \end{cases} \qquad \forall \ell \in \mathbb{N}^*. \tag{6.93}$$

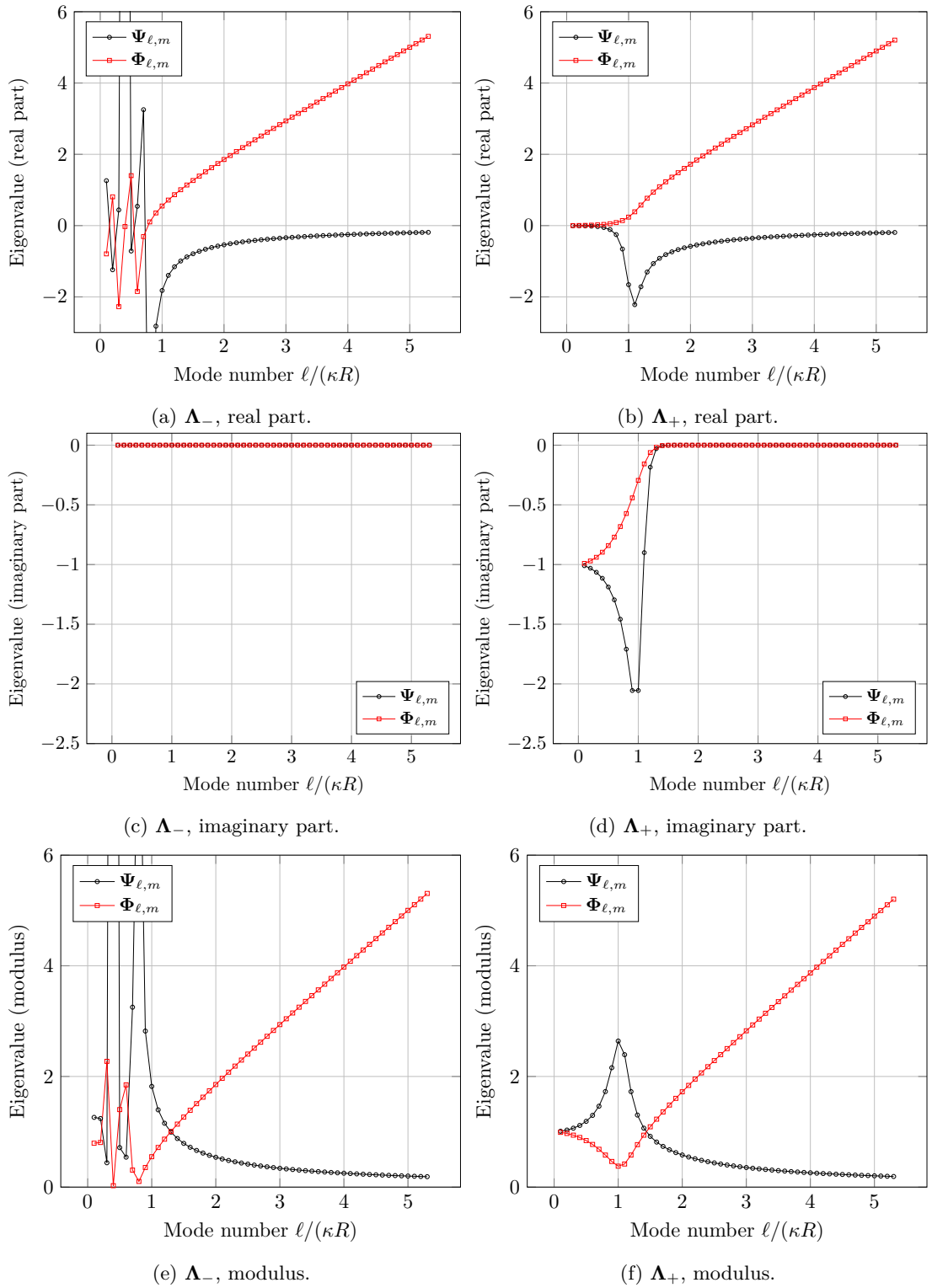

(a) $\mathbf{\Lambda}_-$, real part.

(b) $\mathbf{\Lambda}_+$, real part.

(c) $\mathbf{\Lambda}_-$, imaginary part.

(d) $\mathbf{\Lambda}_+$, imaginary part.

(e) $\mathbf{\Lambda}_-$, modulus.

(f) $\mathbf{\Lambda}_+$, modulus.

Figure 6.5: Real part, imaginary part and modulus (from top to bottom) of the eigenvalues of the operators $\mathbf{\Lambda}_-$ (left column) and $\mathbf{\Lambda}_+$ (right column) with respect to the mode number ℓ. Fixed parameters $\kappa = 5$, $R = 2$.

Proof. To prove this result, we use the reinterpretation of the integral operator in the form of a transmission problem (see (5.90)). For any $\mathbf{J} \in \mathbf{H}^{-1/2}(\mathrm{curl}; S_R)$, we have

$$\mathbf{K}_{3,\sigma}\mathbf{J} := \frac{1}{2}\Big((\mathbf{H}_+ \times \hat{\mathbf{r}})\,|_{S_R} + (\mathbf{H}_- \times \hat{\mathbf{r}})\,|_{S_R}\Big), \tag{6.94}$$

where $(\mathbf{E}_+, \mathbf{H}_+)$ and $(\mathbf{E}_-, \mathbf{H}_-)$ defined respectively in Ω_+ and Ω_- are (here dimensionless) solutions to

$$\begin{cases} \mathbf{curl}\,\mathbf{E}_\pm - \sigma\mathbf{H}_\pm = 0, & \text{in } \Omega_\pm, \\ \mathbf{curl}\,\mathbf{H}_\pm + \sigma\mathbf{E}_\pm = 0, & \text{in } \Omega_\pm, \\ (\mathbf{H}_- \times \hat{\mathbf{r}})\,|_{r=R} - (\mathbf{H}_+ \times \hat{\mathbf{r}})\,|_{r=R} = 0, & \text{on } S_R, \\ \hat{\mathbf{r}} \times (\mathbf{E}_- \times \hat{\mathbf{r}})\,|_{r=R} - \hat{\mathbf{r}} \times (\mathbf{E}_+ \times \hat{\mathbf{r}})\,|_{r=R} = -\mathbf{J}, & \text{on } S_R, \\ \lim_{r\to\infty}\ r\,(\mathbf{H}_+ \times \hat{\mathbf{r}} - \hat{\mathbf{r}} \times (\mathbf{E}_+ \times \hat{\mathbf{r}})) = 0. \end{cases} \tag{6.95}$$

In this coercive case, we would be able to state a result similar to Proposition 6.16: introducing the coefficients $\{E^{\mathbf{\Psi}}_{\pm,\ell,m}, E^{\mathbf{\Phi}}_{\pm,\ell,m}\}_{\ell,m}$ and $\{H^{\mathbf{\Psi}}_{\pm,\ell,m}, H^{\mathbf{\Phi}}_{\pm,\ell,m}\}_{\ell,m}$, the solutions $(\mathbf{E}_+, \mathbf{H}_+)$ in the exterior domain are of the form

$$\begin{cases} \mathbf{E}_+ = \sum_{\ell=1}^{+\infty}\sum_{m=-\ell}^{\ell}\left[E^{\mathbf{\Phi}}_{+,\ell,m}\,\mathbf{curl}\,(\xi_\ell(\mathrm{i}\sigma r)Y_{\ell,m}\hat{\mathbf{r}}) + E^{\mathbf{\Psi}}_{+,\ell,m}(\mathrm{i}\sigma)^{-1}\,\mathbf{curl}\,\mathbf{curl}\,(\xi_\ell(\mathrm{i}\sigma r)Y_{\ell,m}\hat{\mathbf{r}})\right], \\ \mathbf{H}_+ = \sum_{\ell=1}^{+\infty}\sum_{m=-\ell}^{\ell}\left[H^{\mathbf{\Phi}}_{+,\ell,m}\,\mathbf{curl}\,(\xi_\ell(\mathrm{i}\sigma r)Y_{\ell,m}\hat{\mathbf{r}}) + H^{\mathbf{\Psi}}_{+,\ell,m}(\mathrm{i}\sigma)^{-1}\,\mathbf{curl}\,\mathbf{curl}\,(\xi_\ell(\mathrm{i}\sigma r)Y_{\ell,m}\hat{\mathbf{r}})\right]. \end{cases} \tag{6.96}$$

and the solutions $(\mathbf{E}_-, \mathbf{H}_-)$ in the interior domain are of the form

$$\begin{cases} \mathbf{E}_- = \sum_{\ell=1}^{+\infty}\sum_{m=-\ell}^{\ell}\left[E^{\mathbf{\Phi}}_{-,\ell,m}\,\mathbf{curl}\,(\psi_\ell(\mathrm{i}\sigma r)Y_{\ell,m}\hat{\mathbf{r}}) + E^{\mathbf{\Psi}}_{-,\ell,m}(\mathrm{i}\sigma)^{-1}\,\mathbf{curl}\,\mathbf{curl}\,(\psi_\ell(\mathrm{i}\sigma r)Y_{\ell,m}\hat{\mathbf{r}})\right], \\ \mathbf{H}_- = \sum_{\ell=1}^{+\infty}\sum_{m=-\ell}^{\ell}\left[H^{\mathbf{\Phi}}_{-,\ell,m}\,\mathbf{curl}\,(\psi_\ell(\mathrm{i}\sigma r)Y_{\ell,m}\hat{\mathbf{r}}) + H^{\mathbf{\Psi}}_{-,\ell,m}(\mathrm{i}\sigma)^{-1}\,\mathbf{curl}\,\mathbf{curl}\,(\psi_\ell(\mathrm{i}\sigma r)Y_{\ell,m}\hat{\mathbf{r}})\right]. \end{cases} \tag{6.97}$$

From the equations inside the two domains $\Omega_\pm$ and Lemma 6.17, we have

$$\begin{cases} \mathrm{i}E^{\mathbf{\Phi}}_{\pm,\ell,m} - H^{\mathbf{\Psi}}_{\pm,\ell,m} = 0, \\ \mathrm{i}H^{\mathbf{\Phi}}_{\pm,\ell,m} + E^{\mathbf{\Psi}}_{\pm,\ell,m} = 0. \end{cases} \tag{6.98}$$

Using Proposition 6.18, from the continuity requirement on the tangential component of $\mathbf{H}$, we get

$$\begin{aligned} H^{\mathbf{\Phi}}_{-,\ell,m}\psi_\ell(\mathrm{i}\sigma R) - H^{\mathbf{\Phi}}_{+,\ell,m}\xi_\ell(\mathrm{i}\sigma R) = 0, \\ H^{\mathbf{\Psi}}_{-,\ell,m}\psi'_\ell(\mathrm{i}\sigma R) - H^{\mathbf{\Psi}}_{+,\ell,m}\xi'_\ell(\mathrm{i}\sigma R) = 0, \end{aligned} \tag{6.99}$$

so that, using the above relations, we have

$$\begin{aligned} E^{\mathbf{\Psi}}_{-,\ell,m}\psi_\ell(\mathrm{i}\sigma R) - E^{\mathbf{\Psi}}_{+,\ell,m}\xi_\ell(\mathrm{i}\sigma R) = 0, \\ E^{\mathbf{\Phi}}_{-,\ell,m}\psi'_\ell(\mathrm{i}\sigma R) - E^{\mathbf{\Phi}}_{+,\ell,m}\xi'_\ell(\mathrm{i}\sigma R) = 0. \end{aligned} \tag{6.100}$$

Now, using Proposition 6.13 and introducing the families $\{J^{\mathbf{\Psi}}_{\ell,m}, J^{\mathbf{\Phi}}_{\ell,m}\}_{\ell,m}$, we can expand $\mathbf{J}$ as (the rescaling of the coefficients is chosen adequately in order to simplify some expressions in the following)

$$\mathbf{J} = \sum_{\ell=1}^{+\infty}\sum_{m=-\ell}^{\ell} R^{-1}(\ell(\ell+1))^{1/2}\left(J^{\mathbf{\Psi}}_{\ell,m}\mathbf{\Psi}_{\ell,m} + J^{\mathbf{\Phi}}_{\ell,m}\mathbf{\Phi}_{\ell,m}\right), \tag{6.101}$$

so that using again Proposition 6.18, from the continuity requirement on the tangential component of $\mathbf{E}$, we get

$$\begin{aligned} E^{\mathbf{\Phi}}_{-,\ell,m}\psi_\ell(\mathrm{i}\sigma R) - E^{\mathbf{\Phi}}_{+,\ell,m}\xi_\ell(\mathrm{i}\sigma R) &= -J^{\mathbf{\Phi}}_{\ell,m}, \\ E^{\mathbf{\Psi}}_{-,\ell,m}\psi'_\ell(\mathrm{i}\sigma R) - E^{\mathbf{\Psi}}_{+,\ell,m}\xi'_\ell(\mathrm{i}\sigma R) &= -J^{\mathbf{\Psi}}_{\ell,m}. \end{aligned} \tag{6.102}$$

Eliminating the coefficients $E^{\mathbf{\Psi}}_{-,\ell,m}$ and $E^{\mathbf{\Phi}}_{-,\ell,m}$ using the relations we obtained previously we write

$$\begin{aligned} \left(\frac{\xi'_\ell(\mathrm{i}\sigma R)}{\psi'_\ell(\mathrm{i}\sigma R)}\psi_\ell(\mathrm{i}\sigma R) - \xi_\ell(\mathrm{i}\sigma R)\right) E^{\mathbf{\Phi}}_{+,\ell,m} &= -J^{\mathbf{\Phi}}_{\ell,m}, \\ \left(\frac{\xi_\ell(\mathrm{i}\sigma R)}{\psi_\ell(\mathrm{i}\sigma R)}\psi'_\ell(\mathrm{i}\sigma R) - \xi'_\ell(\mathrm{i}\sigma R)\right) E^{\mathbf{\Psi}}_{+,\ell,m} &= -J^{\mathbf{\Psi}}_{\ell,m}, \end{aligned} \tag{6.103}$$

which can be further simplified using the Wronskian identities

$$\begin{aligned} \psi_\ell(z)\chi'_\ell(z) - \psi'_\ell(z)\chi_\ell(z) &= 1, \\ \psi_\ell(z)\xi'_\ell(z) - \psi'_\ell(z)\xi_\ell(z) &= \mathrm{i}. \end{aligned} \tag{6.104}$$

into

$$\begin{aligned} E^{\mathbf{\Phi}}_{+,\ell,m} &= -\mathrm{i}\psi'_\ell(\mathrm{i}\sigma R)J^{\mathbf{\Phi}}_{\ell,m}, \\ E^{\mathbf{\Psi}}_{+,\ell,m} &= +\mathrm{i}\psi_\ell(\mathrm{i}\sigma R)J^{\mathbf{\Psi}}_{\ell,m}. \end{aligned} \tag{6.105}$$

By definition, we have

$$\begin{aligned} \mathbf{K}_{3,\sigma}\mathbf{J} := &-\frac{1}{2R}\sum_{\ell=1}^{+\infty}\sum_{m=-\ell}^{\ell}\left(\ell(\ell+1)\right)^{1/2}\left(H^{\mathbf{\Phi}}_{-,\ell,m}\psi_\ell(\mathrm{i}\sigma R) + H^{\mathbf{\Phi}}_{+,\ell,m}\xi_\ell(\mathrm{i}\sigma R)\right)\mathbf{\Psi}_{\ell,m} \\ &+\frac{1}{2R}\sum_{\ell=1}^{+\infty}\sum_{m=-\ell}^{\ell}\left(\ell(\ell+1)\right)^{1/2}\left(H^{\mathbf{\Psi}}_{-,\ell,m}\psi'_\ell(\mathrm{i}\sigma R) + H^{\mathbf{\Psi}}_{+,\ell,m}\xi'_\ell(\mathrm{i}\sigma R)\right)\mathbf{\Phi}_{\ell,m}, \end{aligned} \tag{6.106}$$

which, using again the continuity of $\mathbf{H}$ at the interface, is readily simplified into

$$\mathbf{K}_{3,\sigma}\mathbf{J} := \frac{1}{R}\sum_{\ell=1}^{+\infty}\sum_{m=-\ell}^{\ell}\left(\ell(\ell+1)\right)^{1/2}\left(-H^{\mathbf{\Phi}}_{+,\ell,m}\xi_\ell(\mathrm{i}\sigma R)\mathbf{\Psi}_{\ell,m} + H^{\mathbf{\Psi}}_{+,\ell,m}\xi'_\ell(\mathrm{i}\sigma R)\mathbf{\Phi}_{\ell,m}\right), \tag{6.107}$$

and further, using again the relations between the coefficients of $\mathbf{H}$ and $\mathbf{E}$,

$$\mathbf{K}_{3,\sigma}\mathbf{J} := \sum_{\ell=1}^{+\infty}\sum_{m=-\ell}^{\ell}R^{-1}\left(\ell(\ell+1)\right)^{1/2}\left(-\mathrm{i}E^{\mathbf{\Psi}}_{+,\ell,m}\xi_\ell(\mathrm{i}\sigma R)\mathbf{\Psi}_{\ell,m} + \mathrm{i}E^{\mathbf{\Phi}}_{+,\ell,m}\xi'_\ell(\mathrm{i}\sigma R)\mathbf{\Phi}_{\ell,m}\right), \tag{6.108}$$

and finally, we get

$$\mathbf{K}_{3,\sigma}\mathbf{J} := \sum_{\ell=1}^{+\infty}\sum_{m=-\ell}^{\ell}R^{-1}\left(\ell(\ell+1)\right)^{1/2}\left(\psi_\ell(\mathrm{i}\sigma R)\xi_\ell(\mathrm{i}\sigma R)J^{\mathbf{\Psi}}_{\ell,m}\mathbf{\Psi}_{\ell,m} + \psi'_\ell(\mathrm{i}\sigma R)\xi'_\ell(\mathrm{i}\sigma R)J^{\mathbf{\Phi}}_{\ell,m}\mathbf{\Phi}_{\ell,m}\right). \tag{6.109}$$

Hence, since we can choose any $\mathbf{J}$ above, we readily obtain the claimed eigenvalues. ■

Properties of the eigenvalues We can check directly on the analytical expression of the eigenvalues that the operator $\mathbf{K}_{3,\sigma}$ has indeed the correct properties.

Proposition 6.23 (**Positivity**). *The eigenvalues are all real and strictly positive*

$$k^{\mathbf{\Psi}}_\ell > 0, \qquad k^{\mathbf{\Phi}}_\ell > 0, \qquad \forall \ell \in \mathbb{N}^*. \tag{6.110}$$

Proof. Let $\ell \in \mathbb{N}^*$. From Rayleigh's formulas [54, p. 10.49], we have, for complex arguments $z \in \mathbb{C}$,

$$\begin{aligned} j_\ell(z) &= z^\ell \left(-\frac{1}{z}\frac{\mathrm{d}}{\mathrm{d}z}\right)^\ell \frac{\sin z}{z}, \\ y_\ell(z) &= z^\ell \left(-\frac{1}{z}\frac{\mathrm{d}}{\mathrm{d}z}\right)^\ell \frac{\cos z}{z}, \end{aligned} \tag{6.111}$$

so that using the relation $h_\ell^{(1)}(z) = j_\ell(z) + \mathrm{i} y_\ell(z)$ and Definition 6.15 of the Riccati-Bessel functions we obtain, for a real x

$$\begin{aligned} \psi_\ell(\mathrm{i}x) &= (\mathrm{i}x)^{\ell+1} \left(-\frac{1}{x}\frac{\mathrm{d}}{\mathrm{d}x}\right)^\ell \frac{\sinh x}{x}, \\ \xi_\ell(\mathrm{i}x) &= -(\mathrm{i}x)^{\ell+1} \left(-\frac{1}{x}\frac{\mathrm{d}}{\mathrm{d}x}\right)^\ell \frac{e^{-x}}{x}. \end{aligned} \tag{6.112}$$

By induction on ℓ, one can prove that for any $\ell \in \mathbb{N}^*$,

$$\operatorname{sign}\left[\left(-\frac{1}{x}\frac{\mathrm{d}}{\mathrm{d}x}\right)^\ell \frac{\sinh x}{x}\right] = 1, \qquad \text{and} \qquad \operatorname{sign}\left[\left(-\frac{1}{x}\frac{\mathrm{d}}{\mathrm{d}x}\right)^\ell \frac{e^{-x}}{x}\right] = (-1)^\ell. \tag{6.113}$$

The sign of k_ℓ^α, $\alpha \in \{\boldsymbol{\Psi}, \boldsymbol{\Phi}\}$, is then readily checked to be positive. ∎

Proposition 6.24 (**Asymptotic behaviour**). *We have at infinity*

$$2k_\ell^{\boldsymbol{\Psi}} \sim \left(\frac{\ell}{\sigma R}\right)^{-1}, \qquad 2k_\ell^{\boldsymbol{\Phi}} \sim \frac{\ell}{\sigma R}, \qquad \text{as } \ell \to \infty. \tag{6.114}$$

Proof. Recall that from [46, Eq. (2.37) and (2.38)] we have, for $z \in \mathbb{C}$,

$$\begin{cases} \psi_\ell(z) \sim \frac{z^{\ell+1}}{(2\ell+1)!!}, \\ \psi_\ell(z) \sim (\ell+1)\frac{z^\ell}{(2\ell+1)!!}, \end{cases} \qquad \text{and} \qquad \begin{cases} \xi_\ell(z) \sim -\mathrm{i}\frac{(2\ell-1)!!}{z^\ell}, \\ \xi_\ell(z) \sim \mathrm{i}\ell\frac{(2\ell-1)!!}{z^{\ell+1}}, \end{cases} \qquad \ell \to +\infty, \tag{6.115}$$

with the notation $(2\ell+1)!! = 1 \cdot 3 \cdots (2\ell+1)$. The result is then readily established. ∎

Numerical illustration We represent the (positive and real) eigenvalues of the operator $\mathbf{K}_{3,\sigma}$ for $\sigma = 5$ in Figure 6.6 for a sphere S_R of radius $R = 2$. The regularizing (respectively de-regularizing) action of $\mathbf{K}_{3,\sigma}$ on $\boldsymbol{\Psi}_{\ell,m}$ (respectively $\boldsymbol{\Phi}_{\ell,m}$) is clear from the asymptotic behaviour for large ℓ that one can infer from the graph. Note also that the eigenvalues are close to $1/2$ for low mode numbers ℓ, which will give 1 for the operator $2\mathbf{K}_{3,\sigma}$ from our choice of renormalization by the factor 2.

6.2.4 A general integral operator

We now study a general integral operator of convolution type, with a kernel that is rotation invariant. In particular, following an original idea of Francis Collino, we prove the relationship between the eigenvalues of the scalar and vector versions of this integral operator with the same kernel. We then apply this result to Riesz potentials. These operators are not used 'as is' in the method but are rather essential ingredients to the construction of some transmission operators.

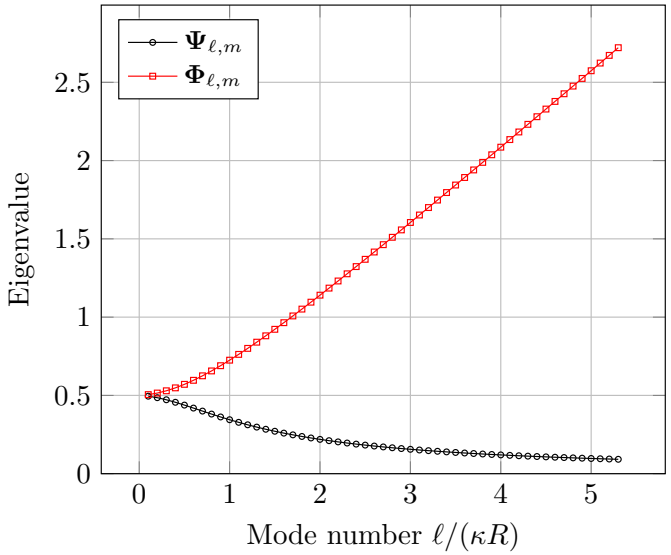

Figure 6.6: Eigenvalues of the operator $\mathbf{K}_{3,\sigma}$ with respect to the mode number ℓ. Fixed parameters $\sigma = 5$, $R = 2$.

6.2.4.1 A first diagonalization result

Let K be a *radial* kernel defined on $\mathbb{R}^+$, by which we mean that it is rotation invariant. Given a scalar field f defined on the sphere S_R of radius R, we define the scalar operator P_K as

$$P_K f(\mathbf{x}) = \int_{S_R} K(|\mathbf{x}-\mathbf{y}|) f(\mathbf{y}) \mathrm{d}s(\mathbf{y}). \qquad \forall \mathbf{x} \in S_R, \tag{6.116}$$

and, similarly, given a tangential vector field $\mathbf{f}$ defined on the sphere S_R, we define the vector operator $\mathbf{P}_K$ as

$$\mathbf{P}_K \mathbf{f}(\mathbf{x}) = \int_{S_R} K(|\mathbf{x}-\mathbf{y}|) \mathbf{f}(\mathbf{y}) \mathrm{d}s(\mathbf{y}), \qquad \forall \mathbf{x} \in S_R. \tag{6.117}$$

We will rely on the following lemma.

Lemma 6.25. *The unique vector field* $\mathbf{J}^{\mathbf{\Psi}}_{\ell,m}$ *in* $\mathbf{L}^2_t(S^2)$ *satisfying*

$$\begin{cases} \mathrm{div}_{S^2} \mathbf{J}^{\mathbf{\Psi}}_{\ell,m} = Y_{\ell,m}, \\ \mathrm{curl}_{S^2} \mathbf{J}^{\mathbf{\Psi}}_{\ell,m} = 0, \end{cases} \tag{6.118}$$

is

$$\mathbf{J}^{\mathbf{\Psi}}_{\ell,m} = -(\ell(\ell+1))^{-1/2} \, \mathbf{\Psi}_{\ell,m}. \tag{6.119}$$

Similarly, the unique vector field $\mathbf{J}^{\mathbf{\Phi}}_{\ell,m}$ *in* $\mathbf{L}^2_t(S^2)$ *satisfying*

$$\begin{cases} \mathrm{curl}_{S^2} \mathbf{J}^{\mathbf{\Phi}}_{\ell,m} = Y_{\ell,m}, \\ \mathrm{div}_{S^2} \mathbf{J}^{\mathbf{\Phi}}_{\ell,m} = 0, \end{cases} \tag{6.120}$$

is

$$\mathbf{J}^{\mathbf{\Phi}}_{\ell,m} = (\ell(\ell+1))^{-1/2} \, \mathbf{\Phi}_{\ell,m}. \tag{6.121}$$

Proof. From the following identities [110, Eq. (2.4.184), (2.4.187) and (2.4.193)]

$$\begin{aligned} \operatorname{div}_{S^2} \mathbf{curl}_{S^2} &= \operatorname{curl}_{S^2} \mathbf{grad}_{S^2} = 0, \\ \operatorname{div}_{S^2} \mathbf{grad}_{S^2} &= -\operatorname{curl}_{S^2} \mathbf{curl}_{S^2} = \Delta_{S^2}, \end{aligned} \tag{6.122}$$

it is straightforward to check that (6.119) and (6.121) are indeed respective solutions to (6.118) and (6.120). The unicity follows from Proposition 6.13 which states that any vector tangent field in $\mathbf{L}^2_t(S^2)$ can be decomposed on the basis of vector spherical harmonics. ■

We are going to apply this lemma to the potential $\mathbf{P}_K$. Before doing so we first need to establish two technical lemmas.

Lemma 6.26. *We have, on S_R,*

$$\operatorname{div}_{S^2} \mathbf{P}_K \mathbf{f} = P_{K-L[K]} \operatorname{div}_{S^2} \mathbf{f}, \tag{6.123}$$

where $L[K]$ is defined as

$$L[K](r) = \frac{1}{2}\Big(\frac{r}{R}\Big)^2 K(r) + R^{-2} \int_0^r sK(s)\mathrm{d}s, \qquad \forall r \in \mathbb{R},\ r > 0. \tag{6.124}$$

Proof. Let $\mathbf{u} = u_r \hat{\mathbf{r}} + u_\theta \hat{\boldsymbol{\theta}} + u_\phi \hat{\boldsymbol{\phi}}$ a vector field in $\mathbb{R}^3$ in spherical coordinates $(\hat{\mathbf{r}}, \hat{\boldsymbol{\theta}}, \hat{\boldsymbol{\phi}})$. The expression for the divergence of $\mathbf{u}$ at a point (r, θ, ϕ) in this basis is

$$\operatorname{div} \mathbf{u} = \frac{1}{r^2}\partial_r(r^2 u_r) + \frac{1}{r} \operatorname{div}_{S^2} \mathbf{u}. \tag{6.125}$$

Let $\mathbf{x} \in S_R$ and $\hat{\mathbf{x}} = \frac{\mathbf{x}}{|\mathbf{x}|}$, we have

$$\operatorname{div}_{S^2} \mathbf{P}_K \mathbf{f}(\mathbf{x}) = |\mathbf{x}| \operatorname{div} \mathbf{P}_K \mathbf{f}(\mathbf{x}) - |\mathbf{x}|^{-1} \partial_{|\mathbf{x}|}(|\mathbf{x}|^2 \mathbf{P}_K \mathbf{f} \cdot \hat{\mathbf{x}})(\mathbf{x}). \tag{6.126}$$

We are going to compute each term separately.

1. Computation of $\operatorname{div} \mathbf{P}_K \mathbf{f}(\mathbf{x})$. Recall that for a scalar field a and a vector field $\mathbf{u}$ in $\mathbb{R}^3$ the following identity holds

$$\operatorname{div}(a\mathbf{u}) = a \operatorname{div}(\mathbf{u}) + \mathbf{grad}(a) \cdot \mathbf{u}, \tag{6.127}$$

from which we deduce

$$\begin{aligned} \operatorname{div}_{\mathbf{x}} \left(K(|\mathbf{x}-\mathbf{y}|)\mathbf{f}(\mathbf{y})\right) &= K(|\mathbf{x}-\mathbf{y}|) \operatorname{div}_{\mathbf{x}} \mathbf{f}(\mathbf{y}) + \mathbf{grad}_{\mathbf{x}} K(|\mathbf{x}-\mathbf{y}|) \cdot \mathbf{f}(\mathbf{y}), \\ &= \mathbf{grad}_{\mathbf{x}} K(|\mathbf{x}-\mathbf{y}|) \cdot \mathbf{f}(\mathbf{y}), \end{aligned} \tag{6.128}$$

so that

$$\operatorname{div} \mathbf{P}_K \mathbf{f}(\mathbf{x}) = \int_{S_R} \mathbf{grad}_{\mathbf{x}} K(|\mathbf{x}-\mathbf{y}|) \cdot \mathbf{f}(\mathbf{y})\ \mathrm{d}s(\mathbf{y}). \tag{6.129}$$

Using $\mathbf{grad}_{\mathbf{x}} K(|\mathbf{x}-\mathbf{y}|) = -\mathbf{grad}_{\mathbf{y}} K(|\mathbf{x}-\mathbf{y}|)$ and the fact that the field $\mathbf{f}(\mathbf{y})$ is tangent to S_R we get successively

$$\begin{aligned} \operatorname{div} \mathbf{P}_K \mathbf{f}(\mathbf{x}) &= \int_{S_R} -\mathbf{grad}_{\mathbf{y}} K(|\mathbf{x}-\mathbf{y}|) \cdot \mathbf{f}(\mathbf{y})\ \mathrm{d}s(\mathbf{y}), \\ &= \int_{S_R} R^{-1} \mathbf{grad}_{S^2} K(|\mathbf{x}-\mathbf{y}|) \cdot \mathbf{f}(\mathbf{y})\ \mathrm{d}s(\mathbf{y}), \end{aligned} \tag{6.130}$$

from which we readily obtain

$$\begin{aligned} \operatorname{div} \mathbf{P}_K \mathbf{f}(\mathbf{x}) &= \int_{S_R} R^{-1} K(|\mathbf{x}-\mathbf{y}|) \operatorname{div}_{S^2} \mathbf{f}(\mathbf{y}) \, \mathrm{d}s(\mathbf{y}), \\ &= R^{-1} \, P_K \operatorname{div}_{S^2} \mathbf{f}. \end{aligned} \tag{6.131}$$

2. Computation of $\partial_{|\mathbf{x}|}(|\mathbf{x}|^2 \mathbf{P}_K \mathbf{f} \cdot \hat{\mathbf{x}})(\mathbf{x})$. Let $\mathbf{y} \in S_R$ and $\hat{\mathbf{y}} = \frac{\mathbf{y}}{|\mathbf{y}|}$, we have

$$\partial_{|\mathbf{x}|}(|\mathbf{x}|^2 K(|\mathbf{x}-\mathbf{y}|)) = |\mathbf{x}|^2 \partial_{|\mathbf{x}|}(|\mathbf{x}-\mathbf{y}|) K'(|\mathbf{x}-\mathbf{y}|) + 2|\mathbf{x}| K(|\mathbf{x}-\mathbf{y}|), \tag{6.132}$$

Now

$$\partial_{|\mathbf{x}|}(|\mathbf{x}-\mathbf{y}|) = |\mathbf{x}-\mathbf{y}|^{-1} \left(|\mathbf{x}| - |\mathbf{y}| \hat{\mathbf{x}} \cdot \hat{\mathbf{y}} \right), \tag{6.133}$$

and since $|\mathbf{x}| = |\mathbf{y}| = R$ and $(1 - \hat{\mathbf{x}} \cdot \hat{\mathbf{y}}) = \frac{|\mathbf{x}-\mathbf{y}|^2}{2R^2}$, we get

$$\partial_{|\mathbf{x}|}(|\mathbf{x}-\mathbf{y}|) = \frac{|\mathbf{x}-\mathbf{y}|}{2R}, \tag{6.134}$$

so that, by definition of $L[K]$, we obtain

$$\begin{aligned} \partial_{|\mathbf{x}|}(|\mathbf{x}|^2 K(|\mathbf{x}-\mathbf{y}|)) &= \frac{R}{|\mathbf{x}-\mathbf{y}|} \left(\frac{1}{2} |\mathbf{x}-\mathbf{y}|^2 K'(|\mathbf{x}-\mathbf{y}|) + 2|\mathbf{x}-\mathbf{y}| K(|\mathbf{x}-\mathbf{y}|) \right), \\ &= R^3 \frac{L[K]'(|\mathbf{x}-\mathbf{y}|)}{|\mathbf{x}-\mathbf{y}|}. \end{aligned} \tag{6.135}$$

Now we compute

$$\begin{aligned} \partial_{|\mathbf{x}|}(|\mathbf{x}|^2 \mathbf{P}_K \mathbf{f} \cdot \hat{\mathbf{x}})(\mathbf{x}) &= \int_{S_R} \partial_{|\mathbf{x}|} \left(|\mathbf{x}|^2 K(|\mathbf{x}-\mathbf{y}|) \right) \mathbf{f}(\mathbf{y}) \cdot \hat{\mathbf{x}} \, \mathrm{d}s(\mathbf{y}), \\ &= \int_{S_R} R^3 \frac{L[K]'(|\mathbf{x}-\mathbf{y}|)}{|\mathbf{x}-\mathbf{y}|} \hat{\mathbf{x}} \cdot \mathbf{f}(\mathbf{y}) \, \mathrm{d}s(\mathbf{y}), \end{aligned} \tag{6.136}$$

and from $\hat{\mathbf{y}} \cdot \mathbf{f}(\mathbf{y}) = 0$, we get

$$\begin{aligned} \partial_{|\mathbf{x}|}(|\mathbf{x}|^2 \mathbf{P}_K \mathbf{f} \cdot \hat{\mathbf{x}})(\mathbf{x}) &= \int_{S_R} R^3 \frac{L[K]'(|\mathbf{x}-\mathbf{y}|)}{|\mathbf{x}-\mathbf{y}|} (\hat{\mathbf{x}} - \hat{\mathbf{y}}) \cdot \mathbf{f}(\mathbf{y}) \, \mathrm{d}s(\mathbf{y}), \\ &= \int_{S_R} R^2 \frac{L[K]'(|\mathbf{x}-\mathbf{y}|)}{|\mathbf{x}-\mathbf{y}|} (\mathbf{x} - \mathbf{y}) \cdot \mathbf{f}(\mathbf{y}) \, \mathrm{d}s(\mathbf{y}), \\ &= \int_{S_R} -R^2 \, \mathbf{grad}_{\mathbf{y}} \, L[K](|\mathbf{x}-\mathbf{y}|) \cdot \mathbf{f}(\mathbf{y}) \, \mathrm{d}s(\mathbf{y}). \end{aligned} \tag{6.137}$$

Using again the fact that the field $\mathbf{f}$ is tangent to S_R we finally obtain

$$\begin{aligned} \partial_R(R \mathbf{P}_K \mathbf{f} \cdot \hat{\mathbf{r}})(\mathbf{x}) &= \int_{S_R} -R \, \mathbf{grad}_{S^2} \, L[K](|\mathbf{x}-\mathbf{y}|) \cdot \mathbf{f}(\mathbf{y}) \, \mathrm{d}s(\mathbf{y}), \\ &= \int_{S_R} R L[K](|\mathbf{x}-\mathbf{y}|) \operatorname{div}_{S^2} \mathbf{f}(\mathbf{y}) \, \mathrm{d}s(\mathbf{y}), \\ &= R P_{L[K]} \operatorname{div}_{S^2} \mathbf{f}(\mathbf{x}). \end{aligned} \tag{6.138}$$

Finally we have

$$\operatorname{div}_{S^2} \mathbf{P}_K \mathbf{f} = P_K \operatorname{div}_{S^2} \mathbf{f} - P_{L[K]} \operatorname{div}_{S^2} \mathbf{f}. \tag{6.139}$$

■

Lemma 6.27. *We have, on S_R,*

$$\operatorname{curl}_{S^2} \mathbf{P}_K \mathbf{f} = P_K \operatorname{curl}_{S^2} \mathbf{f}. \tag{6.140}$$

Proof. Let $\mathbf{x} \in S_R$, we have

$$\operatorname{curl}_{S^2} \mathbf{P}_K \mathbf{f}(\mathbf{x}) = \mathbf{x} \cdot \mathbf{curl}\, \mathbf{P}_K \mathbf{f}(\mathbf{x}), \tag{6.141}$$

so that

$$\operatorname{curl}_{S^2} \mathbf{P}_K \mathbf{f}(\mathbf{x}) = \int_{S_R} \mathbf{curl}_{\mathbf{x}} \left(K(|\mathbf{x}-\mathbf{y}|)\mathbf{f}(\mathbf{y})\right) \cdot \mathbf{x}\, \mathrm{d}s(\mathbf{y}). \tag{6.142}$$

Recall that for a scalar field a and a vector field $\mathbf{u}$ in $\mathbb{R}^3$ the following identity holds

$$\mathbf{curl}(a\mathbf{u}) = a\ \mathbf{curl}(\mathbf{u}) + \mathbf{grad}(a) \times \mathbf{u}, \tag{6.143}$$

from which we deduce

$$\begin{aligned} \mathbf{curl}_{\mathbf{x}} \left(K(|\mathbf{x}-\mathbf{y}|)\mathbf{f}(\mathbf{y})\right) &= K(|\mathbf{x}-\mathbf{y}|)\, \mathbf{curl}_{\mathbf{x}}\, \mathbf{f}(\mathbf{y}) + \mathbf{grad}_{\mathbf{x}}\, K(|\mathbf{x}-\mathbf{y}|) \times \mathbf{f}(\mathbf{y}), \\ &= \mathbf{grad}_{\mathbf{x}}\, K(|\mathbf{x}-\mathbf{y}|) \times \mathbf{f}(\mathbf{y}), \end{aligned} \tag{6.144}$$

so that

$$\operatorname{curl}_{S^2} \mathbf{P}_K \mathbf{f}(\mathbf{x}) = \int_{S_R} (\mathbf{grad}_{\mathbf{x}}\, K(|\mathbf{x}-\mathbf{y}|) \times \mathbf{f}(\mathbf{y})) \cdot \mathbf{x}\, \mathrm{d}s(\mathbf{y}). \tag{6.145}$$

Using the fact that $\mathbf{grad}_{\mathbf{x}}\, K(|\mathbf{x}-\mathbf{y}|)$ is directed along $\mathbf{x}-\mathbf{y}$, we deduce

$$\begin{aligned} \operatorname{curl}_{S^2} \mathbf{P}_K \mathbf{f}(\mathbf{x}) &= \int_{S_R} (\mathbf{grad}_{\mathbf{x}}\, K(|\mathbf{x}-\mathbf{y}|) \times \mathbf{f}(\mathbf{y})) \cdot (\mathbf{x}+\mathbf{y}-\mathbf{x})\, \mathrm{d}s(\mathbf{y}), \\ &= \int_{S_R} (\mathbf{grad}_{\mathbf{x}}\, K(|\mathbf{x}-\mathbf{y}|) \times \mathbf{f}(\mathbf{y})) \cdot \mathbf{y}\, \mathrm{d}s(\mathbf{y}). \end{aligned} \tag{6.146}$$

Using $\mathbf{grad}_{\mathbf{x}}\, K(|\mathbf{x}-\mathbf{y}|) = -\,\mathbf{grad}_{\mathbf{y}}\, K(|\mathbf{x}-\mathbf{y}|)$ and a simple property of the triple product we get

$$\operatorname{curl}_{S^2} \mathbf{P}_K \mathbf{f}(\mathbf{x}) = \int_{S_R} \mathbf{grad}_{\mathbf{y}}\, K(|\mathbf{x}-\mathbf{y}|) \cdot (\mathbf{y} \times \mathbf{f}(\mathbf{y}))\ \mathrm{d}s(\mathbf{y}). \tag{6.147}$$

Since $\mathbf{y} \times \mathbf{f}(\mathbf{y})$ is tangent to S_R we write

$$\operatorname{curl}_{S^2} \mathbf{P}_K \mathbf{f}(\mathbf{x}) = \int_{S_R} R^{-1}\, \mathbf{grad}_{S^2}\, K(|\mathbf{x}-\mathbf{y}|) \cdot (\mathbf{y} \times \mathbf{f}(\mathbf{y}))\ \mathrm{d}s(\mathbf{y}). \tag{6.148}$$

Finally, we obtain

$$\begin{aligned} \operatorname{curl}_{S^2} \mathbf{P}_K \mathbf{f}(\mathbf{x}) &= \int_{S_R} -R^{-1} K(|\mathbf{x}-\mathbf{y}|)\, \operatorname{div}_{S^2} (\mathbf{y} \times \mathbf{f}(\mathbf{y}))\ \mathrm{d}s(\mathbf{y}), \\ &= \int_{S_R} K(|\mathbf{x}-\mathbf{y}|)\, \operatorname{curl}_{S^2} \mathbf{f}(\mathbf{y})\, \mathrm{d}s(\mathbf{y}), \\ &= P_K \operatorname{curl}_{S^2} \mathbf{f}(\mathbf{x}). \end{aligned} \tag{6.149}$$

■

We are now able to state the following abstract diagonalization result.

Proposition 6.28. *Assuming that the two scalar potentials are diagonalized by the scalar spherical harmonics, such that*

$$\begin{aligned} P_K Y_{\ell,m} &= p_K(\ell)\ Y_{\ell,m}, \\ P_{L[K]} Y_{\ell,m} &= p_{L[K]}(\ell)\ Y_{\ell,m}, \end{aligned} \tag{6.150}$$

where $L[K]$ is given in (6.124)*, the operator $\mathbf{P}_K$ given in* (6.117) *is diagonalized by $\mathbf{\Psi}_{\ell,m}$ and $\mathbf{\Phi}_{\ell,m}$. The respective eigenvalues, with $2\ell+1$ multiplicity, read*

$$p_K^{\mathbf{\Psi}}(\ell) = p_K(\ell) - p_{L[K]}(\ell) \qquad \textit{and} \qquad p_K^{\mathbf{\Phi}}(\ell) = p_K(\ell). \tag{6.151}$$

Proof. Using Lemmas 6.27 and 6.27 and the properties of the spherical harmonic $Y_{\ell,m}$, we have, on S_R,

$$\operatorname{div}_{S^2} \mathbf{P}_K \mathbf{\Phi}_{\ell,m} = P_{K-L[K]} \operatorname{div}_{S^2} \mathbf{\Phi}_{\ell,m} = (\ell(\ell+1))^{-1/2}\ P_{K-L[K]} \operatorname{div}_{S^2} \mathbf{curl}_{S^2}\, Y_{\ell,m} = 0,$$

$$\begin{aligned} \text{and} \qquad \operatorname{curl}_{S^2} \mathbf{P}_K \mathbf{\Phi}_{\ell,m} &= P_K \operatorname{curl}_{S^2} \mathbf{\Phi}_{\ell,m} = -(\ell(\ell+1))^{-1/2} P_K \Delta_{S^2} Y_{\ell,m}, \\ &= (\ell(\ell+1))^{1/2} P_K Y_{\ell,m} = (\ell(\ell+1))^{1/2} p_K^{\mathbf{\Phi}}(\ell) Y_{\ell,m}, \end{aligned} \tag{6.152}$$

besides,

$$\begin{aligned} \operatorname{div}_{S^2} \mathbf{P}_K \mathbf{\Psi}_{\ell,m} &= P_{K-L[K]} \operatorname{div}_{S^2} \mathbf{\Psi}_{\ell,m} = (\ell(\ell+1))^{-1/2} P_{K-L[K]} \Delta_{S^2} Y_{\ell,m}, \\ &= -(\ell(\ell+1))^{1/2} P_{K-L[K]} Y_{\ell,m} = -(\ell(\ell+1))^{1/2} p_K^{\mathbf{\Psi}} Y_{\ell,m}, \end{aligned} \tag{6.153}$$

$$\text{and} \qquad \operatorname{curl}_{S^2} \mathbf{P}_K \mathbf{\Psi}_{\ell,m} = P_K \operatorname{curl}_{S^2} \mathbf{\Psi}_{\ell,m} = (\ell(\ell+1))^{-1/2}\ P_K \operatorname{curl}_{S^2} \mathbf{grad}_{S^2}\, Y_{\ell,m} = 0.$$

The result is then a strict application of Lemma 6.25 which yields that

$$\begin{aligned} \mathbf{P}_K \mathbf{\Phi}_{\ell,m} &= p_K^{\mathbf{\Phi}}(\ell) \mathbf{\Phi}_{\ell,m}, \\ \mathbf{P}_K \mathbf{\Psi}_{\ell,m} &= p_K^{\mathbf{\Psi}}(\ell) \mathbf{\Psi}_{\ell,m}. \end{aligned} \tag{6.154}$$

■

We will also use the scalar potential P_K composed with surface differential operators. The corresponding diagonalization result is stated in the following proposition.

Proposition 6.29. *Assume that the scalar potential P_{K_α} is diagonalized by the scalar spherical harmonics, such that*

$$P_K Y_{\ell,m} = p_K(\ell)\ Y_{\ell,m}. \tag{6.155}$$

The operator $\mathbf{curl}_{S^2}\, P_K \operatorname{curl}_{S^2}$ is diagonalized by $\mathbf{\Phi}_{\ell,m}$ with associated eigenvalues

$$p_K^C(\ell) = \ell(\ell+1) p_K(\ell), \tag{6.156}$$

and

$$\mathbf{\Psi}_{\ell,m} \in \operatorname{Ker}\left(\mathbf{curl}_{S^2}\, P_K \operatorname{curl}_{S^2}\right). \tag{6.157}$$

Similarly, the operator $-\mathbf{grad}_{S^2}\, P_K \operatorname{div}_{S^2}$ is diagonalized by $\mathbf{\Psi}_{\ell,m}$ with associated eigenvalues

$$p_K^G(\ell) = \ell(\ell+1) p_K(\ell), \tag{6.158}$$

and

$$\mathbf{\Phi}_{\ell,m} \in \operatorname{Ker}\left(\mathbf{grad}_{S^2}\, P_K \operatorname{div}_{S^2}\right). \tag{6.159}$$

Proof. The fact that

$$\begin{aligned} \boldsymbol{\Psi}_{\ell,m} &\in \mathrm{Ker}\left(\mathbf{curl}_{S^2} P_K \,\mathrm{curl}_{S^2}\right), \\ \boldsymbol{\Phi}_{\ell,m} &\in \mathrm{Ker}\left(\mathbf{grad}_{S^2} P_K \,\mathrm{div}_{S^2}\right), \end{aligned} \tag{6.160}$$

readily follows from

$$\mathrm{div}_{S^2}\,\mathbf{curl}_{S^2} = \mathrm{curl}_{S^2}\,\mathbf{grad}_{S^2} = 0. \tag{6.161}$$

Besides, we compute using simple properties of the scalar and vector spherical harmonics

$$\begin{aligned} \mathbf{curl}_{S^2} P_K \,\mathrm{curl}_{S^2}\, \boldsymbol{\Phi}_{\ell,m} &= \left(\ell(\ell+1)\right)^{-1/2} \mathbf{curl}_{S^2} P_K \,\mathrm{curl}_{S^2}\, \mathbf{curl}_{S^2}\, Y_{\ell,m}, \\ &= -\left(\ell(\ell+1)\right)^{-1/2} \mathbf{curl}_{S^2} P_K \Delta_{S^2} Y_{\ell,m} = \left(\ell(\ell+1)\right)^{1/2} \mathbf{curl}_{S^2} P_K Y_{\ell,m}, \\ &= \left(\ell(\ell+1)\right)^{1/2} p_K(\ell)\, \mathbf{curl}_{S^2}\, Y_{\ell,m} = \ell(\ell+1) p_K(\ell) \boldsymbol{\Phi}_{\ell,m}(\mathbf{y}). \end{aligned} \tag{6.162}$$

The corresponding proof for $\mathbf{grad}_{S^2} P_K \,\mathrm{div}_{S^2}$ is similar. ■

6.2.4.2 Application to Riesz potentials

We now apply the previous rather general results to the specific case of Riesz potentials for which the diagonalization of the scalar potential is known explicitly.

Diagonalization results Recall that the kernel $G_{3,s,0}$, for a real s in the open interval $(1,3)$, is written (we consider $d=3$ in this chapter)

$$G_{3,s,0}(r) = \frac{\Gamma(\frac{3-s}{2})}{2^s \pi^{\frac{3}{2}} \Gamma(\frac{s}{2})}\, r^{s-3}, \qquad \forall r \in \mathbb{R}^+. \tag{6.163}$$

Proposition 6.30. *Let $s \in (1,3)$. The operator $P_{G_{3,s,0}}$ given in (6.116) with $K = G_{3,s,0}$ is diagonalized by $Y_{\ell,m}$. The respective eigenvalues $g_s(\ell)$, with $2\ell+1$ multiplicity, read*

$$g_s(\ell) = R^{s-1}\, \frac{\Gamma(\frac{s-1}{2})}{2\sqrt{\pi}\Gamma(\frac{s}{2})} \frac{\Gamma(\frac{3}{2}+\ell-\frac{s}{2})}{\Gamma(\frac{1}{2}+\ell+\frac{s}{2})}. \tag{6.164}$$

Proof. Let $s \in (1,3)$, $\mathbf{x}, \mathbf{y} \in S_R$ and $\hat{\mathbf{x}} = \frac{\mathbf{x}}{|\mathbf{x}|} = \frac{\mathbf{x}}{R}$, $\hat{\mathbf{y}} = \frac{\mathbf{y}}{|\mathbf{y}|} = \frac{\mathbf{y}}{R}$. We have

$$G_{3,s,0}(|\mathbf{x}-\mathbf{y}|) = \frac{\Gamma(\frac{3-s}{2})}{2^s \pi^{\frac{3}{2}} \Gamma(\frac{s}{2})} |\mathbf{x}-\mathbf{y}|^{s-3} = \frac{\Gamma(\frac{3-s}{2})}{8\pi^{\frac{3}{2}} \Gamma(\frac{s}{2})} R^{s-3} \left(\frac{1-\hat{\mathbf{x}}\cdot\hat{\mathbf{y}}}{2}\right)^{\frac{s-3}{2}}. \tag{6.165}$$

Let us first study the kernel $\left(\frac{1-\hat{\mathbf{x}}\cdot\hat{\mathbf{y}}}{2}\right)^{\frac{s-3}{2}}$. Using the orthogonality of Legendre polynomials

$$\int_{-1}^{1} P_\ell(t) P_n(t) \mathrm{d}t = \frac{2}{2\ell+1} \delta_{\ell,n}, \tag{6.166}$$

we write

$$\left(\frac{1-\hat{\mathbf{x}}\cdot\hat{\mathbf{y}}}{2}\right)^{\frac{s-3}{2}} = \sum_{\ell=0}^{+\infty} c_\ell P_\ell(\hat{\mathbf{x}}\cdot\hat{\mathbf{y}}), \tag{6.167}$$

where

$$c_n := \frac{2n+1}{2} \int_{-1}^{1} P_n(t) \left(\frac{1-t}{2}\right)^{\frac{s-3}{2}} \mathrm{d}t, \qquad \forall n \in \mathbb{N}. \tag{6.168}$$

Besides, using the addition theorem [46, Th. 2.8],

$$P_n(\hat{\mathbf{x}}\cdot\hat{\mathbf{y}}) = \frac{4\pi}{2n+1}\sum_{p=-n}^{n} Y_{n,p}(\hat{\mathbf{x}})\overline{Y_{n,p}(\hat{\mathbf{y}})}, \qquad \forall n\in\mathbb{N}, \tag{6.169}$$

we obtain

$$\left(\frac{1-\hat{\mathbf{x}}\cdot\hat{\mathbf{y}}}{2}\right)^{\frac{s-3}{2}} = \sum_{n=0}^{+\infty} c_n \frac{4\pi}{2n+1}\sum_{p=-n}^{n} Y_{n,p}(\hat{\mathbf{x}})\overline{Y_{n,p}(\hat{\mathbf{y}})}. \tag{6.170}$$

Finally, using the orthogonality of the spherical harmonics, we readily obtain that

$$\begin{aligned}\int_{S^2}\left(\frac{1-\hat{\mathbf{x}}\cdot\hat{\mathbf{y}}}{2}\right)^{\frac{s-3}{2}} Y_{\ell,m}(\hat{\mathbf{y}})\mathrm{d}\sigma(\hat{\mathbf{y}}) &= \sum_{n=0}^{+\infty} c_n \frac{4\pi}{2n+1}\sum_{p=-n}^{n} Y_{n,p}(\hat{\mathbf{x}})\int_{S^2}\overline{Y_{n,p}(\hat{\mathbf{y}})}Y_{\ell,m}(\hat{\mathbf{y}})\mathrm{d}\sigma(\hat{\mathbf{y}}),\\ &= \left[2\pi\int_{-1}^{1} P_n(t)\left(\frac{1-t}{2}\right)^{\frac{s-3}{2}}\mathrm{d}t\right] Y_{\ell,m}(\hat{\mathbf{x}}).\end{aligned} \tag{6.171}$$

Back to the potential $P_{G_{3,s,0}}$, we write

$$\begin{aligned}P_{G_{3,s,0}}Y_{\ell,m}(\mathbf{x}) &= \int_{S_R} G_{3,s,0}(|\mathbf{x}-\mathbf{y}|)Y_{\ell,m}(\mathbf{y})\mathrm{d}\sigma(\mathbf{y}),\\ &= \frac{\Gamma(\frac{3-s}{2})}{8\pi^{\frac{3}{2}}\Gamma(\frac{s}{2})}R^{s-1}\int_{S^2}\left(\frac{1-\hat{\mathbf{x}}\cdot\hat{\mathbf{y}}}{2}\right)^{\frac{s-3}{2}} Y_{\ell,m}(\hat{\mathbf{y}})\mathrm{d}\sigma(\hat{\mathbf{y}}),\\ &= \left[\frac{\Gamma(\frac{3-s}{2})}{4\sqrt{\pi}\Gamma(\frac{s}{2})}R^{s-1}\int_{-1}^{1} P_\ell(t)\left(\frac{1-t}{2}\right)^{\frac{s-3}{2}}\mathrm{d}t\right] Y_{\ell,m}(\mathbf{x}),\end{aligned} \tag{6.172}$$

which confirms that the spherical harmonics are indeed eigenfunctions of $P_{G_{3,s,0}}$. The eigenvalues, which have $2\ell+1$ multiplicity, can be computed explicitly using Bonnet recursion formula [54, p. 18.9], for $x\in[-1,1]$, $\ell\geq 1$,

$$(\ell+1)\,P_{\ell+1}(x) = (2\ell+1)\,x\,P_\ell(x) - \ell\,P_{\ell-1}(x), \tag{6.173}$$

together with the initialization

$$P_0(x) = 1, \qquad P_1(x) = x. \tag{6.174}$$

If we denote by

$$p_\ell^\beta := \int_{-1}^{1} P_\ell(t)\left(\frac{1-t}{2}\right)^{\beta}\mathrm{d}t, \tag{6.175}$$

we find the recurrence relation, for $\ell\geq 1$,

$$(\ell+1)p_{\ell+1}^\beta - (2\ell+1)p_\ell^\beta + 2(2\ell+1)p_\ell^{\beta+1} + \ell p_{\ell-1}^\beta = 0. \tag{6.176}$$

It is a tedious (hence omitted) computation to show by induction that

$$p_\ell^\beta = 2\frac{\Gamma(\beta+1)}{\Gamma(-\beta)}\frac{\Gamma(\ell-\beta)}{\Gamma(2+\ell+\beta)}. \tag{6.177}$$

Using this expression with $\beta=\frac{s-3}{2}$, one gets to the desired result. ■

We consider now the following three operators, parametrized by the real index s supposed to belong to the open interval $(1,3)$,

$$\begin{aligned}
\langle \mathbf{V}_{3,s,0}\boldsymbol{\phi},\boldsymbol{\psi}\rangle_{S_R} &= \frac{2\sqrt{\pi}\,\Gamma(\frac{s}{2})}{\Gamma(\frac{s-1}{2})}\,\kappa^{s-1}\int_{S_R}\int_{S_R}\mathrm{G}_{3,s,0}(|\mathbf{x}-\mathbf{y}|)\boldsymbol{\phi}(\mathbf{y})\cdot\boldsymbol{\psi}(\mathbf{x})\,\mathrm{d}\sigma(\mathbf{x})\mathrm{d}\sigma(\mathbf{y}),\\
\langle \mathbf{Q}^G_{3,s,0}\boldsymbol{\phi},\boldsymbol{\psi}\rangle_{S_R} &= \frac{2\sqrt{\pi}\,\Gamma(\frac{s}{2})}{\Gamma(\frac{s-1}{2})}\,\kappa^{s-3}\int_{S_R}\int_{S_R}\mathrm{G}_{3,s,0}(|\mathbf{x}-\mathbf{y}|)\,\mathrm{div}_{S_R}\,\boldsymbol{\phi}(\mathbf{y})\,\mathrm{div}_{S_R}\,\boldsymbol{\psi}(\mathbf{x})\,\mathrm{d}\sigma(\mathbf{x})\mathrm{d}\sigma(\mathbf{y}),\\
\langle \mathbf{Q}^C_{3,s,0}\boldsymbol{\phi},\boldsymbol{\psi}\rangle_{S_R} &= \frac{2\sqrt{\pi}\,\Gamma(\frac{s}{2})}{\Gamma(\frac{s-1}{2})}\,\kappa^{s-3}\int_{S_R}\int_{S_R}\mathrm{G}_{3,s,0}(|\mathbf{x}-\mathbf{y}|)\,\mathrm{curl}_{S_R}\,\boldsymbol{\phi}(\mathbf{y})\,\mathrm{curl}_{S_R}\,\boldsymbol{\psi}(\mathbf{x})\,\mathrm{d}\sigma(\mathbf{x})\mathrm{d}\sigma(\mathbf{y}).
\end{aligned} \tag{6.178}$$

We have, with our notations, for $s\in(1,3)$,

$$\begin{aligned}
\mathbf{V}_{3,s,0} &= \frac{2\sqrt{\pi}\,\Gamma(\frac{s}{2})}{\Gamma(\frac{s-1}{2})}\,\kappa^{s-1}\,\mathbf{P}_{G_{3,s,0}},\\
\mathbf{Q}^G_{3,s,0} &= -\frac{2\sqrt{\pi}\,\Gamma(\frac{s}{2})}{\Gamma(\frac{s-1}{2})}\,\kappa^{s-3}R^{-2}\,\mathbf{grad}_{S^2}\;P_{G_{3,s,0}}\;\mathrm{div}_{S^2},\\
\mathbf{Q}^C_{3,s,0} &= \frac{2\sqrt{\pi}\,\Gamma(\frac{s}{2})}{\Gamma(\frac{s-1}{2})}\,\kappa^{s-3}R^{-2}\,\mathbf{curl}_{S^2}\;P_{G_{3,s,0}}\;\mathrm{curl}_{S^2}\,.
\end{aligned} \tag{6.179}$$

Proposition 6.31. *Let $s\in(1,3)$. The operator $\mathbf{V}_{3,s,0}$ is diagonalized by $\boldsymbol{\Psi}_{\ell,m}$ and $\boldsymbol{\Phi}_{\ell,m}$. The respective eigenvalues, with $2\ell+1$ multiplicity, read*

$$v_s^{\boldsymbol{\Psi}}(\ell) = v_s(\ell) + \frac{s^2-1}{2(\kappa R)^2}\,v_{s+2}(\ell) \qquad \textit{and} \qquad v_s^{\boldsymbol{\Phi}}(\ell) = v_s(\ell), \tag{6.180}$$

where

$$v_s(\ell) = (\kappa R)^{s-1}\,\frac{\Gamma(\frac{3}{2}+\ell-\frac{s}{2})}{\Gamma(\frac{1}{2}+\ell+\frac{s}{2})}. \tag{6.181}$$

Proof. Let $s\in(1,3)$. We can compute explicitly the kernel $L[G_{3,s,0}]$ from (6.124): for $r\in\mathbb{R}^+$, we have

$$\left(\frac{\Gamma(\frac{3-s}{2})}{2^s\pi^{\frac{3}{2}}\Gamma(\frac{s}{2})}\right)^{-1} L[G_{3,s,0}](r) = R^{-2}\frac{1}{2}r^{s-1} + R^{-2}\int_0^r t^{s-2}\mathrm{d}t = \frac{s+1}{2(s-1)}\frac{r^{s-1}}{R^2}, \tag{6.182}$$

which rewrites

$$L[G_{3,s,0}](r) = \left(\frac{\Gamma(\frac{3-s}{2})}{2^s\pi^{\frac{3}{2}}\Gamma(\frac{s}{2})}\right)\left(\frac{\Gamma(\frac{1-s}{2})}{2^{s+2}\pi^{\frac{3}{2}}\Gamma(\frac{s+2}{2})}\right)^{-1}\frac{s+1}{2(s-1)}R^{-2}\,G_{0,s+2}(r). \tag{6.183}$$

Using the recurrence relation $\Gamma(z+1)=z\Gamma(z)$ of the Gamma function [54, (5.5.1)], valid for $z\in\mathbb{C}$, the prefactor simplifies into

$$L[G_{3,s,0}](r) = -\frac{s(s+1)}{2R^2}\,G_{0,s+2}(r). \tag{6.184}$$

From Proposition 6.30 we have

$$\begin{aligned}
P_{L[G_{3,s,0}]}Y_{\ell,m} &= -\frac{s(s+1)}{2R^2}\,g_{s+2}(\ell)Y_{\ell,m},\\
P_{G_{3,s,0}}Y_{\ell,m} &= g_s(\ell)Y_{\ell,m}.
\end{aligned} \tag{6.185}$$

Using now Proposition 6.28 one gets, for all $\ell \in \mathbb{N}^*$, $-\ell \leq m \leq \ell$,

$$\begin{aligned}
\mathbf{V}_{3,s,0}\mathbf{\Phi}_{\ell,m} &= \frac{2\sqrt{\pi}\,\Gamma(\frac{s}{2})}{\Gamma(\frac{s-1}{2})}\,\kappa^{s-1}\,\left(g_s(\ell) + \frac{s(s+1)}{2R^2}\,g_{s+2}(\ell)\right)\mathbf{\Phi}_{\ell,m},\\
\mathbf{V}_{3,s,0}\mathbf{\Psi}_{\ell,m} &= \frac{2\sqrt{\pi}\,\Gamma(\frac{s}{2})}{\Gamma(\frac{s-1}{2})}\,\kappa^{s-1}\,g_s(\ell)\,\mathbf{\Psi}_{\ell,m},
\end{aligned} \tag{6.186}$$

which simplifies into

$$\begin{aligned}
\mathbf{V}_{3,s,0}\mathbf{\Phi}_{\ell,m} &= (\kappa R)^{s-1}\left(\frac{\Gamma(\frac{3}{2}+\ell-\frac{s}{2})}{\Gamma(\frac{1}{2}+\ell+\frac{s}{2})} + \frac{s(s+1)}{2}\,\frac{\Gamma(\frac{s}{2})}{\Gamma(\frac{s-1}{2})}\,\frac{\Gamma(\frac{s+1}{2})}{\Gamma(\frac{s+2}{2})}\frac{\Gamma(\frac{3}{2}+\ell-\frac{s+2}{2})}{\Gamma(\frac{1}{2}+\ell+\frac{s+2}{2})}\right)\mathbf{\Phi}_{\ell,m},\\
\mathbf{V}_{3,s,0}\mathbf{\Psi}_{\ell,m} &= (\kappa R)^{s-1}\,\frac{\Gamma(\frac{3}{2}+\ell-\frac{s}{2})}{\Gamma(\frac{1}{2}+\ell+\frac{s}{2})}\,\mathbf{\Psi}_{\ell,m}.
\end{aligned} \tag{6.187}$$

One finally gets to (6.180) by using once again the recurrence relation of the Gamma function. ■

Proposition 6.32. *Let $s \in (1,3)$. The operator $\mathbf{Q}^C_{3,s,0}$ is diagonalized by $\mathbf{\Phi}_{\ell,m}$. The associated eigenvalues with $2\ell+1$ multiplicity, read*

$$q^C_s(\ell) = \frac{\ell(\ell+1)}{(\kappa R)^2}\,v_s(\ell), \qquad \forall \ell \in \mathbb{N}^*, \tag{6.188}$$

and

$$\mathbf{\Psi}_{\ell,m} \in \operatorname{Ker}\mathbf{Q}^C_{3,s,0}, \qquad \forall \ell \in \mathbb{N}^*,\ -\ell \leq m \leq \ell. \tag{6.189}$$

Similarly, the operator $\mathbf{Q}^G_{3,s,0}$ is diagonalized by $\mathbf{\Psi}_{\ell,m}$. The associated eigenvalues with $2\ell+1$ multiplicity, read

$$q^G_s(\ell) = \frac{\ell(\ell+1)}{(\kappa R)^2}\,v_s(\ell), \qquad \forall \ell \in \mathbb{N}^*, \tag{6.190}$$

and

$$\mathbf{\Phi}_{\ell,m} \in \operatorname{Ker}\mathbf{Q}^G_{3,s,0}, \qquad \forall \ell \in \mathbb{N}^*,\ -\ell \leq m \leq \ell. \tag{6.191}$$

Proof. Let $s \in (1,3)$. From Proposition 6.30 we have, for all $\ell \in \mathbb{N}^*$, $-\ell \leq m \leq \ell$,

$$P_{G_{3,s,0}}Y_{\ell,m} = g_s(\ell)Y_{\ell,m}. \tag{6.192}$$

Using now Proposition 6.29 one readily get $\mathbf{\Psi}_{\ell,m} \in \operatorname{Ker}\mathbf{Q}^C_{3,s,0}$ and $\mathbf{\Phi}_{\ell,m} \in \operatorname{Ker}\mathbf{Q}^G_{3,s,0}$; besides, for all $\ell \in \mathbb{N}^*$, $-\ell \leq m \leq \ell$,

$$\begin{aligned}
\mathbf{Q}^C_{3,s,0}\mathbf{\Phi}_{\ell,m} &= \frac{2\sqrt{\pi}\,\Gamma(\frac{s}{2})}{\Gamma(\frac{s-1}{2})}\,\kappa^{s-1}\,\frac{\ell(\ell+1)}{(\kappa R)^2}\,g_s(\ell)\,\mathbf{\Phi}_{\ell,m},\\
\mathbf{Q}^G_{3,s,0}\mathbf{\Psi}_{\ell,m} &= \frac{2\sqrt{\pi}\,\Gamma(\frac{s}{2})}{\Gamma(\frac{s-1}{2})}\,\kappa^{s-1}\,\frac{\ell(\ell+1)}{(\kappa R)^2}\,g_s(\ell)\,\mathbf{\Psi}_{\ell,m},
\end{aligned} \tag{6.193}$$

which simplify to the desired result. ■

We can now apply the above results to the transmission operator $\mathrm{T}_0^{\mathrm{Riesz}}$ defined in (5.112).

Corollary 6.33. *The operator* $\mathrm{T}_0^{\mathrm{Riesz}}$ *is diagonalized by* $\boldsymbol{\Psi}_{\ell,m}$ *and* $\boldsymbol{\Phi}_{\ell,m}$*. The respective eigenvalues, with* $2\ell+1$ *multiplicity, read*

$$\begin{cases} t^{\mathrm{Riesz},\boldsymbol{\Psi}}(\ell) = {\theta_\ell}^{-1} + {\theta_\ell}^{-1}\, q^G_{5/2}(\ell)^2, \\ t^{\mathrm{Riesz},\boldsymbol{\Phi}}(\ell) = 1 + q^C_{5/2}(\ell)^2, \end{cases} \qquad \forall \ell \in \mathbb{N}^*, \tag{6.194}$$

where

$$\theta_\ell := 1 + \frac{\ell(\ell+1)}{(\kappa R)^2}, \qquad \forall \ell \in \mathbb{N}^*. \tag{6.195}$$

Proof. Recall the definition of the transmission operator

$$\mathrm{T}_0^{\mathrm{Riesz}} = \Theta^{-1} + \left(\mathbf{Q}^G_{3,5/2,0}\right)^* \Theta^{-1}\, \mathbf{Q}^G_{3,5/2,0} + \left(\mathbf{Q}^C_{3,5/2,0}\right)^* \mathbf{Q}^C_{3,5/2,0}, \tag{6.196}$$

where

$$\Theta = \mathrm{Id} - \kappa^{-2}\, \mathbf{grad}_{S_R}\, \mathrm{div}_{S_R}. \tag{6.197}$$

Using simple properties of the surface differential operators together with Proposition 6.11, we obtain

$$\begin{aligned} &\Theta \boldsymbol{\Psi}_{\ell,m} = \theta_\ell \boldsymbol{\Psi}_{\ell,m}, \\ &\Theta \boldsymbol{\Phi}_{\ell,m} = \boldsymbol{\Psi}_{\ell,m}. \end{aligned} \qquad \forall \ell \in \mathbb{N}^*,\ -\ell \le m \le \ell. \tag{6.198}$$

The result is then a direct application of Proposition 6.32. ∎

Properties of the eigenvalues The explicit formulas for the eigenvalues give us insights on the properties of the associated operators. This is especially valuable since we were not able to prove some of these properties for a general surface Σ.

We begin with the easiest property, namely the positivity of the eigenvalues, hence of the associated integral operators.

Proposition 6.34 (**Positivity**). *For* $s \in (1,3)$*, the following eigenvalues are all real and strictly positive*

$$v_s(\ell) > 0, \qquad v_s^{\boldsymbol{\Psi}}(\ell) > 0, \qquad v_s^{\boldsymbol{\Phi}}(\ell) > 0, \qquad q_s^G(\ell) > 0, \qquad q_s^C(\ell) > 0, \qquad \forall \ell \in \mathbb{N}^*. \tag{6.199}$$

Proof. The (strict) positivity, for $s < 5$, and any $\ell \in \mathbb{N}^*$ of $v_s(\ell)$ defined in (6.181) stems from the positivity of the Gamma function Γ for positive real arguments (which can be seen for instance from its integral representation, see [54, (5.9.1)]) The positivity of the other eigenvalues, for s in the interval $(1,3)$, follows readily. ∎

As a direct corollary, we readily obtain the following result for the eigenvalues of our transmission operator $\mathrm{T}_0^{\mathrm{Riesz}}$.

Corollary 6.35. *The eigenvalues of* $\mathrm{T}_0^{\mathrm{Riesz}}$ *are all real and strictly positive*

$$t^{\mathrm{Riesz},\boldsymbol{\Psi}}(\ell) > 0, \qquad t^{\mathrm{Riesz},\boldsymbol{\Phi}}(\ell) > 0, \qquad \forall \ell \in \mathbb{N}^*. \tag{6.200}$$

The asymptotic behaviour of the eigenvalues is given by the following proposition, which explains our choice of renormalization coefficients and our claim (5.98) on the order of the integral operators considered.

Proposition 6.36 (**Asymptotic behaviour**). *Let $s \in (1,3)$. We have, at infinity*

$$\begin{aligned} v_s(\ell) \ &\sim \ v_s^{\mathbf{\Psi}}(\ell) \ \sim \ v_s^{\mathbf{\Phi}}(\ell) \ \sim \ \left(\frac{\ell}{\kappa R}\right)^{1-s}, \qquad \ell \to \infty, \\ q_s^G(\ell) \sim q_s^C(\ell) \ &\sim \ \left(\frac{\ell}{\kappa R}\right)^{3-s}, \qquad \ell \to \infty. \end{aligned} \tag{6.201}$$

Proof. We recall the Stirling formula

$$\Gamma(1+x) \ \sim \ \frac{1}{\sqrt{2\pi x}}\Big(\frac{x}{e}\Big)^x, \qquad x \to \infty. \tag{6.202}$$

The claimed result then stems from, as $\ell \to \infty$,

$$\frac{\Gamma(\frac{3}{2}+\ell-\frac{s}{2})}{\Gamma(\frac{1}{2}+\ell+\frac{s}{2})} = \frac{\Gamma(\frac{1}{2}+\ell+\frac{s}{2}-(s-1))}{\Gamma(\frac{1}{2}+\ell+\frac{s}{2})} \ \sim \ \frac{\big(-\frac{1}{2}+\ell+\frac{s}{2}\big)^{\left(-\frac{1}{2}+\ell+\frac{s}{2}\right)-(s-1)}}{\big(-\frac{1}{2}+\ell+\frac{s}{2}\big)^{\left(-\frac{1}{2}+\ell+\frac{s}{2}\right)}} \ \sim \ \ell^{(1-s)}. \tag{6.203}$$

■

As a direct corollary, we readily obtain the following result for the eigenvalues of our transmission operator $\mathrm{T}_0^{\mathrm{Riesz}}$.

Corollary 6.37. *We have, at infinity*

$$t^{\mathrm{Riesz},\mathbf{\Psi}}(\ell) \ \sim \ \left(\frac{\ell}{\kappa R}\right)^{-1}, \qquad t^{\mathrm{Riesz},\mathbf{\Phi}}(\ell) \ \sim \ \frac{\ell}{\kappa R}, \qquad \text{as } \ell \to \infty. \tag{6.204}$$

Proof. We have, by direct application of Proposition 6.36,

$$q_{5/2}^G(\ell) \sim q_{5/2}^C(\ell) \ \sim \ \left(\frac{\ell}{\kappa R}\right)^{1/2}, \qquad \ell \to \infty. \tag{6.205}$$

and

$$\theta_\ell = 1 + \frac{\ell(\ell+1)}{(\kappa R)^2} \ \sim \ \left(\frac{\ell}{\kappa R}\right)^2, \qquad \ell \to \infty. \tag{6.206}$$

so that

$$\begin{aligned} t^{\mathrm{Riesz},\mathbf{\Psi}}(\ell) = {\theta_\ell}^{-1} \ + {\theta_\ell}^{-1} \, {q_{5/2}^G(\ell)}^2 \ &\sim \ \left(\frac{\ell}{\kappa R}\right)^{-1}, \qquad \ell \to \infty, \\ t^{\mathrm{Riesz},\mathbf{\Phi}}(\ell) = 1 + {q_{5/2}^C(\ell)}^2 \ &\sim \ \frac{\ell}{\kappa R}, \qquad \ell \to \infty. \end{aligned} \tag{6.207}$$

■

From the previous result, we are also able to prove the mapping properties of the operator $\mathrm{T}_0^{\mathrm{Riesz}}$ in this spherical setting.

Proposition 6.38 (**Mapping properties**). *The transmission operator $\mathrm{T}_0^{\mathrm{Riesz}}$ is a continuous mapping from $\mathbf{H}^{-1/2}(\mathrm{curl}; S_R)$ to $\mathbf{H}^{-1/2}(\mathrm{div}; S_R)$.*

Proof. Let $\mathbf{J} \in \mathbf{H}^{-1/2}(\mathrm{curl}; S_R)$ and denote by $\left(J^{\alpha}_{\ell,m}\right)_{\ell,m}$ for $\alpha \in \{\mathbf{\Psi}, \mathbf{\Phi}\}$ its associated coefficients on the basis $\mathbf{\Psi}_{\ell,m}$ and $\mathbf{\Phi}_{\ell,m}$ so that

$$\mathbf{J} = \sum_{\ell=1}^{+\infty} \sum_{m=-\ell}^{\ell} \left(J^{\mathbf{\Psi}}_{\ell,m} \mathbf{\Psi}_{\ell,m} + J^{\mathbf{\Phi}}_{\ell,m} \mathbf{\Phi}_{\ell,m} \right), \tag{6.208}$$

Since the operator $\mathrm{T}_0^{\mathrm{Riesz}}$ is diagonalized on the same basis according to Corollary 6.33, we have

$$\mathrm{T}_0^{\mathrm{Riesz}} \mathbf{J} = \sum_{\ell=1}^{+\infty} \sum_{m=-\ell}^{\ell} \left(t_\ell^{\mathrm{Riesz},\mathbf{\Psi}} J^{\mathbf{\Psi}}_{\ell,m} \mathbf{\Psi}_{\ell,m} + t_\ell^{\mathrm{Riesz},\mathbf{\Phi}} J^{\mathbf{\Phi}}_{\ell,m} \mathbf{\Phi}_{\ell,m} \right), \tag{6.209}$$

By definition of the norm on $\mathbf{H}^{-1/2}(\mathrm{div}; S_R)$

$$\begin{aligned} \|\mathrm{T}_0^{\mathrm{Riesz}} \mathbf{J}\|^2_{\mathbf{H}^{-1/2}(\mathrm{div};S_R)} = \sum_{\ell=1}^{+\infty} \sum_{m=-\ell}^{\ell} \Big(& (\ell(\ell+1))^{+1/2} |J^{\mathbf{\Psi}}_{\ell,m}|^2 |t_\ell^{\mathrm{Riesz},\mathbf{\Psi}}|^2 \\ & + (\ell(\ell+1))^{-1/2} |J^{\mathbf{\Phi}}_{\ell,m}|^2 |t_\ell^{\mathrm{Riesz},\mathbf{\Phi}}|^2 \Big). \end{aligned} \tag{6.210}$$

From Proposition 6.37, there exists a constant C, independent of ℓ, such that

$$|t_\ell^{\mathrm{Riesz},\mathbf{\Psi}}|^2 \leq C \, (\ell(\ell+1))^{-1}, \qquad |t_\ell^{\mathrm{Riesz},\mathbf{\Phi}}|^2 \leq C \, (\ell(\ell+1)), \tag{6.211}$$

hence

$$\begin{aligned} \|\mathrm{T}_0^{\mathrm{Riesz}} \mathbf{J}\|^2_{\mathbf{H}^{-1/2}(\mathrm{div};S_R)} &= \sum_{\ell=1}^{+\infty} \sum_{m=-\ell}^{\ell} \left((\ell(\ell+1))^{-1/2} |J^{\mathbf{\Psi}}_{\ell,m}|^2 + (\ell(\ell+1))^{+1/2} |J^{\mathbf{\Phi}}_{\ell,m}|^2 \right), \\ &\leq C \, \|\mathbf{J}\|^2_{\mathbf{H}^{-1/2}(\mathrm{curl};S_R)}. \end{aligned} \tag{6.212}$$

■

Numerical illustration We illustrate the previous analysis with the numerical representation of these eigenvalues. We report in Figure 6.7 the eigenvalues of the *inverse* of some integral operators $\mathbf{V}_{3,s,\sigma}$ with respect to the mode number ℓ. We represented the eigenvalues for three values of $s \in \{3/2, 2, 5/2\}$ (from top to bottom in the Figure), and for two values of $\sigma \in \{0, 5\}$. For these particular results, the sphere S_R has a radius $R = 2$ and we set $\kappa = 5$ (we chose $\sigma = 5$ so that it is equal to κ).

Of course, we do not have analytical expressions for the eigenvalues of $\mathbf{V}_{3,s,\sigma}$ for $\sigma > 0$. Inspecting the proof of Proposition 6.30, one finds that their computation can be performed numerically as it boils down to evaluate

$$\frac{2\sqrt{\pi}\,\Gamma(\frac{s}{2})}{\Gamma(\frac{s-1}{2})} \, (\kappa R)^{s-1} \int_{-1}^{1} 2\pi P_\ell(t) G_{3,s,\sigma}\left(\sqrt{2(1-t)}\right) \mathrm{d}t \tag{6.213}$$

which is what we did here.

We chose to represent the inverse of the eigenvalues for better visualization, since these operators $\mathbf{V}_{3,s,\sigma}$ are all regularizing, their eigenvalues tend to 0 which makes less interpretable graphs. We observe numerically that the eigenvalues are indeed strictly positive and have the expected asymptotic behaviour for large ℓ: respectively powers of $\ell/\kappa R$ in $\{1/2, 1, 3/2\}$ for s in $\{3/2, 2, 5/2\}$.

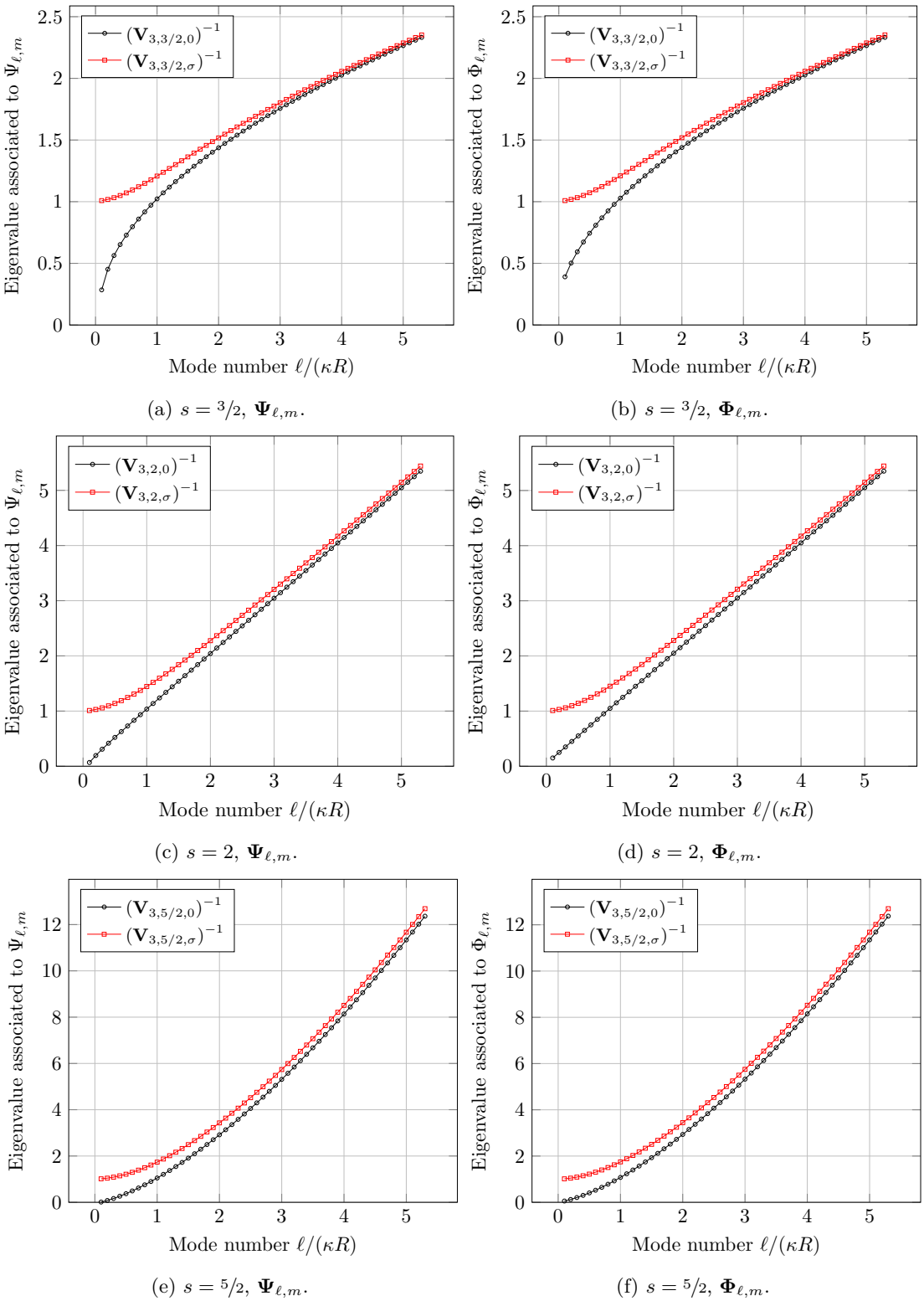

(a) $s = 3/2$, $\mathbf{\Psi}_{\ell,m}$. (b) $s = 3/2$, $\mathbf{\Phi}_{\ell,m}$.

(c) $s = 2$, $\mathbf{\Psi}_{\ell,m}$. (d) $s = 2$, $\mathbf{\Phi}_{\ell,m}$.

(e) $s = 5/2$, $\mathbf{\Psi}_{\ell,m}$. (f) $s = 5/2$, $\mathbf{\Phi}_{\ell,m}$.

Figure 6.7: Eigenvalues associated to each $\mathbf{\Psi}_{\ell,m}$ (left column) and $\mathbf{\Phi}_{\ell,m}$ (right column) of some integral operators with respect to the mode number ℓ. Fixed parameters $\kappa = \sigma = 5$, $R = 2$.

A key observation to make is that, for $\sigma = 0$, the eigenvalues of the inverse operators associated to low mode numbers ℓ are very small. Hence the ones of the operators $\mathbf{V}_{3,s,0}$ are very large, which is not a desirable behaviour, and it gets worse as κR increases. In contrast, for $\sigma > 0$, we observe that the eigenvalues associated to low mode numbers ℓ are (close to) 1, which is adequate and stems from the rapid decay at infinity of the associated Kernel. We have already commented on this aspect in the preceding chapter.

We remark that these graphs are numerical evidence that the Bessel operators ($\sigma > 0$) are indeed compact perturbations of the Riesz operators ($\sigma = 0$).

Finally notice that the eigenvalues associated to either $\mathbf{\Psi}_{\ell,m}$ (left column) or $\mathbf{\Phi}_{\ell,m}$ (right column) are very similar. One can barely notice the discrepancy for the smallest values of the mode number ℓ.

Chapter 7

Numerical results using integral impedance operators

Contents

In this chapter, we consider the discretization of some integral operators defined in Chapter 5 and provide some illustrative numerical results on very simple geometries. In the continuity of the numerical analysis performed in Chapter 4, we consider conformal Galerkin discretization strategies.

This chapter is divided into two parts. The first part concerns the acoustic setting, in two and three dimensions. Our results can be seen as a complement to the work (in the 2D case) presented in [91, Chap. 8]. We report results using four transmission operators. The first two are *local* operators: the identity operator Id of Després; and a positive operator based on second order surface differential operators. The other two are *non-local* operators that satisfy the theoretical requirements of the convergence analysis of Chapter 3: the operator $\mathrm{T}_0^{\mathrm{Bessel}} = \frac{2}{\kappa_0} W_{d,\kappa_0}$, where W_{d,κ_0} was defined in (5.21) which stems from standard potential theory; and

the operator $\mathrm{T}_0^{\mathrm{Riesz}} = \mathrm{Id} + W_{2,5/2,0}^* W_{2,5/2,0}$ already numerically tested in [91], where $W_{2,5/2,0}$ was defined in (5.44), which is based on Riesz potentials.

The second part is devoted to the electromagnetic setting, in three dimensions. We discuss the three operators that were already considered in Chapter 6. The first one is the basic reference given by the *local* identity operator Id of Després. The other two are *non-local* operators that satisfy the theoretical requirements of the convergence analysis of Chapter 3: the operator $\mathrm{T}_0^{\mathrm{Bessel}} = 2\mathbf{K}_{3,\kappa_0}$, defined in (5.82), which stems from standard potential theory; and the operator $\mathrm{T}_0^{\mathrm{Riesz}}$, defined in (5.112), which is based on Riesz potentials.

For all these transmission operators we briefly give some details on their implementation in practice. However, we discuss in more depth the discretization of the operator $\mathrm{T}_0^{\mathrm{Riesz}}$ which caused some difficulties that can be of interest. As we shall see, the nature of the issue lies in the lack of discrete $\inf - \sup$ condition for the L^2 duality between standard (low-order) Raviart-Thomas and Nedelec surface finite elements. This fact is well-known in the integral equation community, it arises especially when devising efficient preconditioners of the so called EFIE equation. Fortunately, a remedy is available, it is based on Buffa-Christiansen dual finite elements constructed on a barycentric refinement of the mesh [24]. It is interesting to see here a different application of these elements in the context of domain decomposition. We believe that our encountering of this problem is not fortuitous and one would almost inevitably stumble on it when trying to derive integral operators with the correct properties for a transmission operator. In this respect, even though the outcome of our numerical tests were somehow disappointed, the discussion of the issue seems of importance.

The numerical experiments reported in this chapter aims at illustrating the interest of using non-local operators satisfying the requirements of the convergence theory of Chapter 3. Overall, we illustrate numerically the theoretical results of the convergence analysis when a transmission operator satisfying the adequate properties is used. Importantly, we show the h-uniform convergence rate of both the relaxed Jacobi and the Gmres algorithms if a non-local operator is used as transmission operator. This is not true if one uses a local operator, one can observe in some cases a strong deterioration of the convergence rate as the mesh is refined. In particular, we show the slow convergence of the relaxed Jacobi algorithm when using local operators, which is due to the highly oscillating modes. The Gmres algorithm succeeds to some extent in mitigating the effect of those modes.

If the numerical results illustrate the theoretical analysis, from an application standpoint, the performance of the non-local operators in 3D is somehow disappointing (in 2D, they are very efficient). Our interpretation is that the boundary element method that is used to approximate the integral operators is inadequate in this context.

The research code that was used to run the tests was developed specifically to test the method and uses standard (low-order) finite elements. The code is primarily written in Julia [16]. The meshes are generated by Gmsh [77] which is conveniently interfaced with the Julia code through the Julia API. The computation of every integral operators considered in this work is performed by external routines written in C++ or Fortran by Xavier Claeys and Francis Collino, as indicated in what follows. These routines were also interfaced with the Julia code. The code was validated on standard scattering test cases.

A word of warning: in all the numerical experiments we present below and in subsequent chapters, the tuning of the parameters associated to each operator is not optimal (this stands also for the operators we advocate) and is guided by simple heuristics. As a matter of fact, we shall hardly change them between different test cases. We therefore acknowledge that, in some cases, we might be wary of the results as it would be possible to obtain much better convergence that what is reported here by simply adjusting a few parameters. Our point of view is that a robust method should not be too much sensitive on the choice of its parameters. This way of

proceeding simplifies in some sense the discussion but one could argue against it.

7.1 Acoustic setting

In the acoustic setting, we report and compare results using four transmission operators:

- two *local* operators:
  - the identity operator Id of Després;
  - a positive operator based on second order surface differential operators, namely

$$\mathrm{Id} - \frac{1}{2{\kappa_0}^2}\Delta_\Sigma; \tag{7.1}$$

- two *non-local* operators that satisfy the theoretical requirements of the convergence analysis of Chapter 3:
  - the operator, for $d \in \{2, 3\}$,

$$\mathrm{T}_0^{\mathrm{Bessel}} = \frac{2}{\kappa_0}\, W_{d,\kappa_0} \tag{7.2}$$

    where W_{d,κ_0} was defined in (5.19) and stems from standard potential theory. To the best of our knowledge, this operator was not previously tested numerically;
  - in the two dimensional case only, the operator

$$\mathrm{T}_0^{\mathrm{Riesz}} = \mathrm{Id} + W^*_{2,5/2,0} W_{2,5/2,0}, \tag{7.3}$$

    where $W_{2,5/2,0}$ was defined in (5.44), which is based on Riesz potentials. This operator was already tested in [91], but the values of the parameters of the version used in our numerical experiments are different than the ones used in this reference. Although this operator can be quasi-localized by truncation, we use the full operator in our numerical experiments. It is included in this analysis for the sake of comparison.

7.1.1 Discretization strategy

The discretization of the integral operators in the acoustic setting follows standard practice, see [124, Chap. 4] for a reference.

The (elliptic) hypersingular operator W_{d,κ_0} in the definition of $\mathrm{T}_0^{\mathrm{Bessel}}$ is a variation of a rather standard operator. As a result, and it is a strong advantage, several freely available codes are available to compute the matrices of W_{d,κ_0} in both 2D and 3D. We chose to use the BemTool library [1], mainly developed by Xavier Claeys and written in C++.

The operator $W_{2,5/2,0}$ in the definition of $\mathrm{T}_0^{\mathrm{Riesz}}$ is uncommon and requires specific quadrature routines. The matrices of this operator are computed thanks to a Fortran routine written by Francis Collino, only available for the 2D case. This operator was already used in previous work [91] were extensive results in other configurations were reported. In contrast to this reference, the parameters involved in the definition of this operator are not optimized in the results we present.

[1] https://github.com/xclaeys/BemTool

7.1.2 Numerical experiments

The purpose of this section is to provide some numerical results in the acoustic setting illustrating the convergence of domain decomposition methods using the integral operators previously described.

7.1.2.1 Test case and implementation details

We consider a model test case in 2D or 3D, that will be repeatedly used in the following (Chapters 7, 8 and 11). Of course, we shall also consider several variations of this test case.

Test Case Helmholtz. *The domain Ω is a disk $d = 2$ or ball $d = 3$ of radius $R = 1$ with a boundary denoted $\Gamma := \partial\Omega$ and an outward unit normal vector ν. The model problem we consider is*

$$\begin{cases} \text{Find } u \in H^1(\Omega) \text{ such that} \\ \left(-\operatorname{div} \frac{1}{\rho_r}\ \mathbf{grad} - \frac{{\kappa_0}^2}{\lambda_r}\right) u = 0, & \text{in } \Omega, \\ \left(\rho_r^{-1}\,\partial_\nu - \mathrm{i}\kappa_0\right) u = \left(\rho_r^{-1}\,\partial_\nu - \mathrm{i}\kappa_0\right) u_{\mathrm{inc}}, & \text{on } \Gamma, \end{cases} \tag{7.4}$$

where u_{inc} is a plane wave in the direction $\mathbf{d}$ which is always set to be the unit vector in the x direction, and is written at a point $\mathbf{x}$

$$u_{\mathrm{inc}}(\mathbf{x}) := e^{\mathrm{i}\kappa_0 \mathbf{d}\cdot\mathbf{x}}. \tag{7.5}$$

By default, the medium of propagation is supposed uniform ($\rho_r \equiv 1$ and $\lambda_r \equiv 1$) and the reference wavenumber is set to the value $\kappa_0 = 1$.

By default, the domain Ω is partitioned into $J = 2$ non-overlapping domains Ω_j, $j \in \{1, 2\}$, separated by a circular or spherical interface Σ at $R = 0.5$.

We provide below various figures reporting convergence results for the relaxed Jacobi algorithm and the restarted Gmres algorithm for this test case. To simplify the discussion, the relaxation parameter of the Jacobi algorithm is taken to be $r = \frac{1}{2}$ throughout all the numerical experiments presented in this work. For the same reason of simplification of the discussion, the restart of the Gmres algorithm is set to 20 iterations. Increasing this number typically yields faster convergence but increases the burden on the memory of the machine induced by the larger Krylov subspaces.

For both these iterative algorithms, the relative errors that are reported are computed in the broken H^1 norm, defined at the iteration n as

$$(\text{relative error})^2 = \frac{\sum_{j=1}^{J} \|\mathfrak{u}_h^n - u_h\|^2_{H^1(\Omega_{j,h})}}{\sum_{j=1}^{J} \|\mathfrak{u}_h^0 - u_h\|^2_{H^1(\Omega_{j,h})}}, \tag{7.6}$$

where $\mathfrak{u}_h^n$ is the volume solution at iteration n, $\mathfrak{u}_h^0$ is the initial volume solution (taken to be zero in practice) and u_h is the exact discrete volume solution of the full (undecomposed) problem.

This choice of volume (energy) norm deserves some comments. First, it is not completely standard practice, since the quantity that is in general reported is usually the L^2 (or rather the ℓ^2) norm of the residual of the linear system, which stems from a problem posed on the interface. This is justified by the fact that this quantity is easy to compute and readily available in standard implementations of the Gmres algorithm.

Instead of the norm of the residual, we chose to represent an error in the volume of the domain, computed in the natural energy norm. The reason for this is that our choice of norm is completely independent of the choice of transmission operator and is not too much sensible to

the mesh partition. Of course, it is not possible to monitor the convergence that way in real-life applications since the computation of the norm requires access to the exact discrete solution, but our focus here is on the (fair) comparison of different methods.

In all test runs that were performed throughout this work, the convergence was stopped if a maximum number of 10^4 iterations (sometimes increased to 10^5) was not enough to get to the set tolerance. Besides, when we report a number of iterations to achieve a certain tolerance for the relative error, this tolerance is set to 10^{-8}.

7.1.2.2 Convergence history

2D The full convergence history of the relative broken H^1 error for the Jacobi and GMRES algorithms are provided for this test case in Figure 7.1 as an illustrative example of typical convergence.

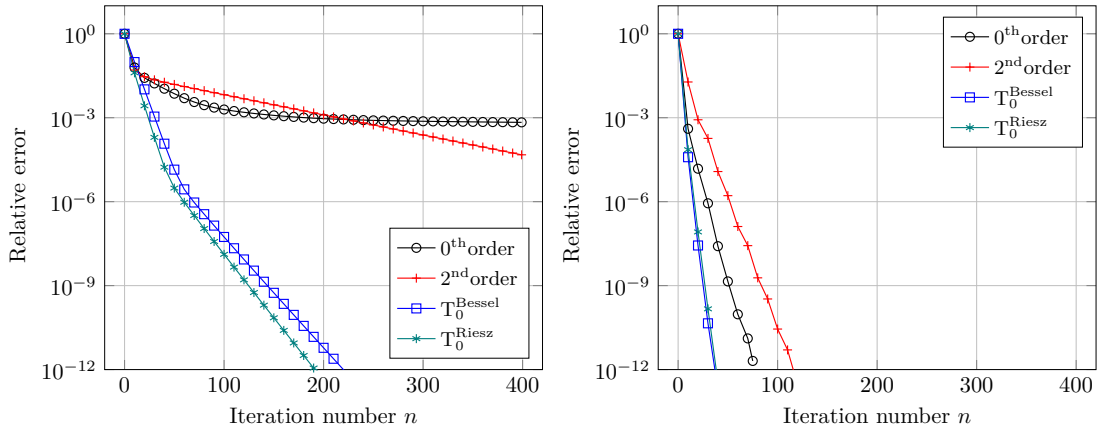

(a) Relaxed Jacobi algorithm

(b) GMRES algorithm

Figure 7.1: Helmholtz 2D. An example of convergence history. Fixed parameters $\kappa_0 = 1$, $N_\lambda = 40$, disk of radius $R = 1$.

For the Jacobi algorithm, we note that the convergence associated to Després transmission condition seems to be stalling. In fact, the convergence does not stop, but becomes really slow.

We observe on this first example an important effect that is rather general and which is the presence of seemingly different convergence regimes. For instance for the Després condition (operator Id), we notice a first short regime (10 first iterations) of rather fast convergence, a second part with a slower rate (up to iteration 100) and a third regime of very slow convergence. For the other operators we observe two main regimes, the first one being quite fast while the asymptotic regime is slightly slower.

The presence of such regimes can be explained by Fourier analysis. In fact, if we were to decompose the source term (a plane wave) in the Hilbert basis, we would realize that most of the energy is concentrated on the propagative modes, since they have the largest coefficients in the expansion (the highest coefficients corresponds to the modes that are close to the wavenumber κ_0). As for the evanescent modes, their energy (and coefficient) decreases (exponentially) as the number of the mode increases. The first regime can therefore be interpreted for all operators as the convergence of the propagative modes which are mainly present in the components of the error at the beginning of the convergence and have relatively small convergence rates. At some point, the main modal contribution in the error will come from the modes that have the

smallest convergence rate, hence control the rest of the convergence. And in fact those modes are very different in nature when we consider local operators (0^{th} and 2^{nd} orders) or non local ones ($\mathrm{T}_0^{\text{Bessel}}$ and $\mathrm{T}_0^{\text{Riesz}}$). For local operators the modes with the smaller convergence rate are the evanescent modes while for the non local ones they are the grazing modes. In both cases, these are the modes that yield the asymptotic convergence rate that we observe.

This effect is corroborated by the results in Figure 7.2, which represents the modulus of the absolute error between the exact discrete solution (the finite element solution of the undecomposed problem) and the discrete solution obtained using the DD algorithm. The convergence of the Jacobi algorithm was stopped for a relative residual of 10^{-6} which is enough to get to the asymptotic regime. The test case is the same, but with a higher frequency $\kappa_0 = 10$ (and a mesh constructed to have $N_\lambda = 40$ points per wavelength) for a better visualization.

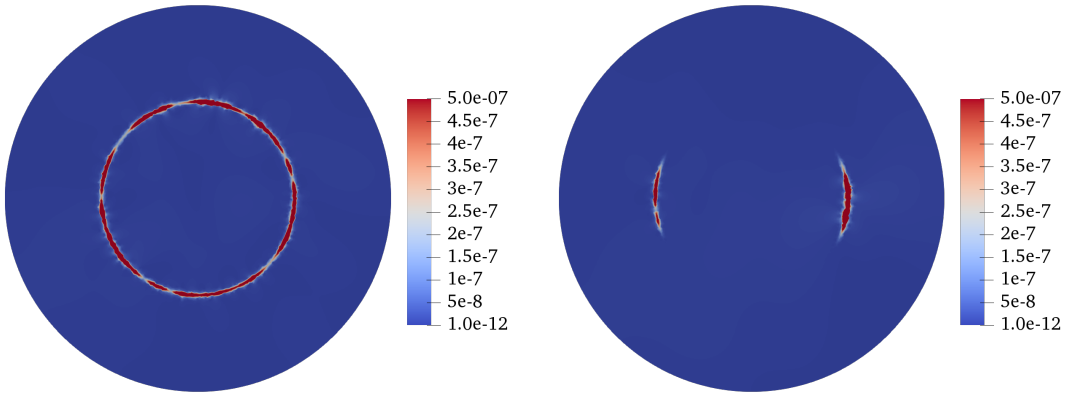

(a) Operator 0^{th}order

(b) Operator 2^{nd}order

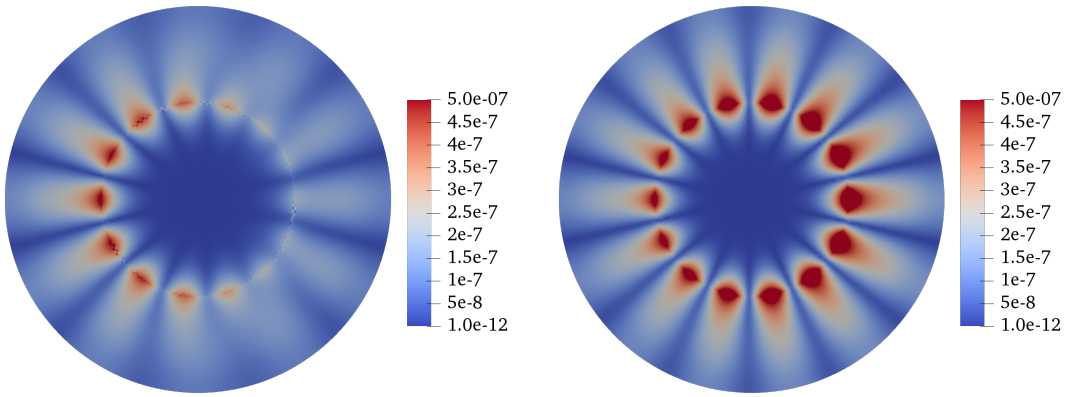

(c) Operator $\mathrm{T}_0^{\text{Bessel}}$

(d) Operator $\mathrm{T}_0^{\text{Riesz}}$

Figure 7.2: Helmholtz 2D. Absolute error modulus. Fixed parameters $\kappa_0 = 10$, $N_\lambda = 40$, disk of radius $R = 1$, Jacobi algorithm.

We observe that for the local operators, the error is highly concentrated near the interface, rapidly decreasing away from it, which are characteristics of evanescent modes. In contrast, for

the two integral operators, the main components seem to come from grazing modes: oscillatory modes concentrated near the interface and slowly decreasing away from it.

3D The full convergence history of the relative broken H^1 error for the Jacobi and GMRES algorithms are provided for this test case in Figure 7.3 as an illustrative example of typical convergence.

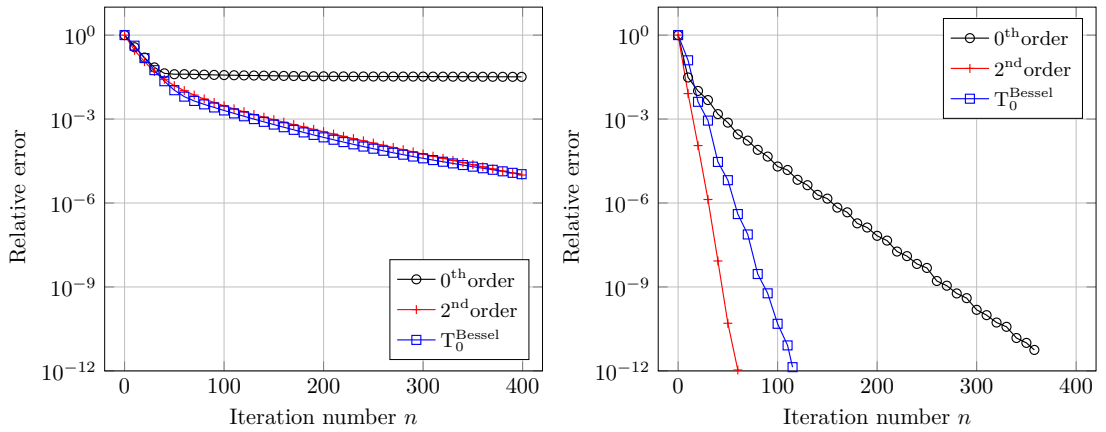

(a) Relaxed Jacobi algorithm (b) GMRES algorithm

Figure 7.3: Helmholtz 3D. An example of convergence history. Fixed parameters $\kappa_0 = 1$, $N_\lambda = 40$, ball of radius $R = 1$.

The convergence of the algorithm in the case of the identity operator is very similar to the 2D case. This is not true for the second-order operator which performs rather well, even better than the non-local operator for the GMRES algorithm. In comparison to the 2D case, the non-local operator seems to struggle a little to converge for the relaxed Jacobi algorithm. The situation is less clear than in the 2D case, but such results do not contradict the analysis.

7.1.2.3 h-uniform geometric convergence

The purpose of the subsequent numerical experiments is to illustrate the main theoretical result on geometric convergence, namely the fact that (suitable) non-local operators allow for uniform convergence rate with respect to the mesh parameter h. This is an important feature for a DD method to have that can save flops and time in several situations. Firstly, when the domain of propagation is large with respect to the wavelength of the problem, the mesh needs to be refined to limit the pollution effect. Besides, realistic meshes are not uniform in general and may exhibit local refinements to capture geometrical details or domain heterogeneities. Finally, for some applications, computations are often done with one single mesh that is used to compute different solutions at different frequencies. This is due to the fact that the engineering time required to mesh some geometries can be quite large in proportion of the total time dedicated to run the test case. In particular producing good quality meshes is not a simple task that is quite time consuming for engineers. As a result, the mesh can be uniformly quite refined for the lowest frequencies considered.

2D We report the number of iterations to reach convergence with respect to mesh refinement in Figure 7.4 for the (relaxed) Jacobi and GMRES algorithms. The refinement of the mesh is

indicated by the number of points per wavelength N_λ which is inversely proportional to the typical mesh size. In Figure 7.4b we also report the number of GMRES iterations that are required to achieve the same error to solve the full (undecomposed) linear system (line plot labelled 'No DDM'). This is to be read as an indication of the conditioning of the original linear system rather than an actual method of resolution. We see that this iteration count has a growth which is approximately quadratic with respect to N_λ, illustrating the deterioration of the matrix conditioning as the mesh is refined.

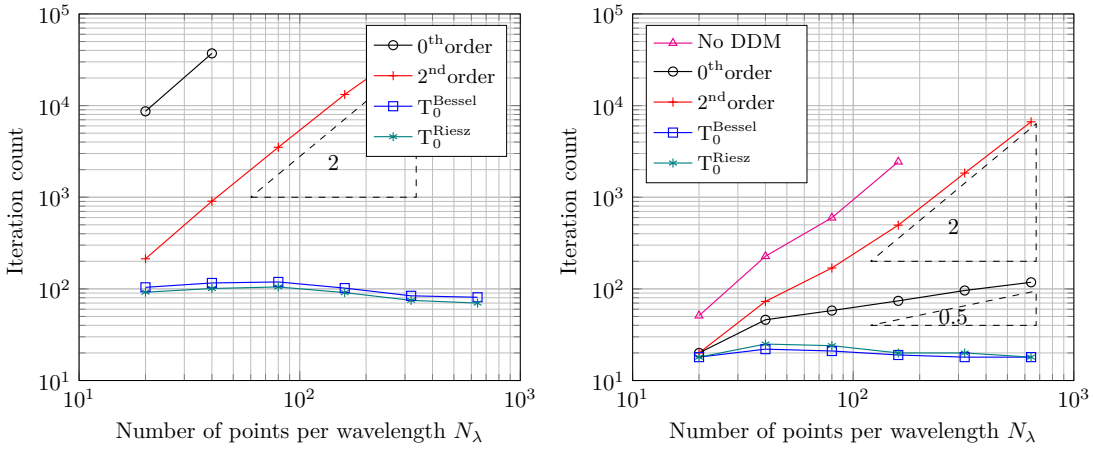

(a) Relaxed Jacobi algorithm

(b) GMRES algorithm

Figure 7.4: Helmholtz 2D. Number of iterations with respect to the number of mesh points per wavelength N_λ. Fixed parameters $\kappa_0 = 1$, 2D, disk of radius $R = 1$.

For the two local operators the convergence is not uniform with respect to the mesh refinement and a large number of iterations is required to get to the set tolerance. The growth of the iteration count appears to be quasi quadratic with respect to N_λ for the Jacobi algorithm and quasi linear for the GMRES algorithm. For small mesh size the convergence may not even be reached within 10^5 iterations. In contrast, the non-local operators T_0^{Bessel} and T_0^{Riesz} exhibit uniform convergence in all cases, with a very moderate number of iterations required to reach the set tolerance.

3D Figure 7.5 reports the number of iterations to reach convergence with respect to mesh refinement in the 3D case. For the Jacobi algorithm, no results are presented for the identity operator because it would not converge to the required precision in under 10^5 iterations.

Again, for the Jacobi algorithm with the second operator the convergence is not uniform with respect to the mesh refinement. The growth of the iteration count appears to be quasi quadratic with respect to N_λ. In comparison, as predicted by the theory, the iteration count associated to the non-local operator T_0^{Bessel} does not grow.

For the GMRES algorithm, the iteration count associated to the identity operator grows sub-linearly, similarly as for the 2D case. And again, the number of GMRES iterations required to solve the full (undecomposed) linear system (line plot labelled 'No DDM') grows (super) linearly with N_λ. For the two other operators, the iteration count is reduced and does not clearly grow. This was expected for the non-local operator T_0^{Bessel} but seems surprising for the second order operator, especially in view of the results in the 2D case. Such efficiency might be due to the specific test case, with the spherical geometry.

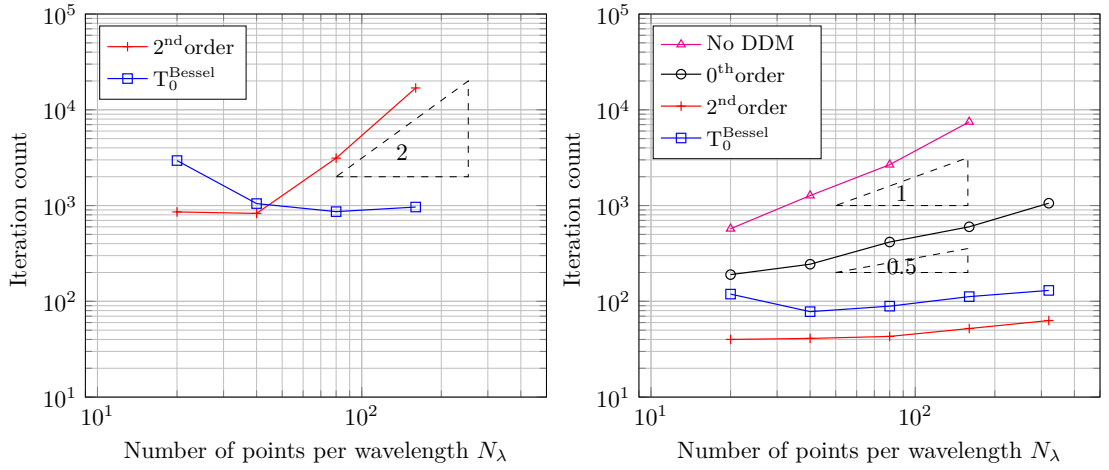

(a) Relaxed Jacobi algorithm

(b) GMRES algorithm

Figure 7.5: Helmholtz 3D. Number of iterations with respect to the number of mesh points per wavelength N_λ. Fixed parameters $\kappa_0 = 1$, ball of radius $R = 1$.

7.2 Electromagnetic setting

We turn now to the discretization strategy of the domain decomposition method applied to Maxwell equations. We compare the three operators that were already considered in Chapter 6 together with a naive local operator based on second order tangential differential operators, namely

- a *local* operator:
  - the identity operator Id of Després;
  - a positive operator based on second order surface differential operators, namely

$$\mathrm{Id} - \frac{1}{2{\kappa_0}^2}\,\mathbf{curl}_\Sigma\,\mathrm{curl}_\Sigma; \tag{7.7}$$

- two *non-local* operators that satisfy the theoretical requirements of the convergence analysis of Chapter 3:
  - the operator $T_0^{\text{Bessel}} = 2\mathbf{K}_{3,\kappa_0}$, defined in (5.82), which stems from standard potential theory.
  - the operator T_0^{Riesz}, defined in (5.112), which is based on Riesz potentials.

The discretization of the operator $\mathbf{K}_{3,\kappa_0}$ using standard boundary elements is fairly straightforward and similar in spirit to the acoustic setting that was just described. In contrast, the discretization strategy that shall be adopted for the T_0^{Riesz} operator is much more involved. This is due to a commonly uncountered difficulty in the numerical analysis of electromagnetic integral equations, namely the lack of a discrete inf − sup condition on the duality between standard Nedelec and Raviart-Thomas (or equivalently Rao-Wilton-Glisson) boundary elements. A remedy was found by Buffa and Christiansen in their celebrated paper [24] that rely on an L^2-dual finite element subspace constructed on the dual mesh (see also [2, 93]). We shall try to explain where lies the difficulty and then exploit their technique in our context.

7.2.1 Discretization strategy

7.2.1.1 Variational formulations

Since the discretization strategy consists in using a Galerkin formulation, the volume unknown $\mathbf{E} \in \mathbf{H}(\mathbf{curl}; \Omega)$, solution of the interior local sub-problems, will be approximated using standard (in our case, first order) volume Nedelec edge elements (on tetrahedrons). The tangential trace $\nu \times (\mathbf{E} \times \nu) \in \mathbf{H}^{-1/2}(\mathrm{curl}; \Sigma)$ on the interface will naturally be approximated by surface Nedelec edge elements (on triangles).

Operator $\mathrm{T}_0^{\mathrm{Bessel}}$ The operator $2\mathbf{K}_{3,\sigma}$ is defined variationally, for any $\boldsymbol{\phi}, \boldsymbol{\psi} \in \mathbf{H}^{-1/2}(\mathrm{curl}; \Sigma)$, by

$$\begin{aligned} \langle \mathbf{K}_{3,\sigma} \boldsymbol{\phi}, \boldsymbol{\psi} \rangle_\Sigma = \sigma & \int_\Sigma \int_\Sigma \mathrm{G}_\sigma(x-y)\ (\nu(y) \times \boldsymbol{\phi}(y)) \cdot (\nu(x) \times \boldsymbol{\psi}(x))\ \mathrm{d}\sigma(x)\mathrm{d}\sigma(y) \\ & + \sigma^{-1} \int_\Sigma \int_\Sigma \mathrm{G}_\sigma(x-y)\ \mathrm{curl}_\Sigma\, \boldsymbol{\phi}(y)\, \mathrm{curl}_\Sigma\, \boldsymbol{\psi}(x)\ \mathrm{d}\sigma(x)\mathrm{d}\sigma(y). \end{aligned} \tag{7.8}$$

The two variables $\boldsymbol{\phi}$ and $\boldsymbol{\psi}$ can be approximated using Nedelec finite elements. Since this is a discrete subspace of the continuous space for which the above operator is coercive, the discrete approximation of the operator is also a continuous and positive isomorphism from the discrete approximation space to its dual.

Operator $\mathrm{T}_0^{\mathrm{Riesz}}$ Let a $\boldsymbol{\phi} \in \mathbf{H}^{-1/2}(\mathrm{curl}; \Sigma)$ be given. At least formally, and at the price of introducing three auxiliary variables, one can write the following variational system to compute the action of the operator $\mathrm{T}_0^{\mathrm{Riesz}}$: we seek $\mathrm{T}_0^{\mathrm{Riesz}}\boldsymbol{\phi}$, $\boldsymbol{\varphi}_0$, $\boldsymbol{\varphi}_c$ and $\boldsymbol{\varphi}_g$, such that

$$\begin{cases} \langle \mathrm{T}_0^{\mathrm{Riesz}} \boldsymbol{\phi}, \boldsymbol{\psi} \rangle_\Sigma = \displaystyle\int_\Sigma \boldsymbol{\varphi}_0 \cdot \boldsymbol{\psi} + \iint_{\Sigma\times\Sigma} \frac{\mathrm{curl}_\Sigma\, \boldsymbol{\varphi}_c\, \mathrm{curl}_\Sigma\, \boldsymbol{\psi}}{|\mathbf{x}-\mathbf{y}|^{1/2}} + \iint_{\Sigma\times\Sigma} \frac{\mathrm{div}_\Sigma\, \boldsymbol{\varphi}_g\, \mathrm{div}_\Sigma\, \boldsymbol{\psi}}{|\mathbf{x}-\mathbf{y}|^{1/2}}, \\ \displaystyle\int_\Sigma \left(\boldsymbol{\varphi}_0 \cdot \boldsymbol{\varphi}_0^t + \mathrm{div}_\Sigma\, \boldsymbol{\varphi}_0\, \mathrm{div}_\Sigma\, \boldsymbol{\varphi}_0^t\right) = \int_\Sigma \boldsymbol{\phi} \cdot \boldsymbol{\varphi}_0^t, \\ \displaystyle\int_\Sigma \boldsymbol{\varphi}_c \cdot \boldsymbol{\varphi}_c^t = \iint_{\Sigma\times\Sigma} \frac{\mathrm{curl}_\Sigma\, \boldsymbol{\phi}\, \mathrm{curl}_\Sigma\, \boldsymbol{\varphi}_c^t}{|\mathbf{x}-\mathbf{y}|^{1/2}}, \\ \displaystyle\int_\Sigma \left(\boldsymbol{\varphi}_g \cdot \boldsymbol{\varphi}_g^t + \mathrm{div}_\Sigma\, \boldsymbol{\varphi}_g\, \mathrm{div}_\Sigma\, \boldsymbol{\varphi}_g^t\right) = \iint_{\Sigma\times\Sigma} \frac{\mathrm{div}_\Sigma\, \boldsymbol{\phi}\, \mathrm{div}_\Sigma\, \boldsymbol{\varphi}_g^t}{|\mathbf{x}-\mathbf{y}|^{1/2}}, \end{cases} \tag{7.9}$$

for all test functions $\boldsymbol{\psi}$, $\boldsymbol{\varphi}_0^t$, $\boldsymbol{\varphi}_c^t$ and $\boldsymbol{\varphi}_g^t$ elements of suitable test spaces.

By construction, the tangential trace $\boldsymbol{\phi}$ of the volume unknown is approximated by Nedelec surface finite elements. As a result, we can readily spot a possible issue regarding the discretization of the right-hand-side of the fourth equation in the previous system. Indeed, the Nedelec finite elements are not div_Σ conforming (they are actually constructed to be curl_Σ conforming). By symmetry (that stems from the symmetry of the operator), since the associated test variable $\boldsymbol{\psi}$ will also be approximated by Nedelec finite elements, the discretization of the third term in the right-hand-side of the first equation in the system might also be problematic.

Discarding for the moment this issue, we now address the delicate question of the choice of approximation spaces for the auxiliary variables $\boldsymbol{\varphi}_c$, $\boldsymbol{\varphi}_0$ and $\boldsymbol{\varphi}_g$. Note that these unknowns are respectively elements of $\mathbf{L}^2(\Sigma)$, $\mathbf{H}^{1/2}(\Sigma)$ and $\mathbf{H}^1(\Sigma)$. The unknown $\boldsymbol{\varphi}_c$ needs to be curl_Σ conforming, which can be seen from the presence of the second term in the right-hand-side of the first equation. It follows that a natural choice is to use Nedelec elements for both $\boldsymbol{\varphi}_c$ and $\boldsymbol{\varphi}_c^t$. Similarly, from the left-hand-sides of the second and fourth equations, we shall require the unknowns $\boldsymbol{\varphi}_0$ and $\boldsymbol{\varphi}_g$ (and their associated test functions respectively $\boldsymbol{\varphi}_0^t$ and $\boldsymbol{\varphi}_g^t$) to be div_Σ

conforming. A natural choice would then be to use Raviart-Thomas finite elements. However, this choice for $\boldsymbol{\varphi}_0$ and $\boldsymbol{\varphi}_0^t$ leads to another issue, as the bilinear form associated to both the first term in the right-hand-side of the first equation and the right-hand-side of the second equation does not satisfy a discrete Babuska-Brezzi $\inf - \sup$ condition. We shall give some more detail on the nature of this problem in the next sub-section and give a possible remedy.

7.2.1.2 Buffa-Christiansen space

Because of its ubiquity, we take a short detour in order to clearly expose the issue and a possible solution as proposed by A. Buffa and S. Christiansen in [24].

The problem stems from the lack of discrete stability of the bilinear form (ν is the outward unit normal vector to Σ)

$$(\boldsymbol{\varphi}, \boldsymbol{\varphi}^t) \mapsto \int_\Sigma (\nu \times \boldsymbol{\varphi}) \cdot \boldsymbol{\varphi}^t, \tag{7.10}$$

if $\boldsymbol{\varphi}$ spans either the Raviart-Thomas or equivalently the Nedelec finite element spaces. Actually, the associated matrix has a non-zero kernel.

To cope with this difficulty we rely on the discrete approximation space described in [24] which is L^2-dual to the Nedelec finite element space and div_Σ-conforming. More precisely, we rely on the result given by Proposition 3.14 in [24] which states that the L^2 duality between the Nedelec and this new space does satisfy a discrete $\inf - \sup$ condition. In the following, we refer to this space (and the associated finite elements) as the Buffa-Christiansen space (and finite elements). We point out that we use here the div_Σ-conforming version of the dual space, i.e. adopting the notations of [24], our Buffa-Christiansen space is $Y_h^1 \times \nu$, which is L^2 dual to the Nedelec space $X_h^1 \times \nu$.

Numerical illustration We propose below a little numerical experiment to try to illustrate the issue and its solution. To do so, we consider a revealing (albeit simple) generalized eigenvalue problem.

Let us denote by M_α, for $\alpha \in \{\mathrm{NED}, \mathrm{RT}, \mathrm{BC}\}$, the matrix associated to the bilinear form

$$(\boldsymbol{\varphi}_\alpha, \boldsymbol{\varphi}_{\mathrm{NED}}) \mapsto \int_\Sigma \boldsymbol{\varphi}_\alpha \cdot \boldsymbol{\varphi}_{\mathrm{NED}}, \tag{7.11}$$

where $\boldsymbol{\varphi}_{\mathrm{NED}}$, $\boldsymbol{\varphi}_{\mathrm{RT}}$, $\boldsymbol{\varphi}_{\mathrm{BC}}$ span respectively the Nedelec, Raviart-Thomas and Buffa-Christiansen finite element spaces. Here Σ is taken to be the unit sphere S^2.

The two eigenvalue problems we consider are, for $\alpha \in \{\mathrm{RT}, \mathrm{BC}\}$,

$$\begin{bmatrix} 0 & M_\alpha \\ M_\alpha^T & 0 \end{bmatrix} \begin{bmatrix} \boldsymbol{\varphi}_{\mathrm{NED}} \\ \boldsymbol{\phi}_{\mathrm{NED}} \end{bmatrix} = \lambda_\alpha \begin{bmatrix} M_{\mathrm{NED}} & 0 \\ 0 & M_{\mathrm{NED}} \end{bmatrix} \begin{bmatrix} \boldsymbol{\varphi}_{\mathrm{NED}} \\ \boldsymbol{\phi}_{\mathrm{NED}} \end{bmatrix}, \tag{7.12}$$

where $\boldsymbol{\varphi}_{\mathrm{NED}}$ and $\boldsymbol{\phi}_{\mathrm{NED}}$ are elements of the Nedelec space. We report in Figure 7.6 the sorted eigenvalues λ_α, for $\alpha \in \{\mathrm{RT}, \mathrm{BC}\}$.

We clearly see a non-zero null-space associated to the case $\alpha = \mathrm{RT}$ with approximately a third of the eigenvalues below machine precision. In contrast for $\alpha = \mathrm{BC}$, the eigenvalues stay bounded away from zero. The eigenvalues of the continuous problem are -1 and 1, we observe that the quality of the approximation is rather similar in both cases (expect for the kernel). If the mesh is refined (not illustrated here) the situation stays the same.

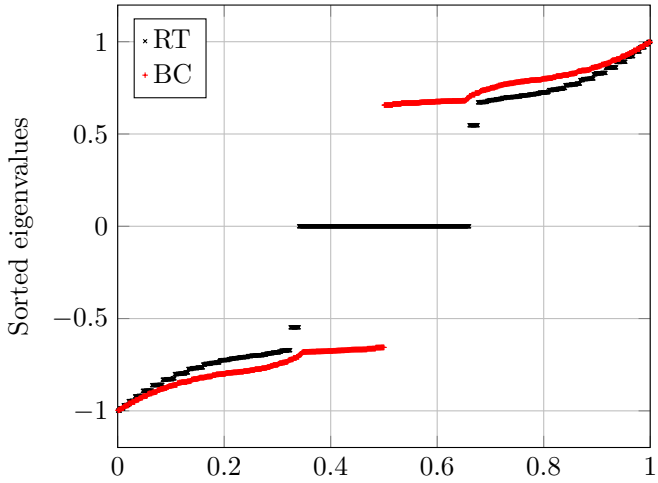

Figure 7.6: Sorted eigenvalues λ_α, for $\alpha \in \{\mathrm{RT}, \mathrm{BC}\}$, of the two generalized eigenvalue problems illustrating the lack of discrete stability of the bilinear form $(\boldsymbol{\varphi}, \boldsymbol{\varphi}^t) \mapsto \int_\Sigma (\nu \times \boldsymbol{\varphi}) \cdot \boldsymbol{\varphi}^t$.

7.2.1.3 Appropriate discretization of $\mathrm{T}_0^{\mathrm{Riesz}}$

It is straightforward to see that by choosing the Buffa-Christiansen space to approximate the unknown $\boldsymbol{\varphi}_0$ and its dual variable $\boldsymbol{\varphi}_0^t$ we readily solve one of our aforementioned issue. It turns out that this space is also the key to solve the other difficulty. The first step to do so, is to represent the tangential trace $\boldsymbol{\phi}$ by an element of the Buffa-Christiansen space, denoted $\boldsymbol{\xi}_g$, which is by construction div_Σ conforming. This new representation is then simply substituted in the right-hand-side of the fourth equation of the above system, which by construction also satisfy a discrete inf − sup condition. To retain the symmetry of the operator, we are led to introduce yet another unknown, denoted $\boldsymbol{\vartheta}_g$, also approximated by Buffa-Christiansen elements, to deal with the discretization of the third term in the right-hand-side of the first equation of the above system.

Finally, at the expense of having now five auxiliary unknowns, we consider the following variational definition of the transmission operator: we seek $\mathrm{T}_0^{\mathrm{Riesz}}\boldsymbol{\phi}$, $\boldsymbol{\varphi}_0$, $\boldsymbol{\varphi}_c$, $\boldsymbol{\varphi}_g$, $\boldsymbol{\xi}_g$ and $\boldsymbol{\vartheta}_g$, such that

$$
\begin{cases}
\langle \mathrm{T}_0^{\mathrm{Riesz}}\boldsymbol{\phi}, \boldsymbol{\psi}\rangle_\Sigma = \displaystyle\int_\Sigma \boldsymbol{\varphi}_0 \cdot \boldsymbol{\psi} + \iint_{\Sigma\times\Sigma} \frac{\mathrm{curl}_\Sigma\, \boldsymbol{\varphi}_c\, \mathrm{curl}_\Sigma\, \boldsymbol{\psi}}{|\mathbf{x}-\mathbf{y}|^{1/2}} + \int_\Sigma \boldsymbol{\vartheta}_g \cdot \boldsymbol{\psi}, \\
\displaystyle\int_\Sigma \left(\boldsymbol{\varphi}_0 \cdot \boldsymbol{\varphi}_0^t + \mathrm{div}_\Sigma\, \boldsymbol{\varphi}_0\, \mathrm{div}_\Sigma\, \boldsymbol{\varphi}_0^t\right) = \int_\Sigma \boldsymbol{\phi} \cdot \boldsymbol{\varphi}_0^t, \\
\displaystyle\int_\Sigma \boldsymbol{\varphi}_c \cdot \boldsymbol{\varphi}_c^t = \iint_{\Sigma\times\Sigma} \frac{\mathrm{curl}_\Sigma\, \boldsymbol{\phi}\, \mathrm{curl}_\Sigma\, \boldsymbol{\varphi}_c^t}{|\mathbf{x}-\mathbf{y}|^{1/2}}, \\
\displaystyle\int_\Sigma \boldsymbol{\xi}_g \cdot \boldsymbol{\xi}_g^t = \int_\Sigma \boldsymbol{\phi} \cdot \boldsymbol{\xi}_g^t, \\
\displaystyle\int_\Sigma \left(\boldsymbol{\varphi}_g \cdot \boldsymbol{\varphi}_g^t + \mathrm{div}_\Sigma\, \boldsymbol{\varphi}_g\, \mathrm{div}_\Sigma\, \boldsymbol{\varphi}_g^t\right) = \iint_{\Sigma\times\Sigma} \frac{\mathrm{div}_\Sigma\, \boldsymbol{\xi}_g\, \mathrm{div}_\Sigma\, \boldsymbol{\varphi}_g^t}{|\mathbf{x}-\mathbf{y}|^{1/2}}, \\
\displaystyle\int_\Sigma \boldsymbol{\vartheta}_g \cdot \boldsymbol{\vartheta}_g^t = \iint_{\Sigma\times\Sigma} \frac{\mathrm{div}_\Sigma\, \boldsymbol{\varphi}_g\, \mathrm{div}_\Sigma\, \boldsymbol{\vartheta}_g^t}{|\mathbf{x}-\mathbf{y}|^{1/2}},
\end{cases}
\tag{7.13}
$$

for all test functions $\boldsymbol{\psi}$, $\boldsymbol{\varphi}_0^t$, $\boldsymbol{\varphi}_c^t$, $\boldsymbol{\varphi}_g^t$, $\boldsymbol{\xi}_g^t$ and $\boldsymbol{\vartheta}_g^t$. The unknowns $\mathrm{T}_0^{\mathrm{Riesz}}\boldsymbol{\phi}$ and $\boldsymbol{\varphi}_c$ are sought as

elements of the Nedelec space while the unknowns $\boldsymbol{\varphi}_0$, $\boldsymbol{\varphi}_g$, $\boldsymbol{\xi}_g$ and $\boldsymbol{\vartheta}_g$ are sought as elements of the Buffa-Christiansen space. Similarly, the test functions $\boldsymbol{\psi}$ and $\boldsymbol{\varphi}_c^t$ span the Nedelec space while the test functions $\boldsymbol{\varphi}_0^t$, $\boldsymbol{\varphi}_g^t$, $\boldsymbol{\xi}_g^t$ and $\boldsymbol{\vartheta}_g^t$ span the Buffa-Christiansen space.

A careful inspection would reveal that the above system does define a self-adjoint operator. It would remain to prove rigorously that it is indeed a positive isomorphism, uniformly continuous with respect to the mesh parameter.

7.2.1.4 Singular quadrature

The numerical integration of the singularity in the operator $2\mathbf{K}_{3,\kappa_0}$ is standard and can be tackled using different strategies, for instance Sauter-Schwab techniques, see [124].

In contrast, the singularity that is present (several times) in the definition of the operator $\mathrm{T}_0^{\mathrm{Riesz}}$ is more challenging. The strategy that is adopted in the routine implemented by Francis Collino rests in part on the works of Lenoir and Salles [92]. However, while their method allows to evaluate singular integrals analytically, the implementation uses their technique when a singularity needs to be evaluated but switches to numerical approximation otherwise.

7.2.2 Numerical experiments

The purpose of this section is to provide some numerical results in the electromagnetic setting illustrating the convergence of domain decomposition methods using the integral operators previously described.

7.2.2.1 Test case and implementation details

We consider a model test case in 3D, that will be repeatedly used in the following (Chapters 7, 8 and 11). Of course, we shall also consider several variations of this test case.

Test Case Maxwell. *The domain Ω is a ball of radius $R = 1$ with a boundary denoted $\Gamma := \partial\Omega$ and an outward unit normal vector ν. The model problem we consider is*

$$\begin{cases} \text{Find } \mathbf{u} \in \mathbf{H}_\Gamma(\mathbf{curl};\Omega) \text{ such that} \\ \left(\mathbf{curl}\, \frac{1}{\mu_r}\, \mathbf{curl} - {\kappa_0}^2 \epsilon_r\right) \mathbf{u} = 0, & \text{in } \Omega, \\ (\mu_r^{-1}\, \mathbf{curl}\, \mathbf{u}) \times \nu - \mathrm{i}\kappa_0 \nu \times (\mathbf{u} \times \nu) = (\mu_r^{-1}\, \mathbf{curl}\, \mathbf{u}_{\mathrm{inc}}) \times \nu - \mathrm{i}\kappa_0 \nu \times (\mathbf{u}_{\mathrm{inc}} \times \nu), & \text{on } \Gamma, \end{cases} \tag{7.14}$$

where $\mathbf{u}_{\mathrm{inc}}$ is a plane wave in the direction $\mathbf{d}$ which is always set to be the unit vector in the x direction, and is written at a point $\mathbf{x}$

$$\mathbf{u}_{\mathrm{inc}}(\mathbf{x}) := (0,0,-1)^T\, e^{\mathrm{i}\kappa_0 \mathbf{d}\cdot\mathbf{x}}. \tag{7.15}$$

By default, the medium of propagation is supposed uniform ($\mu_r \equiv 1$ and $\epsilon_r \equiv 1$) and the reference wavenumber is set to the value $\kappa_0 = 1$.

By default, the domain Ω is partitioned into $J = 2$ non-overlapping domains Ω_j, $j \in \{1,2\}$, separated by a spherical interface Σ at $R = 0.5$.

We provide below various figures reporting convergence results for the relaxed Jacobi algorithm and the restarted GMRES algorithm for this test case. The relative errors that are reported are now computed in the broken $\mathbf{H}(\mathbf{curl})$ norm, defined at the iteration n as

$$(\text{relative error})^2 = \frac{\sum_{j=1}^J \|\mathbb{u}_h^n - u_h\|^2_{\mathbf{H}(\mathbf{curl};\Omega_{j,h})}}{\sum_{j=1}^J \|\mathbb{u}_h^0 - u_h\|^2_{\mathbf{H}(\mathbf{curl};\Omega_{j,h})}}, \tag{7.16}$$

where $\mathfrak{v}_h^n$ is the volume solution at iteration n, $\mathfrak{v}_h^0$ is the initial volume solution (taken to be zero in practice) and u_h is the exact discrete volume solution of the full (undecomposed) problem.

7.2.2.2 Convergence history

The full convergence history of the relative broken $\mathbf{H}(\mathbf{curl})$ error for the Jacobi and GMRES algorithms are provided for this test case in Figure 7.7 as an illustrative example of typical convergence.

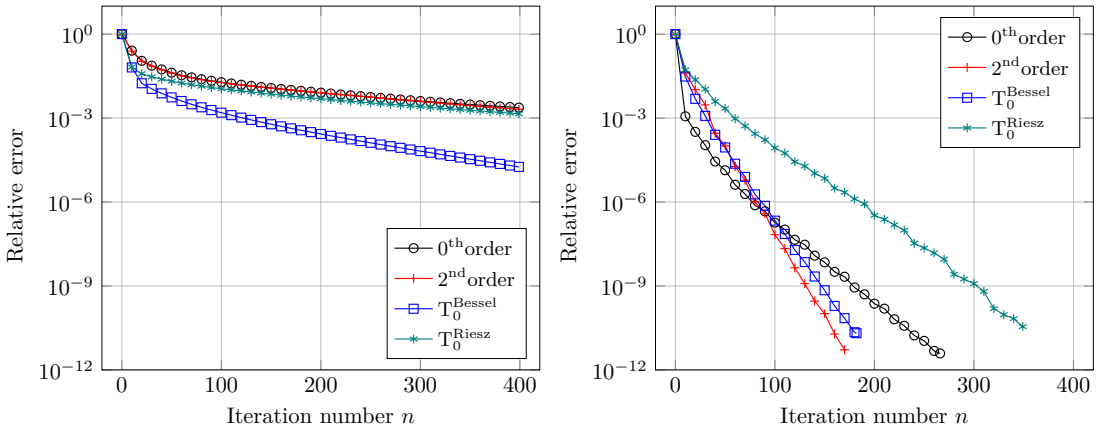

(a) Relaxed Jacobi algorithm

(b) GMRES algorithm

Figure 7.7: Maxwell 3D. An example of convergence history. Fixed parameters $\kappa_0 = 1$, $N_\lambda = 40$, ball of radius $R = 1$.

Looking at those graphs, the interest in using non-local operators, which are much more costly, is not clear. It appears the operator $\mathrm{T}_0^{\text{Riesz}}$ performs the worst. Again, we emphasize that this is not in contradiction with the convergence theory of Chapter 3 or the modal analysis of Chapter 6 (note that in these numerical experiments, the wavenumber is considerably lower than for the numerical illustrations of the modal analysis).

7.2.2.3 h-uniform linear convergence

We report the number of iterations to reach convergence with respect to mesh refinement in Figure 7.8 for the (relaxed) Jacobi and GMRES algorithms. The refinement of the mesh is indicated by the number of points per wavelength N_λ which is inversely proportional to the typical mesh size.

In Figure 7.8b we also report the number of GMRES iterations that are required to achieve the same error to solve the full (undecomposed) linear system (line plot labelled 'No DDM'). There is only one point, which corresponds to the coarsest mesh, since the algorithm was not able to converge in under 10^5 iterations as the mesh was refined. Similarly, as in the acoustic setting, no results are presented for the Jacobi algorithm for the identity operator because it would not converge to the required precision in under 10^5 iterations.

We observe the robustness of the non-local operators with respect to the mesh refinement. Unfortunately, we cannot observe the deterioration of the convergence of the relaxed Jacobi algorithm associated with the zeroth-order local operator since no results are available for this case. When the GMRES algorithm is used, the very mild deterioration of the results for the identity

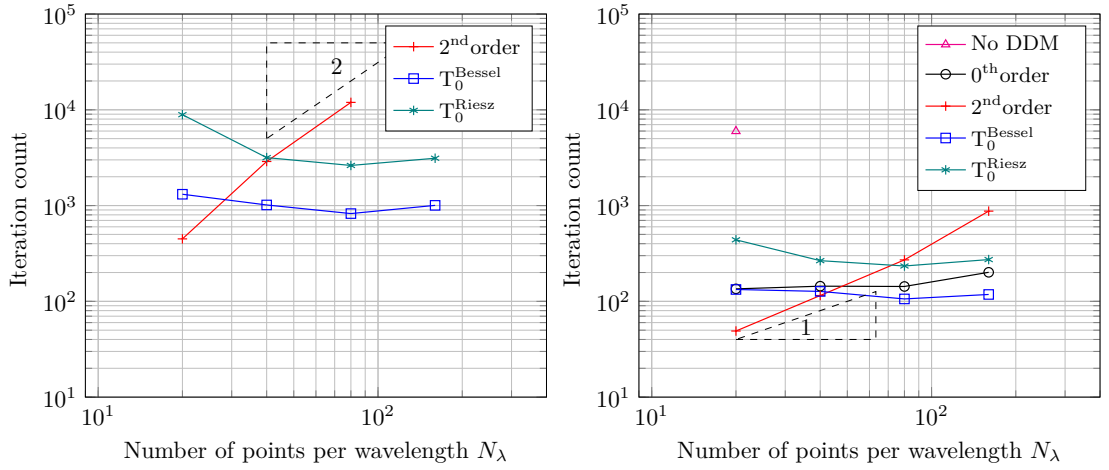

(a) Relaxed Jacobi algorithm (b) GMRES algorithm

Figure 7.8: Maxwell 3D. Number of iterations with respect to the number of mesh points per wavelength N_λ. Fixed parameters $\kappa_0 = 1$, ball of radius $R = 1$.

operator is not pronounced enough to conclude. We see again that the GMRES algorithm is able to mitigate the effect of the evanescent modes (which are the ones damaging the convergence of the relaxed Jacobi algorithm) quite effectively.

In contrast, the deterioration of the convergence for the second-order operator is very clear, the growth in iteration count is quadratic for the relaxed Jacobi algorithm and linear for the GMRES algorithm.

7.2.2.4 On the performance of the non-local operators

Overall, the results in 3D using non-local operators both for the Helmholtz and Maxwell equations are somehow disappointing at this point. We stress though that the results do not contradict the theory. If those non-local operators do have all the required theoretical properties to ensure convergence of the domain decomposition algorithms, they somehow perform poorly in practice, especially in view of their rather heavy computational cost.

If it is essential to bear in mind that these tests are rather academic, and we nevertheless expect some robustness when the test configuration changes, we acknowledge that those results raise legitimate questions. We could first suspect implementation errors, given in particular the complexity of the implementation of the operator T_0^{Riesz}. We performed numerous tests to investigate the issue, which are not reported here because of their low interest. We checked for instance the agreement of the eigenvalues of the operators computed numerically with the values computed using the analytical expressions found in Chapter 6.

The main conclusion of our investigations is that the poor efficiency of the non-local operators is due to the discretization strategy that is used to compute them. We suspect, without being able to argue rigorously, that the discrepancy in the approximation properties of, on one side, the finite element method (FEM) used to solve the local sub-problems, and on the other side, the boundary element method (BEM) used to compute the transmission operators do not cope well with each other. In other words, the issue originates from a pure discrete effect, that is only observed in 3D.

Although it may not be related, this is reminiscent of another discrete effect affecting the

convergence of the domain decomposition method and not completely understood, that was observed in [91, Sec. 7.2.1.1] when a lumped mass matrix was used to approximate the identity term present in the transmission operator $\mathrm{T}_0^{\mathrm{Riesz}}$.

A new approach needed? The poor performance of the non-local operators we considered so far is however a good motivation to look for new ways to construct non-local operators (with adequate properties), which is the purpose of the next chapter. As a matter of fact it is during our investigations of the issue that we thought of the new approach. The new class of non-local operators considered next is *not* based on integral operators and is found to perform rather well in practice. Besides such operators are easy to implement and have a moderate computational cost, making them a promising approach.

Chapter 8

Transmission operators based on auxiliary elliptic problems

Contents

In this chapter we propose a novel realization of a suitable non-local transmission operator based on elliptic auxiliary problems that are solved in the vicinity of the interface on which the boundary operator is defined. This idea appears to be new. We emphasize that the main principle behind this construction is rather general (we will provide an abstract definition) and could be applied in other contexts than the ones we are primarily interested in (namely the acoustic and the electromagnetic settings), for instance for elasticity.

If the underlying continuous operator is of very similar theoretical nature as the operators based on integral representations discussed in the preceding chapters, it presents a certain number of advantages in comparison. To begin with, most (if not all) of the computational technology required to implement a domain decomposition method using this operator should be already at hand (that is mainly the finite element method). This is in contrast to integral operators which require to interface (or implement) a boundary element code. This feature might be a

definitive advantage for someone wishing to implement a domain decomposition method in an already available finite element code, which does not necessarily have the technology for integral operators (singular quadratures for instance). In fact, it is our intuition that it is precisely because the realization of this operator solves similar problems as the original problem that makes it so efficient in practice in our numerical experiments (particularly for low frequency problems).

The computational footprint of the operator is naturally reduced by solving the auxiliary problems only in close vicinity of the boundary on which the operator is defined. Moreover, this truncation process is guaranteed to preserve the essential properties of the operator. Again, this is in contrast to integral operators for which the quasi-localization process (sometimes) invalidates our theoretical proofs. In addition, we remark that some of the tools that could be used to reduce the computational complexity of using integral operators, namely the fast multipole method (FMM) or $\mathcal{H}$-matrices, are again quite advanced technology compared to what is needed here.

Another motivation for using the operator described in this chapter appears when considering heterogeneous problems. The definition of the operator is in fact much more natural than for integral operators for instance. If some parameters appear in its definition, their tuning can be performed by following rather simple heuristics that we shall try to justify in this chapter. In particular, note that because the domain of the auxiliary problem is located around the interface of interest, we need to impose a boundary condition on the fictitious boundary we introduced. In this chapter, we shall compare on a model (but representative) problem, the different options to choose from.

This chapter is organized as follows. We first provide in Section 8.1 a definition of this novel transmission operator in the abstract framework introduced in Chapter 3. This abstract definition is particularized for the two main applications we have in mind, namely the Helmholtz and Maxwell equations. We then study in Section 8.2 some of the parameters that come in the definition of this transmission operator in the particular geometric configuration of the half-space. This permits explicit computations using Fourier analysis and allows to get some insights on the mechanisms at play. We finally provide in Section 8.3 some numerical results that highlight the rather good performance of this new operator.

8.1 Definition at the continuous level

8.1.1 Abstract definition

We consider the boundary Σ of a bounded Lipschitz domain Ω_- subset of $\mathbb{R}^d$, $d \in \{2, 3\}$ and we set $\Omega_+ := \mathbb{R}^d \setminus \overline{\Omega_-}$. We assume that the domain Ω_- is connected and simply connected (all its Betti numbers are zero) so that Σ is also connected and simply connected. We denote by ν the unit outward normal vector defined on Σ from Ω_- to Ω_+.

Besides, we introduce two strips $\mathcal{B}_i \subset \Omega_-$ and $\mathcal{B}_e \subset \Omega_+$ so that $\mathcal{B}_i$ (respectively $\mathcal{B}_e$) has two disconnected (and not intersecting) boundaries Σ and Σ_i (respectively Σ_e), see Figure 8.1. We do not exclude the case $\Sigma_i = \emptyset$ for which we have $\mathcal{B}_i = \Omega_-$. We denote by ν_i (respectively ν_e) the outward unit normal vector to $\mathcal{B}_i$ (respectively $\mathcal{B}_e$).

Strong formulation We suppose (this is not restrictive) that the coefficients a and n of the model problem are defined in $\mathcal{B}_j$, for $j \in \{i, e\}$. Because its definition depends on the coefficient a, recalling (3.29), we define a variant of the γ_1 operator as (simple formal substitution $\mathsf{a} \to \Re(\mathsf{a})$)

$$\tilde{\gamma}_{1,\kappa} := {\kappa_0}^{-1} \, \gamma_{\mathrm{D}^*,\kappa} \, \Re(\mathsf{a}) \, \mathrm{D}, \qquad \kappa \in \{\Sigma, \Sigma_i, \Sigma_e\}. \tag{8.1}$$

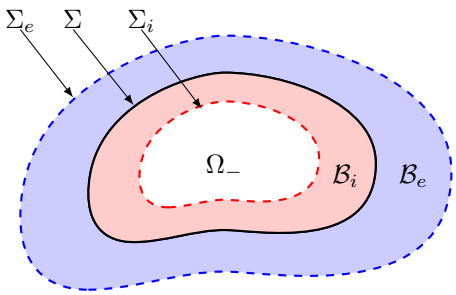

Figure 8.1: Definitions of the domain in which the auxiliary problems are defined.

This variant $\tilde{\gamma}_{1,\kappa}$ obviously enjoys the same mapping properties as the original operator $\gamma_{1,\kappa}$.

We define two operators, for $j \in \{i, e\}$

$$\begin{aligned} \mathcal{T}_j \ &: \mathrm{X}_0(\Sigma) \to \mathrm{X}_1(\Sigma), \\ &\mathrm{x}_0 \mapsto \tilde{\gamma}_{1,\Sigma}\, u_j, \end{aligned} \tag{8.2}$$

where

$$\begin{cases} u_j \in \mathrm{U}_{\Sigma_j}(\mathrm{D}; \mathcal{B}_j) \text{ such that} & \\ [\mathrm{L}_{\Re(\mathsf{a})} + {\kappa_0}^2 \Re(\mathsf{n})] u_j = 0, & \text{in } \mathcal{B}_j, \\ [\tilde{\gamma}_{1,\Sigma_j} + \gamma_{0,\Sigma_j}] u_j = 0, & \text{on } \Sigma_j, \\ \gamma_{0,\Sigma}\, u_j = \mathrm{x}_0, & \text{on } \Sigma. \end{cases} \tag{8.3}$$

Compared to the model wave propagation problems we considered previously, this problem is elliptic (by the positivity assumption on the real part of the coefficients a and n), hence the above definition makes sense. This is further justified below, by adopting a variational approach.

Weak formulation To provide a weak formulation of the above operator we first need to define the subspace

$$\mathrm{U}_{\Sigma_j,\Sigma 0}(\mathrm{D}; \mathcal{B}_j) := \left\{ u \in \mathrm{U}_{\Sigma_j}(\mathrm{D}; \mathcal{B}_j) \mid \gamma_{0,\Sigma}\, u = 0 \right\}, \qquad j \in \{i, e\}. \tag{8.4}$$

Let $j \in \{i, e\}$, for all $u, v \in \mathrm{U}_{\Sigma_j}(\mathrm{D}; \mathcal{B}_j)$, we define

$$a_{\mathcal{B}_j}(u, v) := {\kappa_0}^{-1} (\Re(\mathsf{a})\, \mathrm{D}u, \mathrm{D}v)_{L^2(\mathcal{B}_j)^{m_1}} + \kappa_0\, (\Re(\mathsf{n}) u, v)_{L^2(\mathcal{B}_j)^{m_0}} + (\gamma_{0,\Sigma_j}\, u, \gamma_{0,\Sigma_j}\, v)_{L^2(\Sigma_j)^{m_0}}. \tag{8.5}$$

Now, let us consider the mapping

$$\mathrm{y}_0 \in \mathrm{X}_0(\Sigma) \quad \mapsto \quad u_{\mathrm{y}_0} \in \mathrm{U}_{\Sigma_j}(\mathrm{D}; \mathcal{B}_j), \tag{8.6}$$

such that

$$\begin{cases} a_{\mathcal{B}_j}(u_{\mathrm{y}_0}, v) = 0, & \forall v \in \mathrm{U}_{\Sigma_j,\Sigma 0}(\mathrm{D}; \mathcal{B}_j), \\ \gamma_{0,\Sigma}\, u_{\mathrm{y}_0} = \mathrm{y}_0. \end{cases} \tag{8.7}$$

The well-posedness of the problem appearing in (8.7) stems from the surjectivity of the trace operator $\gamma_{0,\Sigma}$ which allows to get a lifting of the inhomogeneous source term imposed at the essential boundary condition. The well-posedness of the said problem is then readily obtained from Lax-Milgram Lemma, since the bilinear form $a_{\mathcal{B}_j}$ is coercive on $\mathrm{U}_{\Sigma_j}(\mathrm{D}; \mathcal{B}_j)$ from our positivity assumption on the real part of the coefficients a and n.

An equivalent variational formulation of (8.2) is: for any $\mathrm{x}_0 \in \mathrm{X}_0(\Sigma)$, we define $\mathcal{T}_j \mathrm{x}_0 \in \mathrm{X}_1(\Sigma)$ as the unique solution of

$$\langle \mathcal{T}_j \mathrm{x}_0, \mathrm{x}_0^t \rangle_\Sigma = a_{\mathcal{B}_j}(u_{\mathrm{x}_0}, u_{\mathrm{x}_0^t}), \qquad \forall \mathrm{x}_0^t \in \mathrm{X}_0(\Sigma). \tag{8.8}$$

Transmission operators The required properties for a candidate transmission operator are all inherited from those of the auxiliary problem, which can be clearly seen from (8.8). This is the purpose of the following proposition.

Proposition 8.1. *The operator $\mathcal{T}_j$, $j \in \{i, e\}$, is a self-adjoint positive isomorphism from $\mathrm{X}_0(\Sigma)$ to $\mathrm{X}_1(\Sigma)$.*

Proof. Let $j \in \{i, e\}$. Recalling the symmetry, positivity and boundedness of the coefficients (3.78), we immediately obtain the symmetry, continuity and coerciveness of the bilinear form $a_{\mathcal{B}_j}$.

Indeed, from (8.8) and the symmetry of the bilinear form $a_{\mathcal{B}_j}$ we have, for any $\mathrm{x}_0, \mathrm{x}_0^t \in \mathrm{X}_0(\Sigma)$,

$$\langle \mathcal{T}_j \mathrm{x}_0, \mathrm{x}_0^t \rangle_\Sigma = a_{\mathcal{B}_j}(u_{\mathrm{x}_0}, u_{\mathrm{x}_0^t}) = a_{\mathcal{B}_j}(u_{\mathrm{x}_0^t}, u_{\mathrm{x}_0}) = \langle \mathcal{T}_j \mathrm{x}_0^t, \mathrm{x}_0 \rangle_\Sigma, \tag{8.9}$$

hence $\mathcal{T}_j$ is self-adjoint.

Besides, from (8.8) and the continuity and coerciveness of the bilinear form $a_{\mathcal{B}_j}$ we have,

$$\min(1, \mathsf{a}_-, \mathsf{n}_-) \, \|u_{\mathrm{x}_0}\|^2_{\mathrm{U}_{\Sigma_j}(\mathrm{D};\mathcal{B}_j)} \leq \langle \mathcal{T}_j \mathrm{x}_0, \overline{\mathrm{x}_0} \rangle_\Sigma \leq \max(1, \mathsf{a}_+, \mathsf{n}_+) \, \|u_{\mathrm{x}_0}\|^2_{\mathrm{U}_{\Sigma_j}(\mathrm{D};\mathcal{B}_j)}. \tag{8.10}$$

Using the continuity of the trace operator as well as the well-posedness of the problem (8.7), we deduce the existence of two strictly positive constants $c_- > 0$ and $c_+ > 0$ such that

$$c_- \, \|\mathrm{x}_0\|^2_{\mathrm{X}_0(\Sigma)} \leq \langle \mathcal{T}_j \mathrm{x}_0, \overline{\mathrm{x}_0} \rangle_\Sigma \leq c_+ \, \|\mathrm{x}_0\|^2_{\mathrm{X}_0(\Sigma)}. \tag{8.11}$$

■

It is easy to see from the discussion above that any linear combination of $\mathcal{T}_i$ and $\mathcal{T}_e$ would work as a transmission operator, hence we let

$$\mathrm{T}_0^{\mathrm{Aux}} := \alpha_i \mathcal{T}_i + \alpha_e \mathcal{T}_e, \tag{8.12}$$

for any $\alpha_i \geq 0$, $\alpha_e \geq 0$. Besides, it is natural to require $\alpha_i + \alpha_e = 1$. For no more than simple reasons of symmetry, we chose in our numerical simulations $\alpha_i = \alpha_e = \frac{1}{2}$.

Of course, if one implements a domain decomposition method that requires a $\mathbf{T}_{1,\|}$-type transmission operator it is possible to use

$$\mathrm{T}_1^{\mathrm{Aux}} := \beta_i \mathcal{T}_i^{-1} + \beta_e \mathcal{T}_e^{-1}, \tag{8.13}$$

for any $\beta_i \geq 0$, $\beta_e \geq 0$ such that $\beta_i + \beta_e = 1$.

Alternative definitions Besides using different values of $\alpha_i \geq 0$ and $\alpha_e \geq 0$, one could alter the definitions of $\mathcal{T}_i$ and $\mathcal{T}_e$ in a number of different ways without harming their essential properties.

For a start, as we already mentioned, other (positive) coefficients can be chosen in the equation in (8.3) and in (8.7). Our intuition (which was corroborated to some extend by our numerical experiments) is that our choice to use $\Re(\mathsf{a})$, $\Re(\mathsf{n})$ and κ_0 as we did is somewhat sensible. In some sense, this is justified by the commonly mentioned heuristic to use a transmission operator that is close to, or somehow resembles, the exact propagative Dirichlet-to-Neumann operator, if we

adopt the terminology of the acoustic setting. By sticking to the real parts of the coefficients of the original equation, we obtain an operator whose principal part is the same (or close to, if the imaginary parts do not vanish) as the exact propagative Dirichlet-to-Neumann operator (one must also require that $\alpha_i + \alpha_e = 1$). This reasoning does not motivate to keep the lower order term in the acoustic setting, but it does indeed in the electromagnetic case since the **curl** operator has a non-zero null space. In some sense, keeping this term is the same as choosing Bessel potentials over Riesz potentials when we discussed integral operators. Finally, note that we do not claim that the choice of coefficients we made is optimal, but it is a reasonable rule of thumb to start from.

Another possible modification that one can think of is to consider a different kind of boundary condition on Σ_i (and Σ_e). For instance homogeneous Neumann (a natural boundary condition in a Galerkin discretization) or homogeneous Dirichlet (which eliminates some degrees of freedom of the auxiliary problems) boundary conditions. It appears that the choice we made, namely a Robin boundary condition, is worth the (slight) additional complexity of implementation. We shall get back on this aspect in a subsequent section.

Finally, we have some liberty in the definition of the strips $\mathcal{B}_i$ and $\mathcal{B}_e$. Obviously, to make the transmission operator the least expensive to compute, one would like to choose it as thin as possible (ideally a few layers of cells in a mesh). Roughly speaking, because the source of the auxiliary problem is only present on the boundary Σ and the problem is purely dissipative, the solution is exponentially decaying away from it. As a result, having a large domain (thicker than the skin-depth of the problem) does not necessarily affect much the operator. We shall also discuss this important aspect in what follows.

8.1.2 Application to standard propagation problems

We briefly give below the definition of the above abstract transmission operators in view of application to either Helmholtz or Maxwell equations.

Example 1: Helmholtz. *In the acoustic setting, the two operators are a elliptic (or dissipative) version of conventional Dirichlet-to-Neumann maps. They are written, for $j \in \{i, e\}$,*

$$\begin{aligned} \mathcal{T}_j \ &: H^{1/2}(\Sigma) \to H^{-1/2}(\Sigma), \\ &\mathrm{x}_0 \mapsto {\kappa_0}^{-1} \Re\left(\rho_r^{-1}\right) \partial_{\nu_j} p_j, \end{aligned} \tag{8.14}$$

where

$$\begin{cases} p_j \in H^1(\mathcal{B}_j) \text{ such that} & \\ \left[-\operatorname{div} \Re\left(\rho_r^{-1}\right) \mathbf{grad} + {\kappa_0}^2 \Re\left(\lambda_r^{-1}\right)\right] p_j = 0, & \text{in } \mathcal{B}_j, \\ \Re\left(\rho_r^{-1}\right) \partial_{\nu_j} p_j + \kappa_0 p_j = 0, & \text{on } \Sigma_j, \\ p_j = \mathrm{x}_0, & \text{on } \Sigma. \end{cases} \tag{8.15}$$

We denoted by ν_j the outward unit vector to $\mathcal{B}_j$ either on Σ or on Σ_j.

Example 2: Maxwell. *In the electromagnetic setting, the two operators are a elliptic (or dissipative) version of conventional Electric-to-Magnetic maps. They are written, for $j \in \{i, e\}$,*

$$\begin{aligned} \mathcal{T}_j \ &: \mathbf{H}^{-1/2}(\mathrm{curl}; \Sigma) \to \mathbf{H}^{-1/2}(\mathrm{div}; \Sigma), \\ &\mathrm{x}_0 \mapsto {\kappa_0}^{-1} \Re\left(\mu_r^{-1}\right) \mathbf{curl}\, \mathbf{E}_j \times \nu_{j,\Sigma}, \end{aligned} \tag{8.16}$$

where

$$\begin{cases} \mathbf{E}_j \in \mathbf{H}_{\Sigma_j}(\mathbf{curl}; \mathcal{B}_j) \text{ such that} & \\ \left[\mathbf{curl}\, \Re\left(\mu_r^{-1}\right) \mathbf{curl} + {\kappa_0}^2 \Re\left(\epsilon_r\right)\right] \mathbf{E}_j = 0, & \text{in } \mathcal{B}_j, \\ \Re\left(\mu_r^{-1}\right)\ \mathbf{curl}\, \mathbf{E}_j \times \nu_j + \kappa_0\, \nu_j \times (\mathbf{E}_j \times \nu_j) = 0, & \text{on } \Sigma_j, \\ \nu_j \times (\mathbf{E}_j \times \nu_j) = \mathrm{x}_0, & \text{on } \Sigma. \end{cases} \tag{8.17}$$

Again, we denoted by ν_j the outward unit vector to $\mathcal{B}_j$ respectively on Σ and on Σ_j.

In both cases, provided there exists a continuous right inverse to respectively the Dirichlet trace and the tangential trace, the above problems are well posed using the Lax-Milgram Lemma.

Note that one could rather use a different coefficient instead of $\Re(\rho_r^{-1})$, for instance $\Re(\rho_r)^{-1}$ or $|\rho_r|^{-1}$, which are different if the imaginary part does not vanish. Of course, this comment also stands for the other coefficients and apply to both the acoustic and electromagnetic settings. This may later have a strong influence on the efficiency of the domain decomposition method associated to the transmission operator. However, as far as the convergence theory is concerned, any positive coefficient can be chosen.

Connection with the previously defined integral operators If the medium of propagation is

1. *unbounded*: the strips are extended to the whole domain so that we have $\mathcal{B}_i = \Omega_-$ and $\mathcal{B}_e = \Omega_+ = \mathbb{R}^d \setminus \overline{\Omega_-}$,

2. *uniform*: the (positive) coefficients $\Re(\mathsf{n})$ and $\Re(\mathsf{a})$ are constant in the whole of $\mathbb{R}^d$ so that we can define the positive and real parameter $\kappa = \kappa_0 \sqrt{\frac{\Re(\mathsf{n})}{\Re(\mathsf{a})}}$,

then the connection with the previously defined integral operators is possible. Indeed, we (formally) have in this case, in the acoustic setting

$$\begin{aligned} (2\kappa V_{d,\kappa})^{-1} &= \frac{1}{2}\left(\mathcal{T}_i + \mathcal{T}_e\right), \\ \frac{2}{\kappa} W_{d,\kappa} &= \frac{1}{2}\left(\mathcal{T}_i^{-1} + \mathcal{T}_e^{-1}\right)^{-1}, \end{aligned} \tag{8.18}$$

where $V_{d,\kappa}$ and $W_{d,\kappa}$ were defined in (5.19), and already reinterpreted as equivalent transmission problems in (5.25) and in (5.26); and in the electromagnetic setting

$$\begin{aligned} (2\mathbf{U}_{3,\kappa})^{-1} &= \frac{1}{2}\left(\mathcal{T}_i + \mathcal{T}_e\right), \\ 2\mathbf{K}_{3,\kappa} &= \frac{1}{2}\left(\mathcal{T}_i^{-1} + \mathcal{T}_e^{-1}\right)^{-1}, \end{aligned} \tag{8.19}$$

where $\mathbf{U}_{3,\kappa}$ and $\mathbf{K}_{3,\kappa}$ were defined in (5.82), and already reinterpreted as equivalent transmission problems in (5.89) and in (5.90).

Of course in practice the operators $\mathcal{T}_i$ and $\mathcal{T}_e$ will necessarily be computed in a bounded domain so the above identities will not be true. Besides we propose to use a standard finite element method to compute these operators whereas the integral operators require a boundary element method, which does make a significant difference in practice.

8.2 Quantitative analysis for a model problem

We have already commented on the parameters on which one can play to modulate the action of the operators $\mathcal{T}_i$ and $\mathcal{T}_e$. We provide in this section some more quantitative computations to study precisely their influence. The two main questions we are trying to answer are:

- What is the effect on the operators of the type of boundary condition (among Dirichlet, Neumann and Robin) that is imposed on the fictitious boundaries Σ_i and Σ_e?
- What is the asymptotic behaviour of the operators if the width of the strips $\mathcal{B}_i$ and $\mathcal{B}_e$ shrinks to 0?

8.2.1 The periodic wave-guide

Model problem We consider the theoretical (because unbounded) configuration of an infinite wave guide of width L, see Figure 8.2. The domain of the problem is

$$\Omega := \left\{ (x,y) \in \mathbb{R}^2 \mid -\frac{L}{2} < x < \frac{L}{2} \right\}. \tag{8.20}$$

We consider the Helmholtz equation in 2D in the wave-guide with periodic boundary conditions (in absence of source terms)

$$\begin{cases} (-\Delta - \kappa^2)u = 0, & \text{in } \Omega, \\ u(-\frac{L}{2}, y) = u(\frac{L}{2}, y), & y \in \mathbb{R}, \end{cases} \tag{8.21}$$

where we require the solution u to satisfy the Sommerfeld radiation condition at infinity

$$\lim_{r \to +\infty} (\partial_r - \mathrm{i}\kappa)\, u = 0, \qquad r = |x|. \tag{8.22}$$

Partition The domain Ω is divided in the upper Ω_+ and lower Ω_- regions

$$\Omega_+ := \left\{ (x,y) \in \mathbb{R}^2 \mid y > 0 \right\}, \qquad \text{and} \qquad \Omega_- := \left\{ (x,y) \in \mathbb{R}^2 \mid y < 0 \right\}, \tag{8.23}$$

and the interface is denoted

$$\Sigma := \left(-\frac{L}{2}, \frac{L}{2} \right) \times \{0\}. \tag{8.24}$$

Transmission operator To define our domain decomposition we need to introduce our transmission operator. The domain of the auxiliary problem that defines the transmission operator is now bounded in the y-direction, for a positive parameter $\delta > 0$, let

$$\mathcal{B}_{\pm,\delta} := \{ (x,y) \in \Omega_\pm \mid 0 \le |y| \le \delta \}. \tag{8.25}$$

We consider the operators, indexed by the truncation parameter δ and the type of boundary condition $* \in \{D, N, R\}$,

$$\mathcal{T}^{(*)}_{\pm,\delta} \ : \ \mathrm{x}_0 \mapsto \mp \kappa^{-1} \partial_y v^{(*)}_\pm |_{y=0}, \tag{8.26}$$

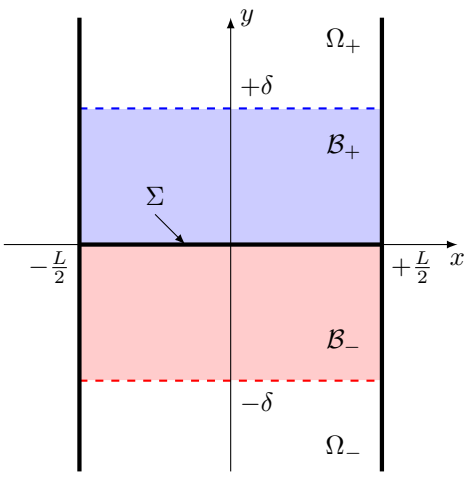

Figure 8.2: Sketch of the periodic wave guide configuration.

where $v_\pm^{(*)}$ solves the (elliptic) problem

$$\begin{cases} \left(-\Delta + \kappa^2\right) v_\pm^{(*)} = 0, & \text{in } \mathcal{B}_{\pm,\delta}, \\ v_\pm^{(*)}(-\frac{L}{2}, y) = v_\pm^{(*)}(\frac{L}{2}, y), & |y| \leq \delta, \\ v_\pm^{(*)}(x, 0) = \mathrm{x}_0(x), & -\frac{L}{2} \leq x \leq \frac{L}{2}, \end{cases}$$
$$\text{and at } y = \pm\delta, \qquad \begin{cases} v_\pm^{(D)}(x, \delta) = 0, \\ \partial_y v_\pm^{(N)}(x, \delta) = 0, \\ [\pm\partial_y + \kappa] v_\pm^{(R)}(x, \delta) = 0, \end{cases} \qquad -\frac{L}{2} \leq x \leq \frac{L}{2}. \tag{8.27}$$

The transmission operator is then, for $* \in \{D, N, R\}$,

$$\mathcal{T}_\delta^{(*)} := \frac{1}{2}\left(\mathcal{T}_{+,\delta}^{(*)} + \mathcal{T}_{-,\delta}^{(*)}\right). \tag{8.28}$$

In the following, our main interest lies in the impact on the convergence of the domain decomposition algorithms of both the type of boundary conditions (either Dirichlet (D), Neumann (N) or Robin (R)) that is imposed on the fictitious boundaries and the width $\delta > 0$.

Interface problem We consider, in this particular two-domain partition, the interface problem (3.222) and the associated relaxed Jacobi algorithm (3.225) (for $\sigma = 1$) from Chapter 3. We specify below our notations for this particular setting.

By linearity it is enough to study the homogeneous problem, which corresponds to study the convergence of the error. We therefore consider the interface problem, for $* \in \{D, N, R\}$ (the dependence in δ will be kept implicit in the notations),

$$\begin{cases} \text{Find } \mathbb{x} \in H^{-1/2}(\Sigma)^2 \text{ such that,} \\ \left(\mathrm{Id} - \mathbf{\Pi}\mathbf{S}^{(*)}\right)\mathbb{x} = 0, \end{cases} \tag{8.29}$$

where the exchange operator $\mathbf{\Pi}$ and the scattering operator $\mathbf{S}^{(*)}$ have the block representation

$$\mathbf{\Pi} := \begin{bmatrix} 0 & \mathrm{Id} \\ \mathrm{Id} & 0 \end{bmatrix}, \qquad \text{and} \qquad \mathbf{S}^{(*)} := \begin{bmatrix} \mathbf{S}_-^{(*)} & 0 \\ 0 & \mathbf{S}_+^{(*)} \end{bmatrix}, \tag{8.30}$$

with the local scattering operators $\mathbf{S}_-^{(*)}$ and $\mathbf{S}_+^{(*)}$ such that

$$\mathbf{S}_\pm^{(*)} \ : \ \mathrm{x}_0 \mapsto \left(\pm\kappa^{-1}\partial_y - \mathrm{i}\mathcal{T}_\delta^{(*)}\right) \ u_\pm^{(*)}|_{y=0}, \tag{8.31}$$

where $u_\pm^{(*)}$ is solution to

$$\begin{cases} (-\Delta - \kappa^2)u_\pm^{(*)} = 0, & \text{in } \Omega_\pm, \\ \left(\mp\kappa^{-1}\partial_y - \mathrm{i}\mathcal{T}_\delta^{(*)}\right) \ u_\pm^{(*)}|_{y=0} = \mathrm{x}_0, & \text{on } \Sigma, \end{cases} \tag{8.32}$$

and

$$\lim_{r\to+\infty} (\partial_r - \mathrm{i}\kappa) \ u_\pm^{(*)} = 0, \qquad r = |x|. \tag{8.33}$$

Iterative algorithm Given a couple of traces $\mathbb{x}^0$ in $H^{-1/2}(\Sigma)^2$ (the initial error) and a relaxation parameter $r \in (0,1)$ the relaxed Jacobi algorithm is,

$$\mathbb{x}^{n+1} = \left[(1-r)\mathrm{Id} + r\mathbf{\Pi}\mathbf{S}^{(*)}\right]\mathbb{x}^n, \qquad n \in \mathbb{N}. \tag{8.34}$$

8.2.2 Symbol of the transmission operator

Similarly as in Chapter 6, because of the separable geometry, we are able to conduct a quantitative study. Exploiting the periodic boundary conditions in the x direction, the main tool for this is the Hilbert basis $\left(e^{ik_m x}\right)_{m\in\mathbb{N}}$ of $L^2(\Sigma)$ where we introduced the mode numbers

$$k_m = m\frac{2\pi}{L}, \qquad m \in \mathbb{N}. \tag{8.35}$$

By symmetry, we need only to study the operator in the upper half-region. The system defining the operator $\mathcal{T}_{+,\delta}^{(*)}$ becomes, for each mode $m \in \mathbb{N}$,

$$\begin{cases} \left(-\partial_y^2 + \mu_m^2\right)\hat{v}_m^{(*)} = 0, & \text{in } \mathcal{B}_{+,\delta}, \\ \hat{v}_m^{(*)}(0) = \hat{x}_{0,m}, & \text{at } y = 0, \end{cases}$$
$$\text{and at } y = \delta, \qquad \begin{cases} \hat{v}_m^{(D)}(\delta) = 0, \\ \partial_y \hat{v}_m^{(N)}(\delta) = 0, \\ [\partial_y + \kappa]\hat{v}_m^{(R)}(\delta) = 0, \end{cases} \tag{8.36}$$

where

$$\mu_m^2 = k_m^2 + \kappa^2, \qquad m \in \mathbb{N}, \tag{8.37}$$

and $(\hat{v}_m^{(*)})_{m\in\mathbb{N}}$ are the coefficients of $v^{(*)}$ on the modal basis $\left(e^{ik_m x}\right)_{m\in\mathbb{N}}$. We introduced in addition the coefficients $(\hat{x}_{0,m})_{m\in\mathbb{N}}$ of the decomposition of x_0 on the same modal basis. It follows that

$$\hat{v}_m^{(*)} \in \mathrm{vect}\left\{y \mapsto e^{\mu_m y}, \ y \mapsto e^{-\mu_m y}\right\}, \qquad m \in \mathbb{N}, \tag{8.38}$$

where we chose $\mu_m := \sqrt{k_m^2 + \kappa^2}$ and it remains to determine the two constants by using the boundary conditions at $y = 0$ and $y = \delta$. We consider successively the three types of boundary

conditions and find that,

$$\begin{cases} \hat{v}_m^{(D)}(y) = \hat{x}_{0,m}\, \dfrac{e^{-\mu_m(y-\delta)} - e^{\mu_m(y-\delta)}}{e^{\mu_m\delta} - e^{-\mu_m\delta}}, & 0 \le y \le \delta, \\ \hat{v}_m^{(N)}(y) = \hat{x}_{0,m}\, \dfrac{e^{-\mu_m(y-\delta)} + e^{\mu_m(y-\delta)}}{e^{\mu_m\delta} + e^{-\mu_m\delta}}, & 0 \le y \le \delta, \\ \hat{v}_m^{(R)}(y) = \hat{x}_{0,m}\, \dfrac{(\mu_m+\kappa)e^{-\mu_m(y-\delta)} + (\mu_m-\kappa)e^{\mu_m(y-\delta)}}{(\mu_m+\kappa)e^{\mu_m\delta} + (\mu_m-\kappa)e^{-\mu_m\delta}}, & 0 \le y \le \delta. \end{cases} \tag{8.39}$$

It is convenient to rewrite the three cases in the following common notation

$$\hat{v}_m^{(*)}(y) = \hat{x}_{0,m}\, \frac{e^{-\mu_m y} + \alpha_m^{(*)} e^{\mu_m y}}{1 + \alpha_m^{(*)}}, \qquad 0 \le y \le \delta, \tag{8.40}$$

where $\alpha^{(*)}$ is given by

$$\begin{cases} \alpha_m^{(D)} = -e^{-2\mu_m\delta}, \\ \alpha_m^{(N)} = e^{-2\mu_m\delta}, \\ \alpha_m^{(R)} = \dfrac{\kappa^{-1}\mu_m - 1}{\kappa^{-1}\mu_m + 1} e^{-2\mu_m\delta}, \end{cases} \tag{8.41}$$

By symmetry, the symbol of the transmission operator $\mathcal{T}_\delta^{(*)}$ is then (the dependence in δ will be kept implicit in the notations),

$$\hat{T}_m^{(*)} = \kappa^{-1}\mu_m\, \frac{1 - \alpha_m^{(*)}}{1 + \alpha_m^{(*)}}, \qquad m \in \mathbb{N}. \tag{8.42}$$

8.2.3 Modal convergence factor

Symbol of the propagative DtN operator We consider the operators

$$\Lambda_\pm \ : \ \mathrm{x}_0 \mapsto \mp\kappa^{-1}\partial_y u|_{y=0}, \tag{8.43}$$

where u solves the (propagative) problem in the sub-domain $\Omega_\pm$

$$\begin{cases} \left(-\Delta - \kappa^2\right) u = 0, & \text{in } \Omega_\pm, \\ u(-\frac{L}{2}, y) = u(\frac{L}{2}, y), & \text{on } \partial\Omega_\pm \setminus \Sigma, \\ u(x,0) = \mathrm{x}_0(x), & -\frac{L}{2} \le x \le \frac{L}{2}, \end{cases} \tag{8.44}$$

with suitable decay at infinity $y \to +\infty$ (Sommerfeld radiation condition).

By symmetry, we need only to study the operator in the upper half-region. The system associated to Λ_+ becomes, for each mode $m \in \mathbb{N}$,

$$\begin{cases} \left(-\partial_y^2 + \xi_m^2\right) \hat{u}_m = 0, & \text{in } \Omega_+, \\ \hat{u}_m(0) = \hat{x}_{0,m}, & \text{at } y = 0, \end{cases} \tag{8.45}$$

where

$$\xi_m^2 = k_m^2 - \kappa^2, \qquad m \in \mathbb{N}, \tag{8.46}$$

and $(\hat{u}_m)_{m\in\mathbb{N}}$ are the coefficients of u on the modal basis $\left(e^{ik_m x}\right)_{m\in\mathbb{N}}$. We introduced in addition the coefficients $(\hat{x}_{0,m})_{m\in\mathbb{N}}$ of the decomposition of x_0 on the same modal basis. From the decay assumption at infinity and the Dirichlet boundary condition at $y = 0$, it follows that

$$\hat{u}_m(y) = \hat{x}_{0,m} e^{-\xi_m y}, \qquad 0 \le y, \qquad m \in \mathbb{N}, \tag{8.47}$$

where we chose (out time convention is $e^{-\mathrm{i}\omega t}$)

$$\xi_m := \begin{cases} -\mathrm{i}\sqrt{\kappa^2 - k_m^2}, & \text{if } k_m \le \kappa, \\ \sqrt{k_m^2 - \kappa^2}, & \text{if } \kappa \le k_m, \end{cases} \qquad m \in \mathbb{N}. \tag{8.48}$$

By symmetry, the symbol of the operators $\Lambda_\pm$ is then

$$\hat{\Lambda}_{\pm,m} = \kappa^{-1}\xi_m = \begin{cases} -\mathrm{i}\sqrt{1 - \left(\frac{k_m}{\kappa}\right)^2}, & \text{if } k_m \le \kappa, \\ \frac{k_m}{\kappa}\sqrt{1 - \left(\frac{\kappa}{k_m}\right)^2}, & \text{if } \kappa \le k_m, \end{cases} \qquad m \in \mathbb{N}. \tag{8.49}$$

Remark 8.2. *It may happen (for countable discrete values of L) that there exists a m such that $k_m = \kappa$, which means that the problem under consideration is ill-posed. We exclude such cases in what follows.*

Symbol of the scattering operators From the definitions of the operators $\Lambda_\pm^{(*)}$ and the scattering operators $\mathbf{S}_\pm^{(*)}$, we formally have

$$\mathbf{S}_\pm^{(*)} = -\left(\Lambda_\pm + \mathrm{i}\mathcal{T}_\delta^{(*)}\right)\left(\Lambda_\pm - \mathrm{i}\mathcal{T}_\delta^{(*)}\right)^{-1}, \tag{8.50}$$

so that the symbol of the local scattering operators $\mathbf{S}_\pm^{(*)}$ are, for $* \in \{D, N, R\}$,

$$\hat{S}_{\pm,m}^{(*)} = \frac{-\hat{\Lambda}_{\pm,m}^{(*)} - \mathrm{i}\hat{T}_m^{(*)}}{\hat{\Lambda}_{\pm,m}^{(*)} - \mathrm{i}\hat{T}_m^{(*)}}, \qquad \forall m \in \mathbb{N}. \tag{8.51}$$

We introduce the ratio (well-defined since $\hat{T}_m^{(*)} > 0$)

$$\hat{Z}_{\pm,m}^{(*)} = -\frac{\hat{\Lambda}_{\pm,m}^{(*)}}{\hat{T}_m^{(*)}}, \qquad \forall m \in \mathbb{N}, \tag{8.52}$$

and we can rewrite

$$\hat{S}_{\pm,m}^{(*)} = -\frac{\hat{Z}_{\pm,m}^{(*)} - \mathrm{i}}{\hat{Z}_{\pm,m}^{(*)} + \mathrm{i}}, \qquad \forall m \in \mathbb{N}. \tag{8.53}$$

We can distinguish two regimes

- The propagative regime $k_m < \kappa$ for which

$$\hat{\Lambda}_{\pm,m} \in -\mathrm{i}\mathbb{R}^+, \qquad \text{and since} \qquad \hat{T}_m^{(*)} \in \mathbb{R}^+, \qquad \text{we have} \qquad \hat{Z}_{\pm,m}^{(*)} \in \mathrm{i}\mathbb{R}^+. \tag{8.54}$$

  Hence

$$\hat{S}_{\pm,m}^{(*)} = -\frac{\hat{Z}_{\pm,m}^{(*)} - 1}{\hat{Z}_{\pm,m}^{(*)} + 1} \in [-1, 1]\,. \tag{8.55}$$

- The evanescent regime $k_m > \kappa$ for which

$$\hat{\Lambda}_{\pm,m} \in \mathbb{R}^+, \qquad \text{and since} \qquad \hat{T}_m^{(*)} \in \mathbb{R}^+, \qquad \text{we have} \qquad \hat{Z}_{\pm,m}^{(*)} \in \mathbb{R}^+. \tag{8.56}$$

  Hence

$$\hat{S}_{\pm,m}^{(*)} = \frac{\hat{Z}_{\pm,m}^{(*)} - \mathrm{i}}{\hat{Z}_{\pm,m}^{(*)} + \mathrm{i}}, \qquad |\hat{S}_{\pm,m}^{(*)}| = 1. \tag{8.57}$$

Modal convergence factor Arguing as in Chapter 6, for each $* \in \{D, N, R\}$, the modal factor of convergence of the algorithm (8.34) can be estimated by

$$\hat{\tau}_m^{(*)} = \max_{\pm} \left| (1 - r) \pm r \sqrt{\hat{S}_{+,m}^{(*)} \hat{S}_{-,m}^{(*)}} \right|, \tag{8.58}$$

Asymptotic analysis $\delta \to \infty$: for a fixed mode $m \in \mathbb{N}$ Although it is not our primary interest we first comment on the limit $\delta \to \infty$ for a fixed mode $m \in \mathbb{N}$. It is immediate to check that for $* \in \{D, N, R\}$

$$\hat{T}_m^{(*)} \sim \frac{\mu_m}{\kappa}, \qquad \text{as } \delta \to \infty. \tag{8.59}$$

We simply remark that the limit is independent of the type of boundary condition. This is not surprising considering that when δ is large the boundary on which the condition is imposed is rejected far away from the source of the problem which is dissipative.

Asymptotic analysis $\delta \to 0$: for a fixed mode $m \in \mathbb{N}$ From the previous expressions, we obtain the following asymptotic behaviours, for each mode $m \in \mathbb{N}$,

$$\begin{cases} \hat{T}_m^{(D)} \sim (\delta\kappa)^{-1}, & \text{as } \delta \to 0, \\ \hat{T}_m^{(N)} \sim \delta\kappa, & \text{as } \delta \to 0, \\ \hat{T}_m^{(R)} \sim 1, & \text{as } \delta \to 0. \end{cases} \tag{8.60}$$

From these asymptotic behaviours, one infers that the transmission operator using a Robin boundary condition is — to say the least — better behaved in the limit $\delta \to 0$ than the one using either Dirichlet or Neumann boundary conditions. For a fixed mode m, the transmission condition with the operator using Robin boundary conditions degenerates to the Després conditions. In fact, for the transmission operator $\mathcal{T}_\delta^{(R)}$ we have that the convergence factor associated to each mode $m \in \mathbb{N}$ is bounded away from 1, uniformly with respect to the truncation parameter δ. More precisely, it is a simple (but tedious, hence omitted) computation to show that there exists a positive constant $C_m^{(R)}$ depending only on m (not on δ) such that

$$\hat{\tau}_m^{(R)} \leq 1 - C_m^{(R)}, \qquad \forall \delta > 0. \tag{8.61}$$

Of course, this result is *not* uniform with respect to the mode m and we cannot conclude from this that the convergence factor of the associated algorithm is uniformly bounded with respect to δ. As a matter of fact, we give below evidence that such a result, namely global uniformity of the convergence factor with respect to δ, does not hold.

In contrast, for the transmission operators $\mathcal{T}_\delta^{(D)}$ and $\mathcal{T}_\delta^{(N)}$, it can be shown[1] that

$$\text{propagative regime } k_m \leq \kappa, \quad \begin{cases} \hat{\tau}_m^{(D)} = 1 - \left[2r\sqrt{1-\left(\frac{k_m}{\kappa}\right)^2}\,\kappa\right]\,\delta + \mathcal{O}(\delta^2), \\ \hat{\tau}_m^{(N)} = 1 - \left[2r\frac{1+\left(\frac{k_m}{\kappa}\right)^2}{\sqrt{1-\left(\frac{k_m}{\kappa}\right)^2}}\,\kappa\right]\,\delta + \mathcal{O}(\delta^2), \end{cases}$$

$$\text{evanescent regime } k_m \geq \kappa, \quad \begin{cases} \hat{\tau}_m^{(D)} = 1 - \left[2r(1-r)\left(\left(\frac{k_m}{\kappa}\right)^2 - 1\right)\,\kappa^2\right]\,\delta^2 + \mathcal{O}(\delta^3), \\ \hat{\tau}_m^{(N)} = 1 - \left[2r(1-r)\frac{\left(\left(\frac{k_m}{\kappa}\right)^2+1\right)^2}{\left(\frac{k_m}{\kappa}\right)^2-1}\,\kappa^2\right]\,\delta^2 + \mathcal{O}(\delta^3). \end{cases} \tag{8.62}$$

The above result implies that the global convergence factor converges to 1 at least as fast as $\mathcal{O}(\delta^2)$ when using either the Dirichlet or the Neumann boundary conditions.

8.2.4 Global convergence

The global convergence factor of the algorithm (8.34) can be estimated by

$$\hat{\tau}^{(*)} := \sup_{m\in\mathbb{N}} \hat{\tau}_m^{(*)}. \tag{8.63}$$

From the previous analysis we know already that in the case $* \in \{D, N\}$,

$$\lim_{\delta\to 0} \hat{\tau}^{(D)} = \lim_{\delta\to 0} \hat{\tau}^{(N)} = 1. \tag{8.64}$$

Unfortunately we were not able to derive analytic expressions for this global convergence factor. However, we studied the asymptotic analysis $m \to +\infty$ for a fixed δ and proved that also for $* = R$ we have necessarily $\lim_{\delta\to 0} \hat{\tau}^{(R)} = 1$.

Asymptotic analysis $m \to +\infty$: $\delta > 0$ fixed This amounts to study the limit $k_m \to +\infty$. It is immediate to check that for $* \in \{D, N, R\}$ and a fixed $\delta > 0$

$$\hat{T}_m^{(*)} \;\sim\; \hat{\Lambda}_m^{(*)} \;\sim\; \frac{k_m}{\kappa}, \qquad \text{as } m \to \infty. \tag{8.65}$$

It is then straightforward to show that there exists a positive constant $\hat{\tau}_\infty$ (independent of the boundary condition chosen) such that for each $* \in \{D, N, R\}$

$$\hat{\tau}_m^{(*)} \to \hat{\tau}_\infty < 1, \qquad \text{as } m \to \infty. \tag{8.66}$$

We see here a manifestation of the effect of choosing an operator with the "right" order that adequately deals with the highest frequency modes. Notice that the limit is independent of the type of boundary condition. This is not surprising as the highest modes "do not see", in some sense, the boundary condition.

[1] We used the symbolic computing PYTHON package `SymPy` [102] through the JULIA binding `Sympy.jl` to derive the modal convergence factor estimates.

Asymptotic analysis $m \to +\infty$ and $\delta = m^{-1/2}$ Guided by numerical experiments, we studied the double limit $\delta \to 0$ and $m \to +\infty$ such that $\delta = m^{-1/2}$ for the convergence factor associated to the operator $\mathcal{T}_\delta^{(R)}$. It can be shown that

$$\hat{\tau}_m^{(R)} = 1 - \left[2r(1-r) \left(\frac{2\pi}{L} + \frac{L}{2\pi} \right)^2 \right] \delta + \mathcal{O}(\delta^2). \tag{8.67}$$

The above result implies that the global convergence factor converges to 1 at least as fast as $\mathcal{O}(\delta)$ when using the Robin boundary condition and

$$\lim_{\delta \to 0} \hat{\tau}^{(R)} = 1. \tag{8.68}$$

8.2.5 Mocking the effect of the discretization

We are however unable to consider at the same time both the limit $\delta \to 0$ and $m \to \infty$, as the double asymptotic leads to undetermined behaviour. This is the motivation for the following analysis.

The idea is to mock the effect of discretization. To do so, we filter the admissible modes that belong to the bandwidth of the discrete problem. This amounts in this case to take $m \leq M$ in the definition of k_m for some integer M. Typically, one consider M such that (Nyquist-Shannon criteria)

$$k_M = \frac{2\pi}{\lambda} M \leq \frac{\pi}{h}, \tag{8.69}$$

where $h > 0$ is the typical mesh parameter. In our setting, we make the particular choice to have M such that

$$\delta k_M = \gamma, \tag{8.70}$$

where the positive constant $\gamma > 0$ is supposed to be fixed and we consider the limit

$$M \to +\infty \qquad \Leftrightarrow \qquad \delta \to 0. \tag{8.71}$$

In some sense, this would correspond in a discrete setting to study the effect of mesh refinement $h \to 0$ for a transmission operator whose associated auxiliary problem is defined in a strip made of a fixed number of layers of cells as $h \to 0$.

We obtain the following asymptotic behaviours

$$\begin{cases} \hat{T}_M^{(D)} & \sim & \tanh^{-1}(\gamma)\ \hat{\Lambda}_M, \\ \hat{T}_M^{(N)} & \sim & \tanh(\gamma)\ \hat{\Lambda}_M, \\ \hat{T}_M^{(R)} & \sim & \tanh(\gamma)\ \hat{\Lambda}_M, \end{cases} \qquad \text{as } M \to +\infty. \tag{8.72}$$

It is then straightforward to show that for each $* \in \{D, N, R\}$ there exists a positive constant $\hat{\tau}_\infty^{(*)}$ such that

$$\hat{\tau}_M^{(*)} \to \hat{\tau}_\infty^{(*)} < 1, \qquad \text{as } M \to \infty. \tag{8.73}$$

Again, one sees here the interest of using non-local operators which are pseudo-differential operators of the correct order. This time the limit does depend on the type of boundary condition. However, what is really important here, is to notice that, in this discrete setting, taking the truncation parameter δ to 0 as the discretization parameter goes to 0 (or equivalently $M \to \infty$), does not affect the convergence factor for the highest modes present in the computation.

8.2.6 Numerical investigations

We provide numerical computations to obtain more insight and corroborate the previous analysis.

Modal convergence factor We first report in Figure 8.3 the gap between 1 and the convergence factor $\hat{\tau}_m^{(*)}$ with respect to the mode number δ for different values of δ and for each $* \in \{D, N, R\}$. The parameters of the problem are $L = 1$, the wavenumber is $\kappa = 11\pi$ and the relaxation parameter for the Jacobi algorithm is $r = 0.5$. It follows that the propagative region corresponds to $m \in \mathbb{N}$ such that $m\frac{2\pi}{L} \leq \kappa = 11\pi$, hence $m \leq \frac{11}{2}$. Therefore for this configuration, 6 modes can propagate through the waveguide, the rest are evanescent.

These plots must be read as follows: the convergence is controlled by the mode m with the lowest value on the vertical axis, which corresponds to the mode with a convergence factor which is the closest to one. We see that as δ decreases this minimum value also decreases and the convergence is damaged in all three cases.

Notice that the predicted asymptotic behaviours for the cases using either Dirichlet or Neumann boundary conditions are indeed numerically corroborated. We observe a linear increase of the convergence factor in the propagative region and a quadratic increase in the evanescent region. Besides, the mode number for the lowest point seems to be roughly constant as δ changes.

In contrast for the case with Robin boundary condition, the convergence factor stays constant in the propagative region as δ changes. In the evanescent regime, we observe a linear increase of the convergence factor with respect to δ. Notice that the lowest point moves to the right as δ decreases, which means the most problematic mode (as far as convergence is concerned) changes as δ changes. To investigate this effect more precisely we report the mode numbers at which the maximum modal convergence factor is reached with respect to the width δ of the strips in Figure 8.4. Again, this corroborates the previous analysis, where such mode numbers where found to be proportional to $\delta^{-1/2}$.

We report in Figure 8.5 the gap between 1 and the convergence factor $\hat{\tau}^{(*)}$ with respect to the width of the strip δ. The quantity $\hat{\tau}^{(*)}$ is computed from $\hat{\tau}_m^{(*)}$ as

$$\hat{\tau}^{(*)} = \max_{0 \leq m \leq M_{\max}} \hat{\tau}_m^{(*)}, \tag{8.74}$$

with $M_{\max} = 10^5$ in this case. Since the parameters of the problem are kept the same as before, the value $M_{\max}$ appears sufficient considering that only the first 120 modes were plotted on Figure 8.3. For δ large enough we observe that the convergence factor is constant and is actually the same for all three cases. Both these effects were predicted by the previous analytical analysis and can be explained by the dissipative nature of the auxiliary problems and the fact that for δ large enough the boundary on which the Dirichlet, Neumann of Robin condition imposed is far away from the source of the problem. What is staggering is the fact that at some point the convergence factor actually decreases when the width of the strip is diminished for the transmission operators associated either to Neumann or Robin boundary conditions. This effect may be due to our somehow contrived example and we shall not comment more on it. For sufficiently small δ, the asymptotic is attained and we obtain numerically that the modal convergence factor for the relaxed Jacobi algorithm has the following asymptotic behavior: there exist three positive constants $C^{(*)} > 0$, for $* \in \{D, N, R\}$ such that

$$\begin{cases} \hat{\tau}^{(D)} \sim 1 - C^{(D)}\,\delta^2, \\ \hat{\tau}^{(N)} \sim 1 - C^{(N)}\,\delta^2, \\ \hat{\tau}^{(R)} \sim 1 - C^{(R)}\,\delta, \end{cases} \qquad \text{as } \delta \to 0. \tag{8.75}$$

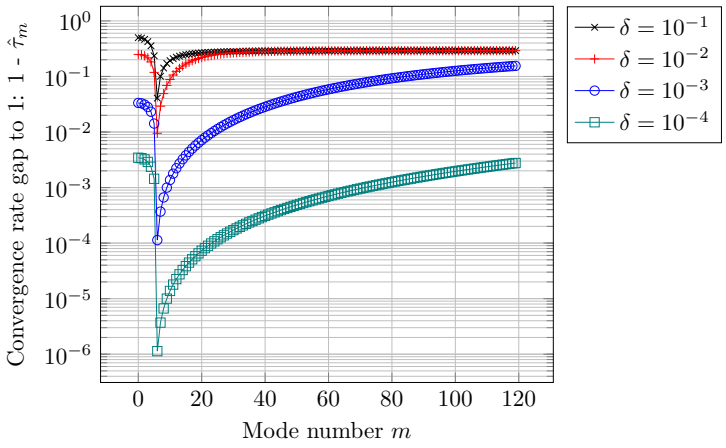

(a) Dirichlet

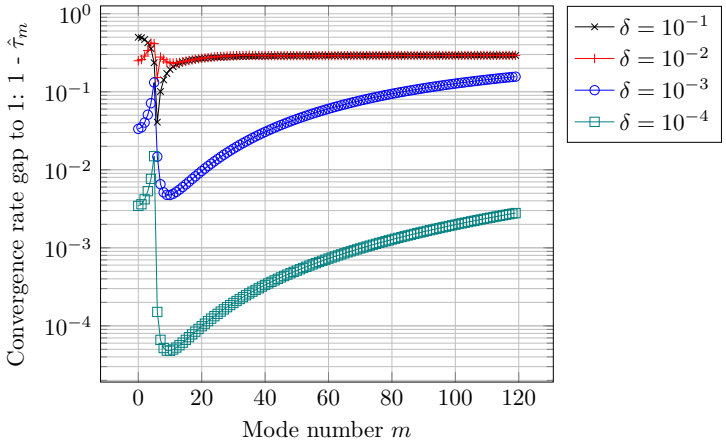

(b) Neumann

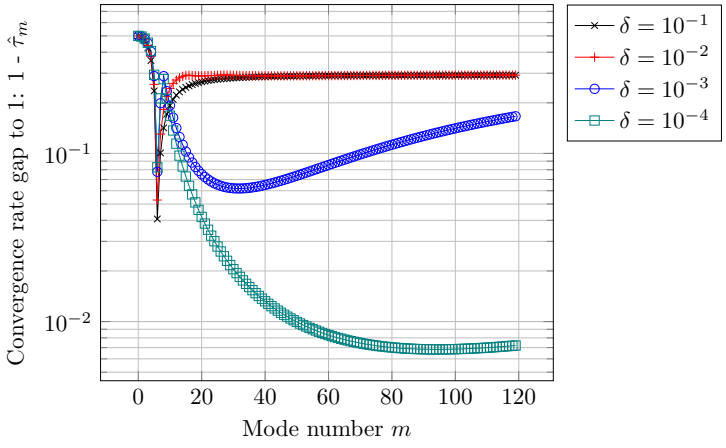

(c) Robin

Figure 8.3: Convergence factor with respect to mode number m for different values of δ and the different types of boundary conditions.

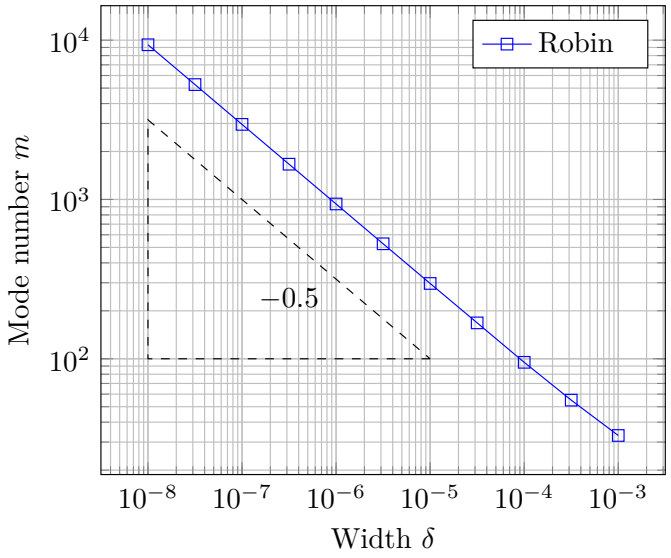

Figure 8.4: Mode number m associated to the maximal modal convergence factor with respect to the truncation parameter δ.

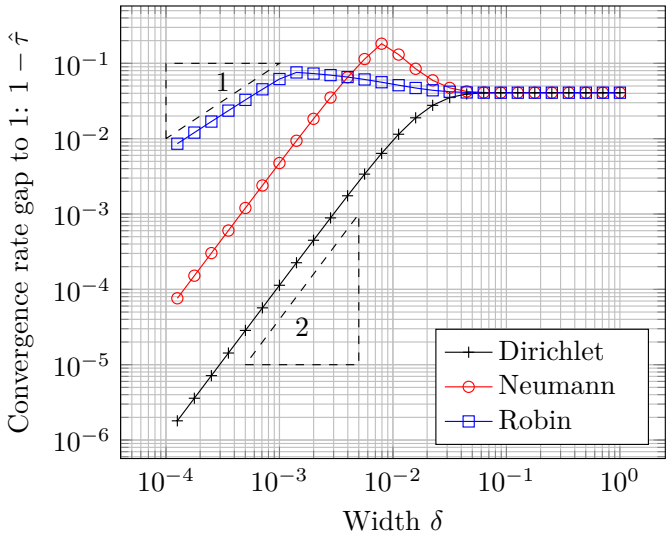

Figure 8.5: Modal convergence factor with respect to the truncation parameter δ.

We observe that, for δ small enough, the convergence factor tends to 1 as fast as $\mathcal{O}(\delta^2)$ for the transmission operators associated to Dirichlet and Neumann boundary condition, while a slower asymptotic of $\mathcal{O}(\delta)$ is observed numerically for the transmission operator associated to Robin boundary condition.

Interpretation as an iteration count It is enlightening to re-interpret the behavior of the convergence factor in terms of the (perhaps more revealing) required number of iterations. From (8.75), we expect the following asymptotic growth in the number of iterations to get to a specific tolerance

$$\begin{cases} N_{\text{it}}^{(D)} & \sim & N_0^{(D)}\, \delta^{-2}, \\ N_{\text{it}}^{(N)} & \sim & N_0^{(N)}\, \delta^{-2}, \\ N_{\text{it}}^{(R)} & \sim & N_0^{(R)}\, \delta^{-1}, \end{cases} \qquad \text{as } \delta \to 0, \tag{8.76}$$

where the positive constants $N_0^{(*)}$ depend on $C^{(*)}$ and on the required tolerance.

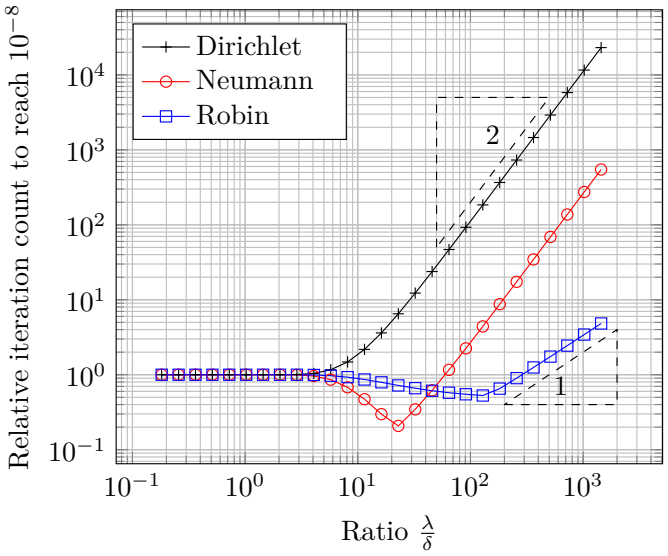

Figure 8.6: Relative iteration count to reach a set tolerance of 10^{-8} in relative error with respect to the ratio $\frac{\lambda}{\delta}$, with $\lambda = \frac{2\pi}{\kappa}$ for the different types of boundary conditions.

This is illustrated in Figure 8.6, where we report the relative iteration count to reach a set tolerance of 10^{-8} in relative error with respect to the ratio $\frac{\lambda}{\delta}$, with $\lambda = \frac{2\pi}{\kappa}$. This is a relative iteration count since we have rescaled the plot by the number of iterations required to reach the set tolerance for sufficiently large δ (note that this number is actually the same for each $* \in \{D, N, R\}$ according to the previous discussion). As a result the vertical coordinate indicates how much the truncation of the strip at δ has affected the iteration count. More precisely, it represents by how much one needs to multiply the asymptotic iteration count for $\delta \to \infty$ in order to get the iteration count for the value of δ that is read on the horizontal axis. Besides, the horizontal coordinate represents the quantity $\frac{\lambda}{\delta}$, where $\lambda = \frac{2\pi}{\kappa}$ is the wavelength of the propagative problem we are trying to solve. This represents he relative size of the width of the strip with respect to the typical length of the problem under consideration. In a discrete setting, if one chooses to take a strip of one layer of cells around the interface (this is the smallest

domain that one can take in practice), this ratio represents in some sense the number of points per wavelength of the mesh.

It is striking to see that, for this particular case ($\kappa = 11\pi$), the iteration count is not affected until the width of the strip gets to about a fourth of a wavelength. Although making a parallel might be questionable, this is not without reminding similar observations in the truncation of the kernel of integral operators as were reported in [44, Fig. 11] for instance. We observe again on this graph the fact that as the width get smaller, the iteration count actually temporarily decreases for the transmission operators associated to Neumann and Robin boundary conditions. At some point, the number of iterations does get to an asymptotic behaviour. We observe a quadratic growth of the number of iterations for the operators associated to Dirichlet and Neumann boundary conditions and a linear growth for the operator associated to Robin boundary condition.

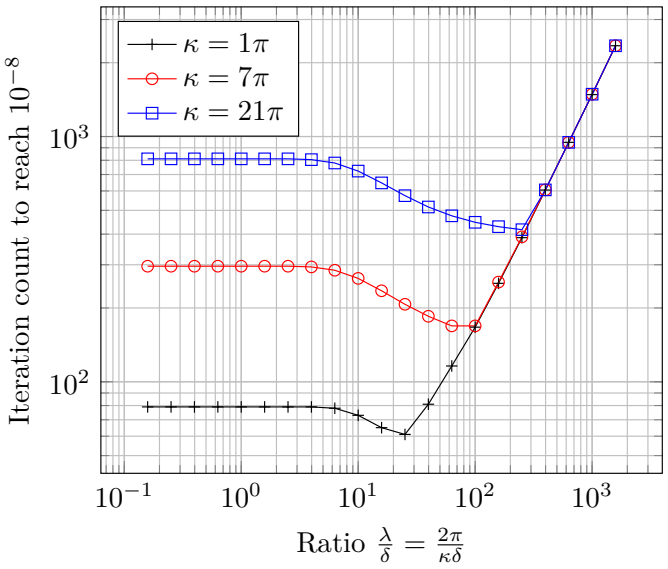

Figure 8.7: Iteration count to reach a set tolerance of 10^{-8} in relative error with respect to the ratio $\frac{\lambda}{\delta}$, with $\lambda = \frac{2\pi}{\kappa}$ for various values of κ in the case of a Robin boundary condition.

We further investigate the observed behaviour with respect to the frequency of the problem under consideration. We report in Figure 8.7 the iteration count to reach a set tolerance of 10^{-8} in relative error with respect to the ratio $\frac{2\pi}{\kappa\delta}$ for various values of the frequency κ in the case of Robin boundary conditions only. Since this is no longer a relative iteration count, we observe, as one can expect, that increasing the frequency increases the iteration count for a fixed δ. Moreover, we see that the tipping point after which the truncation starts to affect the convergence is fairly constant with respect to the frequency. This supports the claim that the truncation at δ should be taken as a (relatively small) fraction of the wavelength of the problem under consideration.

The slight advantage of using a Neumann rather than a Dirichlet boundary condition is not negligible but may be due to the particular setting. The previous analytic analysis as well as this numerical evidence strengthen our conviction that the transmission operator associated to the Robin boundary condition is a better choice than the ones using either Dirichlet or Neumann boundary conditions. We believe that the reasons for the observed better behaviour in this particular setting are profound and can be extrapolated to some extend in more general

configurations.

8.3 Numerical results

We provide in this section numerical results illustrated the interest in using the transmission operators we introduced in this chapter.

8.3.1 Influence of the strip width

We first illustrate on an actual mesh partition how the different types of auxiliary problems one can define (width of the strips, type of boundary condition on the fictitious boundary) actually influence the convergence of the iterative solvers. Recall that we asked ourselves two main questions: How the shrinking of the width of the strips $\mathcal{B}_i$ and $\mathcal{B}_e$ in which the auxiliary problems are posed influence the convergence of the domain decomposition algorithm? What is the best boundary condition to apply on the fictitious boundaries Σ_i and Σ_e that bounds the strips? Without any surprise, our numerical results corroborate the findings of Section 8.2.

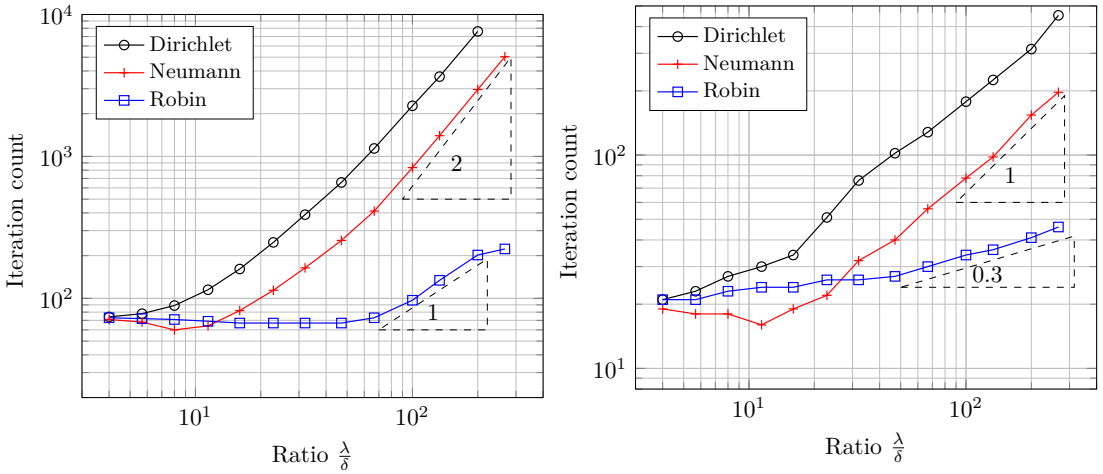

(a) Relaxed Jacobi algorithm

(b) GMRES algorithm

Figure 8.8: Iteration count to reach a set tolerance of 10^{-8} in relative error with respect to the ratio $\frac{\lambda}{\delta}$, with $\lambda = \frac{2\pi}{\kappa_0}$ for the different types of boundary conditions.

This is illustrated in Figure 8.8, where we report the relative iteration count to reach a set tolerance of 10^{-8} in relative error (H^1 norm) with respect to the ratio $\frac{\lambda}{\delta}$, with $\lambda = \frac{2\pi}{\kappa_0}$. The domain is an annulus (or flat torus) comprised between the radius $R_i = 0.5$ and $R_e = 3.5$. This is a configuration without junction points, the interface being placed at $R_\Sigma = 2$ (after the mesh was constructed). The mesh is kept the same in all the computations that appear on the plot, with a fixed number of points per wavelength $N_\lambda = 400$ for a wavenumber $\kappa_0 = 1$. The only parameters that change are the width of the strip that defines the auxiliary problem and the type of boundary condition on the fictitious boundary that is introduced. The construct the strips, the mesh elements are nibbled one by one from the transmission boundary, following an heuristic in order to correspond to the set width. This results in a very rough fictitious interface. For the larger width considered, the auxiliary problem is solved in a domain that is almost as

large as the full domain of propagation, the fictitious boundary is close to the physical boundary. We stress that the mesh is very refined for the frequency considered. As a result, it may not be feasible to get to strips that small in more realistic situations.

The results exhibit a growth in iteration count as the width of the strip get smaller. The qualitative behaviour is similar to the previous analytical study in the planar geometry (infinite wave-guide).

For the Jacobi algorithm we observe a quasi-quadratic growth for sufficiently smaller δ for the Dirichlet and Neumann boundary conditions. In contrast, for the Robin condition, the growth is only linear. Besides, in this latter case the asymptotic behaviour is reached for a much smaller width δ. In fact the iteration count does not seem to be affected by the truncation until the width is smaller than $\frac{1}{50}$ of the wavelength while the tipping point is about a tenth for the Neumann condition and around an eighth for the Dirichlet condition. For large enough strips, the choice of boundary condition does not matter, which we mainly explain by the dissipative nature of the auxiliary problem.

For the GMRES we observe a quasi-linear growth for sufficiently smaller δ for the Dirichlet and Neumann boundary conditions. In contrast, for the Robin condition, the number of iterations only mildly increases and the growth rate is clearly sub-linear.

The worst choice of condition on the fictitious boundary of the auxiliary problem is undeniably to use Dirichlet condition. Despite the temporary gain in the case of the Neumann condition, we observe again a clear advantage in using a Robin condition since it exhibits a much smaller asymptotic growth rate.

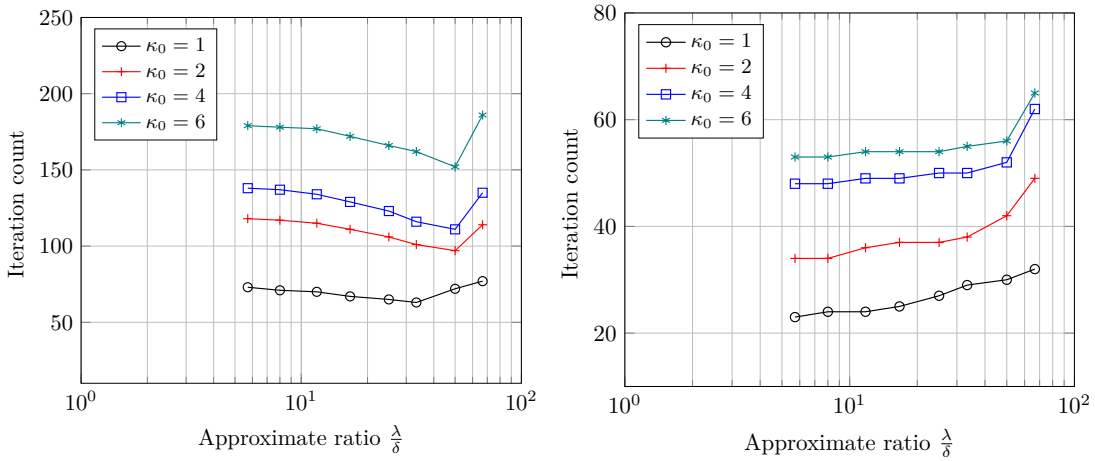

(a) Relaxed Jacobi algorithm

(b) GMRES algorithm

Figure 8.9: Iteration count to reach a set tolerance of 10^{-8} in relative error with respect to the ratio $\frac{\lambda}{\delta}$, with $\lambda = \frac{2\pi}{\kappa_0}$ for the Robin boundary condition.

Influence of the wavenumber We further investigate the observed behaviour with respect to the frequency of the problem under consideration. We report in Figure 8.9 the iteration count to reach a set tolerance of 10^{-8} in relative error with respect to the ratio $\frac{2\pi}{\kappa_0 \delta}$ for various values of the frequency κ_0 in the case of Robin boundary conditions only. The geometry of the problem is kept the same but the number of points per wavelength is fixed to $N_\lambda = 100$ for each wavenumber κ_0 considered. For a fixed wavenumber, the mesh is kept the same as the ratio $\frac{\lambda}{\delta}$ varies. Notice

that because we investigated higher frequencies the mesh is less refined compared to the previous test case.

We observe that as the wavenumber increases, the increase in the number of iterations is approximately uniform with respect to the ratio $\frac{\lambda}{\delta}$. This supports the idea that the width of the auxiliary problem strip can be chosen as a fraction of the wavelength. We observe numerically in the case considered that one can choose this width as small as $\frac{1}{50}$ of the wavelength with only a few more iterations required to reach the tolerance.

8.3.2 Convergence history

As we did for the integral operators, we report the full convergence history of the relative broken H^1 and $\mathbf{H}(\mathbf{curl})$ error for the Jacobi and GMRES algorithms as an illustrative example of typical convergence. For the two dimensional acoustic setting, we consider our first test case which we recall consists in a disk of radius $R = 1$ that is partitioned into 2 domains separated by a circular interface at $R = 0.5$. The results are reported in Figure 8.10. For the three dimensional cases, the domain is a ball of radius $R = 1$ split into two domains separated by a spherical interface at $R = 0.5$. The results for the acoustic and electromagnetic settings are respectively reported in Figure 8.11 and Figure 8.12. In both cases, the wavenumber if taken to be $\kappa_0 = 1$.

These figures are the enriched versions (with the results using the operators based on elliptic auxiliary problems) of respectively Figure 7.1, Figure 7.3 and Figure 7.7. We therefore refer the reader to the comments made in Chapter 7 before resuming the discussion.

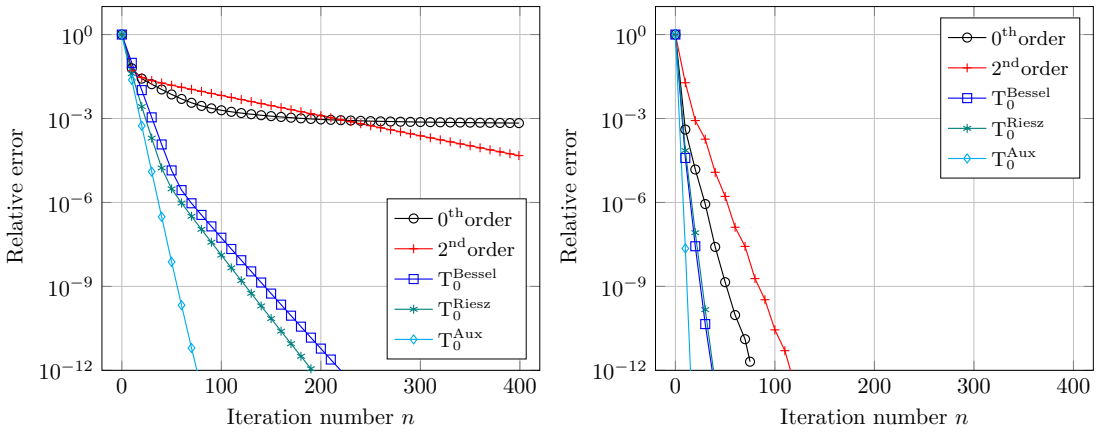

(a) Relaxed Jacobi algorithm

(b) GMRES algorithm

Figure 8.10: Helmholtz 2D. An example of convergence history. Fixed parameters $\kappa_0 = 1$, $N_\lambda = 40$, disk of radius $R = 1$.

We clearly see that the newly defined operator based on elliptic auxiliary problems outperforms all the other transmission operators we are considering (the only exception is the similar performance with the second order local operator in 3D for Helmholtz). This includes 2D Helmholtz where the results using the integral operators were already quite satisfying; but it is especially true for the case of Maxwell equations in 3D: the number of GMRES iterations required to achieve (almost) machine precision is an order of magnitude lower than for the other operators.

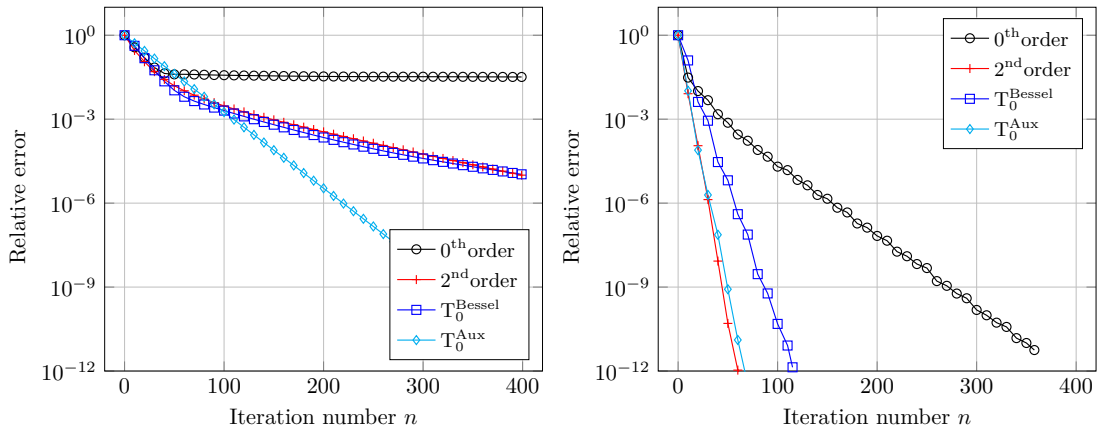

(a) Relaxed Jacobi algorithm (b) GMRES algorithm

Figure 8.11: Helmholtz 3D. An example of convergence history. Fixed parameters $\kappa_0 = 1$, $N_\lambda = 40$, ball of radius $R = 1$.

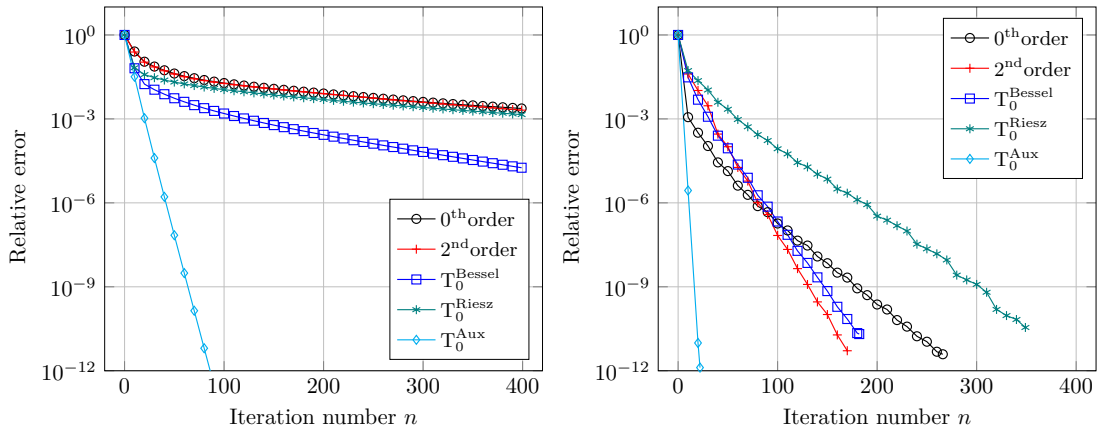

(a) Relaxed Jacobi algorithm (b) GMRES algorithm

Figure 8.12: Maxwell 3D. An example of convergence history. Fixed parameters $\kappa_0 = 1$, $N_\lambda = 40$, 3D, ball of radius $R = 1$.

8.3.3 h-uniform geometric convergence

As we did for the integral operators, we now study the number of iterations required to reach convergence with respect to mesh refinement, for both the relaxed Jacobi and GMRES algorithms. The refinement of the mesh is indicated by the number of points per wavelength N_λ which is inversely proportional to the typical mesh size. In the results given below, the iteration counts that are reported correspond to the number of the iteration for which the relative error in the broken relative energy norms (H^1 for Helmholtz, $\mathbf{H}(\mathbf{curl})$ for Maxwell) is below 10^{-8}.

For the two dimensional acoustic setting, the results are reported in Figure 8.13. The results for the acoustic and electromagnetic settings in 3D are respectively reported in Figure 8.14 and Figure 8.15.

These figures are the enriched versions (with the results using the operators based on elliptic auxiliary problems) of respectively Figure 7.4, Figure 7.5 and Figure 7.8. We therefore refer the reader to the comments made in Chapter 7 before resuming the discussion.

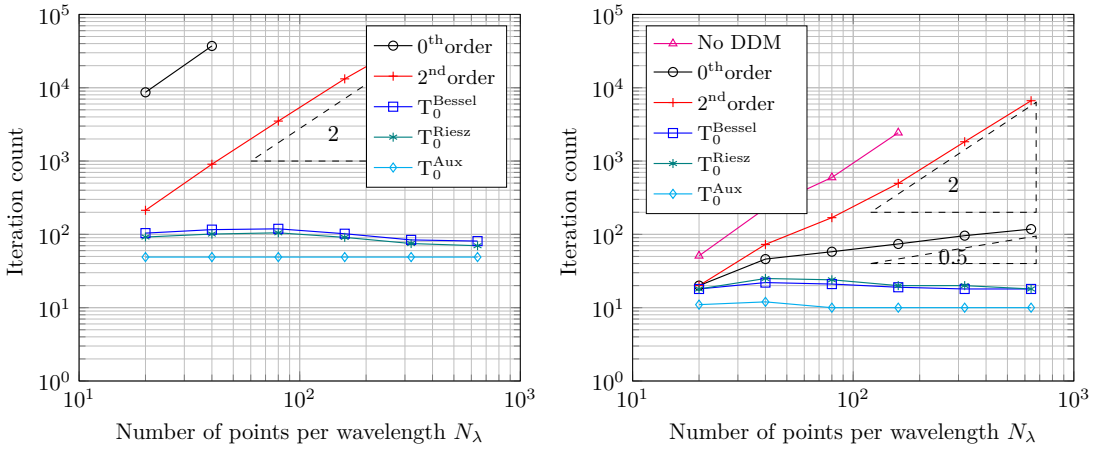

(a) Relaxed Jacobi algorithm

(b) GMRES algorithm

Figure 8.13: Helmholtz 2D. Number of iterations with respect to the number of mesh points per wavelength N_λ. Fixed parameters $\kappa_0 = 1$, disk of radius $R = 1$.

According to these results, the operators based on elliptic auxiliary problems outperform (in the electromagnetic setting, rather spectacularly) the integral operators, in all three configurations considered. We shall point out that we noticed during our numerical experiments that this difference is especially true because the problems are rather low frequency (which is required here to truly investigate the dependency with respect to the mesh parameter). Importantly, we observe that the iteration count for the operator based on elliptic auxiliary problems is fairly independent to the discretization parameter, as expected.

Besides, we notice that the iteration counts for the integral operators actually decreases (in most cases) as the mesh is refined. This can be explained to some extend by realizing that the continuous operators behind the two operators present in the plots are somehow similar while the two discretization methods are radically different. Indeed, roughly speaking, similar (continuous) elliptic problems are hidden behind both operators, the main difference being the boundedness of the domain of the problem. However, for the integral operators, the discretization method uses a standard boundary element method while for the other ones, a standard finite element method is used. As the mesh is refined the operators get closer in some sense and we observe

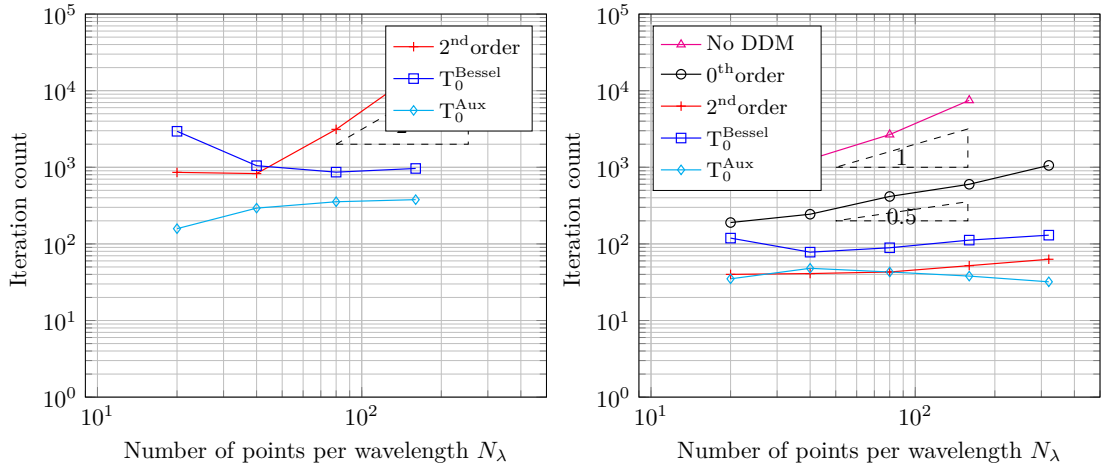

(a) Relaxed Jacobi algorithm (b) GMRES algorithm

Figure 8.14: Helmholtz 3D. Number of iterations with respect to the number of mesh points per wavelength N_λ. Fixed parameters $\kappa_0 = 1$, ball of radius $R = 1$.

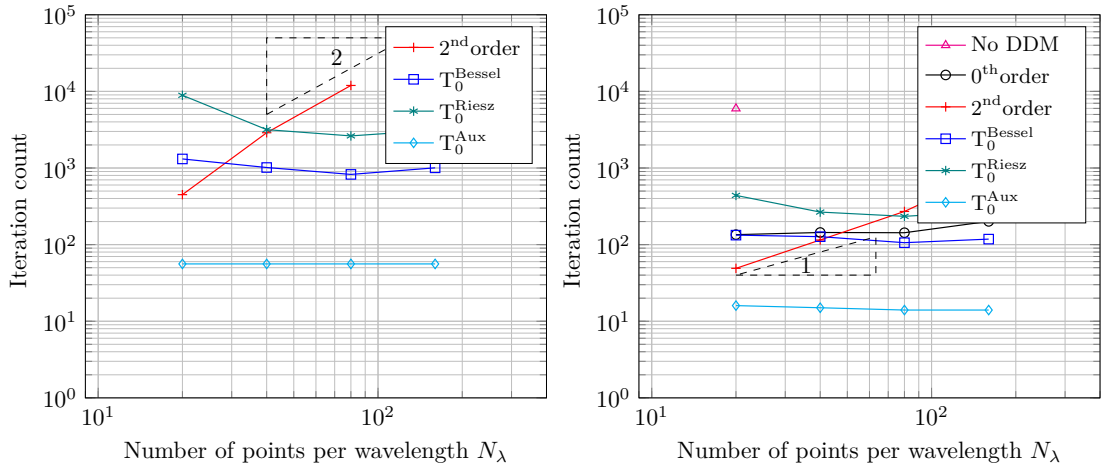

(a) Relaxed Jacobi algorithm (b) GMRES algorithm

Figure 8.15: Maxwell 3D. Number of iterations with respect to the number of mesh points per wavelength N_λ. Fixed parameters $\kappa_0 = 1$, ball of radius $R = 1$.

similar behaviours. In addition, we believe that the observed better behaviour for the operators using explicit auxiliary problems is due to the fact that it is actually discretized by the same method as for the propagative problems.

8.3.4 Frequency

We now report the dependency of the iteration count with respect to the wavenumber κ_0. See Figure 8.16 for the two-dimensional results for the Helmholtz equation, where results are reported for both the relaxed Jacobi and the GMRES algorithms The three-dimensional results are reported in Figure 8.17 for both the acoustic and electromagnetic settings, only for the GMRES algorithm.

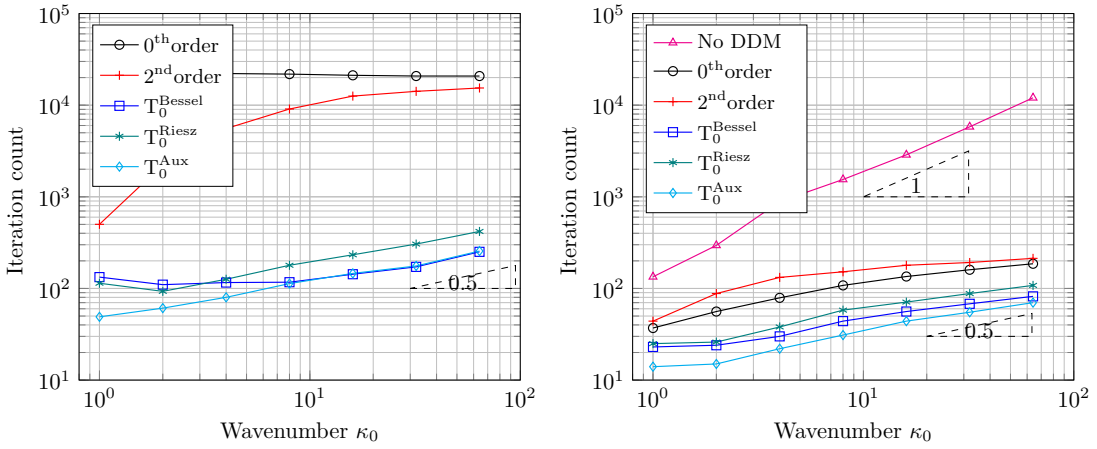

(a) Relaxed Jacobi algorithm

(b) GMRES algorithm

Figure 8.16: Helmholtz 2D. Number of iterations with respect to the wavenumber κ_0. Fixed parameters $J = 2$, $N_\lambda = 30$, disk of radius $R = 1$.

As the wavenumber κ_0 increases, the discrete (as well as the continuous) problem gets harder. This is indicated again by the increase in the iteration count of the GMRES algorithm for the undecomposed problem (line plot labelled 'No DDM'). For this case, the growth is linear (at least for the acoustic setting) with respect to κ_0. In contrast, for all the impedance operators under study, we notice a sub-linear growth of the number of iteration with respect to κ_0. We see numerically that the domain decomposition method mitigates to some extent the effect of an increase in the frequency of the propagation problem.

8.3.5 Scalability of the method: strong scaling

We finally study the dependency of the method with respect to the number of subdomains J of the mesh partition.

The results of a strong scaling test in 2D are provided in Figure 8.18 which reports the iteration count with respect to J varying from 2 to 64 subdomains. The interfaces are concentric circles, with linearly increasing radii. As a result, the computational charge is *not* equilibrated among sub-domains.

We observe numerically a significant increase in the number of iterations required to achieve the set tolerance. This is true for all transmission operators considered. This suggests that,

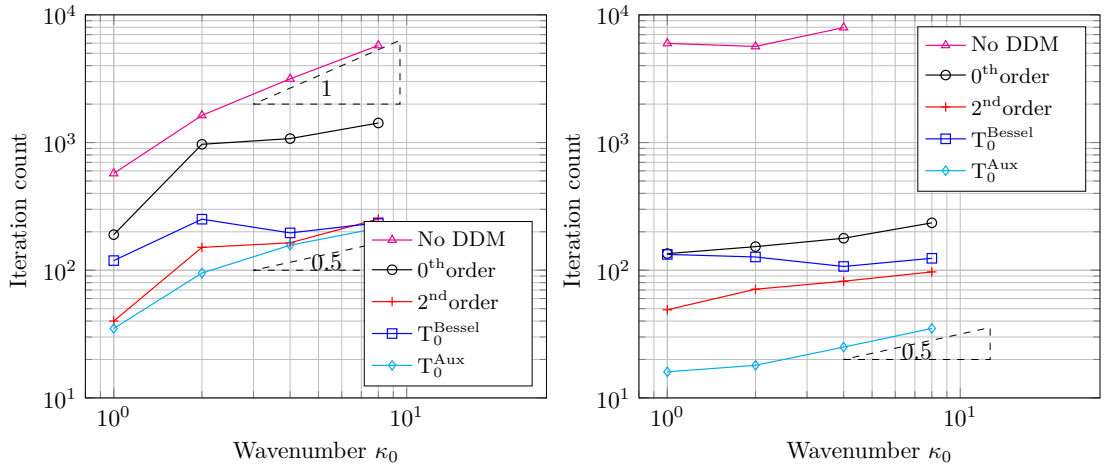

(a) Helmholtz 3D. (b) Maxwell 3D.

Figure 8.17: Number of iterations with respect to the wavenumber κ_0. Fixed parameters $J = 2$, $N_\lambda = 20$, sphere of radius $R = 1$. GMRES algorithm.

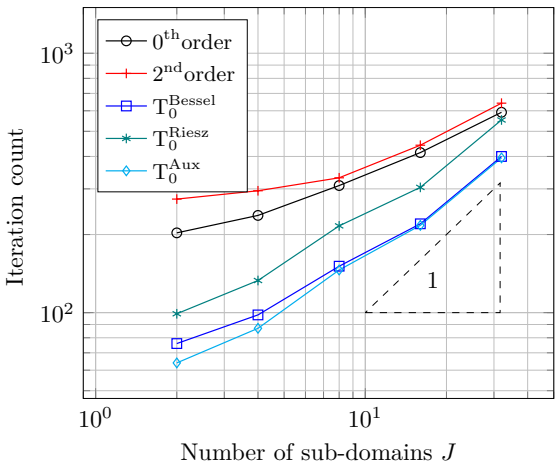

Figure 8.18: Helmholtz 2D. Number of iterations with respect to the number of subdomains J. Fixed parameters $\kappa_0 = 10$, $N_\lambda = 40$, GMRES algorithm, disk of radius $a = 1$.

when the partitioning is performed in consecutive layers, the number of sub-domains should be kept moderate.

Part III

Junctions

Chapter 9

Continuous setting

Contents

In this new part and chapter, we extend the formalism and analysis to allow for the presence of junction points, i.e. points where three (or more) sub-domains abut.

The breakthrough ideas and theoretical foundation that made possible the treatment of junction points originate mainly from the work of Xavier Claeys, notably in [29] (and re-exploited in [33]), but are adapted here to our abstract formalism. We closely follow, in particular in this chapter, the approach (and notations) that were used in Part I of this manuscript so that to precisely highlight these new key ideas. As the reader will soon realize, the definitions of the Cauchy trace space and the scattering operators that we are going to introduce in this chapter are formally very similar to the ones provided in Chapter 3. The main meaningful difference lies in the definition of the single trace space (and, as a result, will require to replace the exchange operator by a new operator realizing the communication between sub-domains). In fact, the striking difference between Chapter 3 and this chapter is that, to define our multi-trace space, we shift from considering a collection of traces at *interfaces* between two sub-domains to a collection of traces at *boundaries* of sub-domains in order to define our multi-trace space. In the

previously described method from Chapter 3 the characterization of the so-called single traces, i.e. continuous traces, was particularly natural and easy. Moreover such a characterization could be done locally at each interface in the form of interface matching conditions. The key point is to realize that in the presence of junctions, this local characterization as matching conditions at every interface is somewhat obsolete and shall be abandoned. However, the space of collections of boundary traces of elements of $\mathrm{U}_\Gamma(\mathrm{D};\Omega)$ does still make sense: this will be our new definition of the single-trace space.

Our aim is to retain the characteristic feature of the class of domain decomposition we consider namely the interface problem formulation (see Proposition 3.24) involving a scattering operator (solving the equation in each sub-domain) and an exchange operator (that performs communications between sub-domains). An immediate and important consequence of the paradigm shift we just described is that the so-called *exchange operator* that realizes communications between sub-domains (recall that it was intimately linked to the single trace space) can no longer be defined as a local operator that simply exchanges data through an interface shared by two sub-domains. Since we will require however that a candidate substitute for this operator still performs communications between sub-domains (this is the operator that performs the coupling of the sub-domains), we refer to it as a *communication operator* to emphasize that it no longer performs a standard exchange of data at the interface.

The breakthrough idea comes from the realization that the exchange operator $\mathbf{\Pi}_\parallel$ actually defines an (orthogonal, for the scalar product stemming from the transmission operator) projector $\mathrm{Id}+\mathbf{\Pi}_\parallel$ (respectively $\mathrm{Id}-\mathbf{\Pi}_\parallel$) onto the single trace space $\mathbb{S}_{0,\parallel}$ (respectively $\mathbb{S}_{1,\parallel}$). In a partition without junctions, defining either this particular communication operator or the orthogonal projectors is very natural and straightforward. However, in a partition that contains junctions, the proper definition (within the multi-trace formalism) of a communication operator seems necessarily intricate. On the other hand, defining orthogonal projectors (for a given scalar product) onto the single trace spaces remains natural (and moreover easy to do after discretization). This is why the new definition of a communication operator explicitly involves an orthogonal projector whose actual computation takes the form of an auxiliary global problem posed on the skeleton of the partition (see Remark 9.24 for more detail). As a result, in the approach which is developed below, the exchange of information or transmission condition at interfaces is somewhat elusive as it is only implicitly defined through the auxiliary global problem. However, as we shall see, this change of point of view is fertile as it allows to deal with more general partitions, including partitions with interior cross points. Moreover, we shall show that the method described in Chapter 3 is actually a particular case of the new approach presented in this chapter, in the absence of interior cross points. In particular the communication operator is exactly the previous standard exchange operator, independently of the choice of the projectors (hence of the underlying scalar product).

Solving the global auxiliary problem posed on the full skeleton could appear frightening at first sight, in particular in view of a parallel implementation of the method. Indeed, the exchange operator is, *a priori*, fully non-local and its action is expensive to compute if no particular attention is given. However, the nature of the problem, namely its positivity and definiteness makes the situation far more favorable than it may seems. In particular, one could resort to iterative methods to solve this problem, for instance a preconditioned conjugate gradient method. As we shall explain, the matrix-vector product required to implement an iterative algorithm only requires communications with neighbouring sub-domains, exactly as in standard methods. The only difference is that this time, we will need to have several communications, as many as we need to have iterations in this inner iterative algorithm, for an actual exchange (as far as the outer global DD method is concerned) to take place. Fortunately, the nature of the problem makes the additional system well conditioned.

Our change of paradigm has also important consequences on the transmission operators we can consider in order to preserve the theory. As a matter of fact, one shall chose the transmission operator as the scalar product that defines the orthogonal projector that is used in the definition of the communication operator. This is sufficient to ensure the consistency between the decomposed problem and the original problem. The question of the necessity of this choice (in particular in a discrete setting) is not fully settled. Besides, since we no longer look at interfaces between two sub-domains, we no longer require any type of two-sided symmetry with respect to interfaces in the transmission operators. As a result, it is natural to define a block diagonal transmission operator whose blocks (one for each sub-domain) are built independently in each sub-domain. This is another valuable feature of the new approach.

Let us now replace our work in the literature associated to the Multi-Trace Formalism (MTF) which we recall was initially introduced in the context of boundary integral equations. We point out that there already exists some literature making connections between the MTF and domain decomposition methods [7, 35, 31, 55]. Note that the former framework of Part I stems from the *local* MTF [83, 84], as was clearly demonstrated in [39, Sec. 7]. In contrast, the framework we are about to describe comes from the *global* version of the MTF [32, 38].

9.1 A motivating numerical experiment

To further motivate the forthcoming analysis, we report here some numerical experiments conducted by Francis Collino on a model problem designed specifically to study cross points.

The test case consists of a 2D disk of radius $R = 1$ which is regularly split into J pie wedges pointing at the center of the disk. Therefore, by construction, there are J boundary cross points and one single interior cross point (the center of the disk) which is shared by all sub-domains. To avoid the specific difficulty posed by nodal discretizations, the discretization strategy that is chosen here rests on a formulation in $\mathbf{H}(\mathrm{div})$. This choice means that in the finite element formulation no degree of freedom is associated to the interior cross-point, which simplifies in many ways the definition of the transmission conditions.

Formulation of the model problem We consider our usual model problem for the Helmholtz equation on the unit disk in 2D. Let $g \in L^2(\Gamma)$ and suppose we are set to solve the model problem, naturally posed in $H^1(\Omega)$,

$$\begin{cases} -\Delta p - {\kappa_0}^2 p = 0, & \text{in } \Omega, \\ (\partial_\nu - \mathrm{i}\kappa_0)\, p = g, & \text{on } \Gamma. \end{cases} \tag{9.1}$$

Instead of looking directly for p we will consider a formulation in $\mathbf{H}(\mathrm{div};\Omega)$, for its gradient $\mathbf{u} := \mathbf{grad}\, p$. The problem in $\mathbf{u}$ is written as

$$\begin{cases} -\mathbf{grad}\,\mathrm{div}\,\mathbf{u} - {\kappa_0}^2 \mathbf{u} = 0, & \text{in } \Omega, \\ \mathrm{div}\,\mathbf{u} - \mathrm{i}\kappa_0 \mathbf{u}\cdot\nu = -\mathrm{i}\kappa_0 g, & \text{on } \Gamma. \end{cases} \tag{9.2}$$

Such a problem is naturally posed in

$$\mathbf{H}_\Gamma(\mathrm{div};\Omega) := \left\{ \mathbf{u} \in L^2(\Omega)^2 \mid \mathrm{div}\,\mathbf{u} \in L^2(\Omega),\ \mathbf{u}\cdot\nu \in L^2(\Gamma) \right\}. \tag{9.3}$$

The variational form of the problem is written as

$$\begin{cases} \text{Find } \mathbf{u} \in \mathbf{H}_\Gamma(\mathrm{div};\Omega) \text{ such that} \\ a(\mathbf{u},\ \mathbf{u}^t) = -\mathrm{i}\kappa_0\, (g,\ \mathbf{u}^t\cdot\nu)_{L^2(\Gamma)}, \qquad \forall \mathbf{u}^t \in \mathbf{H}_\Gamma(\mathrm{div};\Omega), \end{cases} \tag{9.4}$$

where for all $\mathbf{u}, \mathbf{u}^t \in \mathbf{H}_\Gamma(\mathrm{div};\Omega)$, we define

$$a\big(\mathbf{u},\ \mathbf{u}^t\big) := \big(\mathrm{div}\,\mathbf{u},\ \mathrm{div}\,\mathbf{u}^t\big)_{L^2(\Omega)} - {\kappa_0}^2\big(\mathbf{u},\ \mathbf{u}^t\big)_{L^2(\Omega)^2} - \mathrm{i}\kappa_0\big(\mathbf{u}\cdot\nu,\ \mathbf{u}^t\cdot\nu\big)_{L^2(\Gamma)}. \tag{9.5}$$

The unknown $\mathbf{u}$ and the test function will be both discretized using standard (low-order) Raviart-Thomas finite elements. Note that this formulation has many drawbacks, starting from an increased computational cost, but in this way, the natural trace $\mathbf{u}\cdot\nu$ is piecewise constant on the boundary, with one degree of freedom associated to each edge and there will be no issue in the definition of the exchange operator due to the presence of the cross point.

The domain decomposition methods compared We briefly describe here the three domain decomposition methods that we compare.

- The first method is a straightforward extension of the method described previously, where the transmission operator is simply a scalar coefficient which corresponds to Després-like transmission conditions;

- The second method is also a straightforward extension of the method described previously, but uses non-local transmission operators defined on each interface. These transmission operators are constructed by solving elliptic auxiliary problems in the sub-domains adjacent to the interface on which they are defined, in the spirit of the operators introduced in Chapter 8. However, due to the formulation that is adopted, the operators are constructed from Neumann-to-Dirichlet maps and are therefore regularizing.

- The third method compared corresponds to the newly proposed method and will be described in what follows. It uses non-local transmission operators satisfying the requirements of the forthcoming (geometric) convergence analysis. These operators are also regularizing and are computed by solving elliptic auxiliary problems within each sub-domain.

We believe that the first two approaches are the simplest and most natural extensions of the previously defined domain decomposition method that one can consider. In particular, the purpose of the second method is to investigate whether or not it is possible to obtain geometric convergence with non-local transmission operators in presence of junction points.

Convergence history of iterative algorithms We report in Figure 9.1 the convergence histories of the three domain decomposition methods for the relaxed Jacobi algorithm and in Figure 9.2 the corresponding results for the GMRES algorithm. The results are provided for three different mesh refinements.

We see, as expected, the deterioration of the convergence of the iterative algorithms when the Després transmission conditions are used. This was also observed in the absence of cross-points, so this is not a surprise.

The results using the non-local transmission operators also bear a deterioration, albeit less severe, with finer meshes. This result, which contrast with the previous results, was feared but is a strong motivation for the forthcoming analysis. Note that the effect is attenuated for the GMRES algorithm, especially for the 3 sub-domains configuration.

On the contrary, the new approach exhibits a perfectly uniform convergence with respect to the mesh size and converges faster than the other two strategies.

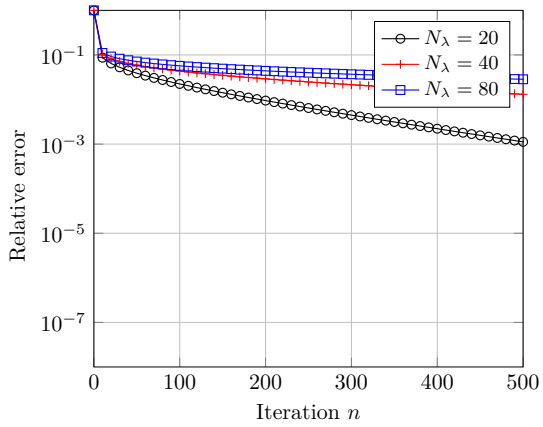

(a) Després transmission operator. $J = 3$.

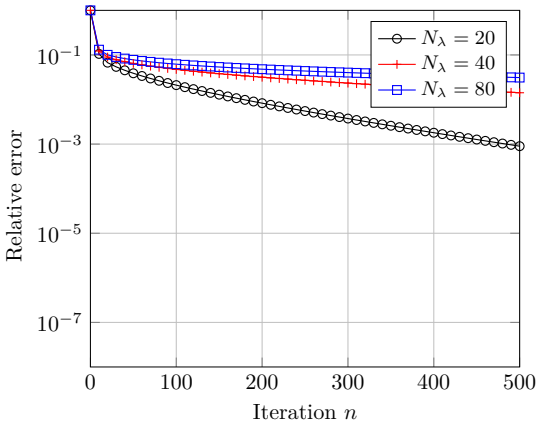

(b) Després transmission operator. $J = 6$.

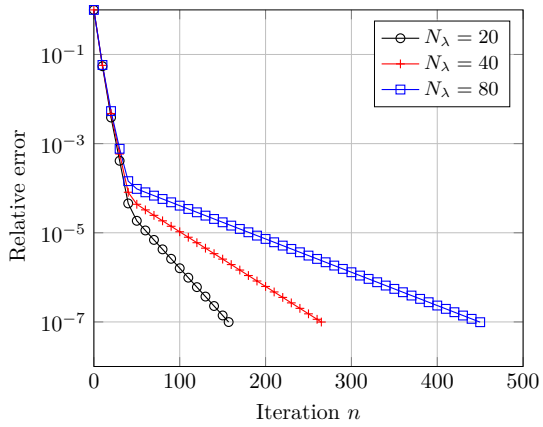

(c) Non-local transmission operator. $J = 3$.

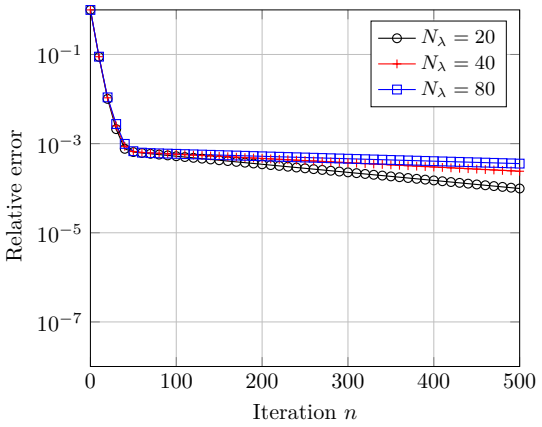

(d) Non-local transmission operator. $J = 6$.

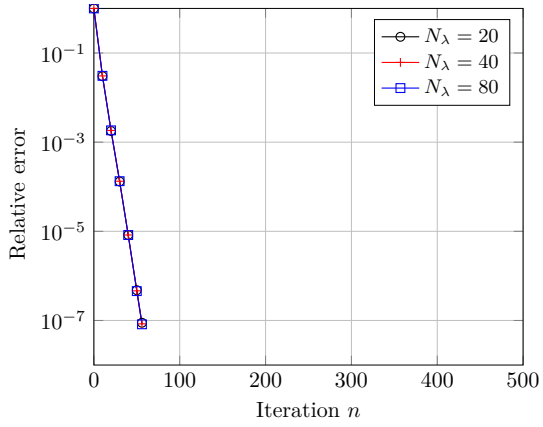

(e) New approach. $J = 3$.

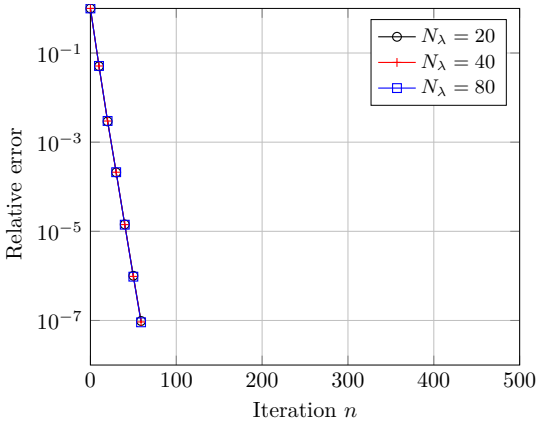

(f) New approach. $J = 6$.

Figure 9.1: Convergence history for the Jacobi algorithm. With 3 (left) and 6 (right) subdomains.

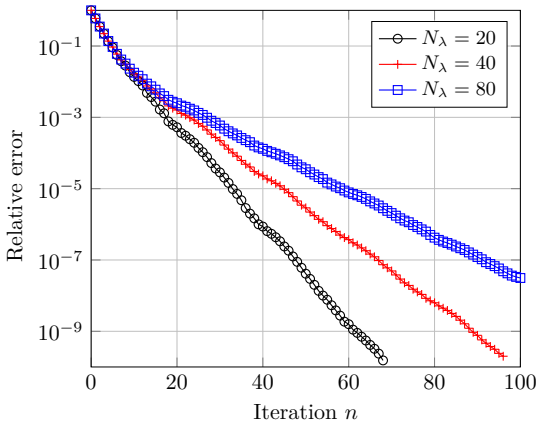

(a) Després transmission operator. $J = 3$.

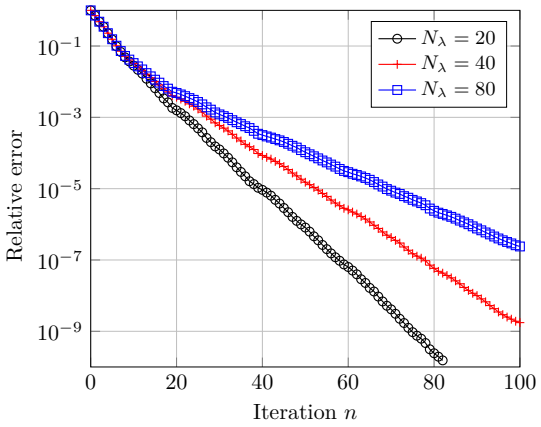

(b) Després transmission operator. $J = 6$.

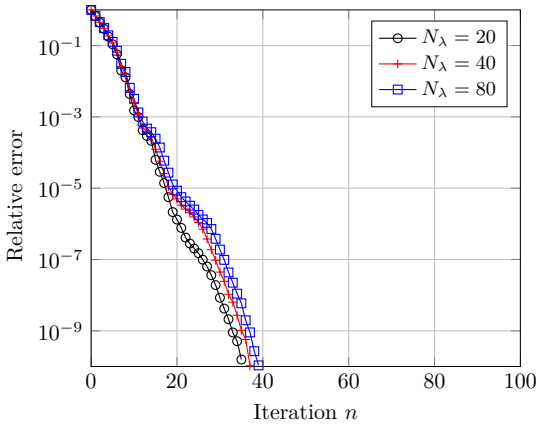

(c) Non-local transmission operator. $J = 3$.

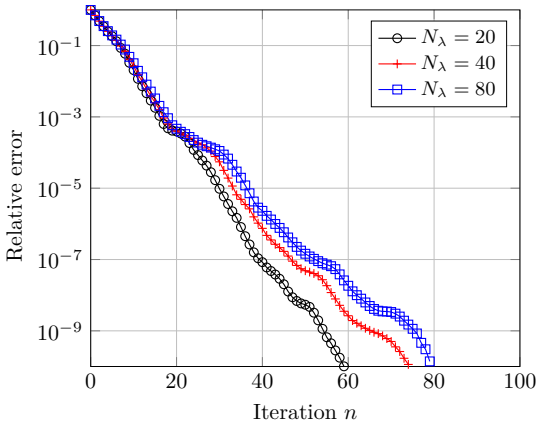

(d) Non-local transmission operator. $J = 6$.

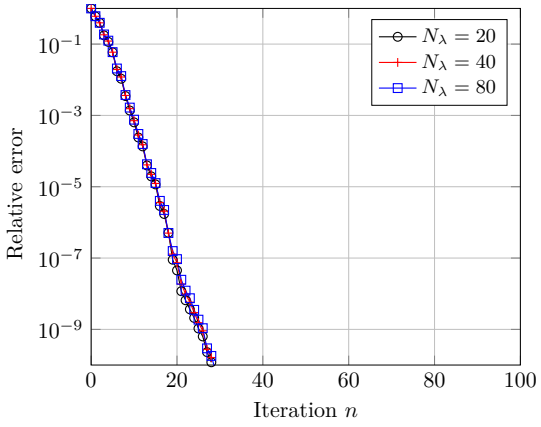

(e) New approach. $J = 3$.

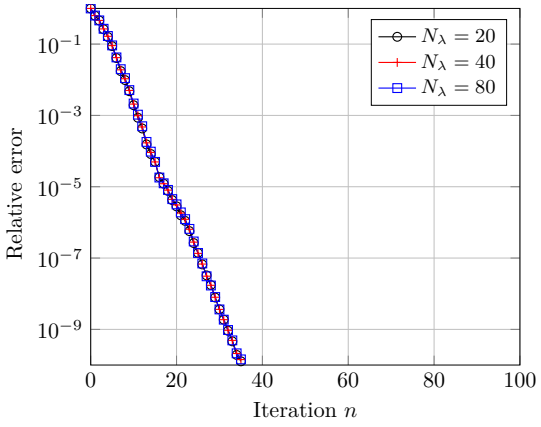

(f) New approach. $J = 6$.

Figure 9.2: Convergence history for the GMRES algorithm. With 3 (left) and 6 (right) subdomains.

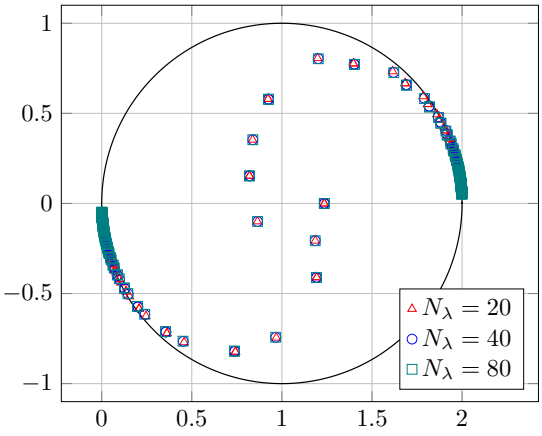

(a) Després transmission operator. $J = 3$.

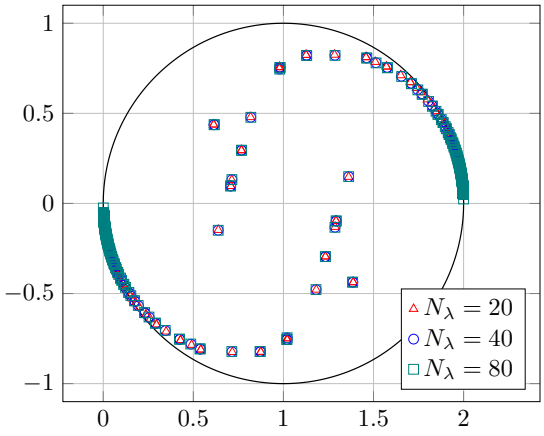

(b) Després transmission operator. $J = 6$.

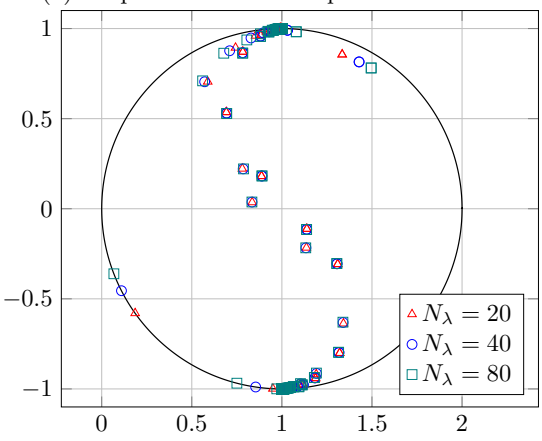

(c) Non-local transmission operator. $J = 3$.

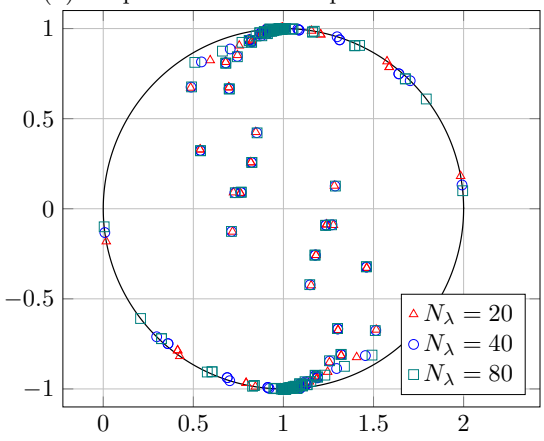

(d) Non-local transmission operator. $J = 6$.

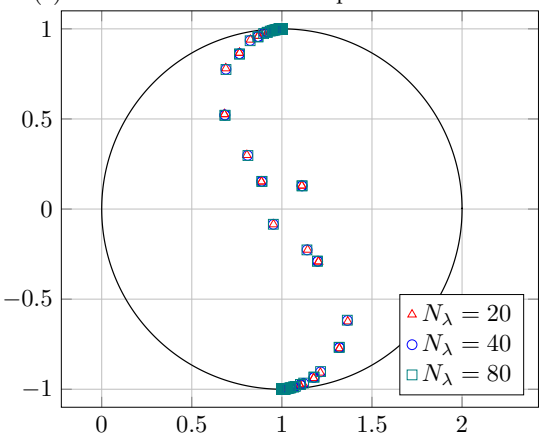

(e) New approach. $J = 3$.

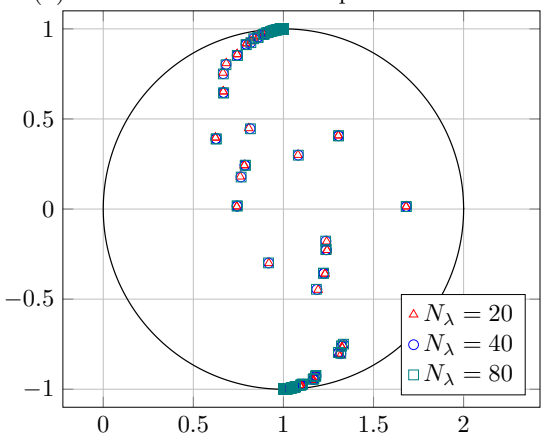

(f) New approach. $J = 6$.

Figure 9.3: Eigenvalues of the iteration matrices. With 3 (left) and 6 (right) sub-domains.

Eigenvalues of the iteration matrix To try to explain those results, we represent in Figure 9.3 the eigenvalues of the iteration operators that are involved in the three domain decomposition methods. Note that for the two methods adopting the previously defined strategy, the iteration operator corresponds to $\mathrm{Id} - \mathbf{\Pi}_{\|}\mathbf{S}_{1,\|}$. The iteration operator takes also the same form in the new approach, as we shall see.

When the Després conditions are used, we see an accumulation near the origin which will damage the convergence of both the GMRES and the relaxed Jacobi algorithms, as expected.

When the non-local transmission operator is used in conjonction of the previous approach, we see that the clusters are next to the two points $(1, 1)$ and $(1, -1)$, which demonstrates that the evanescent modes are well taken into account. However, we see that a few isolated eigenvalues, close to the shifted unit circle, exist, and seem to get closer to the origin as the mesh is refined. This is particularly visible on the configuration with 6 sub-domains.

In contrast, with the new approach, the eigenvalues seem to be uniformly bounded away from the critical points.

Nature of the error We represent in Figure 9.4 the distribution of the error between the exact discrete solution and the discrete solution (obtained with the relaxed Jacobi algorithm). More precisely, the absolute value of the error is represented as the elevation along the z axis, after linear interpolation on the nodes of the mesh. For a better representation, the magnification factor is different for each figure, as indicated by the actual maximum and minimal values of the error on the colorbar. The convergence is stopped before machine precision is reached. In some sense, the nature of the remaining error gives us insight on the components that are troublesome for the convergence.

When Després transmission conditions are used, we see that the error is highly concentrated along each interface and decreases very rapidly away from them. The most likely interpretation is that the main components in the error consist in some sense of "evanescent waves". Note also that the ratio between the maximum and minimum values of the error is very large.

In contrast, the error is highly peaked at the cross point and (slowly) decreasing away from it when the non-local operator is used. The transmission interfaces seem less visible. Note also that the ratio between the maximum and minimum values of the error is much smaller than for the Després transmission conditions.

As for the non-local transmission operator used in conjunction with the new approach, the error is more evenly distributed in the domain, albeit slightly accumulating near the interfaces. More importantly, no accumulation of the error at the cross point can be observed in contrast to the result using also a non-local transmission operator but with the standard exchange operator (Figure 9.4b).

Conclusion on these numerical experiments To sum up, although this is by no means a rigorous proof, these numerical experiments appear to be a numerical counter-example to the claim that the straightforward extension of the iteration operator $\mathrm{Id} - \mathbf{\Pi}_{\|}\mathbf{S}_{1,\|}$ is continuously invertible on the multi-trace space in presence of junction points. Indeed, if it was true, one would expect h-uniform geometric convergence of the iterative algorithms. As a consequence, we do not expect that a result on *geometric* convergence akin to Theorem 3.63 exists for a general configuration. The fact that available proofs (in absence of junction points) failed to yield the result in a general configuration is maybe not fortuitous, after all. Obviously these numerical experiments clearly highlighted that convergence of the algorithms is however indeed possible and do not contradict the convergence results that have been already established, even in presence of junctions, see [49, 78]. This assessment is the starting point and the main motivation for the subsequent approach.

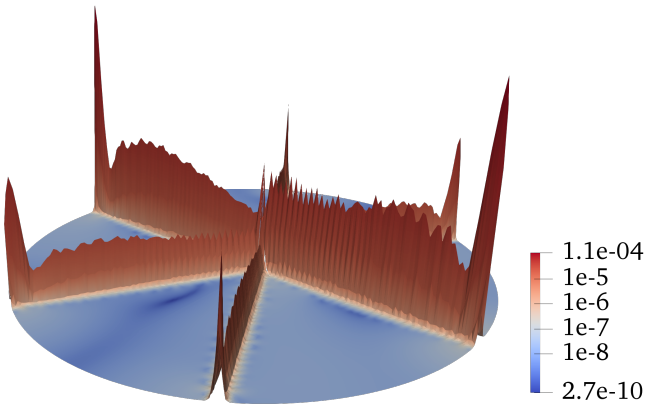

(a) Després transmission operator.

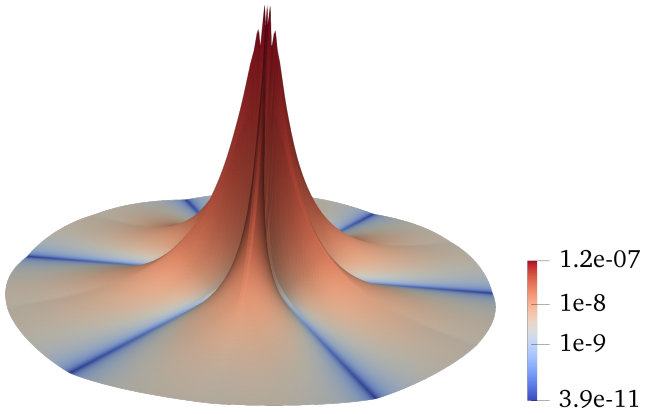

(b) Non-local transmission operator.

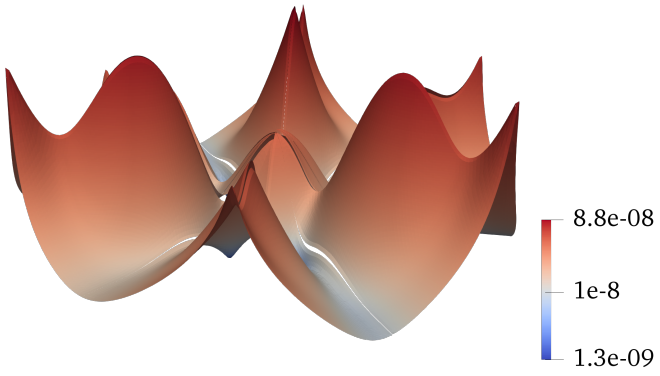

(c) New approach.

Figure 9.4: Nature of the error using different approaches (6 sub-domains configuration). The absolute value of the error on the solution is represented as the elevation (after linear interpolation on the nodes of the mesh). Different magnification factors are used for the three figures.

9.2 Abstract domain decomposition method

We stress that in this Chapter, we do *not* suppose that Assumption 3.11 holds, therefore allowing the presence of *interior* junction points. However, to make the presentation clearer and avoid many technicalities due to the physical boundary conditions, we still require Assumption 3.12 to hold, namely we still exclude the presence of *boundary* cross points (cross points at physical boundary). For instance we allow the example configuration of Figure 3.1b but exclude the one of Figure 3.1a.

The definitions and notations introduced in Section 3.1 are independent of the type of partition and will still be in use in this chapter. Recall that we use the index $\times$ in place of $\parallel$ to differentiate what has a meaning in a configuration that may admit cross-points versus a configuration that excludes cross-points.

9.2.1 Multi-trace formalism

We provide an alternative to the definitions of Section 9.2.1 that allows the treatment of junction points.

9.2.1.1 Multi-trace spaces

We introduce global trace spaces whose elements are a collection of traces on the sub-domain boundaries, with the exception of physical boundaries (hence no longer on interfaces as in Definition 3.16).

Definition 9.1 (**Multi-trace spaces**). *The global multi-trace spaces are defined as*

$$\begin{aligned}
\mathbb{M}_{0,\times}\left(\tilde{\Sigma}\right) &:= \bigtimes_{j=1}^{J} \mathrm{X}_0(\tilde{\Gamma}_j),\\
\mathbb{M}_{1/2,\times}\left(\tilde{\Sigma}\right) &:= \bigtimes_{j=1}^{J} \mathrm{X}_{1/2}(\tilde{\Gamma}_j),\\
\mathbb{M}_{1,\times}\left(\tilde{\Sigma}\right) &:= \bigtimes_{j=1}^{J} \mathrm{X}_1(\tilde{\Gamma}_j),\\
\mathbb{M}_{\times}\left(\tilde{\Sigma}\right) &:= \bigtimes_{j=1}^{J} \mathrm{X}(\tilde{\Gamma}_j) \equiv \mathbb{M}_{0,\times}\left(\tilde{\Sigma}\right) \times \mathbb{M}_{1,\times}\left(\tilde{\Sigma}\right).
\end{aligned} \tag{9.6}$$

Note that because Assumption 3.12 is still assumed to hold, each manifold $\tilde{\Gamma}_j$ is necessarily closed.

Again, we shall omit in the following the dependence in the skeleton ($\mathbb{M}_{\times} := \mathbb{M}_{\times}\left(\tilde{\Sigma}\right)\dots$) for the sake of simplicity.

Remark 9.2 (**Making the link with the free junction case**). *For each $\sigma \in \{0,1\}$, an element of $\mathbb{M}_{\sigma,\times}$ is a tuple composed of exactly J elements (the number of sub-domains in the partition), while an element of $\mathbb{M}_{\sigma,\parallel}$ is a tuple composed of exactly* $\operatorname{card}\mathbb{J}$ *elements (the number of non-empty interfaces between exactly two sub-domains).*

However, if Assumption 3.11 and Assumption 3.12 hold, we can identify the two spaces in a straightforward manner. The key point is to see that if we do not allow the presence of junction points, the interfaces Γ_{jk} are all closed manifolds of dimension $d-1$ and the boundary Γ_j of Ω_j is made of the reunion of several connected components Γ_{jk} for $k \in \mathbb{K}_j$. As a result, the

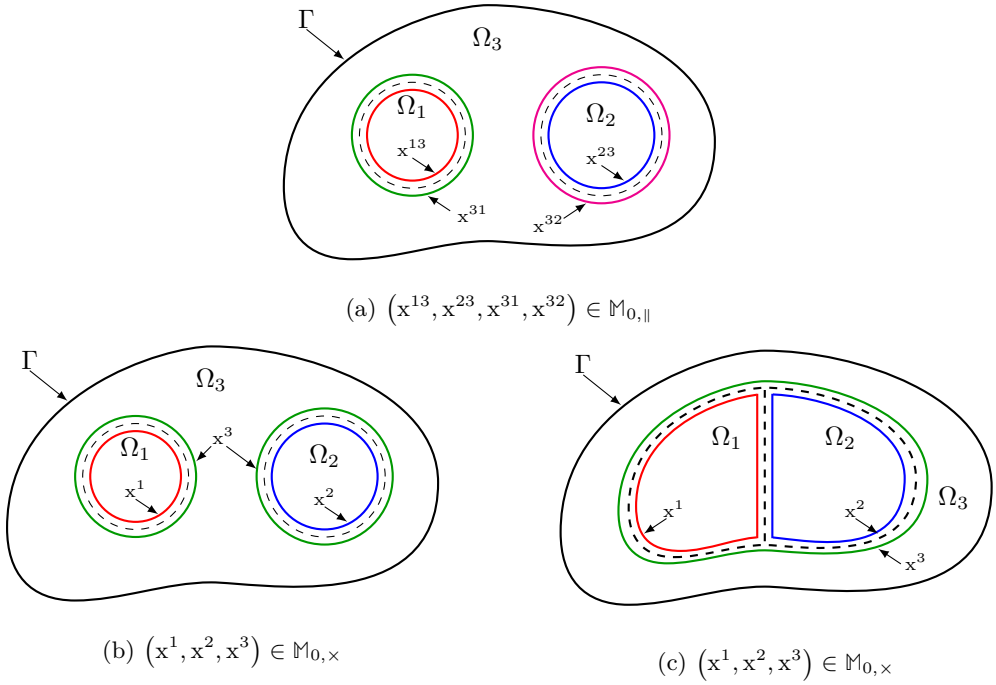

(a) $\left(\mathrm{x}^{13}, \mathrm{x}^{23}, \mathrm{x}^{31}, \mathrm{x}^{32}\right) \in \mathbb{M}_{0,\|}$

(b) $\left(\mathrm{x}^{1}, \mathrm{x}^{2}, \mathrm{x}^{3}\right) \in \mathbb{M}_{0,\times}$

(c) $\left(\mathrm{x}^{1}, \mathrm{x}^{2}, \mathrm{x}^{3}\right) \in \mathbb{M}_{0,\times}$

Figure 9.5: Visual representation of the components of the multi-trace spaces.

identification stems from the continuity and surjectivity properties of the trace operators on closed manifolds and suitably "gathering" and "dividing" traces of different connected components, see Figure 9.5.

More precisely, elements of $\mathbb{M}_{\sigma,\|}$ are identified as elements of $\mathbb{M}_{\sigma,\times}$ by "gathering" together the (disconnected) pieces that belong to a single sub-domain:

$$\begin{aligned} &\textit{For any} \quad (\mathrm{x}_\sigma^{jk})_{(j,k)\in\mathbb{J}} \in \mathbb{M}_{\sigma,\|}, \\ &\textit{let} \quad \mathrm{x}_\sigma^{j} \in \mathrm{X}_\sigma(\Gamma_j),\ \forall j \in \{1,\dots,J\}, \quad \textit{such that} \quad \mathrm{x}_\sigma^{j}|_{\Gamma_{jk}} := \mathrm{x}_\sigma^{jk},\ \forall (j,k)\in\mathbb{J}, \\ &\textit{then} \quad (\mathrm{x}_\sigma^{j})_{j=1}^{J} \in \mathbb{M}_{\sigma,\times}. \end{aligned} \tag{9.7}$$

Similarly, elements of $\mathbb{M}_{\sigma,\times}$ are identified as elements of $\mathbb{M}_{\sigma,\|}$ by "dividing" boundary traces into (disconnected) single interface pieces:

$$\begin{aligned} &\textit{For any} \quad (\mathrm{x}_\sigma^{j})_{j=1}^{J} \in \mathbb{M}_{\sigma,\times}. \\ &\textit{let} \quad \mathrm{x}_\sigma^{jk} \in \mathrm{X}_\sigma(\Gamma_{jk}),\ \forall (j,k)\in\mathbb{J}, \quad \textit{such that} \quad \mathrm{x}_\sigma^{jk} := \mathrm{x}_\sigma^{j}|_{\Gamma_{jk}},\ \forall (j,k)\in\mathbb{J}, \\ &\textit{then} \quad (\mathrm{x}_\sigma^{jk})_{(j,k)\in\mathbb{J}} \in \mathbb{M}_{\sigma,\|}, \end{aligned} \tag{9.8}$$

We emphasize that if Assumption 3.11 and Assumption 3.12 do not hold, the identification above is, in general, no longer possible: "gathering" and "dividing" traces is no longer permitted as we may break out of the natural trace spaces. However the identification remains possible for regular enough functions, that is for instance elements of $\mathbb{M}_{\sigma,\|} \cap \mathbb{M}_{1/2,\|}$ and $\mathbb{M}_{\sigma,\times} \cap \mathbb{M}_{1/2,\times}$.

Note that it is not possible to define a suitable multi-trace space $\mathbb{M}_{0,\|}$ on the geometric configuration represented in Figure 9.5c whereas there is no trouble with our new definition of $\mathbb{M}_{0,\times}$.

Trace operators By construction, the following global trace operators are continuous mappings from the broken solution spaces into the multi-trace spaces

$$\begin{aligned}
\boldsymbol{\gamma}_{0,\times} &: \mathbb{U}(\mathrm{D};\mathcal{P}_\Omega) \to \mathbb{M}_{0,\times},\\
&\quad u \mapsto \left(\gamma_{0,\tilde{\Gamma}_j}\, u|_{\Omega_j}\right)_{j=1}^{J},\\
\boldsymbol{\gamma}_{1,\times} &: \mathbb{U}(\mathrm{D},\mathrm{L}_{\mathsf{a}};\mathcal{P}_\Omega) \to \mathbb{M}_{1,\times},\\
&\quad u \mapsto \left(\gamma_{1,\tilde{\Gamma}_j}\, u|_{\Omega_j}\right)_{j=1}^{J},\\
\boldsymbol{\gamma}_{\times} &: \mathbb{U}(\mathrm{D},\mathrm{L}_{\mathsf{a}};\mathcal{P}_\Omega) \to \mathbb{M}_{\times},\\
&\quad u \mapsto \left(\gamma_{\tilde{\Gamma}_j}\, u|_{\Omega_j}\right)_{j=1}^{J}.
\end{aligned} \tag{9.9}$$

In addition, from Assumption 3.2, the mappings $\boldsymbol{\gamma}_{0,\times}$ and $\boldsymbol{\gamma}_{1,\times}$ are surjective. It is clear that, up to a re-ordering of the elements, we can make the identification $\boldsymbol{\gamma}_\times \equiv (\boldsymbol{\gamma}_{0,\times}, \boldsymbol{\gamma}_{1,\times})$.

Norms and duality pairings In the definitions below, and systematically in the remainder of this document, we shall use the following notations for elements of the multi-trace spaces

$$\begin{aligned}
&\mathbb{x}_0 = (\mathrm{x}_0^j)_{j=1}^J, && \mathbb{y}_0 = (\mathrm{y}_0^j)_{j=1}^J && \in \mathbb{M}_{0,\times},\\
&\mathbb{x}_1 = (\mathrm{x}_1^j)_{j=1}^J, && \mathbb{y}_1 = (\mathrm{y}_1^j)_{j=1}^J && \in \mathbb{M}_{1,\times},\\
&\mathbb{x}_{1/2} = (\mathrm{x}_{1/2}^j)_{j=1}^J, && \mathbb{y}_{1/2} = (\mathrm{y}_{1/2}^j)_{j=1}^J && \in \mathbb{M}_{1/2,\times},\\
&\mathbb{x} = (\mathrm{x}^j)_{j=1}^J \equiv (\mathbb{x}_0, \mathbb{x}_1), && \mathbb{y} = (\mathrm{y}^j)_{j=1}^J \equiv (\mathbb{y}_0, \mathbb{y}_1) && \in \mathbb{M}_{\times},
\end{aligned} \tag{9.10}$$

The multi-trace spaces can be endowed with the norms stemming from their Cartesian product structure. Recalling the definitions of the norms on a single domain given in (3.31), (3.33) and (3.50), we set, for each $\sigma \in \{0, 1/2, 1\}$,

$$\|\mathbb{x}_\sigma\|^2_{\mathbb{M}_{\sigma,\times}} := \sum_{j=1}^{J} \|\mathrm{x}_\sigma^j\|^2_{\mathrm{X}_\sigma(\Gamma_{j,h})}. \tag{9.11}$$

Besides, we introduce the natural norm on $\mathbb{M}_\times$ as follows

$$\|\mathbb{x}\|^2_{\mathbb{M}_\times} := \|\mathbb{x}_0\|^2_{\mathbb{M}_{0,\times}} + \|\mathbb{x}_1\|^2_{\mathbb{M}_{1,\times}}, \qquad \forall \mathbb{x} \equiv (\mathbb{x}_0, \mathbb{x}_1) \in \mathbb{M}_\times. \tag{9.12}$$

Recalling the local duality pairing $\langle\cdot,\cdot\rangle_{\partial\mathcal{O}}$ between the two dual trace spaces (3.28) on a single boundary $\partial\mathcal{O}$, we introduce the duality pairing between multi-trace spaces (which does not involve any complex conjugation operation)

$$\begin{aligned}
\langle\!\langle\cdot,\cdot\rangle\!\rangle_\times &: \mathbb{M}_{1,\times} \times \mathbb{M}_{0,\times} \to \mathbb{C},\\
&\quad (\mathbb{x}_1,\, \mathbb{x}_0) \mapsto \sum_{j=1}^{J} \langle \mathrm{x}_1^j, \mathrm{x}_0^j \rangle_{\tilde{\Gamma}_j}.
\end{aligned} \tag{9.13}$$

Recalling our definition (3.49) of the inner product $(\cdot,\cdot)_{\partial\mathcal{O}}$ on the pivot trace space $\mathrm{X}_{1/2}(\partial\mathcal{O})$ on a single boundary $\partial\mathcal{O}$, we also equip the (pivot) multi-trace space with its natural scalar product

(and associated norm) which reads

$$\begin{aligned} \left(\!\left(\cdot,\cdot\right)\!\right)_{\times} &: \mathbb{M}_{1/2,\times} \times \mathbb{M}_{1/2,\times} \to \mathbb{C}, \\ (\mathbb{x}_{1/2},\, \mathbb{x}_{1/2}) &\mapsto \sum_{j=1}^{J} (\mathrm{x}^j_{1/2}, \mathrm{y}^j_{1/2})_{\tilde{\Gamma}_j}. \end{aligned} \tag{9.14}$$

Recalling the definition (3.73) of the bilinear form $[\cdot,\cdot]_{\partial\mathcal{O}}$ on $\mathrm{X}(\partial\mathcal{O})$ for a single boundary $\partial\mathcal{O}$, we finally define the skew symmetric bilinear form

$$\begin{aligned} \left[\!\left[\cdot,\cdot\right]\!\right]_{\times} &: \mathbb{M}_{\times} \times \mathbb{M}_{\times} \to \mathbb{C}, \\ (\mathbb{x},\, \mathbb{y}) &\mapsto \sum_{j=1}^{J} [\mathrm{x}^j, \mathrm{y}^j]_{\tilde{\Gamma}_j} = \left(\!\left(\mathbb{y}_1, \mathbb{x}_0\right)\!\right)_{\times} - \left(\!\left(\mathbb{x}_1, \mathbb{y}_0\right)\!\right)_{\times}. \end{aligned} \tag{9.15}$$

9.2.1.2 Cauchy-trace spaces

Similarly to Definition 3.18, we define a first subset of the space of multi-trace spaces which is the space of traces of a function whose restriction in each sub-domain satisfies the *homogeneous* PDE and physical boundary conditions on Γ (see (3.130)). In particular, note that no boundary condition on the transmission interface is imposed in the following definition and that the two traces associated to the two sides of a single interface between two sub-domains need not satisfy a matching condition.

Definition 9.3. *Recall that, for each $j = 1, \dots, J$, we introduced in* (3.130) *the subspace $S(\Omega_j)$ of solutions of the homogeneous PDE in Ω_j. For each $j = 1, \dots, J$, the local space of Cauchy traces is defined as*

$$\mathrm{C}_{\times}(\Gamma_j) := \left\{ \mathrm{x}^j \in \mathrm{X}(\Gamma_j) \;\middle|\; \exists u_j \in S(\Omega_j),\ \mathrm{x}^j := \gamma_{\Gamma_j} u_j \right\}. \tag{9.16}$$

The global Cauchy trace space, subspace of $\mathbb{M}_{\times}$, is defined as

$$\mathbb{C}_{\times}\left(\tilde{\Sigma}\right) := \bigtimes_{j=1}^{J} \mathrm{C}_{\times}(\Gamma_j). \tag{9.17}$$

Again, because elements of the Cauchy traces are related to local solutions that satisfy the original equation in each sub-domain, it is natural that they satisfy some sort of energy conservation result, as stated in the following Proposition. We refer the reader to the discussion preceding Proposition 3.19 for the meaning of energy balance in our setting. A similar result in a slightly different setting (in the whole space) can be found in [29, Lem. 6.1].

Proposition 9.4 (**Energy balance interpretation**). *The energy decreases globally in Ω, which translates as*

$$\mathrm{i}\left[\!\left[\mathbb{x}, \overline{\mathbb{x}}\right]\!\right]_{\times} < 0, \qquad \forall \mathbb{x} \in \mathbb{C}_{\times}. \tag{9.18}$$

Proof. Let

$$\mathbb{x} = \left(\mathrm{x}^j\right)_{j=1}^{J} \in \mathbb{C}_{\times}, \qquad \mathrm{x}^j = (\mathrm{x}^j_0, \mathrm{x}^j_1), \quad \forall j \in \{1, \dots, J\}. \tag{9.19}$$

For each $j \in \{1, \dots, J\}$, by definition of the local Cauchy trace space $\mathrm{C}_{\times}$ given in (9.16), let $u_j \in \mathrm{U}_{\Gamma}(\mathrm{D}; \Omega_j)$ be such that

$$\begin{cases} \left(\mathrm{L}_{\mathsf{a}} - {\kappa_0}^2 \mathsf{n}\right) u_j = 0, & \text{in } \Omega_j, \\ (\gamma_{1,\Gamma} - \mathrm{i}\gamma_{0,\Gamma}) u_j = 0, & \text{on } \Gamma, \\ \gamma_{\tilde{\Gamma}_j} u_j = \mathrm{x}^j, & \text{on } \tilde{\Gamma}_j. \end{cases} \tag{9.20}$$

We have, using Lemma 3.6 and the first Green identity (3.104)

$$\begin{aligned} \mathrm{i}\frac{1}{2}[\mathrm{x}^j, \overline{\mathrm{x}^j}]_{\Gamma_j} &= \Im\langle \gamma_{1,\Gamma_j} u_j, \gamma_{0,\Gamma_j} \overline{u_j}\rangle_{\Gamma_j}, \\ &= \Im\Big[-{\kappa_0}^{-1}(\mathrm{L}_{\mathsf{a}} u_j, \overline{u_j})_{L^2(\Omega_j)^{m_0}} + {\kappa_0}^{-1}(\mathsf{a}\,\mathrm{D}u_j, \mathrm{D}\overline{u_j})_{L^2(\Omega_j)^{m_1}} \\ &\qquad -\langle \gamma_{1,\Gamma} u_j, \gamma_{0,\Gamma} \overline{u_j}\rangle_{\Gamma}\Big]. \end{aligned} \tag{9.21}$$

From (9.20), we obtain

$$\begin{aligned} \mathrm{i}\frac{1}{2}[\mathrm{x}^j, \overline{\mathrm{x}^j}]_{\Gamma_j} = \Big[&-\kappa_0(\Im(\mathsf{n}) u_j, \overline{u_j})_{L^2(\Omega_j)^{m_0}} + {\kappa_0}^{-1}(\Im(\mathsf{a})\,\mathrm{D}u_j, \mathrm{D}\overline{u_j})_{L^2(\Omega_j)^{m_1}} \\ &-\|\gamma_{0,\Gamma} u_j\|^2_{L^2(\Gamma)^{m_0}}\Big] \leq 0, \end{aligned} \tag{9.22}$$

from the assumption (3.78). This proves that the energy is conserved locally in each sub-domain, the global result follows by summing over all sub-domains. ■

9.2.1.3 Single-trace spaces

We now introduce the single trace spaces, which are, again in this setting, spaces of traces of functions that are "globally regular" in some (Sobolev) sense in the whole of Ω. In contrast to Definition 3.20, we use as a definition the characterization given by Proposition 3.21. We emphasize that we adopt here an approach that is fundamentally different from the one of Chapter 3.

First, let us define the following global trace operators (see in particular Assumption 3.2 for the definition of the local traces)

$$\begin{aligned} \boldsymbol{\gamma}_{\mathrm{D},\times} \;:\; & \mathbb{U}(\mathrm{D};\mathcal{P}_\Omega) \to \mathbb{M}_{0,\times}, \\ & u \mapsto \Big(\gamma_{\mathrm{D},\tilde{\Gamma}_j} u|_{\Omega_j}\Big)_{j\in\{1,\dots,J\}}, \\ \boldsymbol{\gamma}_{\mathrm{D}^*,\times} \;:\; & \mathbb{U}(\mathrm{D}^*;\mathcal{P}_\Omega) \to \mathbb{M}_{1,\times}, \\ & u \mapsto \Big(\gamma_{\mathrm{D}^*,\tilde{\Gamma}_j} u|_{\Omega_j}\Big)_{j\in\{1,\dots,J\}}. \end{aligned} \tag{9.23}$$

Of course from (3.64), we have $\boldsymbol{\gamma}_{\mathrm{D},\times} = \boldsymbol{\gamma}_{0,\times}$. However, we introduced the operator $\boldsymbol{\gamma}_{\mathrm{D},\times}$ to respect the symmetry in our notations.

Definition 9.5. *The global single-trace spaces are defined as*

$$\begin{aligned} \mathbb{S}_{0,\times}\left(\tilde{\Sigma}\right) &:= \boldsymbol{\gamma}_{\mathrm{D},\times}\,\mathrm{U}_\Gamma(\mathrm{D};\Omega), \\ \mathbb{S}_{1,\times}\left(\tilde{\Sigma}\right) &:= \boldsymbol{\gamma}_{\mathrm{D}^*,\times}\,\mathrm{U}_\Gamma(\mathrm{D}^*;\Omega), \\ \mathbb{S}_{\times}\left(\tilde{\Sigma}\right) &:= \mathbb{S}_{0,\times}\left(\tilde{\Sigma}\right) \times \mathbb{S}_{1,\times}\left(\tilde{\Sigma}\right). \end{aligned} \tag{9.24}$$

Remark 9.6. *Observe that, contrary to Definition 3.20, we have not used matching conditions at every interface to define the single-trace spaces. However, we still have*

$$\begin{aligned} \mathbb{S}_{0,\times} &= \Big\{ \mathbb{x}_0 = (\mathrm{x}_0^j)_{j=1}^J \in \mathbb{M}_{0,\times} \quad | \quad x_0^j|_{\Gamma_{jk}} = x_0^k|_{\Gamma_{jk}},\ \forall (j,k) \in \mathbb{J} \Big\}, \\ \mathbb{S}_{1,\times} &= \Big\{ \mathbb{x}_1 = (\mathrm{x}_1^j)_{j=1}^J \in \mathbb{M}_{1,\times} \quad | \quad x_1^j|_{\Gamma_{jk}} = -x_1^k|_{\Gamma_{jk}},\ \forall (j,k) \in \mathbb{J} \Big\}, \end{aligned} \tag{9.25}$$

where the restriction operation is to be understood in a suitable weak sense, which would be quite delicate to give a meaning to in our abstract setting. It follows that we shall not rely on the above matching conditions when devising our domain decomposition method.

The following lemma, which rests on Assumption 3.3, is in some sense a generalization to the case of junction points of Lemma 3.13.

Lemma 9.7. *We have*

$$\begin{aligned} &\operatorname{Ker}\boldsymbol{\gamma}_{\mathrm{D},\times} \subset \mathrm{U}(\mathrm{D};\Omega), \\ &\operatorname{Ker}\boldsymbol{\gamma}_{\mathrm{D}^*,\times} \subset \mathrm{U}(\mathrm{D}^*;\Omega). \end{aligned} \tag{9.26}$$

Proof. We give the proof of the first result, the proof of the other one takes a very similar route.

Let $u \in \operatorname{Ker}\boldsymbol{\gamma}_{\mathrm{D},\times}$. For any $j \in \{1,\dots,J\}$, we have by definition of the multi-trace operator $\boldsymbol{\gamma}_{\mathrm{D},\times}$ that $u|_{\Omega_j} \in \operatorname{Ker}\gamma_{\mathrm{D},\tilde{\Gamma}_j}$. By Assumption 3.3, there exists a sequence $(\phi_j^n)_{n\in\mathbb{N}}$ of elements of $\mathcal{D}(\Omega_j)^{m_0}$ that converges to $u|_{\Omega_j}$ in $\mathrm{U}(\mathrm{D};\Omega_j)$. For each $n \in \mathbb{N}$, let ϕ^n be such that $\phi^n|_{\Omega_j} = \phi_j^n$. By construction it is clear that all elements of the sequence $(\phi^n)_{n\in\mathbb{N}}$ belong to $\mathcal{D}(\Omega)^{m_0}$. This sequence is a Cauchy sequence, since we have

$$\begin{aligned} \|\phi^p - \phi^q\|^2_{\mathrm{U}(\mathrm{D};\Omega)} &= \sum_{j=1}^{J} \|\phi_j^p - \phi_j^q\|^2_{\mathrm{U}(\mathrm{D};\Omega_j)}, \\ &\le 2\sum_{j=1}^{J} \left(\|\phi_j^p - u|_{\Omega_j}\|^2_{\mathrm{U}(\mathrm{D};\Omega_j)} + \|u|_{\Omega_j} - \phi_j^q\|^2_{\mathrm{U}(\mathrm{D};\Omega_j)} \right), \end{aligned} \tag{9.27}$$

and each term on the right-hand-side converges to 0 by assumption on $(\phi_j^n)_{n\in\mathbb{N}}$. Hence the sequence $(\phi^n)_{n\in\mathbb{N}}$ converges in $\mathrm{U}(\mathrm{D};\Omega)$ (which is complete) say to v. Besides it converges to u in $L_2(\Omega)^{m_0}$. By uniqueness of the limit, it follows that $u = v \in \mathrm{U}(\mathrm{D};\Omega)$ and we are done. ■

We deduce the following corollary, which completes Definition 9.5. It is a characterization of the difference between the U (regular) and the $\mathbb{U}$ (broken) versions of the solution spaces using the single-trace spaces. This result is the analogue of Corollary 3.22 and the two proofs are similar. Notice however that the arguments are different, we use Definition 9.5 instead of Proposition 3.21 and Lemma 9.7 instead of Lemma 3.13.

Corollary 9.8. *We have*

$$\begin{array}{lllcl} \text{(i)} & \forall u \in \mathbb{U}_\Gamma(\mathrm{D};\mathcal{P}_\Omega), & \boldsymbol{\gamma}_{\mathrm{D},\times}u = \boldsymbol{\gamma}_{0,\times}u \in \mathbb{S}_{0,\times} & \Leftrightarrow & u \in \mathrm{U}_\Gamma(\mathrm{D};\Omega), \\ \text{(ii)} & \forall u \in \mathbb{U}_\Gamma(\mathrm{D}^*;\mathcal{P}_\Omega), & \boldsymbol{\gamma}_{\mathrm{D}^*,\times}u \in \mathbb{S}_{1,\times} & \Leftrightarrow & u \in \mathrm{U}_\Gamma(\mathrm{D}^*;\Omega), \\ \text{(iii)} & \forall u \in \mathbb{U}_\Gamma(\mathrm{D},\mathrm{L}_\mathsf{a};\mathcal{P}_\Omega), & \boldsymbol{\gamma}_\times u \in \mathbb{S}_\times & \Leftrightarrow & u \in \mathrm{U}_\Gamma(\mathrm{D},\mathrm{L}_\mathsf{a};\Omega). \end{array} \tag{9.28}$$

Proof. It is clear that one implication ($\Leftarrow$) stems from Definition 9.5. We need only to prove the reverse implication ($\Rightarrow$).

(i) Let $u \in \mathbb{U}_\Gamma(\mathrm{D};\mathcal{P}_\Omega)$ such that $\boldsymbol{\gamma}_{0,\times}u \in \mathbb{S}_{0,\times}$. By Definition 9.5 of $\mathbb{S}_{0,\times}$, there exists $v \in \mathrm{U}_\Gamma(\mathrm{D};\Omega)$ such that $\boldsymbol{\gamma}_{0,\times}(v-u) = 0$. It follows that $w := v - u \in \operatorname{Ker}\boldsymbol{\gamma}_{0,\times} = \operatorname{Ker}\boldsymbol{\gamma}_{\mathrm{D},\times}$ and by Lemma 9.7 we get $w \in \mathrm{U}_\Gamma(\mathrm{D};\Omega)$ so that finally $u = v + w$ does belong to $\mathrm{U}_\Gamma(\mathrm{D};\Omega)$.

(ii) Let $u \in \mathbb{U}_\Gamma(\mathrm{D}^*;\mathcal{P}_\Omega)$ such that $\boldsymbol{\gamma}_{1,\times}u \in \mathbb{S}_{1,\times}$. By Definition 9.5 of $\mathbb{S}_{1,\times}$, there exists $v \in \mathrm{U}_\Gamma(\mathrm{D}^*;\Omega)$ such that $\boldsymbol{\gamma}_{1,\times}(v-u) = 0$. It follows that $w := v - u \in \operatorname{Ker}\boldsymbol{\gamma}_{1,\times} = \operatorname{Ker}\boldsymbol{\gamma}_{\mathrm{D}^*,\times}$ and by Lemma 9.7 we get $w \in \mathrm{U}_\Gamma(\mathrm{D}^*;\Omega)$ so that finally $u = v + w$ does belong to $\mathrm{U}_\Gamma(\mathrm{D}^*;\Omega)$.

(iii) Let $u \in \mathbb{U}_\Gamma(\mathrm{D},\mathrm{L}_\mathsf{a};\mathcal{P}_\Omega)$ such that $\boldsymbol{\gamma}_\times u \in \mathbb{S}_\times$, which is rewritten as from Definition 9.5 as $\boldsymbol{\gamma}_{0,\times}u \in \mathbb{S}_{0,\times}$ and $\boldsymbol{\gamma}_{1,\times}u \in \mathbb{S}_{1,\times}$. We just proved in (i) that from $\boldsymbol{\gamma}_{0,\times}u \in \mathbb{S}_{0,\times}$ we have $u \in \mathrm{U}_\Gamma(\mathrm{D};\Omega)$. If we let $v \in L^2(\Omega)^{m_1}$ such that for each $j \in \{1,\dots,J\}$, $v|_{\Omega_j} = \mathsf{a}\mathrm{D}u|_{\Omega_j}$, we have $\boldsymbol{\gamma}_{1,\times}v \in \mathbb{S}_{1,\times}$ and we just proved in (ii) that then $v \in \mathrm{U}_\Gamma(\mathrm{D}^*;\Omega)$. Hence we get $\mathsf{a}\mathrm{D}u \in \mathrm{U}_\Gamma(\mathrm{D}^*;\Omega)$ and we have $u \in \mathrm{U}_\Gamma(\mathrm{D},\mathrm{L}_\mathsf{a};\Omega)$. ■

The following proposition is the counterpart of Proposition 3.23 and states that the single trace spaces are orthogonal in some sense, providing as a result a helpful characterization of the spaces. Such a result was proven for in [28, Prop. 2.1], [36, Prop. 2.1] and [29, Prop. 4.1] for the acoustic setting and in [37, Prop. 3.1] for the electromagnetic setting.

Proposition 9.9. *The single trace spaces are such that:*

$$\begin{aligned}
&\forall \mathbb{x}_0 \in \mathbb{M}_{0,\times}, && \Big(\mathbb{x}_0 \in \mathbb{S}_{0,\times} && \Leftrightarrow && \langle\!\langle \mathbb{y}_1, \mathbb{x}_0 \rangle\!\rangle_\times = 0, && \forall \mathbb{y}_1 \in \mathbb{S}_{1,\times}\Big),\\
&\forall \mathbb{x}_1 \in \mathbb{M}_{1,\times}, && \Big(\mathbb{x}_1 \in \mathbb{S}_{1,\times} && \Leftrightarrow && \langle\!\langle \mathbb{x}_1, \mathbb{y}_0 \rangle\!\rangle_\times = 0, && \forall \mathbb{y}_0 \in \mathbb{S}_{0,\times}\Big),\\
&\forall \mathbb{x} \in \mathbb{M}_{\times}, && \Big(\mathbb{x} \in \mathbb{S}_{\times} && \Leftrightarrow && [\![\mathbb{x}, \mathbb{y}]\!]_\times = 0, && \forall \mathbb{y} \in \mathbb{S}_{\times}\Big).
\end{aligned} \tag{9.29}$$

Proof. Let $\mathbb{x} \equiv (\mathbb{x}_0, \mathbb{x}_1) \in \mathbb{M}_\times$. By definition,

$$\mathbb{x} \in \mathbb{S}_\times \qquad \Leftrightarrow \qquad \begin{cases} \mathbb{x}_0 \in \mathbb{S}_{0,\times}, \\ \mathbb{x}_1 \in \mathbb{S}_{1,\times}, \end{cases} \tag{9.30}$$

and it is clear that

$$[\![\mathbb{x}, \mathbb{y}]\!]_\times = 0, \ \forall \mathbb{y} \in \mathbb{S}_\times \qquad \Leftrightarrow \qquad \begin{cases} \langle\!\langle \mathbb{y}_1, \mathbb{x}_0 \rangle\!\rangle_\times = 0, \ \forall \mathbb{y}_1 \in \mathbb{S}_{1,\times}, \\ \langle\!\langle \mathbb{x}_1, \mathbb{y}_0 \rangle\!\rangle_\times = 0, \ \forall \mathbb{y}_0 \in \mathbb{S}_{0,\times}, \end{cases} \tag{9.31}$$

so the last result is equivalent to the first two. We give the proof for the first one, it relies on the first Green identity written in local domains and in the whole of Ω. The proof for the second result follows the same route and is omitted for the sake of brevity.

($\Rightarrow$) Let $\mathbb{x}_0 \equiv (\mathrm{x}_0^j)_{j\in\{1,\dots,J\}} \in \mathbb{S}_{0,\times}$, there exists $u_0 \in \mathrm{U}_\Gamma(\mathrm{D};\Omega)$ such that $\gamma_{\mathrm{D},\tilde{\Gamma}_j} u_0 = \mathrm{x}_0^j$ for all $j = 1,\dots,J$. Let $\mathbb{y}_1 \equiv (\mathrm{y}_1^j)_{j\in\{1,\dots,J\}} \in \mathbb{S}_{1,\times}$, there exists $u_1 \in \mathrm{U}_\Gamma(\mathrm{D}^*;\Omega)$ such that $\gamma_{\mathrm{D}^*,\tilde{\Gamma}_j} u_1 = \mathrm{y}_1^j$ for all $j = 1,\dots,J$. We have, applying the first Green identity (3.65) twice (locally and globally)

$$\begin{aligned}
\langle\!\langle \mathbb{y}_1, \mathbb{x}_0 \rangle\!\rangle_\times &:= \sum_{j=1}^J \langle \mathrm{y}_1^j, \mathrm{x}_0^j \rangle_{\tilde{\Gamma}_j} = \sum_{j=1}^J \langle \gamma_{\mathrm{D}^*,\tilde{\Gamma}_j} u_1, \gamma_{\mathrm{D},\tilde{\Gamma}_j} u_0 \rangle_{\tilde{\Gamma}_j}, \\
&= \sum_{j=1}^J \Big[(u_1, \mathrm{D}u_0)_{L^2(\Omega_j)^{m_1}} - (\mathrm{D}^* u_1, u_0)_{L^2(\Omega_j)^{m_0}} - \langle \gamma_{\mathrm{D}^*,\Gamma} u_1, \gamma_{\mathrm{D},\Gamma} u_0 \rangle_\Gamma \Big], \\
&= (u_1, \mathrm{D}u_0)_{L^2(\Omega)^{m_1}} - (\mathrm{D}^* u_1, u_0)_{L^2(\Omega)^{m_0}} - \langle \gamma_{\mathrm{D}^*,\Gamma} u_1, \gamma_{\mathrm{D},\Gamma} u_0 \rangle_\Gamma = 0.
\end{aligned} \tag{9.32}$$

($\Leftarrow$) Let $\mathbb{x}_0 \equiv (\mathrm{x}_0^j)_{j\in\{1,\dots,J\}} \in \mathbb{M}_{0,\times}$ such that $\langle \langle \mathbb{y}_1, \mathbb{x}_0 \rangle \rangle_\Sigma = 0, \ \forall \mathbb{y}_1 \in \mathbb{S}_{1,\times}$. For each $j = 1,\dots,J$, we introduce local liftings $u_0^j \in \mathrm{U}_\Gamma(\mathrm{D};\Omega_j)$ such that $\gamma_{\mathrm{D},\tilde{\Gamma}_j} u_0^j = \mathrm{x}_0^j$. Let $u_0 \in \mathbb{U}_\Gamma(\mathrm{D};\mathcal{P}_\Omega)$ and $v_1 \in L^2(\Omega)^{m_1}$ be such that

$$u_0|_{\Omega_j} = u_0^j, \qquad \text{and} \qquad v_1|_{\Omega_j} = \mathrm{D}u_0^j. \tag{9.33}$$

For any $u_1 \in \mathrm{U}_\Gamma(\mathrm{D}^*;\Omega)$ with vanishing trace $\gamma_{\mathrm{D}^*,\Gamma} u_1 = 0$ on Γ, we set $\mathbb{y}_1 \equiv (\mathrm{y}_1^j)_{j\in\{1,\dots,J\}} \in \mathbb{S}_{1,\times}$

with $\mathrm{y}_1^j = \gamma_{\mathrm{D}^*,\tilde{\Gamma}_j}\, u_1$ for all $j = 1, \dots, J$. We have,using once again the first Green identity (3.65)

$$\begin{aligned}
(\mathrm{D}^* u_1, u_0)_{L^2(\Omega)^{m_0}} &= \sum_{j=1}^{J} (\mathrm{D}^* u_1, u_0^j)_{L^2(\Omega_j)^{m_0}}, \\
&= \sum_{j=1}^{J} \left[-\langle \gamma_{\mathrm{D}^*,\tilde{\Gamma}_j}\, u_1, \gamma_{\mathrm{D},\tilde{\Gamma}_j}\, u_0^j \rangle_{\tilde{\Gamma}_j} + (u_1, \mathrm{D} u_0^j)_{L^2(\Omega_j)^{m_1}} \right], \\
&= \sum_{j=1}^{J} \left[-\langle \mathrm{y}_1^j, \mathrm{x}_0^j \rangle_{\tilde{\Gamma}_j} + (u_1, \mathrm{D} u_0^j)_{L^2(\Omega_j)^{m_1}} \right], \\
&= -\langle\!\langle \mathrm{y}_1, \mathbb{x}_0 \rangle\!\rangle_{\times} + (u_1, v_1)_{L^2(\Omega)^{m_1}} = (u_1, v_1)_{L^2(\Omega)^{m_1}}.
\end{aligned} \tag{9.34}$$

Which proves that $v_1 = \mathrm{D} u_0$ weakly on the whole of Ω, hence $u_0 \in \mathrm{U}_\Gamma(\mathrm{D}; \Omega)$ and $\mathbb{x}_0 \in \mathbb{S}_{0,\times}$. ■

Remark 9.10. *Notice that the proof of the similar result (Proposition 3.23) in absence of junction points was considerably easier. Similarly, for regular enough functions (for which the restriction on parts of the boundary can be properly defined) the orthogonality property can be easily deduced (see Remark 9.6). Indeed, let*

$$\mathrm{x}_0 \equiv (\mathrm{x}_0^j)_{j=1}^J \in \mathbb{M}_{0,\times} \cap \mathbb{M}_{1/2,\times} \qquad \textit{and} \qquad \mathrm{x}_1 \equiv (\mathrm{x}_1^j)_{j=1}^J \in \mathbb{M}_{1,\times} \cap \mathbb{M}_{1/2,\times}, \tag{9.35}$$

we first establish the identity

$$\begin{aligned}
\langle\!\langle \mathbb{x}_1, \mathbb{x}_0 \rangle\!\rangle_{\times} = (\!(\mathbb{x}_1, \mathbb{x}_0)\!)_{\times} &= \sum_{j=1}^{J} (\mathrm{x}_1^j, \mathrm{x}_0^j)_{\tilde{\Gamma}_j} = \sum_{j=1}^{J} \sum_{k \in \mathbb{K}_j} (\mathrm{x}_1^j|_{\Gamma_{jk}}, \mathrm{x}_0^j|_{\Gamma_{jk}})_{\Gamma_{jk}}, \\
&= \sum_{j=1}^{J} \sum_{\substack{k \in \mathbb{K}_j \\ j<k}} \left[(\mathrm{x}_1^j|_{\Gamma_{jk}}, \mathrm{x}_0^j|_{\Gamma_{jk}})_{\Gamma_{jk}} + (\mathrm{x}_1^k|_{\Gamma_{jk}}, \mathrm{x}_0^k|_{\Gamma_{jk}})_{\Gamma_{jk}} \right].
\end{aligned} \tag{9.36}$$

Now, if $\mathrm{x}_0 \in \mathbb{S}_{0,\times}$ and $\mathrm{x}_1 \in \mathbb{S}_{1,\times}$, it follows from Definition 9.5 that $\langle\!\langle \mathbb{x}_1, \mathbb{x}_0 \rangle\!\rangle_{\times} = 0$. Reciprocally, let $\mathrm{x}_0 \in \mathbb{M}_{0,\times}$ such that for any $\mathrm{x}_1 \in \mathbb{S}_{1,\times}$, we have $\langle\!\langle \mathbb{x}_1, \mathbb{x}_0 \rangle\!\rangle_{\times} = 0$. We obtain

$$\langle\!\langle \mathbb{x}_1, \mathbb{x}_0 \rangle\!\rangle_{\times} = \sum_{j=1}^{J} \sum_{\substack{k \in \mathbb{K}_j \\ j<k}} \langle \mathrm{x}_1^{jk}|_{\Gamma_{jk}}, \mathrm{x}_0^{jk}|_{\Gamma_{jk}} - \mathrm{x}_0^{kj}|_{\Gamma_{kj}} \rangle_{\Gamma_{jk}} = 0, \tag{9.37}$$

which holds for any x_1, so that $\mathrm{x}_0^{jk}|_{\Gamma_{jk}} = \mathrm{x}_0^{kj}|_{\Gamma_{kj}}$ for any $(j,k) \in \mathbb{J}$ and finally $\mathrm{x}_0 \in \mathbb{S}_{0,\times}$.

The other result can be obtained analogously.

9.2.1.4 Characterization of the trace of the solution

We are now ready to characterize the solution of the model problem (3.79) entirely through its trace. This is the purpose of the following Proposition, counterpart of Proposition 3.24 but now allowing interior junction points.

Proposition 9.11 (**Equivalent decomposed problem**). *Let $F \in \mathbb{U}_\Gamma(\mathrm{D}; \mathcal{P}_\Omega)$ be any source lifting such that (the choice is not unique)*

$$\begin{cases}
(\mathrm{L}_{\mathsf{a}} - \kappa_0{}^2 \mathsf{n}) F|_{\Omega_j} = f|_{\Omega_j}, & \textit{in } \Omega_j,\ \forall j \in \{1, \dots, J\}, \\
(\gamma_{1,\Gamma} - \mathrm{i}\gamma_{0,\Gamma}) F = g, & \textit{on } \Gamma.
\end{cases} \tag{9.38}$$

Let $u \in \mathbb{U}_\Gamma(\mathrm{D}, \mathrm{L}_\mathsf{a}; \mathcal{P}_\Omega)$. Then, u is solution of the model problem (3.79) *if, and only if,*

$$\boldsymbol{\gamma}_\times u \in (\mathbb{C}_\times + \boldsymbol{\gamma}_\times F) \cap \mathbb{S}_\times. \tag{9.39}$$

Proof. ($\Rightarrow$) Let u be a solution of the model problem (3.79):

$$\begin{cases} \text{Find } u \in \mathrm{U}_\Gamma(\mathrm{D}; \Omega) \text{ such that} & \\ (\mathrm{L}_\mathsf{a} - {\kappa_0}^2 \mathsf{n}) u = f, & \text{in } \Omega, \\ (\gamma_{1,\Gamma} - \mathrm{i}\gamma_{0,\Gamma}) u = g, & \text{on } \Gamma. \end{cases} \tag{9.40}$$

Since u satisfies the PDE in Ω in a distributional sense, by testing for each $j \in \{1, \dots, J\}$ with a test function in $C_0^\infty(\Omega_j)$ (extended by zero outside Ω_j), the restriction $u|_{\Omega_j}$, which ought to be in $\mathrm{U}_\Gamma(\mathrm{D}; \Omega j)$, satisfies the PDE in each sub-domain Ω_j. The physical boundary condition on Γ is not affected by the decomposition since we exclude the case of boundary junction points (Assumption 3.12). We get

$$\begin{cases} (\mathrm{L}_\mathsf{a} - {\kappa_0}^2 \mathsf{n}) u|_{\Omega_j} = f|_{\Omega_j}, & \text{in } \Omega_j, \ \forall j \in \{0, \dots, J\}, \\ (\gamma_{1,\Gamma} - \mathrm{i}\gamma_{0,\Gamma}) u = g, & \text{on } \Gamma. \end{cases} \tag{9.41}$$

Given any $F \in \mathbb{U}_\Gamma(\mathrm{D}; \mathcal{P}_\Omega)$ satisfying (9.38), by Definition 9.3 of the Cauchy trace space $\mathbb{C}_\times$ we get

$$\boldsymbol{\gamma}_\times (u - F) \in \mathbb{C}_\times. \tag{9.42}$$

Besides u is explicitly sought as an element of $\mathrm{U}_\Gamma(\mathrm{D}; \Omega)$ and in addition u satisfy the PDE in the whole of Ω and by Assumption 3.10 necessarily $u \in \mathrm{U}_\Gamma(\mathrm{D}, \mathrm{L}_\mathsf{a}; \Omega)$. By Definition 9.5 on the single trace space $\mathbb{S}_\times$ we get

$$\boldsymbol{\gamma}_\times u \in \mathbb{S}_\times. \tag{9.43}$$

($\Leftarrow$) Conversely, suppose that $u \in \mathbb{U}_\Gamma(\mathrm{D}, \mathrm{L}_\mathsf{a}; \mathcal{P}_\Omega)$ is such that

$$\begin{aligned} &\boldsymbol{\gamma}_\times (u - F) \in \mathbb{C}_\times, \\ &\boldsymbol{\gamma}_\times u \in \mathbb{S}_\times, \end{aligned} \tag{9.44}$$

for any $F \in \mathbb{U}_\Gamma(\mathrm{D}; \mathcal{P}_\Omega)$ satisfying (9.38). From

$$\boldsymbol{\gamma}_\times (u - F) \in \mathbb{C}_\times, \tag{9.45}$$

using Corollary 9.8 we have that

$$\begin{cases} (\mathrm{L}_\mathsf{a} - {\kappa_0}^2 \mathsf{n}) u|_{\Omega_j} = f|_{\Omega_j}, & \text{in } \Omega_j, \ \forall j \in \{0, \dots, J\}, \\ (\gamma_{1,\Gamma} - \mathrm{i}\gamma_{0,\Gamma}) u = g, & \text{on } \Gamma. \end{cases} \tag{9.46}$$

From

$$\boldsymbol{\gamma}_\times u \in \mathbb{S}_\times, \tag{9.47}$$

by Definition 9.5 on the single trace space $\mathbb{S}_\times$ we get that $u \in \mathrm{U}_\Gamma(\mathrm{D}, \mathrm{L}_\mathsf{a}; \Omega)$. It follows that $(\mathrm{L}_\mathsf{a} - {\kappa_0}^2 \mathsf{n}) u$ makes sense in $L^2(\Omega)^{m_0}$ and we can write for any test function $\phi \in \mathcal{D}(\Omega)^{m_0}$

$$\begin{aligned} ((\mathrm{L}_\mathsf{a} - {\kappa_0}^2 \mathsf{n}) u, \phi)_{L^2(\Omega)^{m_0}} &= \sum_{j=1}^{J} ((\mathrm{L}_\mathsf{a} - {\kappa_0}^2 \mathsf{n}) u|_{\Omega_j}, \phi|_{\Omega_j})_{L^2(\Omega_j)^{m_0}}, \\ &= \sum_{j=1}^{J} (f|_{\Omega_j}, \phi|_{\Omega_j})_{L^2(\Omega_j)^{m_0}} = (f, \phi)_{L^2(\Omega)^{m_0}}, \end{aligned} \tag{9.48}$$

where we could write the last equality thanks to Assumption 3.10. Finally, using the same argument for the physical boundary condition on Γ, u is solution of the model problem (3.79). ∎

As in Proposition 3.25, we are again able to write a decomposition of the multi-trace space using the single and Cauchy trace spaces. Such a result was proven in the case of constant coefficients for instance in [32, Prop. 6.1] for the acoustic setting and in [37, Prop. 6.1] for the electromagnetic setting. The extension to variable coefficients for the acoustic setting is available in [29, Prop. 6.1].

Proposition 9.12. *We have the direct sum*

$$\mathbb{M}_\times = \mathbb{C}_\times \oplus \mathbb{S}_\times. \tag{9.49}$$

Proof.

Null intersection $\mathbb{C}_\times \cap \mathbb{S}_\times = \{0\}$. Let $\mathbb{x} \equiv (\mathrm{x}^j)_{j=1}^J \in \mathbb{C}_\times \cap \mathbb{S}_\times$. First, since $\mathbb{x} \in \mathbb{C}_\times$, from Definition 9.3 of the Cauchy trace space $\mathbb{C}_\times$, for all $j \in \{1, \dots, J\}$, we can find a lifting $u_j \in \mathrm{U}_\Gamma(\mathrm{D}; \Omega_j)$ such that

$$\begin{cases} (\mathrm{L}_{\mathsf{a}} - {\kappa_0}^2 \mathsf{n}) u_j = 0, & \text{in } \Omega_j, \\ (\gamma_{1,\Gamma} - \mathrm{i}\gamma_{0,\Gamma}) u_j = 0, & \text{on } \Gamma, \end{cases} \tag{9.50}$$

and

$$\gamma_{\tilde{\Gamma}_j} u_j = \mathrm{x}^j, \qquad \text{on } \tilde{\Gamma}_j. \tag{9.51}$$

Now let $u \in \mathbb{U}_\Gamma(\mathrm{D}; \mathcal{P}_\Omega)$ such that

$$u|_{\Omega_j} = u_j, \qquad \forall j \in \{1, \dots, J\}, \tag{9.52}$$

we remark that u belongs in fact to $\mathbb{U}_\Gamma(\mathrm{D}, \mathrm{L}_{\mathsf{a}}; \mathcal{P}_\Omega)$ (so that its trace $\boldsymbol{\gamma}_\times$ is well defined) and by construction it is such that

$$\boldsymbol{\gamma}_\times u = \mathbb{x} \in \mathbb{C}_\times \cap \mathbb{S}_\times. \tag{9.53}$$

From Proposition 9.11, it follows that u actually satisfies the homogeneous model problem (3.79) in the whole of Ω

$$\boldsymbol{\gamma}_\times u \in \mathbb{C}_\times \cap \mathbb{S}_\times \qquad \Leftrightarrow \qquad \begin{cases} u \in \mathrm{U}_\Gamma(\mathrm{D}; \Omega), \\ (\mathrm{L}_{\mathsf{a}} - {\kappa_0}^2 \mathsf{n}) u = 0, & \text{in } \Omega, \\ (\gamma_{1,\Gamma} - \mathrm{i}\gamma_{0,\Gamma}) u = 0, & \text{on } \Gamma. \end{cases} \tag{9.54}$$

The well-posedness of this problem (Assumption 3.9) yields $u = 0$, hence $\mathbb{x} = \boldsymbol{\gamma}_\times u = 0$.

Decomposition. Let $\mathbb{x} \equiv (\mathbb{x}_0, \mathbb{x}_1) \in \mathbb{M}_\times$ with $\mathbb{x}_0 \equiv (\mathrm{x}_0^j)_{j=1}^J$ and $\mathbb{x}_1 \equiv (\mathrm{x}_1^j)_{j=1}^J$. We wish to construct $\mathbb{y} \in \mathbb{C}_\times$ and $\mathbb{z} \in \mathbb{S}_\times$ such that $\mathbb{x} = \mathbb{y} + \mathbb{z}$. The proof performs explicitly the projection of $\mathbb{x}$ on the subspace $\mathbb{C}_\times$ in parallel to the subspace $\mathbb{S}_\times$. To construct $\mathbb{y}$, we proceed in two steps

1. Lifting of $\mathbb{x}_0$: define

$$\begin{cases} v \in \mathbb{U}_\Gamma(\mathrm{D}, \mathrm{L}_{\mathsf{a}}; \mathcal{P}_\Omega) \text{ such that,} \\ \boldsymbol{\gamma}_{0,\times} v = \mathbb{x}_0. \end{cases} \tag{9.55}$$

   Any such lifting will work, a particular lifting can be constructed for instance by solving coercive (note the change of sign in the equation and the real parts of the coefficients) local problems (which are well-posed):

$$\forall j \in \{1, \dots, J\}, \qquad \begin{cases} v|_{\Omega_j} \in \mathrm{U}_\Gamma(\mathrm{D}; \Omega_j) \text{ such that,} \\ (\mathrm{L}_{\Re(\mathsf{a})} + {\kappa_0}^2 \Re(\mathsf{n})) v|_{\Omega_j} = 0, & \text{in } \Omega_j, \\ (\gamma_{1,\Gamma} - \mathrm{i}\gamma_{0,\Gamma}) v|_{\Omega_j} = 0, & \text{on } \Gamma_j \cap \Gamma, \\ \gamma_{0,\Gamma_j} v|_{\Omega_j} = \mathrm{x}_0^j, & \text{on } \tilde{\Gamma}_j. \end{cases} \tag{9.56}$$

2. Lifting of $\mathbb{x}_1$: define (see (3.83) and (3.98) for the definition of the sesquilinear forms)

$$\begin{cases} w \in \mathrm{U}_\Gamma(\mathrm{D};\Omega) \text{ such that,} \\ a(w, w^t) = \mathbb{o}(v, w^t) - \langle\!\langle \mathbb{x}_1, \boldsymbol{\gamma}_{0,\times} w^t \rangle\!\rangle_{\|}, \qquad \forall w^t \in \mathrm{U}_\Gamma(\mathrm{D};\Omega). \end{cases} \tag{9.57}$$

Such a solution $w \in \mathrm{U}_\Gamma(\mathrm{D};\Omega)$ exists from the well-posedness of the model problem (3.79) (Assumption 3.9).

Let

$$\mathbb{y} \equiv (\mathbb{y}_0, \mathbb{y}_1) := \boldsymbol{\gamma}_\times(v - w). \tag{9.58}$$

Notice that, using the first Green identity (3.104) in each sub-domain Ω_j in (9.57), we have

$$\forall j \in \{1, \dots, J\}, \qquad \begin{cases} (\mathrm{L}_{\mathsf{a}} - {\kappa_0}^2 \mathsf{n})(v|_{\Omega_j} - w|_{\Omega_j}) = 0, & \text{in } \Omega_j, \\ (\gamma_{1,\Gamma} - \mathrm{i}\gamma_{0,\Gamma})(v|_{\Omega_j} - w|_{\Omega_j}) = 0, & \text{on } \Gamma_j \cap \Gamma. \end{cases} \tag{9.59}$$

It follows that $v - w \in \mathbb{U}_\Gamma(\mathrm{D};\mathcal{P}_\Omega)$ satisfies the PDE in each sub-domain Ω_j (and the physical boundary condition), Definition 9.3 of the Cauchy trace space $\mathbb{C}_\times$ yields $\mathbb{y} \in \mathbb{C}_\times$.

Now, let

$$\mathbb{z} \equiv (\mathbb{z}_0, \mathbb{z}_1) := \mathbb{x} - \mathbb{y}. \tag{9.60}$$

We have, by construction,

$$\mathbb{z}_0 = \mathbb{x}_0 - \mathbb{y}_0 = \mathbb{x}_0 - (\boldsymbol{\gamma}_{0,\times} v - \boldsymbol{\gamma}_{0,\times} w) = \boldsymbol{\gamma}_{0,\times} w. \tag{9.61}$$

Since $w \in \mathrm{U}_\Gamma(\mathrm{D};\Omega)$, by Definition 9.5 $\mathbb{z}_0 = \boldsymbol{\gamma}_{0,\times} w \in \mathbb{S}_{0,\times}$. To prove that $\mathbb{z}_1 \in \mathbb{S}_{1,\times}$, we take any $\mathbb{s}_0 \in \mathbb{S}_{0,\times}$ and we denote by $u_{\mathbb{s}_0} \in \mathrm{U}_\Gamma(\mathrm{D};\Omega)$ any lifting such that $\boldsymbol{\gamma}_{0,\times} u_{\mathbb{s}_0} = \mathbb{s}_0$, which exists by Definition 9.5. Using again the first Green identity (3.104) in each sub-domain, we have that

$$\langle\!\langle \boldsymbol{\gamma}_{1,\times}(v - w), \mathbb{s}_0 \rangle\!\rangle_\times = a(v - w, u_{\mathbb{s}_0}), \qquad \forall \mathbb{s}_0 \in \mathbb{S}_{0,\times}. \tag{9.62}$$

Hence, we deduce from (9.57) that

$$\langle\!\langle \mathbb{z}_1, \mathbb{s}_0 \rangle\!\rangle_\times = \langle\!\langle \mathbb{x}_1 - \mathbb{y}_1, \mathbb{s}_0 \rangle\!\rangle_\times = \langle\!\langle \mathbb{x}_1 - \boldsymbol{\gamma}_{1,\times}(v - w), \mathbb{s}_0 \rangle\!\rangle_\times = 0, \qquad \forall \mathbb{s}_0 \in \mathbb{S}_{0,\times}. \tag{9.63}$$

Therefore, using Proposition 9.9, we obtain $\mathbb{z}_1 \in \mathbb{S}_{1,\times}$ and $\mathbb{z} \in \mathbb{S}_\times$. Finally we have the constructed the decomposition

$$\mathbb{x} = \mathbb{y} + \mathbb{z}, \qquad \text{with} \qquad \begin{cases} \mathbb{y} \in \mathbb{C}_\times, \\ \mathbb{z} \in \mathbb{S}_\times. \end{cases} \tag{9.64}$$

■

Remark 9.13. *Note that the mechanism of the proof for the null intersection is very similar to the one in Chapter 3. In contrast, even though the general idea for the proof of the decomposition remains the same, the arguments used are significantly different. In particular, we are no longer able to explicitly interpret the underlying problem as a transmission problem since the notion of a jump is more delicate in the present setting. Note though that the problem* (3.161) *is stricly equivalent to the problem* (9.56)*, while the problem* (3.162) *has the same variational formulation as problem* (9.57)*.*

9.2.2 Reformulation as an interface problem

In this section, repeating the steps of Chapter 3, we exploit the above characterization (see Proposition 9.11) of the trace of the solution to equivalently recast the original problem (3.79) as a problem posed on the skeleton $\tilde{\Sigma}$ of the partition (see (9.99)).

9.2.2.1 Transmission operators and associated scalar products

Again, we start by introducing a key ingredient of our formulation, the transmission operators. Note that we have been unable in this new setting to introduce an equivalent operator to the operator $\mathbf{Z}$ from (3.173) in Chapter 3.

Definition 9.14 (**Transmission operators**). *We call* transmission *operators any* continuous *and* injective *mapping such that*

$$\begin{aligned} \mathbf{T}_{0,\times} &: \mathbb{M}_{0,\times} \to \mathbb{M}_{1,\times}, \\ \mathbf{T}_{1,\times} &: \mathbb{M}_{1,\times} \to \mathbb{M}_{0,\times}. \end{aligned} \tag{9.65}$$

Scalar products We have equipped our multi-trace spaces with the norm stemming from the Cartesian product structure of the multi-trace space. We now introduce different, albeit equivalent, norms.

Unless stated otherwise, we shall assume that the following assumption holds, thereby allowing us to define a scalar product (and associated norm) on the multi-trace spaces.

Assumption 9.15. *We suppose that the transmission operators are* self-adjoint positive definite isomorphisms *between the multi-trace spaces. In addition, we suppose to have the following relation*

$$\mathbf{T}_{1,\times} = (\mathbf{T}_{0,\times})^{-1}. \tag{9.66}$$

We can equip the multi-trace spaces $\mathbb{M}_{0,\times}$ and $\mathbb{M}_{1,\times}$respectively with the following scalar products

$$\begin{aligned} \mathrm{t}_{0,\times}(\mathbb{x}_0, \mathbb{y}_0) &:= \langle\!\langle \mathbf{T}_{0,\times}\mathbb{x}_0, \overline{\mathbb{y}_0} \rangle\!\rangle_\times, \qquad \forall \mathbb{x}_0, \mathbb{y}_0 \in \mathbb{M}_{0,\times}, \\ \mathrm{t}_{1,\times}(\mathbb{x}_1, \mathbb{y}_1) &:= \langle\!\langle \mathbb{y}_1, \mathbf{T}_{1,\times}\overline{\mathbb{x}_1} \rangle\!\rangle_\times, \qquad \forall \mathbb{x}_1, \mathbb{y}_1 \in \mathbb{M}_{1,\times}. \end{aligned} \tag{9.67}$$

Norms We can then endow the multi-trace spaces $\mathbb{M}_{0,\times}$ and $\mathbb{M}_{1,\times}$with the norms induced by the previous scalar products. Hence we define

$$\begin{aligned} \|\mathbb{x}_0\|^2_{\mathbf{T}_{0,\times}} &:= \mathrm{t}_{0,\times}(\mathbb{x}_0, \mathbb{x}_0), \qquad \forall \mathbb{x}_0 \in \mathbb{M}_{0,\times}, \\ \|\mathbb{x}_1\|^2_{\mathbf{T}_{1,\times}} &:= \mathrm{t}_{1,\times}(\mathbb{x}_1, \mathbb{x}_1), \qquad \forall \mathbb{x}_1 \in \mathbb{M}_{1,\times}. \end{aligned} \tag{9.68}$$

Remark 9.16. *Since the transmission operators are supposed to be continuous and coercive (by assumption 9.15), the norms defined in* (9.68) *are equivalent to the ones previously defined in* (9.11).

Generalized Robin operators We introduce similar operators as in Chapter 3. As before, the transmission operators are used to combine the two types of traces in the so-called generalized impedance multi-trace operator (Definition 9.17, counterpart of Definition 3.27), which in turn are used in the definition of the scattering operators (Definition 9.19, counterpart of Definition 3.29).

Definition 9.17 (**Generalized Robin operators**). *For each $\sigma \in \{0,1\}$, we introduce the global operators,*

$$\begin{aligned} \mathbf{R}^{\pm}_{\sigma,\times} &: \mathbb{M}_\times \to \mathbb{M}_{\sigma,\times}, \\ \aleph \equiv (\aleph_0, \aleph_1) &\mapsto \begin{cases} \pm\mathbf{T}_{1,\times}\aleph_1 - \mathrm{i}\aleph_0, & \text{if } \sigma = 0, \\ \pm\aleph_1 - \mathrm{i}\mathbf{T}_{0,\times}\aleph_0, & \text{if } \sigma = 1, \end{cases} \end{aligned} \tag{9.69}$$

9.2.2.2 Scattering operators

The definition of the scattering operators can be straightforwardly deduced in our new formalism from the one of Chapter 3. The required modifications are only minor but we stated them regardless for the sake of completeness.

Because of the abstract setting, we need again to first make the following assumption (which puts constraints on the transmission operators) before proceeding.

Assumption 9.18. *For each $\sigma \in \{0,1\}$ and for any $\aleph_\sigma \in \mathbb{M}_{\sigma,\times}$, $f \in L^2(\Omega)^{m_0}$, $g \in L^2(\Gamma)^{m_0}$, the transmission operators are such that the following problem is well-defined:*

$$\begin{cases} \text{Find } u_\sigma \in \mathbb{U}_\Gamma(\mathrm{D};\mathcal{P}_\Omega) \text{ such that} & \\ (\mathrm{L}_\mathsf{a} - {\kappa_0}^2\mathsf{n})u_\sigma|_{\Omega_j} = f|_{\Omega_j}, & \text{in } \Omega_j,\ \forall j \in \{1,\dots,J\}, \\ (\gamma_{1,\Gamma} - \mathrm{i}\gamma_{0,\Gamma})u_\sigma = g, & \text{on } \Gamma, \\ \mathbf{R}^{+}_{\sigma,\times}\boldsymbol{\gamma}_\times u_\sigma = \aleph_\sigma, & \text{on } \tilde{\Sigma}. \end{cases} \tag{9.70}$$

Upon satisfying the above assumption, we can now safely define the scattering operators.

Definition 9.19 (**Scattering operators**). *For each $\sigma \in \{0,1\}$, we define the global scattering operators,*

$$\begin{aligned} \mathbf{S}_{\sigma,\times} &: \mathbb{M}_{\sigma,\times} \to \mathbb{M}_{\sigma,\times}, \\ \aleph_\sigma &\mapsto \mathbf{R}^{-}_{\sigma,\times}\boldsymbol{\gamma}_\times u_\sigma, \end{aligned} \tag{9.71}$$

where $u_\sigma \in \mathbb{U}_\Gamma(\mathrm{D};\mathcal{P}_\Omega)$ is such that

$$\begin{cases} (\mathrm{L}_\mathsf{a} - {\kappa_0}^2\mathsf{n})u_\sigma|_{\Omega_j} = 0, & \text{in } \Omega_j,\ \forall j \in \{1,\dots,J\}, \\ (\gamma_{1,\Gamma} - \mathrm{i}\gamma_{0,\Gamma})u_\sigma = 0, & \text{on } \Gamma, \\ \mathbf{R}^{+}_{\sigma,\times}\boldsymbol{\gamma}_\times u_\sigma = \aleph_\sigma, & \text{on } \tilde{\Sigma}. \end{cases} \tag{9.72}$$

From the above definition, we readily obtain a characterization of the Cauchy trace space $\mathbb{C}_\times$ (Definition 9.3) as the kernel of an operator involving the generalized Robin operators $\mathbf{R}^{\sigma}_{\pm,\times}$ and the scattering operator $\mathbf{S}_{\sigma,\times}$.

Proposition 9.20 (**Characterization of the Cauchy trace space**). *For each $\sigma \in \{0,1\}$, we have the following characterization of the Cauchy-trace space* (9.3)*:*

$$\mathbb{C}_\times = \mathrm{Ker}\left(\mathbf{R}^{-}_{\sigma,\times} - \mathbf{S}_{\sigma,\times}\mathbf{R}^{+}_{\sigma,\times}\right). \tag{9.73}$$

Proof. ($\Rightarrow$) Let $\aleph \in \mathbb{C}_\times$. From Definition 9.3 of the Cauchy trace space $\mathbb{C}_\times$, there exists $u \in \mathrm{U}_\Gamma(\mathrm{D};\Omega_j)$ such that $\boldsymbol{\gamma}_\times u = \aleph$ and

$$\begin{cases} (\mathrm{L}_\mathsf{a} - {\kappa_0}^2\mathsf{n})u|_{\Omega_j} = 0, & \text{in } \Omega_j,\ \forall j \in \{1,\dots,J\} \\ (\gamma_{1,\Gamma} - \mathrm{i}\gamma_{0,\Gamma})|_{\Omega_j} = 0, & \text{on } \Gamma \cap \Gamma_j. \end{cases} \tag{9.74}$$

If, for any $\sigma \in \{0,1\}$, we let $\mathbb{y} := \mathbf{R}^+_{\sigma,\times}\boldsymbol{\gamma}_\times u = \mathbf{R}^+_{\sigma,\times}\mathbb{x}$, by Definition 9.19 of the scattering operator $\mathbf{S}_{\sigma,\times}$, we have $\mathbf{R}^-_{\sigma,\times}\boldsymbol{\gamma}_\times u := \mathbf{S}_{\sigma,\times}\mathbb{y}$ which is rewritten as $\mathbf{R}^-_{\sigma,\times}\mathbb{x} = \mathbf{S}_{\sigma,\times}\mathbf{R}^+_{\sigma,\times}\mathbb{x}$.

($\Leftarrow$) Let $\sigma \in \{0,1\}$ and $\mathbb{x} \in \mathbb{M}_\times$ be such that $\mathbf{R}^-_{\sigma,\times}\mathbb{x} = \mathbf{S}_{\sigma,\times}\mathbf{R}^+_{\sigma,\times}\mathbb{x}$. By Assumption 9.18, there exists $u_\sigma \in \mathrm{U}_\Gamma(\mathrm{D};\Omega_j)$ such that

$$\begin{cases} (\mathrm{L}_\mathsf{a} - \kappa_0{}^2\mathsf{n})u_\sigma|_{\Omega_j} = 0, & \text{in } \Omega_j,\ \forall j \in \{1,\dots,J\}, \\ (\gamma_{1,\Gamma} - \mathrm{i}\gamma_{0,\Gamma})u_\sigma = 0, & \text{on } \Gamma, \\ \mathbf{R}^+_{\sigma,\times}\boldsymbol{\gamma}_\times u_\sigma = \mathbf{R}^+_{\sigma,\times}\mathbb{x}, & \text{on } \tilde{\Sigma}, \end{cases} \tag{9.75}$$

and from Definition 9.19 of the scattering operator $\mathbf{S}_{\sigma,\times}$ we have $\mathbf{R}^-_{\sigma,\times}\boldsymbol{\gamma}_\times u_\sigma := \mathbf{S}_{\sigma,\times}\mathbf{R}^+_{\sigma,\times}\mathbb{x}$. It follows that

$$\begin{cases} \mathbf{R}^+_{\sigma,\times}\boldsymbol{\gamma}_\times u_\sigma = \mathbf{R}^+_{\sigma,\times}\mathbb{x}, \\ \mathbf{R}^-_{\sigma,\times}\boldsymbol{\gamma}_\times u_\sigma = \mathbf{R}^-_{\sigma,\times}\mathbb{x}. \end{cases} \tag{9.76}$$

It remains to prove that $\boldsymbol{\gamma}_\times u_\sigma = \mathbb{x}$. We give the proof for $\sigma = 1$, the other proof follows the same lines. By Definition 9.17 of the generalized Robin operators $\mathbf{R}^\pm_{\sigma,\times}$, the system (9.75) is rewritten as

$$\begin{cases} \boldsymbol{\gamma}_{1,\times}u_1 - \mathrm{i}\mathbf{T}_{0,\times}\boldsymbol{\gamma}_{0,\times}u_1 = \mathbb{x}_1 - \mathrm{i}\mathbf{T}_{0,\times}\mathbb{x}_0, \\ -\boldsymbol{\gamma}_{1,\times}u_1 - \mathrm{i}\mathbf{T}_{0,\times}\boldsymbol{\gamma}_{0,\times}u_1 = -\mathbb{x}_1 - \mathrm{i}\mathbf{T}_{0,\times}\mathbb{x}_0, \end{cases} \tag{9.77}$$

so that taking linear combinations we get

$$\begin{cases} \mathbf{T}_{0,\times}\,(\boldsymbol{\gamma}_{0,\times}u_1 - \mathbb{x}_0) = 0, \\ (\boldsymbol{\gamma}_{1,\times}u_1 - \mathbb{x}_1) = 0, \end{cases} \quad \Rightarrow \quad \begin{cases} \boldsymbol{\gamma}_{0,\times}u_1 = \mathbb{x}_0, \\ \boldsymbol{\gamma}_{1,\times}u_1 = \mathbb{x}_1, \end{cases} \quad \Rightarrow \quad \boldsymbol{\gamma}_\times u_1 = \mathbb{x}, \tag{9.78}$$

using the injectivity assumption on the transmission operator $\mathbf{T}_{0,\times}$ (Definition 9.14). ■

9.2.2.3 Communication operator

We define below an operator that plays the role of a communication operator in that it couples all local sub-problems together and will be used in the algorithm to exchange information between the subdomains. However, contrary to its counterpart $\boldsymbol{\Pi}_\parallel$ (Definition 3.31) in Chapter 3, this communication operator $\boldsymbol{\Pi}_{\sigma,\times}$ is no longer local and does not simply swap data at an interface. This is the reason why we no longer refer to it as an *exchange* operator, but prefer the term *communication*. We emphasize that the definition of this new operator is the key difference with the previous formalism that allows to make the leap forward in the clean treatment of junction points.

Helped by the following lemma, which is a direct consequence of Proposition 9.9, we are able to introduce orthogonal projectors onto the single trace spaces in Definition 9.22 before defining the communication operators in Definition 9.23.

Lemma 9.21. *For any $\sigma \in \{0,1\}$, the space $\mathbb{S}_\sigma$ is a closed subspace of $\mathbb{M}_{\sigma,\times}$.*

Definition 9.22 (**Orthogonal projectors**). *For each $\sigma \in \{0,1\}$, in the Hilbert space equipped with the norm stemming from the transmission operator $(\mathbb{M}_{\sigma,\times}, \|\cdot\|_{\mathbf{T}_{\sigma,\times}})$, we introduce the following orthogonal projectors*

$$\mathbf{P}_{\sigma,\times} : \mathbb{M}_{\sigma,\times} \to \mathbb{S}_\sigma \qquad \textit{and} \qquad \mathbf{P}^\perp_{\sigma,\times} : \mathbb{M}_{\sigma,\times} \to \mathbb{S}^\perp_\sigma \qquad \textit{satisfying} \qquad \mathrm{Id} = \mathbf{P}^\perp_{\sigma,\times} + \mathbf{P}_{\sigma,\times}. \tag{9.79}$$

Definition 9.23 (**Communication operators**). *We define the communication operators as*

$$\begin{aligned} \boldsymbol{\Pi}_{0,\times} &:= \mathrm{Id} - 2\mathbf{P}_{0,\times} : \mathbb{M}_{0,\times} \to \mathbb{M}_{0,\times}, \\ \boldsymbol{\Pi}_{1,\times} &:= 2\mathbf{P}_{1,\times} - \mathrm{Id} : \mathbb{M}_{1,\times} \to \mathbb{M}_{1,\times}. \end{aligned} \tag{9.80}$$

To compare with the theory of Chapter 3, observe that what was previously a property (see Proposition 3.34) is now a definition (Definition 9.22).

We emphasize that the orthogonal projectors, and therefore the communication operators, depend on our choice of norms (9.68) hence are intrinsically linked to the transmission operators (9.65).

The formal change of sign between the different values of σ will be explained when we explore the connections between the above operators and the usual communication operator $\mathbf{\Pi}_{\|}$ given in Definition 3.31 (see Section 9.2.3).

Remark 9.24 (**Practical computation of the projection**). *In practice, given $\mathbb{x}_\sigma \in \mathbb{M}_{\sigma,\times}$, for any $\sigma \in \{0,1\}$, one can compute $\mathbf{P}_{\sigma,\times}\mathbb{x}_\sigma \in \mathbb{S}_\sigma$ by solving the following coercive problem*

$$\mathrm{t}_{\sigma,\times}(\mathbf{P}_{\sigma,\times}\mathbb{x}_\sigma, \mathbb{y}_\sigma) = \mathrm{t}_{\sigma,\times}(\mathbb{x}_\sigma, \mathbb{y}_\sigma), \qquad \forall \mathbb{y}_\sigma \in \mathbb{S}_\sigma. \tag{9.81}$$

Of course this problem is global and is posed on the whole skeleton $\tilde{\Sigma}$. Here the choice of the scalar product $\mathrm{t}_{\sigma,\times}(\cdot,\cdot)$ does matter: it should be chosen so that the orthogonal projection in (9.81) *is easy to compute. This variational problem makes the operator $\mathbf{\Pi}_{\sigma,\times}$ a priori non-local. For certain choices of impedance, this communication operator may couple distant subdomain that are not a priori adjacent. This will be a salient feature of this new strategy, and a key difference in comparison with existing literature and the method described in Chapter 3.*

Admittedly, this non-locality raises a computational difficulty. We remark however that the variational problem (9.81) *is symmetric positive definite. Current literature offers very efficient scalable two level DDM preconditioners for tackling such a problem, see [127, §4.3], [113, §2.1] or [58, §6.4]. We shall present in the following the strategy that was adopted to solve* (9.81) *in practice in our numerical experiments, which is based on a (preconditioned) conjugate gradient algorithm. The key point being that the DD algorithm remains fully parallelizable, in particular on distributed-memory architectures, with only communications between neighbouring sub-domains.*

Remark 9.25. *For future reference, we give alternative expressions of the projectors in terms of the communication operators:*

$$\begin{aligned} \mathbf{P}_{1,\times} &= \frac{1}{2}\left(\mathrm{Id} - \mathbf{\Pi}_{1,\times}\right) \qquad \textit{and} \qquad \mathbf{P}_{1,\times}{}^{\perp} = \frac{1}{2}\left(\mathrm{Id} + \mathbf{\Pi}_{1,\times}\right), \\ \mathbf{P}_{\sigma,\times} &= \frac{1}{2}\left(\mathrm{Id} + \mathbf{\Pi}_{0,\times}\right) \qquad \textit{and} \qquad \mathbf{P}_{0,\times}{}^{\perp} = \frac{1}{2}\left(\mathrm{Id} - \mathbf{\Pi}_{0,\times}\right), \end{aligned} \tag{9.82}$$

The following proposition is immediate from the definition of the communication operators $\mathbf{\Pi}_{\sigma,\times}$ by simple properties of projectors.

Proposition 9.26 (**Isometric property**). *Let $\sigma \in \{0,1\}$, the communication operator $\mathbf{\Pi}_{\sigma,\times}$ is an involution*

$$\mathbf{\Pi}_{\sigma,\times}^2 = \mathrm{Id}, \qquad \textit{in } \mathbb{M}_{\sigma,\times}, \tag{9.83}$$

and an isometry of $\mathbb{M}_{\sigma,\times}$, for the norm induced by $\mathbf{T}_{\sigma,\times}$,

$$\|\mathbf{\Pi}_{\sigma,\times}\mathbb{x}_\sigma\|_{\mathbf{T}_{\sigma,\times}} = \|\mathbb{x}_\sigma\|_{\mathbf{T}_{\sigma,\times}}, \qquad \forall \mathbb{x}_\sigma \in \mathbb{M}_{\sigma,\times}. \tag{9.84}$$

As a consequence of Proposition 9.9 we have the following important decompositions. A similar result in a slightly different geometric configuration (in the whole space) and for the acoustic setting is available in [29, Prop. 4.2].

Proposition 9.27 (**Orthogonal decompositions of multi-trace spaces**). *For the scalar products on the multi-trace spaces* (9.67)*, the following direct sums hold and are orthogonal:*

$$\begin{aligned} \mathbb{M}_{0,\times} &:= \mathbb{S}_{0,\times} \oplus \mathbf{T}_{1,\times}\, \mathbb{S}_{1,\times}, \\ \mathbb{M}_{1,\times} &:= \mathbb{S}_{1,\times} \oplus \mathbf{T}_{0,\times}\, \mathbb{S}_{0,\times}. \end{aligned} \tag{9.85}$$

Proof. We prove the first result, the proofs for the other results are similar.

Decomposition Let $\mathbb{x}_0 \in \mathbb{M}_{0,\times}$ and set

$$\mathbb{y}_0 := \mathbf{P}_{0,\times}\mathbb{x}_0, \qquad \mathbb{z}_0 := \mathbb{x}_0 - \mathbb{y}_0. \tag{9.86}$$

By definition of the orthogonal projector (9.79), we have $\mathbb{y}_0 \in \mathbb{S}_{0,\times}$ and

$$\mathrm{t}_{0,\times}(\mathbb{y}_0, \mathbb{s}_0) = \mathrm{t}_{0,\times}(\mathbb{x}_0, \mathbb{s}_0), \quad \forall \mathbb{s}_0 \in \mathbb{S}_{0,\times}, \qquad \Leftrightarrow \qquad \langle\!\langle \mathbf{T}_{0,\times}\mathbb{z}_0, \mathbb{s}_0 \rangle\!\rangle_\times = 0, \quad \forall \mathbb{s}_0 \in \mathbb{S}_{0,\times}. \tag{9.87}$$

From Proposition 9.9, we have $\mathbf{T}_{0,\times}\mathbb{z}_0 \in \mathbb{S}_{1,\times}$ hence $\mathbb{z}_0 \in \mathbf{T}_{1,\times}\mathbb{S}_{1,\times}$.

Orthogonality Let $\mathbb{x}_0 \in \mathbb{S}_{0,\times}$ and $\mathbb{y}_1 \in \mathbb{S}_{1,\times}$, then $\overline{\mathbb{y}_1} \in \mathbb{S}_{1,\times}$. We have, by definition (9.67),

$$\mathrm{t}_{0,\times}(\mathbb{x}_0, \mathbf{T}_{1,\times}\mathbb{y}_1) = \langle\!\langle \mathbf{T}_{0,\times}\mathbb{x}_0, \overline{\mathbf{T}_{1,\times}\mathbb{y}_1} \rangle\!\rangle_\times. \tag{9.88}$$

As direct consequence of (9.66) and the self-adjoint properties of the operators $\mathbf{T}_{0,\times}$ and $\mathbf{T}_{1,\times}$, we get

$$\mathrm{t}_{0,\times}(\mathbb{x}_0, \mathbf{T}_{1,\times}\mathbb{y}_1) = \langle\!\langle \overline{\mathbb{y}_1}, \mathbb{x}_0 \rangle\!\rangle_\times. \tag{9.89}$$

Finally, using Proposition 9.9

$$\mathrm{t}_{0,\times}(\mathbb{x}_0, \mathbf{T}_{1,\times}\mathbb{y}_1) = 0. \tag{9.90}$$

■

Remark 9.28. *It is clear that, if Assumption 3.11 holds, the multi-trace spaces $\mathbb{M}_{0,\|}$, $\mathbb{M}_{1,\|}$ and $\mathbb{M}_\|$ from Definition 3.16 satisfy similar decompositions. We have*

$$\begin{aligned} \mathbb{M}_{0,\|} &:= \mathbb{S}_{0,\|} \oplus \mathbf{T}_{1,\|}\, \mathbb{S}_{1,\|}, \\ \mathbb{M}_{1,\|} &:= \mathbb{S}_{1,\|} \oplus \mathbf{T}_{0,\|}\, \mathbb{S}_{0,\|}. \end{aligned} \tag{9.91}$$

Again, we can characterize the single-trace space $\mathbb{S}_\times$ (Definition 9.5) as the kernel of an operator involving the generalized Robin operators $\mathbf{R}^\sigma_{\pm,\times}$ and the communication operator $\mathbf{\Pi}_{\sigma,\times}$. The following proposition, which follows from Proposition 9.27, is the counterpart of Proposition 3.37. A similar result in a slightly different setting (in the whole space) was proven for instance in [29, Prop. 5.4] for the acoustic setting.

Proposition 9.29 (**Characterization of the single-trace space**). *For each $\sigma \in \{0,1\}$, we have the following characterization of the single-trace space* (9.24)*:*

$$\mathbb{S}_\times = \mathrm{Ker}\left(\mathbf{R}^\pm_{\sigma,\times} - \mathbf{\Pi}_{\sigma,\times}\mathbf{R}^\mp_{\sigma,\times}\right). \tag{9.92}$$

Proof. First note that, for any $\sigma \in \{0,1\}$ and any $\mathbb{x} \in \mathbb{M}_\times$, $\mathbf{R}^+_{\sigma,\times}\mathbb{x} = \mathbf{\Pi}_{\sigma,\times}\mathbf{R}^-_{\sigma,\times}\mathbb{x}$ is equivalent to $\mathbf{R}^-_{\sigma,\times}\mathbb{x} = \mathbf{\Pi}_{\sigma,\times}\mathbf{R}^+_{\sigma,\times}\mathbb{x}$ since the exchange operator $\mathbf{\Pi}_{\sigma,\times}$ is an involution according to Proposition 9.26.

We prove the result for $\sigma = 1$, the other proof formally takes the same route. For all $\mathbb{x} \equiv (\mathbb{x}_0, \mathbb{x}_1) \in \mathbb{M}_\times \equiv \mathbb{M}_{0,\times} \times \mathbb{M}_{1,\times}$ we have, from (9.79)

$$\mathbb{x}_1 \in \mathbb{S}_{1,\times} \quad \Leftrightarrow \quad {\mathbf{P}_{1,\times}}^\perp \mathbb{x}_1 = 0, \tag{9.93}$$

and from (9.79), together with Proposition 9.27,

$$\mathbb{x}_0 \in \mathbb{S}_{0,\times} \quad \Leftrightarrow \quad \mathbf{T}_{0,\times}\mathbb{x}_0 \in \mathbf{T}_{0,\times}\mathbb{S}_{0,\times} = {\mathbb{S}_{1,\times}}^\perp \quad \Leftrightarrow \quad \mathbf{P}_{1,\times}\mathbf{T}_{0,\times}\mathbb{x}_0 = 0. \tag{9.94}$$

Hence, by simple properties of projectors, we have

$$\mathbb{x} \in \mathbb{S}_\times \quad \Leftrightarrow \quad {\mathbf{P}_{1,\times}}^\perp \mathbb{x}_1 + \mathrm{i}\mathbf{P}_{1,\times}\, \mathbf{T}_{0,\times}\mathbb{x}_0 = 0. \tag{9.95}$$

This is rewritten as, using the expressions of the projectors in term of the communication operator $\mathbf{\Pi}_{1,\times}$ from (9.82)

$$\begin{aligned} \mathbb{x} \in \mathbb{S}_\times \quad &\Leftrightarrow \quad (\mathbf{\Pi}_{1,\times} + \mathrm{Id})\mathbb{x}_1 + \mathrm{i}(\mathbf{\Pi}_{1,\times} - \mathrm{Id})\, \mathbf{T}_{0,\times}\mathbb{x}_0 = 0, \\ &\Leftrightarrow \quad \mathbb{x}_1 - \mathrm{i}\mathbf{T}_{0,\times}\mathbb{x}_0 = \mathbf{\Pi}_{1,\times}(-\mathbb{x}_1 - \mathrm{i}\mathbf{T}_{0,\times}\mathbb{x}_0). \end{aligned} \tag{9.96}$$

Finally, using Definition 9.17 of the generalized Robin operators, we get

$$\mathbb{x} \in \mathbb{S}_\times \quad \Leftrightarrow \quad \big(\mathbf{R}^{\pm}_{1,\times} - \mathbf{\Pi}_{1,\times}\mathbf{R}^{\pm}_{1,\times}\big)\,\mathbb{x} = 0. \tag{9.97}$$

■

9.2.2.4 Equivalent interface problem

With the help of the scattering operators $\mathbf{S}_{\sigma,\times}$ and exchange operator $\mathbf{\Pi}_{\sigma,\times}$ we are now in a position to recast the original problem (3.79) as a problem for the trace of the solution posed on the skeleton $\tilde{\Sigma}$. Importantly, it takes formally the same form as before (see Proposition 3.38). Unsurprisingly its proof follows very closely the one of its counterpart of Chapter 3 because it relies on the two characterisations (Propositions 9.20 and 9.29) of the Cauchy trace space $\mathbb{C}_\times$ and single trace space $\mathbb{S}_\times$, but we restate it here for completeness.

Proposition 9.30 (**Equivalent interface problem**). *Let $\sigma \in \{0,1\}$. Let $F_\sigma \in \mathbb{U}_\Gamma(\mathrm{D};\mathcal{P}_\Omega)$ be the (unique) source lifting such that*

$$\begin{cases} (\mathrm{L}_{\mathsf{a}} - \kappa_0{}^2\mathsf{n})F_\sigma|_{\Omega_j} = f|_{\Omega_j}, & \text{in } \Omega_j,\ \forall j \in \{1,\dots,J\}, \\ (\gamma_{1,\Gamma}\ - \mathrm{i}\gamma_{0,\Gamma}\,)F_\sigma = g, & \text{on } \Gamma, \\ \mathbf{R}^{+}_{\sigma,\times}\boldsymbol{\gamma}_\times F_\sigma = 0, & \text{on } \tilde{\Sigma}. \end{cases} \tag{9.98}$$

Consider the problem

$$\begin{cases} \text{Find } \mathbb{x}_\sigma \in \mathbb{M}_{\sigma,\times}, \\ (\mathrm{Id} - \mathbf{\Pi}_{\sigma,\times}\mathbf{S}_{\sigma,\times})\,\mathbb{x}_\sigma = \mathbf{\Pi}_{\sigma,\times}\mathbf{R}^{-}_{\sigma,\times}\boldsymbol{\gamma}_\times F_\sigma. \end{cases} \tag{9.99}$$

If $u \in \mathrm{U}_\Gamma(\mathrm{D};\Omega)$ is solution of the model problem (3.79), then its trace $\mathbb{x}_\sigma := \mathbf{R}^{+}_{\sigma,\times}\boldsymbol{\gamma}_\times u$ satisfies the interface problem (9.99).

Reciprocally, if $\mathbb{x}_\sigma \in \mathbb{M}_{\sigma,\times}$ is solution of the interface problem (9.99) and if $v_\sigma \in \mathbb{U}_\Gamma(\mathrm{D};\mathcal{P}_\Omega)$ is the (unique) solution of

$$\begin{cases} (\mathrm{L}_{\mathsf{a}} - \kappa_0{}^2\mathsf{n})v_\sigma|_{\Omega_j} = 0, & \text{in } \Omega_j,\ \forall j \in \{1,\dots,J\}, \\ (\gamma_{1,\Gamma}\ - \mathrm{i}\gamma_{0,\Gamma}\,)v_\sigma = 0, & \text{on } \Gamma, \\ \mathbf{R}^{+}_{\sigma,\times}\boldsymbol{\gamma}_\times v_\sigma = \mathbb{x}_\sigma, & \text{on } \tilde{\Sigma}, \end{cases} \tag{9.100}$$

then $u \in \mathbb{U}_\Gamma(\mathrm{D};\mathcal{P}_\Omega)$ defined as $u_\sigma := v_\sigma + F_\sigma$ is solution of the model problem (3.79).

Proof. Let F_σ be the unique solution (by Assumption 9.18) of (9.98), then it satisfies (9.38). We will rely on the characterization given by Proposition 9.11, which states that $u \in \mathrm{U}_\Gamma(\mathrm{D},\mathrm{L}_{\mathsf{a}};\Omega)$ is solution of the model problem (3.79) if, and only if,

$$\boldsymbol{\gamma}_\times u \in (\mathbb{C}_\times + \boldsymbol{\gamma}_\times F_\sigma) \cap \mathbb{S}_\times. \tag{9.101}$$

($\Rightarrow$) Let $u \in \mathrm{U}_\Gamma(\mathrm{D};\Omega)$ be the solution of the model problem (3.79), then $\boldsymbol{\gamma}_\times u \in (\mathbb{C}_\times + \boldsymbol{\gamma}_\times F_\sigma) \cap \mathbb{S}_\times$. From Propositions 9.20 and 9.29 we have

$$\begin{cases} \boldsymbol{\gamma}_\times(u - F_\sigma) \in \mathbb{C}_\times, \\ \boldsymbol{\gamma}_\times u \in \mathbb{S}_\times, \end{cases} \quad \Leftrightarrow \quad \begin{cases} \mathbf{R}^{-}_{\sigma,\times}\boldsymbol{\gamma}_\times(u - F_\sigma) = \mathbf{S}_{\sigma,\times}\mathbf{R}^{+}_{\sigma,\times}\boldsymbol{\gamma}_\times(u - F_\sigma), \\ \mathbf{R}^{+}_{\sigma,\times}\boldsymbol{\gamma}_\times u = \mathbf{\Pi}_{\sigma,\times}\mathbf{R}^{-}_{\sigma,\times}\boldsymbol{\gamma}_\times u. \end{cases} \tag{9.102}$$

hence using $\mathbf{R}^+_{\sigma,\times}\boldsymbol{\gamma}_\times F_\sigma = 0$ from (9.98) we deduce

$$\begin{cases} \mathbf{R}^-_{\sigma,\times}\boldsymbol{\gamma}_\times u = \mathbf{S}_{\sigma,\times}\mathbf{R}^+_{\sigma,\times}\boldsymbol{\gamma}_\times u + \mathbf{R}^-_{\sigma,\times}\boldsymbol{\gamma}_\times F_\sigma, \\ \mathbf{R}^+_{\sigma,\times}\boldsymbol{\gamma}_\times u = \boldsymbol{\Pi}_{\sigma,\times}\mathbf{R}^-_{\sigma,\times}\boldsymbol{\gamma}_\times u. \end{cases} \tag{9.103}$$

Eliminating $\mathbf{R}^-_{\sigma,\times}\boldsymbol{\gamma}_\times u$ it is then immediate that

$$\mathbf{R}^+_{\sigma,\times}\boldsymbol{\gamma}_\times u = \boldsymbol{\Pi}_{\sigma,\times}\mathbf{S}_{\sigma,\times}\mathbf{R}^+_{\sigma,\times}\boldsymbol{\gamma}_\times u + \boldsymbol{\Pi}_{\sigma,\times}\mathbf{R}^-_{\sigma,\times}\boldsymbol{\gamma}_\times F_\sigma, \tag{9.104}$$

hence its trace $\mathbb{x}_\sigma := \mathbf{R}^+_{\sigma,\times}\boldsymbol{\gamma}_\times u$ satisfies the interface problem (9.99).

($\Leftarrow$) Reciprocally, let $\mathbb{x}_\sigma \in \mathbb{M}_{\sigma,\times}$ be solution of the interface problem (9.99) and let $v_\sigma \in \mathbb{U}_\Gamma(\mathrm{D};\mathcal{P}_\Omega)$ be the unique solution (by Assumption 9.18) to (9.100). Then, by definition of the Cauchy trace space $\mathbb{C}_\times$ (Definition 3.18), its trace $\boldsymbol{\gamma}_\times v_\sigma \in \mathbb{C}_\times$. If we set $u_\sigma := v_\sigma + F_\sigma$, we readily obtain $\boldsymbol{\gamma}_\times(u_\sigma - F_\sigma) \in \mathbb{C}_\times$. Besides, using $\mathbb{x}_\sigma = \mathbf{R}^+_{\sigma,\times}\boldsymbol{\gamma}_\times v_\sigma$ from (9.100), we rewrite (9.99) as

$$(\mathrm{Id} - \boldsymbol{\Pi}_{\sigma,\times}\mathbf{S}_{\sigma,\times})\,\mathbb{x}_\sigma = \boldsymbol{\Pi}_{\sigma,\times}\mathbf{R}^-_{\sigma,\times}\boldsymbol{\gamma}_\times F_\sigma, \quad \Leftrightarrow \quad (\mathrm{Id} - \boldsymbol{\Pi}_{\sigma,\times}\mathbf{S}_{\sigma,\times})\,\mathbf{R}^+_{\sigma,\times}\boldsymbol{\gamma}_\times v_\sigma = \boldsymbol{\Pi}_{\sigma,\times}\mathbf{R}^-_{\sigma,\times}\boldsymbol{\gamma}_\times F_\sigma. \tag{9.105}$$

Using Proposition 9.20 we get

$$\mathbf{R}^+_{\sigma,\times}\boldsymbol{\gamma}_\times v_\sigma - \boldsymbol{\Pi}_{\sigma,\times}\mathbf{R}^-_{\sigma,\times}\boldsymbol{\gamma}_\times v_\sigma = \boldsymbol{\Pi}_{\sigma,\times}\mathbf{R}^-_{\sigma,\times}\boldsymbol{\gamma}_\times F_\sigma. \tag{9.106}$$

Finally, using the fact that $\mathbf{R}^+_{\sigma,\times}\boldsymbol{\gamma}_\times F_\sigma = 0$ from (9.98) and the definition of u_σ yield

$$\mathbf{R}^+_{\sigma,\times}\boldsymbol{\gamma}_\times u_\sigma = \boldsymbol{\Pi}_{\sigma,\times}\mathbf{R}^-_{\sigma,\times}\boldsymbol{\gamma}_\times u_\sigma. \tag{9.107}$$

Proposition 9.29 then gives $\boldsymbol{\gamma}_\times u_\sigma \in \mathbb{S}_\times$. Finally we indeed have $\boldsymbol{\gamma}_\times u_\sigma \in (\mathbb{C}_\times + \boldsymbol{\gamma}_\times F_\sigma) \cap \mathbb{S}_\times$. ■

Remark 9.31. *Again, it is perhaps worth mentioning an alternative equivalent interface problem, exchanging the order of composition of* $\mathbf{S}_{\sigma,\times}$ *and* $\boldsymbol{\Pi}_{\sigma,\times}$. *Let* $\sigma \in \{0,1\}$ *and consider instead the alternative interface problem*

$$\begin{cases} \textit{Find } \mathbb{x}_\sigma \in \mathbb{M}_{\sigma,\times}, \\ (\mathrm{Id} - \mathbf{S}_{\sigma,\times}\boldsymbol{\Pi}_{\sigma,\times})\,\mathbb{x}_\sigma = \mathbf{R}^-_{\sigma,\times}\boldsymbol{\gamma}_\times F_\sigma. \end{cases} \tag{9.108}$$

If $u \in \mathrm{U}_\Gamma(\mathrm{D};\Omega)$ *is solution of the model problem* (3.79)*, then its trace* $\mathbb{x}_\sigma := \mathbf{R}^-_{\sigma,\times}\boldsymbol{\gamma}_\times u$ *satisfies the interface problem* (9.108)*. Reciprocally, if* $\mathbb{x}_\sigma \in \mathbb{M}_{\sigma,\times}$ *is solution of the interface problem* (9.108) *and if* $v_\sigma \in \mathbb{U}_\Gamma(\mathrm{D};\mathcal{P}_\Omega)$ *is the (unique) solution of* (9.100) *then* $u \in \mathbb{U}_\Gamma(\mathrm{D};\mathcal{P}_\Omega)$ *defined as* $u_\sigma := v_\sigma + F_\sigma$ *is solution of the model problem* (3.79).

9.2.2.5 Block diagonal transmission operators

Again, we now investigate the particular case of *block diagonal* transmission operators. We emphasize that also in this new framework this sub-case is in fact the *only case of practical interest* as any other alternative would prevent us to get any parallelization of the domain decomposition algorithm. It is interesting to note though that the theory does not rest on this assumption. As a result, one would typically impose the following additional requirement (which is not restrictive) on the transmission operators.

Assumption 9.32 (**Block diagonal transmission operator**). *The operator* $\mathbf{T}_{\sigma,\times}$, $\sigma \in \{0,1\}$, *viewed as an operator matrix of size* $J \times J$, *is diagonal*

$$\mathbf{T}_{\sigma,\times} = diag_{j\in\{1,\dots,J\}}\left(\mathbf{T}^j_{\sigma,\times}\right), \tag{9.109}$$

where, for all $j \in \{1,\dots,J\}$, *we have*

$$\begin{aligned} \mathbf{T}^j_{0,\times} &: \mathrm{X}_0(\Gamma_j) \to \mathrm{X}_1(\Gamma_j), \\ \mathbf{T}^j_{1,\times} &: \mathrm{X}_1(\Gamma_j) \to \mathrm{X}_0(\Gamma_j). \end{aligned} \tag{9.110}$$

We provide an example of a diagonal transmission operator in Figure 9.6. This sketch correspond to the top-right geometrical configuration that is given in Figure 3.1c. The non-zero operators are represented by the hatched areas. For comparison, the sketches of admissible transmission operators for the previous formalism were provided in Figure 3.4.

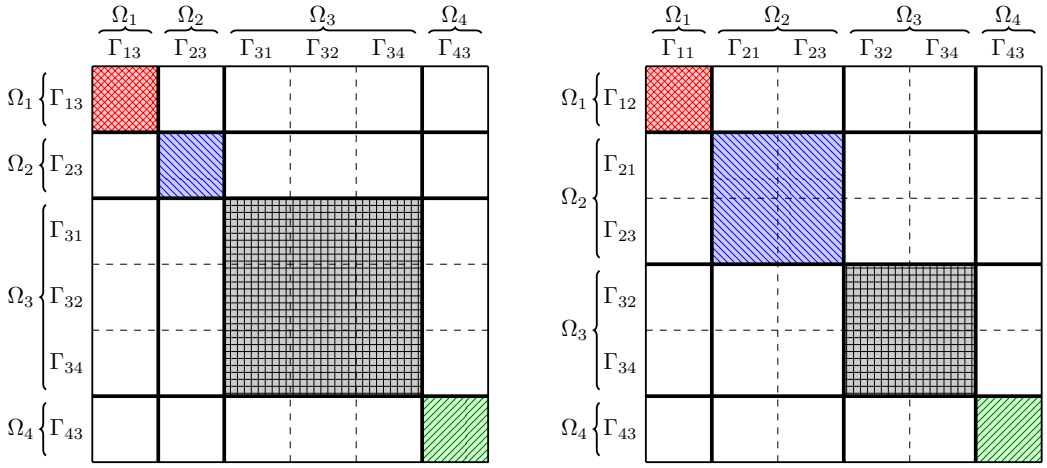

(a) Top right geometric partition in Figure 3.1c. (b) Bottom geometric partition in Figure 3.1c.

Figure 9.6: Sketch of the operator matrix of diagonal transmission operators of the top right geometric partition in Figure 3.1c. The non-zero operators are featured by the hatched areas.

Furthermore, the diagonal structure of the transmission operators implies a diagonal structure for the scattering operator. To see that we first introduce local versions of the Robin operators at an interface.

Definition 9.33 (**Local generalized Robin operators**). *For each* $\sigma \in \{0,1\}$ *and* $j \in \{1,\dots,J\}$, *we introduce the local operators,*

$$\begin{aligned} \mathbf{R}^{j,\pm}_{\sigma,\times} &: \mathrm{X}(\tilde{\Gamma}_j) \to \mathrm{X}_\sigma(\tilde{\Gamma}_j), \\ \mathrm{x} \equiv (\mathrm{x}_0,\mathrm{x}_1) &\mapsto \begin{cases} \pm\mathbf{T}^j_{1,\times}\mathrm{x}_1 - \mathrm{i}\varkappa_0\mathrm{x}_0, & \text{if } \sigma = 0, \\ \pm\mathrm{x}_1 - \mathrm{i}\mathbf{T}^j_{0,\times}\mathrm{x}_0, & \text{if } \sigma = 1, \end{cases} \end{aligned} \tag{9.111}$$

Then, for each $\sigma \in \{0,1\}$, we have

$$\mathbf{S}_{\sigma,\times} = \mathrm{diag}_{j\in\{1,\dots,J\}}\left(\mathbf{S}^j_{\sigma,\times}\right), \tag{9.112}$$

where the local scattering operators are given in the following definition.

Definition 9.34 (**Local scattering operator**). *For each $\sigma \in \{0,1\}$ and $j \in \{1,\dots,J\}$, we define the local scattering operators,*

$$\begin{aligned} \mathbf{S}^j_{\sigma,\times} \ &: \mathrm{X}_\sigma(\tilde\Gamma_j) \to \mathrm{X}_\sigma(\tilde\Gamma_j), \\ &\mathrm{x}^j_\sigma \mapsto \ \mathbf{R}^{j,-}_{\sigma,\times}\, \gamma_{\tilde\Gamma_j}\, u_{\sigma,j}, \end{aligned} \tag{9.113}$$

where, for all $j \in \{1,\dots,J\}$, $u_{\sigma,j} \in \mathrm{U}_\Gamma(\mathrm{D};\Omega_j)$ is such that

$$\begin{cases} (\mathrm{L}_{\mathsf{a}} - {\kappa_0}^2 \mathsf{n}) u_{\sigma,j}|_{\Omega_j} = 0, & \text{in } \Omega_j, \\ (\gamma_{1,\Gamma} - \mathrm{i}\gamma_{0,\Gamma}) u_{\sigma,j} = 0, & \text{on } \Gamma, \\ \mathbf{R}^{j,+}_{\sigma,\times}\, \gamma_{\tilde\Gamma_j}\, u_{\sigma,j} = \mathrm{x}^j_\sigma, & \text{on } \tilde\Gamma_j. \end{cases} \tag{9.114}$$

It is now clear that applying the scattering operator consists in solving local problems locally in each subdomain (hence hopefully in parallel), thereby insuring that the PDE is satisfied locally. It is the communication operator that couples all sub-domains together by exchanging information, thereby insuring the global continuity of the solution.

Besides, we note that satisfying Assumption 9.18 now amounts to satisfy the following assumption.

Assumption 9.35 (**Well-posedness of local sub-problems**). *For each $\sigma \in \{0,1\}$, $j \in \{1,\dots,J\}$ and for any $\mathrm{x}^j_\sigma \in \mathrm{X}_\sigma(\Gamma_j)$, $f \in L^2(\Omega)^{m_0}$, $g \in L^2(\Gamma)^{m_0}$, the transmission operators are such that the following local sub-problems are well-defined:*

$$\begin{cases} \text{Find } u_{\sigma,j} \in \mathrm{U}_\Gamma(\mathrm{D};\Omega_j) \text{ such that} & \\ (\mathrm{L}_{\mathsf{a}} - {\kappa_0}^2 \mathsf{n}) u_{\sigma,j} = f|_{\Omega_j}, & \text{in } \Omega_j, \\ (\gamma_{1,\Gamma} - \mathrm{i}\gamma_{0,\Gamma}) u_{\sigma,j} = g, & \text{on } \Gamma_j \cap \Gamma, \\ \mathbf{R}^{j,+}_{\sigma,\times}\, \gamma_{\Gamma_j}\, u_{\sigma,j} = \mathrm{x}^j_\sigma, & \text{on } \Gamma_j. \end{cases} \tag{9.115}$$

9.2.3 The case of no junctions

We investigate briefly the relations between the interface problems (3.200) and (9.99), as well as the operators involved when, as we shall assume in this section, Assumption 3.11 holds (as well as Assumption 3.12). Beyond all the similarities between the two formalisms, the two methods can actually be equivalent.

First, recall from Remark 9.2 that one can identify the two multi-trace spaces $\mathbb{M}_\times$ and $\mathbb{M}_\parallel$. Using the same process, the spaces $\mathbb{C}_\times$ and $\mathbb{C}_\parallel$ (respectively $\mathbb{S}_\times$ and $\mathbb{S}_\parallel$) can also be identified.

We shall study only the case where diagonal transmission operators are used, in the sense of Assumption 3.40 and Assumption 9.32. A moment of thought will reveal that, in order to have some sort of equivalence between the two formalisms, the main requirement on the transmission operators is to satisfy the kind of symmetry with respect to each interface stated in Proposition 3.41. This motivates the following assumption.

Assumption 9.36 (**Compatibility condition on the transmission operators**). *For each $\sigma \in \{0,1\}$, there exists a family of operators $\left(\mathbf{T}^{jk}_{\sigma,\parallel}\right)_{(j,k)\in\mathbb{J}}$ of self-adjoint positive definite isomorphisms satisfying* (3.213) *such that the operator $\mathbf{T}_{\sigma,\parallel}$ is diagonal in the form of* (3.210)*. In addition, this family $\left(\mathbf{T}^{jk}_{\sigma,\parallel}\right)_{(j,k)\in\mathbb{J}}$ defines another family of operators $\left(\mathbf{T}^{j}_{\sigma,\times}\right)_{j=1}^{J}$ satisfying*

$$\left(\mathbf{T}^j_{\sigma,\times}\mathrm{x}^j_\sigma\right)|_{\Gamma_{jk}} = \mathbf{T}^{jk}_{\sigma,\parallel}\left(\mathrm{x}^j_\sigma|_{\Gamma_{jk}}\right), \qquad \forall \mathrm{x}^j_\sigma \in \mathrm{X}_\sigma\left(\tilde\Gamma_j\right),\ \forall (j,k) \in \mathbb{J}. \tag{9.116}$$

such that the operator $\mathbf{T}_{\sigma,\times}$ is diagonal in the sense of (9.109)*.*

It is straightforward to show that if Assumption 9.36 holds, the Robin trace operators, defined respectively in Definition 3.27 and Definition 9.17, and the scattering operators, defined respectively in Definition 3.29 and Definition 9.19, are equivalent. Of course, the scalar product and norms on the respective multi-trace spaces also coincide. The much more obscure point is the agreement between the exchange and communication operators, which is the subject of the following proposition.

Proposition 9.37 (**Equivalence between the exchange and communication operators**). *If Assumption 3.11 and Assumption 9.36 hold, then we have*

$$\mathbf{\Pi}_{\sigma,\times} \equiv \mathbf{\Pi}_{\shortparallel}, \qquad \forall \sigma \in \{0,1\}, \tag{9.117}$$

with $\mathbf{\Pi}_{\shortparallel}$ *as in Definition 3.31 and* $\mathbf{\Pi}_{\sigma,\times}$ *as in Definition 9.23.*

Proof. Suppose first that $\sigma = 1$. It is straightforward to check that the operator

$$\mathbf{P}_{1,\shortparallel} := \frac{1}{2}\left(\mathrm{Id} - \mathbf{\Pi}_{\shortparallel}\right), \tag{9.118}$$

is a projector. Moreover, the single trace space $\mathbb{S}_{1,\shortparallel}$ is included in its range.

Since Assumption 9.36 holds, the transmission operator $\mathbf{T}_{0,\shortparallel}$ is diagonal and Proposition 3.41 gives us that it commutes with the exchange operator $\mathbf{\Pi}_{\shortparallel}$ (Assumption 3.36 holds). It follows that $\mathbf{T}_{0,\shortparallel}\mathbb{S}_{0,\shortparallel}$ is included in the kernel of the projector $\mathbf{P}_{1,\shortparallel}$. From the decomposition of the multi-trace space (9.91), we have that $\mathrm{Rg}\,\mathbf{P}_{1,\shortparallel} = \mathbb{S}_{1,\shortparallel}$ and $\mathrm{Ker}\,\mathbf{P}_{1,\shortparallel} = \mathbf{T}_{0,\shortparallel}\mathbb{S}_{0,\shortparallel}$.

Using the same arguments, $\mathbf{T}_{1,\shortparallel}$ commutes with $\mathbf{\Pi}_{\shortparallel}$. It follows (see Proposition 3.54) that $\mathbf{\Pi}_{\shortparallel}$, hence the projector $\mathbf{P}_{1,\shortparallel}$, is self-adjoint with respect to the scalar product induced by $\mathbf{T}_{1,\shortparallel}$. As a result, the projector $\mathbf{P}_{1,\shortparallel}$ is an orthogonal projector with respect to this scalar product. Therefore, $\mathbf{P}_{1,\shortparallel} \equiv \mathbf{P}_{1,\times}$ and $\mathbf{\Pi}_{\shortparallel} \equiv \mathbf{\Pi}_{1,\times}$.

For the cases $\sigma \in \{0\}$ the arguments are similar but notice that, for instance for $\sigma = 0$, we need to introduce (note the formal change of sign)

$$\mathbf{P}_{0,\shortparallel} := \frac{1}{2}\left(\mathrm{Id} + \mathbf{\Pi}_{\shortparallel}\right), \tag{9.119}$$

to have a projector on the single trace space $\mathbb{S}_{0,\shortparallel}$. This explains the formal change of sign in Definition 9.23 of the communication operators. ■

To sum up, we can state the following proposition which shows that the method introduced in this chapter is actually a true generalization to the configuration with cross points of the method described in Chapter 3.

Proposition 9.38 (**Equivalence between the two formalisms**). *If Assumption 3.11 and Assumption 9.36 hold, the interface problems* (3.200) *and* (9.99) *are equivalent.*

9.3 Iterative domain decomposition methods

Again, one can see (at last) the purpose of our reformulation of the model problem (3.79) in the form of the interface problem (9.99) when we consider iterative solvers to provide an actual practical way of computing a solution. Indeed, iterative methods will construct sequences of (broken) solutions by solving independently (hence hopefully in parallel) local sub-problems and exchanging or communicating information between sub-domains.

9.3.1 Iterative algorithm

Let $\sigma \in \{0,1\}$, F_σ be the solution of (9.98), and define

$$\mathbb{b}_\sigma := \mathbf{\Pi}_{\sigma,\times}\mathbf{R}^-_{\sigma,\times}\boldsymbol{\gamma}_\times F_\sigma. \tag{9.120}$$

In this section, we want to devise (and study the convergence of) an algorithm to solve

$$\begin{cases} \text{Find } \mathbb{x}_\sigma \in \mathbb{M}_{\sigma,\times} \text{ such that,} \\ (\mathrm{Id} - \mathbf{\Pi}_{\sigma,\times}\mathbf{S}_{\sigma,\times})\,\mathbb{x}_\sigma = \mathbb{b}_\sigma. \end{cases} \tag{9.121}$$

Recall that, according to Proposition 9.11, having found such a $\mathbb{x}_\sigma$ solution of (9.121), the global volume solution of the model problem (3.79) can be computed as

$$u_\sigma := v_\sigma + F_\sigma, \tag{9.122}$$

where $v_\sigma \in \mathbb{U}_\Gamma(\mathrm{D};\mathcal{P}_\Omega)$ is such that

$$\begin{cases} (\mathrm{L_a} - \kappa_0{}^2\mathsf{n})v_\sigma|_{\Omega_j} = 0, & \text{in } \Omega_j,\ \forall j \in \{1,\dots,J\}, \\ (\gamma_{1,\Gamma} - \mathrm{i}\gamma_{0,\Gamma})v_\sigma = 0, & \text{on } \Gamma, \\ \mathbf{R}^+_{\sigma,\times}\boldsymbol{\gamma}_\times v_\sigma = \mathbb{x}_\sigma, & \text{on } \tilde{\Sigma}, \end{cases} \tag{9.123}$$

which is well-posed according to Assumption 9.18.

Richardson algorithm We can use again for problem (9.121) a fixed point iteration algorithm, counterpart of (3.225), which is not strictly speaking a Jacobi algorithm any more but rather a Richardson algorithm. Let $\mathbb{x}^0_\sigma \in \mathbb{M}_{\sigma,\times}$ and a relaxation parameter $0 < r \leq 1$ be given, a sequence $(\mathbb{x}^n_\sigma)_{n\in\mathbb{N}}$ in $\mathbb{M}_{\sigma,\times}$ is constructed as follows

$$\mathbb{x}^{n+1}_\sigma = [(1-r)\mathrm{Id} + r\mathbf{\Pi}_{\sigma,\times}\mathbf{S}_{\sigma,\times}]\,\mathbb{x}^n_\sigma + r\,\mathbb{b}_\sigma, \qquad n \in \mathbb{N}. \tag{9.124}$$

Constructing this sequence of traces also constructs a sequence of broken solutions $(v^n_\sigma)_{n\in\mathbb{N}}$ in $\mathbb{U}_\Gamma(\mathrm{D};\mathcal{P}_\Omega)$ when the action of $\mathbf{S}_{\sigma,\times}$ is computed. For each $n \in \mathbb{N}$ the broken solution v^n_σ satisfy

$$\begin{cases} (\mathrm{L_a} - \kappa_0{}^2\mathsf{n})v^n_\sigma|_{\Omega_j} = 0, & \text{in } \Omega_j,\ \forall j \in \{1,\dots,J\}, \\ (\gamma_{1,\Gamma} - \mathrm{i}\gamma_{0,\Gamma})v^n_\sigma = 0, & \text{on } \Gamma, \\ \mathbf{R}^+_{\sigma,\times}\boldsymbol{\gamma}_\times v^n_\sigma = \mathbb{x}^n_\sigma, & \text{on } \tilde{\Sigma}. \end{cases} \tag{9.125}$$

The true solution of the original problem is then (hopefully, if convergence occurs) the limit of the broken solutions $(u^n_\sigma := v^n_\sigma + F_\sigma)_{n\in\mathbb{N}}$ in $\mathbb{U}_\Gamma(\mathrm{D};\mathcal{P}_\Omega)$.

It is clear that this new algorithm is formally very close to its counterpart from Chapter 3.

9.3.2 Convergence analysis

We now turn to the convergence analysis of the previously described iterative method.

It is clear that the new interface problem (9.121) takes the form of the abstract problem (3.230). To prove the geometric convergence of the above fixed point algorithm, we simply need to check that the assumptions of Proposition 3.57 are satisfied in our particular case where $V = \mathbb{M}_{\sigma,\times}$ and $A = \mathbf{\Pi}_{\sigma,\times}\mathbf{S}_{\sigma,\times}$.

To prove the property of contraction of $\mathbf{\Pi}_{\sigma,\times}\mathbf{S}_{\sigma,\times}$, we first need to establish the following lemma, which rests in particular on Assumption 9.15.

Lemma 9.39. *For each $\sigma \in \{0,1\}$, we have,*

$$\|\mathbf{R}^-_{\sigma,\times}\mathbb{x}\|^2_{\mathbf{T}_{\sigma,\times}} - \|\mathbf{R}^+_{\sigma,\times}\mathbb{x}\|^2_{\mathbf{T}_{\sigma,\times}} = 2\mathrm{i}[\![\mathbb{x},\overline{\mathbb{x}}]\!]_\times, \qquad \forall \mathbb{x} \in \mathbb{M}_\times. \tag{9.126}$$

Proof. We prove the equality for $\sigma = 1$, the other proof is similar. Let $\mathbb{x} \equiv (\mathbb{x}_0, \mathbb{x}_1) \in \mathbb{M}_\times$. By Definition 9.17 of the generalized Robin operator $\mathbf{R}^+_{1,\times}$ and by definition of the norms (9.68) we have

$$\begin{aligned} \|\mathbf{R}^+_{1,\times}\mathbb{x}\|^2_{\mathbf{T}_{1,\times}} &= \|\mathbb{x}_1 - \mathrm{i}\mathbf{T}_{0,\times}\mathbb{x}_0\|^2_{\mathbf{T}_{1,\times}}, \\ &= \langle\!\langle \mathbb{x}_1 - \mathrm{i}\mathbf{T}_{0,\times}\mathbb{x}_0,\ \mathbf{T}_{1,\times}\overline{(\mathbb{x}_1 - \mathrm{i}\mathbf{T}_{0,\times}\mathbb{x}_0)}\rangle\!\rangle_\times, \end{aligned} \tag{9.127}$$

using Assumption 9.15 we obtain

$$\|\mathbf{R}^+_{1,\times}\mathbb{x}\|^2_{\mathbf{T}_{1,\times}} = \langle\!\langle \mathbb{x}_1 - \mathrm{i}\mathbf{T}_{0,\times}\mathbb{x}_0,\ \mathbf{T}_{1,\times}\overline{\mathbb{x}_1} + \mathrm{i}\overline{\mathbb{x}_0}\rangle\!\rangle_\times, \tag{9.128}$$

so that using again Assumption 9.15 and the self-adjointness of $\mathbf{T}_{0,\times}$, we get

$$\begin{aligned} \|\mathbf{R}^+_{1,\times}\mathbb{x}\|^2_{\mathbf{T}_{1,\times}} &= \|\mathbb{x}_1\|^2_{\mathbf{T}_{1,\times}} + \|\mathbb{x}_0\|^2_{\mathbf{T}_{0,\times}} - \mathrm{i}\langle\!\langle \overline{\mathbb{x}_1}, \mathbb{x}_0\rangle\!\rangle_\times + \mathrm{i}\langle\!\langle \mathbb{x}_1, \overline{\mathbb{x}_0}\rangle\!\rangle_\times, \\ &= \|\mathbb{x}_1\|^2_{\mathbf{T}_{1,\times}} + \|\mathbb{x}_0\|^2_{\mathbf{T}_{0,\times}} - 2\Im\langle\!\langle \mathbb{x}_1, \overline{\mathbb{x}_0}\rangle\!\rangle_\times. \end{aligned} \tag{9.129}$$

Finally using Lemma 3.6, we obtain

$$\|\mathbf{R}^+_{1,\times}\mathbb{x}\|^2_{\mathbf{T}_{1,\times}} = \|\mathbb{x}_1\|^2_{\mathbf{T}_{1,\times}} + \|\mathbb{x}_0\|^2_{\mathbf{T}_{0,\times}} - \mathrm{i}[\![\mathbb{x},\overline{\mathbb{x}}]\!]_\times. \tag{9.130}$$

Similarly,

$$\|\mathbf{R}^-_{1,\times}\mathbb{x}\|^2_{\mathbf{T}_{1,\times}} = \|\mathbb{x}_1\|^2_{\mathbf{T}_{1,\times}} + \|\mathbb{x}_0\|^2_{\mathbf{T}_{0,\times}} + \mathrm{i}[\![\mathbb{x},\overline{\mathbb{x}}]\!]_\times. \tag{9.131}$$

■

We are now able to prove the property of contraction of the scattering operator $\mathbf{S}_{\sigma,\times}$ (Definition 9.19). A similar result in a slightly different setting (in the whole space but for the scalar equation only) can also be found in [29, Lem. 7.1].

Proposition 9.40 (**Contraction property of the scattering operator**). *Let $\sigma \in \{0,1\}$, the scattering operator $\mathbf{S}_{\sigma,\times}$ is a contraction of $\mathbb{M}_{\sigma,\times}$, for our particular choice of norm* (9.68)*,*

$$\|\mathbf{S}_{\sigma,\times}\mathbb{x}_\sigma\|_{\mathbf{T}_{\sigma,\times}} \leq \|\mathbb{x}_\sigma\|_{\mathbf{T}_{\sigma,\times}}, \qquad \forall \mathbb{x}_\sigma \in \mathbb{M}_{\sigma,\times}. \tag{9.132}$$

Proof. Let $\sigma \in \{0,1\}$ and $\mathbb{x}_\sigma \in \mathbb{M}_{\sigma,\times}$. Let us introduce $u_\sigma \in \mathbb{U}_\Gamma(\mathrm{D};\mathcal{P}_\Omega)$ be such that

$$\begin{cases} (\mathrm{L}_{\mathsf{a}} - \kappa_0{}^2\mathsf{n})u_\sigma|_{\Omega_j} = 0, & \text{in } \Omega_j,\ \forall j \in \{1,\dots,J\}, \\ (\gamma_{1,\Gamma} - \mathrm{i}\gamma_{0,\Gamma})u_\sigma = 0, & \text{on } \Gamma, \\ \mathbf{R}^+_{\sigma,\times}\boldsymbol{\gamma}_\times u_\sigma = \mathbb{x}_\sigma, & \text{on } \tilde{\Sigma}, \end{cases} \tag{9.133}$$

which is well defined thanks to Assumption 9.18. Set $\mathbb{y} = \boldsymbol{\gamma}_\times u_\sigma$, by Definition 9.19 of the scattering operator $\mathbf{S}_{\sigma,\times}$ we have

$$\mathbf{R}^-_{\sigma,\times}\mathbb{y} = \mathbf{S}_{\sigma,\times}\mathbb{x}_\sigma, \tag{9.134}$$

and we also have by construction

$$\mathbb{x}_\sigma = \mathbf{R}^+_{\sigma,\times}\mathbb{y}. \tag{9.135}$$

It follows that

$$\|\mathbf{S}_{\sigma,\times}\mathbb{x}_\sigma\|_{\mathbf{T}_{\sigma,\times}} - \|\mathbb{x}_\sigma\|_{\mathbf{T}_{\sigma,\times}} = \|\mathbf{R}^-_{\sigma,\times}\mathbb{y}\|_{\mathbf{T}_{\sigma,\times}} - \|\mathbf{R}^+_{\sigma,\times}\mathbb{y}\|_{\mathbf{T}_{\sigma,\times}} \tag{9.136}$$

Using Lemma 9.39, we obtain

$$\|\mathbf{S}_{\sigma,\times}\mathbb{x}_\sigma\|_{\mathbf{T}_{\sigma,\times}} - \|\mathbb{x}_\sigma\|_{\mathbf{T}_{\sigma,\times}} = 2\mathrm{i}[\![\mathbb{x},\overline{\mathbb{x}}]\!]_\times. \tag{9.137}$$

Applying the energy conservation results of Proposition 9.4 we finally get

$$\|\mathbf{S}_{\sigma,\times}\mathbb{x}_\sigma\|_{\mathbf{T}_{\sigma,\times}} - \|\mathbb{x}_\sigma\|_{\mathbf{T}_{\sigma,\times}} \leq 0. \tag{9.138}$$

■

Combining both Proposition 9.40 and Proposition 9.26 we get the contraction property we were looking for.

Corollary 9.41 (**Contraction property**). *Let $\sigma \in \{0,1\}$, we have*

$$\|\mathbf{\Pi}_{\sigma,\times}\mathbf{S}_{\sigma,\times}\mathbb{x}_\sigma\|_{\mathbf{T}_{\sigma,\times}} \leq \|\mathbb{x}_\sigma\|_{\mathbf{T}_{\sigma,\times}}, \qquad \forall \mathbb{x}_\sigma \in \mathbb{M}_{\sigma,\times}. \tag{9.139}$$

It remains to prove the isomorphism property of the operator $\mathrm{Id} - \mathbf{\Pi}_{\sigma,\times}\mathbf{S}_{\sigma,\times}$ which is the subject of the following proposition. Once more, the approach follows closely the one from Chapter 3 but is restated in the new formalism for the sake of completeness.

We begin with the following lemma, counterpart of Lemma 3.59.

Lemma 9.42. *For each $\sigma \in \{0,1\}$, the operator $\mathbf{R}^+_{\sigma,\times} - \mathbf{\Pi}_{\sigma,\times}\mathbf{R}^-_{\sigma,\times}$ (respectively the operator $\mathbf{R}^-_{\sigma,\times} - \mathbf{\Pi}_{\sigma,\times}\mathbf{R}^+_{\sigma,\times}$) is surjective from $\mathbb{M}_\times \equiv (\mathbb{M}_{0,\times}, \mathbb{M}_{1,\times})$ onto $\mathbb{M}_{\sigma,\times}$.*

Proof. First note that, for any $\sigma \in \{0,1\}$, the result for the operator $\mathbf{R}^-_{\sigma,\times} - \mathbf{\Pi}_{\sigma,\times}\mathbf{R}^+_{\sigma,\times}$ is equivalent to the result for the operator $\mathbf{R}^+_{\sigma,\times} - \mathbf{\Pi}_{\sigma,\times}\mathbf{R}^-_{\sigma,\times}$ since the communication operator $\mathbf{\Pi}_{\sigma,\times}$ is an involution according to Proposition 9.26.

We prove the results for $\sigma = 1$, the proof for the other case formally takes the same route.

Let $\mathbb{y}_1 \in \mathbb{M}_{1,\times}$. We seek $\mathbb{x} \equiv (\mathbb{x}_0, \mathbb{x}_1) \in \mathbb{M}_\times$ such that

$$\mathbf{R}^+_{1,\times}\mathbb{x} - \mathbf{\Pi}_{1,\times}\mathbf{R}^-_{1,\times}\mathbb{x} = \mathbb{y}_1 \tag{9.140}$$

which, using successively Definition 9.17 of the generalized Robin operators $\mathbf{R}^\pm_{1,\times}$ and Definition 9.22 of the orthogonal projectors $\mathbf{P}_{1,\times}$ and $\mathbf{P}_{1,\times}{}^\perp$, is equivalent to

$$\begin{aligned} & (\mathbb{x}_1 - \mathrm{i}\mathbf{T}_{0,\times}\mathbb{x}_0) - \mathbf{\Pi}_{1,\times}\left(-\mathbb{x}_1 - \mathrm{i}\mathbf{T}_{0,\times}\mathbb{x}_0\right) = \mathbb{y}_1, \\ \Leftrightarrow \quad & (\mathrm{Id} + \mathbf{\Pi}_{1,\times})\,\mathbb{x}_1 + (\mathrm{Id} - \mathbf{\Pi}_{1,\times})\left(-\mathrm{i}\mathbf{T}_{0,\times}\mathbb{x}_0\right) = \mathbb{y}_1, \\ \Leftrightarrow \quad & \mathbf{P}_{1,\times}{}^\perp\mathbb{x}_1 + \mathbf{P}_{1,\times}\left(-\mathrm{i}\mathbf{T}_{0,\times}\mathbb{x}_0\right) = \frac{1}{2}\mathbb{y}_1. \end{aligned} \tag{9.141}$$

Using the usual properties of the projectors $\mathbf{P}_{1,\times}$ and $\mathbf{P}_{1,\times}{}^\perp$ it is then immediate to check that a solution is at hand if $\mathbb{x}_0$ and $\mathbb{x}_1$ satisfy

$$\begin{cases} -\mathrm{i}\mathbf{T}_{0,\times}\mathbb{x}_0 = \frac{1}{2}\mathbf{P}_{1,\times}\,\mathbb{y}_1, \\ \mathbb{x}_1 = \frac{1}{2}\mathbf{P}_{1,\times}{}^\perp\,\mathbb{y}_1, \end{cases} \qquad \Leftrightarrow \qquad \begin{cases} \mathbb{x}_0 = \frac{\mathrm{i}}{2}(\mathbf{T}_{0,\times})^{-1}\mathbf{P}_{1,\times}\,\mathbb{y}_1, \\ \mathbb{x}_1 = \frac{1}{2}\mathbf{P}_{1,\times}{}^\perp\,\mathbb{y}_1. \end{cases} \tag{9.142}$$

■

As a direct corollary to Propositions 9.12, 9.29 and Lemma 9.42 we have the following easy result. Notice that the cornerstone to establish this result is the decomposition $\mathbb{M}_\times = \mathbb{C}_\times \oplus \mathbb{S}_\times$ from Proposition 9.12.

Corollary 9.43. *For each $\sigma \in \{0,1\}$, the operator $\mathbf{R}^+_{\sigma,\times} - \mathbf{\Pi}_{\sigma,\times}\mathbf{R}^-_{\sigma,\times}$ (respectively the operator $\mathbf{R}^-_{\sigma,\times} - \mathbf{\Pi}_{\sigma,\times}\mathbf{R}^+_{\sigma,\times}$) is a bijection from $\mathbb{C}_\times$ to $\mathbb{M}_{\sigma,\times}$.*

Proof. Let $\sigma \in \{0,1\}$. Again, first note that the result for the operator $\mathbf{R}^-_{\sigma,\times} - \mathbf{\Pi}_{\sigma,\times}\mathbf{R}^+_{\sigma,\times}$ is equivalent to the result for the operator $\mathbf{R}^+_{\sigma,\times} - \mathbf{\Pi}_{\sigma,\times}\mathbf{R}^-_{\sigma,\times}$ since the communication operator $\mathbf{\Pi}_{\sigma,\times}$ is an involution according to Proposition 9.26.

From Lemma 9.42, the operator $\mathbf{R}^+_{\sigma,\times} - \mathbf{\Pi}_{\sigma,\times}\mathbf{R}^-_{\sigma,\times}$ is surjective from $\mathbb{M}_\times$ onto $\mathbb{M}_{\sigma,\times}$. From Proposition 9.29 we know that its kernel is $\mathbb{S}_\times$. From Proposition 3.25 we have that $\mathbb{M}_\times = \mathbb{C}_\times \oplus \mathbb{S}_\times$. It follows that the operator $\mathbf{R}^+_{\sigma,\times} - \mathbf{\Pi}_{\sigma,\times}\mathbf{R}^-_{\sigma,\times}$ is invertible on $\mathbb{C}_\times$. ∎

We are finally able to verify that we satisfy in our particular setting the required additional assumption of the abstract result contain in Proposition 3.57. This will be a direct consequence of the following lemma.

Lemma 9.44. *Let $\sigma \in \{0,1\}$ and $\mathbb{b}_\sigma \in \mathbb{M}_{\sigma,\times}$. Consider the two problems*

$$\begin{cases} \text{Find } \mathbb{x}_\sigma \in \mathbb{M}_{\sigma,\times} \text{ such that}: \\ (\mathrm{Id} - \mathbf{\Pi}_{\sigma,\times}\mathbf{S}_{\sigma,\times})\,\mathbb{x}_\sigma = \mathbb{b}_\sigma, \end{cases} \tag{9.143}$$

and

$$\begin{cases} \text{Find } \mathbb{y} \in \mathbb{C}_\times \text{ such that}: \\ \left(\mathbf{R}^+_{\sigma,\times} - \mathbf{\Pi}_{\sigma,\times}\mathbf{R}^-_{\sigma,\times}\right)\mathbb{y} = \mathbb{b}_\sigma. \end{cases} \tag{9.144}$$

If $\mathbb{x}_\sigma \in \mathbb{M}_{\sigma,\times}$ is solution to the problem (9.143)*, then there exists $\mathbb{y} \in \mathbb{C}_\times$ solution to the problem* (9.144) *such that $\mathbb{x}_\sigma = \mathbf{R}^+_{\sigma,\times}\mathbb{y}$.*

Reciprocally, if $\mathbb{y} \in \mathbb{C}_\times$ is solution to the problem (9.144) *then $\mathbb{x}_\sigma = \mathbf{R}^+_{\sigma,\times}\mathbb{y} \in \mathbb{M}_{\sigma,\times}$ is solution to the problem* (9.143)*.*

Proof. Let $\sigma \in \{0,1\}$ and $\mathbb{b}_\sigma \in \mathbb{M}_{\sigma,\times}$.

($\Rightarrow$) Suppose to have $\mathbb{x}_\sigma \in \mathbb{M}_{\sigma,\times}$ a solution to the problem (9.143) and let $u_\sigma \in \mathbb{U}_\Gamma(\mathrm{D};\mathcal{P}_\Omega)$ be such that

$$\begin{cases} (\mathrm{L}_{\mathsf{a}} - \kappa_0{}^2\mathsf{n})u_\sigma|_{\Omega_j} = 0, & \text{in } \Omega_j,\ \forall j \in \{1,\dots,J\}, \\ (\gamma_{1,\Gamma} - \mathrm{i}\gamma_{0,\Gamma})u_\sigma = 0, & \text{on } \Gamma, \\ \mathbf{R}^+_{\sigma,\times}\boldsymbol{\gamma}_\times u_\sigma = \mathbb{x}_\sigma, & \text{on } \tilde{\Sigma}, \end{cases} \tag{9.145}$$

which is well defined thanks to Assumption 9.18 and set

$$\mathbb{y} := \boldsymbol{\gamma}_\times u_\sigma \in \mathbb{M}_\times, \qquad \text{so that by construction} \qquad \mathbb{x}_\sigma = \mathbf{R}^+_{\sigma,\times}\mathbb{y}. \tag{9.146}$$

By Definition 9.3 of the Cauchy trace space $\mathbb{C}_\times$ we also have $\mathbb{y} \in \mathbb{C}_\times$ and the characterization of this space given in Proposition 9.20 yields

$$\left(\mathbf{R}^-_{\sigma,\times} - \mathbf{S}_{\sigma,\times}\mathbf{R}^+_{\sigma,\times}\right)\mathbb{y} = 0. \tag{9.147}$$

Finally, equation (9.143) is rewritten as

$$\left(\mathbf{R}^+_{\sigma,\times} - \mathbf{\Pi}_{\sigma,\times}\mathbf{R}^-_{\sigma,\times}\right)\mathbb{y} = \mathbb{b}_\sigma, \tag{9.148}$$

which finally proves that $\mathbb{y} \in \mathbb{C}_\times$ solves (9.144).

($\Leftarrow$) Suppose to have $\mathbb{y} \in \mathbb{C}_\times$ a solution to the problem (9.144) and set $\mathbb{x}_\sigma := \mathbf{R}^+_{\sigma,\times}\mathbb{y}$. Using the characterization of the Cauchy trace space $\mathbb{C}_\times$ given in Proposition 9.20 we have

$$\left(\mathbf{R}^-_{\sigma,\times} - \mathbf{S}_{\sigma,\times}\mathbf{R}^+_{\sigma,\times}\right)\mathbb{y} = 0. \tag{9.149}$$

Then, equation (9.144) is readily rewritten as

$$\left(\mathrm{Id} - \mathbf{\Pi}_{\sigma,\times}\mathbf{S}_{\sigma,\times}\right)\mathbb{x}_\sigma = \mathbb{b}_\sigma, \tag{9.150}$$

■

Proposition 9.45. *For each $\sigma \in \{0,1\}$, the operator $\mathrm{Id} - \mathbf{\Pi}_{\sigma,\times}\mathbf{S}_{\sigma,\times}$ is an isomorphism on $\mathbb{M}_{\sigma,\times}$.*

Proof. **Injectivity** Let $\sigma \in \{0,1\}$ and $\mathbb{x}_\sigma \in \mathbb{M}_{\sigma,\times}$ be such that

$$\left(\mathrm{Id} - \mathbf{\Pi}_{\sigma,\times}\mathbf{S}_{\sigma,\times}\right)\mathbb{x}_\sigma = 0. \tag{9.151}$$

Using Lemma 9.44, there exists necessarily a $\mathbb{y} \in \mathbb{C}_\shortparallel$ such that $\mathbb{x}_\sigma = \mathbf{R}^+_{\sigma,\times}\mathbb{y}$ and

$$\left(\mathbf{R}^+_{\sigma,\times} - \mathbf{\Pi}_{\sigma,\times}\mathbf{R}^-_{\sigma,\times}\right)\mathbb{y} = 0. \tag{9.152}$$

Using the characterization of $\mathbb{S}_\times$ given in Proposition 9.29 we get from this last equation that $\mathbb{y} \in \mathbb{S}_\times$ so that in fact $\mathbb{y} \in \mathbb{C}_\shortparallel \cap \mathbb{S}_\times$, which is reduced to the singleton $\{0\}$ from Proposition 9.12. Finally from $\mathbb{y} = 0$ we obtain $\mathbb{x}_\sigma = \mathbf{R}^+_{\sigma,\times}\mathbb{y} = 0$.

Surjectivity Let $\sigma \in \{0,1\}$ and $\mathbb{b}_\sigma \in \mathbb{M}_{\sigma,\times}$. From Lemma 9.44 we know that to find a $\mathbb{x}_\sigma \in \mathbb{M}_{\sigma,\times}$ such that

$$\left(\mathrm{Id} - \mathbf{\Pi}_{\sigma,\times}\mathbf{S}_{\sigma,\times}\right)\mathbb{x}_\sigma = \mathbb{b}_\sigma, \tag{9.153}$$

it is enough to find a $\mathbb{y} \in \mathbb{C}_\shortparallel$ such that

$$\left(\mathbf{R}^+_{\sigma,\times} - \mathbf{\Pi}_{\sigma,\times}\mathbf{R}^-_{\sigma,\times}\right)\mathbb{y} = \mathbb{b}_\sigma, \tag{9.154}$$

and set $\mathbb{x}_\sigma = \mathbf{R}^+_{\sigma,\times}\mathbb{y}$. The above problem in $\mathbb{y}$ is uniquely solvable by application of Corollary 9.43 and we are done. ■

Note that a similar result in a slightly different geometric configuration (in the whole space) and for the acoustic setting was already established in [29, Cor. 7.1]. We are now ready to state the following important convergence result, see also [29, Sec. 7.3].

Theorem 9.46 (Geometric convergence of the fixed point iteration algorithm). *The sequence of broken solutions $(u^n_\sigma)_{n\in\mathbb{N}}$ computed according to* (9.125)*, converges* geometrically *to u the solution of the model problem* (3.79)*. Specifically, there exist $C > 0$ and $0 < \tau < 1$ such that*

$$\left\|u^n_\sigma - u\right\|_{\mathbb{U}_\Gamma(\mathrm{D};\mathcal{P}_\Omega)} \leq C\tau^n, \qquad \forall n \in \mathbb{N}. \tag{9.155}$$

Proof. Arguing as in the proof of Corollary 3.63, this is a direct application of Proposition 3.57 whose two assumptions are verified in Proposition 9.41 and Proposition 9.45. ■

Remark 9.47. *Arguing as in Section 3.3.3, we remark again that geometric convergence of the relaxed Jacobi algorithm guarantees geometric convergence of the* Gmres *counter-part.*

Chapter 10

Discrete setting

Contents

This chapter is devoted to the numerical analysis of the Galerkin approximation of the domain decomposition method that was described in the previous chapter with one important caveat: we do *not* impose any (geometrical) restriction on the (non-overlapping) partition in sub-domains. In particular, we allow the presence of both interior and boundary junction points. Again, we point out that this is *one* (our) choice of discretization strategy, which we actually implemented and tested numerically (see Chapter 11 for numerical experiments). The ideas presented in this chapter originate from the work of Xavier Claeys for the acoustic setting and are largely based on those described in [33] (which in turn was based upon [29]). We adapted here the proofs to our abstract formalism which allows to seamlessly extend the results to the electromagnetic setting.

The discretization strategy from Chapter 4 of the method described in Chapter 3 used the formulation for $\sigma = 1$. This means that the Lagrange multiplier, solution of the interface problem on which the iterative algorithm is applied, can be identified as an element of the *dual* trace space (in this case $\mathbb{M}_{1,\parallel}$ or $\mathbb{M}_{1,h,\parallel}$). This is a rather natural choice for the Galerkin method considered here and is slightly more efficient compared to the other choices $\sigma \in \{1/2, 1\}$, if carefully implemented. In contrast, we consider in this chapter a discretization strategy of the method presented in Chapter 9 based on the formulation for $\sigma = 0$. This means that the Lagrange multiplier, solution of the interface problem on which the iterative algorithm is applied, can be identified as an element of the *natural* (or primal) trace space (in this case $\mathbb{M}_{0,\times}$ or $\mathbb{M}_{0,h,\times}$). This choice is more natural here because of the new way data is communicated between sub-domains.

10.1 Abstract discrete domain decomposition

In this chapter, we consider the most general configuration for the partitioning. We suppose that the sub-domains are non-overlapping and that the partition is conformal (in the sense of Assumption 4.7), but we do *not* suppose that Assumption 3.11, nor Assumption 3.12 hold, i.e. we allow for the presence of both interior and boundary junction points.

The definitions and notations introduced in Section 3.1 and Section 4.1 are independent of the type of partition and will still be in use in this chapter. Recall that we use the index $\times$ in place of $\parallel$ to differentiate what has a meaning in a configuration that may admit cross-points versus a configuration that excludes cross-point.

10.1.1 Multi-trace formalism

This time, because we allow the presence of junction points in the partition, the definitions below are not a straightforward discretization of the continuous spaces of Chapter 9. The multi-trace formalism is particularly adapted to this general setting, in fact it was created for this exact purpose.

10.1.1.1 Multi-trace spaces

We introduce discrete global trace spaces whose elements are collection of traces *on the whole boundary* $\Gamma_{j,h}$ of each sub-domain $\Omega_{j,h}$ (including, this time, the physical boundary).

Definition 10.1 (**Discrete multi-trace spaces**). *The discrete global multi-trace spaces are defined as*

$$\begin{aligned}
\mathbb{M}_{0,h,\times}(\Sigma_h) &:= \bigtimes_{j=1}^{J} \mathrm{X}_{0,h}(\Gamma_{j,h}),\\
\mathbb{M}_{1,h,\times}(\Sigma_h) &:= \bigtimes_{j=1}^{J} \mathrm{X}_{1,h}(\Gamma_{j,h}),\\
\mathbb{M}_{h,\times}(\Sigma_h) &:= \bigtimes_{j=1}^{J} \mathrm{X}_{h}(\Gamma_{j,h}) \equiv \mathbb{M}_{0,h,\times}(\Sigma_h) \times \mathbb{M}_{1,h,\times}(\Sigma_h).
\end{aligned} \tag{10.1}$$

Beware this time that these discrete spaces are *not* subsets of the continuous spaces $\mathbb{M}_{0,\times}(\Sigma \setminus \Gamma)$, $\mathbb{M}_{1,\times}(\Sigma \setminus \Gamma)$, $\mathbb{M}_{1/2,\times}(\Sigma \setminus \Gamma)$ and $\mathbb{M}_{\times}(\Sigma \setminus \Gamma)$ introduced in the previous chapter. This is because we excluded in the continuous setting the part of the boundary of the sub-domains which was part of the physical boundary (and we were in the restrictive configuration that excludes boundary cross points).

A representation of the components of such multi-trace spaces is available in Figure 10.1.

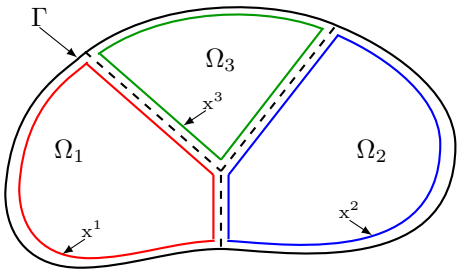

Figure 10.1: Visual representation of the components of a multi-trace space for a partition with both boundary and interior junction points, for instance $\left(\mathrm{x}^1, \mathrm{x}^2, \mathrm{x}^3\right) \in \mathbb{M}_{0,h,\times}$

We introduce the following global trace operator $\boldsymbol{\gamma}_{0,h,\times}$ which is a continuous and surjective mapping from the broken solution space into the Dirichlet multi-trace space

$$\boldsymbol{\gamma}_{0,h,\times} := \left(\gamma_{0,\Gamma_{j,h}}\right)_{j=1}^{J} : \mathbb{V}_h(\mathcal{P}_{\Omega,h}) \to \mathbb{M}_{0,h,\times}. \tag{10.2}$$

Again $\boldsymbol{\gamma}_{0,h,\times}$ is different from its continuous version $\boldsymbol{\gamma}_{0,\times}$ because of the presence of the physical boundary in our multi-trace spaces.

Norms and duality pairings The multi-trace space $\mathbb{M}_{0,\times}$ can be endowed with the norms stemming from its Cartesian product structure. Recalling the definition of the norm on a single domain given in (4.6), we set,

$$\|\mathbb{x}_0\|^2_{\mathbb{M}_{0,h,\times}} := \sum_{j=1}^{J} \|\mathrm{x}_0^j\|^2_{\mathrm{X}_{0,h}(\Gamma_{j,h})}, \qquad \forall \mathbb{x}_0 \equiv (\mathrm{x}_0^j)_{j\in\{1,\dots,J\}} \in \mathbb{M}_{0,h,\times}. \tag{10.3}$$

Recalling the local duality pairing $\langle\cdot,\cdot\rangle_{\partial\mathcal{O}}$ between the two dual trace spaces (4.9) on a single boundary $\partial\mathcal{O}$, we introduce the duality pairing between multi-trace spaces (which does not involve any complex conjugation operation)

$$\begin{aligned} \langle\!\langle\cdot,\cdot\rangle\!\rangle_{\times} &: \mathbb{M}_{1,h,\times} \times \mathbb{M}_{0,h,\times} \to \mathbb{C}, \\ (\mathbb{x}_1,\, \mathbb{x}_0) &\mapsto \sum_{j=1}^{J} \langle \mathrm{x}_1^j, \mathrm{x}_0^j \rangle_{\Gamma_{j,h}}. \end{aligned} \tag{10.4}$$

The space $\mathbb{M}_{1,h,\times}$ is equipped with the corresponding canonical dual norm, namely

$$\|\mathrm{x}_1\|_{\mathbb{M}_{1,h,\times}} := \sup_{\substack{\mathrm{x}_0 \in \mathbb{M}_{0,h,\times} \\ \mathrm{x}_0 \neq 0}} \frac{\langle \mathrm{x}_1, \mathrm{x}_0 \rangle_{\partial\mathcal{O}}}{\|\mathrm{x}_0\|_{\mathbb{M}_{0,h,\times}}}, \qquad \forall \mathrm{x}_1 \in \mathbb{M}_{1,h,\times}. \tag{10.5}$$

Besides, we introduce the natural norm on $\mathbb{M}_{h,\times}$ as follows

$$\|\mathbb{x}\|^2_{\mathbb{M}_{h,\times}} := \|\mathbb{x}_0\|^2_{\mathbb{M}_{0,h,\times}} + \|\mathbb{x}_1\|^2_{\mathbb{M}_{1,h,\times}}, \qquad \forall \mathbb{x} \equiv (\mathbb{x}_0, \mathbb{x}_1) \in \mathbb{M}_{h,\times}. \tag{10.6}$$

Lifting operators With the help of Assumption 4.2, it is clear that one can construct a (trace preserving) continuous lifting operator

$$\mathbb{E}_{h,\times} \ : \mathbb{M}_{0,h,\times} \to \mathbb{V}_h(\mathcal{P}_{\Omega,h}). \tag{10.7}$$

We shall require in the forthcoming analysis the continuity constant of this lifting operator, denoted $|||\mathbb{E}_{h,\times}|||$, and such that

$$\| \mathbb{E}_{h,\times} \, \mathbb{x}_0 \|_{\mathbb{U}_\Gamma(\mathrm{D};\mathcal{P}_{\Omega,h})} \leq |||\mathbb{E}_{h,\times}||| \, \|\mathbb{x}_0\|_{\mathbb{M}_{0,h,\times}}, \qquad \forall \mathbb{x}_0 \in \mathbb{M}_{0,h,\times}. \tag{10.8}$$

10.1.1.2 Cauchy-trace spaces

We first define the discrete version of the Cauchy trace space from Definition 9.3, resorting to weak formulations in this discrete setting. The bilinear a_j was defined in (3.97) and the broken version $\mathbb{a}$ was defined in (3.98).

Definition 10.2 (**Discrete Cauchy-trace space**). *For each $j = 1, \ldots, J$, the local space of discrete Cauchy traces $\mathrm{C}_{h,\times}(\Gamma_{j,h})$ is defined as the subset of $\mathrm{X}_h(\Gamma_{j,h})$ such that: for all $\mathrm{x} \in \mathrm{X}_h(\Gamma_{j,h})$,*

$$\begin{aligned} & \mathrm{x} \equiv (\mathrm{x}_0^j, \mathrm{x}_1^j) \in \mathrm{C}_{h,\times}(\Gamma_{j,h}) \\ \Leftrightarrow \quad & \exists u_j \in \mathrm{V}_h(\Omega_{j,h}) \text{ such that} \\ & \qquad \begin{cases} a_j(u_j, v_j) = \langle \mathrm{x}_1^j, \gamma_{0,\Gamma_{j,h}} v_j \rangle_{\Gamma_{j,h}}, & \forall v_j \in \mathrm{V}_h(\Omega_{j,h}), \\ \mathrm{x}_0^j = \gamma_{0,\Gamma_{j,h}} u_j. \end{cases} \end{aligned} \tag{10.9}$$

The global discrete Cauchy trace space is defined as

$$\mathbb{C}_{h,\times}(\Sigma_h) := \bigtimes_{j=1}^{J} \mathrm{C}_{h,\times}(\Gamma_{j,h}), \tag{10.10}$$

or, equivalently,

$$\begin{aligned} & \mathbb{x} \equiv (\mathbb{x}_0, \mathbb{x}_1) \in \mathbb{C}_{h,\times}(\Sigma_h) \\ \Leftrightarrow \quad & \exists \mathbb{u} \in \mathbb{V}_h(\mathcal{P}_{\Omega,h}) \text{ such that } \begin{cases} \mathbb{a}(\mathbb{u}, \mathbb{v}) = \langle\!\langle \mathbb{x}_1, \boldsymbol{\gamma}_{0,h,\times} \mathbb{v} \rangle\!\rangle_\times, & \forall \mathbb{v} \in \mathbb{V}_h(\mathcal{P}_{\Omega,h}), \\ \mathbb{x}_0 = \boldsymbol{\gamma}_{0,h,\times} \mathbb{u}, \end{cases} \end{aligned} \tag{10.11}$$

which we identify as a subspace of $\mathbb{M}_{h,\times}$ in a straightforward manner.

10.1.1.3 Single-trace spaces

Our definition of the single-trace space is again here fundamentally different from the one of Chapter 4 (or Chapter 3). Indeed, it is clear that a generalization of Definition 4.11, using simple matching conditions at each interface, is not possible since we now include the physical boundary in the definition of the multi-trace spaces. However, our new definition exploits what were previously properties of the single-trace space. To see this, we refer the reader to Proposition 4.12 and Proposition 4.15.

Definition 10.3 (**Discrete single-trace spaces**). *The global discrete single-trace spaces are defined as*

$$\begin{aligned} & \mathbb{S}_{0,h,\times}(\Sigma_h) := \boldsymbol{\gamma}_{0,h,\times} \mathrm{V}_h(\Omega), \\ & \mathbb{S}_{1,h,\times}(\Sigma_h) := \left\{ \mathbb{x}_1 \in \mathbb{M}_{1,h,\times} \quad | \quad \langle\!\langle \mathbb{x}_1, \mathbb{x}_0 \rangle\!\rangle_\times = 0, \ \forall \mathbb{x}_0 \in \mathbb{S}_{0,h,\times} \right\}, \\ & \mathbb{S}_{h,\times}(\Sigma_h) \ := \ \mathbb{S}_{0,h,\times}(\Sigma_h) \ \times \ \mathbb{S}_{1,h,\times}(\Sigma_h). \end{aligned} \tag{10.12}$$

The definition of $\mathbb{S}_{0,h,\times}$ should be compared with Definition 9.5 from the previous chapter in the continuous setting, it is similar in spirit. Note that $\mathbb{S}_{1,h,\times}$ can be seen as the annihilator of $\mathbb{S}_{0,h,\times}$ in $\mathbb{M}_{1,h,\times}$ for the duality induced by $\langle\!\langle \cdot, \cdot \rangle\!\rangle_\times$, since it consists of all the functionals of $\mathbb{M}_{1,h,\times}$ whose restriction to $\mathbb{S}_{0,h,\times}$ vanishes. As a result it is isomorphic to the orthogonal complement of $\mathbb{S}_{0,h,\times}$.

The following lemma is a direct corollary of Lemma 9.7.

Lemma 10.4. *We have*

$$\operatorname{Ker} \boldsymbol{\gamma}_{0,h,\times} \subset \mathrm{V}_h(\Omega). \tag{10.13}$$

Proof. Let $u_h \in \mathbb{V}_h(\mathcal{P}_{\Omega,h})$ such that $\boldsymbol{\gamma}_{0,h,\times} u_h = 0$. From Lemma 9.7, we have $u_h \in \mathrm{U}_\Gamma(\mathrm{D};\Omega)$ so that from Assumption 4.7, $u_h \in \mathrm{U}_\Gamma(\mathrm{D};\Omega) \cap \mathbb{V}_h(\mathcal{P}_{\Omega,h}) = \mathrm{V}_h(\Omega)$. ■

We deduce the following corollary, which completes Definition 10.3 and makes clear the difference between the $\mathrm{V}_h(\Omega)$ (regular) and the $\mathbb{V}_h(\mathcal{P}_{\Omega,h})$ (broken) versions of the solution spaces using the single-trace space.

Corollary 10.5. *We have*

$$\forall u \in \mathbb{V}_h(\mathcal{P}_{\Omega,h}), \qquad \boldsymbol{\gamma}_{0,h,\times} u \in \mathbb{S}_{0,h,\times} \quad \Leftrightarrow \quad u \in \mathrm{V}_h(\Omega). \tag{10.14}$$

Proof. It is clear that one implication ($\Leftarrow$) stems from Definition 10.3. We need only to prove the reverse implication ($\Rightarrow$).

Let $u \in \mathbb{V}_h(\mathcal{P}_{\Omega,h})$ such that $\boldsymbol{\gamma}_{0,h,\times} u \in \mathbb{S}_{0,h,\times}$. By Definition 10.3 of $\mathbb{S}_{0,h,\times}$, there exists $v \in \mathrm{V}_h(\Omega)$ such that $\boldsymbol{\gamma}_{0,h,\times}(v-u) = 0$. It follows that $w := v - u \in \operatorname{Ker} \boldsymbol{\gamma}_{0,h,\times}$ and by Lemma 10.4 we get $w \in \mathrm{V}_h(\Omega)$ so that finally $u = v + w$ does belong to $\mathrm{V}_h(\Omega)$. ■

10.1.1.4 A first equivalent transmission problem

We are now ready to rewrite the (discrete) approximation (4.19) of the model problem (3.79) This is the purpose of the following proposition, analogue to Proposition 9.11. The broken sesquilinear and linear forms $\mathfrak{o}$ and $\mathbb{I}$ were defined in (3.98) and (3.101). The result is formally very similar to Proposition 4.16, and so are the proofs. However the arguments are from different origins.

Proposition 10.6 (Equivalent discrete transmission problem). *If $u_h \in \mathrm{V}_h(\Omega)$ is solution of the discrete model problem* (4.19) *then there exists $\mathbb{x} \equiv (\mathbb{x}_0, \mathbb{x}_1) \in \mathbb{S}_{h,\times}$ such that*

$$\begin{cases} \mathfrak{o}(u_h, \mathbb{v}) - \mathbb{I}(\mathbb{v}) = \langle\!\langle \mathbb{x}_1, \boldsymbol{\gamma}_{0,h,\times} \mathbb{v} \rangle\!\rangle_\times, & \forall \mathbb{v} \in \mathbb{V}_h(\mathcal{P}_{\Omega,h}), \\ \mathbb{x}_0 = \boldsymbol{\gamma}_{0,h,\times} u_h. \end{cases} \tag{10.15}$$

Reciprocally, if $u_h \in \mathbb{V}_h(\mathcal{P}_{\Omega,h})$ and $\mathbb{x} \equiv (\mathbb{x}_0, \mathbb{x}_1) \in \mathbb{S}_{h,\times}$ are such that (10.15) *is satisfied then u_h is solution of the discrete model problem* (4.19).

Proof. ($\Rightarrow$) Let $u_h \in \mathrm{V}_h(\Omega)$ be the solution of the (discrete) approximation (4.19) of the model problem (3.79). Since $u_h \in \mathrm{V}_h(\Omega)$, from Definition 10.3 we immediately have

$$\mathbb{x}_0 := \boldsymbol{\gamma}_{0,h,\times} u_h \in \mathbb{S}_{0,h,\times}. \tag{10.16}$$

Now, we introduce $\mathbb{x}_1 \in \mathbb{M}_{1,h,\times}$ such that

$$\langle\!\langle \mathbb{x}_1, \mathbb{x}_0^t \rangle\!\rangle_\times = \mathfrak{o}(u_h, \mathbb{x}_0^t) - \mathbb{I}(\mathbb{x}_0^t), \qquad \forall \mathbb{x}_0^t \in \mathbb{M}_{0,h,\times}. \tag{10.17}$$

Let us show that $\mathbb{x}_1$ is independent of the particular lifting $\mathbb{E}_{h,\times}$. Let $\mathbb{v} \in \mathbb{V}_h(\mathcal{P}_{\Omega,h})$, we have

$$\boldsymbol{\gamma}_{0,h,\times}\left(\mathbb{v} - \mathbb{E}_{h,\times}\,\boldsymbol{\gamma}_{0,h,\times}\mathbb{v}\right) = 0 \in \mathbb{S}_{0,h,\times}, \tag{10.18}$$

so that, by application of Corollary 10.5, we know that $\mathbb{v} - \mathbb{E}_{h,\times}\,\boldsymbol{\gamma}_{0,h,\times}\mathbb{v} \in \mathrm{V}_h(\Omega)$. It follows that

$$\mathbb{o}(u_h, \mathbb{v} - \mathbb{E}_{h,\times}\,\boldsymbol{\gamma}_{0,h,\times}\mathbb{v}) - \mathbb{l}(\mathbb{v} - \mathbb{E}_{h,\times}\,\boldsymbol{\gamma}_{0,h,\times}\mathbb{v}) = a(u_h, \mathbb{v} - \mathbb{E}_{h,\times}\,\boldsymbol{\gamma}_{0,h,\times}\mathbb{v}) - l(\mathbb{v} - \mathbb{E}_{h,\times}\,\boldsymbol{\gamma}_{0,h,\times}\mathbb{v}) = 0, \tag{10.19}$$

hence

$$\mathbb{o}(u_h, \mathbb{E}_{h,\times}\,\boldsymbol{\gamma}_{0,h,\times}\mathbb{v}) - \mathbb{l}(\mathbb{E}_{h,\times}\,\boldsymbol{\gamma}_{0,h,\times}\mathbb{v}) = \mathbb{o}(u_h, \mathbb{v}) - \mathbb{l}(\mathbb{v}), \tag{10.20}$$

and finally, using the surjectivity of the trace $\boldsymbol{\gamma}_{0,h,\times}$ from $\mathbb{V}_h(\mathcal{P}_{\Omega,h})$ into $\mathbb{M}_{0,h,\times}$,

$$\left\langle\!\left\langle \mathbb{x}_1, \boldsymbol{\gamma}_{0,h,\times}\mathbb{v}^t \right\rangle\!\right\rangle_{\times} = \mathbb{o}(u_h, \mathbb{v}^t) - \mathbb{l}(\mathbb{v}^t), \qquad \forall \mathbb{v}^t \in \mathbb{V}_h(\mathcal{P}_{\Omega,h}). \tag{10.21}$$

Let $\mathbb{z}_0 \in \mathbb{S}_{0,h,\times}$, using Definition 10.3, there exists $v^t \in \mathrm{V}_h(\Omega)$ such that $\mathbb{z}_0 = \boldsymbol{\gamma}_{0,h,\times} v^t$. Since $u_h \in \mathrm{V}_h(\Omega)$ satisfies the discrete model problem (4.19), we have

$$\left\langle\!\left\langle \mathbb{x}_1, \mathbb{z}_0 \right\rangle\!\right\rangle_{\times} = \mathbb{o}(u_h, v^t) - \mathbb{l}(v^t) = a(u_h, v^t) - l(v^t) = 0, \tag{10.22}$$

which means, from Definition 10.3, that

$$\mathbb{x}_1 \in \mathbb{S}_{1,h,\times} \qquad \text{and hence} \qquad \mathbb{x} \equiv (\mathbb{x}_0, \mathbb{x}_1) \in \mathbb{S}_{h,\times}. \tag{10.23}$$

($\Leftarrow$) Reciprocally, suppose that there exists $u_h \in \mathbb{V}_h(\mathcal{P}_{\Omega,h})$ and $\mathbb{x} \equiv (\mathbb{x}_0, \mathbb{x}_1) \in \mathbb{S}_{h,\times}$ such that (4.55) holds. We immediately conclude from $\boldsymbol{\gamma}_{0,h,\times} u_h = \mathbb{x}_0 \in \mathbb{S}_{0,h,\times}$ and Corollary 10.5 that $u_h \in \mathrm{V}_h(\Omega)$. Now testing with elements of $\mathrm{V}_h(\Omega)$,

$$a(u_h, v_h) - l(v_h) = \mathbb{o}(u_h, v_h) - \mathbb{l}(v_h) = \left\langle\!\left\langle \mathbb{x}_1, \boldsymbol{\gamma}_{0,h,\times} v_h \right\rangle\!\right\rangle_{\times} = 0, \qquad \forall v_h \in \mathrm{V}_h(\Omega), \tag{10.24}$$

using Definition 10.3 together with the fact that $\mathbb{x}_1 \in \mathbb{S}_{1,h,\times}$. Hence, $u_h \in \mathrm{V}_h(\Omega)$ is the solution of the discrete model problem (4.19). ■

We state now the result on the decomposition of the discrete multi-trace space in the sum of the discrete single-trace and Cauchy-trace spaces, analogue of Proposition 9.12. The following result on the decomposition of the discrete multi-trace spaces is based on similar results available for the acoustic setting, see [33, Prop. 7.1].

Proposition 10.7. *We have the direct sum*

$$\mathbb{M}_{h,\times} = \mathbb{C}_{h,\times} \oplus \mathbb{S}_{h,\times}. \tag{10.25}$$

In addition, if we denote by $\mathbf{P}_{\mathbb{C}_{h,\times}}$ *the projector from* $\mathbb{M}_{h,\times}$ *onto* $\mathbb{C}_{h,\times}$*, then we have the following estimate*

$$\alpha_{\mathbf{P}_{\mathbb{C}_{h,\times}}} := \sup_{\substack{\mathbb{x}\in\mathbb{M}_{h,\times} \\ \mathbb{x}\neq 0}} \frac{\|\mathbf{P}_{\mathbb{C}_{h,\times}}\mathbb{x}\|_{\mathbb{M}_{\times}}}{\|\mathbb{x}\|_{\mathbb{M}_{\times}}} \leq \left(1 + \alpha^{-2}_{\mathbb{M}_{h,\times}} \,|||a|||^2\, |||\mathbb{E}_{h,\times}|||^2\right)^{1/2} [(1 + \alpha_{a,h}\,|||a|||)|||\mathbb{E}_{h,\times}||| + \alpha_{a,h}]. \tag{10.26}$$

Proof.

Null intersection $\mathbb{C}_{h,\times} \cap \mathbb{S}_{h,\times} = \{0\}$. Let $\mathbb{x} \in \mathbb{C}_{h,\times} \cap \mathbb{S}_{h,\times}$. Since $\mathbb{x} \in \mathbb{C}_{h,\times}$, we can find $u \in \mathbb{V}_h(\mathcal{P}_{\Omega,h})$ such that

$$\begin{cases} \mathfrak{a}(u,v) = \langle\!\langle \mathbb{x}_1, \boldsymbol{\gamma}_{0,h,\times} v \rangle\!\rangle_\times, & \forall v \in \mathbb{V}_h(\mathcal{P}_{\Omega,h}), \\ \mathbb{x}_0 = \boldsymbol{\gamma}_{0,h,\times} u. \end{cases} \tag{10.27}$$

Then since $\boldsymbol{\gamma}_{0,h,\times} u = \mathbb{x}_0 \in \mathbb{S}_{0,h,\times}$, $u \in \mathrm{V}_h(\Omega)$ from Proposition 4.12 and since $\mathbb{x}_1 \in \mathbb{S}_{1,h,\times}$, $\langle\!\langle \mathbb{x}_1, \boldsymbol{\gamma}_{0,h,\times} v \rangle\!\rangle_\times = 0$ for all $v \in \mathrm{V}_h(\Omega)$ from Proposition 4.15. Hence we proved that

$$\begin{cases} u \in \mathrm{V}_h(\Omega), \\ a(u,v) = 0, & \forall v \in \mathrm{V}_h(\Omega). \end{cases} \tag{10.28}$$

The well-posedness of this problem (Assumption 4.4) yields $u = 0$, hence $\mathbb{x} = 0$ by continuity of the trace operator $\boldsymbol{\gamma}_{0,h,\times}$.

Decomposition. Let $\mathbb{x} \equiv (\mathbb{x}_0, \mathbb{x}_1) \in \mathbb{M}_{h,\times}$. We define

$$\begin{cases} u \in \mathrm{V}_h(\Omega) \text{ such that,} \\ \mathfrak{a}(u - \mathbb{E}_{h,\times}\, \mathbb{x}_0, v) = -\langle\!\langle \mathbb{x}_1, \boldsymbol{\gamma}_{0,h,\times} v \rangle\!\rangle_\times, & \forall v \in \mathrm{V}_h(\Omega), \end{cases} \tag{10.29}$$

Such a solution exists from the well-posedness of the model problem (4.19) (Assumption 4.4). Now define $\mathbb{y}_1 \in \mathbb{M}_{1,h,\times}$ such that

$$\mathfrak{a}(u - \mathbb{E}_{h,\times}\, \mathbb{x}_0, \mathbb{E}_{h,\times}\, \mathbb{x}_0^t) = -\langle\!\langle \mathbb{y}_1, \mathbb{x}_0^t \rangle\!\rangle_\times, \qquad \forall \mathbb{x}_0^t \in \mathbb{M}_{0,h,\times}, \tag{10.30}$$

By construction, using Definition 10.2, we have

$$\mathbb{y} := (\boldsymbol{\gamma}_{0,h,\times}(\mathbb{E}_{h,\times}\, \mathbb{x}_0 - u), \mathbb{y}_1) \in \mathbb{C}_{h,\times}. \tag{10.31}$$

Besides, Proposition 4.12 yields

$$\langle\!\langle \mathbb{x}_1 - \mathbb{y}_1, \mathbb{z}_0 \rangle\!\rangle_\times = 0, \qquad \forall \mathbb{z}_0 \in \mathbb{S}_{0,h,\times}, \tag{10.32}$$

so that, using Proposition 4.15 and again Proposition 4.12 together with the fact that $u \in \mathrm{V}_h(\Omega)$, we have

$$\mathbb{z} := (\boldsymbol{\gamma}_{0,h,\times} u, \mathbb{x}_1 - \mathbb{y}_1) \in \mathbb{S}_{h,\times}. \tag{10.33}$$

It is then straightforward to check that

$$\mathbb{x} = \mathbb{y} + \mathbb{z}, \qquad \text{with} \qquad \begin{cases} \mathbb{y} \in \mathbb{C}_{h,\times}, \\ \mathbb{z} \in \mathbb{S}_{h,\times}. \end{cases} \tag{10.34}$$

Explicit estimate. We adopt the same notations as for the proof of the decomposition. By definition of the projector $\mathbf{P}_{\mathbb{C}_{h,\times}}$, we have,

$$\mathbb{y} \equiv (\mathbb{y}_0, \mathbb{y}_1) := \mathbf{P}_{\mathbb{C}_{h,\times}} \mathbb{x}, \qquad \text{so that} \qquad \|\mathbf{P}_{\mathbb{C}_{h,\times}} \mathbb{x}\|^2_{\mathbb{M}_\times} = \|\mathbb{y}\|^2_{\mathbb{M}_\times} = \|\mathbb{y}_0\|^2_{\mathbb{M}_{0,\times}} + \|\mathbb{y}_1\|^2_{\mathbb{M}_{1,\times}}. \tag{10.35}$$

By definition of $\mathbb{y}$, we have

$$\begin{aligned} \|\mathbb{y}_0\|_{\mathbb{M}_{0,\times}} &\le \|\, \mathbb{E}_{h,\times}\, \mathbb{x}_0 - u\|_{\mathbb{U}_\Gamma(\mathrm{D};\mathcal{P}_{\Omega,h})}, \\ \|\mathbb{y}_1\|_{\mathbb{M}_{1,\times}} &\le \alpha^{-1}_{\mathbb{M}_{h,\times}}\, |||a|||\, |||E|||\, \|\, \mathbb{E}_{h,\times}\, \mathbb{x}_0 - u\|_{\mathbb{U}_\Gamma(\mathrm{D};\mathcal{P}_{\Omega,h})}. \end{aligned} \tag{10.36}$$

Besides, by definition of u we have

$$\|u\|_{\mathrm{U}_\Gamma(\mathrm{D};\mathcal{P}_{\Omega,h})} = \|u\|_{\mathrm{U}_\Gamma(\mathrm{D};\Omega)} \leq \alpha_{a,h} \left(|||a||| \; |||\mathbb{E}_{h,\times}||| \; \|\mathbb{x}_0\|_{\mathbb{M}_{0,\times}} + \|\mathbb{x}_1\|_{\mathbb{M}_{1,\times}} \right). \tag{10.37}$$

We readily obtain the claimed estimate

$$\begin{aligned} \|\mathbf{P}_{\mathbb{C}_{h,\times}} \mathbb{x}\|^2_{\mathbb{M}_\times} &\leq \left(1 + \alpha^{-2}_{\mathbb{M}_{h,\times}} \; |||a|||^2 \; |||\mathbb{E}_{h,\times}|||^2\right) \left[(1 + \alpha_{a,h} \; |||a|||) \, |||\mathbb{E}_{h,\times}||| \; \|\mathbb{x}_0\|_{\mathbb{M}_{0,\times}} + \alpha_{a,h} \; \|\mathbb{x}_1\|_{\mathbb{M}_{1,\times}}\right]^2, \\ &\leq \left(1 + \alpha^{-2}_{\mathbb{M}_{h,\times}} \; |||a|||^2 \; |||\mathbb{E}_{h,\times}|||^2\right) \left[(1 + \alpha_{a,h} \; |||a|||) |||\mathbb{E}_{h,\times}||| + \alpha_{a,h}\right]^2 \|\mathbb{x}\|^2_{\mathbb{M}_\times}. \end{aligned} \tag{10.38}$$

■

10.1.2 Reformulation as an interface problem

In this section, repeating the steps of Chapter 4, we exploit the above characterization (see Proposition 10.6) of the trace of the solution to equivalently recast the discrete approximation of the original problem (4.19) as a problem (10.85) posed on the skeleton Σ of the partition.

10.1.2.1 Transmission operators and associated scalar products

We start by introducing the key ingredient of our formulation, the transmission operator.

Definition 10.8 (**Transmission operator**). *We call* transmission *operator any* continuous *and* positive definite *bilinear form*

$$\mathrm{t}_{0,h,\times} \; : \; \mathbb{M}_{0,h,\times} \times \mathbb{M}_{0,h,\times} \to \mathbb{R}, \tag{10.39}$$

such that

$$\mathrm{t}_{0,h,\times}(\mathbb{x}_0, \overline{\mathbb{x}_0}) > 0, \qquad \forall \mathbb{x}_0 \in \mathbb{M}_{0,h,\times} \setminus \{0\}. \tag{10.40}$$

For the sake of simplicity, and because it will always be the case in practice, we suppose that this operator is diagonal.

Definition 10.9 (**Diagonal operator**). *The transmission operator* $\mathrm{t}_{0,h,\times}$ *will be called* diagonal *if there exist, for each* $j \in \{1, \ldots, J\}$*, the following local continuous bilinear forms*

$$\mathrm{t}^j_{0,h,\times} \; : \; \mathrm{X}_{0,h}(\Gamma_{j,h}) \times \mathrm{X}_{0,h}(\Gamma_{j,h}) \to \mathbb{C}, \tag{10.41}$$

such that

$$\mathrm{t}_{0,h,\times}(\mathbb{x}_0, \mathbb{y}_0) := \sum_{j=1}^{J} \mathrm{t}^j_{0,h,\times}(\mathrm{x}^j_0, \mathrm{y}^j_0), \qquad \forall \mathbb{x}_0, \mathbb{y}_0 \in \mathbb{M}_{0,h,\times}, \tag{10.42}$$

where we adopted the notation $\mathbb{x}_0 \equiv (\mathrm{x}^j_0)_{j=1}^J$ *and* $\mathbb{y}_0 \equiv (\mathrm{y}^j_0)_{j=1}^J$.

Scalar product and norm We can then endow the multi-trace space $\mathbb{M}_{0,h,\times}$ with the norm induced by the previous scalar product. Hence we define

$$\|\mathbb{x}_0\|^2_{\mathrm{t}_{0,h,\times}} := \mathrm{t}_{0,h,\times}(\mathbb{x}_0, \overline{\mathbb{x}_0}), \qquad \forall \mathbb{x}_0 \in \mathbb{M}_{0,h,\times}. \tag{10.43}$$

Because of the finite dimensional setting, the norms $\|\cdot\|_{\mathbb{M}_{0,h,\times}}$ (defined in (10.3)) and $\|\cdot\|_{\mathrm{t}_{0,h,\times}}$ are always equivalent on $\mathbb{M}_{0,h,\times}$. However, they are not necessarily h-uniformly equivalent. This is why we introduce the continuity constant

$$|||\mathrm{t}_{0,h,\times}||| := \sup_{\substack{\mathrm{x}_0 \in \mathbb{M}_{0,h,\times} \\ \mathrm{x}_0 \neq 0}} \frac{\|\mathrm{x}_0\|_{\mathrm{t}_{0,h,\times}}}{\|\mathrm{x}_0\|_{\mathbb{M}_{0,h,\times}}}, \tag{10.44}$$

and coercivity constant

$$\beta_{\mathrm{t}_{0,h,\times}} := \inf_{\substack{\mathrm{x}_0 \in \mathbb{M}_{0,h,\times} \\ \mathrm{x}_0 \neq 0}} \frac{\|\mathrm{x}_0\|_{\mathrm{t}_{0,h,\times}}}{\|\mathrm{x}_0\|_{\mathbb{M}_{0,h,\times}}}. \tag{10.45}$$

By definition, it follows that

$$\beta_{\mathrm{t}_{0,h,\times}} \, \|\mathbb{x}_0\|_{\mathbb{M}_{0,h,\times}} \leq \|\mathbb{x}_0\|_{\mathrm{t}_{0,h,\times}} \leq |||\mathrm{t}_{0,h,\times}||| \, \|\mathbb{x}_0\|_{\mathbb{M}_{0,h,\times}}, \qquad \forall \mathbb{x}_0 \in \mathbb{M}_{0,h,\times}. \tag{10.46}$$

Generalized Robin operators The transmission operator is used to combine the two types of traces into so-called generalized Robin multi-traces.

Definition 10.10 (**Discrete generalized Robin trace**). *We introduce the global operators,*

$$\mathbf{R}^{\pm}_{0,h,\times} : \mathbb{M}_{h,\times} \to \mathbb{M}_{0,h,\times}, \tag{10.47}$$

where, for any $\mathbb{x} \equiv (\mathbb{x}_0, \mathbb{x}_1) \in \mathbb{M}_{h,\times}$*, we define* $\mathbf{R}^{\pm}_{0,h,\times}$ *as the unique solutions of the following variational problem*

$$\mathrm{t}_{0,h,\times}(\mathbf{R}^{\pm}_{0,h,\times}\mathbb{x}, \mathbb{x}^t_0) = \pm\langle\!\langle \mathbb{x}_1, \mathbb{x}^t_0 \rangle\!\rangle_{\times} - \mathrm{it}_{0,h,\times}(\mathbb{x}_0, \mathbb{x}^t_0), \qquad \forall \mathbb{x}^t_0 \in \mathbb{M}_{0,h,\times}. \tag{10.48}$$

If the transmission operators are diagonal we can define local Robin operators at a single interface: for each $(j,k) \in \mathbb{J}$ *and any* $\mathrm{x} \equiv (\mathrm{x}_0, \mathrm{x}_1) \in \mathrm{X}(\Gamma_{j,h})$*, we define* $\mathbf{R}^{j,\pm}_{0,h,\times}$ *as the unique solution of the following variational problem,*

$$\mathrm{t}^j_{0,h,\times}(\mathbf{R}^{j,\pm}_{0,h,\times}\mathrm{x}, \mathrm{x}^t_0) = \pm\langle \mathbb{x}_1, \mathrm{x}^t_0 \rangle_{\Gamma_{j,h}} - \mathrm{it}^j_{0,h,\times}(\mathrm{x}_0, \mathrm{x}^t_0), \qquad \forall \mathrm{x}^t_0 \in \mathrm{X}_0(\Gamma_{j,h}). \tag{10.49}$$

10.1.2.2 Scattering operators

We are now going to introduce a discrete version of the scattering operator $\mathbf{S}_{0,\times}$ from Definition 9.19 using only weak formulations.

Definition 10.11 (**Discrete scattering operator**). *We define the global scattering operators,*

$$\mathbf{S}_{0,h,\times} : \mathbb{M}_{0,h,\times} \to \mathbb{M}_{0,h,\times}, \tag{10.50}$$

where for any $\mathbb{x}_0 \in \mathbb{M}_{0,h,\times}$ *we define*

$$\mathbf{S}_{0,h,\times}\mathbb{x}_0 = -\mathbb{x}_0 - 2\mathrm{i}\boldsymbol{\gamma}_{0,h,\times}\mathbb{u}_h, \tag{10.51}$$

with $\mathbb{u}_h \in \mathbb{V}_h(\mathcal{P}_{\Omega,h})$ *such that: for all* $\mathbb{v}_h \in \mathbb{V}_h(\mathcal{P}_{\Omega,h})$

$$\mathfrak{d}(\mathbb{u}_h, \mathbb{v}_h) - \mathrm{it}_{0,h,\times}(\boldsymbol{\gamma}_{0,h,\times}\mathbb{u}_h, \boldsymbol{\gamma}_{0,h,\times}\mathbb{v}_h) = \mathrm{t}_{0,h,\times}(\mathbb{x}_0, \boldsymbol{\gamma}_{0,h,\times}\mathbb{v}_h). \tag{10.52}$$

If the transmission operators are diagonal, the scattering operators are themselves diagonal and we have,

$$\begin{aligned} \mathbf{S}_{0,h,\times} &= diag_{j\in\{1,\dots,J\}}\left(\mathbf{S}^j_{0,h,\times}\right), \\ \mathbf{S}^j_{0,h,\times} &: \mathrm{X}_{0,h}(\Gamma_{j,h}) \to \mathrm{X}_{0,h}(\Gamma_{j,h}), \end{aligned} \tag{10.53}$$

where for any $\mathrm{x}^j_0 \in \mathrm{X}_{0,h}(\Gamma_{j,h})$ *we define,*

$$\mathbf{S}^j_{0,h,\times}\mathrm{x}^j_0 = -\mathrm{x}^j_0 - 2\mathrm{i}\gamma_{0,\Gamma_{j,h}}\, u_{j,h}, \tag{10.54}$$

with $u_{j,h} \in \mathrm{V}_h(\Omega_j)$, $j \in \{1,\dots,J\}$, *such that: for all* $v_{j,h} \in \mathrm{V}_h(\Omega_j)$,

$$a_j(u_{j,h}, v_{j,h}) - \mathrm{it}^j_{0,h,\times}(\gamma_{0,\Gamma_j}\, u_{j,h},\, \gamma_{0,\Gamma_j}\, v_{j,h}) = \mathrm{t}^j_{0,h,\times}(\mathrm{x}^j_0,\, \gamma_{0,\Gamma_j}\, v_{j,h}). \tag{10.55}$$

The following proposition shows that the above scattering operators are well-defined. Of course, the result relies on the properties of the transmission operator from Definition 10.8. This proposition is based on a similar result available for the scalar equation, see [33, Lem. 4.4].

Proposition 10.12 (**Well-posedness of local problems**). *Let*

$$\alpha_{s,h} := \inf_{\substack{\mathfrak{u}\in\mathbb{V}_h(\mathcal{P}_{\Omega,h})\\ \mathfrak{u}\neq 0}} \sup_{\substack{\mathfrak{v}\in\mathbb{V}_h(\mathcal{P}_{\Omega,h})\\ \mathfrak{v}\neq 0}} \frac{|\mathfrak{a}(\mathfrak{u},\mathfrak{v}) - \mathrm{it}_{0,h,\times}(\boldsymbol{\gamma}_{0,h,\times}\mathfrak{u},\, \boldsymbol{\gamma}_{0,h,\times}\mathfrak{v})|}{\|\mathfrak{u}\|_{\mathbb{U}_\Gamma(\mathrm{D};\mathcal{P}_\Omega)}\|\mathfrak{v}\|_{\mathbb{U}_\Gamma(\mathrm{D};\mathcal{P}_\Omega)}}. \tag{10.56}$$

We have, for any h,

$$\alpha_{s,h} > 0. \tag{10.57}$$

As a result, for any linear form $\mathbb{l}$ *on* $\mathbb{V}_h(\mathcal{P}_{\Omega,h})$, *the following problem is well-posed:*

$$\begin{cases} \text{Find } \mathfrak{u} \in \mathbb{V}_h(\mathcal{P}_{\Omega,h}) \text{ such that}: \\ \mathfrak{a}(\mathfrak{u},\mathfrak{v}) - \mathrm{it}_{0,h,\times}(\boldsymbol{\gamma}_{0,h,\times}\mathfrak{u},\, \boldsymbol{\gamma}_{0,h,\times}\mathfrak{v}) = \mathbb{l}(\mathfrak{v}), \qquad \forall \mathfrak{v} \in \mathbb{V}_h(\mathcal{P}_{\Omega,h}). \end{cases} \tag{10.58}$$

Proof. Suppose by contradiction that the above $\inf-\sup$ constant vanishes for some $\mathfrak{u} \in \mathbb{V}_h(\mathcal{P}_{\Omega,h})$, then

$$\mathfrak{a}(\mathfrak{u},\mathfrak{v}) - \mathrm{it}_{0,h,\times}(\boldsymbol{\gamma}_{0,h,\times}\mathfrak{u},\, \boldsymbol{\gamma}_{0,h,\times}\mathfrak{v}) = 0, \qquad \forall \mathfrak{v} \in \mathbb{V}_h(\mathcal{P}_{\Omega,h}). \tag{10.59}$$

Testing by $\overline{\mathfrak{u}}$ (see (3.98) for the definition of the sesquilinear form $\mathfrak{a}$), we get

$$\begin{aligned} {\kappa_0}^{-1}(\mathsf{a}\,\mathrm{D}\mathfrak{u}, \mathrm{D}\overline{\mathfrak{u}})_{L^2(\Omega)^{m_1}} - \kappa_0\,(\mathsf{n}\mathfrak{u}, \overline{\mathfrak{u}})_{L^2(\Omega)^{m_0}} \\ - \mathrm{i}(\gamma_{0,\Gamma}\,\mathfrak{u}, \gamma_{0,\Gamma}\,\overline{\mathfrak{u}})_{L^2(\Gamma)^{m_0}} - \mathrm{it}_{0,h,\times}(\boldsymbol{\gamma}_{0,h,\times}\mathfrak{u},\, \boldsymbol{\gamma}_{0,h,\times}\overline{\mathfrak{u}}) = 0. \end{aligned} \tag{10.60}$$

Since the imaginary parts of the coefficients a and n are respectively supposed negative and positive (see (3.78)), retaining only the imaginary part above implies necessarily that

$$\mathrm{t}_{0,h,\times}(\boldsymbol{\gamma}_{0,h,\times}\mathfrak{u},\, \boldsymbol{\gamma}_{0,h,\times}\overline{\mathfrak{u}}) = 0, \tag{10.61}$$

so that by the definiteness of $\mathrm{t}_{0,h,\times}$, we have $\boldsymbol{\gamma}_{0,h,\times}\mathfrak{u} = 0$. From Corollary 10.5, we deduce that $\mathfrak{u} \in \mathrm{V}_h(\Omega)$ and, testing by $v \in \mathrm{V}_h(\Omega)$ in (10.59) we get

$$\mathfrak{a}(\mathfrak{u}, v) - \mathrm{it}_{0,h,\times}(\boldsymbol{\gamma}_{0,h,\times}\mathfrak{u},\, \boldsymbol{\gamma}_{0,h,\times}v) = a(\mathfrak{u}, v) = 0, \qquad \forall v \in \mathrm{V}_h(\Omega). \tag{10.62}$$

The well-posedness of the discrete model problem (4.19) stated in Assumption 4.4 gives that $\mathfrak{u} = 0$ which is a contradiction. ∎

Again, we point out that such a result is valid for our target applications for h small enough, but this is not an issue for the abstract analysis.

A direct consequence of the well-posedness of the above problem (10.52) is the well-posedness of the following local sub-problems in each sub-domain, for diagonal operators.

Corollary 10.13. *If the transmission operator* $\mathrm{t}_{0,h,\times}$ *are diagonal, for all* $j \in \{1, \dots, J\}$ *and any linear form* l_j *on* $\mathrm{V}_h(\Omega_{j,h})$*, the problem*

$$\begin{cases} \text{Find } u_j \in \mathrm{V}_h(\Omega_{j,h}) \text{ such that}: \\ a_j(u_j, v_j) - \mathrm{it}^j_{0,h,\times}(\gamma_{0,\Gamma_{j,h}} u_j,\, \gamma_{0,\Gamma_{j,h}} v_j) = l_j(v_j) \qquad \forall v_j \in \mathrm{V}_h(\Omega_{j,h}), \end{cases} \tag{10.63}$$

is well posed.

We are able to provide an equivalent discrete characterization to the one from Proposition 9.20, which is similar to [33, Lem. 7.2].

Proposition 10.14 (**Characterization of the discrete Cauchy trace space**)**.** *We have the following characterization of the Cauchy-trace space* (10.2)*:*

$$\mathbb{C}_{h,\times} = \mathrm{Ker}\left(\mathbf{R}^-_{0,h,\times} - \mathbf{S}_{0,h,\times}\mathbf{R}^+_{0,h,\times}\right). \tag{10.64}$$

Proof. From Definition 10.10 and Definition 10.11, $\mathbb{x} \equiv (\mathbb{x}_0, \mathbb{x}_1) \in \mathbb{M}_{h,\times}$ satisfy

$$\mathbf{R}^-_{0,h,\times}\mathbb{x} = \mathbf{S}_{0,h,\times}\mathbf{R}^+_{0,h,\times}\mathbb{x}, \tag{10.65}$$

if, and only if, there exists $\mathbb{u} \in \mathbb{V}_h(\mathcal{P}_{\Omega,h})$ such that

$$\begin{aligned} &\begin{cases} \mathbb{a}(\mathbb{u}, \mathbb{v}) - \mathrm{it}_{0,h,\times}(\boldsymbol{\gamma}_{0,h,\times}\mathbb{u},\, \boldsymbol{\gamma}_{0,h,\times}\mathbb{v}) \\ \qquad = \langle\!\langle \mathbb{x}_1, \boldsymbol{\gamma}_{0,h,\times}\mathbb{v} \rangle\!\rangle_\times - \mathrm{it}_{0,h,\times}(\mathbb{x}_0,\, \boldsymbol{\gamma}_{0,h,\times}\mathbb{v}), & \forall \mathbb{v} \in \mathbb{V}_h(\mathcal{P}_{\Omega,h}), \\ -\langle\!\langle \mathbb{x}_1, \mathbb{x}^t_0 \rangle\!\rangle_\times - \mathrm{it}_{0,h,\times}(\mathbb{x}_0,\, \mathbb{x}^t_0) \\ \qquad = -\langle\!\langle \mathbb{x}_1, \mathbb{x}^t_0 \rangle\!\rangle_\times + \mathrm{it}_{0,h,\times}(\mathbb{x}_0,\, \mathbb{x}^t_0) - 2\mathrm{it}_{0,h,\times}(\boldsymbol{\gamma}_{0,h,\times}\mathbb{u},\, \mathbb{x}^t_0), & \forall \mathbb{x}^t_0 \in \mathbb{M}_{0,h,\times}. \end{cases} \\ &\Leftrightarrow \begin{cases} \mathbb{a}(\mathbb{u}, \mathbb{v}) - \mathrm{it}_{0,h,\times}(\boldsymbol{\gamma}_{0,h,\times}\mathbb{u} - \mathbb{x}_0,\, \boldsymbol{\gamma}_{0,h,\times}\mathbb{v}) = \langle\!\langle \mathbb{x}_1, \boldsymbol{\gamma}_{0,h,\times}\mathbb{v} \rangle\!\rangle_\times, & \forall \mathbb{v} \in \mathbb{V}_h(\mathcal{P}_{\Omega,h}), \\ \mathrm{t}_{0,h,\times}(\mathbb{x}_0,\, \mathbb{x}^t_0) = \mathrm{t}_{0,h,\times}(\boldsymbol{\gamma}_{0,h,\times}\mathbb{u},\, \mathbb{x}^t_0), & \forall \mathbb{x}^t_0 \in \mathbb{M}_{0,h,\times}, \end{cases} \\ &\Leftrightarrow \begin{cases} \mathbb{a}(\mathbb{u}, \mathbb{v}) = \langle\!\langle \mathbb{x}_1, \boldsymbol{\gamma}_{0,h,\times}\mathbb{v} \rangle\!\rangle_\times, \qquad \forall \mathbb{v} \in \mathbb{V}_h(\mathcal{P}_{\Omega,h}), \\ \boldsymbol{\gamma}_{0,h,\times}\mathbb{u} = \mathbb{x}_0, \end{cases} \end{aligned} \tag{10.66}$$

which yields $\mathbb{x} \in \mathbb{C}_{h,\times}$ from Definition 10.2. Note that we used the injectivity of $\mathrm{t}_{0,h,\times}$ to establish the last equivalence. ■

10.1.2.3 Communication operator

Following the approach adopted in Section 9.2.2.3 we start by defining the orthogonal projector onto the single trace space $\mathbb{S}_{0,h,\times}$.

Definition 10.15 (**Discrete orthogonal projector**)**.** *In the Hilbert space* $\left(\mathbb{M}_{0,h,\times},\, \|\cdot\|_{\mathrm{t}_{0,h,\times}}\right)$*, we introduce the following orthogonal projectors*

$$\begin{aligned} &\mathbf{P}_{0,h,\times} : \mathbb{M}_{0,h,\times} \to \mathbb{S}_{0,h,\times} \qquad \textit{and} \qquad \mathbf{P}_{0,h,\times}{}^{\perp} : \mathbb{M}_{0,h,\times} \to \mathbb{S}_{0,h,\times}{}^{\perp}, \\ &\textit{satisfying} \qquad \mathrm{Id} = \mathbf{P}_{0,h,\times}{}^{\perp} + \mathbf{P}_{0,h,\times}. \end{aligned} \tag{10.67}$$

The communication operator is then defined from the projection operator, as stated below.

Definition 10.16 (**Communication operator**). *We define the communication operator as*

$$\boldsymbol{\Pi}_{0,h,\times} := 2\mathbf{P}_{0,h,\times} - \mathrm{Id} \ : \ \mathbb{M}_{0,h,\times} \to \mathbb{M}_{0,h,\times}. \tag{10.68}$$

We emphasize again that the orthogonal projector $\mathbf{P}_{0,h,\times}$, and therefore the communication operator $\boldsymbol{\Pi}_{0,h,\times}$, depend on our choice of norm (10.43) hence are intrinsically linked to the transmission operator $\mathrm{t}_{0,h,\times}$ introduced in (10.39).

Remark 10.17 (**Practical computation of the projection**). *We refer the reader to Remark 9.24 for some important discussion on the practical computation of this projection. In practice, given $\mathbb{x}_0 \in \mathbb{M}_{0,h,\times}$ one can compute $\mathbf{P}_{0,h,\times}\mathbb{x}_0 \in \mathbb{S}_{0,h,\times}$ by solving the following* coercive *problem*

$$\mathrm{t}_{0,h,\times}(\mathbf{P}_{0,h,\times}\mathbb{x}_0,\, \mathbb{y}_0) = \mathrm{t}_{0,h,\times}(\mathbb{x}_0,\, \mathbb{y}_0), \qquad \forall \mathbb{y}_0 \in \mathbb{S}_{0,h,\times}. \tag{10.69}$$

Note that we can give alternative expressions of the projectors in terms of the communication operators:

$$\mathbf{P}_{0,h,\times} = \frac{1}{2}\left(\mathrm{Id} + \boldsymbol{\Pi}_{0,h,\times}\right) \qquad \text{and} \qquad {\mathbf{P}_{0,h,\times}}^{\perp} = \frac{1}{2}\left(\mathrm{Id} - \boldsymbol{\Pi}_{0,h,\times}\right). \tag{10.70}$$

The following proposition is immediate from the definition of the communication operator $\boldsymbol{\Pi}_{0,h,\times}$ by simple properties of projectors. Note that the following two propositions are based on a similar result valid in the acoustic setting only which can be found in [33, Lem. 4.3].

Proposition 10.18 (**Isometric property**). *The communication operator $\boldsymbol{\Pi}_{0,h,\times}$ is an involution*

$${\boldsymbol{\Pi}_{0,h,\times}}^2 = \mathrm{Id}, \qquad \text{in } \mathbb{M}_{0,h,\times}, \tag{10.71}$$

and an isometry of $\mathbb{M}_{0,h,\times}$, for the norm induced by $\mathrm{t}_{0,h,\times}$,

$$\left\|\boldsymbol{\Pi}_{0,h,\times}\mathbb{x}_0\right\|_{\mathrm{t}_{0,h,\times}} = \left\|\mathbb{x}_0\right\|_{\mathrm{t}_{0,h,\times}}, \qquad \forall \mathbb{x}_0 \in \mathbb{M}_{0,h,\times}. \tag{10.72}$$

We are now able to characterize the discrete single-trace space $\mathbb{S}_{h,\times}$ (Definition 10.3) as the kernel of an operator involving the discrete generalized Robin operators $\mathbf{R}^{\pm}_{0,h,\times}$ and the exchange operator $\boldsymbol{\Pi}_{0,h,\times}$.

Proposition 10.19 (**Characterization of the discrete single-trace space**). *We have the following characterization of the single-trace space* (10.12)*:*

$$\mathbb{S}_{h,\times} = \mathrm{Ker}\left(\mathbf{R}^{\pm}_{0,h,\times} - \boldsymbol{\Pi}_{0,h,\times}\mathbf{R}^{\mp}_{0,h,\times}\right). \tag{10.73}$$

Proof. First note that for any $\mathbb{x} \in \mathbb{M}_{h,\times}$, $\mathbf{R}^{+}_{0,h,\times}\mathbb{x} = \boldsymbol{\Pi}_{0,h,\times}\mathbf{R}^{-}_{0,h,\times}\mathbb{x}$ is equivalent to $\mathbf{R}^{-}_{0,h,\times}\mathbb{x} = \boldsymbol{\Pi}_{0,h,\times}\mathbf{R}^{+}_{0,h,\times}\mathbb{x}$ since the exchange operator $\boldsymbol{\Pi}_{0,h,\times}$ is an involution according to Proposition 10.18.

Let $\mathbb{x} \equiv (\mathbb{x}_0, \mathbb{x}_1) \in \mathbb{M}_{h,\times} \equiv \mathbb{M}_{0,h,\times} \times \mathbb{M}_{1,h,\times}$. First, we have the characterization of $\mathbb{S}_{0,h,\times}$ from the orthogonal projector (10.67)

$$\mathbb{x}_0 \in \mathbb{S}_{0,h,\times} \quad \Leftrightarrow \quad {\mathbf{P}_{0,h,\times}}^{\perp}\mathbb{x}_0 = 0. \tag{10.74}$$

Second, we identify the annihilator of $\mathbb{S}_{0,h,\times}$ in $\mathbb{M}_{0,h,\times}$, denoted $\mathbb{S}_{1,h,\times}$, with the orthogonal complement of $\mathbb{S}_{0,h,\times}$ with respect to the scalar product $\mathrm{t}_{0,h,\times}$, denoted ${\mathbb{S}_{0,h,\times}}^{\perp}$. Let us define $\mathbb{x}_0^{\perp} \in \mathbb{M}_{0,h,\times}$ such that

$$\mathrm{t}_{0,h,\times}(\mathbb{x}_0^{\perp},\, \mathbb{x}_0^t) = \left\langle\!\left\langle \mathbb{x}_1, \mathbb{x}_0^t \right\rangle\!\right\rangle_{\times}, \qquad \forall \mathbb{x}_0^t \in \mathbb{M}_{0,h,\times}, \tag{10.75}$$

which is well defined from Definition 10.8. By Definition 10.3 of $\mathbb{S}_{1,h,\times}$, we have

$$\mathrm{t}_{0,h,\times}(\mathbb{x}_0^\perp,\, \mathbb{x}_0^t) = \langle\!\langle \mathbb{x}_1, \mathbb{x}_0^t \rangle\!\rangle_\times = 0, \qquad \forall \mathbb{x}_0^t \in \mathbb{S}_{0,h,\times}, \tag{10.76}$$

so that

$$\mathbb{x}_1 \in \mathbb{S}_{1,h,\times} \quad \Leftrightarrow \quad \mathbb{x}_0^\perp \in {\mathbb{S}_{0,h,\times}}^\perp \quad \Leftrightarrow \quad \mathbf{P}_{0,h,\times}\mathbb{x}_0^\perp = 0. \tag{10.77}$$

Hence, by simple properties of projectors, we have from (10.74) and (10.77),

$$\mathbb{x} \in \mathbb{S}_{h,\times} \quad \Leftrightarrow \quad \mathbf{P}_{0,h,\times}\mathbb{x}_0^\perp - \mathrm{i}\mathbf{P}_{0,h,\times}{}^\perp \mathbb{x}_0 = 0. \tag{10.78}$$

This is rewritten as, using the expressions of the projectors in term of the communication operator $\mathbf{\Pi}_{0,h,\times}$ from (10.70)

$$\begin{aligned} \mathbb{x} \in \mathbb{S}_{h,\times} \quad &\Leftrightarrow \quad (\mathrm{Id} + \mathbf{\Pi}_{0,h,\times})\mathbb{x}_0^\perp - \mathrm{i}(\mathrm{Id} - \mathbf{\Pi}_{0,h,\times})\mathbb{x}_0 = 0, \\ &\Leftrightarrow \quad \mathbb{x}_0^\perp - \mathrm{i}\mathbb{x}_0 = \mathbf{\Pi}_{0,h,\times}(-\mathbb{x}_0^\perp - \mathrm{i}\mathbb{x}_0). \end{aligned} \tag{10.79}$$

Using Definition 10.10 of the generalized Robin operators, we have, for all $\mathbb{x}_0^t \in \mathbb{M}_{0,h,\times}$,

$$\mathrm{t}_{0,h,\times}(\mathbf{R}^\pm_{0,h,\times}\mathbb{x},\, \mathbb{x}_0^t) = \pm\langle\!\langle \mathbb{x}_1, \mathbb{x}_0^t \rangle\!\rangle_\times - \mathrm{i}\mathrm{t}_{0,h,\times}(\mathbb{x}_0,\, \mathbb{x}_0^t) = \mathrm{t}_{0,h,\times}(\pm\mathbb{x}_0^\perp - \mathrm{i}\mathbb{x}_0,\, \mathbb{x}_0^t), \tag{10.80}$$

so that using the injectivity property of $\mathrm{t}_{0,h,\times}$ we have

$$\mathbf{R}^\pm_{0,h,\times}\mathbb{x} = \pm\mathbb{x}_0^\perp - \mathrm{i}\mathbb{x}_0. \tag{10.81}$$

Finally, we get

$$\mathbb{x} \in \mathbb{S}_{h,\times} \quad \Leftrightarrow \quad \left(\mathbf{R}^+_{0,h,\times} - \mathbf{\Pi}_{0,h,\times}\mathbf{R}^-_{0,h,\times}\right)\mathbb{x} = 0. \tag{10.82}$$

■

10.1.2.4 Equivalent interface problem

With the help of the discrete scattering operators $\mathbf{S}_{0,h,\times}$ and exchange operator $\mathbf{\Pi}_{0,h,\times}$ we are now in a position to recast the discrete approximation of the original problem (4.19) as a problem posed on the skeleton Σ_h. The result is formally very similar to Proposition 4.33, and so are the proofs. The main difference lies in the different kind of space the interface problems are posed.

Proposition 10.20 (**Equivalent discrete interface problem**). *Let $\mathbb{F}_h \in \mathbb{V}_h(\mathcal{P}_{\Omega,h})$ be the (unique) source lifting such that*

$$\mathfrak{a}(\mathbb{F}_h, v) - \mathrm{i}\mathrm{t}_{0,h,\times}(\boldsymbol{\gamma}_{0,h,\times}\mathbb{F}_h,\, \boldsymbol{\gamma}_{0,h,\times}v) = \mathbb{l}(v), \qquad \forall \mathbb{v} \in \mathbb{V}_h(\mathcal{P}_{\Omega,h}), \tag{10.83}$$

and define $\mathbb{f} \equiv (\mathbb{f}_0, \mathbb{f}_1) \in \mathbb{M}_{h,\times}$ such that

$$\begin{cases} \langle\!\langle \mathbb{f}_1, \mathbb{x}_0^t \rangle\!\rangle_\times = +\mathrm{i}\mathrm{t}_{0,h,\times}(\boldsymbol{\gamma}_{0,h,\times}\mathbb{F}_h,\, \mathbb{x}_0^t), \qquad \forall \mathbb{x}_0^t \in \mathbb{M}_{0,h,\times}, \\ \mathbb{f}_0 := \boldsymbol{\gamma}_{0,h,\times}\mathbb{F}_h. \end{cases} \tag{10.84}$$

Consider the problem

$$\begin{cases} \textit{Find } \mathbb{x}_0 \in \mathbb{M}_{0,h,\times}, \\ (\mathrm{Id} - \mathbf{\Pi}_{0,h,\times}\mathbf{S}_{0,h,\times})\mathbb{x}_1 = \mathbf{\Pi}_{0,h,\times}\mathbf{R}^-_{0,h,\times}\mathbb{f}. \end{cases} \tag{10.85}$$

If $u_h \in \mathrm{V}_h(\Omega)$ is solution of the (discrete) approximation (4.19) *of the model problem* (3.79) *then $\mathbb{x}_0 = \mathbf{R}^+_{0,h,\times}\mathbb{y} \in \mathbb{M}_{0,h,\times}$ where $\mathbb{y} \equiv (\mathbb{y}_0, \mathbb{y}_1) \in \mathbb{M}_{h,\times}$ is defined as*

$$\begin{cases} \mathbb{a}(u_h, \mathbb{v}_h) - \mathbb{l}(\mathbb{v}_h) = \langle\!\langle \mathbb{y}_1, \boldsymbol{\gamma}_{0,h,\times}\mathbb{v}_h \rangle\!\rangle_\times, & \forall \mathbb{v}_h \in \mathbb{V}_h(\mathcal{P}_{\Omega,h}), \\ \boldsymbol{\gamma}_{0,h,\times} u_h = \mathbb{y}_0, \end{cases} \tag{10.86}$$

solves problem (10.85).

Reciprocally, if $\mathbb{x}_0 \in \mathbb{M}_{0,h,\times}$ is solution of the interface problem (10.85) *and if $\mathbb{v} \in \mathbb{V}_h(\mathcal{P}_{\Omega,h})$ is the (unique) solution of*

$$\mathbb{a}(\mathbb{v}_h, \mathbb{v}^t_h) - \mathrm{it}_{0,h,\times}(\boldsymbol{\gamma}_{0,h,\times}\mathbb{v}_h, \boldsymbol{\gamma}_{0,h,\times}\mathbb{v}^t_h) = \mathrm{t}_{0,h,\times}(\mathbb{x}_0, \boldsymbol{\gamma}_{0,h,\times}\mathbb{v}^t_h), \quad \forall \mathbb{v}^t_h \in \mathbb{V}_h(\mathcal{P}_{\Omega,h}), \tag{10.87}$$

then $u_h \in \mathbb{V}_h(\mathcal{P}_{\Omega,h})$ defined as $u_h := \mathbb{v}_h + \mathbb{F}_h$ is solution of the (discrete) approximation (4.19) *of the model problem* (3.79).

Proof. Let $\mathbb{F}_h$ and $\mathbb{f} \equiv (\mathbb{f}_0, \mathbb{f}_1) \in \mathbb{M}_{h,\times}$ satisfy (10.83) (which are uniquely defined by Proposition 10.12). Note that by construction, it holds that

$$\begin{aligned} & + \langle\!\langle \mathbb{f}_1, \mathbb{x}^t_0 \rangle\!\rangle_\times - \mathrm{it}_{0,h,\times}(\mathbb{f}_0, \mathbb{x}^t_0) = 0, \qquad \forall \mathbb{x}^t_0 \in \mathbb{M}_{0,h,\times}, \\ \Leftrightarrow \quad & \mathbf{R}^+_{0,h,\times}\mathbb{f} = 0, \end{aligned} \tag{10.88}$$

and $\mathbb{F}_h \in \mathbb{V}_h(\mathcal{P}_{\Omega,h})$ is such that

$$\begin{cases} \mathbb{a}(\mathbb{F}_h, \mathbb{v}_h) - \mathbb{l}(\mathbb{v}_h) = \langle\!\langle \mathbb{f}_1, \boldsymbol{\gamma}_{0,h,\times}\mathbb{v}_h \rangle\!\rangle_\times, & \forall \mathbb{v}_h \in \mathbb{V}_h(\mathcal{P}_{\Omega,h}), \\ \boldsymbol{\gamma}_{0,h,\times}\mathbb{F}_h = \mathbb{f}_0. \end{cases} \tag{10.89}$$

($\Rightarrow$) If $u_h \in \mathrm{V}_h(\Omega)$ is solution of the (discrete) approximation (4.19) of the model problem (3.79), then by Proposition 10.6, we know that $\mathbb{y} \equiv (\mathbb{y}_0, \mathbb{y}_1)$ defined in (10.86) above belongs to $\mathbb{C}_{h,\times}$. Besides, from both (10.86) and (10.89), we get

$$\begin{cases} \mathbb{a}(u_h - \mathbb{F}_h, \mathbb{v}_h) = \langle\!\langle \mathbb{y}_1 - \mathbb{f}_1, \boldsymbol{\gamma}_{0,h,\times}\mathbb{v}_h \rangle\!\rangle_\times, & \forall \mathbb{v}_h \in \mathbb{V}_h(\mathcal{P}_{\Omega,h}), \\ \boldsymbol{\gamma}_{0,h,\times}(u_h - \mathbb{F}_h) = \mathbb{y}_0 - \mathbb{f}_0, \end{cases} \tag{10.90}$$

so that by Definition 4.10 of $\mathbb{C}_{h,\times}$, we have $\mathbb{y} - \mathbb{f} \in \mathbb{C}_{h,\times}$. From the characterizations of both the Cauchy trace space stated in Proposition 10.14 and the single trace space stated in Proposition 10.19 we have

$$\begin{cases} \mathbb{y} - \mathbb{f} \in \mathbb{C}_{h,\times}, \\ \mathbb{y} \in \mathbb{C}_{h,\times}, \end{cases} \quad \Leftrightarrow \quad \begin{cases} \mathbf{R}^-_{0,h,\times}(\mathbb{y} - \mathbb{f}) = \mathbf{S}_{0,h,\times}\mathbf{R}^+_{0,h,\times}(\mathbb{y} - \mathbb{f}), \\ \mathbf{R}^+_{0,h,\times}\mathbb{y} = \boldsymbol{\Pi}_{0,h,\times}\mathbf{R}^-_{0,h,\times}\mathbb{y}. \end{cases} \tag{10.91}$$

Hence using $\mathbf{R}^+_{0,h,\times}\mathbb{f} = 0$ we deduce

$$\begin{cases} \mathbf{R}^-_{0,h,\times}\mathbb{y} = \mathbf{S}_{0,h,\times}\mathbf{R}^+_{0,h,\times}\mathbb{y} + \mathbf{R}^-_{0,h,\times}\mathbb{f}, \\ \mathbf{R}^+_{0,h,\times}\mathbb{y} = \boldsymbol{\Pi}_{0,h,\times}\mathbf{R}^-_{0,h,\times}\mathbb{y}. \end{cases} \tag{10.92}$$

Eliminating $\mathbf{R}^-_{0,h,\times}\mathbb{y}$ it is then immediate that

$$\mathbf{R}^+_{0,h,\times}\mathbb{y} = \boldsymbol{\Pi}_{0,h,\times}\mathbf{S}_{0,h,\times}\mathbf{R}^+_{0,h,\times}\mathbb{y} + \boldsymbol{\Pi}_{0,h,\times}\mathbf{R}^-_{0,h,\times}\mathbb{f}. \tag{10.93}$$

hence the quantity $\mathbb{x}_0 := \mathbf{R}^+_{0,h,\times}\mathbb{y}$ satisfies the interface problem (10.85).

($\Leftarrow$) Reciprocally, let $\mathbb{x}_0 \in \mathbb{M}_{0,h,\times}$ be solution of the interface problem (10.85) and let $\mathbb{v}_h \in \mathbb{V}_h(\mathcal{P}_{\Omega,h})$ be the unique solution (by Proposition 10.12) to (10.87). Then, define $\mathbb{z} \equiv (\mathbb{z}_0, \mathbb{z}_1) \in \mathbb{M}_{h,\times}$ such that

$$\begin{cases} \mathfrak{a}(\mathbb{v}_h, \mathbb{v}_h^t) = \langle\!\langle \mathbb{z}_1, \boldsymbol{\gamma}_{0,h,\times} \mathbb{v}_h^t \rangle\!\rangle_\times, & \forall \mathbb{v}_h^t \in \mathbb{V}_h(\mathcal{P}_{\Omega,h}), \\ \boldsymbol{\gamma}_{0,h,\times} \mathbb{v}_h = \mathbb{z}_0, \end{cases} \tag{10.94}$$

so that using (10.89), we get

$$\begin{cases} \mathfrak{a}(\mathbb{v}_h + \mathbb{F}_h, \mathbb{v}_h^t) - \mathbb{l}(\mathbb{v}_h) = \langle\!\langle \mathbb{z}_1 + \mathbb{f}_1, \boldsymbol{\gamma}_{0,h,\times} \mathbb{v}_h \rangle\!\rangle_\times, & \forall \mathbb{v}_h^t \in \mathbb{V}_h(\mathcal{P}_{\Omega,h}), \\ \boldsymbol{\gamma}_{0,h,\times}(\mathbb{v}_h + \mathbb{F}_h) = \mathbb{z}_0 + \mathbb{f}_0. \end{cases} \tag{10.95}$$

If we set

$$\begin{aligned} &u_h := \mathbb{v}_h + \mathbb{F}_h, \\ &\mathbb{y} \equiv (\mathbb{y}_0, \mathbb{y}_1) := \mathbb{z} + \mathbb{f} \equiv (\mathbb{z}_0 + \mathbb{f}_0, \mathbb{z}_1 + \mathbb{f}_1), \end{aligned} \tag{10.96}$$

we obtain

$$\begin{cases} \mathfrak{a}(u_h, \mathbb{v}^t) - \mathbb{l}(\mathbb{v}^t) = \langle\!\langle \mathbb{y}_1, \boldsymbol{\gamma}_{0,h,\times} \mathbb{v}^t \rangle\!\rangle_\times, & \forall \mathbb{v}^t \in \mathbb{V}_h(\mathcal{P}_{\Omega,h}), \\ \boldsymbol{\gamma}_{0,h,\times} u_h = \mathbb{y}_0. \end{cases} \tag{10.97}$$

Using Proposition 10.6 all that remains to prove is that $\mathbb{y} \in \mathbb{C}_{h,\times}$. We have, combining (10.87) and (10.94)

$$\mathrm{t}_{0,h,\times}(\mathbb{x}_0, \mathbb{x}_0^t) = +\langle\!\langle \mathbb{z}_1, \mathbb{x}_0^t \rangle\!\rangle_\times - \mathrm{it}_{0,h,\times}(\mathbb{z}_0, \mathbb{x}_0^t), \qquad \forall \mathbb{x}_0^t \in \mathbb{M}_{0,h,\times}, \tag{10.98}$$

so that $\mathbb{x}_0 = \mathbf{R}^+_{0,h,\times}\mathbb{z}$ by Definition 10.10 of the generalized Robin operator. We can rewrite (9.99) as

$$\begin{aligned} & (\mathrm{Id} - \boldsymbol{\Pi}_{0,h,\times}\mathbf{S}_{0,h,\times})\,\mathbb{x}_0 = \boldsymbol{\Pi}_{0,h,\times}\mathbf{R}^-_{0,h,\times}\mathbb{f}, \\ \Leftrightarrow \quad & (\mathrm{Id} - \boldsymbol{\Pi}_{0,h,\times}\mathbf{S}_{0,h,\times})\,\mathbf{R}^+_{0,h,\times}\mathbb{z} = \boldsymbol{\Pi}_{0,h,\times}\mathbf{R}^-_{0,h,\times}\mathbb{f}. \end{aligned} \tag{10.99}$$

Using Proposition 10.14 we get

$$\mathbf{R}^+_{0,h,\times}\mathbb{z} - \boldsymbol{\Pi}_{0,h,\times}\mathbf{R}^-_{0,h,\times}\mathbb{z} = \boldsymbol{\Pi}_{0,h,\times}\mathbf{R}^-_{0,h,\times}\mathbb{f}. \tag{10.100}$$

Hence using $\mathbf{R}^+_{0,h,\times}\mathbb{f} = 0$ together with the definition of $\mathbb{y}$ we obtain that

$$\mathbf{R}^+_{0,h,\times}\mathbb{y} = \boldsymbol{\Pi}_{0,h,\times}\mathbf{R}^-_{0,h,\times}\mathbb{y}. \tag{10.101}$$

Proposition 10.19 then gives $\mathbb{y} \in \mathbb{C}_{h,\times}$. ■

Remark 10.21. *The interface problem is set in $\mathbb{M}_{0,h,\times}$, the natural trace space, while the corresponding problem in Chapter 4 was set in the dual trace space $\mathbb{M}_{1,h,\|}$, so to speak. Our numerical implementations of both methods reflect this. It is entirely possible to write a similar interface problem in $\mathbb{M}_{1,h,\times}$, however this would require a different communication operator, based on a projector onto $\mathbb{S}_{1,h,\times}$ (and not onto $\mathbb{S}_{0,h,\times}$).*

The reason for our choice is that it is easier to implement a projector onto the single-trace space $\mathbb{S}_{0,h,\times}$ rather than onto $\mathbb{S}_{1,h,\times}$ (in the context of a Galerkin approximation based on standard finite elements). Indeed, it is easy to characterize the single-trace space $\mathbb{S}_{0,h,\times}$ in a finite element context, by requirying all the degrees of freedom associated to the same physical element (vertex, edge) to be equal. Besides, the size of the finite dimensional space $\mathbb{S}_{0,h,\times}$ is in general marginally smaller than the space $\mathbb{S}_{1,h,\times}$, due to the junctions points.

A drawback is the presence of the transmission operator in the right-hand-side of the local problems, which makes the local resolution more expensive. This could be enough to justify a different implementation and could be worth investigating in a future work.

10.2 Iterative discrete domain decomposition methods

10.2.1 Iterative algorithm

Let $\mathbb{F}_h$ be the solution of (10.83) with $\mathbb{f} \equiv (\mathbb{f}_0, \mathbb{f}_1) \in \mathbb{M}_{h,\times}$ defined in (10.84) and set

$$\mathbb{b}_0 := \mathbf{\Pi}_{0,h,\times} \mathbf{R}^-_{0,h,\times} \mathbb{f}. \tag{10.102}$$

In this section, we want to devise (and study the convergence of) an algorithm to solve

$$\begin{cases} \text{Find } \mathbb{x}_0 \in \mathbb{M}_{0,h,\times} \text{ such that,} \\ (\mathrm{Id} - \mathbf{\Pi}_{0,h,\times} \mathbf{S}_{0,h,\times})\, \mathbb{x}_0 = \mathbb{b}_0. \end{cases} \tag{10.103}$$

Having found such a $\mathbb{x}_0$ solution of (10.103), a global volume solution u_h can be computed by solving

$$\begin{cases} \text{Find } \mathbb{v}_h \in \mathbb{V}_h(\mathcal{P}_{\Omega,h}) \text{ such that,} \\ \mathfrak{a}(\mathbb{v}_h, \mathbb{v}^t) - \mathrm{it}_{0,h,\times}(\boldsymbol{\gamma}_{0,h,\times} \mathbb{v}_h, \boldsymbol{\gamma}_{0,h,\times} \mathbb{v}^t) = \mathrm{t}_{0,h,\times}(\mathbb{x}_0, \boldsymbol{\gamma}_{0,h,\times} \mathbb{v}^t), \qquad \forall \mathbb{v}^t \in \mathbb{V}_h(\mathcal{P}_{\Omega,h}). \end{cases} \tag{10.104}$$

Then the global solution of the discrete model problem is $u_h := \mathbb{v}_h + \mathbb{F}_h$.

Richardson algorithm Again, one of the simplest iterative method to solve (10.103) is the Richardson algorithm. Let $\mathbb{x}_0^0 \in \mathbb{M}_{0,h,\times}$ and a relaxation parameter $0 < r \leq 1$ be given, a sequence $(\mathbb{x}_0^n)_{n\in\mathbb{N}}$ in $\mathbb{M}_{0,h,\times}$ is constructed using the Richardson algorithm as follows

$$\mathbb{x}_0^{n+1} = [(1-r)\mathrm{Id} + r\mathbf{\Pi}_{0,h,\times} \mathbf{S}_{0,h,\times}]\, \mathbb{x}_0^n + r\, \mathbb{b}_0, \qquad n \in \mathbb{N}. \tag{10.105}$$

Constructing this sequence of traces also constructs a sequence of broken solutions $(\mathbb{v}_h^n)_{n\in\mathbb{N}}$ in $\mathbb{V}_h(\mathcal{P}_{\Omega,h})$ when the action of $\mathbf{S}_{0,h,\times}$ is computed. For each $n \in \mathbb{N}$ the broken solution $\mathbb{v}_h^n$ satisfy

$$\mathfrak{a}(\mathbb{v}_h^n, \mathbb{v}^t) - \mathrm{it}_{0,h,\times}(\boldsymbol{\gamma}_{0,h,\times} \mathbb{v}_h^n, \boldsymbol{\gamma}_{0,h,\times} \mathbb{v}^t) = \mathrm{t}_{0,h,\times}(\mathbb{x}_0^n, \boldsymbol{\gamma}_{0,h,\times} \mathbb{v}^t), \qquad \forall \mathbb{v}^t \in \mathbb{V}_h(\mathcal{P}_{\Omega,h}). \tag{10.106}$$

The true solution of the original problem is then (hopefully, if convergence occurs) the limit of the broken solutions $(\mathbb{u}_h^n := \mathbb{v}_h^n + \mathbb{F}_h)_{n\in\mathbb{N}}$ in $\mathbb{V}_h(\mathcal{P}_{\Omega,h})$.

10.2.2 Discrete convergence analysis

We now turn to the convergence analysis of the previously described iterative method. As we already remarked in Chapter 4, in this discrete setting there are two independent convergence processes. We study here the convergence with respect to increasing n, the iteration number, of the iterative discrete solution $\mathbb{u}_h^n \in \mathbb{V}_h(\mathcal{P}_{\Omega,h})$ towards the discrete solution $u_h \in \mathrm{V}_h(\Omega)$ of (4.19). The convergence with respect to decreasing h, the discretization parameter, of the discrete solution $u_h \in \mathrm{V}_h(\Omega)$ of (4.19) towards the continuous solution $u \in \mathrm{U}_\Gamma(\mathrm{D};\Omega)$ of (3.79), although a legitimate question, is not addressed here. However, we shall study the behavior of the convergence factor as h goes to 0.

It is clear that the new interface problem (10.103) takes the form of the abstract problem (3.230). To prove the geometric convergence of the above fixed point algorithm, we simply need to check that the assumptions of Proposition 3.57 are satisfied in our particular case where $V = \mathbb{M}_{0,h,\times}$ and $A = \mathbf{\Pi}_{0,h,\times} \mathbf{S}_{0,h,\times}$. A similar result in a slightly different setting can be found in [33, Lem. 5.1].

Proposition 10.22 (**Contraction property of the scattering operator**). *The scattering operator* $\mathbf{S}_{0,h,\times}$ *is a contraction of* $\mathbb{M}_{0,h,\times}$*, for our particular choices of norms* (10.43)*,*

$$\|\mathbf{S}_{0,h,\times}\mathbb{x}_0\|_{\mathrm{t}_{0,h,\times}} \leq \|\mathbb{x}_0\|_{\mathrm{t}_{0,h,\times}}, \qquad \forall \mathbb{x}_0 \in \mathbb{M}_{0,h,\times}. \tag{10.107}$$

Proof. Let $\mathbb{x}_0 \in \mathbb{M}_{0,h,\times}$, we have by definition of $\mathbf{S}_{0,h,\times}$ (see (10.50))

$$\mathbf{S}_{0,h,\times}\mathbb{x}_0 = -\mathbb{x}_0 - 2\mathrm{i}\boldsymbol{\gamma}_{0,h,\times}\mathbb{u}, \tag{10.108}$$

where $\mathbb{u} \in \mathbb{V}_h(\mathcal{P}_{\Omega,h})$ is such that

$$\mathfrak{a}(\mathbb{u},\mathbb{v}) - \mathrm{it}_{0,h,\times}(\boldsymbol{\gamma}_{0,h,\times}\mathbb{u},\, \boldsymbol{\gamma}_{0,h,\times}\mathbb{v}) = \mathrm{t}_{0,h,\times}(\mathbb{x}_0,\, \boldsymbol{\gamma}_{0,h,\times}\mathbb{v}), \qquad \forall \mathbb{v} \in \mathbb{V}_h(\mathcal{P}_{\Omega,h}). \tag{10.109}$$

We have, by definition of the norm (10.43),

$$\begin{aligned}
\|\mathbf{S}_{0,h,\times}\mathbb{x}_0\|^2_{\mathrm{t}_{0,h,\times}} =& \mathrm{t}_{0,h,\times}(-\mathbb{x}_0 - 2\mathrm{i}\boldsymbol{\gamma}_{0,h,\times}\mathbb{u},\, \overline{-\mathbb{x}_0 - 2\mathrm{i}\boldsymbol{\gamma}_{0,h,\times}\mathbb{u}}) \\
=& \mathrm{t}_{0,h,\times}(\mathbb{x}_0,\, \overline{\mathbb{x}_0}) + 4\mathrm{t}_{0,h,\times}(\boldsymbol{\gamma}_{0,h,\times}\mathbb{u},\, \overline{\boldsymbol{\gamma}_{0,h,\times}\mathbb{u}}) \\
& - 2\mathrm{i}\mathrm{t}_{0,h,\times}(\mathbb{x}_0,\, \overline{\boldsymbol{\gamma}_{0,h,\times}\mathbb{u}}) + 2\mathrm{i}\mathrm{t}_{0,h,\times}(\boldsymbol{\gamma}_{0,h,\times}\mathbb{u},\, \overline{\mathbb{x}_0}), \\
:=& \|\mathbb{x}_0\|^2_{\mathrm{t}_{0,h,\times}} + 4\|\boldsymbol{\gamma}_{0,h,\times}\mathbb{u}\|^2_{\mathrm{t}_{0,h,\times}} + 4\Im\, \mathrm{t}_{0,h,\times}(\mathbb{x}_0,\, \overline{\boldsymbol{\gamma}_{0,h,\times}\mathbb{u}}).
\end{aligned} \tag{10.110}$$

Besides, by definition of $\mathbb{u}$ (testing by $\mathbb{u}$ in (10.109)) and the bilinear form $\mathfrak{a}$ (see (4.16)) we have

$$\begin{aligned}
\Im\, \mathrm{t}_{0,h,\times}(\mathbb{x}_0,\, \overline{\boldsymbol{\gamma}_{0,h,\times}\mathbb{u}}) = \kappa_0{}^{-1}(\Im(\mathsf{a})\,\mathrm{D}\mathbb{u}, \mathrm{D}\overline{\mathbb{u}})_{L^2(\Omega)^{m_1}} - \kappa_0\, (\Im(\mathsf{n})\mathbb{u}, \overline{\mathbb{u}})_{L^2(\Omega)^{m_0}} \\
- \|\gamma_{0,\Gamma}\,\mathbb{u}\|^2_{L^2(\Gamma)^{m_0}} - \|\boldsymbol{\gamma}_{0,h,\times}\mathbb{u}\|^2_{\mathrm{t}_{0,h,\times}},
\end{aligned} \tag{10.111}$$

which yields, since the imaginary parts of the coefficients a and n are respectively supposed negative and positive (see (3.78)),

$$\begin{aligned}
\|\mathbf{S}_{0,h,\times}\mathbb{x}_0\|^2_{\mathrm{t}_{0,h,\times}} - \|\mathbb{x}_0\|^2_{\mathrm{t}_{0,h,\times}} = \kappa_0{}^{-1}(\Im(\mathsf{a})\,\mathrm{D}\mathbb{u}, \mathrm{D}\overline{\mathbb{u}})_{L^2(\Omega)^{m_1}} \\
- \kappa_0\, (\Im(\mathsf{n})\mathbb{u}, \overline{\mathbb{u}})_{L^2(\Omega)^{m_0}} - \|\gamma_{0,\Gamma}\,\mathbb{u}\|^2_{L^2(\Gamma)^{m_0}} \leq 0.
\end{aligned} \tag{10.112}$$

■

Combining both Proposition 10.18 and Proposition 10.22 we get the contraction property we were looking for.

Corollary 10.23 (**Contraction property**). *We have*

$$\|\boldsymbol{\Pi}_{0,h,\times}\mathbf{S}_{0,h,\times}\mathbb{x}_0\|_{\mathrm{t}_{0,h,\times}} \leq \|\mathbb{x}_0\|_{\mathrm{t}_{0,h,\times}}, \qquad \forall \mathbb{x}_0 \in \mathbb{M}_{0,h,\times}. \tag{10.113}$$

The second requirement of Proposition 3.57 to obtain geometric convergence is verified next. A similar result valid in the acoustic setting only can be found in [33, Prop. 5.2].

Proposition 10.24. *The operator* $\mathrm{Id} - \boldsymbol{\Pi}_{0,h,\times}\mathbf{S}_{0,h,\times}$ *is an isomorphism on* $\mathbb{M}_{0,h,\times}$*.*

Proof. Since $\mathbb{M}_{0,h,\times}$ is finite dimensional, we only need to prove injectivity. Let $\mathbb{x}_0 \in \mathbb{M}_{0,h,\times}$ be such that

$$(\mathrm{Id} - \boldsymbol{\Pi}_{0,h,\times}\mathbf{S}_{0,h,\times})\,\mathbb{x}_0 = 0. \tag{10.114}$$

Define (which exists from Proposition 10.12)

$$\begin{cases} u \in \mathbb{V}_h(\mathcal{P}_{\Omega,h}) \text{ such that} \\ \mathfrak{a}(u,\mathbb{v}) - \mathrm{it}_{0,h,\times}(\boldsymbol{\gamma}_{0,h,\times}u,\, \boldsymbol{\gamma}_{0,h,\times}\mathbb{v}) = \mathrm{t}_{0,h,\times}(\mathbb{x}_0,\, \boldsymbol{\gamma}_{0,h,\times}\mathbb{v}), \qquad \forall \mathbb{v} \in \mathbb{V}_h(\mathcal{P}_{\Omega,h}). \end{cases} \tag{10.115}$$

Then let $\mathbb{y} \equiv (\mathbb{y}_0, \mathbb{y}_1) \in \mathbb{M}_{h,\times}$ such that

$$\begin{cases} \langle\!\langle \mathbb{y}_1, \mathbb{x}_0^t \rangle\!\rangle_\times = \mathrm{it}_{0,h,\times}(\boldsymbol{\gamma}_{0,h,\times}\mathbb{u},\, \mathbb{x}_0^t) + \mathrm{t}_{0,h,\times}(\mathbb{x}_0,\, \mathbb{x}_0^t), & \forall \mathbb{x}_0^t \in \mathbb{M}_{0,h,\times}, \\ \mathbb{y}_0 = \boldsymbol{\gamma}_{0,h,\times}\mathbb{u}. \end{cases} \tag{10.116}$$

By construction

$$\begin{cases} \mathbb{a}(u, \mathbb{v}) = \langle\!\langle \mathbb{y}_1, \boldsymbol{\gamma}_{0,h,\times}\mathbb{v} \rangle\!\rangle_\times, & \forall \mathbb{v} \in \mathbb{V}_h(\mathcal{P}_{\Omega,h}), \\ \boldsymbol{\gamma}_{0,h,\times} u = \mathbb{y}_0, \end{cases} \tag{10.117}$$

so that $\mathbb{y} \in \mathbb{C}_{h,\times}$ and Proposition 10.14 yields

$$\left(\mathbf{R}^-_{0,h,\times} - \mathbf{S}_{0,h,\times}\mathbf{R}^+_{0,h,\times}\right)\mathbb{y} = 0. \tag{10.118}$$

Besides,

$$\langle\!\langle \mathbb{y}_1, \mathbb{x}_0^t \rangle\!\rangle_\times - \mathrm{it}_{0,h,\times}(\mathbb{y}_0,\, \mathbb{x}_0^t) = \mathrm{t}_{0,h,\times}(\mathbb{x}_0,\, \mathbb{x}_0^t), \qquad \forall \mathbb{x}_0^t \in \mathbb{x}_0, \tag{10.119}$$

so that by Definition 10.10 of the generalized Robin operators

$$\mathbf{R}^+_{0,h,\times}\mathbb{y} = \mathbb{x}_0. \tag{10.120}$$

Now (10.114) is rewritten as

$$\left(\mathbf{R}^+_{0,h,\times} - \boldsymbol{\Pi}_{0,h,\times}\mathbf{R}^-_{0,h,\times}\right)\mathbb{y} = 0, \tag{10.121}$$

and Proposition 10.19 yields $\mathbb{y} \in \mathbb{S}_{h,\times}$. Finally $\mathbb{y} \in \mathbb{C}_{h,\times} \cap \mathbb{S}_{h,\times}$, hence from Proposition 10.7, $\mathbb{y} = 0$ and $\mathbb{x}_0 = \mathbf{R}^+_{0,h,\times}\mathbb{y} = 0$. ■

We finally give the geometric convergence result. A similar result valid in the acoustic setting only can be found in [33, Th. 6.1].

Theorem 10.25 (Geometric convergence of the discrete Richardson algorithm). *The sequence of broken solutions* $(\mathbb{u}_h^n)_{n\in\mathbb{N}}$ *computed according to* (10.106)*, converges* geometrically *to* u_h *the solution of the discrete approximation of the model problem* (4.19)*. Specifically, there exist* $C > 0$ *and* $0 < \tau < 1$*, which might depend on* h*, such that*

$$\|\mathbb{u}_h^n - u_h\|_{\mathbb{U}_\Gamma(\mathrm{D};\mathcal{P}_{\Omega,h})} \leq C\,\tau^n, \qquad \forall n \in \mathbb{N}. \tag{10.122}$$

Proof. Arguing as in the proof of Corollary 3.56, this is direct application of the abstract result in Proposition 3.57. The assumptions of the latter result are systematically checked in Proposition 10.23 and Proposition 10.24. ■

Of course, as we already remarked in Chapter 4, this theorem is less important than its counterpart in the continuous setting. Indeed, if one uses an iterative algorithm applied to a finite dimensional system of equations, one will always get geometric convergence (or no convergence at all). This is why the forthcoming discrete stability analysis, which addresses the question of the behavior of the geometric convergence factor as h goes to 0, is particularly relevant.

10.2.3 Discrete stability

We have seen that in the discrete setting, the Richardson algorithm is (geometrically) convergent provided that the transmission operator defines a scalar product on the multi-trace space. The important question of discrete stability remains, namely can we get h-uniform (geometric) convergence.

Explicit bounds To provide answers to this question we need explicit bounds with respect to the discretization parameter h on the convergence factor.

Again, the main ingredient we need is an estimate on the continuity constant of the inverse of the operator $\mathrm{Id} - \mathbf{\Pi}_{0,h,\times}\mathbf{S}_{0,h,\times}$. From Proposition 10.24 we already know that the following quantity is strictly positive,

$$\zeta_{h,\times} := \inf_{\substack{\mathbb{x}_0 \in \mathbb{M}_{0,h,\times} \\ \mathbb{x}_0 \neq 0}} \frac{\|(\mathrm{Id} - \mathbf{\Pi}_{0,h,\times}\mathbf{S}_{0,h,\times})\mathbb{x}_0\|_{\mathbb{M}_{0,h,\times}}}{\|\mathbb{x}_0\|_{\mathbb{M}_{0,h,\times}}} > 0. \tag{10.123}$$

The estimate is provided by the following proposition, similar to [33, Prop. 7.1 and 7.3].

Proposition 10.26 (**Explicit discrete estimate**). *We have*

$$\begin{aligned}\zeta_{h,\times} \geq 2\frac{\beta_{\mathrm{t}_{0,h,\times}}}{|||\mathrm{t}_{0,h,\times}|||}\,(1+|||\mathrm{t}_{0,h,\times}|||)^{-1}\Big(1+\beta_{\mathrm{t}_{0,h,\times}}^{-1}\Big)^{-1/2} \\ \Big(1+|||a|||^2\,|||\mathbb{E}_{h,\times}|||^2\Big)^{-1/2}\Big[\Big(1+\alpha_{a,h}^{-1}\,|||a|||\Big)|||\mathbb{E}_{h,\times}||| + \alpha_{a,h}^{-1}\Big]^{-1} > 0.\end{aligned} \tag{10.124}$$

Proof. Let $\mathbb{b}_0 \in \mathbb{M}_{0,h,\times}$. We need to provide an explicit construction of $\mathbb{c}_0 \in \mathbb{M}_{0,h,\times}$ such that

$$(\mathrm{Id} - \mathbf{\Pi}_{0,h,\times}\mathbf{S}_{0,h,\times})\,\mathbb{c}_0 = \mathbb{b}_0, \tag{10.125}$$

in order to estimate its norm. The construction below follows closely the steps taken in the proof of Proposition 4.39, itself based on Remark 3.62.

1. First we look for a solution to

$$\begin{cases}\text{Find } \mathbb{y} \in \mathbb{M}_{h,\times} \text{ such that :} \\ \Big(\mathbf{R}^+_{0,h,\|} - \mathbf{\Pi}_{0,h,\times}\mathbf{R}^-_{0,h,\|}\Big)\,\mathbb{y} = \mathbb{b}_0.\end{cases} \tag{10.126}$$

Inspired by (9.142) from the proof of Lemma 9.42, we construct first $\mathbb{x}_0 \in \mathbb{M}_{0,h,\times}$ such that

$$\mathrm{t}_{0,h,\|}(\mathbb{x}_0,\, \mathbb{x}_0^t) = \frac{\mathrm{i}}{2}\langle\!\langle \mathbf{P}_{0,h,\times}{}^{\perp}\mathbb{b}_0, \mathbb{x}_0^t\rangle\!\rangle_{\times}, \qquad \forall \mathbb{x}_0^t \in \mathbb{M}_{0,h,\times}, \tag{10.127}$$

and we have, using the fact that $\mathbf{P}_{0,h,\times}{}^{\perp}$ is a projector,

$$\|\mathbb{x}_0\|_{\mathbb{M}_{0,h,\times}} \leq \frac{1}{2}\beta_{\mathrm{t}_{0,h,\times}}^{-1/2}\,\|\mathbb{b}_0\|_{\mathbb{M}_{0,h,\times}}. \tag{10.128}$$

Then we construct $\mathbb{x}_1 \in \mathbb{M}_{0,h,\times}$ such that

$$\langle\!\langle \mathbb{x}_1, \mathbb{x}_0^t\rangle\!\rangle_{\times} = \frac{1}{2}\langle\!\langle \mathbf{P}_{0,h,\times}\mathbb{b}_0, \mathbb{x}_0^t\rangle\!\rangle_{\times}, \qquad \forall \mathbb{x}_0^t \in \mathbb{M}_{0,h,\times}, \tag{10.129}$$

and we have

$$\|\mathbb{x}_1\|_{\mathbb{M}_{0,h,\times}} \leq \frac{1}{2}\|\mathbb{b}_0\|_{\mathbb{M}_{0,h,\times}}. \tag{10.130}$$

Now, set $\mathbb{x} := (\mathbb{x}_0, \mathbb{x}_1) \in \mathbb{M}_{h,\times}$, so that

$$\|\mathbb{x}\|_{\mathbb{M}_{\|}} \leq \frac{1}{2}\Big(1+\beta_{\mathrm{t}_{0,h,\times}}^{-1}\Big)^{1/2}\|\mathbb{b}_0\|_{\mathbb{M}_{0,h,\times}}. \tag{10.131}$$

Now let us check that it is a solution to (10.126): by definition, we have, for any $\mathbb{x}_0^t \in \mathbb{M}_{0,h,\times}$

$$\begin{aligned}
\mathrm{t}_{0,h,\|}(\mathbf{R}^+_{0,h,\|}\mathbb{x},\, \mathbb{x}_0^t) &= \langle\!\langle \mathbb{x}_1, \mathbb{x}_0^t \rangle\!\rangle_\times - \mathrm{it}_{0,h,\|}(\mathbb{x}_0,\, \mathbb{x}_0^t) = \langle\!\langle \frac{1}{2}\mathbb{b}_0, \mathbb{x}_0^t \rangle\!\rangle_\times, \\
\mathrm{t}_{0,h,\|}(\mathbf{R}^-_{0,h,\|}\mathbb{x},\, \mathbb{x}_0^t) &= -\langle\!\langle \mathbb{x}_1, \mathbb{x}_0^t \rangle\!\rangle_\times - \mathrm{it}_{0,h,\|}(\mathbb{x}_0,\, \mathbb{x}_0^t) = -\langle\!\langle \frac{1}{2}\mathbf{\Pi}_{0,h,\times}\mathbb{b}_0, \mathbb{x}_0^t \rangle\!\rangle_\times,
\end{aligned} \tag{10.132}$$

from which we deduce, using the involution property of the exchange operator $\mathbf{\Pi}_{0,h,\times}$ (Proposition 10.18),

$$\left(\mathbf{R}^+_{0,h,\|} - \mathbf{\Pi}_{0,h,\times}\mathbf{R}^-_{0,h,\|}\right)\mathbb{x} = \mathbb{b}_0. \tag{10.133}$$

2. From the previous solution $\mathbb{x} \in \mathbb{M}_{h,\times}$, Proposition 10.7 yields the existence of $\mathbb{y} \in \mathbb{C}_{h,\times}$ and $\mathbb{z} \in \mathbb{S}_{h,\times}$ such that

$$\mathbb{x} = \mathbb{y} + \mathbb{z}, \tag{10.134}$$

and we have

$$\|\mathbb{y}\|_{\mathbb{M}_\|} \le\ \alpha_{\mathbb{P}_{\mathbb{C}_{h,\times}}}\ \|\mathbb{x}\|_{\mathbb{M}_\|} \le \frac{1}{2}\,\alpha_{\mathbb{P}_{\mathbb{C}_{h,\times}}}\,\left(1+\beta^{-1}_{\mathrm{t}_{0,h,\times}}\right)^{1/2}\|\mathbb{b}_0\|_{\mathbb{M}_{0,h,\times}}. \tag{10.135}$$

Using the characterization of the single-trace space $\mathbb{S}_{h,\times}$ provided by Proposition 10.19, we have

$$\left(\mathbf{R}^+_{0,h,\|} - \mathbf{\Pi}_{0,h,\times}\mathbf{R}^-_{0,h,\|}\right)\mathbb{z} = 0, \tag{10.136}$$

so that the projection $\mathbb{y} \in \mathbb{C}_{h,\times}$ of $\mathbb{x}$ satisfies the same equation:

$$\left(\mathbf{R}^+_{0,h,\|} - \mathbf{\Pi}_{0,h,\times}\mathbf{R}^-_{0,h,\|}\right)\mathbb{y} = \mathbb{b}_0. \tag{10.137}$$

3. Set

$$\mathbb{c}_0 = \mathbf{R}^+_{0,h,\|}\mathbb{y}, \tag{10.138}$$

we have

$$\begin{aligned}
\|\mathbb{c}_0\|_{\mathbb{M}_{0,h,\times}} &\le \left(\|\mathbb{y}_1\|_{\mathbb{M}_{0,h,\times}} + |||\mathrm{t}_{0,h,\times}|||\ \|\mathbb{y}_0\|_{\mathbb{M}_{0,h,\times}}\right), \\
&\le (1 + |||\mathrm{t}_{0,h,\times}|||)\,\|\mathbb{y}\|_{\mathbb{M}_\|}, \\
&\le \frac{1}{2}\alpha_{\mathbb{P}_{\mathbb{C}_{h,\times}}}\,(1 + |||\mathrm{t}_{0,h,\times}|||)\left(1+\beta^{-1}_{\mathrm{t}_{0,h,\times}}\right)^{1/2}\|\mathbb{b}_0\|_{\mathbb{M}_{0,h,\times}}.
\end{aligned} \tag{10.139}$$

Using the characterization of the Cauchy trace space $\mathbb{C}_{h,\times}$ provided by Proposition 10.19, we obtain from $\mathbb{y} \in \mathbb{C}_{h,\times}$,

$$\mathbf{R}^-_{0,h,\|}\mathbb{y} = \mathbf{S}_{0,h,\times}\mathbf{R}^+_{0,h,\|}\mathbb{y}. \tag{10.140}$$

Therefore, we get

$$(\mathrm{Id} - \mathbf{\Pi}_{0,h,\times}\mathbf{S}_{0,h,\times})\,\mathbb{c}_0 = (\mathrm{Id} - \mathbf{\Pi}_{0,h,\times}\mathbf{S}_{0,h,\times})\,\mathbf{R}^+_{0,h,\|}\mathbb{y} = \left(\mathbf{R}^+_{0,h,\|} - \mathbf{\Pi}_{0,h,\times}\mathbf{R}^-_{0,h,\|}\right)\mathbb{y} = \mathbb{b}_0, \tag{10.141}$$

and $\mathbb{c}_0$ is the (unique, by Proposition 10.24) solution of the original problem.

We obtained above an estimate using the norm $\|\cdot\|_{\mathbb{M}_{0,h,\times}}$ however we wish to establish a bound in the norm induced by $\mathrm{t}_{0,h,\times}$. From (10.46) we have

$$\|\mathbb{c}_0\|_{\mathrm{t}_{0,h,\times}} \le \frac{1}{2}\alpha_{\mathbb{P}_{\mathbb{C}_{h,\times}}}\,\frac{|||\mathrm{t}_{0,h,\times}|||}{\beta_{\mathrm{t}_{0,h,\times}}}\,(1 + |||\mathrm{t}_{0,h,\times}|||)\left(1+\beta^{-1}_{\mathrm{t}_{0,h,\times}}\right)^{1/2}\|\mathbb{b}_0\|_{\mathrm{t}_{0,h,\times}}. \tag{10.142}$$

The claimed estimate can then readily obtained from the expression of $\alpha_{\mathbb{P}_{\mathbb{C}_{h,\times}}}$ provided in Proposition 10.7. ■

h-uniform convergence The question of h-uniform stability is settled by the following proposition, similar to [33, Cor. 8.2].

Proposition 10.27. *If the partition is independent of h, see Assumption 4.5, and under the following additional assumptions:*

1. *In addition to Assumption 4.4, we suppose that the stability constant $\alpha_{a,h}$ of the original problem is h-uniform, namely*
$$\alpha_a^\star := \liminf_{h\to 0} \alpha_{a,h} > 0, \tag{10.143}$$
2. *In addition to the requirements of Definition 10.8, we suppose that the transmission operators are h-uniformly stable, namely*
$$|||\mathfrak{t}_{0,\times}||| := \limsup_{h\to 0} |||\mathfrak{t}_{0,h,\times}||| < +\infty, \qquad \text{and} \qquad \beta^\star_{\mathfrak{t}_{0,h,\times}} := \liminf_{h\to 0} \beta_{\mathfrak{t}_0} > 0, \tag{10.144}$$
3. *We suppose that the stability constant $\alpha_{s,h}$ of the decomposed problem, defined in Proposition 10.12, is h-uniform, namely*
$$\alpha^\star_{s,\times} := \liminf_{h\to 0} \alpha_{s,h} > 0, \tag{10.145}$$
4. *In addition to Assumption 4.2, we suppose that the discrete lifting is h-uniformly stable, namely*
$$|||\mathbb{E}||| := \limsup_{h\to 0} |||\mathbb{E}_{h,\times}||| < +\infty, \tag{10.146}$$

the sequence of broken solutions $(\mathfrak{u}_h^n)_{n\in\mathbb{N}}$ computed according to (10.106)*, converges geometrically and* h-uniformly *to u_h the solution of the discrete model problem* (4.19)*. Specifically, there exist $C > 0$ and $0 < \tau < 1$, independent of h, such that*
$$\|\mathfrak{u}_h^n - u_h\|_{\mathbb{U}_\Gamma(\mathrm{D};\mathcal{P}_{\Omega,h})} \le C\tau^n, \qquad \forall n \in \mathbb{N}. \tag{10.147}$$

Proof. At each iteration $n \in \mathbb{N}$, we can define an error on the trace $\epsilon_0^n \in \mathbb{M}_{0,h,\times}$ such that
$$\epsilon_0^n = \mathfrak{x}_0^n - \mathfrak{x}_0, \tag{10.148}$$
where the sequence $(\mathfrak{x}_0^n)_{n\in\mathbb{N}}$ is computed through (10.105) and $\mathfrak{x}_0$ is the solution of (10.103). It follows that, the sequence $(\epsilon_0^n)_n$ satisfies the recurrence relation
$$\epsilon_0^{n+1} = [(1-r)\mathrm{Id} + r\boldsymbol{\Pi}_{0,h,\times}\mathbf{S}_{0,h,\|}]\,\epsilon_0^n, \qquad n \in \mathbb{N}, \tag{10.149}$$
and is such that, for all $\mathfrak{v}^t \in \mathbb{V}_h(\mathcal{P}_{\Omega,h})$,
$$\mathfrak{d}(\mathfrak{u}_h^n - u_h, \mathfrak{v}^t) - \mathrm{it}_{0,h,\|}(\boldsymbol{\gamma}_{0,h,\times}(\mathfrak{u}_h^n - u_h), \boldsymbol{\gamma}_{0,h,\times}\mathfrak{v}^t) = \langle\!\langle \epsilon_0^n, \boldsymbol{\gamma}_{0,h,\times}\mathfrak{v}^t \rangle\!\rangle_\times. \tag{10.150}$$
We use again the convexity identity (3.233) from the proof of Theorem 3.49 and we get
$$\|\epsilon_0^{n+1}\|^2_{\mathfrak{t}_{0,h,\times}} = (1-r)\|\epsilon_0^n\|^2_{\mathfrak{t}_{0,h,\times}} + r\|\boldsymbol{\Pi}_{0,h,\times}\mathbf{S}_{0,h,\|}\epsilon_0^n\|^2_{\mathfrak{t}_{0,h,\times}} - r(1-r)\|\left(\mathrm{Id} - \boldsymbol{\Pi}_{0,h,\times}\mathbf{S}_{0,h,\|}\right)\epsilon_0^n\|^2_{\mathfrak{t}_{0,h,\times}}. \tag{10.151}$$
Since $\boldsymbol{\Pi}_{0,h,\times}\mathbf{S}_{0,h,\|}$ is a contraction in $\mathbb{M}_{0,h,\times}$ from Corollary 10.23, we have
$$\|\boldsymbol{\Pi}_{0,h,\times}\mathbf{S}_{0,h,\|}\epsilon_0^n\|_{\mathfrak{t}_{0,h,\times}} \le \|\epsilon_0^n\|_{\mathfrak{t}_{0,h,\times}}, \tag{10.152}$$

and from Proposition 10.26 we have

$$\|\epsilon_0^n\|_{\mathrm{t}_{0,h,\times}} \leq \zeta_{h,\times} \, \| \left(\mathrm{Id} - \mathbf{\Pi}_{0,h,\times}\mathbf{S}_{0,h,\|}\right) \epsilon_0^n\|_{\mathrm{t}_{0,h,\times}}, \tag{10.153}$$

hence

$$\|\epsilon_0^n\|_{\mathrm{t}_{0,h,\times}} \leq \tau^n \|\epsilon_0^0\|_{\mathrm{t}_{0,h,\times}}, \tag{10.154}$$

where $\tau = \sqrt{1 - r(1-r)\zeta_{h,\times}^2}$ with $\zeta_{h,\times}$ defined in (10.123). By the stability of the problem (10.150), we have

$$\|\mathfrak{u}_h^n - u_h\|_{\mathbb{U}_\Gamma(\mathrm{D};\mathcal{P}_{\Omega,h})} \leq \left(\alpha_{s,\times}^\star\right)^{-1} \|\epsilon_0^n\|_{\mathrm{t}_{0,h,\times}} \leq \left(\alpha_{s,\times}^\star\right)^{-1} \tau^n \|\epsilon_0^0\|_{\mathrm{t}_{0,h,\times}}, \tag{10.155}$$

From problem (10.150) with $n = 0$, we also get

$$\|\epsilon_0^0\|_{\mathrm{t}_{0,h,\times}} \leq \beta_{\mathrm{t}_{0,h,\times}}^{-1/2} \; \left(|||a||| + |||\mathrm{t}_{0,h,\times}|||\right) \|\mathfrak{u}_h^0 - u_h\|_{\mathbb{U}_\Gamma(\mathrm{D};\mathcal{P}_{\Omega,h})}. \tag{10.156}$$

Finally, we have the estimate

$$\frac{\|\mathfrak{u}_h^n - u_h\|_{\mathbb{U}_\Gamma(\mathrm{D};\mathcal{P}_{\Omega,h})}}{\|\mathfrak{u}_h^0 - u_h\|_{\mathbb{U}_\Gamma(\mathrm{D};\mathcal{P}_{\Omega,h})}} \leq \beta_{\mathrm{t}_{0,h,\times}}^{-1/2} \; \left(\alpha_{s,\times}^\star\right)^{-1} \left(|||a||| + |||\mathrm{t}_{0,h,\times}|||\right) \left(1 - r(1-r)\zeta_{h,\times}^2\right)^{n/2}, \tag{10.157}$$

and the bound is h-uniform from all the above assumptions. ■

Remark 10.28. *Again, it should be noted that the stable lifting $\mathbb{E}_{h,\times}$ is a purely theoretical tool, whose existence (and stability) are solely required for the purposes of analysis. In particular, the implementation of the method does* not *require in general the actual implementation of $\mathbb{E}_{h,\times}$.*

The assumptions of the previous proposition deserves some discussion. We refer the reader to the comments made following Proposition 4.40 which also apply in this setting. Note in particular that the stability of the constant $\alpha_{s,h,\times}$ with respect to the mesh parameter h is available for the scalar equation, see [33, Lem. 4.4].

Remark 10.29. *Arguing as in Section 3.3.3, let us remark once again that h-uniform geometric convergence of the relaxed Jacobi algorithm guarantees h-uniform geometric convergence of the* GMRES *counter-part.*

10.3 Matrix and vector representation

In this section we will describe in more concrete terms the implementation of the iterative scheme, writing all equations in matrix form. This will help gain a real insight on the implementation details underlying the solution strategy we propose. In this section, we assume that the finite dimensional spaces are constructed using standard finite element spaces defined on simplicial mesh triangulations.

Approximation spaces First of all, we set a few matrix notations.

Let $j \in \{1, \ldots, J\}$, we assume to have a finite dimensional basis of $\mathrm{V}_h(\Omega_{j,h})$ consisting of $N(\Omega_{j,h}) := \dim \; \mathrm{V}_h(\Omega_{j,h})$ shape functions denoted $\varphi_{l,\Omega_{j,h}}$, $l \in \{1, \ldots, N(\Omega_{j,h})\}$. In practice, each $\varphi_{l,\Omega_{j,h}}$ will refer to the usual $\mathbb{P}_k$ Lagrange shape functions [65, Sec. 1.2.3] in the acoustic setting or to the volume Nedelec edge functions [65, Sec. 1.2.8] in the electromagnetic setting.

According to our assumptions from Chapter 4, this also defines a basis of $\mathrm{X}_{0,h}(\Gamma_{j,h})$ consisting of $N(\Gamma_{j,h}) := \dim \; \mathrm{X}_{0,h}(\Gamma_{j,h})$ shape functions denoted $\varphi_{l,\Gamma_{j,h}}$, $l \in 1, \ldots, N(\Gamma_{j,h})$. Note that we

assume that each shape function on $\Gamma_{j,h}$ is obtained by taking the natural trace (i.e. the Dirichlet or tangential trace) of some shape function on $\Omega_{j,h}$ so that for any $m \in \{1, \ldots, N(\Gamma_{j,h})\}$ there exists a $n \in \{1, \ldots, N(\Omega_{j,h})\}$ such that $\varphi_{m,\Gamma_{j,h}} = \varphi_{n,\Omega_{j,h}}|_{\Gamma_{j,h}}$.

With the previous notations, the dimension of the multi-trace space $\mathbb{M}_{0,h,\times}$ will be

$$M(\Sigma_h) := \dim \mathbb{M}_{0,h,\times} = \sum_{j=1}^{J} N(\Omega_{j,h}). \tag{10.158}$$

Let us denote by ψ_m, $m \in \{1, \ldots, M(\Sigma_h)\}$ the basis functions of the multi-trace space $\mathbb{M}_{0,h,\times}$. The single-trace space $\mathbb{S}_{0,h,\times}$ is a sub-space of $\mathbb{M}_{0,h,\times}$ whose dimension will be denoted $N(\Sigma_h) := \dim \mathbb{S}_{0,h,\times}$. Note that by construction, $N(\Sigma_h) < M(\Sigma_h)$.

Let us denote by $\widetilde{\psi}_n$, $n \in \{1, \ldots, N(\Sigma_h)\}$ the basis functions of the single-trace space $\mathbb{S}_{0,h,\times}$. We introduce in addition the (surjective) mapping Φ which associates to each index $m \in \{1, \ldots, M(\Sigma_h)\}$ the (unique) index $n := \Phi(m) \in \{1, \ldots, N(\Sigma_h)\}$ so that the two basis functions ψ_m and $\widetilde{\psi}_n$ are associated to the same geometrical element (a node in the acoustic setting, an edge in the electromagnetic setting).

Matrices For each sub-domain $\Omega_{j,h}$, $j \in \{1, \ldots, J\}$, we introduce the local matrices $\mathbf{A}_j$ of size $N(\Omega_{j,h}) \times N(\Omega_{j,h})$, such that

$$(\mathbf{A}_j)_{m,n} := a_j(\varphi_{n,\Omega_{j,h}}, \varphi_{m,\Omega_{j,h}}), \qquad \forall m, n \in \{1, \ldots, N(\Omega_{j,h})\}, \tag{10.159}$$

where the local sesquilinear form a_j is defined in (3.97). The local contributions of the right-hand side are represented by vectors $\mathbf{f}_j$ of size $N(\Omega_{j,h})$ defined by

$$(\mathbf{f}_j)_m := l_j(\varphi_{m,\Omega_{j,h}}), \qquad \forall m \in \{1, \ldots, N(\Omega_{j,h})\}, \tag{10.160}$$

where the local linear form l_j is defined in (3.100). We also introduce the local impedance matrices $\mathbf{T}_j$, of size $N(\Gamma_{j,h}) \times N(\Gamma_{j,h})$, such that

$$(\mathbf{T}_j)_{m,n} := \mathrm{t}^j_{0,h,\times}(\varphi_{n,\Gamma_{j,h}}, \varphi_{m,\Gamma_{j,h}}), \qquad \forall m, n \in \{1, \ldots, N(\Gamma_{j,h})\}. \tag{10.161}$$

It will be convenient also to define boolean local trace matrices $\mathbf{B}_j$ of size $N(\Gamma_{j,h}) \times N(\Omega_{j,h})$, which restrict a vector representing a local solution to the vector representing its trace on the boundary of the local sub-domain. The entries of these matrices are defined by

$$(\mathbf{B}_j)_{m,n} := \begin{cases} 1, & \text{if } \varphi_{m,\Gamma_{j,h}} = \varphi_{n,\Omega_{j,h}}|_{\Gamma_{j,h}}, \\ 0, & \text{otherwise,} \end{cases} \quad \forall m \in \{1, \ldots, N(\Gamma_{j,h})\},\ n \in \{1, \ldots, N(\Omega_{j,h})\}. \tag{10.162}$$

Besides, let us define for each $j \in \{1, \ldots, J\}$, the boolean matrix $\mathbf{R}_j$ of size $N(\Gamma_{j,h}) \times M(\Sigma_h)$, which restricts a vector representing a global multi-trace to the vector representing the local trace contribution on the boundary of the local sub-domain $\Omega_{j,h}$. The entries of these matrices are defined by

$$(\mathbf{R}_j)_{m,n} := \begin{cases} 1, & \text{if } m = n - \sum_{k<j} N(\Omega_{k,h}), \\ 0, & \text{otherwise,} \end{cases} \quad \forall m \in \{1, \ldots, N(\Gamma_{j,h})\},\ n \in \{1, \ldots, M(\Sigma_h)\}. \tag{10.163}$$

Let us also define the matrix $\mathbf{Q}$ of size $M(\Sigma_h) \times N(\Sigma_h)$ which constructs a multi-trace vector from a single-trace vector. The entries of this matrix are defined by

$$(\mathbf{Q})_{m,n} := \begin{cases} 1, & \text{if } n = \Phi(m), \\ 0, & \text{otherwise,} \end{cases} \quad \forall m \in \{1, \ldots, M(\Sigma_h)\},\ n \in \{1, \ldots, N(\Sigma_h)\}. \tag{10.164}$$

The local contributions

$$\mathbf{Q}_j := \mathbf{R}_j \mathbf{Q}, \qquad \forall j \in \{1, \ldots, J\}, \tag{10.165}$$

will also prove useful. Finally, we introduce a diagonal matrix $\mathbf{D}$

$$\mathbf{D} := \operatorname{diag}\left(\frac{1}{\operatorname{mult}(n)}\right)_{n=1}^{N(\Sigma_h)}. \tag{10.166}$$

where we defined

$$\operatorname{mult}(n) := \operatorname{card}\ \big\{l \in \{1, \ldots, M(\Sigma_h)\} \mid n = \Phi(l)\big\}, \tag{10.167}$$

which corresponds to the number of sub-domains to which the degree of freedom indexed by n is associated to.

One can then define the matrices of the local sub-problems

$$\mathbf{K}_j := \mathbf{A}_j - \mathrm{i}\mathbf{B}_j^* \mathbf{T}_j \mathbf{B}_j, \qquad \forall j \in \{1, \ldots, J\}. \tag{10.168}$$

From Proposition 10.12, these matrices are invertible.

10.3.1 Scattering operator

Assuming that the above local matrices are assembled for each sub-domain, the evaluation of the scattering operator $\mathbf{S}_{0,h,\times}$ takes the form of Algorithm 10.1. Note that everything is parallel, the global multi-trace vectors $\mathbf{x}$ and $\mathbf{s}$ respectively input and output of the algorithm can be distributed on the cluster nodes on a distributed-memory architecture.

Algorithm 10.1 Evaluation of the scattering operator $\mathbf{S}_{0,h,\times}$

function GLOBALSCATTERING($\mathbf{x}$) ▷ Input size: $M(\Sigma_h)$
  $\mathbf{s} \leftarrow 0$ ▷ size: $M(\Sigma_h)$
  for $j = 1, \ldots, J$ **do** ▷ Parallel loop
    $\mathbf{x}_j \leftarrow \mathbf{R}_j \mathbf{x}$ ▷ Local contribution of the multi-trace (size: $M(\Gamma_{j,h})$)
    $\mathbf{u}_j \leftarrow \mathbf{K}_j^{-1} \mathbf{B}_j^* \mathbf{T}_j \mathbf{x}_j$ ▷ Local solve (size: $N(\Omega_{j,h})$)
    $\mathbf{s}_j \leftarrow -\mathbf{x}_j - 2\mathrm{i}\mathbf{B}_j \mathbf{u}_j$ ▷ Local scattering (size: $N(\Gamma_{j,h})$)
    $\mathbf{s} \leftarrow \mathbf{s} + \mathbf{R}_j^* \mathbf{s}_j$
  end for
  return s ▷ Output size: $M(\Sigma_h)$
end function

10.3.2 Communication operator

The definition of the communication operator $\mathbf{\Pi}_{0,h,\times}$ requires to solve a projection problem. This projection step in the algorithm is a global coercive problem posed on the skeleton of the partition. We discuss here, first, the naive assembly of the full operator and then we propose an efficient algorithm to solve the problem by means of a conjugate gradient algorithm.

Explicit expression of the communication operator From the definitions of the above matrices, we can introduce the Galerkin matrix of the full transmission operator $\mathrm{t}_{0,h,\times}$ on $\mathbb{M}_{0,h,\times}$. It is of size $M(\Sigma_h) \times M(\Sigma_h)$ and admits the expression

$$\mathbf{T}_{\Sigma_h} := \sum_{j=1}^{J} \mathbf{R}_j^* \mathbf{T}_j \mathbf{R}_j, \tag{10.169}$$

and its restriction on $\mathbb{S}_{0,h,\times}$, of size $N(\Sigma_h) \times N(\Sigma_h)$, reads

$$\widetilde{\mathbf{T}}_{\Sigma_h} := \mathbf{Q}^* \mathbf{T}_{\Sigma_h} \mathbf{Q}. \tag{10.170}$$

The orthogonal projection (for the scalar product defined by the transmission operator, see Definition 10.15) from the global multi-trace space $\mathbb{M}_{0,h,\times}$ onto the single-trace space $\mathbb{S}_{0,h,\times}$ can be computed as follows. For a given vector $\mathbf{x}$ of size $M(\Sigma_h)$ representing an element of $\mathbb{M}_{0,h,\times}$, the problem to solve is rewritten as: Find $\mathbf{y}$ such that

$$\mathbf{Q}^* \mathbf{T}_{\Sigma_h} \mathbf{Q}\, \mathbf{y} = \mathbf{Q}^* \mathbf{T}_{\Sigma_h}\, \mathbf{x}, \tag{10.171}$$

where $\mathbf{y}$ is a vector of size $N(\Sigma_h)$ representing the projection $\mathbf{P}_{0,h,\times}\mathbf{x}$ in $\mathbb{S}_{0,h,\times}$. Recalling the definition of the communication operator $\mathbf{\Pi}_{0,h,\times}$ from (10.68), the matrix representing this operator can then be written as

$$2\,(\mathbf{Q}^* \mathbf{T}_{\Sigma_h} \mathbf{Q})^{-1} \mathbf{Q}^* \mathbf{T}_{\Sigma_h} - \mathrm{Id}. \tag{10.172}$$

A naive implementation of the method consists in assembling the above matrix by computing the inverse of $\widetilde{\mathbf{T}}_{\Sigma_h}$ using a direct method, which is expensive to compute. In addition, the inverse of this (sparse, since block-diagonal) matrix is, at first glance, a dense matrix, and even though the dimension of the domain (the skeleton) is reduced (from d to $d-1$), the required storage may be rather large. Fortunately the evaluation of the above matrix *need not* to be realized in practice, as indicated below.

A preconditioned conjugate gradient algorithm A possibility to solve the global problem (10.171) is to use an iterative method. Since the problem is symmetric positive definite, a natural choice is to use a conjugate gradient algorithm. At each iteration of the outer domain decomposition algorithm, the projection problem will therefore be solved iteratively using an inner CG algorithm. It turns out that it is possible to solve the projection problem using this method rather efficiently provided we use a preconditioner on the inner CG. The preconditioner that we propose (and used in our numerical experiments) is

$$\mathbf{D}\mathbf{Q}^* \mathbf{T}^{-1} \mathbf{Q}\mathbf{D}. \tag{10.173}$$

Note that we need to compute the inverse of the local transmission operator matrices, but it is not more expensive than solving the local problems. Besides, the (Cholesky) factorization can be done once for all. The presence of the diagonal matrix $\mathbf{D}$ follows heuristic considerations and is found to improve the efficiency of the preconditioner.

To solve the projection problem (10.171) with the CG algorithm, the matrix $\mathbf{Q}^* \mathbf{T}^{-1} \mathbf{Q}$ need not to be (and is not) fully assembled, it is enough to be able to evaluate its action, as indicated in Algorithm 10.2. Similarly, the matrix-vector product routine associated to the preconditioner (10.173) can be found in Algorithm 10.3. We can then define in Algorithm 10.4 the routine that evaluates the action of $\mathbf{\Pi}_{0,h,\times}$.

Algorithm 10.2 Evaluation of $\mathbf{Q}^*\mathbf{T}_{\Sigma_h}\mathbf{Q}$ for the CG algorithm

function MatVec($\mathbf{x}$) ▷ Input size: $M(\Sigma_h)$
  $\mathbf{y} \leftarrow 0$ ▷ size: $N(\Sigma_h)$
  for $j = 1, \ldots, J$ **do**
    $\mathbf{y}_j \leftarrow \mathbf{Q}_j^*\mathbf{T}_j\mathbf{Q}_j\mathbf{x}$ ▷ Parallel
    $\mathbf{y} \leftarrow \mathbf{y} + \mathbf{y}_j$ ▷ Reduction
  end for
  return $\mathbf{y}$ ▷ Output size: $N(\Sigma_h)$
end function

Algorithm 10.3 Preconditioner for the CG algorithm

function MatVec($\mathbf{x}$) ▷ Input size: $M(\Sigma_h)$
  $\mathbf{y} \leftarrow 0$ ▷ size: $N(\Sigma_h)$
  for $j = 1, \ldots, J$ **do**
    $\mathbf{y}_j \leftarrow \mathbf{D}\mathbf{Q}_j^*\mathbf{T}_j^{-1}\mathbf{Q}_j\mathbf{D}\mathbf{x}$ ▷ Parallel
    $\mathbf{y} \leftarrow \mathbf{y} + \mathbf{y}_j$ ▷ Reduction
  end for
  return $\mathbf{y}$ ▷ Output size: $N(\Sigma_h)$
end function

Algorithm 10.4 Evaluation of the communication operator $\mathbf{\Pi}_{0,h,\times}$

function GlobalExchange($\mathbf{x}$) ▷ Input size: $M(\Sigma_h)$
  $\mathbf{y} \leftarrow 0$ ▷ size: $N(\Sigma_h)$
  for $j = 1, \ldots, J$ **do**
    $\mathbf{y}_j \leftarrow \mathbf{Q}_j^*\mathbf{T}_j\mathbf{R}_j\mathbf{x}$ ▷ Parallel
    $\mathbf{y} \leftarrow \mathbf{y} + \mathbf{y}_j$ ▷ Reduction
  end for
  $\mathbf{z} \leftarrow \mathbf{Q}(\mathbf{Q}^*\mathbf{T}_{\Sigma_h}\mathbf{Q})^{-1}\mathbf{y}$ ▷ Using preconditioned CG to compute the inverse
  return $2\mathbf{z} - \mathbf{x}$ ▷ Output size: $M(\Sigma_h)$
end function

The key point is that the end result is a projection step routine that is naturally parallel (with the same level of parallelization as the outer algorithm) and which converges in only a few iterations. The communications occur at the reduction steps as indicated in the algorithms. We note that only neighbouring sub-domains (*i.e.* sub-domains that share at least a vertex in the acoustic setting, or an edge in the electromagnetic setting) need to communicate, exactly as in the usual domain decomposition algorithms. As a result, we insists that no all-to-all communication is required in the domain decomposition algorithm.

10.3.3 Richardson algorithm

The assembly of the local matrices $\mathbf{A}_j$, $\mathbf{T}_j$ and the source terms $\mathbf{f}_j$ can be pre-computed before starting the iterative algorithm. In addition, the factorizations of $\mathbf{K}_j$ (LU) and $\mathbf{T}_j$ (Choleksy) shall also be performed. The last pre-computations possible are provided by Algorithm 10.5 which describes the computation of the lifting of the source terms represented by the local vectors $\mathbf{v}_j$ and the computation of the right-hand-side $\mathbb{b}_0$ represented by the vector $\mathbf{b}$ of the skeleton problem (10.103). Except for the application of the exchange operator, all the computations are independent and can be performed in parallel.

Algorithm 10.5 Lifting of the source

$\mathbf{b} \leftarrow 0$ ▷ size: $M(\Sigma_h)$
for $j = 1, \dots, J$ **do** ▷ Parallel loop
  $\mathbf{v}_j \leftarrow \mathbf{K}_j^{-1}\mathbf{f}_j$ ▷ Local solve (size: $N(\Omega_{j,h})$)
  $\mathbf{b} \leftarrow \mathbf{b} - 2\mathrm{i}\,\mathbf{R}_j^*\mathbf{B}_j\mathbf{v}_j$ ▷ Skeleton problem right-hand-side $\mathbb{b}_0$
end for
$\mathbf{b} \leftarrow$ GlobalExchange($\mathbf{b}$) ▷ Application of $\mathbf{\Pi}_{0,h,\times}$

After choosing a relaxation parameter $r \in (0, 1)$ and maximum number of iterations $n_{\max} \in \mathbb{N}^*$, the iterative Richardson algorithm (10.105) takes the form of Algorithm 10.6 below. The only place where communications occurs are in the global exchange step. Of course, this basic algorithm can be completed by the computation of the residual for instance, and the iterations can be stopped if it is below a certain tolerance for some norm.

Algorithm 10.6 Richardson algorithm

$\mathbf{x} \leftarrow 0$ ▷ Initialization (size: $M(\Sigma_h)$)
for $n = 1, \dots, n_{\max}$ **do**
  $\mathbf{s} \leftarrow$ GlobalScattering($\mathbf{x}$) ▷ Application of $\mathbf{S}_{0,h,\times}$ (size: $M(\Sigma_h)$)
  $\mathbf{p} \leftarrow$ GlobalExchange($\mathbf{s}$) ▷ Application of $\mathbf{\Pi}_{0,h,\times}$ (size: $M(\Sigma_h)$)
  $\mathbf{x} \leftarrow (1 - r)\mathbf{x} + r\mathbf{p} + r\mathbf{b}$ ▷ Iteration (size: $M(\Sigma_h)$)
end for

Having found an approximation $\mathbf{x}$ of the solution of the skeleton problem (10.103) *via* the Richardson algorithm, the global (broken) solution, represented by local vectors $\mathbf{u}_j$, can then be computed thanks to Algorithm 10.7. The local liftings of the source $\mathbf{v}_j$ have been computed thanks to Algorithm 10.5.

10.3.4 GMRES algorithm

We can also solve the linear system given by (10.103) iteratively using the Gmres algorithm. To define the algorithm, it suffices to provide a definition for a right-hand-side and a matrix-vector

Algorithm 10.7 Evaluation of the global broken solution

for $j = 1, \ldots, J$ **do** ▷ Parallel loop
  $\mathbf{w}_j \leftarrow \mathbf{K}_j^{-1} \mathbf{B}_j^* \mathbf{T}_j \mathbf{R}_j \mathbf{x}$ ▷ Local solve (size: $N(\Omega_{j,h})$)
  $\mathbf{u}_j \leftarrow \mathbf{v}_j + \mathbf{w}_j$ ▷ Local solution (size: $N(\Omega_{j,h})$)
end for

product routine. The right-hand-side is denoted by $\mathbf{b}$ and can be computed (offline) according to Algorithm 10.5. The matrix-vector product procedure, which takes as input a global multi-trace vector $\mathbf{x}$, is given in Algorithm 10.8. Notice again here that apart from the computation of the global exchange step which ensures coupling between subdomains, all operations are local to the sub-domains. Having found an approximation $\mathbf{x}$ of the solution of the skeleton problem (10.103) *via* the GMRES algorithm, the global (broken) solution, represented by local vectors $\mathbf{u}_j$, can then be computed thanks to Algorithm 10.7.

Algorithm 10.8 Matrix-vector product for the GMRES algorithm

function MATVEC($\mathbf{x}$) ▷ Input size: $M(\Sigma_h)$
  $\mathbf{s} \leftarrow$ GLOBALSCATTERING($\mathbf{x}$) ▷ Application of $\mathbf{S}_{0,h,\times}$ (size: $M(\Sigma_h)$)
  $\mathbf{p} \leftarrow$ GLOBALEXCHANGE($\mathbf{s}$) ▷ Application of $\mathbf{\Pi}_{0,h,\times}$ (size: $M(\Sigma_h)$)
  return $\mathbf{x} - \mathbf{p}$ ▷ Output size: $M(\Sigma_h)$
end function

Chapter 11

Numerical results

Contents

In this chapter, we investigate numerically the performance of the method presented in the previous two chapters on more realistic mesh partitions generated by an automatic graph partitioner.

After some details on the implementation and the test cases in Section 11.1, we provide some extensive testing both for the acoustic (2D and 3D) and electromagnetic (3D) settings. Some illustrative convergence history results are provided in Section 11.2. We then investigate the stability of the convergence with respect to mesh refinement in Section 11.3, which has been a strong leitmotiv throughout this work, and the numerical results confirm the theoretical predictions. To study more precisely the robustness of the approach with increasingly more complex problems, we report results with respect to increasing frequency in Section 11.4 and for heterogeneous media (only in 2D) in Section 11.5. The scalability of the method is then investigated in Section 11.6 with strong and weak scaling tests. If the method is not optimal in the sense that the number of iteration grows with the number of sub-domains, we observe that the increase remains moderate and is an acceptable result for wave propagation problems.

We provide in Section 11.7 some results to compare the previous and new strategies in the case of *boundary* junction points only (i.e. there are no *interior* junction points). Note importantly that in the case where there are no junction points, the two methods are actually identical (with the caveat that the Lagrange multipliers on the physical boundary, that are introduced in the second strategy, need to be eliminated, see Section 9.2.3) so there is no interest in performing a comparison. Besides, in the case of interior junction points, because of our choice of using a nodal discretization method, there does not exist a natural and straightforward cross-point treatment (see [71] on this matter) and therefore the comparison of the two strategies is actually not possible because one is simply not properly defined.

In a last section, we report some numerical results to sustain our claim that the projection step introduced in the new approach is not prohibitive. In a first part, we show the sparsity pattern of the newly defined communication operator. This is a visual representation of the actual communications of data that take place between sub-domains. We observe that far apart sub-domains are only weakly coupled by the coercive problem posed on the skeleton that is implicitly defined behind the projection step. In a second part, we report the number of conjugate gradient iterations that are necessary to actually solve this coercive problem. We see that the solution, which can take place in parallel, requires only a moderate number of iterations, provided that the system is preconditioned. This is not the only way to solve the skeleton problem, other methods could be applied, hopefully even more efficiently but that will be the subject of future works.

Although we do not claim that the approach we advocate is the fastest or the least expensive strategy in a general configuration, we stress that the overall impression given by our numerical experiments is a general robustness of the domain decomposition approach when the operator based on elliptic auxiliary problem is used, and which rests on strong theoretical foundations. Besides, the treatment of junction points previously described provides a satisfactory solution for nodal based discretization strategies even if less computationally expensive transmission operators (e.g. local operators) are preferred.

11.1 Implementation details and test cases

The method presented in the previous two chapters was also implemented in the research code written in Julia that was briefly described in Chapter 7. We gather here some general information that apply to the numerical experiments reported in this chapter.

11.1.1 Test cases and mesh partitioning

We use again here the tests cases described in Chapter 7. However the way the partitioning of the mesh is performed is radically different. One of the big advantages of allowing junction points is our ability to deal with much more general mesh partitions.

The meshes used in the numerical experiments below are all generated by Gmsh [77] and partitioned using the autimatic graph partitionner Metis [89] through the Julia API. In some sense, despite the simplicity of the model problems we consider, the way the partitioning is performed is somehow closer to realistic applications than the partitions we used up to now. Of course, the partitioner naturally generates junctions points (and junctions curves in 3D), of both boundary and interior types, see Figure 11.1 for examples of 2D mesh partitions we consider.

The automatic partitioning aims at constructing equilibrated partitions (comparable number of cells in all sub-domains) with minimal contact surfaces between sub-domains. These are very desirable features in view of distributed computing, in particular for load balancing and to minimize communications between cores. However, this choice has many important consequences. First, we emphasize that as a result we do not have any control on the geometry of the partition,

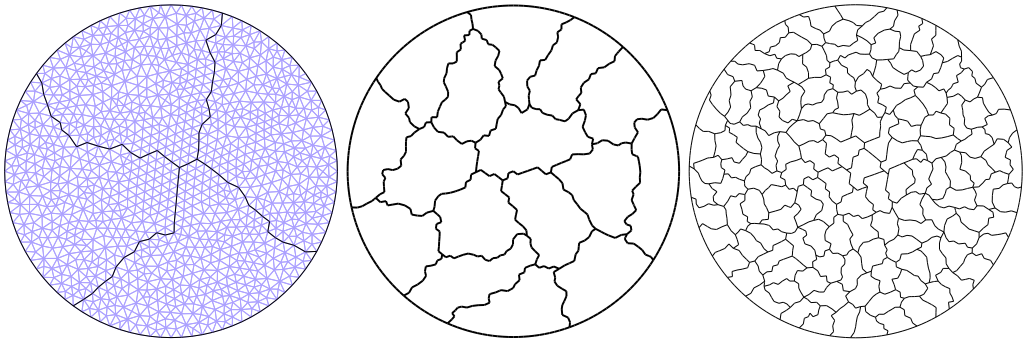

(a) $J = 4$. (b) $J = 16$. (c) $J = 128$.

Figure 11.1: Examples of 2D mesh partitions.

in particular on the smoothness of the interfaces which is therefore really rough (variations of the size of the mesh cells and re-entrant corners). Also note that in the partitions, almost all junctions, points or curves, are shared by exactly three sub-domains. Configurations with four (or more) sub-domains hardly ever happen. Notice finally that the geometry of the skeleton changes when the mesh is refined. This happens in our numerical experiments when we increase the number of points per wavelength N_λ or when we increase the wavenumber κ_0 (N_λ being fixed).

11.1.2 Transmission operators

We report and compare results using transmission operators that were already considered in Chapter 7 and Chapter 8.

Note that with the new approach it is no longer necessary to define a transmission operator by interface $\Gamma_{jk} := \partial\Omega_j \cap \partial\Omega_k$ between two sub-domains Ω_j and Ω_k. We need only one transmission operator per sub-domain Ω_j defined on its boundary $\Gamma_j := \partial\Omega_j$. The definition of transmission operators based on local tangential operators or on integral operators is straightforward and restricted to the said boundary Γ_j. However, for the operator based on the resolution of an elliptic auxiliary problem, the domain of resolution can be limited to one single sub-domain Ω_j (and no longer on the two sub-domains on both sides of the interface). This corresponds to use $\alpha_i = 1$ and $\alpha_e = 0$ in (8.12). This is obviously more economical and it also means fewer communications in the pre-processing step for a parallel implementation on a distributed architecture.

In the acoustic setting, we compare results for four transmission operators

- two *local* operators:
  - the identity operator Id of Després;
  - a positive operator based on second order surface differential operators, namely

$$\mathrm{Id} - \frac{1}{2{\kappa_0}^2}\Delta_\Sigma; \tag{11.1}$$

- two *non-local* operators that satisfy the theoretical requirements of the convergence analysis of Chapter 3:

  - the operator, for $d \in \{2, 3\}$,
$$\mathrm{T}_0^{\mathrm{Bessel}} = \frac{2}{\kappa_0}\, W_{d,\kappa_0} \tag{11.2}$$
where W_{d,κ_0} was defined in (5.19) and stems from standard potential theory.
  - the operator $\mathrm{T}_0^{\mathrm{Aux}}$, defined in (8.12) (with $\alpha_i = 1$ and $\alpha_e = 0$), which is based on the resolution of auxiliary elliptic problems.

In the electromagnetic setting, we compare results for four transmission operators

- a *local* operator:
  - the identity operator Id of Després;
  - a positive operator based on second order surface differential operators, namely
$$\mathrm{Id} - \frac{1}{2{\kappa_0}^2}\, \mathbf{curl}_\Sigma \,\mathrm{curl}_\Sigma; \tag{11.3}$$
- two *non-local* operators that satisfy the theoretical requirements of the convergence analysis of Chapter 3:
  - the operator $\mathrm{T}_0^{\mathrm{Bessel}} = 2\mathbf{K}_{3,\kappa_0}$, defined in (5.82), which stems from standard potential theory.
  - the operator $\mathrm{T}_0^{\mathrm{Aux}}$, defined in (8.12) (with $\alpha_i = 1$ and $\alpha_e = 0$), which is based on the resolution of auxiliary elliptic problems.

11.2 Convergence history

Similarly as was done in the numerical results in the free-junction setting, we first report convergence histories for both the Richardson (the fixed point iteration algorithm does no longer identify with the Jacobi algorithm) and GMRES algorithms.

We consider our acoustic and electromagnetic test cases from Chapter 7. The only difference being now that the domain is split roughly (using a mesh partitioner) into four quarters in 2D, see Figure 11.1a; and in eight parts in 3D. The interest of such partitioning is the presence of pure interior junction points where at least three domains share a common vertex.

The full convergence history in the relative H^1 error (7.6) is provided in Figure 11.2 for the acoustic 2D results and in Figure 11.3 for the acoustic 3D results. The full convergence history in the relative $\mathbf{H}(\mathbf{curl})$ error (7.16) is provided in Figure 11.4 for the Maxwell 3D results.

Note that we recover qualitatively the previous results observed in a two-domain configuration without junction points. The local operators perform the worst while we notice that the non-local operators T_0^E have the best overall performance, with the non-local operators T_0^B somewhere in-between. Moreover, the GMRES attenuates the discrepancies between the transmission operators compared to the Richardson algorithm.

11.3 h-uniform geometric convergence

We present now the influence of mesh refinement on the number of iterations to reach a set tolerance, for the different transmission operators under study and the two iterative algorithms. The refinement of the mesh is indicated by the number of points per wavelength N_λ which is inversely proportional to the typical mesh size. We also report the number of GMRES iterations

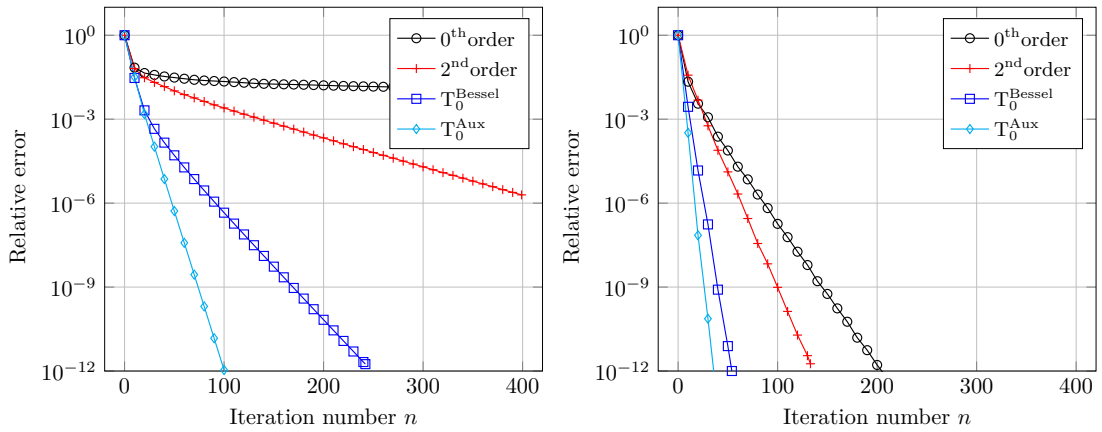

(a) Richardson algorithm (b) GMRES algorithm

Figure 11.2: Helmholtz 2D. An example of convergence history. Fixed parameters $\kappa_0 = 5$, $J = 4$, $N_\lambda = 40$.

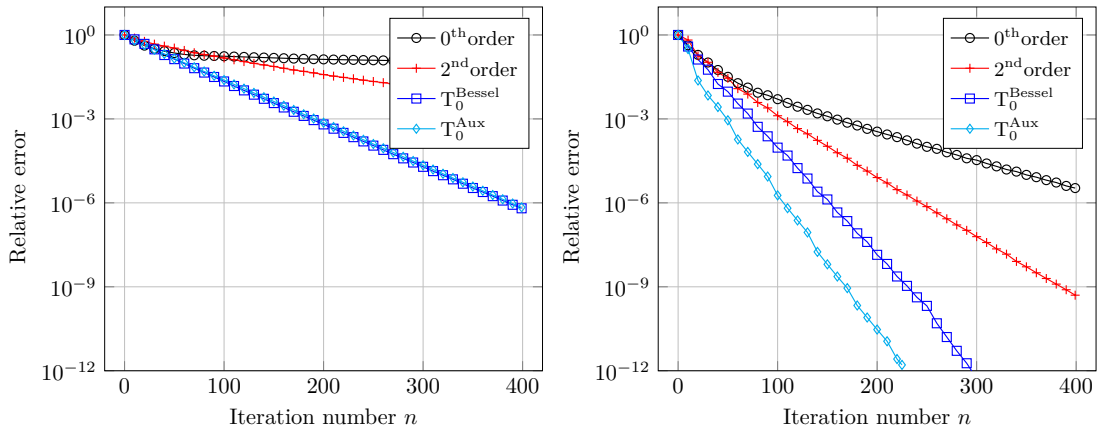

(a) Richardson algorithm (b) GMRES algorithm

Figure 11.3: Helmholtz 3D. An example of convergence history. Fixed parameters $\kappa_0 = 5$, $J = 4$, $N_\lambda = 40$.

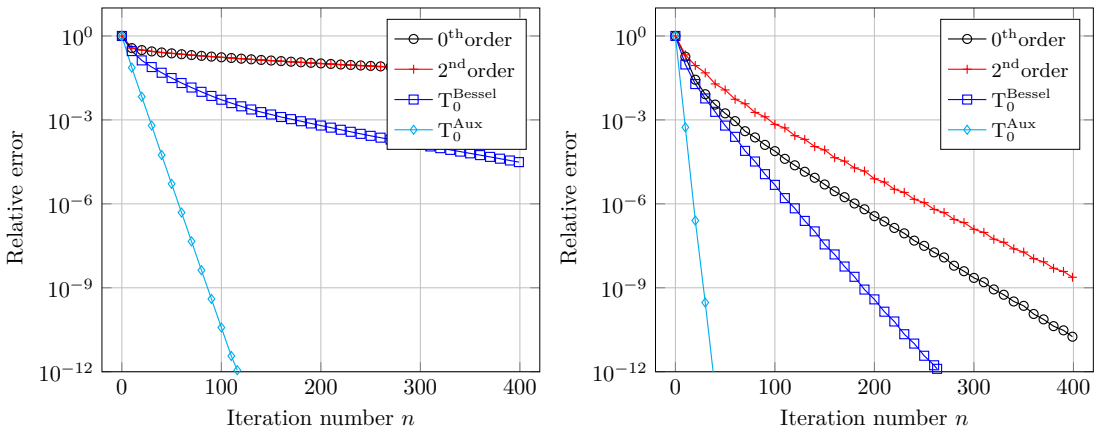

(a) Richardson algorithm (b) GMRES algorithm

Figure 11.4: Maxwell 3D. An example of convergence history. Fixed parameters $\kappa_0 = 5$, $J = 4$, $N_\lambda = 40$

that are required to achieve the same error to solve the full (undecomposed) linear system (line plot labelled 'No DDM'). Recall that this is to be read as an indication of the conditioning of the original linear system rather than an actual method of resolution.

It shall be noted that this numerical test does not fall exactly in the theory developed previously as far as the stability with respect to the mesh parameter is concerned. This is due to the use of an automatic mesh partitioner, which produces different geometries for different meshes. The skeleton and therefore the geometry of the interfaces between sub-domains may change greatly when N_λ changes. Moreover, the transmission interfaces get rougher as the mesh is refined, with geometrical details of the size of the mesh cells. This situation is different from the previously reported results of Chapter 7 and Chapter 8 where the underlying interface was converging to a perfect sphere as the mesh was refined.

Helmholtz 2D We report the number of iterations to reach convergence with respect to mesh refinement in Figure 11.5 for the Richardson and GMRES algorithms. We see that the iteration count 'No DDM' has a growth which is approximately quadratic with respect to N_λ, illustrating the deterioration of the matrix conditioning as the mesh is refined. For the local operators the convergence is not uniform with respect to mesh refinement and a large number of iterations is required to get to the set tolerance. The growth of the iteration count appears to be quasi quadratic with respect to N_λ for the Richardson algorithm and quasi linear for the GMRES algorithm. For small mesh size the convergence may not even be reached within 10^5 iterations. In contrast, the non-local operators T_0^{Bessel} and T_0^{Aux} exhibit uniform convergence in all cases, with a very moderate number of iterations required to reach the set tolerance.

Helmholtz 3D We report the number of iterations to reach convergence with respect to mesh refinement in Figure 11.6 for the Richardson and GMRES algorithms. Again in this case, we clearly identify the non-uniformity of the convergence with respect to the number of point per wavelength for the zeroth order local operator. On the contrary, the non-local operators T_0^{Bessel} and T_0^{Aux} exhibit h-uniform convergence. It shall be noticed however the quasi-uniformity of the convergence for the second order operator if the GMRES algorithm is used, which is not explained, while the deterioration is quadratic when the Richardson algorithm is used.

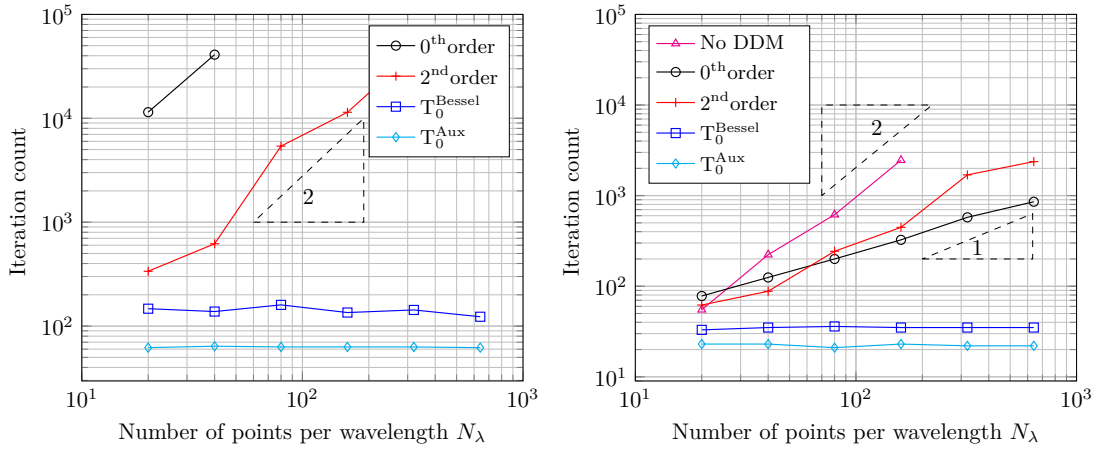

(a) Richardson algorithm (b) GMRES algorithm

Figure 11.5: Helmholtz 2D. Number of iterations with respect to the number of mesh points per wavelength N_λ. Fixed parameters $\kappa_0 = 1$, $J = 4$, disk of radius $R = 1$.

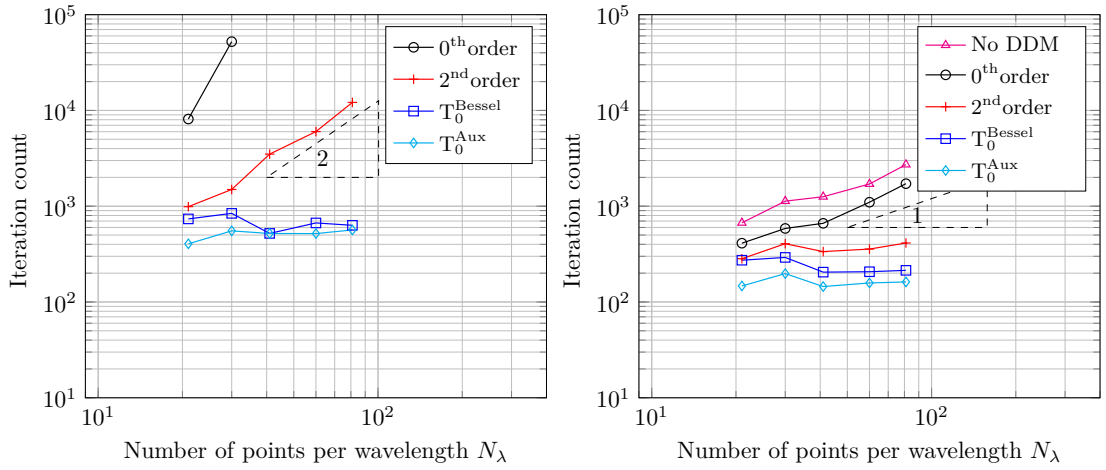

(a) Richardson algorithm (b) GMRES algorithm

Figure 11.6: Helmholtz 3D. Number of iterations with respect to the number of mesh points per wavelength N_λ. Fixed parameters $\kappa_0 = 1$, $J = 8$, sphere of radius $R = 1$.

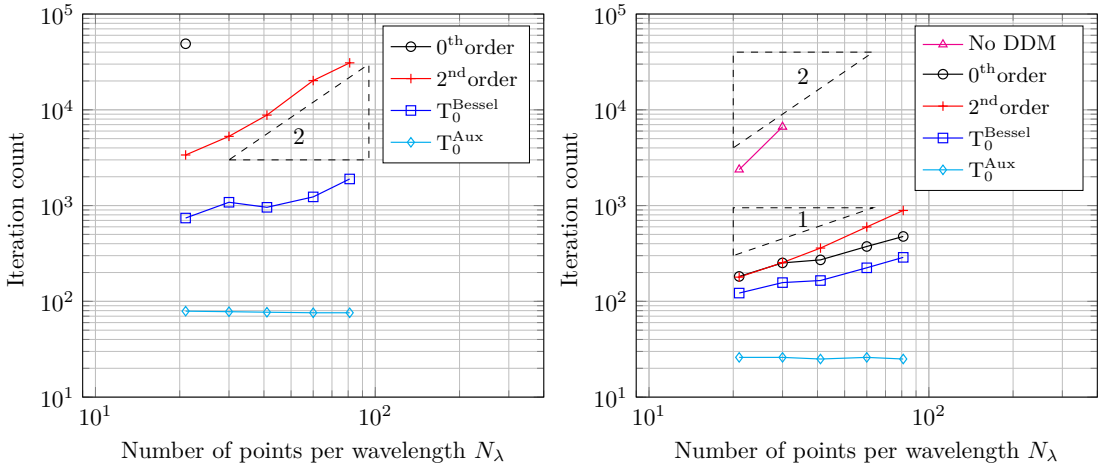

(a) Richardson algorithm

(b) GMRES algorithm

Figure 11.7: Maxwell 3D. Number of iterations with respect to the number of mesh points per wavelength N_λ. Fixed parameters $\kappa_0 = 1$, $J = 8$, sphere of radius $R = 1$.

Maxwell 3D We report the number of iterations to reach convergence with respect to mesh refinement in Figure 11.7 for the Richardson and GMRES algorithms. We see for this case the increased difficulty of the original problem that can be deduced for the large number of GMRES iterations required to solve the undecomposed problem. For the two local operators the number of iterations depend strongly on the mesh refinement, while for the non-local operator based on the resolution of auxiliary problems, the convergence is independent of the mesh size. It seems however, that the iteration count actually increases when the mesh is refined for the non-local operator T_0^E. This is not fully understood and may be due to the increasing roughness and geometrical singularities of the transmission interface, although we note that such an effect was not observed for the non-local operators based on integral formulations in the acoustic setting.

11.4 Influence of the frequency

We now study the dependency of the iteration counts with respect to the wavenumber κ_0 when the GMRES algorithm is used. In addition, we provide results with the Jacobi algorithm only for the acoustic 2D case. To keep the test simple, we chose to keep a fixed number of points per wavelength as the frequency changes, so that the size of the linear system increases as the frequency changes but pollution effect is not taken into account here.

The results for the acoustic setting are given in Figure 11.8 for the two-dimensional case and in Figure 11.9 for the three-dimensional case. The corresponding results for the electromagnetic setting can be found in Figure 11.10.

As the wavenumber κ_0 increases, the discrete (as well as the continuous) problem gets harder. This is indicated again by the increase in the iteration count of the GMRES algorithm for the undecomposed problem (line plot labelled 'No DDM'). For this case, the growth is linear with respect to κ_0. In contrast, for all the impedance operators under study, we notice a sub-linear growth of the number of iteration with respect to κ_0. The iteration count is especially moderate for the non-local operators. Notice also that the difference in iteration counts between the integral operator based on the potential theory and the non-local operator based on the resolution of

auxiliary problems is diminished as the frequency increases.

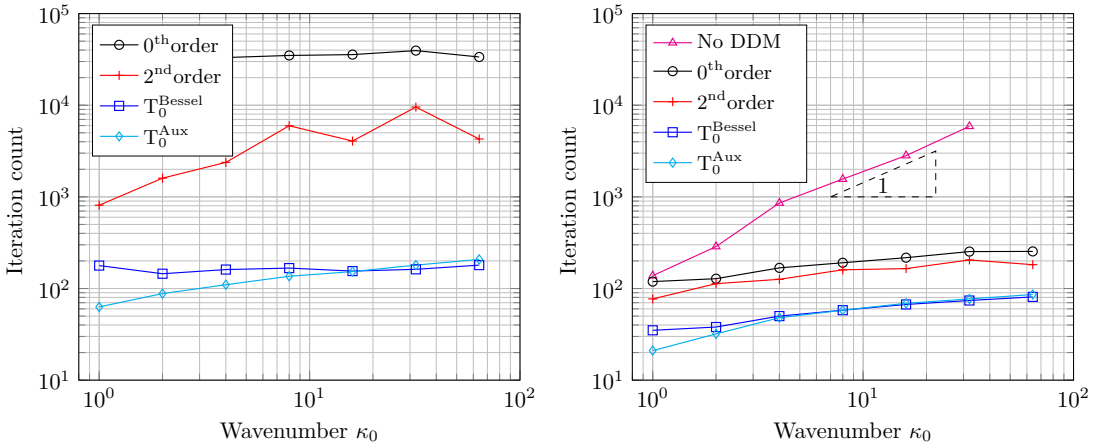

(a) Richardson algorithm

(b) GMRES algorithm

Figure 11.8: Helmholtz 2D. Number of iterations with respect to the wavenumber κ_0. Fixed parameters $J = 4$, $N_\lambda = 30$, disk of radius $R = 1$.

11.5 Influence of domain heterogeneity

We provide some results in heterogeneous medium for the Helmholtz equation in 2D. The nature of the test case is slightly different to the previous ones and is motivated by scattering problems for coated objects. More precisely, we study the evolution of the iteration count with respect to different contrast in μ_r and ϵ_r respectively. The domain is a circular strip contained between the circles of radius $R = 1$ and $R = 1.5$. The medium characteristics change at $R = 1.25$:

- for $R > 1.25$, μ_r and ϵ_r are constant equal to 1 and is intended to represent the vacuum;
- for $R < 1.25$, either μ_r or ϵ_r take a lower or higher value and is intended to represent the coating material.

At $R = 1.5$, the usual first order absorbing boundary condition is applied. Besides, two different boundary conditions are considered at the object boundary $R = 1$, either the sound-hard (Dirichlet) or the sound-soft (Neumann) boundary conditions. As a result, this test has the additional benefit to highlight that these two boundary conditions can also be taken into account seamlessly by the new method. The source of the problem comes from an impinging plane wave, as the one defined previously for the usual test case considered.

The partition is composed of $J = 20$ sub-domains so that some interfaces are cut by the discontinuity in the medium and the results are provided for the GMRES algorithm. When no results are provided, it means that the algorithm did not converge in under 10^5 iterations.

In Figure 11.11 the frequency in the vacuum is taken to be $\kappa_0 = 1$ with $N_\lambda = 640$ points per wavelength (the vacuum one). The value of the relative coefficients μ_r and ϵ_r is *higher* in the material.

In Figure 11.12 the frequency in the vacuum is taken to be $\kappa_0 = 32$ with $N_\lambda = 20$ points per wavelength (the vacuum one). The value of the relative coefficients μ_r and ϵ_r is *lower* in the material (notice the inverse in the horizontal axis label in the plots).

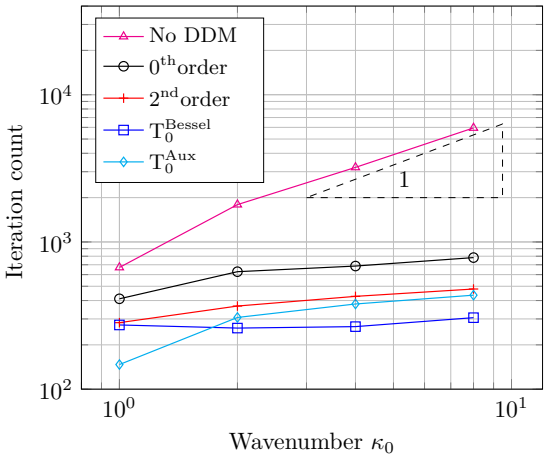

(a) GMRES algorithm

Figure 11.9: Helmholtz 3D. Number of iterations with respect to the wavenumber κ_0. Fixed parameters $J = 8$, $N_\lambda = 20$, sphere of radius $R = 1$.

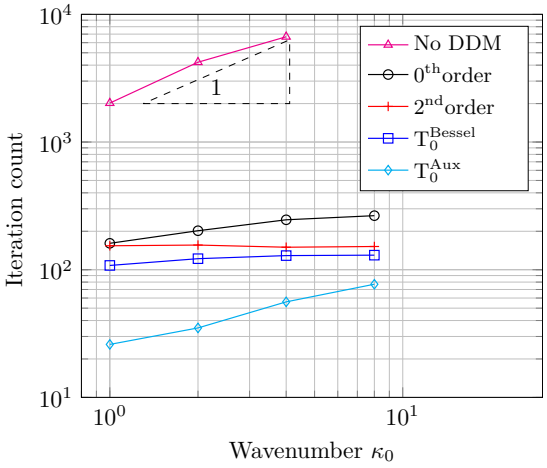

(a) GMRES algorithm

Figure 11.10: Maxwell 3D. Number of iterations with respect to the wavenumber κ_0. Fixed parameters $J = 8$, $N_\lambda = 20$, sphere of radius $R = 1$.

It is clear that the local operator perform the worse, even though as the strength of the discontinuity increases, the difference is dimished in the case where the frequency is higher inside the material. The best results are obtained for the non-local operator based on the resolution of the auxiliary problems and this is particularly true for the case where the frequency is smaller inside the material. Notice that in some cases, the algorithm using the non-local operator based on an integral formulation simply did not converge in under 10^5 iterations.

11.6 Scalability of the method

We now study the dependency of the method with respect to the number of subdomains J of the mesh partition for the Helmholtz equation. The numerical experiments presented now are obtained on the test cases presented in Chapter 7.

11.6.1 Strong scaling

We start with a strong scaling test in 2D, which consists in increasing the number of subdomains for a fixed size problem. The results at a rather high frequency ($\kappa_0 = 20$) are provided in Figure 11.13a and at a lower frequency ($\kappa_0 = 2$) in Figure 11.13b. These figures report the iteration count with respect to J varying from 2 to 1024 subdomains. In both cases the GMRES algorithm is used.

One can notice a sub-linear increase in the number of iterations to get to a converged solution for all the transmission operators under study. Notice that for the strong scaling test the undecomposed linear system is kept the same as J is increased. It follows that at some point it is no longer useful to split the initial domain into too many pieces and one is better off with moderate size sub-problems.

Interestingly, we see in Figure 11.13b that the number of iterations levels out for the coercive DtN operator, in a regime where the size of the sub-problems gets really small compared to the wavelength of the problem.

11.6.2 Weak scaling

A weak scaling test was also performed, this time with a domain increasing in size as the number of sub-domains J grows for both the 2D and 3D cases. More precisely, the size of the domain is chosen to grow like $J^{1/d}$ where d is the dimension of ambiant space, so as to keep a fixed size (in terms of DOFs) for the local subdomains. In 2D the domain is a disk of radius increasing from $R = 1$ to $R = 16$, and in 3D the domain is a sphere of radius increasing from $R = 1$ to $R = 3.7$. The frequency is set $\kappa_0 = 5$ and the GMRES algorithm is used. Notice that the number of points per wavelength is kept constant, despite the fact that the size of the problem increases, as a result the pollution effect is not taken into account here.

The growth of the number of iteration to reach the set tolerance also appears to scale like $J^{1/d}$ and the phenomenon seems to apply to all the transmission operators considered. This non-optimality can be understood in this wave context from the fact that the waves need to travel longer as the size of the global domain increases.

11.7 Comparison with the previous method

We present below a comparison of the new approach with a communication operator based on a projection against the more usual method where the exchange is defined localy. This

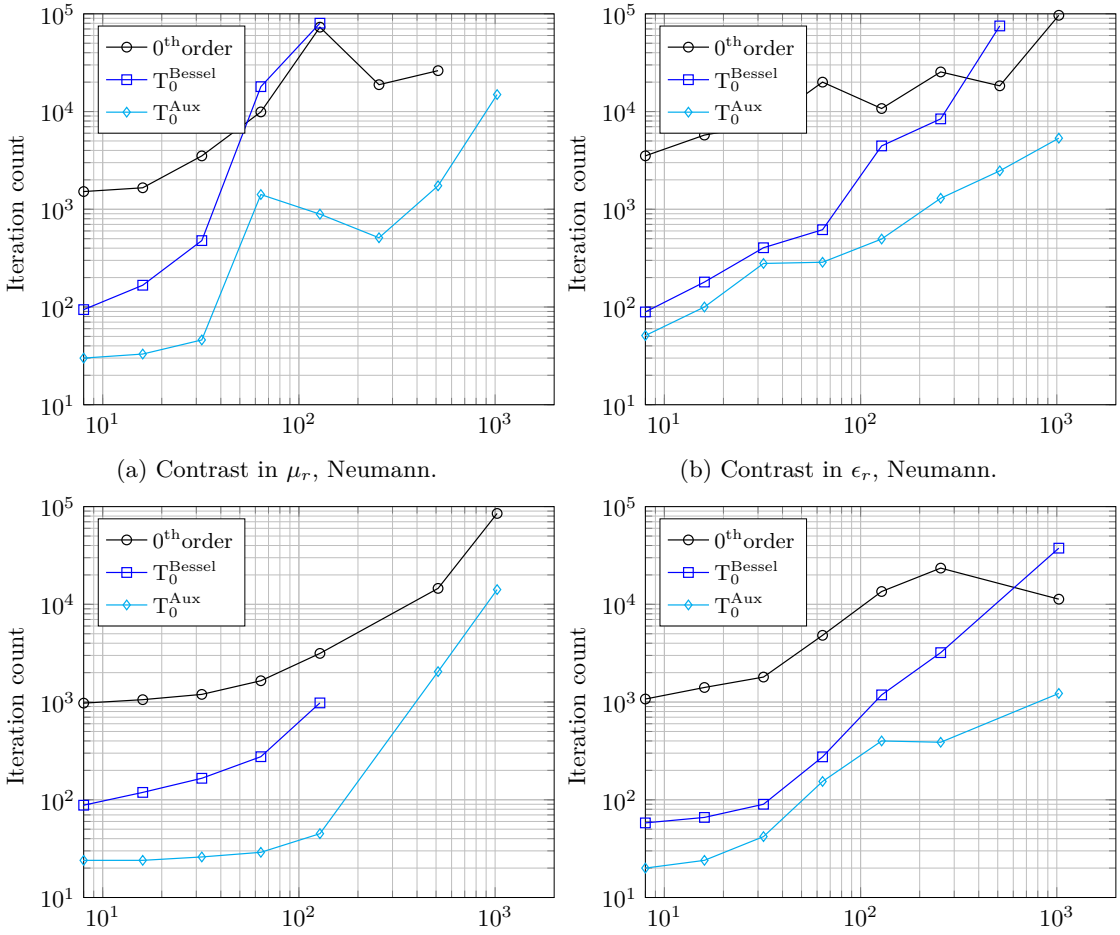

(a) Contrast in μ_r, Neumann.

(b) Contrast in ϵ_r, Neumann.

(c) Contrast in μ_r, Dirichlet.

(d) Contrast in ϵ_r, Dirichlet.

Figure 11.11: Helmholtz 2D. Evolution of the iteration count for heterogeneous medium. Fixed parameters $\kappa_0 = 1$, $N_\lambda = 640$, $J = 20$, GMRES algorithm.

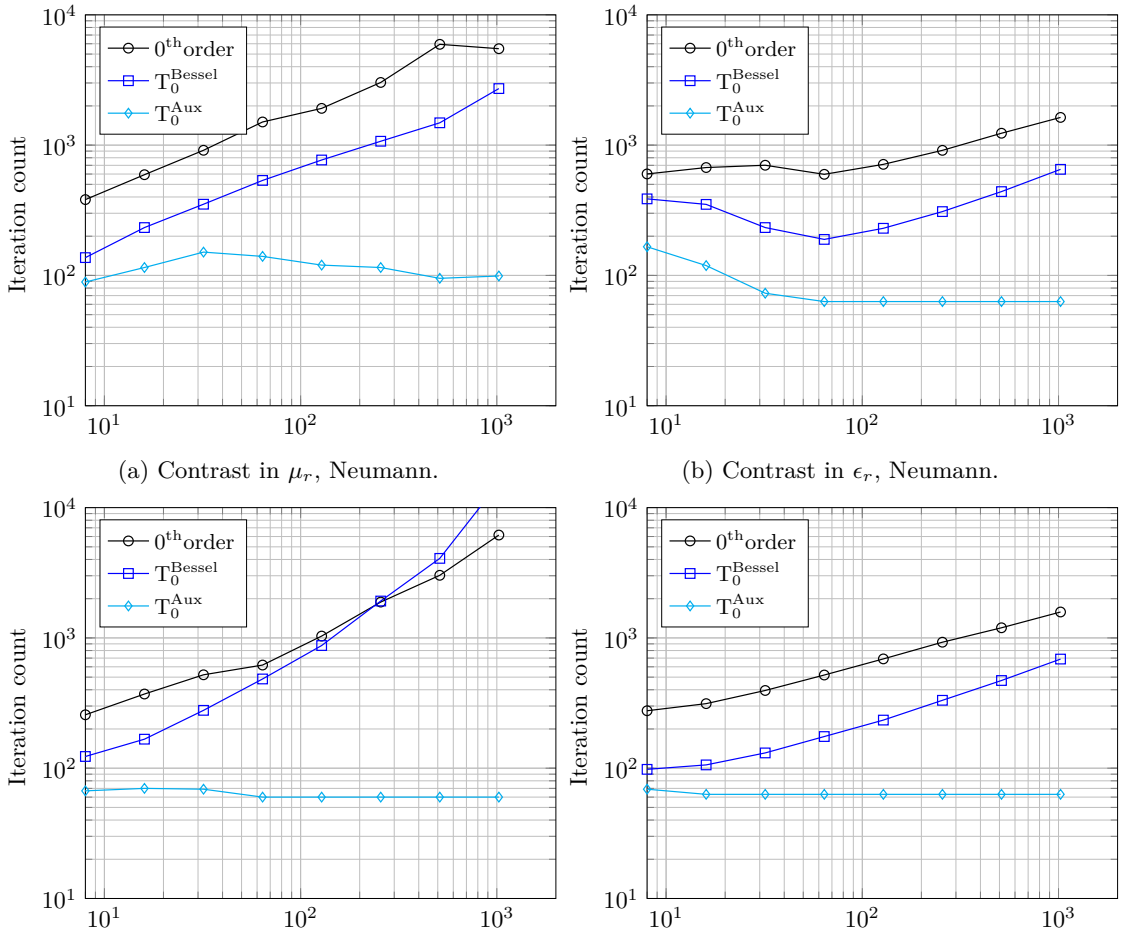

(a) Contrast in μ_r, Neumann.

(b) Contrast in ϵ_r, Neumann.

(c) Contrast in μ_r, Dirichlet.

(d) Contrast in ϵ_r, Dirichlet.

Figure 11.12: Helmholtz 2D. Evolution of the iteration count for heterogeneous medium. Fixed parameters $\kappa_0 = 32$, $N_\lambda = 20$, $J = 20$, GMRES algorithm.

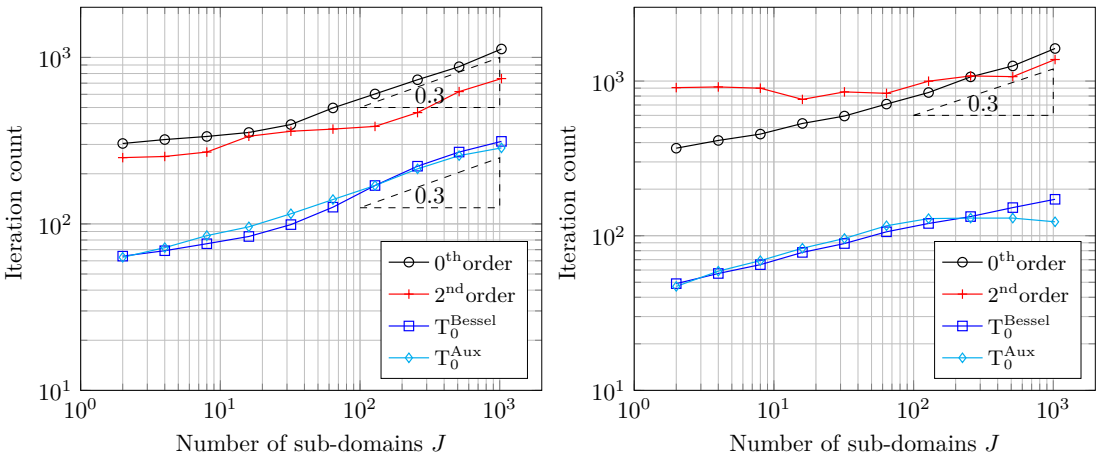

(a) $\kappa_0 = 20$, $N_\lambda = 50$, $R = 1$ (b) $\kappa_0 = 2$, $N_\lambda = 100$, $R = 4$

Figure 11.13: Helmholtz 2D. Number of iterations with respect to the number of subdomains J (Strong scaling). Disk of radius R, GMRES algorithm.

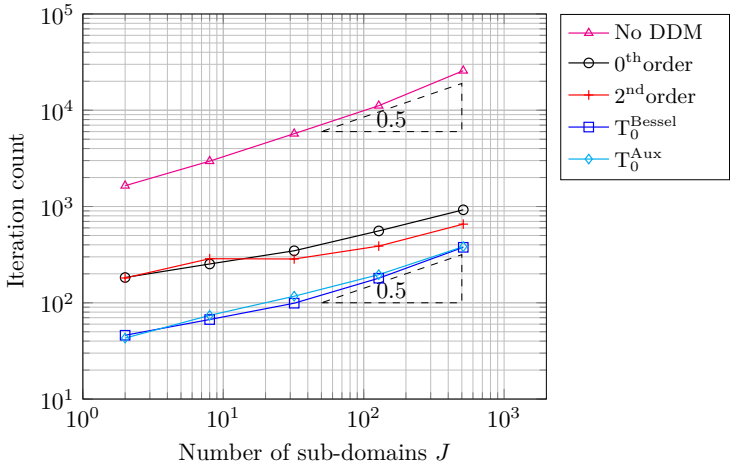

Figure 11.14: Helmholtz 2D. Number of iterations with respect to the number of subdomains J (Weak scaling). Fixed parameters $\kappa_0 = 5$, $N_\lambda = 40$, disk of increasing radius. GMRES algorithm.

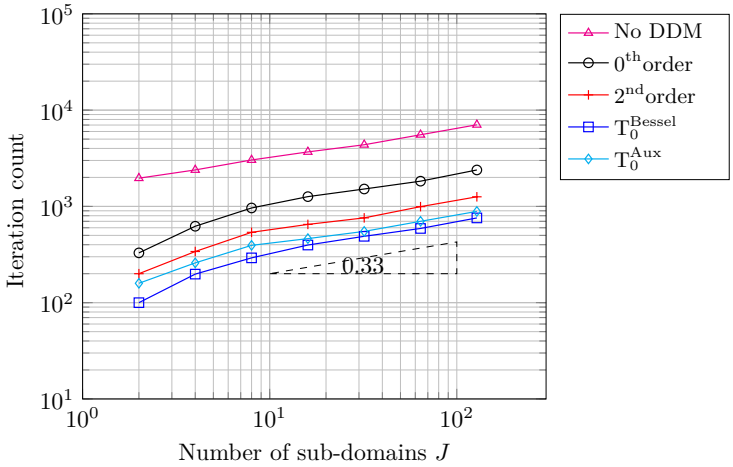

Figure 11.15: Helmholtz 3D. Number of iterations with respect to the number of subdomains J (Weak scaling). Fixed parameters $\kappa_0 = 2$, $N_\lambda = 30$, sphere of increasing radius. GMRES algorithm.

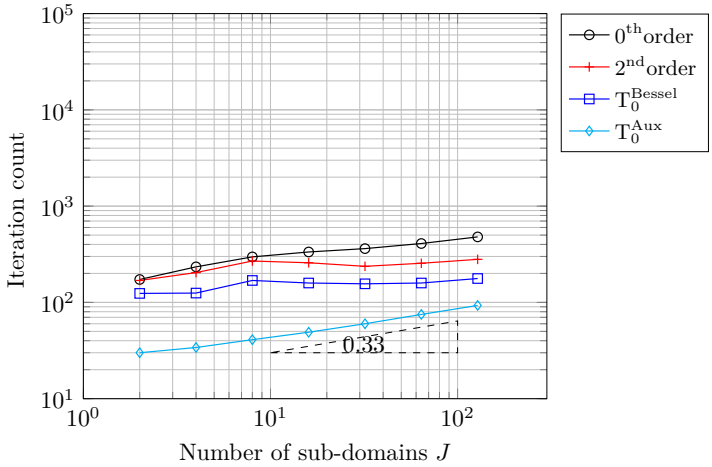

Figure 11.16: Maxwell 3D. Number of iterations with respect to the number of subdomains J (Weak scaling). Fixed parameters $\kappa_0 = 2$, $N_\lambda = 30$, sphere of increasing radius. GMRES algorithm.

comparison is carried out in the configuration with only *boundary* cross-points. Indeed, the two methods are identical in absence of cross-points (with the caveat that the Lagrange multipliers defined on the physical boundary in the new approach shall be first eliminated), hence not worth comparing. Besides, in the presence of *interior* cross-points, the definition of the discrete transmission conditions is not straightforward and natural for our nodal finite element method.

This comparison is conducted for the 2D Helmholtz equation only. The test case is constructed from the one described in Chapter 7 and consists in a disk of radius $R = 1$, split roughly (using a mesh partitioner) in half, which creates two sub-domains and two junction points with the physical boundary. Note that in this case there are no degrees of freedom (DOF) that are shared with more than two subdomains.

It is worth noting that actually, this setting is *not* covered by our analysis of Chapter 3 of Chapter 4 due to the presence of boundary junction points. However, the extension of the method with the local exchange operator is straightforward. The transmission interface is restricted to the common interface between the two sub-domains, on which the transmission operators are defined. Note that this interface is not a closed manifold, which complicates the functional analysis and invalidates the convergence analysis we conducted.

On the other side, the newly proposed method is well-defined, see Chapter 10, and the (geometric) convergence result stands.

h-uniform geometric convergence We report the number of iterations to reach convergence with respect to mesh refinement in Tables 11.1 and 11.2 respectively for the Richardson and GMRES algorithms. In Table 11.2 we also report the number of GMRES iterations that are required to achieve the same error to solve the full (undecomposed) linear system (column labelled 'No DDM'). We see that this iteration count has a growth which is approximately quadratic with respect to N_λ, illustrating the deterioration of the matrix conditioning as the mesh is refined.

For the local operators the convergence is not uniform with respect to mesh refinement and a large number of iterations is required to get to the set tolerance. For small mesh size the convergence may not even be reached within 10^5 iterations. The growth appears to be quasi linear with respect to N_λ.

For the (elliptic) hypersingular operator T_0^B used in conjunction with the local exchange operator ($\mathbf{\Pi}_\parallel$), the convergence is not uniform with respect to the mesh size. The number of iterations slightly increases as the typical mesh size decreases, especially for the Richardson algorithm. This is a very interesting effect and may be due to the loss of continuity of the integral operator defined on open curves. These observations are moreover in agreement with the results reported in [91, Sec. 9.2]. In contrast, when used with the newly introduced communication operator ($\mathbf{\Pi}_{0,\times}$), the integral operator is defined on closed curves and is a continuous mapping between the trace spaces — we recover the uniform convergence.

The other non-local operator T_0^E exhibit uniform convergence for both strategies, with a very moderate number of iterations required to reach the set tolerance. In fact, in terms of iteration count, it outperforms all other operators. It seems that this operator has the correct properties (in contrast to the other non-local operator which is based on integral formulations) to ensure a stable convergence of the algorithm.

From those results, we do believe that it should be possible to derive a convergence analysis and state a geometrical convergence result for a domain decomposition method based on the usual point-to-point exchange operator even in the presence of *boundary* junction points. These numerical results are at least some evidence to support this claim. In contrast, we believe that there is no hope to extend such a result in the presence of *interior* junction points. The numerical results (using a mixed-hybrid finite element formulation) presented at the beginning of Chapter 9 support this idea.

	local ($\mathbf{\Pi}_{\|}$)				projection ($\mathbf{\Pi}_{0,\times}$)			
N_λ	0^{th}ord	2^{nd}ord	$\mathrm{T}_0^{\text{Bessel}}$	$\mathrm{T}_0^{\text{Aux}}$	0^{th}ord	2^{nd}ord	$\mathrm{T}_0^{\text{Bessel}}$	$\mathrm{T}_0^{\text{Aux}}$
20	9845	799	159	52	10121	818	158	61
40	44068	591	154	55	44417	582	154	62
80	·	3260	176	54	·	3256	172	61
160	·	12804	190	54	·	12853	145	61
320	·	50522	272	54	·	50615	169	61
640	·	·	387	54	·	·	151	61

Table 11.1: Helmholtz 2D. Number of iterations with respect to the number of mesh points per wavelength N_λ. Fixed parameters $\kappa_0 = 1$, $J = 2$, Richardson algorithm.

	No DDM	local ($\mathbf{\Pi}_{\|}$)				projection ($\mathbf{\Pi}_{0,\times}$)			
N_λ	$\emptyset$	0^{th}ord	2^{nd}ord	$\mathrm{T}_0^{\text{Bessel}}$	$\mathrm{T}_0^{\text{Aux}}$	0^{th}ord	2^{nd}ord	$\mathrm{T}_0^{\text{Bessel}}$	$\mathrm{T}_0^{\text{Aux}}$
20	44	16	16	16	15	42	52	22	18
40	227	59	60	33	16	102	76	30	19
80	654	105	73	39	16	163	80	32	19
160	2474	179	533	40	16	279	392	32	19
320	9559	295	1605	48	16	464	·	34	18
640	41888	475	314	47	16	730	359	34	19

Table 11.2: Helmholtz 2D. Number of iterations with respect to the number of mesh points per wavelength N_λ. Fixed parameters $\kappa_0 = 1$, $J = 2$, GMRES algorithm.

	No DDM	local ($\mathbf{\Pi}_{\|}$)				projection ($\mathbf{\Pi}_{0,\times}$)			
κ_0	$\emptyset$	0^{th}ord	2^{nd}ord	$\mathrm{T}_0^{\text{Bessel}}$	$\mathrm{T}_0^{\text{Aux}}$	0^{th}ord	2^{nd}ord	$\mathrm{T}_0^{\text{Bessel}}$	$\mathrm{T}_0^{\text{Aux}}$
1	149	51	53	32	15	81	57	30	19
2	268	91	40	36	18	110	48	35	26
4	811	126	114	41	27	136	123	44	39
8	1563	133	147	46	33	154	154	49	48
16	2926	160	152	54	40	192	157	59	56
32	5846	183	168	59	48	213	189	67	64

Table 11.3: Helmholtz 2D. Number of iterations with respect to the wavenumber κ_0. Fixed parameters $J = 2$, $N_\lambda = 30$, GMRES algorithm.

Influence of the frequency We report the number of iterations to reach convergence with respect to the wavenumber κ_0 in Table 11.3 for the GMRES algorithm. As the wavenumber κ_0 increases, the discrete (as well as the continuous) problem gets harder. This is indicated again by the increase in the iteration count of the GMRES algorithm for the undecomposed problem (column 'No DDM'). For this case, the growth is linear with respect to κ_0. In contrast, for all the impedance operators under study, we notice a sub-linear growth of the number of iteration with respect to κ_0. The increase in the iteration count is especially moderate for the non-local operators.

Comparison of the two approaches If we compare the two alternatives of using a local exchange operator $\mathbf{\Pi}_{\|}$ or a non-local communication operator $\mathbf{\Pi}_{0,\times}$ for a fixed impedance operator, we notice for this test case, a small but not significant advantage of the local exchange operator. This is due to the fact that the method using the non-local communication operator requires a Lagrange multiplier at each DOF of the boundaries of the subdomains, even on the boundary on which a physical condition is imposed. This feature is essential for some impedance operators defined by integral operators that require a closed boundary to be properly defined, as the hypersingular operator for instance. However, when used in conjunction to a local operator, this introduces somewhat redundant and unnecessary DOFs, that could be eliminated, hence a larger linear system and a worse convergence. The only counter-example to this effect is the hypersingular operator T_0^E for the reason that was previously alluded to, namely the loss of continuity on open curves. For this operator, the performance is better when used in conjunction with the non-local communication operator $\mathbf{\Pi}_{0,\times}$.

11.8 Exchange operator

The purpose of this last section is to provide some numerical evidence to support our claim that the projection step that occurs in the definition of the newly introduced communication operator is not prohibitive.

11.8.1 Sparsity patterns

The actual transmission of information between sub-domains that is induced by the projection-based communication operator is somehow elusive. We provide below a visual interpretation of such transmissions of data that we find instructive.

We represent in Figure 11.17 the sparsity patterns (i.e. the absolute value of the non-zero coefficients) of the communication operator matrices (see (10.172) for the definition of these matrices) for several transmission operators: the Euclidian inner product Id, the identity 0^{th}order and the elliptic hypersingular operator $\mathrm{T}_0^{\text{Bessel}}$ and for several different partitions $J \in \{2, 3, 4, 8\}$ of the same mesh.

The utilisation of the Euclidian inner product Id deserves some comments. This is a pure discrete operator define algebraicaly, which consists in using literaly an identity matrix as a transmission operator. It is therefore close to the operator which would be obtained for a lumped mass matrix. We include this operator in this comparison because it possess interesting properties.

The domain is a disk or radius $R = 1$, the wavenumber of the problem is $\kappa_0 = 1$ and the mesh is constructed to have roughly $N_\lambda = 20$ DOFs per wavelength (the size of the problem is deliberately small to be able to actually represent the matrix of the communication operator). The number of sub-domains ranges from $J = 2$ to $J = 8$ on the same mesh, which as a result increases the size of the skeleton (hence the number of elements in the exchange operator matrix).

As expected, the patterns for Id is really sparse, while the ones for 0^{th}order is denser and the patterns for $\mathrm{T}_0^{\text{Bessel}}$ is almost completely dense.

- Id: we can formally decompose the exchange matrix associated to Id in two parts: the diagonal part whose non-zero elements correspond to degrees of freedom on the physical boundary (which are not boundary junction points); and the off-diagonal part which is symmetric and which corresponds to exchange between sub-domains for degrees of freedom belonging to more than one-subdomain. For two subdomains ($J = 2$) we can clearly visually identify the standard point-to-point exchange. For more sub-domains, we notice columns (and lines) with more than one single non-zero element.

- 0^{th}order: for the exchange matrix associated to Després transmission conditions, we first notice the loss of symmetry. The exchange matrix is in fact self-adjoint with respect to the scalar product induced by the mass matrix. The identity blocks that were present in the matrix associated to Id and which correspond to degrees of freedom on the physical boundary are still present. Besides, some of the off-diagonal part remain the same as for Id, these correspond to interior degrees of freedom on the transmission boundary that belong to exactly two sub-domains. The main difference with the previous operator comes from the non-zero columns stemming from cross-points. For two sub-domains, there are only two boundary cross points which are shared by two sub-domains. For the other geometrical configurations, there are interior cross points in addition to boundary cross points. We clearly visualize here that only the cross-points (interior or boundary) have global contributions on the whole skeleton. This feature is a manifestation of the coupling of all the sub-domains through the cross-points. Very similar sparsity patterns can be observed for second order operators.

- $\mathrm{T}_0^{\text{Bessel}}$: again, the matrix is not symmetric for the same reason given above. Besides, one can again locate the degrees of freedom that belong to the physical boundary, by the diagonal identity blocks. The main difference from the previous operator is the fact that all the degrees of freedom that belong to a true transmission boundary (hence geometrically belong to at least two sub-domains) have global contributions on the whole skeleton. What is perhaps more surprising is the fact that no information is sent from the degrees of freedom that belong to the physical boundary to the other degrees of freedom, but they do receive some data from the other ones. Notice that the blocks corresponding to pure interior sub-domains (such cases occurs for $J = 8$) are, as a result, fully populated. Very similar sparsity patterns can be observed for other non-local operators.

We report in Figure 11.18 the sparsity pattern of the exchange matrices for the transmission operator $\mathrm{T}_0^{\text{Aux}}$ for two frequencies $\kappa_0 = 10$ and $\kappa_0 = 40$. The domain is a disk or radius $a = 1$ partitioned into $J = 10$ subdomains, with a mesh constructed in order to have roughly $N_\lambda = 10$ (respectively $N_\lambda = 2$) DOFs per wavelength for $\kappa_0 = 10$ (respectively $\kappa_0 = 40$). Again, the size of the problem is dramatically small for the frequencies considered (and not realistic) but this is for the sake of illustration. Notice however that the sizes of the two matrices are comparable.

The purpose of this figure is to show that, even for non-local transmission operators, the exchange matrix can become sparse as the relative size of the domain increases with respect to the wavelength of the problem $\frac{2\pi}{\kappa_0}$ (which we recall is taken as the characteristic length of the dissipative problems associated to the non-local operators). For the case with the largest frequency ($\kappa_0 = 40$), some sub-domains (that do not share common degrees of freedom) are not directly coupled (although they are indirectly by their common neighbours). Obviously this remark stands only in a discrete setting and the effect is due to finite precision arithmetic. Finally, we point out that a similar effect can be observed on the exchange matrices associated

to transmission operator based on local operators such as 0^{th}order and 2^{nd}order, namely the apparent direct de-coupling of far apart sub-domains (which were at first sight coupled by global contributions stemming from cross points).

11.8.2 Inner conjugate gradient

We investigate numerically (in 2D) in the following our claim that the (preconditionned) inner CG algorithm that is used in order to solve the projection problem only requires a few iterations to complete.

We report in Figure 11.19 the evolution of the maximum number of iterations to reach convergence for the inner CG solver with respect to mesh refinement. The maximum is taken over all solves during one run of the outer GMRES algorithm. In Figure 11.20 the evolution with respect to the wavenumber κ_0 is investigated. Finally, Figure 11.21 and Figure 11.23 report respectively the evolution of the maximum number of iterations of inner CG in a strong and weak scaling tests, namely with respect to increasing number of sub-domains J in the partition.

We observe a clear but moderate increase in the number of required iterations when the mesh is refined (the discrete size of the problem increases). In contrast, the maximum iteration count stays fairly constant as the wavenumber of the problem increases. As far as the strong and weak scaling tests are concerned, we notice that the maximum number of iterations steadily increases as we increase the number of problems but sort of levels off once we reach about ten sub-domains.

We see that the operator $\mathrm{T}_0^{\text{Bessel}}$ is consistently more advantageous than the other non-local operator $\mathrm{T}_0^{\text{Aux}}$ as less iterations of inner CG are required. As for the local operators, they generally exhibit lower iteration counts in comparison to non-local operators (except for the second order operator in the strong and weak scaling tests).

Note that we did not report inner CG iteration counts associated to the transmission operator Id as the projection can in this case be computed explicitly without requiring the inner algorithm. As a matter of fact, if one would nevertheless use a CG algorithm to solve the associated problem, the algorithm would converge to machine precision in exactly one iteration.

Finally, we remark that we observed numerically that the (relative) tolerance of the inner CG algorithm needs to be smaller than the (relative) tolerance of the outer algorithm in order to be able to (globally) converge. In all our numerical experiments, we set the tolerance of the inner algorithm to machine precision (10^{-14}) as a safety measure, but we remark that it should be possible to save a few inner iterations by using a larger tolerance at the start of the outer iterations or if the required global precision is not too small. This speculation has however not been investigated further.

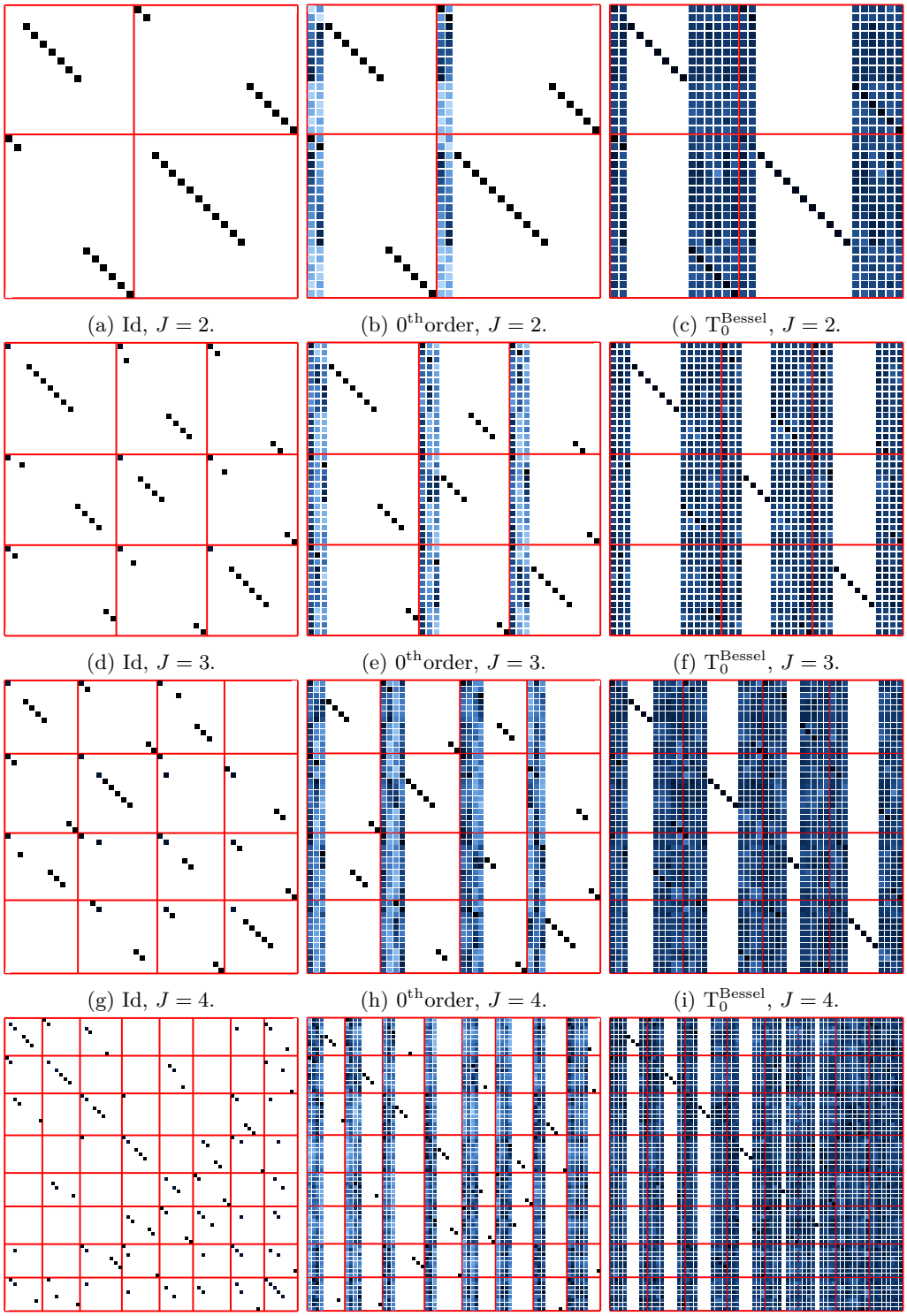

(a) Id, $J = 2$. (b) 0^{th}order, $J = 2$. (c) $\mathrm{T}_0^{\text{Bessel}}$, $J = 2$.

(d) Id, $J = 3$. (e) 0^{th}order, $J = 3$. (f) $\mathrm{T}_0^{\text{Bessel}}$, $J = 3$.

(g) Id, $J = 4$. (h) 0^{th}order, $J = 4$. (i) $\mathrm{T}_0^{\text{Bessel}}$, $J = 4$.

(j) Id, $J = 8$. (k) 0^{th}order, $J = 8$. (l) $\mathrm{T}_0^{\text{Bessel}}$, $J = 8$.

Figure 11.17: Sparsity pattern of exchange matrices. The darker the element, the bigger. The saturation scales logarithmically from 10^{-12} (white) to 1 (black). The red lines delimit subdomain contributions. Disk of radius $a = 1$, $\kappa_0 = 1$, $N_\lambda = 20$

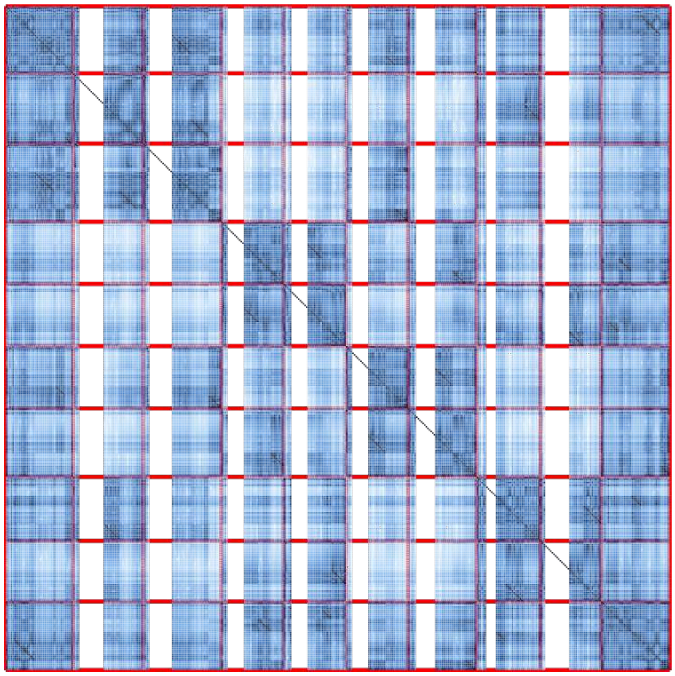

(a) $\mathrm{T}_0^{\mathrm{Aux}}$, $J = 10$, $\kappa_0 = 10$, $N_\lambda = 10$.

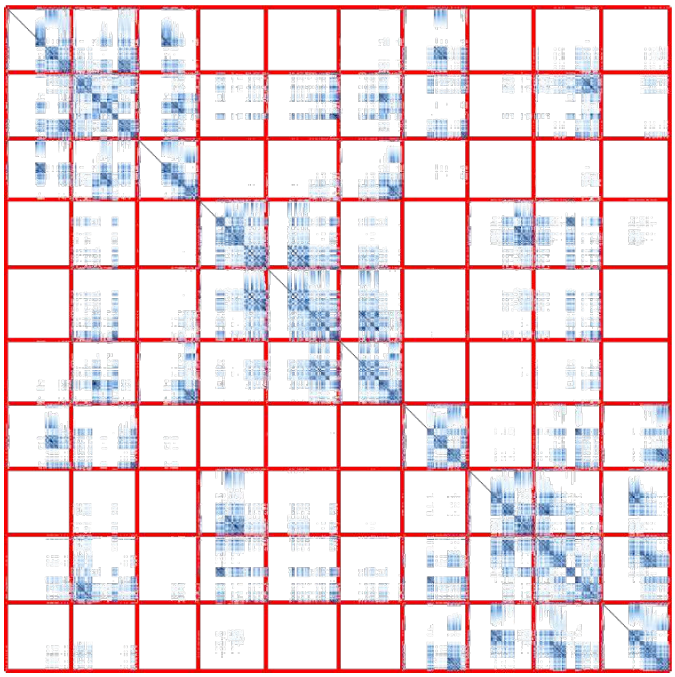

(b) $\mathrm{T}_0^{\mathrm{Aux}}$, $J = 10$, $\kappa_0 = 40$, $N_\lambda = 2$.

Figure 11.18: Sparsity pattern of exchange matrices. The darker the element, the bigger. The saturation scales logarithmically from 10^{-12} (white) to 1 (black). The red lines delimit subdomains contributions. Disk of radius $a = 1$.

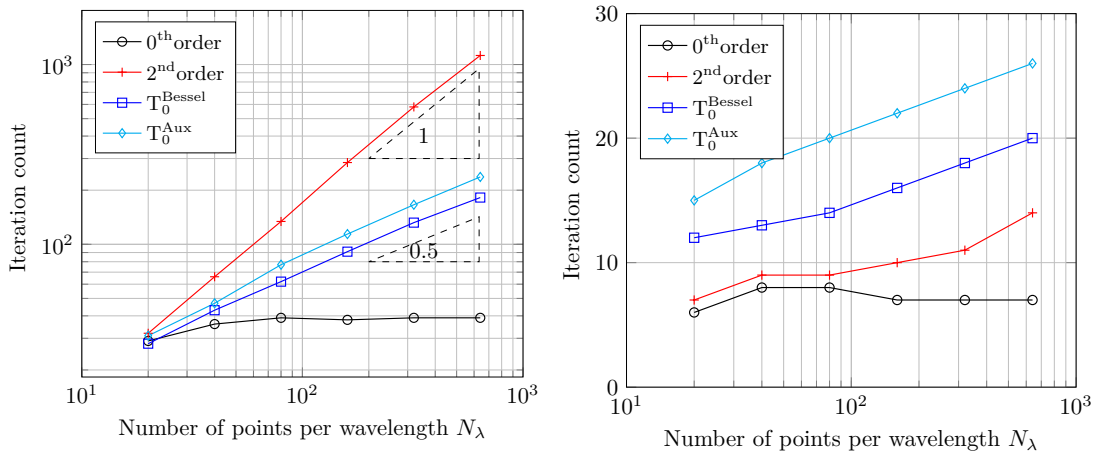

(a) Without preconditioning.

(b) With preconditioning.

Figure 11.19: Helmholtz 2D. Maximum number of iterations of inner CG with respect to the number of mesh points per wavelength N_λ. Fixed parameters $\kappa_0 = 1$, $J = 4$, disk of radius $R = 1$.

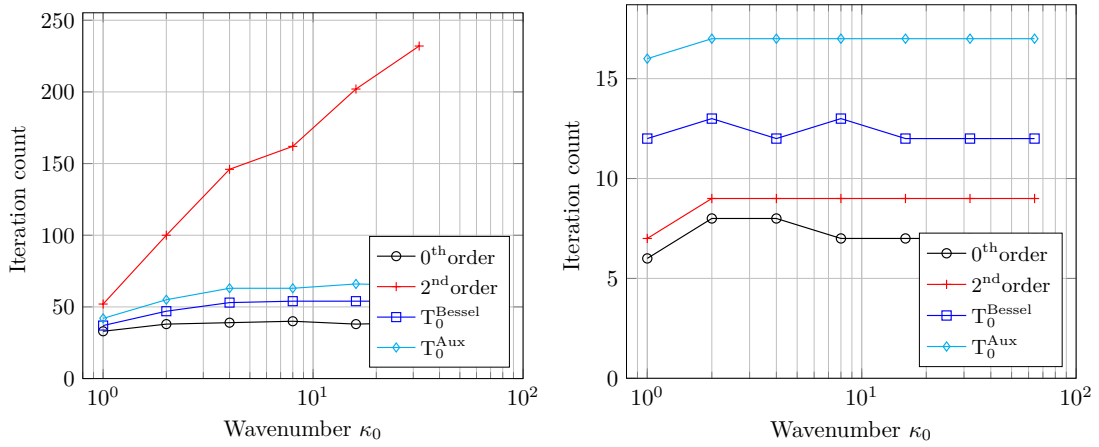

(a) Without preconditioning.

(b) With preconditioning.

Figure 11.20: Helmholtz 2D. Maximum number of iterations of inner CG with respect to the wavenumber κ_0. Fixed parameters $J = 4$, $N_\lambda = 30$, disk of radius $R = 1$.

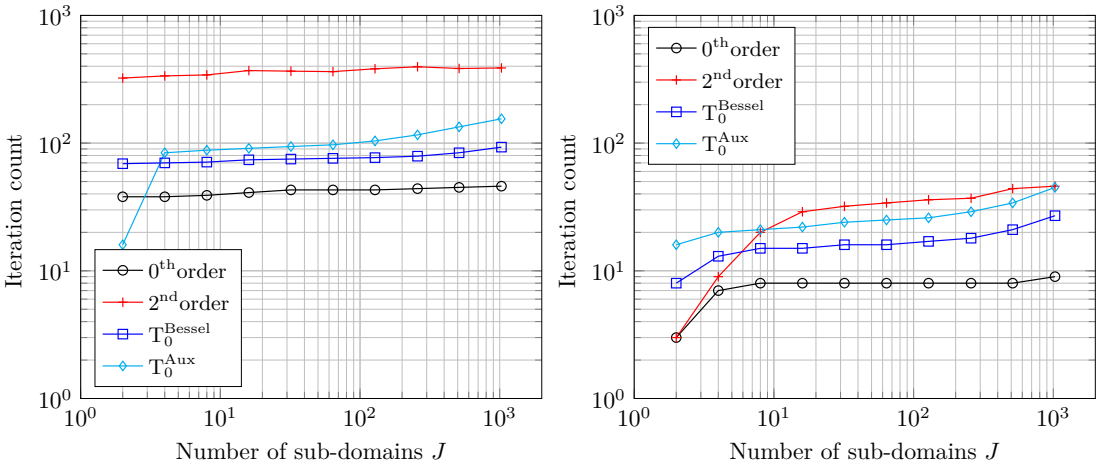

(a) Without preconditioning. (b) With preconditioning.

Figure 11.21: Helmholtz 2D. Maximum number of iterations of inner CG with respect to the number of subdomains J (Strong scaling). Fixed parameters $\kappa_0 = 20$, $N_\lambda = 50$, disk of radius $R = 1$.

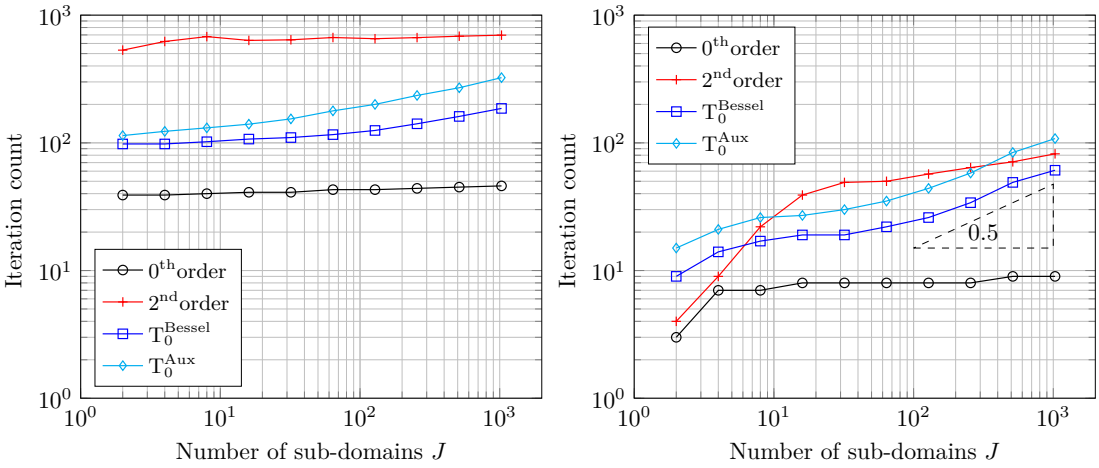

(a) Without preconditioning. (b) With preconditioning.

Figure 11.22: Helmholtz 2D. Maximum number of iterations of inner CG with respect to the number of subdomains J (Strong scaling). Fixed parameters $\kappa_0 = 2$, $N_\lambda = 100$, disk of radius $R = 4$.

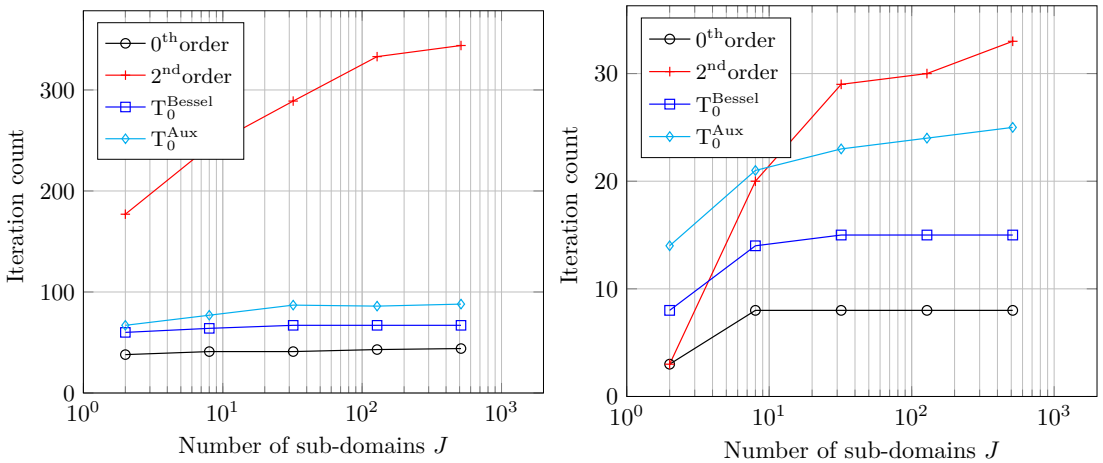

(a) Without preconditioning.

(b) With preconditioning.

Figure 11.23: Helmholtz 2D. Maximum number of iterations of inner CG with respect to the number of subdomains J (Weak scaling). Fixed parameters $\kappa_0 = 5$, $N_\lambda = 40$, disk of increasing radius as $J^{1/d}$.

Conclusion and outlook

Outcomes and main conclusions

A unified formalism for wave propagation problems We proposed a new abstract formalism that unifies the analysis of convergence of a wide class of non-overlapping domain decomposition methods for time-harmonic wave propagation problems. As we have shown, the formalism encompasses both the acoustic and electromagnetic settings, and should be able to be extended to elasticity without much difficulties. We proved the geometric convergence of standard fixed point algorithms, provided non-local transmission operators with simple suitable properties are used.

Stable convergence The geometric convergence proof follows at the discrete level for standard discretization methods, and the convergence rate is proved to be stable with the mesh parameter. This is in contrast with transmission conditions based on local operators for which the discrete convergence factor tends to 1 as the mesh is refined.

A novel treatment of junction points We have developed, within the abstract formalism, a new approach that applies to general geometric configurations, including those with junctions, that is found to generalize the pre-existing approach. The new method can be applied with various transmission operators, including local ones, provided these transmission operators define a scalar product on the trace space.

The geometric convergence proof is recovered if suitable non-local transmission operators are used, and stays stable with respect to the discretization parameter. Besides, the method remains amenable to straightforward parallelization, including the case of distributed-memory architectures.

Novel non-local transmission operators We have proposed several non-local transmission operators suited to the electromagnetic setting which possess explicit integral representations. Somehow unexpectedly, the straightforward discretization of these operators using the boundary element method produced disappointing results in regards to the computation cost.

This motivated to investigate alternative routes to design well-suited non-local transmission operators. A successful alternative strategy is proposed, based on the resolution of elliptic auxiliary problems in the vicinity of the transmission interfaces. Non-local transmission operators built from those auxiliary problems possess many advantages:

1. They satisfy the theoretical requirements of the convergence analysis hence imply guaranteed h-stable (geometric) convergence on arbitrary partitions, including ones with junctions;

2. Their definition is generic, with simple adaptations to the acoustic or electromagnetic settings, including the case of heterogeneous media. Their parameters are easy to choose and do not require complicated tuning to get efficiency. Besides, they are applicable to sub-domains of arbitrary geometry, including ones with rough boundaries generated by automatic graph partitioners, without any additional treatment;

3. Their implementation in practice is straightforward with a computational cost that remains moderate, for instance using standard finite elements, and does not require sophisticated technologies.

If we do not claim that they yield the fastest convergence in every situation — and we acknowledge that competitive alternatives exist with regards to this criteria — we believe that the robustness of the strategy is unmatched, at the expense of a moderate but increased computational cost.

Outlook and possible extensions

The approach that has been developed to tackle the difficulties generated by the presence of junctions in general partitions is rather new. We believe that further work in this direction are required to obtain a mature method. Besides, many interesting questions can be addressed, for instance: How to couple the strategy with integral equations (FEM-BEM coupling)? How to cope with non-conformal meshes? Can we improve the convergence with a second level?

Projection onto the single-trace space The computation of an orthogonal projection is at the heart of the evaluation of the new communication operator and it may be the main computational bottleneck of the new approach if no particular care is taken. Fortunately, the favorable nature of the problem should make it easy to tackle and we have already presented a first possible route based on a preconditioned conjugate gradient algorithm that proved successful. However, some other different approaches can be proposed, which could be even more efficient.

Distributed parallelism Our research code was initially built to test out ideas and is unfortunately not (yet) able to run on a distributed memory machine. Yet, leveraging such distributed architecture is actually one of the main purpose of domain decomposition. This is why a distributed-memory implementation of the method able to run more industrial-like test cases to further test the approach would be a nice addition to this work.

Bibliography

[1] M. Ainsworth, J. Guzmán, and F.-J. Sayas. "Discrete extension operators for mixed finite element spaces on locally refined meshes". In: *Math. Comput.* 85 (2016), pp. 2639–2650.

[2] F. P. Andriulli, K. Cools, H. Bagci, F. Olyslager, A. Buffa, et al. "A Multiplicative Calderon Preconditioner for the Electric Field Integral Equation". In: *IEEE Transactions on Antennas and Propagation* 56.8 (Aug. 2008), pp. 2398–2412. DOI: 10.1109/TAP.2008.926788.

[3] X. Antoine, M. Darbas, and Y. Lu. "An Improved Surface Radiation Condition for High-Frequency Acoustics Scattering Problems". In: *Computer Methods in Applied Mechanics and Engineering* 195 (Aug. 2006), pp. 4060–4074. DOI: 10.1016/j.cma.2005.07.010.

[4] T. Apel. "Interpolation of non-smooth functions on anisotropic finite element meshes". In: *ESAIM: M2AN* 33.6 (1999), pp. 1149–1185. DOI: 10.1051/m2an:1999139.

[5] T. Apel and J. M. Melenk. "Interpolation and Quasi-Interpolation in h - and hp -Version Finite Element Spaces". In: *Encyclopedia of Computational Mechanics Second Edition*. American Cancer Society, 2017, pp. 1–33. DOI: 10.1002/9781119176817.ecm2002m. eprint: https://onlinelibrary.wiley.com/doi/pdf/10.1002/9781119176817.ecm2002m.

[6] F. Assous, P. Ciarlet, and S. Labrunie. *Mathematical foundations of computational electromagnetism*. Vol. 158. Applied Mathematical Sciences. Springer, 2018.

[7] A. Ayala, X. Claeys, V. Dolean, and M. J. Gander. "Closed form inverse of local multitrace operators". In: *Domain Decomposition Methods in Science and Engineering XXIII*. Springer, 2017, pp. 107–115.

[8] J. Ball, Y. Capdeboscq, and B. T. Xiao. "On uniqueness for time harmonic anisotropic Maxwell's equations with pievewise regular coefficients". In: *Mathematical Models and Methods in Applied Sciences* 22 (2012), p. 1250036.

[9] A. Bamberger, B. Engquist, L. Halpern, and P. Joly. "Higher Order Paraxial Wave Equation Approximations in Heterogeneous Media". In: *SIAM Journal on Applied Mathematics* 48.1 (1988), pp. 129–154.

[10] A. Bamberger, P. Joly, and J. E. Roberts. "Second-Order Absorbing Boundary Conditions for the Wave Equation: A Solution for the Corner Problem". In: *SIAM Journal on Numerical Analysis* 27.2 (1990), pp. 323–352. DOI: 10.1137/0727021. eprint: https://doi.org/10.1137/0727021.

[11] B. Beckermann. "Image numérique, GMRES et polynômes de Faber". In: *Comptes Rendus Mathematique* 340.11 (2005), pp. 855–860. DOI: https://doi.org/10.1016/j.crma.2005.04.027.

[12] A. Bendali, Y. Boubendir, and M. Fares. "A FETI-like domain decomposition method for coupling finite elements and boundary elements in large-size problems of acoustic scattering". In: *Computers & Structures* 85.9 (2007). High Performance Computing for Computational Mechanics, pp. 526–535. DOI: https://doi.org/10.1016/j.compstruc.2006.08.029.

[13] A. Bendali and Y. Boubendir. "Dealing with cross-points in a non-overlapping domain decomposition solution of the Helmholtz equation". In: *Mathematical and Numerical Aspects of Wave Propagation WAVES 2003: Proceedings of The Sixth International Conference on Mathematical and Numerical Aspects of Wave Propagation*. Ed. by G. Cohen, P. Joly, E. Heikkola, and P. Neittaanmäki. 2003, pp. 319–324.

[14] A. Bendali and Y. Boubendir. "Méthode de décomposition de domaine et éléments finis nodaux pour la résolution de l'équation d'Helmholtz". In: *Comptes Rendus Mathematique* 339.3 (2004), pp. 229–234. DOI: https://doi.org/10.1016/j.crma.2004.06.002.

[15] A. Bendali and Y. Boubendir. "Non-overlapping Domain Decomposition Method for a Nodal Finite Element Method". In: *Numerische Mathematik* 103.4 (June 2006), pp. 515–537. DOI: 10.1007/s00211-006-0010-9.

[16] J. Bezanson, A. Edelman, S. Karpinski, and V. B. Shah. "Julia: A fresh approach to numerical computing". In: *SIAM review* 59.1 (2017), pp. 65–98.

[17] Y. Boubendir, X. Antoine, and C. Geuzaine. "A Quasi-Optimal Non-Overlapping Domain Decomposition Algorithm for the Helmholtz Equation". In: *J. Comp. Phys.* 213.2 (2012), pp. 262–280.

[18] Y. Boubendir. "Techniques de décomposition de domaine et méthodes d'équations intégrales". PhD thesis. Toulouse, INSA, 2002.

[19] Y. Boubendir, C. Jerez-Hanckes, C. Pérez-Arancibia, and C. Turc. "Domain Decomposition Methods based on quasi-optimal transmission operators for the solution of Helmholtz transmission problems". In: (Sept. 2017).

[20] A. Buffa and P. Ciarlet Jr. "On traces for functional spaces related to Maxwell's equations Part I: An integration by parts formula in Lipschitz polyhedra". In: *Mathematical Methods in the Applied Sciences* 24.1 (2001), pp. 9–30. DOI: 10.1002/1099-1476(20010110)24:1<9::AID-MMA191>3.0.CO;2-2.

[21] A. Buffa and P. Ciarlet Jr. "On traces for functional spaces related to Maxwell's equations Part II: Hodge decompositions on the boundary of Lipschitz polyhedra and applications". In: *Mathematical Methods in the Applied Sciences* 24.1 (2001), pp. 31–48. DOI: 10.1002/1099-1476(20010110)24:1<31::AID-MMA193>3.0.CO;2-X.

[22] A. Buffa, M. Costabel, and C. Schwab. "Boundary element methods for Maxwell's equations on non-smooth domains". In: *Numerische Mathematik* 92.4 (2002), pp. 679–710. DOI: 10.1007/s002110100372.

[23] A. Buffa, R. Hiptmair, T. von Petersdorff, and C. Schwab. "Boundary Element Methods for Maxwell Transmission Problems in Lipschitz Domains". In: *Numerische Mathematik* 95.3 (Sept. 2003), pp. 459–485. DOI: 10.1007/s00211-002-0407-z.

[24] A. Buffa and S. H. Christiansen. "A Dual Finite Element Complex on the Barycentric Refinement". In: *Mathematics of Computation* 76.260 (2007), pp. 1743–1769.

[25] A. Buffa and R. Hiptmair. "Galerkin Boundary Element Methods for Electromagnetic Scattering". In: *Topics in Computational Wave Propagation: Direct and Inverse Problems*. Ed. by M. Ainsworth, P. Davies, D. Duncan, B. Rynne, and P. Martin. Berlin, Heidelberg: Springer Berlin Heidelberg, 2003, pp. 83–124. DOI: 10.1007/978-3-642-55483-4_3.

[26] P. Chevalier. "Méthodes numériques pour les tubes hyperfréquences. Résolution par décomposition de domaine". PhD thesis. Paris 6, 1998.

[27] P. Ciarlet. "Analysis of the Scott-Zhang interpolation in the fractional order Sobolev spaces". In: *Journal of Numerical Mathematics* 21.3 (2013), pp. 173–180. DOI: 10.1515/jnum-2013-0007.

[28] X. Claeys. *A single trace integral formulation of the second kind for acoustic scattering.* Tech. rep. 14. Switzerland: Seminar for Applied Mathematics, ETH Zürich, 2011.

[29] X. Claeys. "A new variant of the Optimised Schwarz Method for arbitrary non-overlapping subdomain partitions". In: *ESAIM: M2AN* (2021). DOI: 10.1051/m2an/2020083. Forthcoming.

[30] X. Claeys, F. Collino, P. Joly, and E. Parolin. "A discrete domain decomposition method for acoustics with uniform exponential rate of convergence using non-local impedance operators". In: *Domain Decomposition Methods in Science and Engineering XXV*. Springer International Publishing, 2020.

[31] X. Claeys, V. Dolean, and M. Gander. "An introduction to multi-trace formulations and associated domain decomposition solvers". In: *Applied Numerical Mathematics* 135 (2019), pp. 69–86. DOI: https://doi.org/10.1016/j.apnum.2018.07.006.

[32] X. Claeys and R. Hiptmair. "Multi-trace boundary integral formulation for acoustic scattering by composite structures". In: *Comm. Pure Appl. Math.* 66.8 (2013), pp. 1163–1201. DOI: 10.1002/cpa.21462.

[33] X. Claeys and E. Parolin. *Robust treatment of cross points in Optimized Schwarz Methods.* 2020. arXiv: 2003.06657 [math.NA].

[34] X. Claeys, B. Thierry, and F. Collino. "Integral equation based optimized Schwarz method for electromagnetics". In: *Domain decomposition methods in science and engineering XXIV*. Vol. 125. Lect. Notes Comput. Sci. Eng. Springer, Cham, 2018, pp. 187–194.

[35] X. Claeys. "Essential spectrum of local multi-trace boundary integral operators". In: *IMA Journal of Applied Mathematics* 81.6 (2016), pp. 961–983.

[36] X. Claeys and R. Hiptmair. *Boundary integral formulation of the first kind for acoustic scattering by composite structures.* Tech. rep. 2011.

[37] X. Claeys and R. Hiptmair. "Electromagnetic scattering at composite objects: a novel multi-trace boundary integral formulation". In: *ESAIM: Mathematical Modelling and Numerical Analysis* 46.6 (2012), pp. 1421–1445.

[38] X. Claeys and R. Hiptmair. "Integral equations on multi-screens". In: *Integral equations and operator theory* 77.2 (2013), pp. 167–197.

[39] X. Claeys and P. Marchand. "Boundary integral multi-trace formulations and Optimised Schwarz Methods". In: *Computers & Mathematics with Applications* (2020).

[40] P. Clément. "Approximation by finite element functions using local regularization". In: 9 (Aug. 1975).

[41] F. Collino, G. Delbue, P. Joly, and A. Piacentini. "A new interface condition in the non-overlapping domain decomposition method for the Maxwell equations". In: *Comput. Methods Appl. Mech. Engrg.* 148.1-2 (1997), pp. 195–207.

[42] F. Collino, S. Ghanemi, and P. Joly. "Domain decomposition method for harmonic wave propagation: a general presentation". In: *CMAME* 184.24 (2000), pp. 171–211.

[43] F. Collino, P. Joly, M. Lecouvez, and B. Stupfel. "Quasi-local transmission conditions for non-overlapping domain decomposition methods for the Helmholtz equation". In: *Comptes Rendus Physique* 15.5 (2014), pp. 403–414. DOI: 10.1016/j.crhy.2014.04.005.

[44] F. Collino, P. Joly, and M. Lecouvez. "Exponentially convergent non overlapping domain decomposition methods for the Helmholtz equation". In: *ESAIM: M2AN* 54.3 (2020), pp. 775–810. DOI: 10.1051/m2an/2019050.

[45] M. Crouzeix and A. Greenbaum. "Spectral Sets: Numerical Range and Beyond". In: *SIAM Journal on Matrix Analysis and Applications* 40.3 (2019), pp. 1087–1101. DOI: 10.1137/18M1198417. eprint: https://doi.org/10.1137/18M1198417.

[46] D.Colton and R.Kress. *Inverse acoustic and electromagnetic scattering theory. 3rd ed.* English. Vol. 93. New York, Springer, 2013, pp. xiv + 405.

[47] B. Després. "Décomposition de domaine et problème de Helmholtz". In: *C. R. Acad. Sci. Paris Sér. I Math.* 311.6 (1990), pp. 313–316.

[48] B. Després. "Domain decomposition method and the Helmholtz problem". In: *Mathematical and numerical aspects of wave propagation phenomena (Strasbourg, 1991)*. SIAM, Philadelphia, PA, 1991, pp. 44–52.

[49] B. Després. "Méthodes de décomposition de domaine pour la propagation d'ondes en régime harmonique. Le théorème de Borg pour l'équation de Hill vectorielle". PhD thesis. Université Paris IX Dauphine, 1991.

[50] B. Després. "Domain decomposition method and the Helmholtz problem (Part II)". In: *Second international conference on mathematical and numerical aspect of wave propagation phenomena SIAM* (1993), pp. 197–206.

[51] B. Després, P. Joly, and J. Roberts. "A domain decomposition method for the harmonic Maxwell equations. Iterative methods in linear algebra". In: *Iterative Methods in Linear Algebra* (1992), pp. 245–252.

[52] B. Després, A. Nicolopoulos, and B. Thierry. "Corners and stable optimized domain decomposition methods for the Helmholtz problem". working paper or preprint. May 2020.

[53] A.-S. B.-B. Dhia, L. Chesnel, and P. C. Jr. "T-Coercivity for the Maxwell Problem with Sign-Changing Coefficients". In: *Communications in Partial Differential Equations* 39.6 (2014), pp. 1007–1031. DOI: 10.1080/03605302.2014.892128. eprint: https://doi.org/10.1080/03605302.2014.892128.

[54] *NIST Digital Library of Mathematical Functions*. http://dlmf.nist.gov/, Release 1.0.18 of 2018-03-27. F. W. J. Olver, A. B. Olde Daalhuis, D. W. Lozier, B. I. Schneider, R. F. Boisvert, C. W. Clark, B. R. Miller and B. V. Saunders, eds.

[55] V. Dolean and M. J. Gander. "Multitrace formulations and Dirichlet-Neumann algorithms". In: *Domain decomposition methods in science and engineering XXII*. Springer, 2016, pp. 147–155.

[56] V. Dolean, M. J. Gander, S. Lanteri, J.-F. Lee, and Z. Peng. "Effective transmission conditions for domain decomposition methods applied to the time-harmonic curl-curl Maxwell's equations". In: *Journal of Computational Physics* 280 (Jan. 2015), pp. 232–247.

[57] V. Dolean, M. Gander, and L. Gerardo-Giorda. *Optimized Schwarz Methods for Maxwell equations*. SIAM J. Sci. Comput., 31(3): 2193-2213, 2009. 2009.

[58] V. Dolean, P. Jolivet, and F. Nataf. *An introduction to domain decomposition methods*. Algorithms, theory, and parallel implementation. Society for Industrial and Applied Mathematics (SIAM), Philadelphia, PA, 2015.

[59] M. El Bouajaji, X. Antoine, and C. Geuzaine. "Approximate local magnetic-to-electric surface operators for time-harmonic Maxwell's equations". In: *Journal of Computational Physics* 279.15 (2014), pp. 241–260.

[60] M. El Bouajaji, V. Dolean, M. J. Gander, and S. Lanteri. "Comparison of a One and Two Parameter Family of Transmission Conditions for Maxwell's Equations with Damping". In: *Domain Decomposition Methods in Science and Engineering XX*. Ed. by R. Bank, M. Holst, O. Widlund, and J. Xu. Berlin, Heidelberg: Springer Berlin Heidelberg, 2013, pp. 271–278.

[61] M. El Bouajaji, B. Thierry, X. Antoine, and C. Geuzaine. "A quasi-optimal domain decomposition algorithm for the time-harmonic Maxwell's equations". In: *Journal of Computational Physics* 294 (2015), pp. 38–57.

[62] M. El Bouajaji, V. Dolean, M. Gander, and A. LANTERI. "Optimized Schwarz Methods for the Time-Harmonic Maxwell Equations with Damping". In: *SIAM Journal on Scientific Computing* 34 (July 2012), A2048–A2071. DOI: 10.1137/110842995.

[63] B. Engquist and A. Majda. "Absorbing Boundary Conditions for the Numerical Simulation of Waves". In: *Mathematics of Computation* 31.139 (1977), pp. 629–651.

[64] B. Engquist and H.-K. Zhao. "Absorbing boundary conditions for domain decomposition". In: *Applied Numerical Mathematics* 27.4 (1998). Special Issue on Absorbing Boundary Conditions, pp. 341–365. DOI: https://doi.org/10.1016/S0168-9274(98)00019-1.

[65] A. Ern and J. Guermond. *Theory and Practice of Finite Elements*. Applied Mathematical Sciences. Springer New York, 2004.

[66] C. Farhat, M. Lesoinne, P. LeTallec, K. Pierson, and D. Rixen. "FETI-DP: a dual–primal unified FETI methodpart I: A faster alternative to the two-level FETI method". In: *International journal for numerical methods in engineering* 50.7 (2001), pp. 1523–1544.

[67] M. Gander. "Optimized Schwarz Methods for Helmholtz Problems". In: *Thirteenth International Conference on Domain Decomposition Methods*. 2001, pp. 245–252.

[68] M. Gander et al. "Schwarz methods over the course of time". In: *Electron. Trans. Numer. Anal* 31.5 (2008), pp. 228–255.

[69] M. Gander, L. Halpern, and F. Nataf. "Optimized schwarz methods". In: *Twelfth International Conference on Domain Decomposition Methods*. 2000, pp. 15–27.

[70] M. Gander and F. Kwok. "Best Robin Parameters for Optimized Schwarz Methods at Cross Points". In: *SIAM Journal on Scientific Computing* 34 (Jan. 2012). DOI: 10.1137/110837218.

[71] M. Gander and F. Kwok. "On the Applicability of Lions' Energy Estimates in the Analysis of Discrete Optimized Schwarz Methods with Cross Points". In: *Lecture Notes in Computational Science and Engineering* 91 (Jan. 2013). DOI: 10.1007/978-3-642-35275-1_56.

[72] M. Gander, F. Magoulès, and F. Nataf. "Optimized Schwarz Methods without Overlap for the Helmholtz Equation". In: *SIAM Journal on Scientific Computing* 24.1 (2002), pp. 38–60.

[73] M. Gander and K. Santugini. "Cross-points in domain decomposition methods with a finite element discretization". In: *Electron. Trans. Numer. Anal.* 45 (2016), pp. 219–240.

[74] M. Gander and H. Zhang. "A Class of Iterative Solvers for the Helmholtz Equation: Factorizations, Sweeping Preconditioners, Source Transfer, Single Layer Potentials, Polarized Traces, and Optimized Schwarz Methods". In: *SIAM Review* 61 (Feb. 2018). DOI: 10.1137/16M109781X.

[75] M. Gander, L. Halpern, and F. Magoulès. "An optimized Schwarz method with twosided Robin transmission conditions for the Helmholtz equation". In: *International Journal for Numerical Methods in Fluids* 55 (Sept. 2007), pp. 163–175. DOI: 10.1002/fld.1433.

[76] M. Gander and H. Zhang. "Optimized Schwarz Methods with Overlap for the Helmholtz Equation". In: *Lecture Notes in Computational Science and Engineering* 98 (Jan. 2014), pp. 207–215. DOI: 10.1007/978-3-319-05789-7__17.

[77] C. Geuzaine and J.-F. Remacle. "Gmsh: A 3-D Finite Element Mesh Generator with Built-in Pre- and Post-Processing Facilities". In: *International Journal for Numerical Methods in Engineering* 79 (Sept. 2009), pp. 1309–1331. DOI: 10.1002/nme.2579.

[78] S. Ghanemi. "Méthodes de Décomposition de Domaines avec conditions de transmission non locales pour des problèmes de propagation d'ondes". PhD thesis. Université Paris IX Dauphine, 1996.

[79] Girault, V. and Lions, J.-L. "Two-grid finite-element schemes for the transient Navier-Stokes problem". In: *ESAIM: M2AN* 35.5 (2001), pp. 945–980. DOI: 10.1051/m2an:2001145.

[80] Y. Goldman, P. Joly, and M. Kern. "The electric field in the conductive halfspace as a model in mining and petroleum prospection". In: *Math. Meth. Appl. Sc.* 11 (1989), pp. 373–401.

[81] Z. Guan-Quan. "High-order approximation of one-way wave equations". In: *J. Comput. Math.* 3 (1985), pp. 90–97.

[82] T. Hagstrom, R. Tewarson, and A. Jazcilevich. "Numerical experiments on a domain decomposition algorithm for nonlinear elliptic boundary value problems". In: *Applied Mathematics Letters* 1.3 (1988), pp. 299–302. DOI: https://doi.org/10.1016/0893-9659(88)90097-3.

[83] R. Hiptmair and C. Jerez-Hanckes. "Multiple traces boundary integral formulation for Helmholtz transmission problems". In: *Advances in Computational Mathematics* 37.1 (2012), pp. 39–91.

[84] R. Hiptmair, C. Jerez-Hanckes, J.-F. Lee, and Z. Peng. "Domain decomposition for boundary integral equations via local multi-trace formulations". In: *Domain decomposition methods in science and engineering XXI*. Springer, 2014, pp. 43–57.

[85] R. Hiptmair and C. Schwab. "Natural Boundary Element Methods for the Electric Field Integral Equation on Polyhedra". In: *SIAM J. Numerical Analysis* 40 (May 2002), pp. 66–86. DOI: 10.1137/S0036142901387580.

[86] F. Ihlenburg. *Finite element analysis of acoustic scattering*. Vol. 132. Applied Mathematical Sciences. Springer-Verlag, New York, 1998, pp. xiv+224. DOI: 10.1007/b98828.

[87] P. Joly and M. Kern. *Etude mathematique du couplage air sous-sol dans la diffusion d'un champ electrique en milieu conducteur tridimensionnel*. Tech. rep. RR-0556. INRIA, Aug. 1986.

[88] P. Joly, S. Lohrengel, and O. Vacus. "Un résultat d'existence et d'unicité pour l'équation de Helmholtz avec conditions aux limites absorbantes d'ordre 2". In: *Comptes Rendus de l'Académie des Sciences - Series I - Mathematics* 329.3 (1999), pp. 193–198. DOI: https://doi.org/10.1016/S0764-4442(00)88592-4.

[89] G. Karypis and V. Kumar. "A fast and high quality schema for partitioning irregular graphs". In: *Siam Journal on Scientific Computing* 20 (Jan. 1999).

[90] A. Klawonn, O. B. Widlund, and M. Dryja. "Dual-Primal Feti Methods for Three-Dimensional Elliptic Problems with Heterogeneous Coefficients". In: *SIAM Journal on Numerical Analysis* 40.1 (2003), pp. 159–179.

[91] M. Lecouvez. "Méthodes itératives de décomposition de domaine sans recouvrement avec convergence géométrique pour l'équation de Helmholtz". PhD thesis. École polytechnique, 2015.

[92] M. Lenoir and N. Salles. "Evaluation of 3-D Singular and Nearly Singular Integrals in Galerkin BEM for Thin Layers". In: *SIAM Journal on Scientific Computing* 36 (2012), pp. 3057–3078. DOI: 10.1137/120866567.

[93] W.-D. Li, W. Hong, H.-X. Zhou, and Z. Song. "Novel Buffa-Christiansen Functions for Improving CFIE With Impedance Boundary Condition". In: 60 (Aug. 2012), pp. 3763–3771.

[94] P.-L. Lions. "On the Schwarz alternating method. I". In: *First international symposium on domain decomposition methods for partial differential equations*. Vol. 1. 1988, pp. 1–42.

[95] P.-L. Lions. "On the Schwarz alternating method. II: Stochastic interpretation and order properties". In: *Second international symposium on domain decomposition methods for partial differential equations*. Vol. 628. 1989, pp. 47–70.

[96] P.-L. Lions. "On the Schwarz alternating method. III: a variant for nonoverlapping subdomains". In: *Third international symposium on domain decomposition methods for partial differential equations*. Vol. 6. 1990, pp. 202–223.

[97] F. Magoulès, P. Iványi, and B. H. V. Topping. "Non-overlapping Schwarz methods with optimized transmission conditions for the Helmholtz equation". In: *Comput. Methods Appl. Mech. Engrg.* 193.45-47 (2004), pp. 4797–4818. DOI: 10.1016/j.cma.2004.05.004.

[98] F. Magoulès, F. X. Roux, and S. Salmon. "Optimal discrete transmission conditions for a non-overlapping domain decomposition method for the Helmholtz equation". In: *SIAM Journal on Scientific Computing* 25.5 (2004), pp. 1497–1515. DOI: 10.1137/S1064827502415351.

[99] F. Magoulès, P. Iványi, and B. Topping. "Convergence analysis of Schwarz methods without overlap for the Helmholtz equation". In: *Computers & Structures* 82.22 (2004), pp. 1835–1847. DOI: https://doi.org/10.1016/j.compstruc.2004.02.025.

[100] J. Mandel and M. Brezina. "Balancing domain decomposition for problems with large jumps in coefficients". In: *Mathematics of Computation* 65 (Oct. 1996), pp. 1387–1401. DOI: 10.1090/S0025-5718-96-00757-0.

[101] W. McLean. *Strongly Elliptic Systems and Boundary Integral Equations*. First Edition. Cambridge University Press, 2000.

[102] A. Meurer, C. P. Smith, M. Paprocki, O. ertík, S. B. Kirpichev, et al. "SymPy: symbolic computing in Python". In: *PeerJ Computer Science* 3 (Jan. 2017), e103. DOI: 10.7717/peerj-cs.103.

[103] F. A. Milinazzo, C. A. Zala, and G. H. Brooke. "Rational square-root approximations for parabolic equation algorithms". In: *The Journal of the Acoustical Society of America* 101.2 (1997), pp. 760–766. DOI: 10.1121/1.418038. eprint: https://doi.org/10.1121/1.418038.

[104] A. Modave, C. Geuzaine, and X. Antoine. "Corner treatments for high-order local absorbing boundary conditions in high-frequency acoustic scattering". In: *Journal of Computational Physics* 401 (2020), p. 109029. DOI: https://doi.org/10.1016/j.jcp.2019.109029.

[105] A. Modave, A. Royer, X. Antoine, and C. Geuzaine. "An optimized Schwarz domain decomposition method with cross-point treatment for time-harmonic acoustic scattering". working paper or preprint. Jan. 2020.

[106] P. K. Mogensen and A. N. Riseth. "Optim: A mathematical optimization package for Julia". In: *Journal of Open Source Software* 3.24 (2018), p. 615. DOI: 10.21105/joss.00615.

[107] P. Monk. *Finite Element Methods for Maxwell's Equations*. Numerical mathematics and scientific computation. Clarendon Press; Oxford University Press, 2003.

[108] F. Nataf. "Absorbing boundary conditions and perfectly matched layers in wave propagation problems". In: *Direct and Inverse problems in Wave Propagation and Applications*. Vol. 14. Radon Ser. Comput. Appl. Math. de Gruyter, 2013, pp. 219–231.

[109] F. Nataf, F. Rogier, and E. de Sturler. "Optimal interface conditions for domain decomposition methods". In: (1994).

[110] J.-C. Nédélec. *Acoustic and Electromagnetic equations*. Applied Mathematical Sciences. New-York: Springer-Verlag, 2001.

[111] A. Nicolopoulos. "Formulations variationnelles d'équations de Maxwell résonantes et problmes aux coins en propagation d'ondes". PhD thesis. Sorbonne Université, 2019.

[112] N. Ortner and P. Wagner. "A Survey on Explicit Representation Formulae for Fundamental Solutions of Linear Partial Differential Operators". In: *Acta Applicandae Mathematica* 47.1 (1997), pp. 101–124. DOI: 10.1023/A:1005784017770.

[113] C. Pechstein. *Finite and boundary element tearing and interconnecting solvers for multiscale problems*. Vol. 90. Lecture Notes in Computational Science and Engineering. Springer, Heidelberg, 2013, pp. xiv+312. DOI: 10.1007/978-3-642-23588-7.

[114] Z. Peng and J.-F. Lee. "Non-conformal domain decomposition method with second-order transmission conditions for time-harmonic electromagnetics". In: *Journal of Computational Physics* 229 (Aug. 2010), pp. 5615–5629. DOI: 10.1016/j.jcp.2010.03.049.

[115] Z. Peng and J.-F. Lee. "A Scalable Nonoverlapping and Nonconformal Domain Decomposition Method for Solving Time-Harmonic Maxwell Equations in $\mathbb{R}^3$". In: *SIAM Journal on Scientific Computing* 34 (Jan. 2012). DOI: 10.1137/100817978.

[116] Z. Peng, V. Rawat, and J.-F. Lee. "One way domain decomposition method with second order transmission conditions for solving electromagnetic wave problems". In: *Journal of Computational Physics* 229 (Feb. 2010), pp. 1181–1197. DOI: 10.1016/j.jcp.2009.10.024.

[117] A. Piacentini and N. Rosa. "An improved domain decomposition method for the 3D Helmholtz equation". In: *Computer Methods in Applied Mechanics and Engineering* 162.1 (1998), pp. 113–124. DOI: https://doi.org/10.1016/S0045-7825(97)00336-8.

[118] A. Quarteroni and A. Valli. *Domain Decomposition Methods for Partial Differential Equations*. Jan. 1999.

[119] V. Rawat and J.-F. Lee. "Nonoverlapping Domain Decomposition with Second Order Transmission Condition for the Time-Harmonic Maxwell's Equations". In: *SIAM Journal on Scientific Computing* 32.6 (2010), pp. 3584–3603. DOI: 10.1137/090777220. eprint: https://doi.org/10.1137/090777220.

[120] J. Roberts and J.-M. Thomas. "Mixed and hybrid methods". In: *Finite Element Methods (Part 1)*. Vol. 2. Handbook of Numerical Analysis. Elsevier, 1991, pp. 523–639. DOI: https://doi.org/10.1016/S1570-8659(05)80041-9.

[121] A. A. Rodriguez and L. Gerardo-Giorda. "New Nonoverlapping Domain Decomposition Methods for the Harmonic Maxwell System". In: *SIAM Journal on Scientific Computing* 28.1 (2006), pp. 102–122. DOI: 10.1137/040608696. eprint: https://doi.org/10.1137/040608696.

[122] Y. Saad and M. H. Schultz. "GMRES: A Generalized Minimal Residual Algorithm for Solving Nonsymmetric Linear Systems". In: *SIAM Journal on Scientific and Statistical Computing* 7.3 (1986), pp. 856–869. DOI: 10.1137/0907058. eprint: https://doi.org/10.1137/0907058.

[123] Y. Saad. *Iterative Methods for Sparse Linear Systems*. Second. Society for Industrial and Applied Mathematics, 2003. DOI: 10.1137/1.9780898718003. eprint: https://epubs.siam.org/doi/pdf/10.1137/1.9780898718003.

[124] S. Sauter and C. Schwab. *Boundary element methods*. Vol. 39. Springer Series in Computational Mathematics. Translated and expanded from the 2004 German original. Springer-Verlag, Berlin, 2011, pp. xviii+561. DOI: 10.1007/978-3-540-68093-2.

[125] H. A. Schwarz. *Ueber einen Grenzübergang durch alternirendes Verfahren*. Zürcher u. Furrer, 1870.

[126] L. Scott and S. Zhang. "Finite element interpolation of nonsmooth functions satisfying boundary conditions." English. In: *Math. Comput.* 54.190 (1990), pp. 483–493.

[127] A. Toselli and O. Widlund. *Domain decomposition methods—algorithms and theory*. Vol. 34. Springer Series in Computational Mathematics. Springer-Verlag, Berlin, 2005, pp. xvi+450. DOI: 10.1007/b137868.

[128] F. Vico, L. Greengard, and Z. Gimbutas. "Boundary integral equation analysis on the sphere". In: *Numerische Mathematik* 128.3 (Oct. 2014), pp. 463–487. DOI: 10.1007/s00211-014-0619-z.

ECOLE
DOCTORALE
DE MATHEMATIQUES
HADAMARD

Titre : Méthodes de décomposition de domaine sans recouvrement avec opérateurs de transmission non-locaux pour des problèmes de propagation d'ondes harmoniques

Mots clés : Méthodes de décomposition de domaine, ondes harmoniques, points de jonction.

Résumé : Les premiers travaux de B. Després, puis M. Gander, F. Magoules et F. Nataf ont montré qu'il est nécessaire, du moins dans le contexte des équations d'ondes, d'utiliser des conditions de transmission de type impédante pour le couplage des sous-domaines afin d'obtenir la convergence des méthodes de décomposition de domaine sans-recouvrement. L'approche standard considérée dans la littérature utilise un opérateur d'impédance local permettant une convergence algébrique dans les meilleurs cas. Des travaux ultérieurs dus à F. Collino, S. Ghanemi et P. Joly puis F. Collino, P. Joly et M. Lecouvez ont permis de montrer que l'utilisation d'opérateurs d'impédance non-locaux, comme par exemple des opérateurs intégraux avec des noyaux singuliers adaptés, peut permettre une convergence géométrique des méthodes de décomposition de domaine.
Cette thèse prolonge ces travaux (qui ont principalement concerné l'équation de Helmholtz scalaire) pour dans un premier temps étendre l'analyse au cas de la propagation d'ondes électromagnétiques. De plus, l'analyse numérique de la méthode est pour la première fois effectuée, démontrant la stabilité du taux de convergence par rapport au paramètre de discrétisation, et ainsi la robustesse de l'approche. Plusieurs opérateurs intégraux sont ensuite proposés comme opérateurs de transmission pour les équations de Maxwell dans le même esprit que ceux construits pour le cas de l'acoustique. Une alternative aux opérateurs intégraux, fondée sur la résolution de problèmes auxiliaires elliptiques, est par ailleurs proposée et étudiée. De nombreuses expériences numériques ont été menées, illustrant le haut potentiel de cette nouvelle approche. À partir de récents travaux de X. Claeys, la dernière partie de ce travail consiste à exploiter le formalisme multi-trace afin d'étendre l'analyse au cas des partitions comportant des points de jonction, problème ayant attiré beaucoup d'attention récemment. Cette nouvelle approche met en jeu un nouvel opérateur permettant la communication d'informations entre sous-domaines, qui a vocation à remplacer l'opérateur point-à-point classique. Une preuve de convergence géométrique de l'algorithme itératif associé, également uniforme par rapport au paramètre de discrétisation, est disponible et l'on montre que l'on retrouve l'algorithme classique en l'absence de point de jonction.

Title : Non overlapping domain decomposition methods with non-local transmission operators for harmonic wave propagation problems

Keywords : Domain decomposition methods, harmonic waves, junction points.

Abstract : The pioneering work of B. Després then M. Gander, F. Magoules and F. Nataf have shown that it is mandatory, at least in the context of wave equations, to use impedance type transmission conditions in the coupling of subdomains in order to obtain convergence of non-overlapping domain decomposition methods (DDM). In the standard approach considered in the literature, the impedance operator involved in the transmission conditions is local and leads to algebraic convergence of the DDM in the best cases. In later works, F. Collino, S. Ghanemi and P. Joly then F. Collino, P. Joly and M. Lecouvez have observed that using non local impedance operators such as integral operators with suitable singular kernels could lead to a geometric convergence of the DDM.
This thesis extends these works (that mainly concerned the scalar Helmholtz equation) with the extension of the analysis to electromagnetic wave propagation. Besides, the numerical analysis of the method is performed for the first time, proving the stability of the convergence rate with respect to the discretization parameter, hence the robustness of the approach. Several integral operators are then proposed as transmission operators for Maxwell equations in the spirit of those constructed for the acoustic setting. An alternative to integral operators, based on the resolution of elliptic auxiliary problems, is also advocated and analyzed. Extensive numerical results are conducted, illustrating the high potential of the new approach. Based on a recent work by X. Claeys, the last part of this work consists in exploiting the multi-trace formalism to extend the convergence analysis to the case of partitions with junction points, which is a difficult problem that attracted a lot of attention recently. The new approach relies on a new operator that communicates information between sub-domains, which replaces the classical point-to-point exchange operator. A proof of geometrical convergence of the associated iterative algorithm, again uniform with respect to the discretization parameter, is available and we show that one recovers the standard algorithm in the absence of junction points.

Institut Polytechnique de Paris
91120 Palaiseau, France